HCV assembly : from clustering of viral assembly factors to envelopment and lipidation of particles

Solène Denolly

N°d'ordre NNT : 2018LYSE1085

THESE de DOCTORAT DE L'UNIVERSITE DE LYON
opérée au sein de
l'Université Claude Bernard Lyon 1

Ecole Doctorale N° 340
Biologie moléculaire, intégrative et cellulaire

Spécialité de doctorat : **Science de la Vie**
Discipline : Virologie

Soutenue publiquement le 31/05/2018, par :
Solène DENOLLY

HCV assembly: from clustering of viral assembly factors to envelopment and lipidation of particles

---

Devant le jury composé de :

Berlioz-Torrent, Clarisse Directrice de Recherche Institut Cochin Rapportrice

Martin, Annette Directrice de Recherche Institut Pasteur Rapportrice

Schuster, Catherine Directrice de Recherche Institut de Recherche sur les Maladies Virales et Hépatiques Examinatrice

Faure, Mathias Professeur Centre International de Recherche en Infectiologie Examinateur

Pietschmann, Thomas Professeur Twincore Examinateur

Cosset, François-Loïc Directeur de Recherche Centre International de Recherche en Infectiologie Directeur de thèse

HCV assembly: from clustering of viral assembly factors to envelopment and lipidation of particles

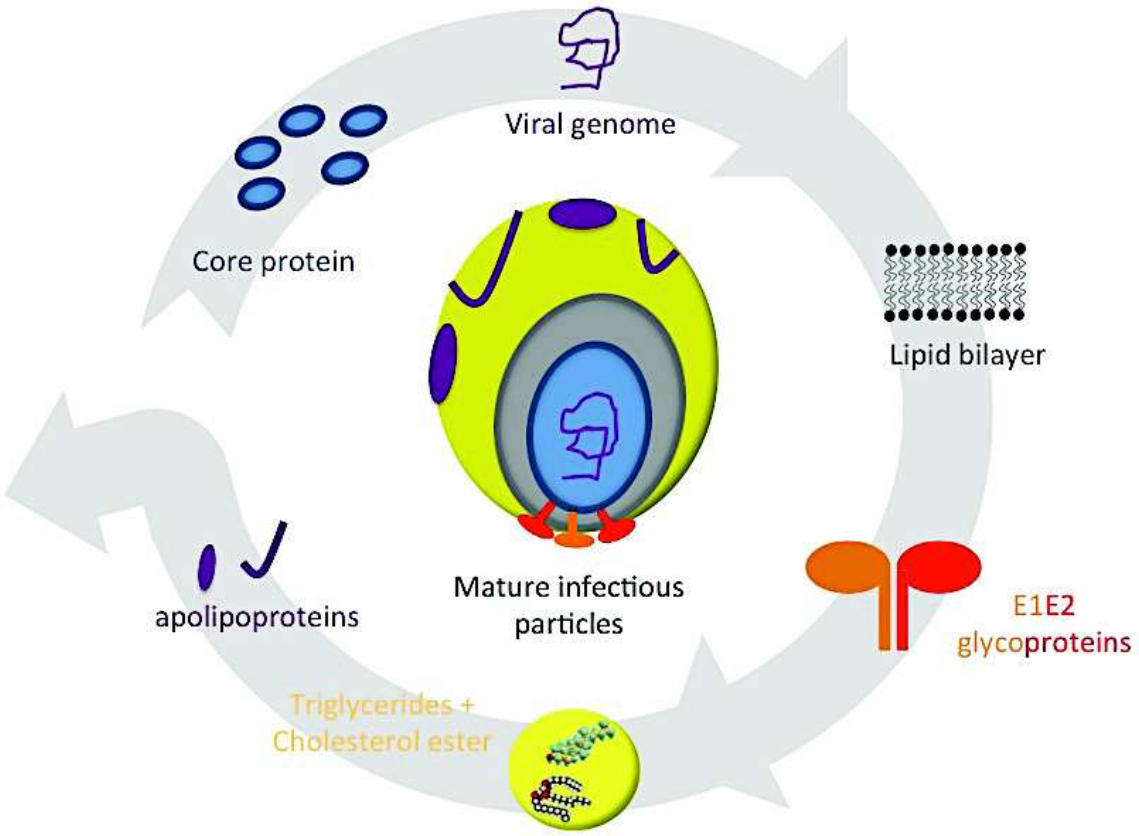

Remerciements

Je tiens tout d'abord à remercier les membres de mon Jury pour le temps qu'ils ont pris pour évaluer mon travail et pour leur précieuses aides sur ce manuscrit.

Je voudrais ensuite remercier très chaleureusement François-Loïc pour tout ce que tu m'as appris, toute ton aide, tes encouragements et ton soutien. J'ai énormément appris à tes côtés sur la recherche, la science, le métier de chercheur… Je te remercie également pour l'indépendance que tu m'as offerte. Tu as toujours été présent tout en me laissant prendre des initiatives, en me poussant à suivre mes idées et en me poussant à faire des propositions. Je repense souvent à tous les mails où tu me disais « Proposition ? » ! Merci également pour toutes les opportunités que tu m'as offertes. Merci pour nos réunions biblio hebdomadaire qui m'ont permis d'apprendre beaucoup, de développer mon esprit critique… En résumé, tu es la personne qui a permis que ma thèse se déroule de la meilleure des façons. Enfin, merci d'avoir pris du temps pour relire et m'aider pour l'écriture de ce manuscrit

Immense merci à toi, Bertrand !! Tu as également joué un rôle très important dans la réussite de ma thèse. C'est toi qui m'as appris à « maniper » en P1, en P2, en P3… J'ai beaucoup appris à tes côtés. Ton rôle a été vraiment déterminant pour mes premiers pas au labo, alors que je n'étais qu'un « bébé » au laboratoire. Je te remercie pour ta patience, ton aide, ton soutien également. Merci pour tout le temps que tu as passé pour moi, en réunion, en manip, en congrès… Merci pour ta relecture de cette thèse.

Merci ensuite à Chloé. Merci pour ta bonne humeur, merci pour ton investissement au quotidien qui a grandement contribué à la réussite de notre papier sur la p7. C'est un vrai plaisir de travailler ensemble. Tu es un véritable soutien pour moi en qui j'ai toute confiance.

Merci ensuite à Nelly et Christelle. Merci pour votre travail et votre investissement pour la réussite de notre projet « sérum humain ». C'est également un vrai plaisir pour moi d'animer ce groupe de travail.

Merci aussi à Fouzia. Merci pour ton travail et ton investissement qui m'ont beaucoup aidé. Nous n'avons pas travaillé ensemble très longtemps mais j'en garde un super souvenir !

Merci ensuite à tous les membres de l'équipe. Membres actuels … membres partis. Merci car vous m'avez tous aidé de près ou de loin. Merci à tous pour les bons moments passés ensemble, pour votre soutien également. Merci pour tout ce que vous m'avez également appris. Merci Didier, merci Floriane pour tous vos précieux conseils, avis.
Merci à mes collègues de bureau pour leur discussion, leur bonne humeur. Merci à Jimena, Fouzia, Natalia, Margot, Camille, Bertrand, Sonia, Vincent, Florian, Greg, Fanny. Merci Florian et Sonia de partager votre expérience de thésard ! Merci Vincent pour tous ces moments du quotidien de thésard vécus ensemble (dans le bureau ou au P3) et merci pour ta bonne humeur marseillaise… Merci Natalia pour ta relecture de ce manuscrit et ton enthousiasme communicatif !

Merci aussi à tous les « piliers du laboratoire », merci pour tout ce que vous faites au quotidien pour rendre la vie plus facile à tous. Merci pour votre temps pour l'organisation du laboratoire !

Merci également à « mes » stagiaires, Alexandra d'abord, puis Amélie maintenant. J'ai également beaucoup appris à vos côtés. Au-delà de votre travail, nos discussions scientifiques ont été et le sont encore, très enrichissantes. C'est un véritable échange et un véritable plaisir pour moi d'avoir travaillé avec vous.

Merci à François Pénin de votre temps pour nos discussions, votre partage très enrichissants sur la p7, sur le VHC et sur les structures et propriétés des protéines. Nos échanges m'ont beaucoup appris, ont beaucoup fait avancer mon travail.
Merci à Mathias Faure et Mathieu Clavière pour votre expertise, pour les manips que vous avez faites pour nous aider à y voir plus clair sur nos mutants.
Merci à Thomas Bourlet et Bruno Pozzetto. Merci pour votre collaboration, merci pour votre investissement pour nos dosages de core. Ils nous ont grandement permis d'avancer et d'améliorer nos résultats.
Merci à Maryse Guérin pour votre collaboration, nos nombreuses discussions au téléphone et vos précieux conseils.
Merci à Yves Gouriou. Merci pour tout le temps que tu as passé sur nos cellules à essayer de comprendre comment marche p7.
Merci à Baptiste Panthu. Merci de m'avoir associé à ton travail. Merci pour nos discussions dans le train, sur le quai et au labo…

Merci à tous mes amis, à tous mes proches, pour votre soutien et vos encouragements tout au long de ma thèse. Merci à tous pour m'avoir écouté, m'avoir aidé. Vous avez tous contribué à votre façon à la réussite de cette thèse.
Merci aussi Cyril. Tu es arrivé en fin de parcours mais ta présence à mes côtés est un véritable soutien.

Enfin je voudrais remercier ma famille. Plus particulièrement, Papa, Maman, Corentin, vous avez été mes soutiens de la première heure, vous m'avez toujours encouragée, poussée. Merci à vous pour tout. Vous avez toujours cru en moi donc tout simplement un grand merci.

Je finirai par dédier ce manuscrit à Florence.

Abstract

Hepatitis C virus (HCV) is detected in the sera of infected patients as infectious particles of very-low densities. HCV is an enveloped virus whose assembly of viral particles occurs at the endoplasmic reticulum membrane. Its genome is translated as a polyprotein that is further cleaved in ten mature proteins corresponding to either structural or non-structural (NS) proteins with specific functions in viral RNA replication and virion assembly. In addition, specific protein precursors, representing non-cleaved parts of the polyprotein, are also detected in infected cells, underscoring additional functions. Our laboratory is interested at better understanding the mechanisms of assembly, envelopment and secretion of infectious particles, in which I have been involved during my PhD.

In a first project addressing the early steps of HCV assembly, we found that the E2 and core structural proteins colocalize with NS5A and NS4B non-structural proteins and viral RNA, highlighting the functional connection between replication complexes and NS2-based assembly sites. We also demonstrated how the direct-acting antiviral drug daclatasvir, an NS5A inhibitor, blocks this process by preventing the delivery of viral genome to assembly site, which induces clustering of both structural and non-structural proteins.

In a second and main PhD project, we focused on the role of p7, the HCV viroporin, in assembly of infectious particles. Particularly, we investigated the role of the delayed cleavage between E2 and p7 in this process. Using biochemical assays, we showed that p7 dose-dependently slows down the ER-to-Golgi traffic, leading to intracellular retention of E2, which suggests that timely E2p7 cleavage and p7 liberation are critical events to control E2 levels. In addition, using mutants that accelerated the cleavage between E2 and p7, we showed that E2p7 cleavage controls E2 intracellular expression and secretion levels of subviral particles and infectious virions. Finally, we also highlighted that the regulation of E2p7 cleavage controls the unmasking of novel functions localized at p7 amino-terminal extremity. Specifically, we found that this part of the protein governs the specific infectivity of the infectious particles by coordinating the interaction of NS2 with NS5A and E2, which allows the encountering of the nucleocapsid components with the glycoproteins at the assembly site but also the envelopment of the nucleocapsid.

In a third project, we aimed at characterizing how HCV particles acquire their lipidated forms. We discovered specific functions and factors from serum, producer cells, and HCV sequences that modulate lipidation of viral particles during their assembly and secretion. Specifically we found that acquisition of lipids could occur in the extracellular medium and requires lipoproteins as lipid source as well as an seric protein factor as mediator of lipids transfer. Interestingly we also demonstrate that hypervariable region I of E2 is involved in the regulation of the lipidation level of particles.

Altogether, through my involvement in these different projects, I have contributed at better understanding the steps of HCV assembly and the mechanisms modulating i) the

transfer of viral RNAs from replication complexes to assembly sites, ii) the encountering of the nucleocapsids and glycoproteins followed by virion envelopment, and finally, iii) the acquisition of lipids by viral particles; all these steps being essential for the formation of fully infectious particles.

Résumé

Le virus de l'hépatite C (VHC) est détecté dans les sérum de patients infectés sous forme de particules infectieuses de très faibles densités. Le VHC est un virus enveloppé dont l'assemblage de particules virales (PV) se produit au niveau de la membrane du réticulum endoplasmique. Son génome est traduit en une polyprotéine qui est ensuite clivée en dix protéines matures correspondant à des protéines structurales ou non structurales (NS) avec des fonctions spécifiques dans la réplication de l'ARN viral et l'assemblage du virion. De plus, des précurseurs de protéines, représentant des parties non clivées de la polyprotéine, sont également détectés dans des cellules infectées, soulignant des fonctions supplémentaires. Notre laboratoire s'intéresse à mieux comprendre les mécanismes d'assemblage, d'enveloppement et de sécrétion des particules infectieuses, dans lesquels j'ai été impliqué durant mon doctorat.

Dans un premier projet portant sur les premières étapes de l'assemblage, nous avons démontré que les protéines structurales E2 et core co-localisaient avec les protéines non structurales NS4B et NS5A et l'ARN viral, soulignant la connexion fonctionnelle entre les complexes de réplication et les sites d'assemblage. Nous avons également démontré comment le daclatasvir, un inhibiteur de NS5A et molécule antivirale à action directe, bloque ce processus en empêchant la distribution du génome viral au site d'assemblage, ce qui induit le regroupement des protéines structurales et non structurales.

Dans un deuxième et principal projet de thèse, nous nous sommes concentrés sur le rôle de p7, la viroporine du VHC, dans l'assemblage de particules infectieuses. En particulier, nous avons étudié le rôle du clivage retardé entre E2 et p7 dans ce processus. En utilisant des techniques biochimiques, nous avons montré que p7 ralentissait de façon dose-dépendante le trafic ER-Golgi, conduisant à une rétention intracellulaire de E2. Ceci suggère que le clivage E2p7 et la libération de p7 sont des événements critiques pour contrôler les niveaux d'E2. En outre, en utilisant des mutants avec un clivage entre E2 et p7 accéléré, nous avons montré que le clivage E2p7 contrôle l'expression intracellulaire E2 et les niveaux de sécrétion de particules sous-virales et de virions infectieux. Enfin, nous avons également montré que la régulation du clivage E2p7 contrôle le démasquage de nouvelles fonctions localisées à l'extrémité amino-terminale p7. Plus précisément, nous avons démontré que cette partie de la protéine régit l'infectivité spécifique des particules infectieuses en coordonnant l'interaction de NS2 avec NS5A et E2. La régulation de ces interactions permet la rencontre des composants de la nucléocapside avec les glycoprotéines au site d'assemblage, mais aussi l'enveloppement du nucléocapside.

Dans un troisième projet, nous avons cherché à caractériser la façon dont les particules de VHC acquièrent leurs formes lipidées. Nous avons découvert des fonctions et des facteurs spécifiques du sérum, des cellules productrices et des séquences du VHC qui modulent la lipidation des particules virales au cours de leur assemblage et de leur sécrétion. En effet, nous avons constaté que l'acquisition de lipides pourrait se produire dans le milieu extracellulaire et nécessiter des lipoprotéines comme source de lipides ainsi qu'un facteur sérique comme médiateur du transfert des lipides. De manière intéressante, nous avons pu démontrer que la région hypervariable I de E2 est impliquée dans la régulation du niveau de lipidation des particules.

Au total, grâce à mon implication dans ces différents projets, j'ai contribué à mieux comprendre les étapes de l'assemblage du VHC et les mécanismes modulant i) le transfert des ARN viraux des complexes de réplication vers les sites d'assemblage, ii) la rencontre des nucléocapsides et des glycoprotéines enfin, iii) l'acquisition de lipides par des particules virales, toutes ces étapes étant essentielles à la formation de particules entièrement infectieuses.

Table of contents

List of abbreviations

A

Alb	Albumin
ALT	Alanine aminoransferase
Apo	Apolipoprotein

B

BVDV	Bovine Viral Diarrhea Virus

C

CE	Cholesterol Ester
CETP	Cholesterol Ester Transport Protein
CF	CarboxyFluorescein
CLDN1	Claudin-1

D

DAAs	Direct Acting Antivirals
DCV	Daclatasvir
DGAT1	Diacylglycerol O-acyltransferase 1
DI	Domain I
DII	Domain II
DIII	Domain III
DMV	Double Membrane Vesicle
DRM	Detergent-Resistant Membranes
dsRNA	double-stranded RNA

E

EGFR	Epidermal Growth Factor Receptor
eIF	eukaryotic Initiation Factor
eLVP	empty Lipo-Viral Particles
EMCV	EncephaloMyoCarditis Virus
endoH	endoglycosydase H
ER	Endoplasmic Reticulum
ERGIC	ER Golgi Intermediate Compartment
ESCRT	Endosomal Sorting Complexes Required for Transport

F

Fah	fumarylacetoacetate hydrolase
FCS	Fetal Calf Serum
FRG	$Fah^{-/-}$ $Rag2^{-/-}$, $\gamma\text{-}c^{-/-}$

G

GFP	Green Fluorescent Protein
GP	Glycoprotein
Gt	Genotype

H

HBV	Hepatitis B Virus

HCC	HepatoCellular Carcinoma
HCV	Hepatitis C Virus
HCVcc	Cell-culture grown HCV
HCVfrg	Mice FRG HCV particles
HCVpp	HCV pseudoparticles
HCVsgr	HCV subgenomic replicon
HCVsp	Patient serum-derived HCV particles
HDL	High-Density Lipoproteins
HIV	Human Immunodeficient Virus
HL	Hepatic Lipase
HS	Human Serum
HSA	Human Serum Albumin
HSPG	Heparan Sulfate ProteoGlycans
Huh7.5	Human hepatoma cells 7.5
HVRI	HyperVariable Region I

I

IAV	Influenza A Virus
IDL	Intermediate-Density Lipoproteins
IFN	Interferon
IL	Interleukin
IRES	Internal Ribosome Entry Site
ISG	IFN-Stimulated Genes

J

JFH-1	Japanese Fulminant Hepatitis

K

kDa	kiloDalton
KO	Knock-Out

L

LCAT	Lecithin:Cholesterol AcylTransferase
LDL	Low-Density Lipoproteins
LDLr	Low-Density Lipoprotein receptor
LDs	Lipids Droplets
LPDS	LipoProtein-Depleted Serum
LPL	LipoProtein Lipase
LVP	Lipo-Viro-Particle

M

Mir	microRNA
MLV	Murine Leukemia Virus
MTP	Microsomal Triglyceride-Transfer Protein

N

NMR	Nuclear Magnetic Resonance
NPC1L1	Niemann-Pick C1-like 1
NS	Non-Structural

O

OCLN	Occludin
ORF	Open Reading Frame

P

PI4KIIIα	Phosphatidyl-Inositol-4-Kinase-III α
PI4P	Phosphatidyl-Inositol-4-Phosphate

R

RBV	Ribavirin
RNA	RiboNucleic Acid

S

sE2	soluble E2
SP	Signal Peptidase
SR-BI	Scavenger Receptor B1

T

TG	TriGlycerides
TMD	TransMembrane Domain

U

uPA-SCID	Urokinase Plasminogen Activator/Severe Combined ImmunoDeficiency
UTR	UnTranslated Regions

V

VLDL	Very-Low-Density Lipoproteins
VLDL-R	VLDL receptor
VLP	Virus-Like-Particles
VSV-G	Vesicular Stomatitis Virus glycoprotein G
VSV-Gts	thermosensitive VSV-G

W

WHO	World Health Organization

INTRODUCTION

I- THE LIVER: KEY ORGAN FOR HCV INFECTION

I.1- The liver

The liver is a vital organ involved in several functions related to metabolism of carbohydrates, proteins and lipids, and also the clearance of toxins and pathogens and the regulation of the immune response. Lipids, peptides, carbohydrates and nutrients are delivered to the liver via gut-derived portal venous blood, passing first through sinusoidal lining cells before finally being taken up and metabolized by hepatocytes.
The liver is composed of smaller histological structures called lobules, roughly hexagonal in shape, which are surrounded by branches of the hepatic artery (which provides oxygen) and the portal vein (which provides nutrients) (Figure 1). These two vessels merge into sinusoids, which are distensible vascular channels lined with sinusoidal endothelial cells (SECs) and bound circumferentially by hepatocytes (Figure 1). These cells are separated from hepatocytes by the space of Disse (Figure 2).

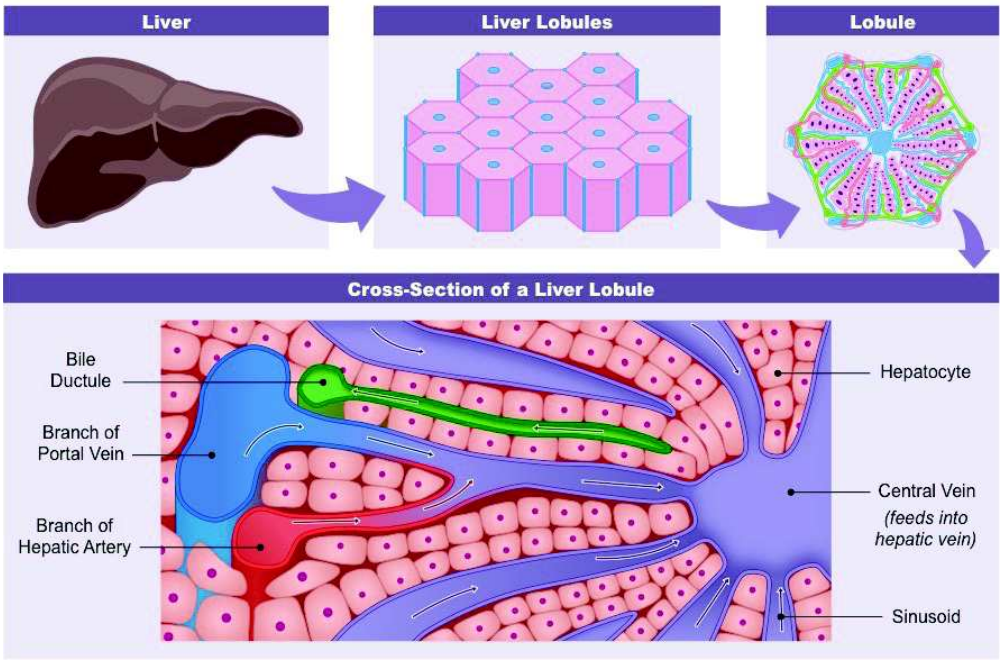

Figure **1: Liver structure.** Liver is composed of hexagonal lobules, which are surrounded by branches of artery or vein. These vessels merged into sinusoids that are bounded by hepatocytes. http://ib.bioninja.com.au/options/option-d-human-physiology/d3-functions-of-the-liver/liver-structure.html

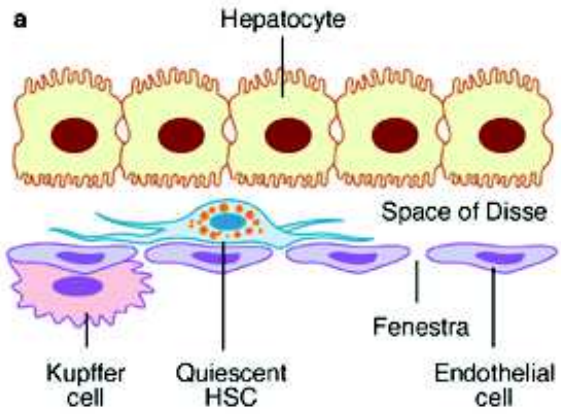

Figure 2: Sinusoid organization. The subendothelial space of Disse separates the epithelial component (hepatocytes) from the sinusoidal endothelium. The tissue macrophages – Kupffer cells – are found in the sinusoids, whereas the hepatic stellate cells (HSCs) are perisinusoidal in location. (Hui & Friedman, 2003)

The liver structure is also conditioned by its secretory functions, particularly, with respect to the synthesis and secretion of bile. Hepatocytes are arranged in polarized "plates" with their apical surfaces facing and surrounding the sinusoids. The basal faces of adjoining hepatocytes are welded together by junctional complexes, such as tight and gap junction as well as desmosomes, to form with adjoining hepatocytes small bile ducts, the canaliculis. Bile produced by hepatocytes drains into the canaliculi that unite to form larger bile ducts, which lead to the gallbladder and ultimately drained into the duodenum.

I.2- The lipoproteins

I.2.1- The lipoprotein structure

Neutral lipids, such as cholesterol ester (CE) and triglycerides (TG) are insoluble in water and therefore need a special way of transport, called lipoproteins. These lipoproteins are composed of a core of hydrophobic lipids surrounded by a monolayer of phospholipids, providing an amphipathic interface with the hydrophilic environment of the plasma. In addition to phospholipids, the external layer is made of unesterified cholesterol and some proteins called apolipoproteins (Figure 3).

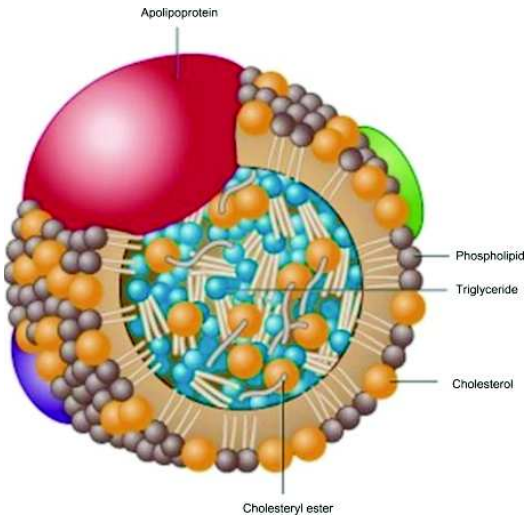

Figure 3: Lipoprotein structure. Phospholipids are oriented with their polar head outside. Free cholesterol and apolipoprotein are inserted within the phospholipid monolayer. Triglyceride and cholesterol ester are found inside the lipoprotein. (Alagona, 2010)

Size, density and content of CE and TG are used to separate and characterize plasma lipoproteins. They are divided in five categories: chylomicrons, very-low-density lipoproteins (VLDL), intermediate-density lipoproteins (IDL), low-density lipoproteins (LDL) and high-density lipoproteins (HDL) (Figure 4) (Wasan et al., 2008).

Characteristics	Chylomicrons	Very low-density lipoproteins	Low density lipoproteins	High density lipoproteins
Density (g per mL)	< 0.95	0.95–1.006	1.019–1.063	1.063–1.210
Particle diameter (nm)	> 75	30–80	18–25	5–12
Protein composition (% dry weight)	1–2	8–10	20–25	52–60
Triacylglycerol composition (% dry weight)	80–88	45–53	5–9	2–3
Cholesterol composition (% dry weight)	2–4	17–27	43–50	12–25
Phospholipid composition (% dry weight)	7–9	17 – 19	19–21	17–24
Function	Transport of exogenous triacylglycerol and cholesterol	Transport of endogenous triacylglycerol	Cholesterol transport to all tissues	Reverse cholesterol transport

Figure 4: Characteristics of lipoproteins found in plasma. (Wasan et al., 2008)

I.2.2- Apolipoproteins

Apolipoproteins are divided in six classes (A-B-C-D-E-H) and several subclasses (Figure 5). They have several functions: they have a structural role, they help in the formation of the lipoproteins, serve as ligands for lipoproteins receptors and act as activators/inhibitors of specific enzymes (Figure 5) (Feingold & Grunfeld, 2000). The large majority of apolipoproteins are composed of amphipathic helices (Segrest et al., 1992) and are exchangeable between different lipoproteins, implying their reversible binding to lipoprotein particles. In contrast apoB remains bound to lipoprotein particles from its biosynthesis to catabolism.

Apolipo-protein	Plasma concentration (mg per dL)	Present on chylomicrons	Distribution into lipoproteins during fasted state (%)			Molecular weight (kDa)	Function
			VLDL	LDL	HDL		
ApoA1	130	Transiently	0	0	100	29.0	LCAT activator; substrate for SRB1
ApoA2	40	No	0	0	100	17.4	Structure; hepatic lipase inhibitor; substrate for SRB1
ApoA4	15	Yes	0	0	0	44.5	LCAT activator
ApoB48	Transient	Exclusively	0	0	0	241	Chylomicron structure
ApoB100	80–250	No	6–12	88–94	0	512	Structure; receptor ligand
ApoC1	3–6	No	3	0	97	6.6	LCAT activator
ApoC2	3–12	No	40	0	60	9.0	Lipoprotein lipase activator
ApoC3	12	No	30	10	60	9.0	Hepatic lipase inhibitor
ApoD	10–12	No	0	0	100	19.0	Many postulated
ApoE	5–7	Yes	40	10	50	34.0	Substrate for LDLr; chylomicron remnant receptor

Figure 5: Characteristics of apolipoproteins. Adapted from (Wasan et al., 2008)
LCAT: Lecithin-cholesterol acyltransferase; SRB1: Scavenger Receptor B1; LDLr: LDL receptor

I.2.3- Lipoproteins metabolism

I.2.3.1- Exogenous pathway

The intestine absorbs the dietary lipids, mainly composed of triglycerides but also cholesterol found in the bile, secreted by the liver. Following absorption, these lipids are assembled with apoB-48 in lipoprotein complexes, name chylomicrons (van Greevenbroek & de Bruin, 1998). The nascent chylomicrons are secreted into the lymphatic vessels and drained into the bloodstream. Maturation of chylomicrons occurs in the blood with the exchange of apoC-II and apoE with HDL. The presence of apoC-II activates the lipoprotein lipase (LPL), resulting in the hydrolyzation of TG in glycerol and fatty acids. The products of these reactions are taken up by the peripheral tissue. The remnant chylomicrons continue circulating and because of the presence of apoE, they interacts with receptors in the liver, such as the low-density lipoprotein receptor (LDLr) (Mortimer et al., 1995), heparan sulfate proteoglycans (HSPG) (Bishop et al., 2007, Dallinga-Thie et al., 2010) or the Scavenger Receptor B1 (SR-BI) (Out et al., 2004), resulting in their absorption by the liver (Figure 6, left).

I.2.3.2- Endogenous pathway

In the endogenous pathway, cholesterol is manly synthesized by the liver and is secreted into the bile or incorporated, as free and esterified forms into VLDL, which are then secreted into the plasma. Secreted nascent VLDL particles, containing apoB-100 and apoE, are then matured by acquisition of more apoE and apoC from HDL particles. Similar to chylomicron metabolism, VLDLs circulate in the bloodstream until they encounter LPL, residing on endothelial cells (Eckel, 1989). After hydrolysis by LPL, VLDL remnants or IDL continue circulating until their reabsorption via apoE on the surface of the liver. Alternatively, they can also be further hydrolyzed by the hepatic lipase (HL), resulting in the release of LDL (IDL remnants). LDLs are either absorbed by the liver or the peripheral tissue through the interaction of apoE or apoB-100 with the LDLr. In the liver, LDL is converted into bile acids and secreted into the intestine; in non-hepatic tissues, LDL is hydrolyzed and the resulting components are used for cell membrane synthesis or storage.
ApoA-I is synthesized and secreted from hepatocytes. This apolipoprotein is attached to ATP-binding cassette transporter A1 (ABCA1), a cellular cholesterol efflux pump, and lipidated by free cholesterol and phospholipids (Wang et al., 2000). ApoA-I is also associated with lecithin acyl cholesterol acyltransferase (LCAT), which esterifies cholesterol, allowing the formation of nascent HDL. LCAT catalyzes the formation of CE from unesterified cholesterol at the surface of HDL by transferring fatty acids from phosphatidylcholine (PC) to cholesterol(Jonas, 2000). The nascent HDLs receive more CE and become spherical in shape and increase in size: smaller HDLs are called HDL3 whereas the larger ones are designated HDL2. HDL2 is able to deliver cholesterol to the

peripheral tissues or the liver, through the interaction with the scavenger receptor class B type I (SR-BI).
Exchange of CE for TG could occur between HDL and apoB-containing lipoproteins (such as VLDL or LDL) with the action of the CE Transport Protein (CETP) via a non-enzymatic process (Cucuianu et al., 2007). Newly acquired CE in LDL and VLDL is then taken up by the hepatic LDLr for excretion in the bile (Morton & Greene, 1997) (Figure 6 right).

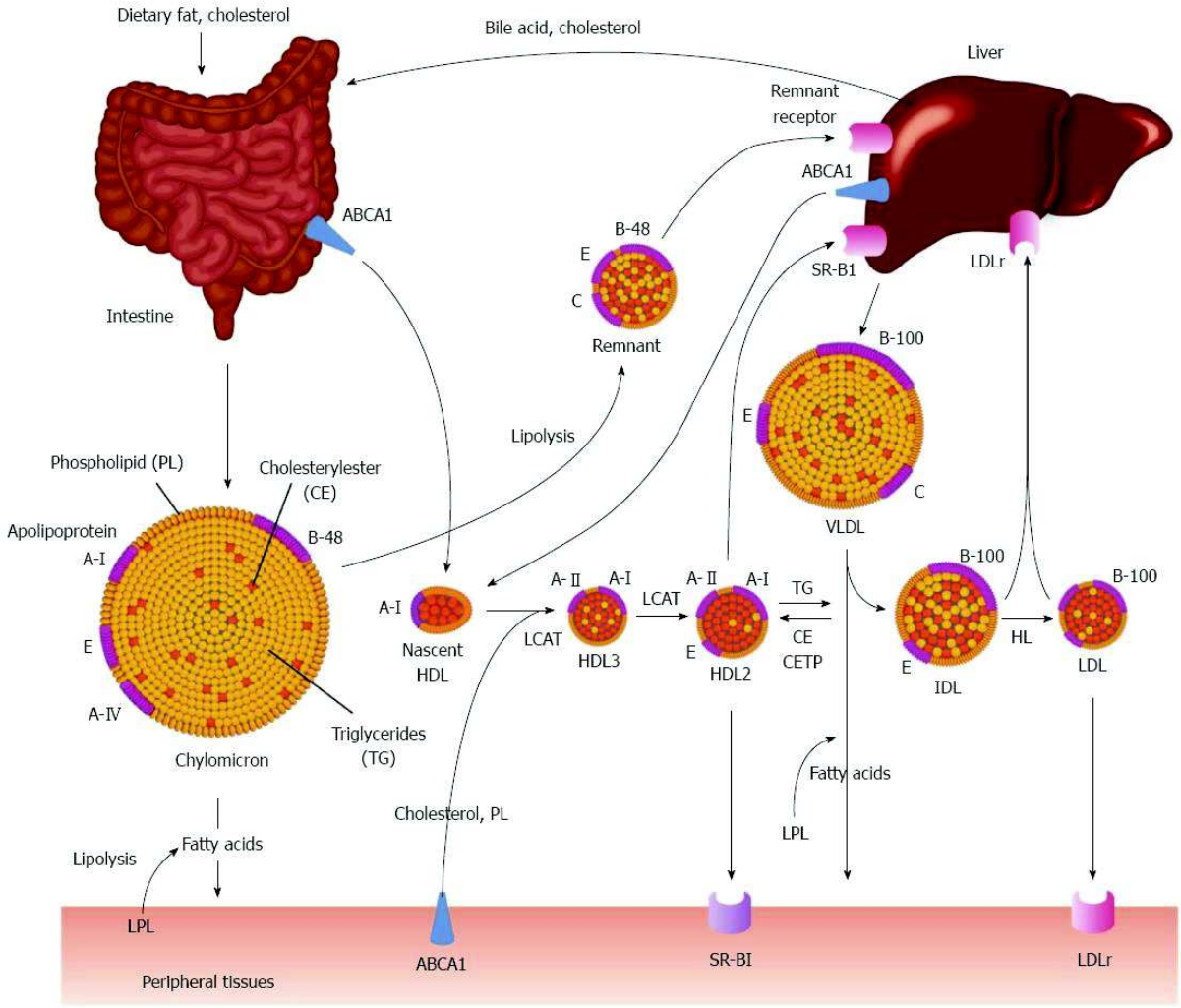

Figure 6: Lipoproteins metabolism. (Aizawa et al., 2015). See text for more details

II- HEPATITIS C VIRUS INFECTION

II.1- HCV prevalence and epidemiology

Hepatitis C is a global liver disease with 71 million chronically infected people. Its prevalence varies between 0.5 and 2.9% (Figure 7) (Manns et al., 2017), depending on the region. The highest prevalence is observed in Egypt (10% in 2015; (Estes et al., 2015)) due to the use of contaminated syringes during a massive treatment campaign to eradicate schistosomiasis, a parasitic disease causing chronic illness.

HCV is a bloodborne virus. It is most commonly transmitted among drug users by sharing injection equipment, reuse or inadequate sterilization of medical equipment (more particularly syringes and needles), transfusion of unscreened blood and blood products (WHO 2017). HCV can also be transmitted sexually and can be passed from an infected mother to her baby; however, these modes of transmission are now much less common (WHO 2017). It is difficult to diagnosed since the acute phase is asymptomatic and an estimated 45-85% of infected people are undiagnosed (Smith et al., 2012).

Approximately 399 000 people die each year from hepatitis C, mostly from cirrhosis and hepatocellular carcinoma (WHO 2017).

The estimates obtained from mathematical modeling suggest that worldwide, in 2015, there were 1.75 million new HCV infections (WHO 2017).

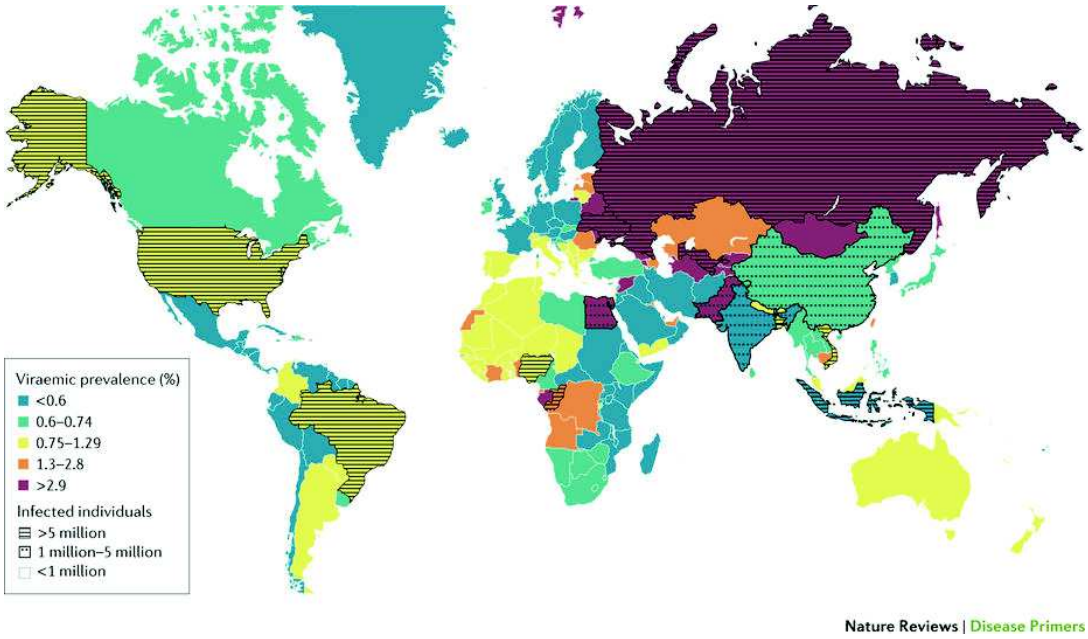

Figure 7: HCV prevalence map. (Manns et al., 2017)

II.2- Immune responses

HCV persistent infection is due to the ability of HCV to evade and restrict both the cellular innate anti-viral response and HCV specific adaptive immune response.

II.2.1- Innate immune responses

Innate immunity is the first-line antiviral defense of the host and induces the production of interferons (iFNs) and cytokines. HCV infection is recognized by several pattern recognition receptors (PRRs) sensed by pathogen-associated molecular patterns (PAMPs). Indeed, the viral double-stranded RNA (dsRNA) is recognized by the endosomal Toll-like receptor (TLR) 3 whereas the poly (U) motif of the genome is recognized by the retinoic acid-inducible gene I (RIG-I). TLR2 is able to sense HCV core and NS3 proteins. In addition, viral RNA is recognized by TRL7 and TLR8. All these recognitions induce the activation of specific cellular pathways leading to the synthesis and secretion of IFN-β but also the expression of several IFN-inducible genes (ISG) (Figure 8). Some of these ISG lead to the inhibition of viral and host RNA translation, as well as the degradation of viral and cellular RNA (Chan & Ou, 2017).
However, it is clear that HCV attenuates the IFN response at multiple levels. For example, HCV NS3/4A proteins cleave protein involved downstream RIG-I and TLR-3 mediated signaling pathway. E2 and NS5A, HCV proteins are also able to block protein kinase R (PKR), another PRR activated by HCV virus (Horner & Gale, 2013)(Figure 9). In addition, HCV induced autophagy is a way to suppress innate immunes responses (Chan & Ou, 2017). In conclusion, the ability of HCV to restrict the cellular antiviral control severely impacts the cellular ability to trigger efficient adaptive responses. However, it has been demonstrated that hepatocytes have developed an unconventional mechanism to stimulate adaptive immune response. Indeed, the plasmacytoid dendritic cells (pDC), which are the major IFN-α secreting cells, are able to secrete IFN-α without direct contact with infectious particles. They are activated by viral-RNA containing exosomes that are secreted by infected hepatocytes (Dreux et al., 2012).

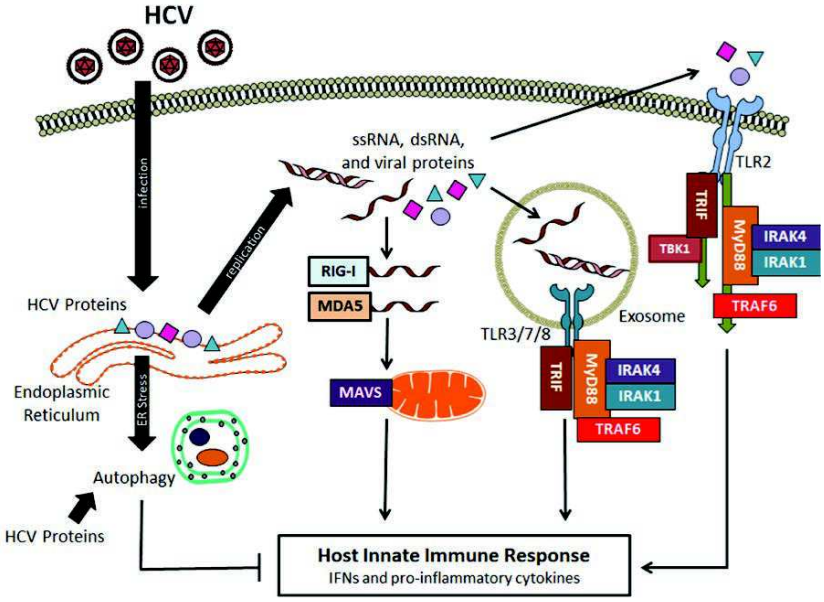

Figure 8: HCV recognition by the host and HCV induced autophagy. After infection HCV products can activate several pathways leading to production of interferon and cytokines. To prevent this production, HCV activates several mechanism including autophagy. Adapted from (Chan & Ou, 2017)
ssRNA: single stranded RNA; dsRNA: double-stranded RNA; TRL: Toll-like Receptor; RIG-I: retinoic acid-inducible gene I; MDA5: melanoma differentiation-associated protein 5 ; IRAKs: Interleukin (IL)-1 receptor-associated kinases; MAVS: Mitochondrial antiviral signaling protein; MyD88: Myeloid differentiation primary-response protein 88;; TRAF6: Tumor necrosis factor receptor-associated factor 6; TRIF: Toll/IL-1 receptor

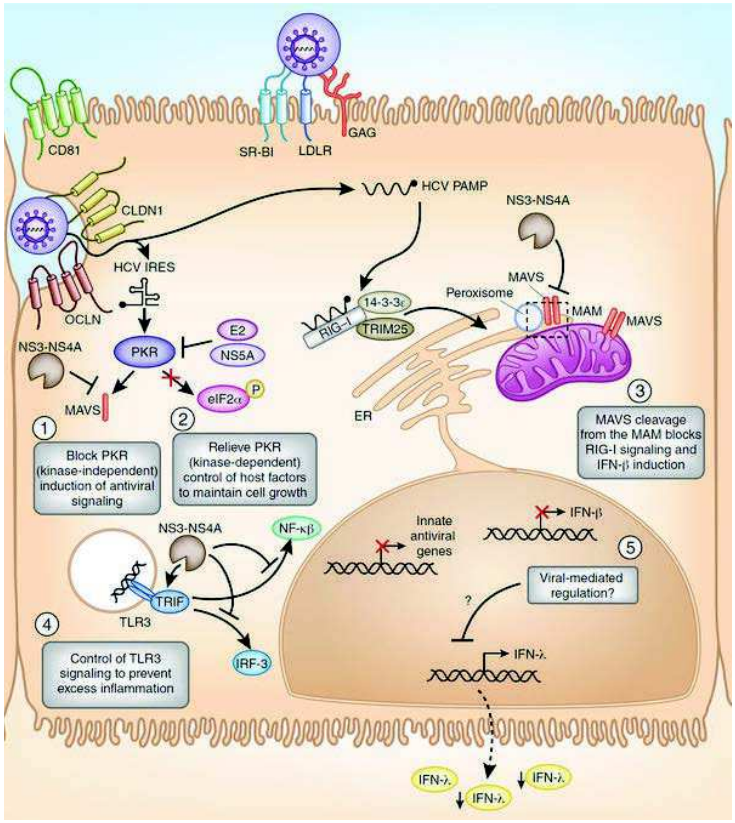

Figure 9: HCV control of IFN induction and immune evasion. The proposed regulation is shown here, where the HCV NS3/4A protease cleaves the signaling adaptors MAVS and TRIF to inactivate (1) PKR, (3) RIG-I, and (4) TLR3 signaling pathways to prevent induction of immunomodulatory innate antiviral genes and IFN-β allowing for HCV replication. (5) HCV infection control of IFN-λ induction is not yet defined; (2) HCV E2 and NS5A proteins inactivate PKR kinase-dependent activation of the host translation factor eIF2α to reactivate protein translation during infection. Adapted from (Horner & Gale, 2013)

II.2.2- Adaptive immune responses

II.2.2.1- Cellular adaptive immune responses

Several reports have shown that HCV elimination is associated with CD4+ and CD8+ T cell responses. These cells are able to recognize several epitopes among HCV proteins (Thimme et al., 2002, Thimme et al., 2001). $CD4^+$ T cells are non-cytotoxic T lymphocytes that regulate $CD8^+$ T and B-lymphocytes function through secretion of interleukine 2 (IL2). $CD8^+$ T cells are cytotoxic lymphocytes that target specifically the infected cells and induce their apoptosis.

HCV-specific T cell responses usually appear 4 to 8 weeks after the beginning of the acute phase of infection (Thimme et al., 2012). The initiation of the cellular adaptive response is correlated with a rise in serum alanine aminotransferase (ALT). At this stage, a high viremia is observed, which then decreases simultaneously with T cells responses (Figure 10A).
However, the HCV-specific T cell responses are usually weak or not sustained, likely due to the viral control of the innate immune responses preventing the stimulation of the adaptive immune system but also due to emergence of viral escape mutations and impaired CD8+ T cells functions (caused by the lack of CD4+ T cells or expression of inhibitory receptors) (Heim & Thimme, 2014, Thimme et al., 2012). The absence of a strong T cell response usually results in maintenance of viremia and in disease progression to chronicity (Figure 10A).
In contrast, effective CD4+ and CD8+ T cell response can persistently resolve virus infection (figure 10) and in this case, a second infection will result in low HCV titers and a more rapid viral clearance (Figure 10B).

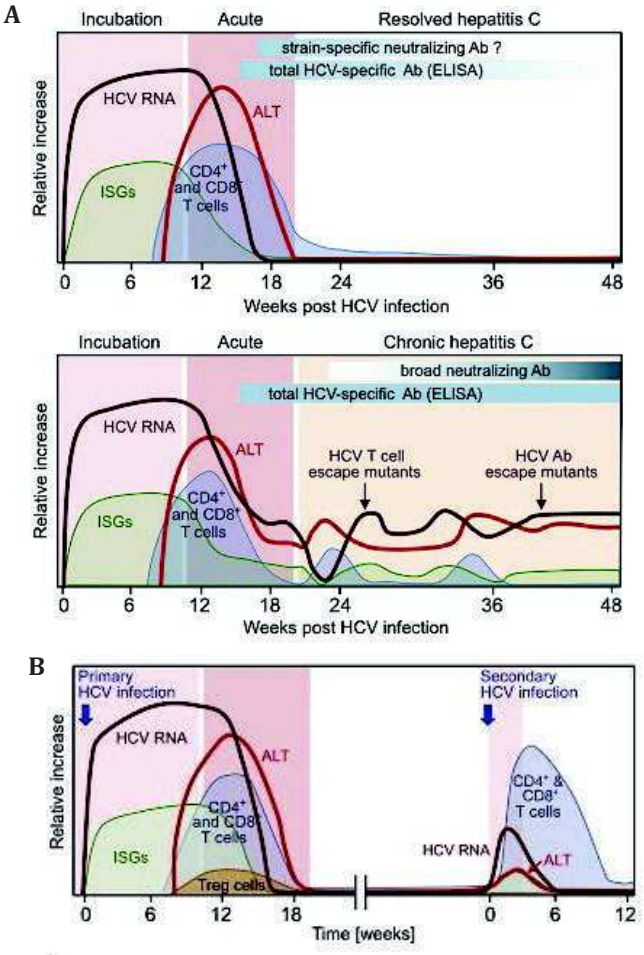

Figure 10: HCV course of infection. (A) Clinical parameters observed after infection with either resolved infection (upper panel) or infection moving to chronicity (lower panel). (B) Due to a strong T cells response, a secondary infection will result in a more rapid viral clearance. Adapted from (Park & Rehermann, 2014)
Brown: viral RNA; red: alanine aminotransferase (ALT); blue: T cells responses; green: Interferon-stimulated gene
(ISGs)

II-2.3.2- Humoral adaptive immune responses

The second arm of the adaptive immune responses is mediated by B-lymphocytes (or B cells). After antigen recognition and presentation by antigen presenting cells (APC), the antigen-specific cells subsets proliferate and differentiate to plasmocytes that secrete antigen-specific antibodies, including neutralizing antibodies. Antibodies play a key role during virus infection by preventing virus binding to cell receptors. Using different models, multiple epitopes targeted by neutralizing antibodies have been identified in the hypervariable region 1 (HVR-1) of the viral glycoproteins that form HCV envelope (Farci et al., 1994).

The role of this response remains not fully understood. On the one hand, some studies have reported the ineffectiveness of HCV neutralizing antibodies to resolve HCV infection both in chimpanzees and humans (Yu et al., 2004). On the other hand, other studies predicted an important role of these antibodies in delaying HCV infection (Thimme et al., 2012). For example anti-HCV immunoglobulins were shown to delay or prevent HCV infection in chimpanzee if inoculated before or simultaneously to virus challenge (Farci et al., 1994). In addition studies that analysed the neutralizing responses in patient cohorts infected by a single source of viral inoculum, showed strong neutralizing responses during acute phase of infections and a correlation of this response with resolution of infections (Lavillette et al., 2005b, Pestka et al., 2007).
The presence of neutralizing antibodies in chronically infected patients highlights the existence of a tight balance between the host neutralizing response and the generation of escape variants (von Hahn et al., 2007). Indeed, the selective pressure of the neutralizing antibodies on E2 epitopes such as HVRI likely contributes to the constant generation of HVRI/E2 quasi-species that can evade the host neutralizing response. This is consistent with studies suggesting that HVRI-mediated quasi species diversity is a relevant indicator of chronic infection (Farci et al., 2000).
Multiple mechanisms have been suggested to explain the failure or the attenuation of the humoral immune response. For example, interaction of HCV glycoproteins with high-density lipoprotein receptor or the scavenger receptor B1 (SR-BI) involved in viral entry may result in escape to neutralizing antibodies (Bartosch et al., 2005, Dreux et al., 2006). Another mechanism proposed is cell-cell transmission (Timpe et al., 2008). Indeed transmission of genome between infected cells and naïve cells could occur in presence of neutralizing antibodies suggesting that cell-cell transmission could be a way to transmit infectivity and to escape neutralizing antibodies at the same time.

II.3- Pathogenesis

HCV infection is a long-term viral infection that develops and persists during several decades in patients.

Commonly, the first stages of infection correspond to an acute hepatitis syndrome that can evolve six months after infection into a chronic liver disease in 70% of cases (Heim, 2013). Serious liver damages including hepatic steatosis and fibrosis are observed in 15-25% of patients after a long and progressive disease evolution that can last many years. Hepatocellular carcinoma appears in about 3% of cirrhotic patients per year and constitute the final stage of the infection disease (Figure 11).

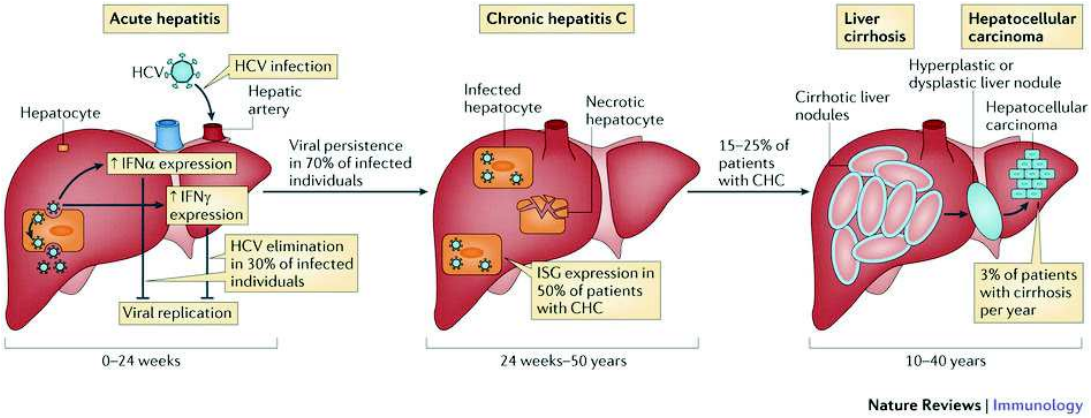

Figure 11: HCV pathogenesis and course of infection. During infection, acute infection progress in 70% of the case toward a chronic liver disease leading to the development of cirrhosis and hepatocellular carcinoma. (Heim, 2013)

Acute hepatitis is often asymptomatic, so it is difficult to be diagnosed. Less than 1% of patients develop a fulminant acute hepatitis C. Viral RNA can be detected between 1 and 3 weeks after HCV exposure (Orland et al., 2001). Between 4 and 12 weeks after viral exposure, elevated alanine aminotransferase level in the blood is the first sign of liver injury (Santantonio et al., 2008). Diagnosis of acute HCV infection is confirmed by detection of HCV RNA and anti-HCV antibody seroconversion, which occurs 4-10 weeks after HCV infection (Post et al., 2004).

Clearance of acute HCV infection may be caused by a complex interplay between host and viral factors, such as sex (men are more prompt to develop chronic disease), viral genotype (genotype 1 was shown to be associated with an increased probability of clearance) as well as genetic polymorphism (IL28B) (Tillmann et al., 2010). The dynamics of viral loads seems to be quite diverging after 3-4 months of infection, ranging from clearance to viral persistence of the virus and could be a way to improve diagnosis (Hajarizadeh et al., 2013)

Chronic hepatitis C is defined by the persistence of viral RNA for at least 6 months after the first infection (Farci et al., 1996). During the 10-15 first years of infection, liver diseases progress slowly. Several parameters have been shown to modulate the risk of developing fibrosis, such as sex (men (Poynard & Bedossa, 1997), ethnicity (black people (Wiley et al., 2002)), age superior to 40 (Minola et al., 2002), and insulin resistance (Hui et al., 2003)).

HCV is the causative agent of cirrhosis with a probability of about 16% after 20 years of infection and 41% after 30 years of infection (Hajarizadeh et al., 2013). As HCV infection is not cytopathic, virus-induced damages are attributed to the reaction of the immune system against the infection, such as cell dysfunction and modification of inflammatory signaling pathways (Wu et al., 2014).

The development of HCC could occur although HCV-infected patients do not have the same risk of developing liver cancer. Genotype 1 is associated with a higher rate of HCC development, likely due to the core protein that displays oncogenic properties *in vitro*. The age of patients could also influence the development of HCC (Ahmad et al., 2011).

II.4- Therapies

Nowadays there is no vaccine is available against HCV. Yet, in the past few years, HCV therapy has profoundly evolved. Before 2011, bi-therapy was used by a combination of pegylated-IFN (peg-IFN) and ribavirin (RBV). This treatment was unspecific, induced important side effects in patients and its efficiency was restricted to particular HCV genotypes. Since 2011, several direct acting antivirals (DAAs) have been approved. These molecules target the NS3/4A protease, the NS5B polymerase and the NS5A protein. The use of these DAAs (in combination) lead to sustained virological responses (SVR), with rates higher than 90% within short periods of time (8-12 weeks).

II.4.1- NS3 inhibitors

In 2011, two new DAAs have been approved by the Food and Drug Administration (FDA) and the European Medicines Agency (EMA) for the treatment of HCV infection: telaprevir (Lin et al., 2006) and boceprevir (Tong et al., 2006). These two molecules target the NS3/4A protease activity through binding to NS3 active site. In addition, with peg-IFN and RBV, they have improved the SVR from 40% to 70% in patients infected by HCV genotype 1. However, these compounds increased the side effects of peg-IFN and RBV and act only on genotype 1. In addition, they have a low genetic barrier to resistance and many drug-drug interactions that is they could reduce the effect of treatment of other pathologies, such as HIV in the case of co-infection HCV/HIV.
A second wave of anti-proteases emerged in 2013 with simeprevir (Raboisson et al., 2008), licensed for the treatment of infection with genotype 1 or 4 but can also act on several other genotypes with exception of genotype 3 (Moreno et al., 2012). Another inhibitor, paritaprevir, was approved in 2014 in combination with other DAAs as well as with a cytochrome CYP3A4 inhibitor (ritonavir), since paritaprevir is metabolized by this cytochrome. Finally, grazoprevir, in combination with elbasvir, an NS5A inhibitor, was approved in 2016 for treatment of genotype 1 and 4 and clinical demonstrated SVR in up to 97% for genotype 1 and 100% for genotype 4.

II.4.2- NS5A inhibitors

Ledipasvir was approved in 2014 and, in combination with sofosbuvir, it was the first treatment free from interferon and ribavirin. It does not act with the same efficiency on all genotypes (lower activity of genotype 2 and genotype 3). Daclatasvir (Gao et al.,

2010) was approved in 2015 for use with sofosbuvir (see below). It acts in low concentrations (picomolar) and with broad coverage of HCV genotypes. It was first described to inhibit HCV replication probably by inhibiting the formation of double-membrane vesicles required for the replication of the viral genome (Berger et al., 2014). In addition, some studies reported an action on assembly (Guedj et al., 2013, McGivern et al., 2014) by preventing the delivery of RNA to the core protein, the main component of the HCV nucleocapsid (Boson et al., 2017).
In 2014, ombitasvir was approved in combination with paritaprevir/ritonavir/dasabuvir (see below and above) and this combination therapy is particularly used in patients that are difficult to treat.

II.4.3- NS5B inhibitors

NS5B is the viral RNA-dependent RNA polymerase and is therefore a very interesting target for therapy. NS5B inhibitors could be nucleoside inhibitors, binding to the active site and being integrated into the nascent RNA chain, or non-nucleosides inhibitors, binding outside the active side and resulting in allosteric inhibition of polymerase activity.
The nucleoside inhibitor sofosbuvir (Sofia et al., 2010) was approved in 2013. It is used in combination with peg-IFN/RBV or other DAAs and has a potent activity against all genotypes.

Figure 12: Milestones of HCV therapy. Adapted from http://www.cure-hepc.com/what-drugs-are-used-for-hepatitis-c-treatment/

Today, the combination of DAAS leads to good results but the access of patients to these molecules is limited by their cost. Another issue is the emergence of resistant-associated variants. Therefore, efforts have still to be made in order to find new molecules targeting other proteins and/or alternative steps of the viral life cycle. In this context, p7 is a good candidate. Indeed as p7 is a viroporin (see part IV), with an ion channel activity, thus a great target for designing new antivirals. In addition some molecules may have effect on different viroporins of several viruses. As an example, amantadine-derivatives are able to block both p7 of HCV and M2 of IAV (see part IV.1.4).

II.4.4- Vaccine

As for HIV, the generation of an efficient HCV vaccine remains a major challenge today to constraint the pandemic, by preventing the primary infection but also the reinfection after treatment with DAAs (Walker, 2017).

Some strategies for the development of vaccines were based on the use of recombinant E1/E2 in order to induce neutralizing antibodies. In this context, immunization of human volunteers with recombinant E1/E2 resulted in the production of broad cross-neutralizing responses (Law et al., 2013). However since neutralizing antibodies act by recognizing native E1E2 heterodimers (Giang et al., 2012), it is important to generate a vaccine that express native E1E2 structures.

A vaccine consisting in modified vaccinia virus Ankara allowing NS3-NS5B expression was also designed (Swadling et al., 2014). This vaccine is in clinical trial for immunogenicity and protection against virus persistence. However it was found that protection against HCV was more closely correlated with immune responses against the viral structural proteins rather than the non-structural proteins (Dahari et al., 2010).

Other strategies are based on the development of viral vectors harboring HCV glycoproteins E1 and E2 since they present conformational epitopes targeted by neutralizing antibodies. Several approaches have been described (figure 13). The first one was the production of virus-like-particles (VLP) in insect cells using a baculovirus system that expressed core, E1 and E2 (Baumert et al., 1998). However in this context it seems that glycosylated forms of E1 and E2 are not the same as in HCV virions due to the use of insect cells (Baumert et al., 1999). Another approach was the development of chimeric HBV/HCV VLP. Indeed subviral particles expressing HBs protein fused to full-length E1 and E2 protein could be produced by replacing the transmembrane domain (TMD) of the HBsAg protein with the TMD of HCV genotype 1a E1 and E2 proteins (Patient et al., 2009). These kinds of particles were immunogenic in rabbit (Beaumont et al., 2013). Some other used an alternative approach by replacing the immunogenic determinant of HBsAg with HVRI of HCV E2 (Netter et al., 2001). Retroviral HCV-like particles were also developed, composed of capsid of MLV and E1E2 glycoproteins. This kind of particles could induce a strong neutralizing response in mice and macaques (Garrone et al., 2011). Finally another approach was the development of VLP produced in human hepatocyte-derived cells using adenoviral expression systems (Earnest-Silveira et al., 2016). This method has the advantage of producing particles that are morphologically typical of HCV virions. The immunogenicity of a vaccine combining genotype 1a/1b/2a/3a HCV VLP is currently under evaluation.

HCV VLP type	Genotype	*In-vitro* cell line for production	Neutralization HCVcc or HCVpp (Genotype)	Binding of human NAb	DC maturation	Memory B cell responses	HCV specific CD8+ and/or CD4+ T cell responses
Insect cell derived	1b	Sf9	No Strong antibody response in mice. Neutralization of vaccinia virus-HCV with Baboon immune sera. (Poor antibody responses in Chimpanzees)	Yes	Yes (*in-vitro*)	Yes	Yes (CD4+, CD8+, CTL)
Mammalian cell derived	1a, 1b, 2, 3a	Huh7	Yes (HCVcc 1b and 2)	Yes	Yes (*in-vitro*)	Yes	Yes (CD4+, CD8+, Granzyme B)
CHIMERIC HBsAg/HCV LPs							
(1) HBs-HCV E1 and E2 VLPs	1a	CHO	Yes (HCVcc and HCVpp 1a, 1b, 2a, and 3)	No	No	No	No
(2) HBsAg/HCV HVR1	1a and 1b	Huh7	Yes (HCVpp 1a)	No	No	No	No
RETROVIRAL HCV-LIKE PARTICLES							
(1) RetroVLP^{E1E2} (2) RetroVLP^{NS3} (3) Plasmo-retroVLP^{E1E2} (4) rAdE1E2 (Prime-boost strategies)	1a		Yes (1b, 2a, 2b, 4, and 5)	No	No	No	Yes (CD8+, CTL)

Figure 13: Summary of HCV VLP approaches. (Torresi, 2017)

II.5- Experimental systems

Since its discovery, HCV has raised important technical challenges because of the difficulties to generate suitable cell culture model and/or animal models that allow the study of HCV biology. Several experimental models have been developed to improve the understanding of the virus life cycle, pathogenesis and virus-host interactions. Initially, HCV was only studied through the use of serum-derived HCV patients (HCVsp). Then, the development of sub-genomic replicons (HCVsgr) allowed the study of viral replication whereas the generation of soluble E2 envelope glycoproteins (sE2) helped to identify the first HCV cellular receptors. More robust infectious systems followed, such as HCV pseudoparticles (HCVpp), allowing the study of virus entry into cells, and ultimately, the development of HCV cell culture systems (HCVcc). The development of relevant small animal models as alternatives to the chimpanzee model form further steps allowing the study of HCV infection *in vivo*.

II.5.1- Serum derived HCV particles (HCVsp)

The first tool used to study HCV infection was based on *ex vivo* characterization of patients' sera derived particles. However, no productive infection was observed in any tested cell lines or primary hepatocytes. The proportion of viruses and viral RNA produced and released, after infection of primary liver cells, was very low although these cells are able to support HCV entry and replication (Fournier et al., 1998).

II.5.2- Sub-genomic replicons (HCVsgr)

In 1999, a major advance allowed the study of HCV replication. Lohmann et al. established cell lines constitutively expressing and replicating a subgenomic HCV RNA derived from a cDNA isolated from the liver of a chronically infected patient with a genotype 1b HCV strain (Con1) (Lohmann et al., 1999a). The term subgenomic was employed to define these replicons as only the HCV non-structural (NS) protein-encoding sequence was used to generate these systems initially.
Most replicons used are bicistronic: they express an antibiotic resistance gene under control of HCV Internal Ribosomal Entry Site (IRES) and the HCV NS proteins NS3-4A-4B-5A-5B under control of EncephaloMyoCarditis Virus (EMCV) IRES (Figure 14).
Huh7 cell lines are transfected with *in vitro* transcribed RNAs and are selected with the corresponding antibiotics, which results in the production of cell lines stably replicating HCV. Moreover, studies identified a number of adaptive mutations, increasing replication efficiency, acquired by the replicon after serial passages of these cell lines. These mutations are mostly found in NS3, NS4B and NS5A proteins. Such subgenomic replicons are available for several HCV genotypes/subtypes.
The replicon model strongly contributed to the development of DAAs, allowing totest the effect of several molecules on the replication of several genotypes.

Figure 14: Subgenomic replicon. Scheme of HCV subgenomic replicon organization. This gene encode for a resistant gene (here Neo: neomycin) under the control of HCV IRES and the non structural proteins NS3-NS5B under the control of EMCV IRES.

II.5.3- Soluble E2 (sE2)

Envelope glycoproteins are essential for viral attachment to target cells and for membrane fusion. Therefore, their study is essential to understand viral entry mechanisms. In addition, these proteins are essential for the generation of neutralizing antibodies. However, the study of the two glycoproteins of HCV, E1 and E2, is difficult as these proteins have been shown to easily misfold and form aggregates (Dubuisson, 2000). Another difficulty to study HCV envelope glycoproteins is linked to their transmembrane domains that result in their retention at the endoplasmic reticulum (ER) membrane (Cocquerel et al., 1999). In order to bypass these problems, soluble forms of E2 were generated through the removal of its transmembrane domain. It allows the secretion of the ectodomain of HCV E2 (Cerino et al., 1997, Rosa et al., 1996).
This soluble protein allowed the discovery of the first two cell entry receptors: (CD81) (Pileri et al., 1998) and the Scavenger Receptor B1 (SR-BI) (Scarselli et al., 2002).
Despite these major advances, it has been demonstrated that the correct folding of E1 and E2 is tightly linked to their association as heterodimeric complexes (Cocquerel et al., 2003, Owsianka et al., 2001). Thus, the use of systems studying E1E2 as a full heterodimer complex incorporated onto viral particles remains an essential goal.

II.5.4- HCV pseudoparticles (HCVpp)

In 2003, the generation of a system allowing the study of HCV entry mechanism was for the first time described. It consisted of defective retroviral particles harboring HCV envelope glycoproteins on their surface (Bartosch et al., 2003, Drummer et al., 2003, Hsu et al., 2003). These particles, named HCV pseudoparticles (HCVpp), can be produced by co-transfection of 293T cells with three expression plasmids encoding: (i) the HCV glycoproteins E1 and E2, (ii) gag-pol protein of Human Immunodeficiency Virus (HIV) or Murine Leukemia Virus (MLV), (iii) a retroviral genome containing a reporter gene such as GFP or Luciferase in order to measure the entry of HCVpp into target cells (Bartosch et al., 2003)(Figure 15). Owing to the presence of a reporter gene and the absence of replication and propagation, this system is easy to manipulate in a biosafety level 2 laboratory (in contrast to full HCV replicative virus).
The HCV pseudoparticles assay allowed effective production of viral particles that efficiently enter Huh7 hepatoma cell lines and primary human hepatocytes (Bartosch et al., 2003, Lavillette et al., 2005b). Moreover, HCVpp harboring E1E2 from the six major

genotypes were successfully generated, allowing testing of neutralizing antibodies or drugs targeting entry (Lavillette et al., 2005b).

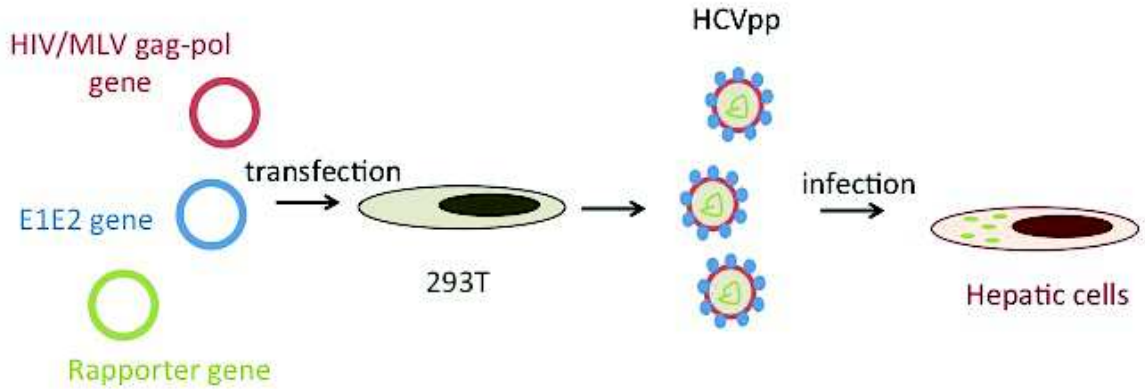

Figure 15: HCV pseudoparticles. Retroviral particles bearing HCV glycoproteins are produced by transfecting HEK293T cells with expression vectors encoding for E1E2, the retroviral core protein and a retroviral derived genome encoding for a reporter gene, which will be expressed upon naïve cells infection.

Although the HCVpp are still very useful for the study of host-virus interaction for viral entry, the particles are produced in 293T, and thus, are not associated with lipoproteins, in contrast to particles detected in patient sera. Another limiting point is that these particles do not allow the study of assembly since they assemble in a similar manner to retroviruses.

II.5.5- HCV cell culture system (HCVcc)

In 2003, a study described the ability of an HCV RNA derived from a genotype 2a HCV subgenomic replicon to efficiently replicate in cell culture without any adaptive mutations (Kato et al., 2001). This replicon, called JFH-1 for Japanese Fulminant Hepatitis 1, was isolated from a Japanese patient that cleared the virus after having developed a fulminant hepatitis (Kato et al., 2001). In 2005, the development of a cell cultured system (HCVcc) based on the transfection into highly permissive Huh7 cells-derived clones of a full-length RNA genome deriving from the JFH1 replicon led to the production of infectious viral particles both *in vitro* and *in vivo* (Lindenbach et al., 2005, Wakita et al., 2005, Zhong et al., 2005). The development of this model constituted a major achievement and offered for the first time the possibility to study the complete HCV life cycle.

The particularity of this JFH1 sequence remained elusive for a long time although a recent study indicates that this strain had lost a function required for replication in human hepatocytes but that needs to be lost for efficient replication in huh7.5 cells. Indeed, HCV needs to stimulate phosphatidylinositol 4-kinase IIIα (PI4KIIIα) to create a phosphatidylinositol 4-phosphate (PI4P)-enriched membrane microenvironment for its replication. However, this enzyme is activated in Huh7.5 cells even in absence of HCV infection. Therefore, to replicate in these cells, HCV needs to adapt by losing this function in order to prevent over-activation of this PI4KIIIα kinase (Harak et al., 2016).

Over the years, the HCVcc model has been highly improved. Serial passages of the JFH1 virus allowed the selection of adaptive mutations improving virus production and virus titers (Kaul et al., 2007, Yi et al., 2007). Moreover, highly permissible cell clones deriving from Huh7 allowed a greater robustness of the system and a better virus production. Huh7.5 (Lindenbach et al., 2005) or Huh7.5.1 (Zhong et al., 2005) clones were notably selected for their high ability to replicate HCV subgenomic replicons and harbor a defect in their interferon triggering system through inactivation of RIG-I pathway.
In order to allow the study of several viral strains, several groups developed chimeric JFH1 genomes. Combination of the NS3-5B region of JFH1 with the C-NS2 region from J6 (genotype 2a isolate) resulted in the J6/JFH1 genome (displaying chimerization between NS2 and NS3) (Lindenbach et al., 2006) or Jc1 (chimerization at position 846, at the end of the first transmembrane domain of NS2) (Pietschmann et al., 2006). These chimeras were characterized by enhanced spread and production of viral particles. The group of J. Bukh used the J6/JFH1 chimeric strain and replaced the C-NS2 region from other genotypes (Gottwein et al., 2010, Gottwein et al., 2007, Gottwein et al., 2009, Jensen et al., 2008, Russell et al., 2009, Scheel et al., 2008), but also the NS3/4A, NS5A or NS5B sequences from other genotypes in order to allow the study of DAAs.
Recently, full-length HCV gt1a (Li et al., 2012b) and gt2b (Ramirez et al., 2014) infectious culture systems have been developed. These viruses are able to replicate efficiently in cell culture, allowing for the first time to analyze and compare specificities of HCV types or sub-types in a full life cycle context.

II.5.6- HCV animal models

II.5.6.1- Natural animal models

The development of an animal model to study HCV infection is critical in order to have a complete understanding of the host-virus interactions.
Chimpanzee and a non-rodent small mammal, the *Tupaia belangeri,* are the only natural permissive animal models that support HCV infection. Chimpanzee infection is less pathogenic than in human but was essential to understand some aspects of the immune responses mechanisms, to evaluate the potential of vaccine candidates and of neutralizing antibodies. However, the limited number of animals used in the study of cohorts, due to their high costs, ethical considerations and absence of a similar course of disease compared to humans pointed out the need for alternative, complementary and efficient animal models
The treeshrew *Tupaia belangeri* was shown to be susceptible to the HCV infection. Indeed, HCV can use the tupaia set of receptors for entry (Tong et al., 2011). However, infection *in vivo* seems to be very weak. Indeed, HCV RNA was undetectable in animal sera as well as anti-HCV antibodies (Amako et al., 2010). In addition the use of these animals raised similar concerns than for chimpanzees since these animals are rare, inducing high costs and small cohorts.

II.5.6.2- Humanized animal models

Mice and rats are commonly used animal models in laboratories. However these animals do not support HCV infection, as the murine CD81 and OCLN have been identified as responsible for restricting species tropism (Ploss et al., 2009).

II.5.6.2.1- Genetically humanized mouse model

In 2011, a study showed that transduction of Rosa26-FLuc mice with adenoviral vectors encoding for the two receptors mediating the host tropism, CD81 and OCLN, allowed viral entry (Dorner et al., 2011). This model was suitable to evaluate neutralizing antibodies, cellular pathways used for entry as well as vaccine candidates. However, HCV was not able to replicate and no viral particles were released in serum, likely due to the innate and adaptive immune responses in mice but also the lack of some proviral factors (Figure 16a).
To overcome these restrictions, the same group developed a new Rosa26-FLuc mouse system, combining the expression of HCV entry factors and disruption of a receptor involved in innate immunity ($STAT^{-/-}$ mice)(Dorner et al., 2013). In these mice, the entire HCV life cycle could be recapitulated, even if the production of infectious particles was low. Despite the lack of innate immune responses, some immunological features could be detected in the infected mice, such as liver infiltration of IFN-producing NK cells and CD8+ T cells, which is consistent with observations made in patients. Another study compared different murine strains and described that the host genetic background plays a key role in the ability of these models to maintain a chronic HCV infection (Figure 16b).
However, the high level of transgene expression and the induction of immune responses against adenoviral transduction could bias this model.

II.5.6.2.2- Xenograft-derived humanized mice model

Mice model harboring a humanized liver via xenotransplantation offers the possibility to study human hepatocytes *in vivo*. A widely used model is an immunodeficient SCID mouse that overexpresses a lethal transgene in hepatocytes, the urokinase-type plasminogen activator (uPA) (Billerbeck et al., 2013, Mailly et al., 2013). In this system, there is no control for the destruction of mouse hepatocytes, thus engraftment of human hepatocytes into the mouse liver is only possible during the first weeks of life (Meuleman et al., 2005, Vanwolleghem et al., 2010). These mice are able to efficiently support both HCVcc and serum-derived HCV particles infection (Figure 16c), which can be sustained for up to 10 months (Mercer et al., 2001, Vanwolleghem et al., 2010). This model also permitted to validate *in vivo* the effect of some neutralizing antibodies, antiviral compounds or DAAs.
More recently, another humanized liver mouse model, $Fah^{-/-}$ $Rag2^{-/-}$, $\gamma\text{-}c^{-/-}$ (FRG), has been developed. These mice are immune-deficient by introducing mutations in the Rag2

recombinase gene and in the γ-chain of the interleukin receptors (Billerbeck et al., 2013, Mailly et al., 2013). In addition, they do not produce the tyrosine catabolic enzyme fumarylacetoacetate hydrolase (Fah), which results in the accumulation of toxic metabolites that induce liver degeneration (Grompe et al., 1993, Grompe et al., 1995). This degeneration allows the engraftment of human hepatocytes into the mouse livers and the development of a humanized livers (Bissig et al., 2007). Interestingly, this model allows the control of liver degeneration by using the 2-(2-nitro-4-trifluoromethylbenzoyl)-1,3-cyclohexanedione (NTBC) that interferes with the production of toxic metabolites and prevents hepatocytes degradation (Grompe et al., 1993, Grompe et al., 1995). Thus, in contrast to the uPA-SCID model, this efficient control system makes it possible to engraft liver mice at any time during their adult life.
This model was shown to support infection with HCVcc but also with serum derived-HCV particles (Bissig et al., 2010). It allowed studying basics aspects of HCV life cycle and notably the composition and biophysical properties of particles produced as well as the use of entry receptors, which highlighted important differences between this model and the HCVcc model (Calattini et al., 2015).
Finally, some models of double humanized mice (liver and immune systems), such AFC8-huHSC/Hep mice (based on the Balb/c Rag2-/- γ-c-/- (BRG) mice model) or the Fah-deficient NOD.Rag2/IL2gRnull (FRGN) mice, have emerged (Bility et al., 2014, Washburn et al., 2011, Wilson et al., 2014). These models allow the engraftment of human liver and immune system components, thus facilitating the study of human immune responses to HCV infection.

Overall, humanized mouse models clearly constitute the most advanced model to study HCV infection in a natural environment, but there remain important challenges, since the immune system is not fully functional.

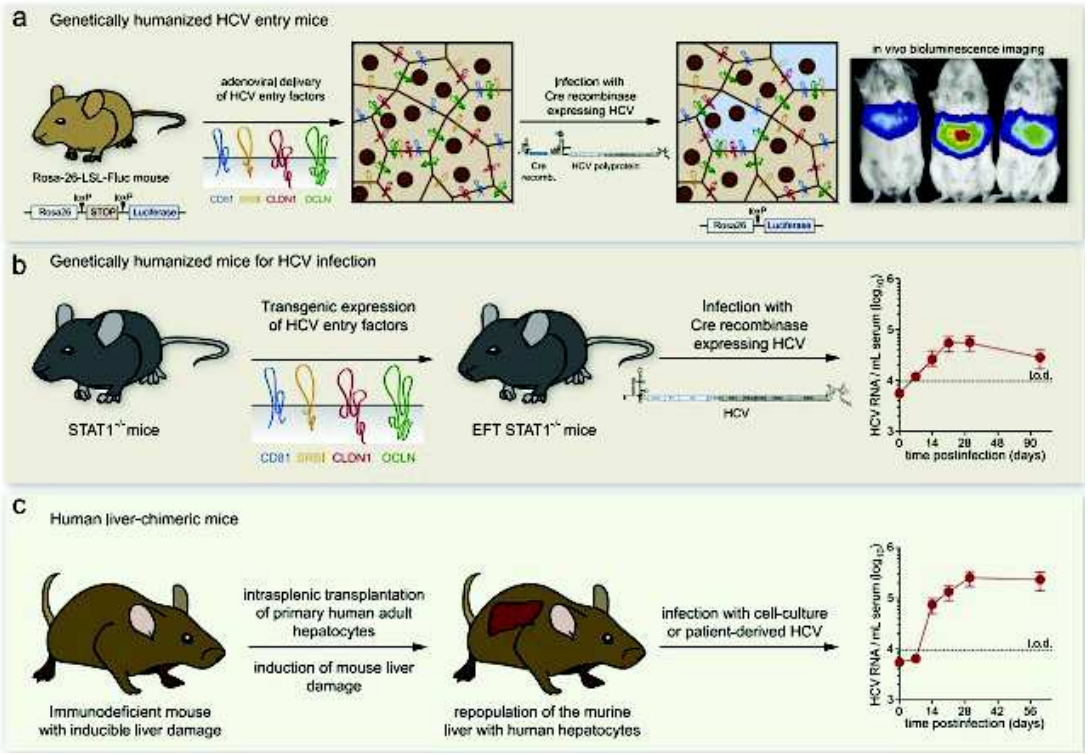

Figure 16: HCV humanized mice model. (a) Immunocompetent luciferase reporter mice become susceptible to entry by adenoviral or transgenic expression of human receptors. Bioluminescence imaging could monitor infection with a genome activating luciferase expression. (b) Genetically humanized mice recapitulating all steps of the HCV life cycle are based on expression of human HCV receptors in STAT1-deficient animals. (c) Human liver-chimeric mice are based on mice with an injured liver being replaced by human liver. (Catanese & Dorner, 2015)

III- HCV life cycle and molecular virology

III.1. Classification and genetic variability

Following sequencing and comparative analysis of the whole HCV genome, HCV was classified in the *Flaviviridae* family (figure 17) (Kapoor et al., 2011) as its genetic organization and polyprotein structure resembled that of pestiviruses and flaviviruses, two other genus of this family (Choo et al., 1991). HCV seems closer to pestiviruses than to flaviviruses regarding the sequence similarity and the glycosylation pattern of its glycoproteins. However, because of the low amino acid and nucleotide sequence homology it was classified in a third genus within the *Flaviviridae*. A fourth genus, *Pegivirus*, was added in *Flaviviridae* , more closely related to *Hepacivirus* (figure 17).

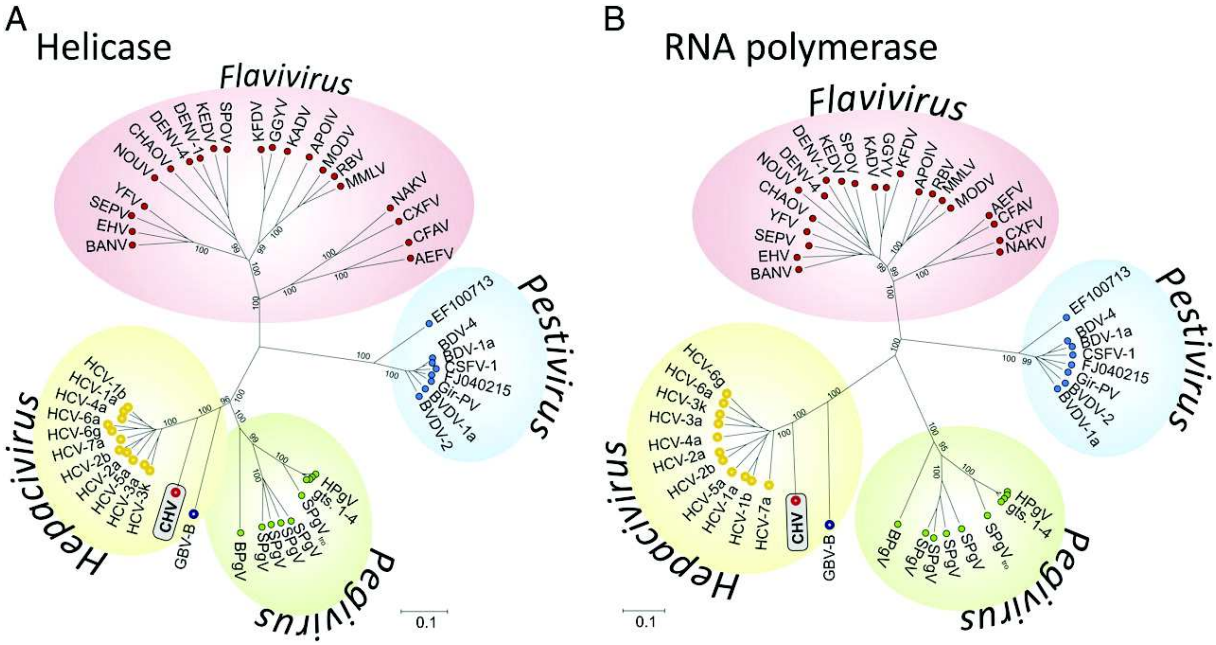

Figure 14: Phylogenetic analysis of *Flaviviridae* family based on helicase (a) or RNA polymerase (b). (Kapoor et al., 2011)

Like all RNA viruses, HCV shows a characteristic high level nucleotide diversity since its RNA-dependent RNA polymerase is highly error-prone and lacks a 5'-3' exonuclease proofreading activity (Steinhauer et al., 1992). Up to 1.4 to 1.9×10^{-3} substitutions per nucleotide and year (Ogata et al., 1991) has resulted in diversification into distinct genotypes, subtypes and quasi-species, allowing rapid virus adaptation to the host responses.

The comparison of two highly conserved domains in its genome, *i.e.*, core and NS5B, are used to determine genotypes and subtypes (figure 18) (Margeridon-Thermet & Shafer, 2010). HCV isolates are classified in 6 major genotypes, with different locations around the world (figure 19). Each genotype, except genotype 5, is subdivided into numerous

subtypes, resulting in more than 100 in total. Genotypes differ from each other by 31% to 33% at the nucleotide level, subtypes about 20% to 25% (Simmonds et al., 2005).

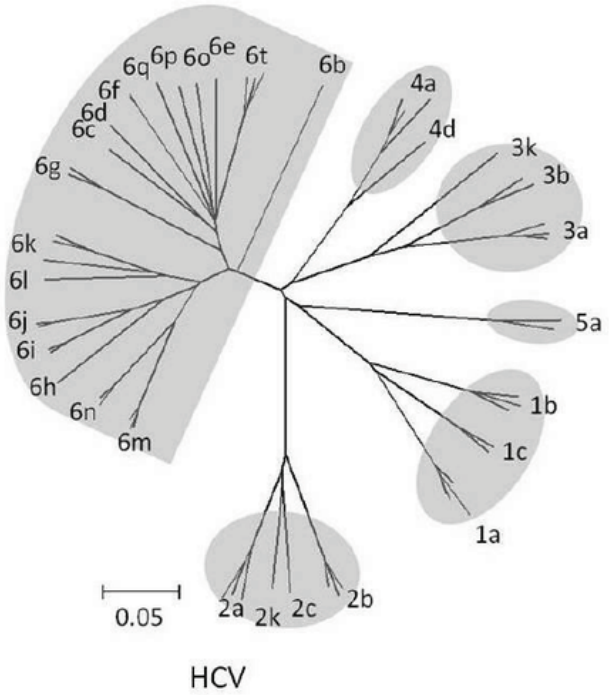

Figure 18: Different genotype and subtype of HCV. Phylogenetic tree of the relationship among HCV genotypes. These relationships are based on nucleotide sequences of the NS5B region. (Margeridon-Thermet & Shafer, 2010)

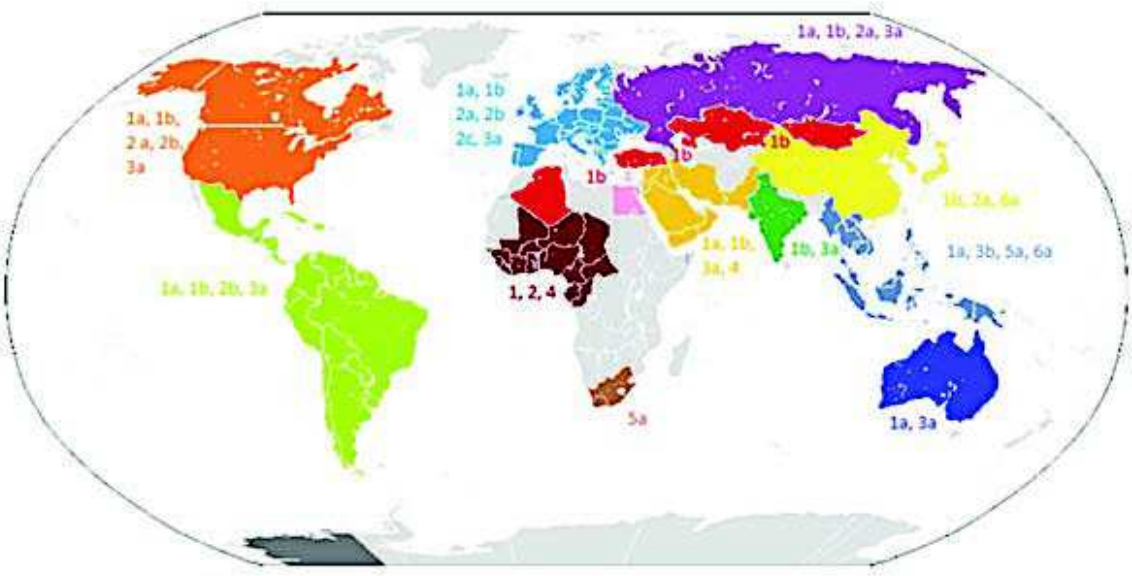

Figure 19: HCV genotype by location. https://www.ahcmedia.com/articles/139945-hepatitis-c-infection-for-primary-care-providers

III.2- Viral particle structure and composition

III.2.1- Infectious particles

HCV is an enveloped virus that is heterogeneous in morphology and size of particles. Indeed, immunocapture of particles with E2 antibodies reveals particles of about 50-60nm and about 80-90 nm (Catanese et al., 2013, Piver et al., 2017). They do not display a symmetrical arrangement (figure 20) (Piver et al., 2017). Therefore, there is actually no clear model of HCV particle structure. Similarly, the arrangement of the structural proteins onto the virion surface remains elusive. HCV particles harbor on their membrane the two envelope glycoproteins, E1E2. This envelope surrounds a nucleocapsid, composed of the multimerized core protein and the viral genome, namely a positive stranded RNA.

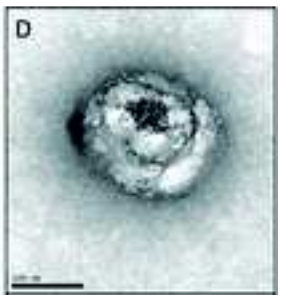

Figure 20: Electron micrographs of particles from serum of HCV-infected patients. Adapted from (Piver et al., 2017).

One particularity of HCV (shared with pegiviruses particles) is the very low and heterogeneous buoyant density of its viral particles, as determined by density gradient analysis. Indeed, in sera from patients or infected animals, most particles are found in densities between 1.00 and 1.10 g/mL (Andre et al., 2002, Nielsen et al., 2006) (figure 21). This density is mainly due to the very distinct lipid compositions, as HCV particles are able to associate with serum lipoproteins (see part I). Indeed, serum-derived HCV particles have been found to be associated with apoB, apoC-I and apoE (Diaz et al., 2006, Thomssen et al., 1992).

HCVcc infectious particles are found in densities between 1.00 and 1.15g/mL; yet, in contrast to serum-derived HCV particles, HCVcc RNA, representing physical particles, is found in densities between 1.1 and 1.2g/mL, indicating their low specific infectivity (Dao Thi et al., 2012, Gastaminza et al., 2006, Lindenbach et al., 2005, Merz et al., 2011) (figure 20). These HCVcc particles are associated with apoC-I (Meunier et al., 2008) and apoE . However, their association with apoB remains unclear (Boyer et al., 2014, Catanese et al., 2013, Merz et al., 2011). The difference between HCVcc and HCV particles derived from patients' sera is attributed to some defective lipoprotein metabolism pathway in Huh7 cells (Icard et al., 2009, Meex et al., 2011, Merz et al., 2011), which will be discussed in Results section. To complement on this point, it was shown that long-term culture of Huh7.5 with human serum could restore the secretion

of VLDL pathway (Steenbergen et al., 2013) and could increase the production of JFH1 infectious particles, with particles associated to apoB and more lipidated.
Interestingly, HCV-derived from humanized liver mice, called HCVfrg, have a lower density than HCVcc and display two peaks of viral RNA (figure 21), suggesting an intermediate maturation between HCVcc and HCV particles found in patients' sera (Calattini et al., 2015). In addition, it was observed that the most HCVfrg particles are enriched in apoE.

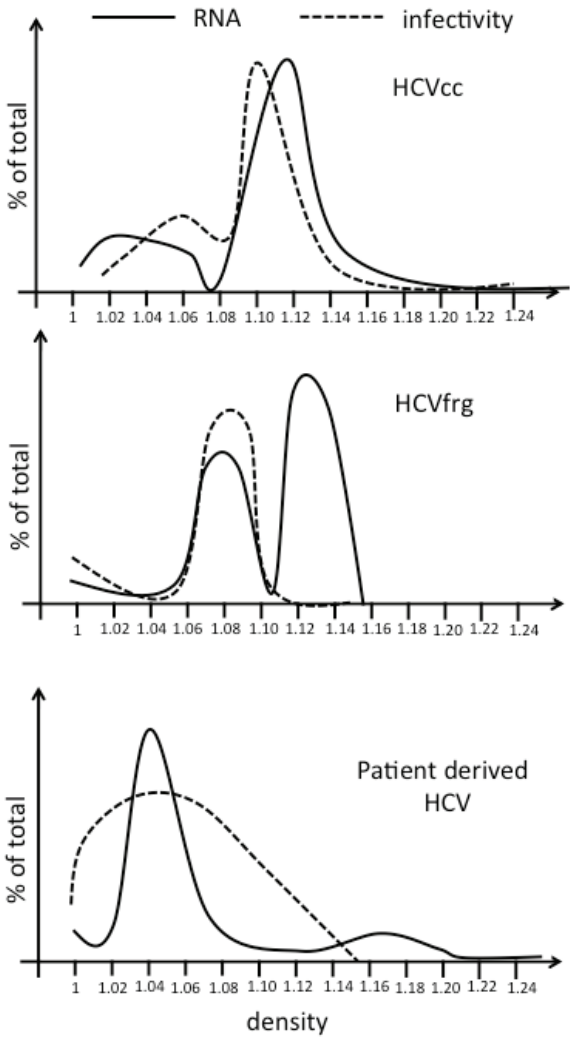

Figure 21: Density profile of RNA and infectivity of different HCV particles. In dotted lines is represented the infectivity and in full lines the physical particles assessed by RNA.

Because of these different lipogenic properties, HCV particles are sometime called lipo-viro-particles.
Interestingly, the association of HCV with lipoproteins is still poorly understood and two models of association have emerged in the literature. The first model consists of a single

particle model, with HCV particle sharing its envelope with an LDL particle (figure 22 right panel). The second model consists of (at least) two particles, with an HCV particle interacting with lipoprotein(s), such as HDL or LDL (figure 22 left panel). Indeed, apoE was found to interact with E2 (Boyer et al., 2014, Lee et al., 2014) and could mediate the interaction of lipoprotein with viral particles.
Recent images of particles, obtained by electron microscopy (Piver et al., 2017) argues in favor of the single particle model, although further experiments have to be done to confirm this point.

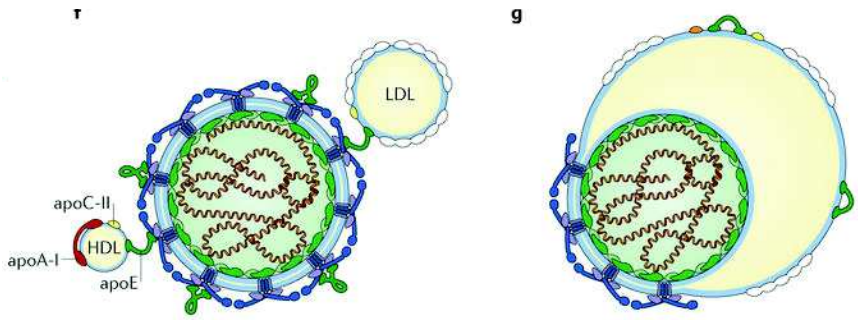

Figure 22: Model of HCV particles. In left a two-article model, which proposes that HCV particles and serum lipoproteins transiently interact. In right single particle model for LVP structure, illustrating an HCV particle sharing an envelope with an LDL particle. Adapted from (Lindenbach & Rice, 2013)

III.2.2- Non-infectious particles

III.2.2.1- Exosomes

Exosomes are vesicles ranging from 40-100nm with a density of 1.13-1.19 g/mL that are released by a variety of cultured cells. They are formed in multivesicular bodies (MVB) and are released through the fusion of MVB with the plasma membrane (Harding et al., 1984, Pan et al., 1985).
The first description of a link between exosomes and HCV was made in 2004. Indeed, it was discovered that exosomes collected from patients' plasma contain viral RNA. In addition, it was found that in presence of CD81, E1E2 glycoproteins could be secreted in exosomes (Masciopinto et al., 2004). Since this discovery, several studies investigated the role of these exosomes in the life cycle of the virus. Some reports indicated that the exosomes containing viral genomes can transmit infection to naïve cells, as shown using either subgenomic (Longatti et al., 2015) or full-length (Ramakrishnaiah et al., 2013) HCV RNAs. However, in the latter case, even if transmission occurs, it is quite low compared to virion infection although a major difficulty is to separate virions from the exosomes. It was also shown that HCV-infected patients also express negative sense HCV

RNA (replication intermediate viral RNA), in association with Ago2, HSP90, and miR-122 (Bukong et al., 2014).
Finally, it was found that HCV genomes contained in exosomes could be transferred from infected cells to non-permissive plasmacytoid dendritic cells (pDCs), leading to their activation (Dreux et al., 2012) and thus the secretion of interferon. It was also demonstrated that HCV associated with exosomes are less sensitive to neutralizing antibodies (Liu et al., 2014), suggesting a role in exosomes in immune responses with either pro- or antiviral functions.

III.2.2.2- Subviral particles

The expression of E1E2 glycoproteins in cells secreting lipoproteins is sufficient to induce their secretion as particles (Icard et al., 2009). These particles have a density of about 1.06-1.08g/mL. They are found to be associated with apoB and were named empty lipo-viral particles (eLVP) as it was suggested that they could correspond to lipo-viral particle without nucleocapsids. Their role remains elusive although it was proposed that they could serve as a decoy against neutralizing antibodies.

III.2.2.3- Naked nucleocapsids

Non-enveloped nucleocapsids were detected in the plasma of HCV-infected patients (Maillard et al., 2001). These particles have a density between 1.32 to 1.34 g/mL and are heterogeneous in size. Again, the role of these particles is poorly characterized although it was proposed that they could play a role in HCV pathogenesis or immune responses.

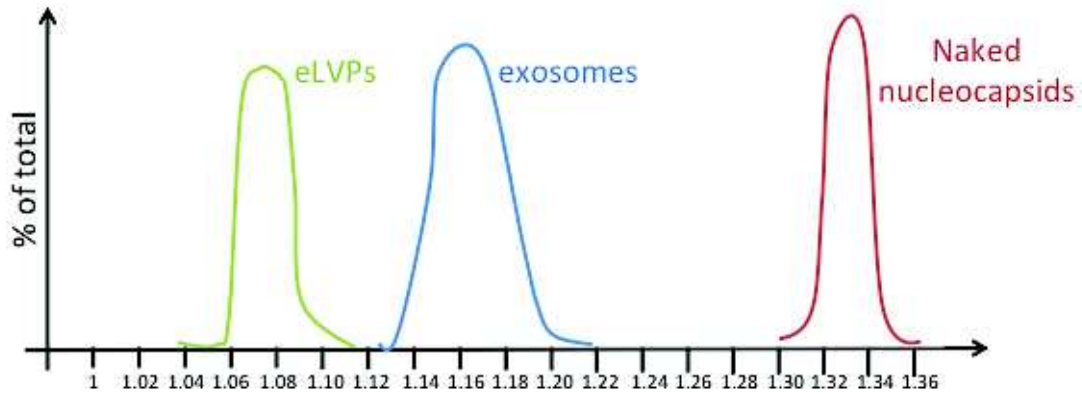

Figure 23: Non-infectious particles of HCV and their density.

III.3- Viral genome and proteins

III.3.1- Viral RNA

The HCV genome is a single positive strand RNA of 9.6kb that encodes a large polyprotein. Two untranslated regions (UTR) at the 5' and 3' extremities of the viral RNA flank the Open-Reading-Frame (ORF).
The ORF encodes a polyprotein of around 3,000 amino acids that is then cleaved to give rise to 10 structural and non-structural proteins. The first part of the polyprotein is cleaved by the cellular signal peptidase (see part III.3.2) whereas the second part is cleaved by the viral proteases. The individual proteins are, in order, 3 structural proteins: core, E1 and E2, which are then followed by the non-structural proteins: p7, NS2, NS3, NS4A, NS4B, NS5A and NS5B (figure 24).

The 5' UTR (341 nucleotides) contains structural features that are conserved among genotypes. It contains 4 structural domains. Domains I and II are essential for RNA replication even if the entire UTR is required to ensure correct RNA synthesis (Kim et al., 2002). Translation is cap-independent and requires an IRES sequence (Tsukiyama-Kohara et al., 1992) constituted by the domains II to IV as well as the beginning of the polyprotein-encoding sequence (Honda et al., 1996). The HCV IRES is critical to recruit the ribosomal subunit 40S and for initiating translation that requires similar initiation factors (eIF4 A, B, F) (Spahn et al., 2001). Liver-specific miR-122 micro-RNA has been shown to enhance translation and replication (Fukuhara et al., 2012, Jopling et al., 2005) and contributes to the restricted tissue tropism of HCV. It has been suggested that miR-122 binding to 5' HCV UTR stabilizes viral RNA (Shimakami et al., 2012, Wilson et al., 2011).

The 3' UTR (200-235 nucleotides) is divided in 3 distinct regions. The first domain is a short variable domain followed by a short polyuridine/ polypyrimidine (polyU/UC) tract. The third domain is a highly conserved domain named 3'X-tail that contains three hairpin structures essential for RNA replication. This 3' UTR is critical for translation, through the stimulation of IRES (figure 24).

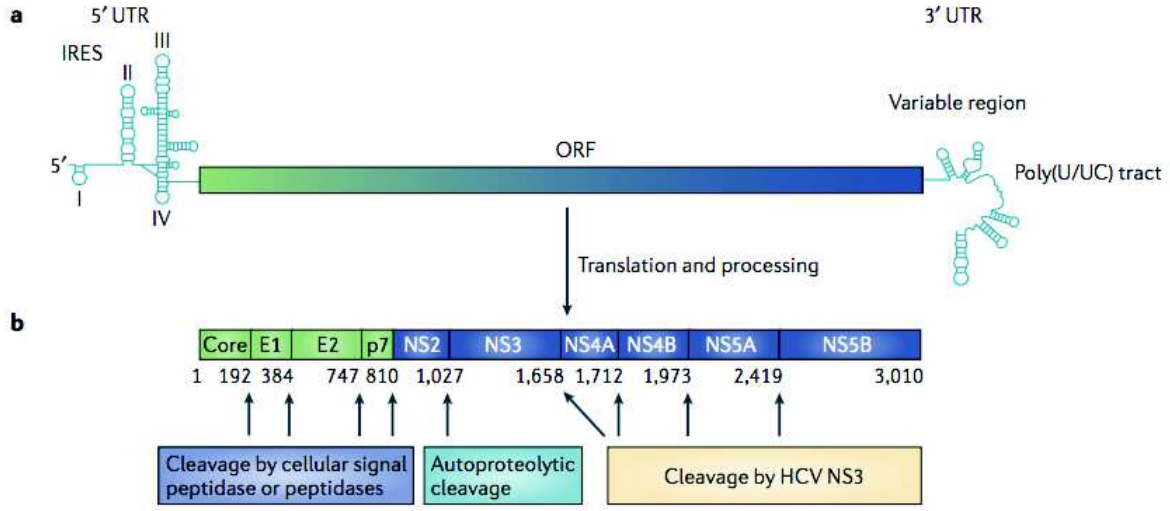

Figure 24: HCV ORF. a. HCV is a positive, single-stranded RNA virus that encodes a large polyprotein of about 3,000 amino acids from a single open reading frame (ORF). The ORF is flanked by two untranslated regions (UTRs), which contain signals for viral protein and RNA synthesis, and for the coordination of both processes. Translation is initiated through an internal ribosomal entry site (IRES) in the 5′ UTR. **b**. In polyprotein maturation, the core–E1, E1–E2, E2–p7 and p7–non-structural 2 (NS2) junctions are cleaved by one or more cellular signal peptidases to yield the structural proteins of the virus. The NS2–NS3 proteins undergo autocatalytic cleavage, which releases the NS3 serine protease. (Arzumanyan et al., 2013)

III.3.2- Polyprotein processing by the cellular signal peptidase

As mentioned above the first part of the polyprotein is cleaved by the cellular signal peptidase, leading to the release of core, E1, E2, and p7. This cleavage is supposed to occur during the translation of the polyprotein in the luminal side of the ER, which is the classical way of action of this protease. However, some viral precursors, resulting for a delayed cleavage, are detected within infected cells (see below). This might be due to a regulation of the cleavage by protein sequences close to the cleavage sites and provides additional functions to HCV proteins, as discussed below.

III.3.2.1- Protein organization

HCV proteins of HCV are released through proteolytic cleavage by the ER signal peptidase (SP) although there are few studies concerning this protein in mammalian cells. SP was first purified in 1986 from dog pancreas (Evans et al., 1986) and was identified as a protein with five subunits (figure 25). SPC 22/23 is a glycoprotein subunit, but its role in cleavage activity remains unknown. SPC18 and SPC21 are supposed to contain the peptidase active site with serine, histidine, and aspartic acid residues important for catalysis that usually occurs close to the ER membrane, in the luminal side (Paetzel et al., 2002). These 3 subunits span the membrane once, with their C-terminal domain in the ER lumen. The two other subunits SPC12 and SPC25 might play additional roles, as their homologues in yeast are not essential for SP cleavage activity (Fang et al., 1996). Indeed, these subunits could interact with the translocon, stabilize the complex or increase the rate of cleavage. These two subunits are two

transmembrane proteins with the N- and C-terminal extremities facing the cytoplasm (figure 25).

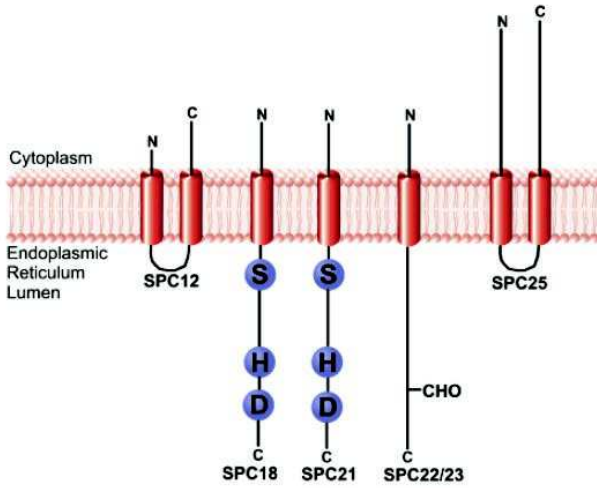

Figure 25: Membrane topology of ER signal peptidase subunits. The ER signal peptidase complex consists of five polypeptides, two of them (SPC21 and SPC18) are weakly homologous to the bacterial, chloroplast, and mitochondrial type I SPases. The active site is located near the membrane surface on the lumenal side of the membrane. (Paetzel et al., 2002)

III.3.2.2- Catalytic mechanism of SP

This mechanism was studied in yeast, using biochemical and mutagenesis analysis. It was shown that a Ser-His-Asp triad, like in classical serine proteases (blue and green residues in figure 26), or a Ser-His dyad, like the Ser-Lys dyad of bacterial SP (blue), are responsible for SP catalytic activity (figure 26) (Chen et al., 1999).

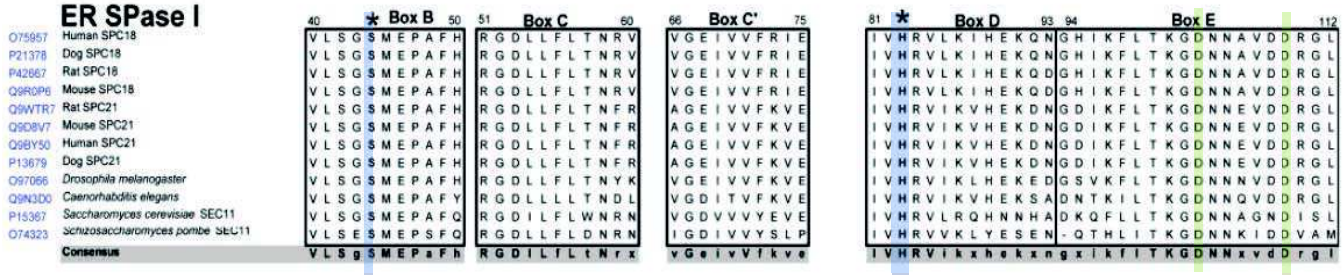

Figure 26: Sequence alignment of ER signal peptidase. Adapted from (Paetzel et al., 2002)

Sequences analysis and mutagenesis have led to the formulation of the (-3,-1) rule for the signal peptidase cleavage of its substrates (von Heijne et al., 1989). Indeed, it was shown that proteins are cleaved only when Ala, Gly, Ser, Cys or Pro residues are found in position 1 and Ala, Gly, Ser, Cys, Thr, Val, Ile, Leu or Pro at position 3 (Dalbey et al., 1997).

III.3.2.3- Signal peptidase and HCV

Interestingly, signal peptidase mediated cleavage is involved in the proteolytic processing of several viral polyproteins, such as flaviviruses, hantaviruses and also HCV.
Furthermore, besides the cleavage of the first part of the HCV polyprotein, it was demonstrated that the SPC12 subunit, which may be not essential for SP cleavage activity, plays a role in the assembly of infectious particles (Suzuki et al., 2013). Indeed, it was shown that this subunit allows the interaction between E2 and NS2.
In addition, a delayed cleavage between E2 and p7 and also between p7 and NS2 is generally detected in most HCV strains (Carrere-Kremer et al., 2002, Lin et al., 1994a, Scull et al., 2015, Shanmugam & Yi, 2013, Steinmann et al., 2007), suggesting an important regulation of the cleavage by virus sequences. In addition, and intriguingly, virus mutants with an IRES between E2 and p7 or between p7 and NS2 are impaired of producing infectious particles (Jones et al., 2007, Shanmugam & Yi, 2013, Stapleford & Lindenbach, 2011), suggesting again a key role of this protease and/or its activity in the viral life cycle.
The cleavage between E2 and p7 has been studied in this thesis (see Results section).

III.3.3- Polyprotein processing by viral proteases

The second part of the polyprotein is cleaved by NS2NS3 and NS3. Indeed, NS2NS3 has an autoprotease activity allowing the release of NS3, which the viral protease that allows release of NS3, NS4B, NS5A and NS5B (figure 24).
Little is known about the mechanism of cleavage between NS2 and NS3. It is supposed to occur at the ER membrane *via* the autoprotease activity of the NS2NS3 precursor in a very efficient way.
After release of NS3, the activity of the NS3 N-terminal part acts as a serine protease that allows the release of its co factor NS4A as well as of NS4B, NS5A and NS5B. The proteolysis of the NS3/4A junction is believed to be a co-translational cis-cleavage whereas the other cleavage events could be achieved by the NS3-4A protease in *trans* (Bartenschlager et al., 1994, Failla et al., 1994, Lin et al., 1994b, Tanji et al., 1994a, Tanji et al., 1994b). It appears that processing at the NS5A/NS5B junction occurs more rapidly than those at the NS4A/NS4B and NS4B/NS5A junctions since rather stable NS4A-NS4B-NS5A processing intermediates can be detected in infected cells (Bartenschlager et al., 1994, Failla et al., 1994, Lin et al., 1994b).

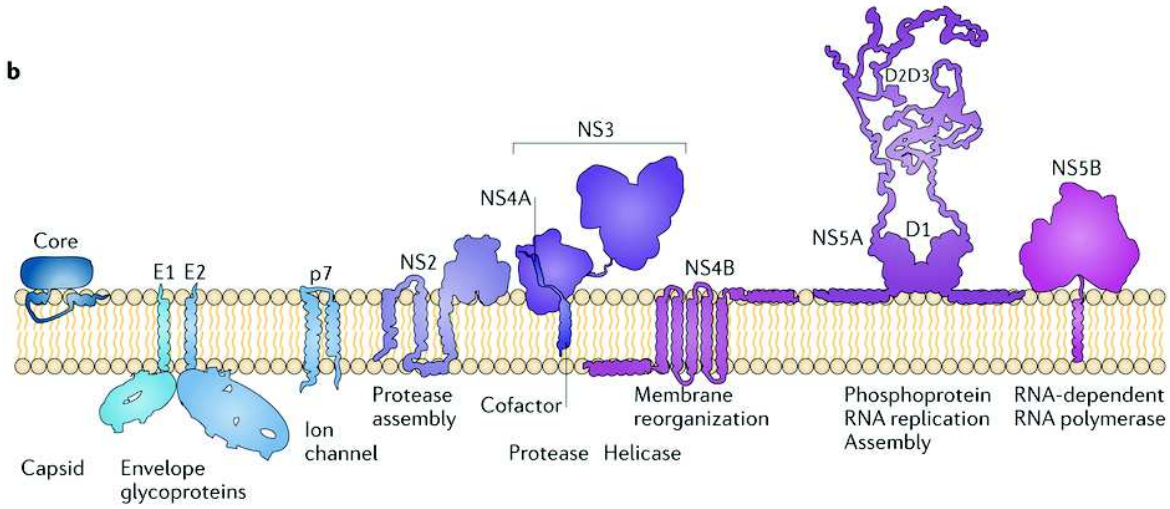

Figure 27. HCV proteins. Adapted from (Bartenschlager et al., 2013)

III.3.4- Structural proteins

III.3.3.1- core protein

The Core protein is the structural protein composing the viral nucleocapsid. It is first released from the polyprotein as an immature form of 23kDa. Then its C-terminal anchoring domain is cleaved by the signal peptide peptidase to allow the release of the mature form of the core protein of about 21 kDa (Okamoto et al., 2008) (figure 27). Before processing, this C-terminal domain is notably required for the translocation of E1 into the ER lumen.

Core is composed of three distinct domains named DI and DII and DIII. DI is constituted by the first 118 amino acids of the protein and is mainly hydrophilic. This domain is involved in nucleocapsid assembly and interacts with the 5'UTR of the viral RNA (Klein et al., 2005). In contrast, DII is hydrophobic and composed of two amphipatic helices (Boulant et al., 2005). The properties of this domain confer the core protein the ability to associate with cellular membranes such as that of lipid droplets (Barba et al., 1997, Miyanari et al., 2007). In parallel, DII is also a structural chaperone for the correct conformation of the DI. The basic domain DIII is cleaved by signal peptide peptidase to give the mature protein and acts as a signal sequence for targeting E1 to the ER membrane (McLauchlan et al., 2002).

Several evidences also showed that the role of Core is not strictly limited to a structural role as it also induces the alteration of the metabolism of lipids or the regulation of several cellular pathways involved on liver pathogenesis (Jackel-Cram et al., 2007).

As a nucleocapsid component, core is able to form dimers and then oligomers (Ai et al., 2009). It seems that core oligomers of core could be formed before the cleavage by signal peptide peptidase, suggesting that oligomeric core complex formation proceeds prior to or upon core attachment to membranes (Ai et al., 2009).

III.3.3.2- E1 and E2 glycoproteins

HCV glycoproteins E1 and E2 are type 1 transmembrane proteins, with a large extracellular domain (160 aa for E1 and 334 aa for E2) and a single C-terminal transmembrane domain (TMD) of 30 amino acids for E1 and 28 amino acids for E2. (figure 28) (Helle et al., 2007).

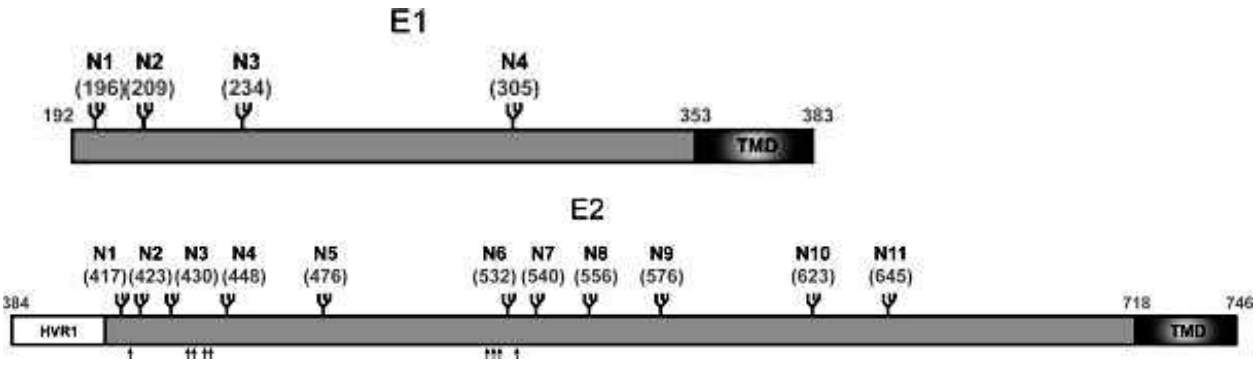

Figure 28: Schematic representation of N-glycosylation sites in HCV glycoproteins E1 and E2. The mutants are named with an N followed by a number relating to the position of the glycosylation site in the sequence. The numbers in parentheses correspond to the positions of the glycosylation sites in the polyprotein of reference strain H (GenBank accession no. AF009606). Epitopes recognized by MAbs 9/27, 3/11, and 1/39 are indicated as dark boxes. Amino acid residues 523, 530, and 535, involved in the formation of the conformation-dependent epitope of H48, are indicated as black bars. TMD, transmembrane domain. Adapted from (Helle et al., 2007)

After their release, E1 and E2, and more precisely their transmembrane domains are matured. During translocation into the ER and before protein cleavage, the two stretches form a hairpin structure into the ER membrane. Cleavage of the E1-E2 and E2-p7 junctions induces E1 and E2 transmembrane rearrangements: the second hydrophobic stretch unfolds toward the cytosol to form a single membrane-spanning domain with the first hydrophobic stretch (figure 29) (Cocquerel et al., 2002). This rearrangement allows the association of E1 and E2 as heterodimer complex.

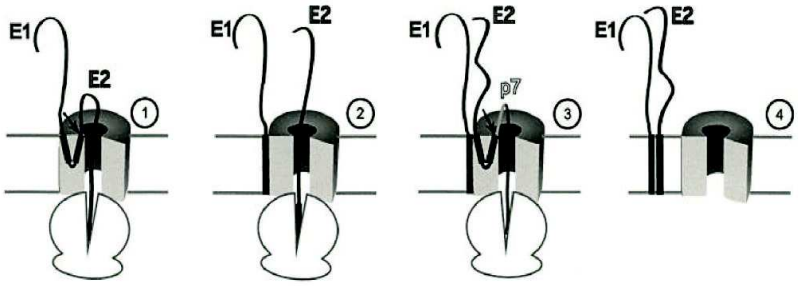

Figure 29: Model of the behavior of the TM domains of HCV envelope glycoproteins E1 and E2 during the early steps of their biogenesis. Adapted from (Cocquerel et al., 2002)

In addition, the E1 and E2 glycoproteins are highly glycosylated, with 5 glycosylation sites present in for E1 and 11 sites in E2 (figure 28). These glycosylations are N-linked high mannose type oligosaccharides (Goffard & Dubuisson, 2003, Zhang et al., 2004).
In cell lysates, E1E2 are mainly glycosylated by high-mannose type glycans but it seems that on the surface of the particles both high mannose and complex glycans are present (Vieyres et al., 2010). These glycosylations have multiple roles. N-glycosylation sites has been shown to be important for the correct folding of the glycoproteins, for interaction with cellular receptors and protection against neutralizing antibodies (Goffard & Dubuisson, 2003, Helle et al., 2007, Helle et al., 2010).
Two structures of the core domain of E2 were resolved recently (Khan et al., 2014, Kong et al., 2013). The E2 ocre is a monomer with a compact and globular architecture consisting of immunoglobulin-like fold and a domain with a central β sheet surrounded by loops, short helices and two β strands. In the core domain of HCV E2, many regions lack regular secondary structure and most of the N-linked glycans are largely disordered In addition, the structure of the N-terminal extremity of E1 was also obtained (El Omari et al., 2014). This protein is arranged as a disulfide linked, domain swapped homodimer. It is composed of a single long α-helix sandwiched by two and three antiparallel β strands. The first two β strands make a hairpin and are involved in domain swapped and homodimer formation.
E2 mediates the attachment and binding to cellular receptors. Indeed, E2 was demonstrated to specifically bind two particular cellular receptors: the scavenger receptor B1 (SR-B1) and the CD81 tetraspanin. The hypervariable region I (HVRI) of E2 is essential for the attachment of viral particles to SR-BI (Bankwitz et al., 2010). Interaction of E2 with CD81 was highly studied (Clayton et al., 2002, Drummer et al., 2006, Flint et al., 1999, Owsianka et al., 2001, Owsianka et al., 2006, Patel et al., 2000, Roccasecca et al., 2003, Witteveldt et al., 2009) as it may play a key role in HCV entry. It was found that the interaction occurs via the large extracellular loop of CD81. In contrast, the role of E1 during binding and cellular entry is poorly characterized. It seems that E1 is not an attachment protein but is involved in the regulation of E2

binding to receptors (Russell et al., 2009, Wahid et al., 2013). Furthermore, E1 and E2 have been shown to be involved in membrane fusion (Drummer et al., 2007, Lavillette et al., 2007).
Finally, E2 is able to interact with apoE (Boyer et al., 2014, Lee et al., 2014), suggesting that E2 plays a key role in the association of viral particles with lipoproteins.

III.3.4- Non-structural proteins

III.3.4.1- p7

This protein involved in assembly and secretion of viral particles is presented in the part IV.

III.3.4.2- NS2

NS2 is a 23kDa non-structural protein. The most recent topology model shows that this protein is composed of 3 transmembrane domains and a cytosolic cysteine protease domain (Jirasko et al., 2010). The structure of its protease domain was resolved (Lorenz et al., 2006) as well as the structure of the two first transmembrane domain (Jirasko et al., 2010). Whereas its N-terminal extremity is cleaved by the cellular signal peptidase, its C-terminal extremity is released through an auto-cleavage (Reed et al., 1995). NS2 is dispensable for replication but it plays a central role in assembly as it interacts with multiple viral proteins, including E2, p7, NS3 and NS5A (Jirasko et al., 2008, Jirasko et al., 2010, Ma et al., 2011, Popescu et al., 2011, Shanmugam & Yi, 2013, Stapleford & Lindenbach, 2011) (figure 30).

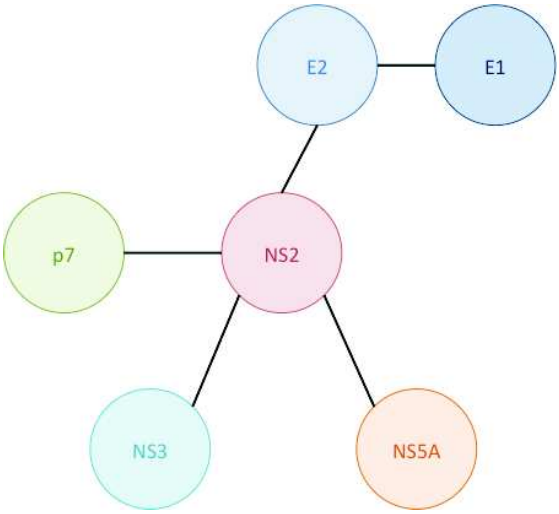

Figure 30: Viral proteins interacting with NS2.

III.3.4.3- NS3-4A

NS3 is a 70kDa protein with two major functions: a serine protease activity encoded by its N-terminal domain and a helicase and NTPase activity encoded by its C-terminal domain. NS3 associates with NS4A, which allows the anchoring of the complex onto the ER membrane in order to form a competent protease complex. This protease cleaves the second part of the viral polyprotein: namely NS3-4A, NS4A-4B, NS4B-5A and NS5A-5B. In addition to the viral proteins, NS3/4A is also able to cleave the RIG-I adaptor MAVS (Meylan et al., 2005) in order to interfere with innate immunity of the host.
In addition, NS3 is essential for RNA replication. Via its helicase activity, it is involved in RNA unwinding (Lindenbach et al., 2007). This function is dependent of the NTPase activity that hydrolyzes ATP to generate energy (Gu & Rice, 2010).
NS3 is also important for virus assembly. Indeed, mutations in the helicase domain that enhance RNA replication may also impair virus assembly, indicating that NS3 orchestrates both functions in a tight coordinated fashion (Chatel-Chaix et al., 2011, Ma et al., 2008). It has been suggested that the NS3-NS4A helicase activity is involved in RNA packaging during nucleocapsid assembly (Lindenbach & Rice, 2013) .

III.3.4.4-NS4B

NS4B is a four transmembrane-containing 27kDa protein, with a N-terminal domain oriented either toward the lumen or toward the cytosol and a cytoplasmic C-terminal domain. NS4B is critical for RNA replication, it is able to oligomerize and interacts with other viral proteins to alter intracellular membranes. It was demonstrated that the NS4B-NS5A precursor is important for the formation of double membrane vesicles, essential for HCV replication (Gouttenoire et al., 2014, Paul et al., 2011, Romero-Brey et al., 2015b). In addition, NS4B is able to interact with NS5A (Biswas et al., 2016) as well as viral RNA (Einav et al., 2008). Moreover, the terminal domains of NS4B both harbor important functions for replication. Although its N-terminal domain possesses a NTPase activity that generate energy essential for replication, its C-terminal domain is important for NS5A hyperphosphorylation (Jones et al., 2009). Similar to NS3, NS4B also plays a key role during virus assembly independently of its function in RNA replication (Han et al., 2013, Jones et al., 2009).

III.3.4.5-NS5A

NS5A is a phosphoprotein that is composed of 3 functional domains. The domain 1 is essential for RNA replication. The other domains are critical for virus assembly and replication. The domain 2 harbors critical residues for RNA replication (Tellinghuisen et al., 2008b) and the domain 3 is likely important for virus assembly through interaction with Core during virus assembly (Appel et al., 2008, Masaki et al., 2008). Two major

forms of this protein co-exist: a phosphorylated form of 56 kDa and a hyperphosphorylated form of 58 kDa (Grakoui et al., 1993). Several residues have been identified as positions for phosphorylation. NS5A is found associated to ER membrane but also at the surface of lipids droplets (Miyanari et al., 2007).
NS5A interacts with PI4KIIIα, this interaction being essential for HCV replication. NS5A is also able to stimulate activity of this kinase (Reiss et al., 2011).
NS5A is a central player in the transition between replication and assembly, possibly via its phosphorylation status (Lindenbach & Rice, 2013, Tellinghuisen et al., 2008a). NS5A is involved in assembly by transferring the viral genome to the site of encapsidation (Boson et al., 2017).
Finally, it has been proposed that NS5A could interact with apoE, allowing assembly and secretion of the viral particles (Benga et al., 2010, Cai et al., 2016, Cun et al., 2010, Lee et al., 2014, Zhang et al., 2016).

III.3.4.6- NS5B

NS5B is the HCV RNA-dependent RNA polymerase. This protein of 68 kDa is inserted into the ER membrane via its unique alpha helical transmembrane domain (Moradpour et al., 2007). A large cytoplasmic domain of around 500 amino acids constitutes a highly conserved enzymatic domain involved in RNA synthesis (Bressanelli et al., 1999). However, this enzyme has a million times lower fidelity than prokaryotic or eukaryotic RNA polymerase since it misses any exonuclease or proof reading activities.
Like many other nucleotides polymerases, NS5B can be compared to a “right hand” with three distinct domains: fingers, thumb and palm (Bressanelli et al., 1999). Contacts between the fingers and the thumb domains form a gap allowing the RNA strand to access to the palm. This domain, which lines up with dTTPs, constitutes the active site of the polymerase and synthesizes new RNA strands. It has been shown that mutations that influence the interactions and contacts between the thumb and fingers domains may significantly increase replication efficiency and thus, virus production (Schmitt et al., 2011). Several viral or cellular proteins regulate the activity of NS5B as NS5A or the cellular cyclophilins that facilitate the NS5B-RNA interactions (Shirota et al., 2002, Watashi et al., 2005).

III.3.5- The HCV life cycle

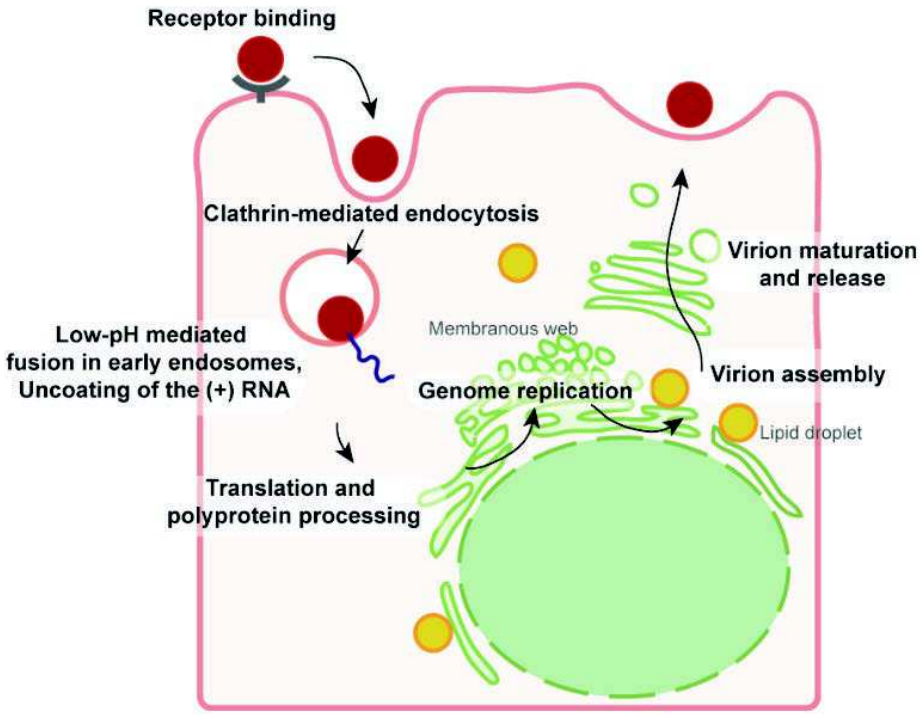

Figure 31: Overview of HCV replication cycle in hepatocytes. The viral particle is represented by a red disk. Viral entry involves a long list of receptors, it occurs by clathrin-mediated endocytosis and terminates with the low-pH induced fusion between viral and endosomal membranes. The released genome is translated into a single polyprotein, which is processed by host and viral proteases into the individual mature proteins. Replication of the viral RNA occurs in vesicles formed by modified ER membranes. Assembly of new virions also occurs at the ER membrane, but in close proximity to lipid droplets. Viral particles bud within the ER lumen and are released via the secretory pathway. Adapted from (Vieyres et al., 2014)

III.3.5.1- HCV entry

HCV particles are transported by the bloodstream and come into contact with the basolateral surface of hepatocytes. Initial attachment of HCV particles occurs via binding to heparan surface proteoglycans (LeFevre & Force, 2014, Shi et al., 2013) or SR-BI (Dao Thi et al., 2012) (figure 32). This initial contact seems to be mediated by apoE rather than by HCV glycoproteins. HCV particles are also able to interact with the LDL-R but it seems that this interaction leads to non-productive entry (Albecka et al., 2012). It was also shown that only low density viral particles could bind to LDL-R, suggesting that interaction with this receptor is due to the particular heterogenicity of HCV particles (Molina et al., 2007). Several studies identified apoE as a main mediator of interaction between LDL-R and HCV particles (Hishiki et al., 2010, Owen et al., 2009). More recently it was also demonstrated that HCV particles could interact with VLDL receptor (VLDL-R) that is not expressed in cell lines used in the majority of the studies, due to the condition of culture (Ujino et al., 2016). The use of VLDL-R might be redundant with the use of LDL-R (Yamamoto et al., 2016).

The steps of HCV entry following the initial attachment of particles involve several cellular factors; yet, the role of each factor remains poorly understood. SR-BI plays a key role in the post binding steps, and it is able to interact with E2 (interaction regulated by HVR-I). One hypothesis is that SR-BI could remove lipidation of particles, via its lipid transfer activity. Another possibility is that SR-BI could prime the particles for interaction with CD81. Indeed, E2 of HCV is able to directly interact with this tetraspanin, while viral particles cannot (Evans et al., 2007). This interaction promotes the activation of Epidermal Growth Factor Receptor (EGFR) (Diao et al., 2012, Lupberger et al., 2011) and associated guanosine triphosphatases such as H-Ras (Zona et al., 2013), which allows CD81 lateral mobility and subsequent association with claudin-1 (CLDN1), leading to internalization of virions with CD81-CLDN1 complexes (Farquhar et al., 2012) and to cell entry (figure 31). In addition, it was also shown that E-cadherin (Li et al., 2016) is involved in HCV entry, probably by regulating the pool of CLDN1 available for interaction with CD81 (figure 32). Interestingly, the localization of CLDN1 in tight junctions is not required for interaction with CD81 (Harris et al., 2010, Harris et al., 2008).

In addition to CLDN1, Occludin (OCLN), another tight junction protein, is essential for HCV entry (Benedicto et al., 2009, Sourisseau et al., 2013) although its role remains elusive. It seems that, like for CLDN1, its localization in tight junction is not required for HCV entry (Fletcher et al., 2014).

The cholesterol transporter Niemann-Pick C1-like 1 (NPC1L1) and the transferrin receptor 1 have also been demonstrated as host factors involved in particle entry; yet, the precise role of either protein remains poorly understood (Martin & Uprichard, 2013, Sainz et al., 2012).

Following interactions with these factors, HCV particles are endocytosed by a clathrin-dependent process (Blanchard et al., 2006). After internalization, virions are transported to endosomes. Acidification of the endosomal compartment is thought to trigger E1E2 conformational changes that induce the fusion of the viral membrane with the endosomal membrane (Op De Beeck et al., 2004, Sharma et al., 2011).

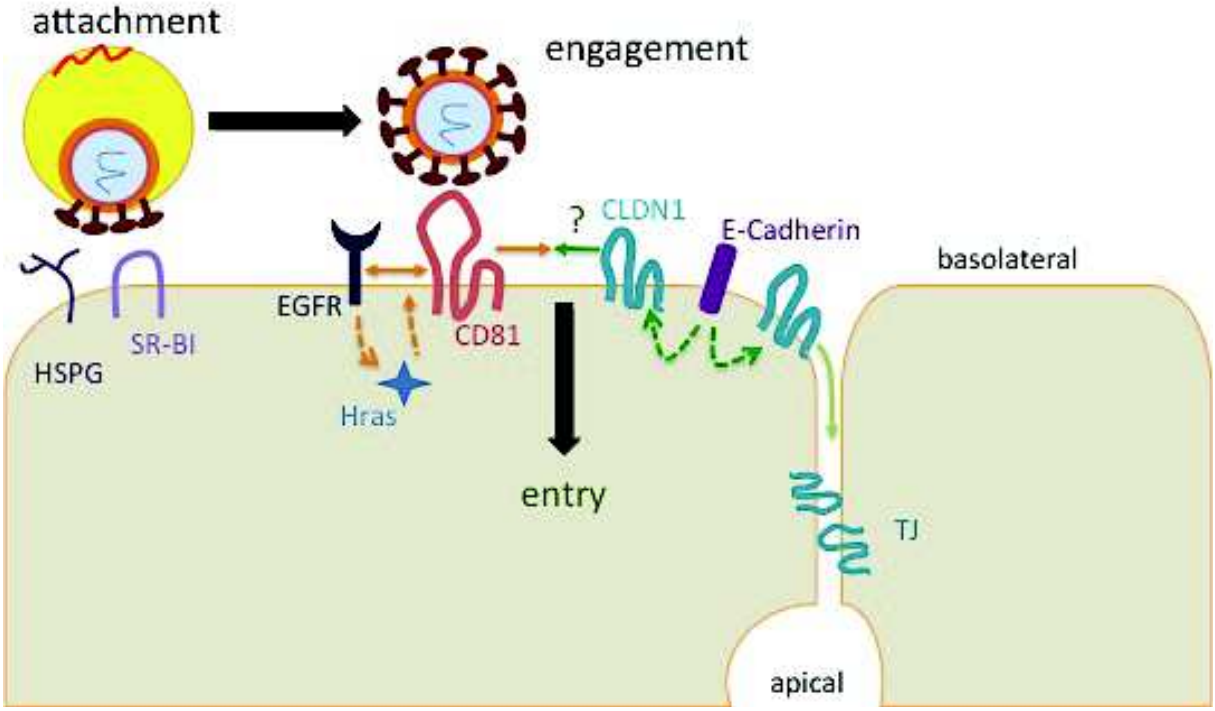

Figure 32: HCV entry. Following attachment to the cell surface, which is mediated by different molecules, including heparan sulfate proteoglycans and SR-BI, the E2 surface glycoprotein harbored by HCV particles interacts with CD81 (engagement), which promotes activation of EGFR and associated guanosine triphosphatases such as H-Ras and allows CD81 lateral mobility and subsequent association with CLDN1 (small orange arrows), leading to internalization of virions and to cell entry. On the other hand, it is proposed that E-cadherin regulates a pool of available CLDN1 molecules for their TJ localization or surface distribution (green arrows). Adapted from (Denolly & Cosset, 2017)

III.3.5.2- HCV replication

HCV replication is mediated after the release of the genome and the translation of the polyprotein. The viral genome is replicated through a negative strand intermediate (Lohmann, 2013).

HCV induces massive rearrangements of the ER membrane in order to create favorable microenvironments for its replication: this is referred to as the "membranous web". It was demonstrated that it is mainly constituted by double-membrane vesicles (DMV) (Romero-Brey et al., 2012) (see part V.1.2).

The incoming positive-stranded viral RNA serves as a template for the synthesis of a single, negative-stranded RNA molecule that remains base-paired with its template to form a double-stranded RNA(Ali et al., 2002). This so-called replicative form (RF) is then copied multiple times to generate progeny positive-stranded RNAs that can be used for translation, synthesis of new RF or packaging into virus particles (reviewed by Bartenschlager et al. 2004). The main actors involved in HCV RNA replication are the non-structural proteins NS3 helicase, which is addressed to the membrane by its cofactor NS4A and responsible for unwinding RNA, and the NS5B replicase, which

catalyses the synthesis of progeny RNAs(Ishido et al., 1998, Lam & Frick, 2006) (Lohmann et al., 1999b), as an RNA-dependent RNA polymerase..

III.3.5.3- HCV assembly and secretion

These steps of HCV life cycle are described in part V and VI.

IV- HCV p7 viroporin

The p7 protein is a small, 63 amino-acid-long protein, consisting of a “hairpin-like” topology involving three helices inducing two trans-membrane segments connected by a hydrophilic, positively-charged cytosolic loo], though alternative folds and topologies have been proposed, e.g., with the p7 C-terminus exposed to the cytosol. As it is able to form an ion channel in either hexameric or heptameric form exhibiting a funnel- or flower-like shape, it was classified as a viroporin, like M2 of influenza virus. Importantly, p7 is dispensable for replication but essential for both assembly and secretion of infectious particles. First, p7 modulates the formation of NS2 complexes with E2, NS3 and NS5A, allowing clustering of assembly components and regulation of early assembly events. Second, p7 allows, in concert with NS2, the regulation of core localization at lipid droplets vs. ER-derived membranes, from where viral particles are released in the secretory pathway. Third, p7 modulates the envelopment of nascent virions. Fourth, p7 may regulate the pH of some intracellular compartments, which could be essential for the protection and secretion of infectious particles. All these fucntions and properties of p7 are described and detailed in this section.

IV.1- Viroporins

IV.1.1- Classification

The existence of viroporins was suggested following the observation that infected cells become more permeable to ions and small molecules (Carrasco, 1978). Viroporins are small proteins that are hydrophobic and able to permeabilize membranes upon oligomerization. Viroporins can be classified into two major groups: class I and class II depending on the number of transmembrane. Subgroups were also proposed depending on their membrane topology (Nieva et al., 2012) (figure 33). Class IA contains a small luminal amino terminal domain with a long cytosolic tail. Class IB contains a small cytosolic amino terminal domain with a long luminal tail. Class IIA are viroporins with N- and C-terminal extremities located in the ER lumen whereas class IIB viroporins extremities are located in the cytosol (figure 33).

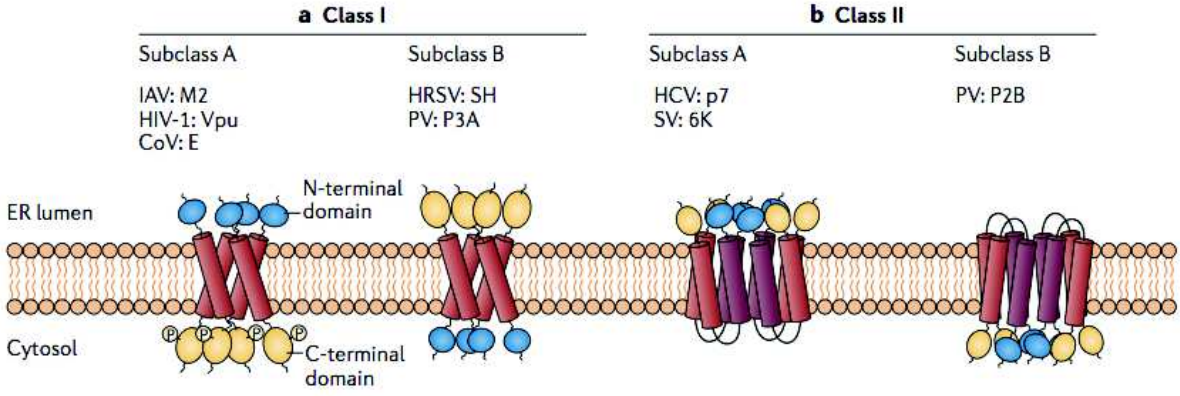

Figure 33: Classification of viroporins according to the number of transmembrane domains and the membrane topology of the constituent monomers. (Nieva et al., 2012)

IV.1.2- Viroporins and cytopathic effects

Viroporins are able to modify cell host membrane permeability and form pores that allow passing of some ions or small molecules. In some cases, the pore could be highly selective for specific ions (e.g. M2 of IAV is highly selective for protons (Pinto et al., 1997) or could be weakly selective, inducing the transfer of all kinds of ions or small molecules (e.g. HCV p7). In addition, several viroporins have been shown to alter calcium homeostasis. It was observed, for example, for picornavirus P2B or rotavirus NSP4 (Aldabe et al., 1996, Hyser et al., 2010), which induces an increase of the cytoplasmic concentration of calcium. Changes in homeostasis could have various effects since Ca^{2+} regulates gene expression, post-translational modifications as well as induction of apoptosis. Several viroporins also affect the trafficking of glycoproteins. It was first observed for poliovirus viroporins (Doedens & Kirkegaard, 1995) but was then described for other viruses such as coxsackievirus 2B (de Jong et al., 2008). Finally, some viroporins are able to prevent acidification of intracellular compartments such as M2 of IAV preventing endosomal acidification.

IV.1.3- Viroporins and the viral life cycle

Viroporins are involved in different steps of viral life cycle. Some of them are involved in virus entry such as IAV M2 (see below) or in replication. Indeed, picornavirus viroporins are involved in the formation of the "viroplasm" that is necessary for the replication of the genome. However, the majority of viroporins are involved in viral assembly and secretion. In addition to p7, coronavirus 3a is involved in the release of virions (Lu et al., 2006), which is also the case of HIV-1 Vpu (see below) and IAV M2 (see below).

IV.1.4- Viroporins as therapeutic targets

As viroporins are involved in several steps of viral life cycles and as they create pores in the membrane, they are good therapeutic targets. In addition, some drugs could impact several viruses, such as amantadine and its derivatives that are able to inhibit HCV p7 and IAV M2 (Kendal & Klenk, 1991). Another molecule called 5-(N,N-hexamethylene) amiloride (HMA) is able to inhibit both HCV p7; HIV-1 Vpu and SARS-CoV E channel activities (Ewart et al., 2002, Premkumar et al., 2004, Wilson et al., 2006). BIT225 (N-(5-(1-methyl-1H-pyrazol-4-yl)-napthalene-2-carbonyl)-guanidine) is a molecule able to inhibit both HCV p7 and HIV Vpu.

IV.1.5- Example of viroporins

Viroporins were first identified in RNA viruses but they are also found in DNA viruses, such as JC polyomavirus and Simian virus 40 (SV40) (Raghava et al., 2011).

ssRNA (+)	ssRNA (-)	dsRNA
Picornaviridae Poliovirus (2B, 3A) Coxsackievirus (2B) Rhinovirus (VP4)	*Orthomyxoviridae* Influenza A virus (M2)	*Reoviridae* Rotavirus (NSP4)
Flaviviridae HCV (p7) BVDV (p7) Dengue (M)		
Togaviridae SFV (6K) Sindbis virus (6K)		
Coronaviridae SARS-CoV (E) (3a) (8a)		
Retroviridae HIV-1 (Vpu)		

Table 1: Example of viroporins.

In the next section, M2 of IAV and Vpu of HIV-1 will be described in more details.

IV.1.5.1- M2 of Influenza A virus (IAV)

M2 is a class IA viroporin with 97 amino acids protein and a tetrameric pore (figure 34) with two residues His37 and Trp41 inside the channels that are essential for the transport of protons.
It has been proposed that M2 is activated during viral entry and triggers the uncoating by conducting protons inside the viral particles (Stauffer et al., 2014, Wharton et al., 1994). In addition to this role, it was shown that M2, by acting as a proton transporter, is able to slow down the trafficking of haemagglutinin and prevents its premature maturation by decreasing the pH of the Golgi apparatus (Henkel et al., 1999, Henkel & Weisz, 1998). Besides, M2 is essential for the budding and scission of the viral particles at the plasma membrane. Indeed, its amphipathic helix mediates a cholesterol-dependent alteration of the membrane curvature. M2 could be localized to the neck of budding virions and mediate their scission (Rossman et al., 2010) .

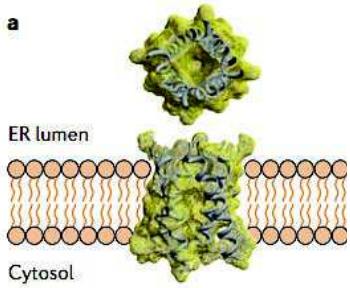

Figure 34: M2 of IAV. Adapted from (Nieva et al., 2012)

IV.1.5.2- Vpu of HIV-1

Vpu (figure 35) is encoded by HIV-1 but not HIV-2, and is a class IA viroporin with 77 or 86 amino acids, with an ion channel activity being specific for monovalent cations such as sodium or potassium(Ewart et al., 1996) and with so far poorly known biological function. Vpu can be found in a variety of oligomers from tetramers to heptamers and it was proposed that it is involved in the regulation of viral particles release(Hsu et al., 2010) (Schubert et al., 1996) . Besides its ion channel activity, it was shown that Vpu modulates the level of expression of several proteins at the plasma membrane, such as CD4(Willey et al., 1992), by degrading this protein via the ubiquitin proteasome pathway. This mechanism prevents the formation of CD4-Env complexes and thus prevents antibody-dependent cell-mediated cytotoxicity (ADCC) that could lead the elimination of infected cells. It also antagonizes the interferon (IFN)-α-induced Bone Marrow Stromal Cell Antigen 2 (BST2) glycoprotein that inhibits the release of viral particles (Neil et al., 2007). In addition, Vpu is able to regulate the localization of Env and Gag as wells as particles formation and budding. Indeed in absence of Vpu, both factors accumulate; yet, in the presence of Vpu, release of particles is enhanced (Handley et al., 2001, Van Damme & Guatelli, 2008).

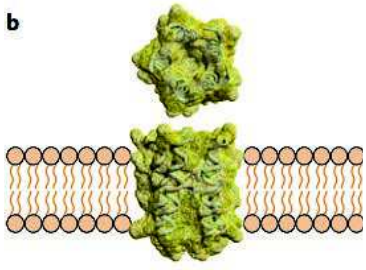

Figure 35: Vpu of HIV. Adapted from (Nieva et al., 2012)

IV.2- Topology and structure of HCV p7

P7 is a 63 amino acid-long protein with two transmembrane domains and a basic loop. It was proposed, using different tag that the extremities of the protein are luminal whereas its loop is cytoplasmic (Carrere-Kremer et al., 2002). However, an alternative topology was proposed with the C-terminal extremity localized towards the cytosol (Isherwood & Patel, 2005). Interestingly, we also showed an alternative, topology of p7 for some mutants of p7 (see Results section) ; yet, as there are no antibodies available against p7, it is quite difficult to conclude on its topology and it is possible that both topologies co-exist.

Four NMR-based structures of the HCV p7 monomer have been described. Three of them were obtained with Gt1b HCV (Cook et al., 2013, Foster et al., 2014, Montserret et al., 2010) and a last one was obtained with Gt5a HCV (OuYang et al., 2013). Even if there are some differences between the structures of Gt1b p7, they all display a "hairpin-like" structure (figure 36) with three or four helical segments with various positions. It appears that in all structures, p7 seems flexible, meaning that the structure could move easily. In contrast, the structure of Gt5a p7 seems quite different from the other p7 (figure 36). It appears that this p7 has a "staple-like" structure, with four helices. Interestingly, this structure was obtained after NMR analysis of the oligomers. Furthermore, the orientation of this structure was proposed in order to fit with a 3D structural model (see below), implying that it could be inversed compared to the 3 others, namely with the loop being in the lumen side of the membrane (figure 38) (Madan & Bartenschlager, 2015). In addition, in contrast to the models of Gt1b p7, the model of OuYang et al. lacks the presence of an unstructured loop (in blue in figure 38).

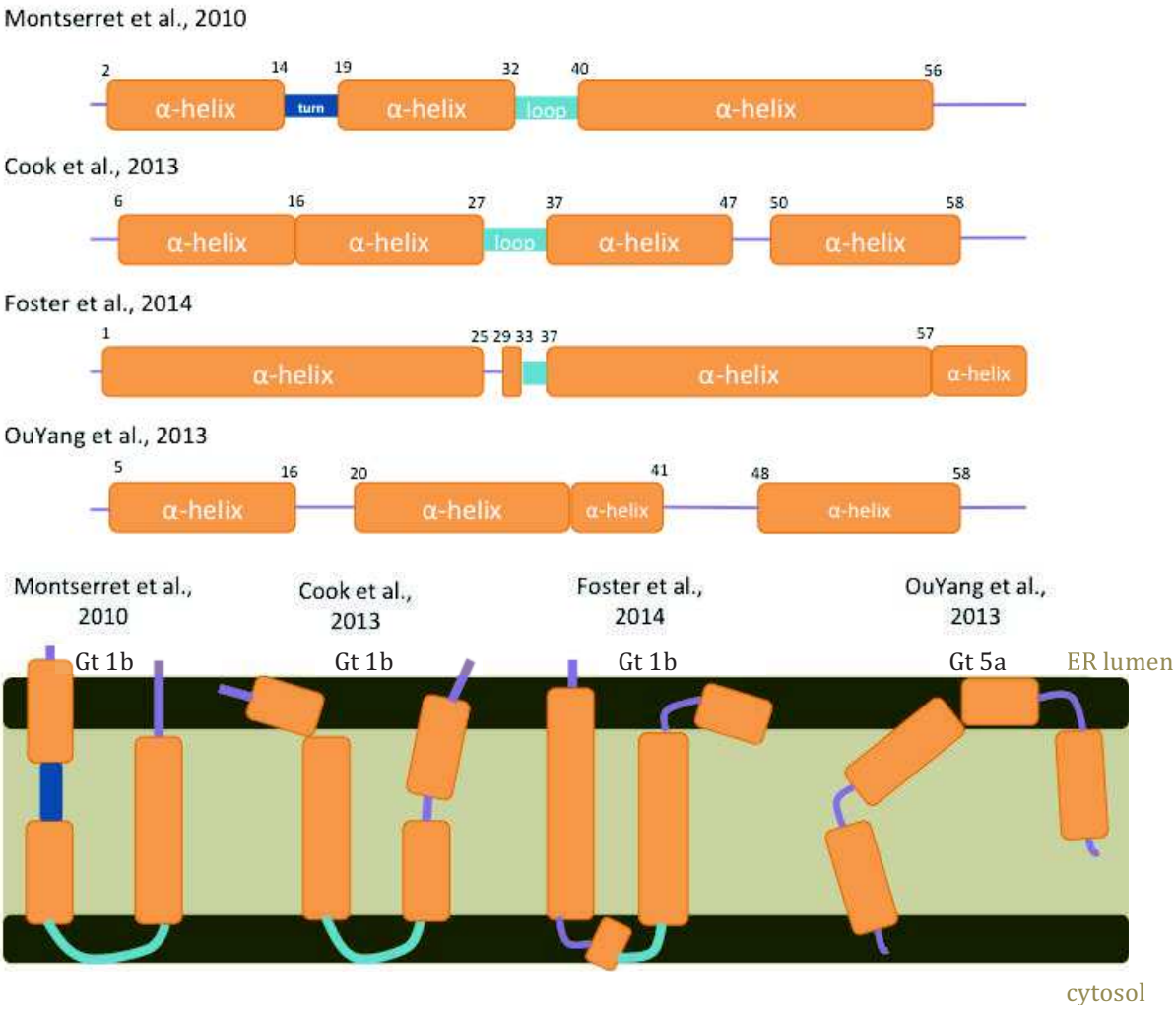

Figure 36: Different topologies of HCV p7 based on literature

P7 is able to form homo-oligomers and assembles as ion channel structures (Clarke et al., 2006, Griffin et al., 2003, Montserret et al., 2010, OuYang et al., 2013, Pavlovic et al., 2003, Premkumar et al., 2004). It appears that p7 might exist in different forms of oligomers as it was observed in hexa- or heptamers (Clarke et al., 2006, Griffin et al., 2003, Montserret et al., 2010). In 2009, the first 3D structure was identified (Luik et al., 2009). It showed that p7 exhibits a flower-shaped complex with 6 petals emerging from a conical base, with the extremity of each monomer exposed towards the tip of the petals. The model of OuYang et al., showed a funnel-like shape that seems to be very closed the flower shape. Other models for the hexameric or heptameric p7 were obtained by molecular dynamics using the structures of the monomers (Chandler et al., 2012, Cook et al., 2013, Foster et al., 2014, Kalita et al., 2015) (figure 37).

.

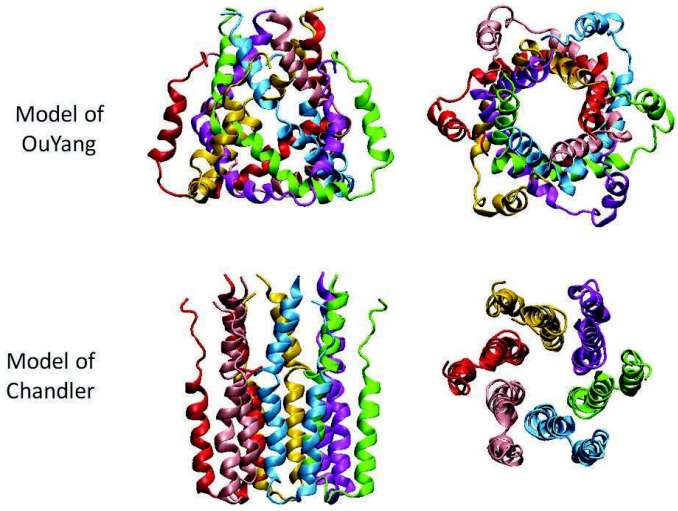

Figure 37: Structural model of oligomers of p7. Top: Model based on (OuYang et al., 2013). Bottom : Model based on (Chandler et al., 2012)

The differences between different models can be attributed to variability between HCV strains and therefore different p7, but also to the protocol used (difference in lipids, detergents…).

IV.3- HCV p7 ion channel activity

P7 was shown to act as a viroporin with poorly selective cation channel activity (Ca2+, K+, Na+, H+) (Chandler et al., 2012, Griffin et al., 2003, Luscombe et al., 2010, Montserret et al., 2010, Pavlovic et al., 2003, Premkumar et al., 2004, Whitfield et al., 2011, Wozniak et al., 2010). These studies mainly used electrophysiological techniques. Some studies reported that p7 could permeabilize liposomes, inducing release of carboxyfluorescein (CF) when added to CF-loaded liposomes (StGelais et al., 2009). However, a study demonstrated that the duality of p7 to transport both protons and large molecules could be due to two conformations of p7 depending on the preparation of samples (Gan et al., 2014). It was also shown that p7 could affect the acidification of vesicles within infected cells (Wozniak et al., 2010).
Mutation of amino acids 33-35 of the dibasic loop to alanine reduces H+ permeability, indicating that these amino acids are essential for the ion channel activity (Wozniak et al., 2010). These mutations were highly used in order to sign the viroporin activity of p7 (Bentham et al., 2013, Griffin et al., 2004, Ma et al., 2011, Shanmugam & Yi, 2013). However, it was shown that these mutations also impacted the topology of NS2, with a change of localization of its C-terminal domain no longer located in the cytosol (Ma et al.,

2011). A defect in E2-p7-NS2 processing was also observed with the same mutation (Ma et al., 2011, Shanmugam & Yi, 2013, Steinmann et al., 2007). In order to overcome these issues, mutations of residues 33-35 to glutamine, instead of alanine, i.e. with an inversion of charge, seem to be more appropriate to study the impact of the on channel (Brohm et al., 2009, Gentzsch et al., 2013, Popescu et al., 2011). The defect caused by the alaninr substitutions of positions 33 and 35 in alanine could be restored in HCV-infected cells by using Bafilomycin A1 (Wozniak et al., 2010) that prevents acidification (inhibiting v-ATPase) or by expressing influenza M2 in *trans* (Wozniak et al., 2010).
A study reported that His 17 of p7 is important for its ion channel activity, based on a motif similar present in influenza M2 (StGelais et al., 2009). However, this amino acid is not conserved in all genotypes and mutation H17A did not impair the production of infectious particles in the JFH1 context (Bentham et al., 2013).
In addition, recent studies indicated that depending on its genotype, p7 could have an activity called either M2-like (activation upon reduced external pH, meaning that it acts only when the pH is low) or pore-like (activation upon any change of external pH, meaning that it acts when pH is below and above a determined pH) in liposome based assays (Atkins et al., 2014, Li et al., 2012a, StGelais et al., 2009).

Several inhibitors of p7 have shown to abolish its ionic channel activity in artificial bilayers and to block the intracellular H+ conductance. These inhibitors include amantadine, rimantadine, NN-DNJ and BIT225 (Bichmann et al., 2014, Griffin et al., 2008, Luscombe et al., 2010, Pavlovic et al., 2005, Wozniak et al., 2010). P7 channel activity sensitivity to these drugs was shown to be genotype specific (Griffin et al., 2008). Additionally, it was observed that the drugs concentrations required to alter channel function in vivo were considerably higher than for isolated membrane vesicles.
Some of these inhibitors (Amantadine and NN-DNJ) were also found to alter the expression of viral glycoproteins in a dose-dependent manner (Griffin et al., 2008). Furthermore, amantadine and rimantadine also appears to have also some effect on HCV entry (Griffin et al., 2008) even if there is still no evidence of the presence of p7 on virions. Docking experiments indicated that the lowest energy positions for docking were the ones corresponding to the loop region (Bichmann et al., 2014).

IV.4- Subcellular localization of p7

P7 exhibits a reticular pattern, colocalizing with specific ER markers (Bentham et al., 2013, Griffin et al., 2005, Haqshenas et al., 2007, Vieyres et al., 2013). One study also indicated that a subset of p7 could also be localized in membranes adjacent to mitochondria and suggested that there were two distinct pools of p7 (Griffin et al., 2005). It seemed that the localization in the ER was independent of p7 signal peptide

and cleavage from E2 suggesting that p7 could be inserted in ER membrane even without signal peptide (Griffin et al., 2005).
P7 was found to colocalize mainly with E2, confirming its reticular localization (Bentham et al., 2013, Vieyres et al., 2013) but also with non-structural viral proteins such as NS2, NS3, NS4A (Vieyres et al., 2013) or NS5A (Bentham et al., 2013). In agreement with the above protein localization studies, foci consisting of p7-core associations were also observed (Bentham et al., 2013, Vieyres et al., 2013).
Importantly, some studies were conducted with p7 expressed as fusion proteins using different tags to overcome the lack of suitable antibodies against p7. It is therefore impossible to evaluate the localization of the native p7 as the presence of the tag could change the phenotype of the protein.

IV.5- Role of p7 in assembly of infectious particles

P7 was shown to be essential for assembly as it is able to interact with NS2, to regulate NS2 localization but also to regulate the localization and envelopment of core as well as the formation of NS2 complexes with other proteins.

IV.5.1- Interaction of p7 with NS2

Several studies reported that p7 interacts with NS2, a protein acting as a central organizer of viral assembly (Hagen et al., 2014, Jirasko et al., 2010, Ma et al., 2011, Popescu et al., 2011, Vieyres et al., 2013). This interaction seems to be genotype-independent, since NS2 (2a) and NS2 (1b) could be co-immuno-precipitated with p7 (1a), even if the lack of sensitivity of the antibody cannot be excluded (Popescu et al., 2011). This interaction seems to involve the transmembrane domains since the first transmembrane domain of NS2 was shown to be essential for this interaction (Popescu et al., 2011). Moreover, a NMR study predicted that W48, located in the second TM of p7, and amino acids 12 and 15 of NS2 are engaged in this interaction (Cook et al., 2013). Interestingly, mutations that affect p7 ion channel activity, such as substitution of aa 33-35 to glutamine (Vieyres et al., 2013) or to alanine (Ma et al., 2011) did not affect this interaction.

IV.5.2- Regulation of NS2 localization

Besides its ability to directly interact with NS2, p7 is able also to regulate the NS2 localization. NS2 accumulates in dotted structures colocalizing with NS5A near lipid droplets (Ma et al., 2011, Popescu et al., 2011). These structures seem to be associated with detergent-resistant membranes (DRM) (Shanmugam et al., 2015), indicating that such structures are localized in a specific cellular compartment. E2 was also detected in the same dots formed by NS2-NS5A (Ma et al., 2011) and NS2 localization in DRM was shown to be essential for the localization of E2 in the DRM (Shanmugam et al., 2015). P7

seems essential for the formation of these structures (Popescu et al., 2011, Shanmugam et al., 2015, Shanmugam & Yi, 2013, Tedbury et al., 2011) since, without p7, NS2 did not accumulate in such dotted structures and showed a more reticular pattern (Ma et al., 2011, Popescu et al., 2011). Controversial results were obtained concerning the role of the ion channel activity in this regulation. One study concluded that mutations that impact the function of p7 ion channel activity such as H17A and G39A, as well as use of rimantadine, an inhibitor of ion channel activity, did not interfere with the formation of dotted structures containing NS2/NS5A (Tedbury et al., 2011). Contrastingly, different set of mutations in p7, namely KR33/35AA and KR33/35QQ produced an altered NS2 reticular distribution pattern (Ma et al., 2011, Shanmugam & Yi, 2013) or a decrease in the number of cells with dotted structures of NS2 (Popescu et al., 2011) respectively. Since these studies did not use the same mutations to impair p7 ion channel activity it can be proposed that the ion channel is not involved in the regulation of NS2 localization but rather, that amino acids 33-35 have another way of action than ion channel function on the regulation of NS2 localization.

IV.5.3- Regulation of NS2 interactions

IV.5.3.1- NS2-E2 interaction:

One study indicated that p7 does not regulate NS2-E2 interaction (Popescu et al., 2011) since deletion of p7 or RR33/35QQ mutation did not affect this interaction. However, other studies showed that p7 is essential for NS2-E2 interaction since the deletion of p7 reduced the amount of E2 immunoprecipitated with NS2 or inhibited the interaction (Ma et al., 2011, Stapleford & Lindenbach, 2011). This difference could be due to the difference in the viruses used or in the tag used to mark p7 and/or NS2. The KR33/35-AA mutation also prevents the NS2-E2 interaction and decrease the interaction between NS2 and E1 (Ma et al., 2011). Yet, this latter result is controversial because other reports indicated that interaction between NS2 and E1 is indirect and only due to E2 heterodimerization with E1 (Stapleford & Lindenbach, 2011).

IV.5.3.2- NS2-NS5A interaction:

P7 seems essential for this interaction. Mutation of amino acids 33-35 of p7 to alanine showed a defect in NS2-NS5A_interaction (Ma et al., 2011) although the same study indicated the inversion of NS2 topology as induced by the KR33/35AA mutation.

IV.5.3.3- NS2-NS3-4A interaction:

P7 is necessary for NS2-NS3 interaction since deletion of p7 inhibited this interaction (Stapleford & Lindenbach, 2011). Mutation of amino acids 33-35 of p7 to alanine also blocked NS2-NS3 interaction (Ma et al., 2011) but as explained above, the same study indicated the inversion of NS2 topology.

IV.5.3.4- Influence of the processing between E2 and p7 on NS2 complexes

The optimal processing between E2 and p7 seems critical for the formation of NS2 complexes with E2 and/or NS3. A complete separation, via the introduction of an IRES between E2 and p7, impairs NS2 interaction with E2 but not with NS3 (Shanmugam & Yi, 2013, Stapleford & Lindenbach, 2011) whereas an impaired cleavage, via mutations in p7 (KR33/35AA) or E2 (A367R), altered the interaction of NS2 with both E2 and NS3 (Shanmugam & Yi, 2013).

The regulation of NS2 complexes by p7 will be discussed in the Results section of this thesis.

IV.5.4- Modulation of core functions by p7

IV.5.4.1- Regulation of core localization

P7, in concert with NS2, is able to modulate the localization of core (Boson et al., 2011). Indeed, depending on the HCV strain, core is mainly localized either at the ER membrane (Jc1 strain) or at the lipid droplet (JFH1 strain) membrane. It was demonstrated that this difference in core localization between Jc1 and JFH1 (ER vs. LD, respectively) is determined by p7 and NS2, through a genetic compatibility between the second transmembrane domain of p7 and the first one of NS2 (Boson et al., 2011). Intriguingly, perturbation of p7 ion channel activity, via the KR33/35AA or QQ mutation, did not change the localization of core when p7 was expressed alone with core (Boson et al., 2011) (unpublished data) whereas the same mutation induced core localization around the lipid droplets in the context of Jc1 HCVcc-infected cells (Gentzsch et al., 2013). This discrepancy between individual protein expression and infected cells could be due to the presence, in the latter case, of other viral proteins as well as functional replication complexes and viral genome that could modulate the above events.

IV.5.4.2- Regulation of capsid envelopment

In addition, functional p7 seems necessary for the final steps of capsid assembly and envelopment by a membrane (Gentzsch et al., 2013). In a context of overexpression of single proteins, interaction between p7 and core has also been described (Hagen et al., 2014).

Finally, alanine scanning in position 33-34-35 showed that p7 protects E2 from degradation in a manner that is independent either of lysosome or acidification of vesicles (Atoom et al., 2013). This phenotype could be linked to a defect in the cleavage of E2-p7 and p7-NS2 junctions as observed in the case of these mutations (Ma et al., 2011). Interaction between p7 and the glycoproteins has also been described (Hagen et al., 2014). This interaction, however, was only documented in the context of overexpression of single proteins, without further confirmation during HCV replication in infected cells.

Besides it was demonstrated that the N-terminal extremity of p7 is essential for the production of infectious particles (Scull et al., 2015). Like for other viroporins, some of the activities of p7 can be complemented in trans by ectopic expression of p7 (Brohm et al., 2009) and this transcomplementation system has been widely used in my studies.

IV.6- Role of p7 in secretion of infectious particles

In addition to its role in assembly, p7, and more particularly its ion channel activity, impacts the secretion of infectious particles (Bentham et al., 2013, Steinmann et al., 2007). Indeed, mutation of the dibasic loop impairs the secretion of infectious particles. In addition, it has been shown that IAV M2 could restore the effect of these mutations, suggesting that p7 exhibits a M2-like function (Bentham et al., 2013, Wozniak et al., 2010). In support of this hypothesis, several studies reported a pH-dependent maturation of the HCV glycoproteins (Atkins et al., 2014, Wozniak et al., 2010) that may be regulated by p7 (Atkins et al., 2014). Intracellular infectious particles are acid-pH sensitive whereas extracellular particles become acid-pH resistant or not, depending on the genotype/strain, and more particularly on the sequence of p7 (Atkins et al., 2014). Because of all this evidence, it was speculated that p7 ion channel might be regarded as a modulator of the pH-mediated maturation process of HCV particles; yet, the mechanism remains poorly defined.

V- Assembly of infectious particles

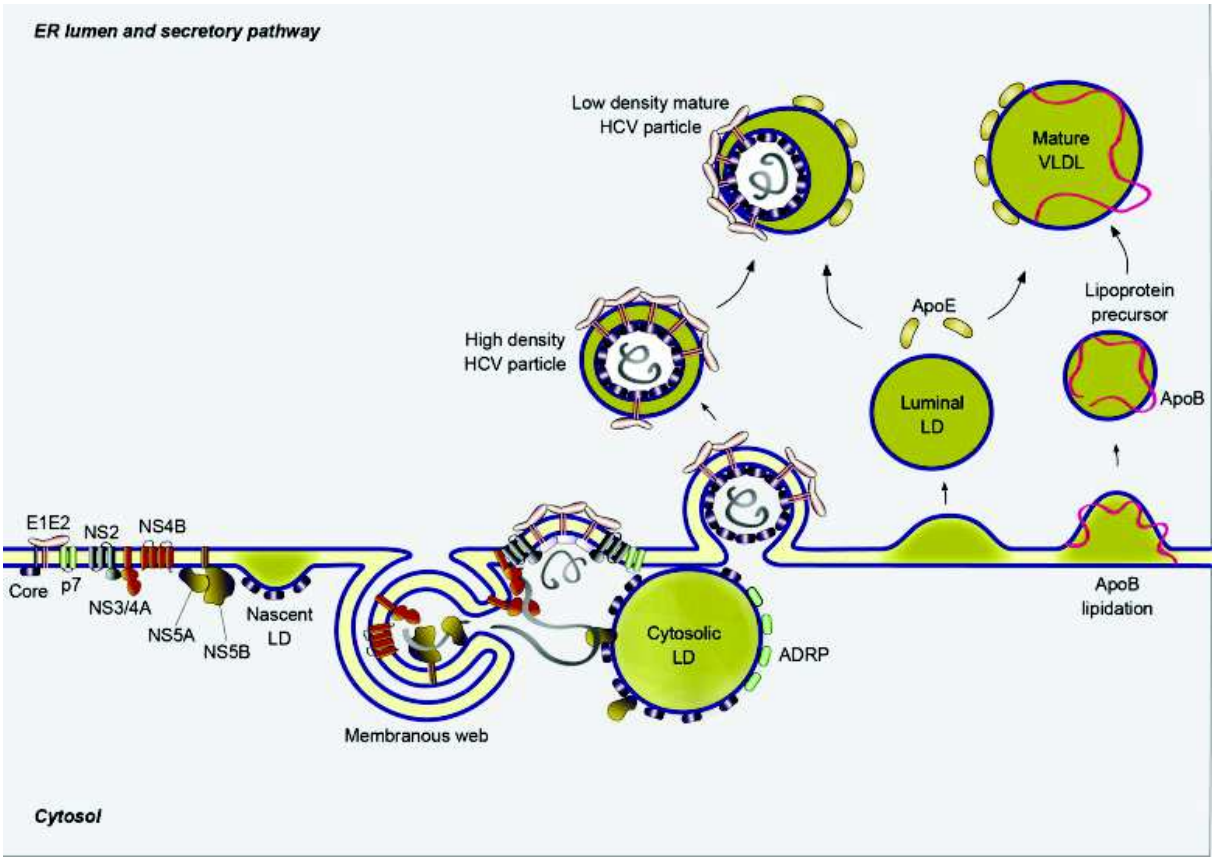

Figure 38: Model of assembly of infectious particles. After the maturation of viral proteins, core is loaded onto LDs. Assembly takes place at the junction between the replication complex called membranous web and LD. The non-structural proteins p7 and NS2 are thought to connect RNA, and the structural proteins core and glycoproteins E1 and E2. Virus budding occurs with encapsidation of the viral RNA and envelopment at the ER membrane. The last steps of assembly and maturation use the lipoproteins pathway but the interplay with this pathway is still unknown. One of the hypothesis is represented here with the fusion of a viral precursor with luminal LD and association with apolipoprotein which are normally used for the maturation of VLDL in the ER lumen. (Dubuisson & Cosset, 2014)

V.1- Key "organelles" for HCV assembly

The current model of HCV assembly is described in this section. Importantly, the assembly events are very difficult to visualize since they are rare and transient. Assembly of infectious particles takes places in the membranous web at ER membranes, near the sites of replications (located in DMVs) and the LDs (figure 38). The nature of assembly sites remains elusive.

V.1.1-Lipid droplets (LDs)

Cytoplasmic lipid droplets are intracellular structures that store neutral lipids (cholesterol ester and triglyceride). They are able to interact with other membrane of the cells.

HCV core and NS5A proteins are associated to LDs(Miyanari et al., 2007, Moradpour et al., 1996). It was shown that HCV assembly efficiency correlates with the colocalization of core and NS5A around same lipid droplets(Appel et al., 2008). Some reports reveal that at least three cellular proteins help the interaction of core and NS5A with LDs: DGAT1 (see part V.3.1.1.) but also Rab18(Salloum et al., 2013) and TIP47(Ploen et al., 2013, Vogt et al., 2013). It was also shown that p7 regulates the localization of core on LDs (Boson et al., 2011, Shavinskaya et al., 2007).
There is still a debate on the precise role of the LDs in assembly and the involvement of core targeting at LDs for assembly. Indeed some studies reported that the interaction of core with LDs is essential for the production of infectious particles (Miyanari et al., 2007) (Boulant et al., 2007) but some other studies reported that HCV species that target core at LDs are less efficient for assembly than those targeting core at ER membranes(Boson et al., 2017, Boson et al., 2011, Shavinskaya et al., 2007). Although the precise role of LDs is still unknown, it is well admitted that assembly occurs in close proximity to LDs.

V.1.2-Double Membrane Vesicles (DMV)

HCV replication induces the remodeling of intracellular membranes and reveals cytoplasmic vesicular structures designated as the membranous web, containing multi-membrane vesicles, single-membrane vesicles or double-membrane vesicles (figure 39).
These latter membrane rearrangements, with an average diameter of 150nm (Romero-Brey et al., 2012), are thought to contain active replication complexes. Indeed, their appearance correlates with viral RNA replication and purified DMVs contain enzymatically-active viral replicase(Paul et al., 2013). Since the outer membrane of DMVs is often linked to the ER, it was confirmed that DMVs are derived from ER-membrane. However, some studies also suggest a role of Golgi fragmentation in HCV replication and membrane modeling (Hansen et al., 2017). In addition, in some cases DMVs are not connected to ER membrane and it is not really known which kind of DMVs contain the active replication
The precise topology of the viral replicase is not fully known. One possibility is represented in figure 40 with the viral replicase found inside the DMVs. This topology should require some proteins to transport HCV RNAs outside the DMVs and this could be mediated by some protein of the nuclear pore complex (Neufeldt et al., 2013).
The DMV are induced by the expression of the NS4B-NS5A precursor (Romero-Brey et al., 2015b), but their formation also require cellular factors. First, several proteins involved in lipid metabolism are required for the formation of DMVs as these structures are enriched with some categories of lipids. Indeed, NS5A is able to recruit and activate the PI4KIIIα kinase, hence allowing the concentration of its product phosphatidylinositol-4-phosphate (PI4P) at DMVs (Reiss et al., 2011) . PI4P is thought to facilitate the release of cholesterol from oxysterol-binding protein (OSBP) (Wang et al., 2014). Both PI4P and cholesterol are found enriched in the membrane of DMVs and seem important for their functionality, and therefore for HCV replication. Besides lipid

metabolism pathways, HCV also hijack autophagy for the formation of DMVs. Several recent studies showed a role of autophagy in viral replication (Sir et al., 2012) (Wang et al., 2017)and particularly in the formation of DMVs. Particularly, it was shown that the ATG5-ATG12-ATG16L1 complex is recruited to the membranous web and may contribute to the formation of DMVs (Fahmy & Labonte, 2017). Other evidence suggest a role of autophagy on the translation of the incoming RNA and the establishment of the initial replication (Dreux et al., 2009b, Guevin et al., 2010).
Importantly, assembly of HCV particles is thought to occur in close proximity to DMVs in order to allow the correct delivery of viral RNA to assembly sites.

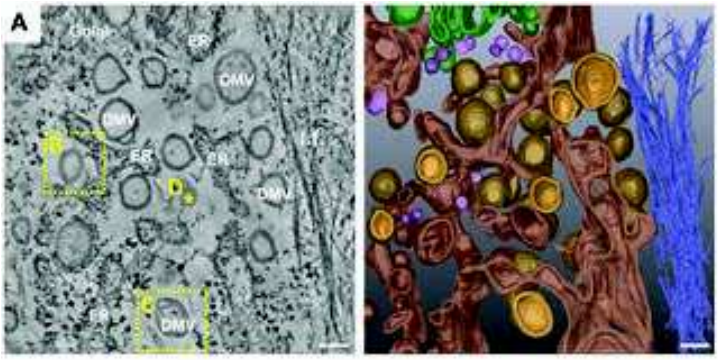

Figure 39: 3D architecture of membrane rearrangements induced 16 h after HCV infection. Left: slice of a dual axis tomogram showing the various membrane alterations. Right: 3D reconstruction of the complete tomogram. Some DMV are attached to ER membrane whereas some other are found without connection to other membranes. Adapted from (Romero-Brey et al., 2012)

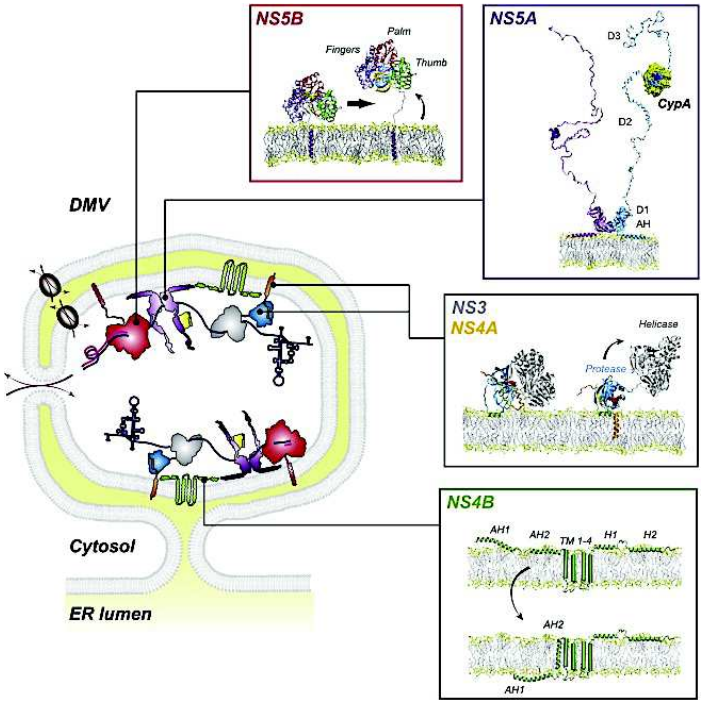

Figure 40: Model of an HCV-Induced Double-Membrane Vesicle (DMV) and Hypothetical 3D Structures of Membrane-Associated HCV Proteins. The DMV contan HCV non structural proteins and RNA and are sites of active RNA replication .Adapted from (Paul et al., 2014)

V.2- Mechanism of HCV assembly:viral factors

V.2.1- core/NS5A association and transfer of RNA

It was first described that the association of core and NS5A at the LD surface could be an important step for initiation of assembly, by allowing the transfer of viral RNA from replication complexes to virion assembly sites (Appel et al., 2008, Masaki et al., 2008, Miyanari et al., 2007). NS5A interacts with core through its DIII domain. In addition, it was also demonstrated that phospohorylation of NS5A could mediate the shift from replication to assembly (Tellinghuisen et al., 2008a). NS5A could be essential for the transfer of viral RNA from replication complexes to core complexes (Boson et al., 2017) (Berger et al., 2014), allowing the initiation of nucleocapsid formation.

The precise role of core localization on LD for assembly events remains controversial. Indeed, the levels of core accumulated on LDs seem to be inversely correlated with the efficiency of production of infectious particles (Appel et al., 2008, Boson et al., 2011, Gentzsch et al., 2013, Shavinskaya et al., 2007). This could reflect a transient localization of core on LDs before its transfer to ER membrane.

V.2.2- NS2 complexes: a plateform for assembly

Another complex that is important for HCV assembly is the NS2-E1E2 complex associated with p7. Indeed, it was demonstrated that p7/NS2 allows the transfer of the HCV glycoproteins to the virion assembly sites (Jirasko et al., 2010, Ma et al., 2011, Popescu et al., 2011, Shanmugam et al., 2015, Shanmugam & Yi, 2013) .

In addition, NS2 is able to interact with NS5A in a transient and weak manner (Jirasko et al., 2010, Ma et al., 2011, Popescu et al., 2011); yet, this interaction could allow the encountering of core and RNA with the glycoproteins, a key step for the initiation of assembly and envelopment of infectious particles. It is thought that the nucleocapsid formations occur concomitantly with its envelopment (Boson et al., 2017, Denolly et al., 2017).

NS2, key organizer of assembly, is also able to interact with NS3 and this protein was shown to be essential for assembly of the viral particles (Jones et al., 2011, Mousseau et al., 2011, Yan et al., 2017). Since mutations that impaired assembly were found in the helicase domain of NS3, it was supposed that NS3 helps assembly via its helicase domain, probably by allowing the unwinding of viral RNA. Yet, it was recently shown that NS3 could also mediate assembly, via its N-terminal domain (Yan et al., 2017).

NS4B also participates in virus assembly (Jones et al., 2009, Tanaka et al., 2013) likely by modulating viral genome encapsidation through its C-terminal extremity (Han et al., 2013).

V.2.3- Budding of particles

After the encountering of all the viral components, the particles bud from the ER membrane. However, the budding force is still unknown. One hypothesis is that the

E1E2 glycoproteins provid this force (Vieyres et al., 2013) since they are able to drive assembly of particles without nucleocapsids (Icard et al., 2009) and since mutations in these glycoproteins impair the envelopment of nuclecapsids (Steinmann et al., 2013).
The mechanisms of scission of HCV particles are still unknown since this event is difficult to observe at the ER membrane. Some studies suggested a role of p7, like for M2 for IAV (Lee et al., 2016). Conversely, ESCRT proteins may also be involved (see below).

V.3- Mechanism of HCV assembly: host factors

Besides the viral proteins, several host factors have been shown to be involved in the HCV assembly. Some of these factors are described in the next section.

V.3.1- Proteins involved in lipid metabolism

V.3.1.1- DGAT1

Diacylglycerol O-acyltransferase 1 (DGAT1) is a protein that catalyzes the conversion of diacylglycerol and fatty acyl CoA to triacylglycerol. This protein was shown to be involved in assembly, likely by facilitating the interaction of core and NS5A with LDs (figure 41) as suggested by the observation that DGAT1 interacts with both core and NS5A proteins in infected cells. Inhibition of DGAT1 activity does not affect the amounts of LDs, since DGAT2 can compensate the defect. However, active DGAT1 seems required for the localization of core at LDs (Camus et al., 2013, Herker et al., 2010) (figure 41).

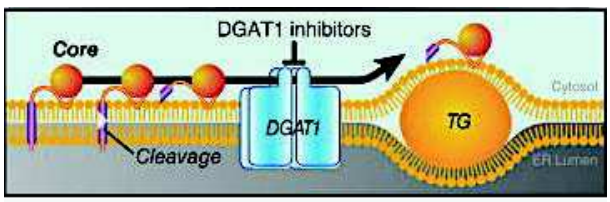

Figure 41: DGAT1 and HCV assembly. Core interacts in the ER with DGAT1 and localizes to lipid droplets in a DGAT1-dependent manner. Adapted from (Herker & Ott, 2012)

V.3.1.2- Proteins involved in VLDL assembly

V.3.1.2.1- VLDL assembly pathway

The assembly of VLDLs proceeds in two steps: cotranslational incorporation of the nascent apoB-100 polypeptide into a precursor lipoprotein particle through the rough

endoplasmic reticulum (ER) followed by the additional posttranslational lipidation via fusion with lipid droplets in the ER and/or the Golgi (Ledford et al., 2006).
Via multiple binding sites within its N-terminal region, apoB-100 interacts with the microsomal triglyceride-transfer protein (MTP) (Hussain et al., 1998, Segrest et al., 1999), which is an apoB-specific molecular chaperone essential for proper folding of apoB-100 during VLDL assembly/secretion (Sundaram & Yao, 2010). MTP is an ER-localized heterodimeric protein that is composed of a unique 97-kDa subunit complexed with the ubiquitous ER-folding enzyme protein disulfide isomerase (PDI) (Berriot-Varoqueaux et al., 2000, Gordon & Jamil, 2000). MTP mediates the transfer of both polar and neutral lipids from the ER membrane or from some other donor sites, such as the Golgi membrane, to nascent apoB during translation. This process called "lipidation", allows proper apoB folding and assembly of an spheric pre-VLDL particles (Berriot-Varoqueaux et al., 2000, Sundaram & Yao, 2010, Wu et al., 1996). Along with the availability of lipids, MTP activity is the most important factor regulating VLDL assembly and secretion (Gordon & Jamil, 2000) (figure 42).
The product of the first steps of VLDL assembly is a relatively small, dense particle, which can be either secreted from the cell as VLDL2 or further lipidated to form a mature, triglyceride- rich VLDL (VLDL1) (Stillemark-Billton et al., 2005). Although it is established that the first step of VLDL assembly occurs in the ER, the location of the additional step(s) during VLDL maturation remains controversial. Whereas a number of studies suggest that the ER is the final site of VLDL maturation (Kulinski et al., 2002, Yamaguchi et al., 2003), other studies implicate the Golgi complex as a second site of maturation (Bamberger & Lane, 1990, Gusarova et al., 2003, Gusarova et al., 2007).

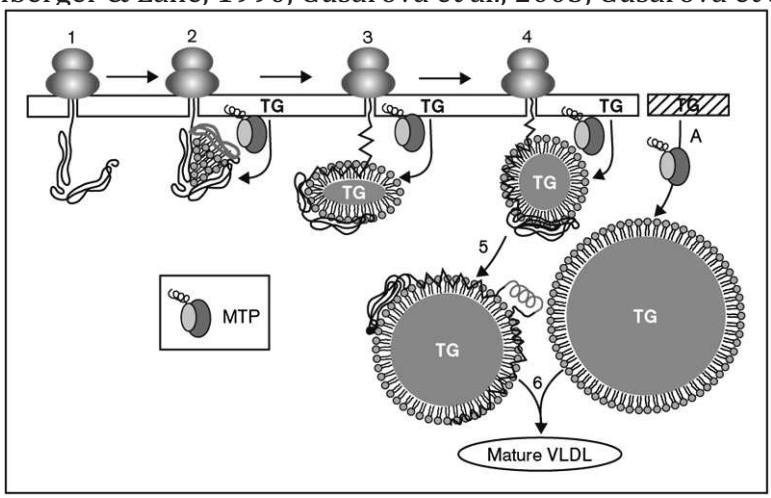

Figure 42: VLDL assembly. After co-translational folding of [alpha]$_1$ domain tertiary structure by apoB, an incomplete lipid binding cavity is formed (step 1). The cavity is lipid-filled by an interaction with microsomal triglyceride transfer protein (MTP) or with a more carboxyl-terminal domain of apoB, thereby allowing recruitment of a small amounts of phospholipids and triglycerids (TG; step 2). Further translocation of apoB concomitant with MTP-mediated lipid transfer forms a neutral lipid core (step 3) and conversion to a spheric emulsion particle (step 4). After release from the ribosome, these first step particles traffic to a distal compartment in the secretory pathway (step 5), where they interact with apoB-free second step precursors that are formed by MTP in the smooth ER (step A). The first and second step precursors fuse to form mature VLDLs (step 6) in a process that may be mediated by one or more [alpha]-helical fusiogenic peptides in apoB. (Shelness & Sellers, 2001).

V.3.1.2.2- VLDL assembly and HCV assembly

Due to the nature of HCV particles, several studies highlighted the role of proteins involved in VLDL assembly in HCV assembly. Indeed, inhibition of MTP results in a decrease of virion assembly (Gastaminza et al., 2008, Huang et al., 2007, Nahmias et al., 2008). In addition, long chain acyl-CoA synthetase 3 (ACSL3) (Yao & Ye, 2008), another enzyme involved in VLDL assembly, and hepatocyte nuclear factor 4α (HNF4α) (Li et al., 2014), a transcription factor that regulates the VLDL secretory pathway, were also shown to modulate the production of infectious particles. Cell death activator Cide-B, another protein involved in the lipidation of VLDL, was shown to be involved in assembly by allowing the interaction between apoE and NS5A (Cai et al., 2016).
Besides these proteins, apoE was found to be essential for the assembly of infectious viral particles (Da Costa et al., 2012, Hueging et al., 2014, Jiang & Luo, 2009). Interestingly, ectopic apoE expression is sufficient to restore the assembly of infectious particles in non-hepatic cell lines (Da Costa et al., 2012, Hueging et al., 2014), suggesting that the VLDL pathway itself might not be essential for the production of infectious particles. It was shown that apoE acts on assembly in a step following capsid envelopment (Hueging et al., 2014, Lee et al., 2014). Recent studies questioned the role of apoE in assembly as they demonstrated that amphipathic α-helices of several different apolipoproteins (Fukuhara et al., 2014) or amphipathic α-helices of NS1 of flavivirus or of Erns of pestivirus (Fukuhara et al., 2017) as well as amphipathic α-helices from some cellular peptides (e.g. Cathelidicin) (Puig-Basagoiti et al., 2016) are able to compensate the effect of KO of apoE and apoB in the assembly of infectious particles. These interesting studies highlight the fact that HCV requires amphipathic α-helices rather than apolipoproteins themselves to promote a crucial assembly event; alternatively, it might have evolved in order to hijacks this metabolic pathway for other purposes.
In conclusion, the available evidence suggests that virion assembly hijacks the VLDL assembly pathway; yet, the exact mechanistic details are missing.

V.3.2- Proteins involved in trafficking

V.3.2.1- ESCRT proteins

V.3.2.1.1- Mode of actions

The Endosomal Sorting Complexes Required for Transport (ESCRT) machinery is constituted of cytosolic proteins complexes, ESCRT-0, ESCRT-I, ESCRT-II, and ESCRT-III. These proteins allow membrane remodeling, inducing membrane bending, budding and scission away from the cytoplasm (reviewed in (Raiborg & Stenmark, 2009)). The ESCRT machinery is used for the delivery of ubiquitinated membrane proteins to

lysosomes. ESCRT-0 initiates the process by interacting with ubiquitin, allowing the concentration of ubiquitylated proteins. ESCRT-I and ESCRT-II are then recruited. They are all able to interact with ubiquitinated proteins and to induce the budding of the growing vesicles. ESCRT-III complex assembles transiently and is involved in budding reactions as well as recruitment of deubiquitinases. Finally, Vps4 is recruited by ESCRT-III, allowing membrane scission by forming two stacked hexameric rings with a central pore (figure 43).

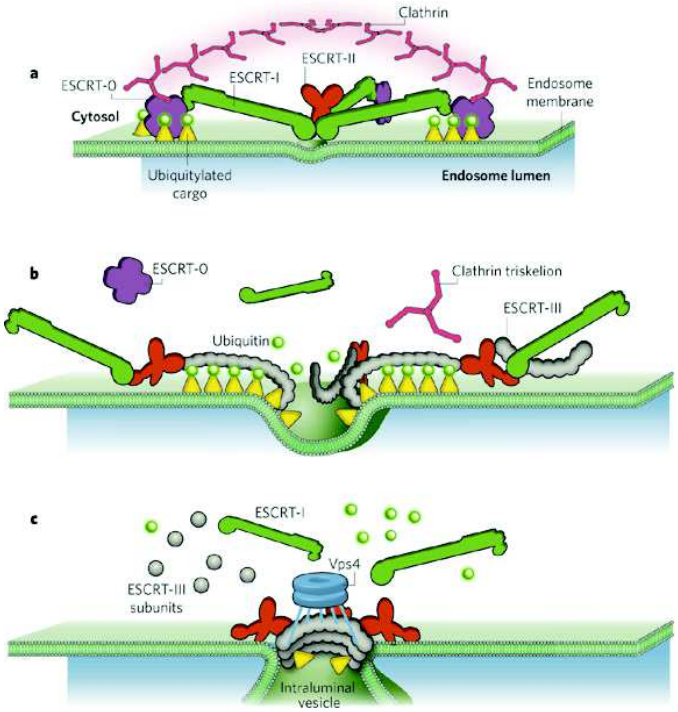

Figure 43: Mechanism of action of ESCRT proteins. **a**. Initial recognition of ubiquitylated cargo is mediated by ESCRT-0, which also serves to recruit ESCRT-I. The elongated ESCRT-I recruits ESCRT-II and may contribute to membrane involution. **b**. ESCRT-III complexes are recruited by binding to the two Vps25 subunits of ESCRT-II and form spiral-shaped filaments that gate cargo into invaginations that ESCRT-III filaments cause. During this process, cargo is deubiquitylated by DUBs that are recruited by ESCRT-II. **c.** As ESCRT-III filaments assemble into circular arrays, the membrane continues to invaginate. Vps4 enters the invagination to disassemble ESCRT-III filaments, ensuring that its subunits are recycled and that the filaments assemble only at the neck of the forming intraluminal vesicle. (Raiborg & Stenmark, 2009)

V.3.2.1.2- HCV assembly and ESCRT proteins

It is well characterized that HIV used a part of ESCRT complex for particles budding evidencing that viruses can hijacks basic cellular mechanisms. In the case of HCV, several studies reported the role of ESCRT pathway in the assembly of virions (Ariumi et al., 2011, Barouch-Bentov et al., 2016, Corless et al., 2010, Tamai et al., 2012). Recently, it was shown that Hrs, member of ESCRT-0 complex, is involved in HCV assembly by interacting with NS2 and NS5A and by regulating capsid envelopment (Barouch-Bentov et al., 2016). Despite the existence of some evidence suggesting a role of ESCRT proteins

in the budding and scission of the viral particles, several pieces of the puzzle are still missing.

V.3.2.2- Adaptor proteins

Adaptor proteins are proteins mediating the sorting of cargo proteins to specific compartments. Four adaptor proteins complexes have been described in mammalian cells, designated AP-1 through AP-4, each composed of 4 subunits. AP2M1 has been shown to be involved in the trafficking of proteins harboring a YXXΦ motif. It was shown that this protein is involved in the regulation of core localization around LDs, by interacting with YXXΦ motif of core and thus regulating the assembly of infectious particles (Neveu et al., 2012).

V.3.2.3- Rab GTPase proteins

Rab GTPases are master regulators of the vesicular transport between organelles. Rab proteins regulate the formation, transport, tethering, and fusion of transport vesicles as a general mechanism for regulating traffic between organelles. More than 50 Rab proteins have been identified, with various intracellular localization and functions. Rab proteins cycle between the cytosol and the membrane. In their GDP-bound form, they are inactive and inserted in membrane. In contrast when they are bound to GTP they are in active states and can interact with effector proteins, helping in trafficking (reviewed in (Hutagalung & Novick, 2011).
Rab32, normally found in mitochondria, was shown to be modulated by HCV: upon infection, the GTP-bound form becomes predominant and interacts with core, allowing its enrichment in some ER membrane domains (Pham et al., 2017). Rab18, normally found in Golgi and LDs, was also shown to regulate the trafficking of core and its recruitment around LDs, and, therefore, the assembly of infectious particles (Dansako et al., 2014).

VI- Secretion and maturation of viral particles

VI.1- Secretion pathway of infectious particles

The nature of the secretion pathway used by HCV is still poorly defined as this step of the life cycle is the least studied. HCV could either use some cellular pathways (such as the conventional secretory pathway) or create its own secretory pathway by perverting the role of several cellular proteins.

VI.1.1- Conventional secretion pathway

After their synthesis in the ER and maturation, secretory proteins traffic through the secretory pathway, a process that requires several transport vesicles. ER-derived vesicles are created by the COPII coat and carry cargos from the ER membrane to the Golgi acceptor membranes, via the ER Golgi intermediate compartment (ERGIC). The cargo will be selected due to specific signals that are recognized by cargo receptors. At the cis-Golgi membrane, these vesicles fuse, allowing the release of the cargo in the Golgi lumen. Proteins can be matured in the different stacks of the Golgi and finally reach the trans-golgi network. From there, these proteins can exit through different ways, such as clathrin-coated vesicles to reach endosomes, or via secretory storage granules (figure 44). Secretion of proteins is dependent on a gradient of pH and $[Ca^{2+}]$.
Interestingly, retrograde transport from Golgi to ER could also occur via COP-I vesicles. The equilibrium between COP-I and COP-II is essential for the neat transport of proteins outside the cells.

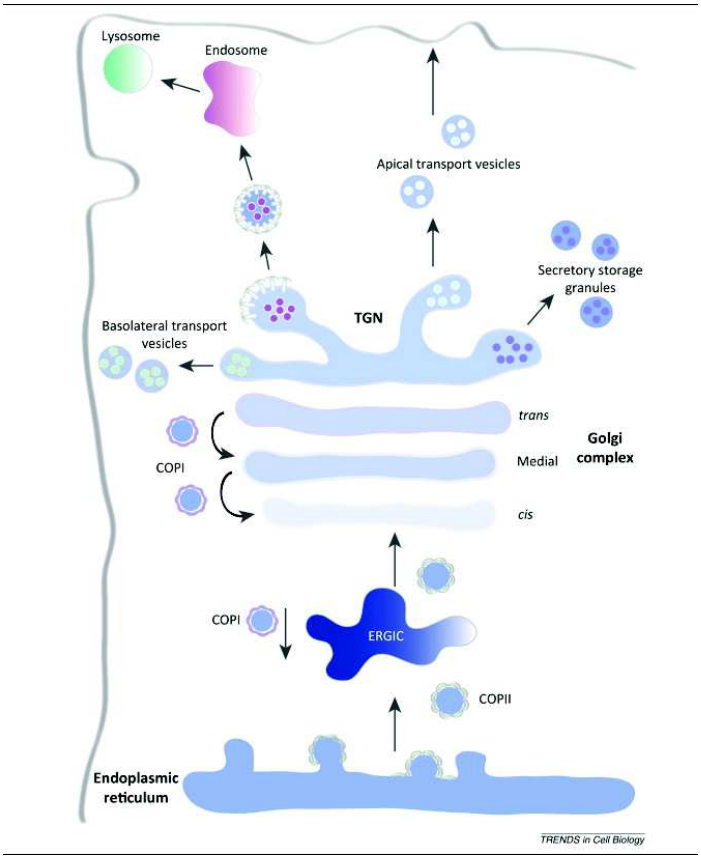

Figure 44: Conventional secretory pathway. Proteins containing a signal sequence are translocated across the endoplasmic reticulum (ER) membrane. After folding in the ER, proteins have two fates: either they become ER-resident proteins or leave the ER in coat protein complex II (COPII)-coated vesicles towards the Golgi apparatus via the ER Golgi intermediate compartment (ERGIC). After traversing the cis and medial Golgi compartments, proteins enter the trans-Golgi network (TGN), an important sorting station. Here proteins have to be sorted and packaged into transport carriers to reach their final destinations. Numerous TGN exit routes have been described: proteins packaged into clathrin-coated vesicles are transported to the endosomes, whereas constitutively secreted cargo or transmembrane proteins are transported towards the apical or basolateral plasma membrane. In specialized cells, proteins leave the TGN to be stored in secretory storage granules. These granules fuse with the plasma membrane primarily in response to an extracellular stimulus. Retrieval of ER proteins is carried out by COPI vesicles. (Kienzle & von Blume, 2014)

VI.1.2- Unconventional secretion pathway

Recently, the concept of unconventional secretion has emerged (reviewed in (Rabouille, 2017)). Indeed, some cytosolic proteins can reach the plasma membrane and be secreted via pores in the plasma membrane (such as for HIV TAT or IL-1β). Some proteins can also subvert some organelles for their secretion such as secretory autophagosomes or endosomes. Finally, some transmembrane proteins can reach the plasma membrane directly from the ER, bypassing the Golgi (figure 45).

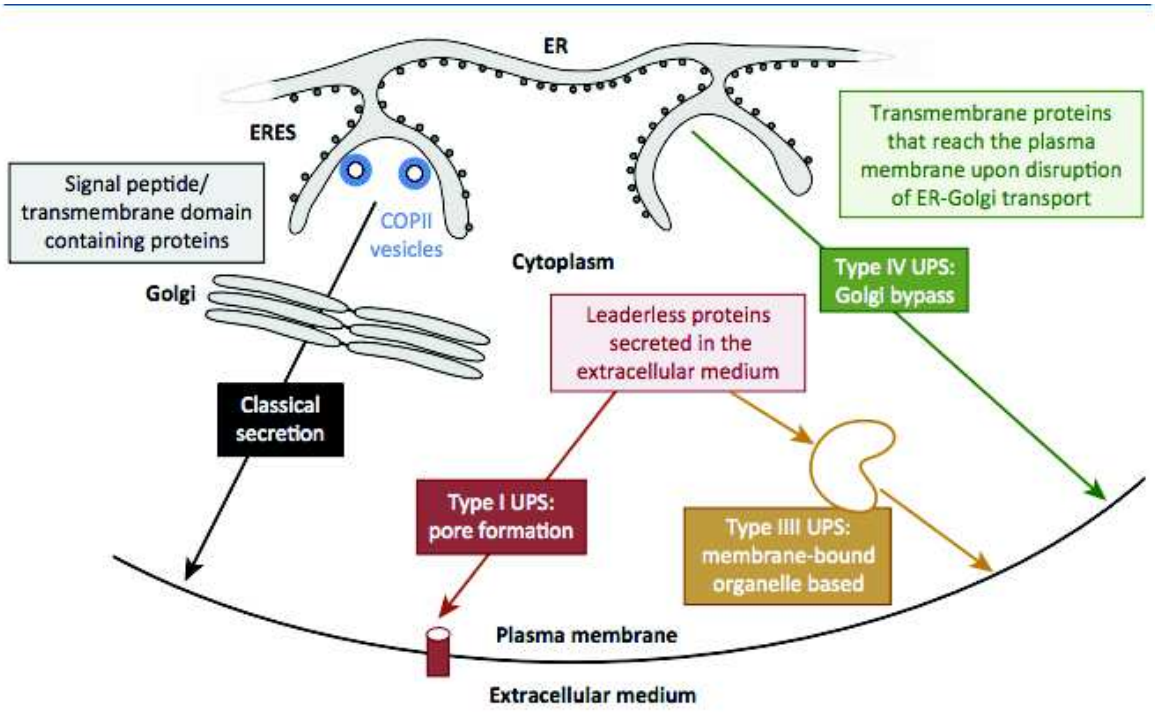

Figure 45: Schematic representation of the 3 types of unconventional secretory pathway. (Rabouille, 2017)

VI.1.3-HCV: Golgi or not Golgi?

VI.1.3.1- Arguments for the use of the Golgi apparatus

Because of the structure of viral particles, several studies proposed that HCV use the secretion pathway of VLDL for its own secretion. Indeed, it was shown that intracellular infectious particles have a higher density than extracellular ones, hence suggesting the acquisition of lipids in a post-ER compartment that could occur during their secretion along with the VLDLs (Gastaminza et al., 2008, Gastaminza et al., 2010). VLDL secretion occurs through the Golgi, using specialized transport vesicles (Tiwari & Siddiqi, 2012).
In addition, it was reported that Brefeldin A, a drug inhibiting the formation of COP-I vesicles and thus the secretion of proteins through a collapse of the Golgi, can inhibit HCV secretion, suggesting a secretion dependent on the Golgi apparatus or at least involving the COP-I vesicles (Coller et al., 2012, Feneant et al., 2015, Gastaminza et al., 2008).

Moreover, using a fluorescent-labeled viral particles, it was shown that HCV colocalizes with Golgi markers (Coller et al., 2012). Several factors linked with the conventional secretory pathway were shown to be involved in the regulation of secretion of infectious particles, such as Arf3, AP1M1,… (Coller et al., 2012) .

To conclude, several pieces of evidence suggest that HCV uses the conventional secretory pathway, or at least components of this pathway, for its own secretion.

VI.1.3.2- Arguments against the use of the Golgi apparatus

Monensin, a drug that inhibits the traffic across the Golgi, was found to be inefficient in blocking the secretion of infectious particles (Feneant et al., 2015, Mankouri et al., 2016). This drug acts as an ionophore by exchanging Na^+ by H^+ and was shown to affect the secretion of apoE (Mankouri et al., 2016), suggesting an alternative secretion route to the VLDL pathway.
Besides, it was shown that glycans attached to the glycoproteins remain mainly non-matured at their surface of glycoproteins (Vieyres et al., 2010). This could be due either to a masking of these glycans precluding their maturation by glycosidases or to a modified Golgi or a Golgi by-pass. Indeed, the maturation of glycans is a process that occurs in the lumen of the Golgi and is very sensitive to ion homeostasis.
Finally, it was shown that HCV induces morphological changes of the Golgi (Hansen et al., 2017), arguing against fully functional organelles. Specifically, NS2 mediates alteration of the trans Golgi network (TGN)(Mankouri et al., 2016).

To conclude, these evidences argue for the use of a modified Golgi or a by-pass of the Golgi apparatus for the secretion of HCV

VI.1.4- Model for HCV secretion pathway after the Golgi apparatus

The group of Hildt identified several factors involved in secretion of infectious particles, allowing them to propose a new model of HCV secretion linked to an exosome-dependent pathway. They showed that an inhibitor of intracellular cholesterol trafficking impairs HCV release as well as functionality of MVBs (Elgner et al., 2016). They also identified that HCV down-regulates α-taxilin, which is a protein interfering with vesicular trafficking and fusion of MVB with plasma membrane (Elgner et al., 2016). HCV also induces a longer half-life of syntaxin 4, a SNARE-protein (Ren et al., 2017). The SNARE (soluble N-ethylmaleimidesensitive factor attachment protein receptor) are proteins complexes that allow the fusion of membranes and participates in vesicles trafficking. Supporting the hypothesis of a trafficking via an exosome-dependent pathway, it was also shown by others that Rab GTPase and protein adaptors involved in endocytic pathway are essential for release of infectious particles (Mankouri et al., 2016, Ostrowski et al., 2010). The Rab7 adaptor protein, called RILP, was also shown to be involved in the regulation of HCV secretion and more precisely the switch from assembly to secretion (Wozniak et al., 2010). Indeed HCV modifies cellular trafficking by cleaving RILP, which redirects Rab7-containing vesicles to a kinesin-dependent trafficking mode promoting virion secretion. To complement this, adaptor protein-1 as well as clathrin are also involved in viral particles egress (Benedicto et al., 2015).
Finally, autophagy was also shown to be involved in the secretion of HCV particles as well as secretion of exosomes (Medvedev et al., 2017, Ren et al., 2017, Shrivastava et al.,

2015). However, although these results seem to indicate that HCV uses vesicles derived from autophagosome and endosomes for its secretion, it is more difficult to imagine how the virus could hijacks exosomes because of their membrane topology since exosomes are able to incorporate cytosolic elements whereas the infectious particles are found in the lumen of the ER.

VI.2- Cell-cell transmission

Besides virus transmission through the cell supernatant, several evidences reported the importance of cell-cell transmission. Indeed in the presence of an excess of neutralizing antibodies, infection of naïve cells still occurs (Timpe et al., 2008). The mechanisms of underlying this mode of infection, constituting an efficient strategy to escape from the host neutralizing response, remains poorly defined even if several studies focused on this step, as indicated below.

The role of apoE is still debated since some studies reported the importance of apoE (Feneant et al., 2015, Gondar et al., 2015, Hueging et al., 2014) whereas other mentioned that the VLDL pathway is not involved in cell-cell spread (Barretto & Uprichard, 2014) In contrast, it was shown that NPC1L1 is involved in this pathway as well as EGFR, SR-BI CLDN1, OCLN and CD81 (Brimacombe et al., 2011, Catanese et al., 2013, Fofana et al., 2013, Lupberger et al., 2011, Witteveldt et al., 2009, Zahid et al., 2013, Zona et al., 2013) . This process was shown to be dependent of pH (Feneant et al., 2015).

Regarding the viral proteins, a report suggested a role of p7 in this pathway (Meredith et al., 2013). In addition, HVRI of E2 was also shown to influence the cell-cell spread (Feneant et al., 2015). One hypothesis could be that the conformation of E2 could modulate the transmission of viral infection either in cell-cell spread or in cell- free infection.

VI.3- Viral particles maturation

Several evidences suggest that there are some differences between infectious intracellular and extracellular HCV particles, suggesting that maturation could occur during the egress or outside the cells.

Indeed, intracellular particles are pH sensitive whereas extracellular particles could become resistant depending on their genotype (Atkins et al., 2014, Wozniak et al., 2010). As above discussed, it was suggested that p7 is involved in this maturation by protecting the glycoproteins from premature fusion similarly as M2 of influenza virus. This could be a result of a change in glycoproteins conformation or of a masking of the glycoproteins by lipids.

In addition, the density of intracellular particles is found to be higher than that of extracellular particles (Gastaminza et al., 2008), indicating again that a maturation occur during virion egress or outside the cells as will be discussed in the Results section.

RESULTS

I-Context and Aims of the Thesis

The assembly of infectious virus particles is a complex process that requires a perfect coordination of all the factors involved as well as a perfect timing. Viruses have set up several smart, step-wise mechanisms to allow the achievement of this process. Its complexity is partly due to the fact that several steps are usually necessary to allow the formation of infectious particles. Indeed, in the case of HCV, core proteins have to interact with the viral genome, which is generated in the replication complexes. The nucleocapsids in formation further need to be enveloped within a lipid bilayer that incorporates the two glycoproteins E1 and E2. After nucleocapsid envelopment, a scission between the viral and cell membrane is required to allow the completion of the particle and its release. As mentioned in the Introduction, HCV particles have the unique particularity to be lipidated, meaning that in addition to the phospholipids and cholesterol usually found in membrane of enveloped viruses, they incorporate both cholesterol esters and triglycerides and apolipoproteins, with a composition close to that of lipoproteins. This particular conformation indicates that HCV particles have to undergo a step of maturation that promotes this specific lipidation.

Besides the core, E1 and E2 structural proteins, almost all the non-structural (NS) proteins encoded by the HCV genome are required to mediate functional assembly. Particularly the p7 and NS2 proteins act as conductors and are responsible for organizing the assembly process. NS5A, another viral NS protein, also plays a key role in assembly. Indeed, it emerges that NS5A is a key player in the switch between replication and assembly, and in the transfer of the synthesized viral genome from the replication complex to the virion assembly sites, as it interacts with both the viral RNA and the core protein. On the other side, NS2 acts as a platform that interact with the E1E2 glycoproteins and with NS5A, which is likely associated with core and RNA. This may allow the regulation of the encountering of the nucleocapsid and the glycoproteins, which initiates virion morphogenesis. Finally, p7 regulates the formation of such “NS2-based platforms” but also modulates the envelopment of the particles. In addition, it is well described that within infected cells, p7 exists also as an E2p7 precursor; yet, the precise function(s) of this precursor remains elusive.

HCV particle assembly occurs at a precise area within infected cells. Indeed, several studies indicate that the cytosolic lipid droplets play a key role in this event, since core and NS5A proteins can localize at their surface. The current model of HCV assembly (see figure 38 in Introduction) proposes that it occurs at an ER membrane-derived site close to replication complex(s) and lipid droplet(s). Although several studies has provided fascinating details on the process of virion assembly, several pieces of the puzzle are still missing to have a full view of the assembly process.

Maturation of HCV particles, through their lipidation, is a central feature of HCV biology; yet, it remains not completely understood. Particularly, the mechanisms but also the location and time of the lipidation of viral particles are poorly defined. Indeed, the *in vitro* models currently used do not allow the reconstitution of same density profile of HCV particle compared to those isolated in sera from infected patients. However, the discovery of these events is essential since lipidation plays a key role in the escape from neutralizing antibodies as well as in shaping the structure and infectivity of viral particles.

In this work, we aimed at better understanding the assembly from the encountering of the viral proteins at assembly sites until the acquisition of lipids.

First, I contributed to a study of the lab led by Bertrand Boson in which we sought to investigate by confocal microscopy the clustering of HCV assembly components and its link with functional assembly of viral particles. To do that, we took advantage of a direct antiviral agent that targets NS5A and that inhibits assembly, which helped us to discover new insights on assembly. This first study allowed to better define the intracellular site of assembly but also to characterize the mode of action of this drug.

Second, we sought to investigate the role of the E2p7 precursor. Indeed, since the amino-terminal extremity of p7 was previously shown to be essential for assembly, we hypothesized that the regulation of the cleavage between E2 and p7 may control the unmasking of a specific, amino-terminal function of p7 in assembly. Specifically, through biochemical, imaging and functional analysis of a series of mutant viruses with modified E2-p7 junction as well as through p7 transcomplementation assays, we wanted to explore how the retarded cleavage between E2 and p7 could regulate their functions associated to virion assembly and/or perturbation of cellular membrane processes. In addition, we aimed at investigating if p7 could share specific functions with viroporins from alternative viruses, such as the reduction of the rate of secretion along the cell secretory pathway.

Third and finally, we sought to better characterize the step of lipidation of HCV particles and we investigated which part of the particle modulates the extent of lipidation and if/how lipidation occurs within the infected liver or in the extracellular milieu. To do that, we compared the density of profiles of viral particles obtained from producer cells cultured or treated in different conditions, particularly by using sera with different lipoprotein compositions. We investigated the viral regulator of lipidation of particles by comparing strains and genetic swaps between different HCV sequences.

Importantly, for all these studies, we compared several HCV strains exhibiting different efficiencies of assembly and/or maturation, which greatly helped to better understand how the sequences of HCV adapt to maintain a global fitness.

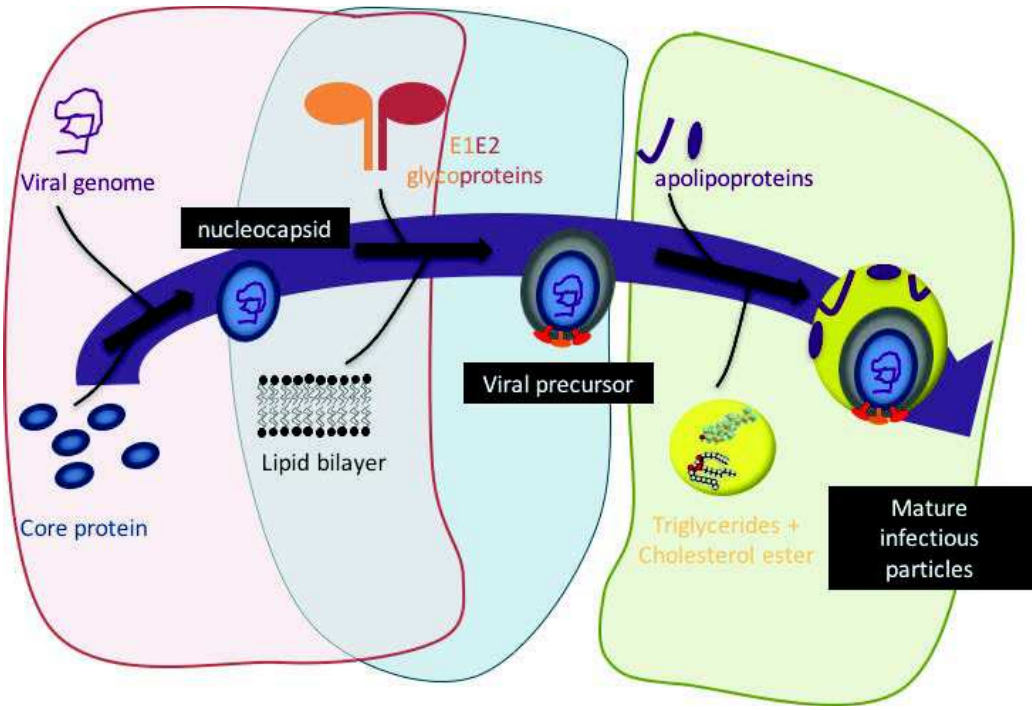

Figure 46: Summary of the steps from HCV particles assembly to maturation studied in this manuscript. The area investigated in the first chapter, *i.e.*, the clustering of virion assembly components, is represented in red; the area covered in the second chapter, *i.e.,* envelopment and secretion of the particles is shown in blue whereas the area investigated in the third chapter, *i.e.,* maturation and lipidation of HCV virions is represented in green.

II-Summary of the findings

The **first chapter in the Result section** of this manuscript focuses on the first steps of HCV assembly, which consists in the clustering of all actors of HCV assembly, structural or non-structural. I have participated to this study led by Bertrand Boson.

1- Connection between replication complexes and assembly components close to lipid droplets

Using imaging, biochemical and functional studies, we further investigated the model previously proposed suggesting that assembly sites are closely associated with lipid droplet and replication complexes. First, using time course analysis, we showed accumulation of core punctae at ER membrane. By comparing two HCV strains with a differential efficiency of assembly, we found a relation between the infectivity levels and the presence of E2/core/NS4B as well as E2/core/NS5A clustered structures. We also detected the presence of positive strand HCV RNAs in structures containing both core and NS5A or NS4B.

2- Daclatasvir, a NS5A inhibitor, induces the clustering of HCV assembly components by preventing the transfer of viral genome to assembly sites

Upon short time (6h) treatment of infected cells with the NS5A inhibitor, daclatasvir, we found an enlargement of core-dotted structures containing E2 and NS5A or NS4B, a shown by confocal microscopy. In addition, we found a reduced colocalization of core with positive strand of viral RNA in a manner correlating with a decreased production of infectious particles. We therefore proposed that the high clustering levels of both structural and non-structural proteins represent assembly platform that are inactive for promoting virion assembly due to the lack of transfer of the HCV genome from replication complexes to nucleocapsid formation sites.

***Publication**: Boson B, Denolly S, Turlure F, Chamot C, Dreux M, Cosset F-L (2017) Daclatasvir Prevents Hepatitis C Virus Infectivity by Blocking Transfer of the Viral Genome to Assembly Sites. Gastroenterology 152: 895-907.e14*

The **second chapter of this manuscript** focuses on the role of p7 in HCV assembly and, more particularly, in later steps of assembly, consisting in the transfer of viral nucleocapsids to virion envelopment site and the completion of their envelopment.

3- Free p7 slows down the cell secretory pathway

Using biochemical assays, we demonstrated that free p7, *i.e.*, not associated in the E2p7 precursor, can slow down the cell secretory pathway in a dose-dependent manner. More particularly we showed that this induces the retention of HCV glycoprotein in the ER and increasing the efficiency of assembly.

4- Processing of E2p7 precursor unmasks a novel p7 function that regulates the encountering of the nucleocapsid with glycoproteins, the levels of secretion of viral particles types, and their specific infectivity

By studying several HCV mutants that accelerate the E2p7 processing, we discovered a new function of the amino-terminal extremity of p7. Our imaging data demonstrated that p7 N-terminus could be exposed to the cytosol, which could modulate the encountering of NS5A and NS2 and thus, the encountering of the nucleocapsid, associated with NS5A, with the E1E2 glycoproteins, associated with NS2. In addition, we showed that this part of p7 regulates the level of secretion of HCV particles types, namely subviral particles, non-infectious particles as well as infectious particles by regulating the quality of envelopment and thus the specific infectivity of the latter particles.

***Publication**: Denolly S, Mialon C, Bourlet T, Amirache F, Penin F, Lindenbach B, Boson B, Cosset F-L (2017) The amino-terminus of the hepatitis C virus (HCV) p7 viroporin and its cleavage from glycoprotein E2-p7 precursor determine specific infectivity and secretion levels of HCV particle types. PLoS Pathog 13: e1006774*

The **last chapter** focuses on the lipidation of infectious particles and more particularly the viral factor and host factors that modulate the quality of lipidation.

5- Lipidation of infectious particles could occur in the extracellular medium and is regulated by the HVRI sequence of E2

Using different HCVcc culture conditions, we showed that the association of viral particles with neutral lipids could occur in the extracellular milieu, depending of its lipid and lipoprotein content. In addition, we showed that short time incubation of 2-6h of HCVcc particles produced in serum-free medium with human serum is sufficient to induce a low-density profile to these particles, close to that generally observed in HCV-infected patients' sera. These results indicated that the acquisition of lipids and the shift to low-density particles could occur after their release from infected cells or, alternatively, at a post-assembly level. Moreover, by comparing two strains and using swap mutants, we demonstrated that hypervariable region I of E2 primarily influences the level of lipidation of particles.

Publication: ***Denolly, S,*** *Granier C, Fontaine N, Pozzetto B, Bourlet T, Guérin M, and Cosset F-L (2018) A serum protein factor mediates lipid acquisition by HCV particles in the extracellular milieu. In preparation.*

III- Daclatasvir Prevents Hepatitis C Virus Infectivity by Blocking Transfer of the Viral Genome to Assembly Sites

Bertrand Boson, Solène Denolly, Fanny Turlure, Christophe Chamot, Marlène Dreux, François-Loïc Cosset

Gastroenterology 2017

Gastroenterology 2017;152:895–907

Daclatasvir Prevents Hepatitis C Virus Infectivity by Blocking Transfer of the Viral Genome to Assembly Sites

Bertrand Boson,[1] Solène Denolly,[1] Fanny Turlure,[1] Christophe Chamot,[2] Marlène Dreux,[1] and François-Loïc Cosset[1]

[1]CIRI - International Center for Infectiology Research, Team EVIR, Inserm, U1111, Université Claude Bernard Lyon 1, CNRS, UMR5308, Ecole Normale Supérieure de Lyon, Univ Lyon, F-69007, Lyon, France; and [2]Plateau Technique Imagerie/Microcopie, Lyon Bio Image, SFR-BioSciences, ENS de Lyon, Inserm US8, CNRS UMS3444, UCBL, France

BACKGROUND & AIMS: Daclatasvir is a direct-acting antiviral agent and potent inhibitor of NS5A, which is involved in replication of the hepatitis C virus (HCV) genome, presumably via membranous web shaping, and assembly of new virions, likely via transfer of the HCV RNA genome to viral particle assembly sites. Daclatasvir inhibits the formation of new membranous web structures and, ultimately, of replication complex vesicles, but also inhibits an early assembly step. We investigated the relationship between daclatasvir-induced clustering of HCV proteins, intracellular localization of viral RNAs, and inhibition of viral particle assembly. **METHODS:** Cell-culture–derived HCV particles were produced from Huh7.5 hepatocarcinoma cells in presence of daclatasvir for short time periods. Infectivity and production of physical particles were quantified and producer cells were subjected to subcellular fractionation. Intracellular colocalization between core, E2, NS5A, NS4B proteins, and viral RNAs was quantitatively analyzed by confocal microscopy and by structured illumination microscopy. **RESULTS:** Short exposure of HCV-infected cells to daclatasvir reduced viral assembly and induced clustering of structural proteins with non-structural HCV proteins, including core, E2, NS4B, and NS5A. These clustered structures appeared to be inactive assembly platforms, likely owing to loss of functional connection with replication complexes. Daclatasvir greatly reduced delivery of viral genomes to these core clusters without altering HCV RNA colocalization with NS5A. In contrast, daclatasvir neither induced clustered structures nor inhibited HCV assembly in cells infected with a daclatasvir-resistant mutant (NS5A-Y93H), indicating that daclatasvir targets a mutual, specific function of NS5A inhibiting both processes. **CONCLUSIONS:** In addition to inhibiting replication complex biogenesis, daclatasvir prevents viral assembly by blocking transfer of the viral genome to assembly sites. This leads to clustering of HCV proteins because viral particles and replication complex vesicles cannot form or egress. This dual mode of action of daclatasvir could explain its efficacy in blocking HCV replication in cultured cells and in treatment of patients with HCV infection.

Keywords: Chronic Hepatitis C; Direct-Acting Antiviral Agent; DAA.

Hepatitis C virus (HCV) infection is a leading cause of chronic liver diseases worldwide. With 180 million people persistently infected, chronic HCV infection, which induces end-stage liver diseases such as liver cirrhosis and hepatocellular carcinoma, presents a public health problem of high socioeconomic impact. No protective vaccine exists against HCV. However, the development of direct-acting antivirals targeting different proteins and functions in HCV life cycle has dramatically changed the treatment options for chronic hepatitis C, leading to new hopes to cure HCV.

HCV has a positive-sense single-strand RNA (RNA[+]) genome encoding viral proteins, including an assembly module (C–non-structural [NS] 2) encompassing the capsid protein (core); E1 and E2 surface glycoproteins that are incorporated in viral particles; the p7 viroporin and NS2 protein that support virion assembly; and a replication module encompassing the NS proteins NS3, NS4A, NS4B, NS5A, and NS5B, which are sufficient to support viral RNA replication and also contribute to virion formation through an unclear process.

The recent development of direct-acting antiviral has benefited greatly from discoveries in HCV molecular virology and host–virus interactions.[1] The primary targets of direct-acting antiviral[2] include the serine protease activity of NS3/NS4A, the multifunctional RNA-binding phosphoprotein NS5A, and the RNA-dependent RNA polymerase NS5B. Daclatasvir (DCV) and DCV-related molecules were discovered through screening of compounds inhibiting HCV subgenomic replicons.[3] In addition to being effective inhibitors of HCV replication, with 50% effective concentration values in the pM range, recent studies have reported that DCV acts on a distinct stage of replication, namely viral particle assembly.[4–6] Exposure of cell-culture–derived HCV infected cells to DCV for short time periods decreased production of infectious particles before decay of intracellular HCV RNA and polyprotein levels.

Although DCV's mode of action is unclear, it specifically targets NS5A,[3,7] particularly its domain I (DI), which has functions associated with genome replication,[8] in line with identified DCV-resistant mutations in DI (eg, L31 and Y93).[3]

Abbreviations used in this paper: **CHX, cycloheximide; DCV, daclatasvir; DI, domain I; DMV, double membrane vesicle; ER, endoplasmic reticulum; HCV, hepatitis C virus; LD, lipid droplet; MOI, multiplicity of infection; NS, non-structural protein; PBS, phosphate-buffered saline; RC, replication complex; SIM, structured illumination microscopy.**

Most current article

0016-5085/$36.00
http://dx.doi.org/10.1053/j.gastro.2016.11.047

Importantly, DCV inhibits formation of double-membrane vesicles (DMVs) that contain the HCV RNA replication complex (RC)[6,9] and are induced by non-structural proteins, particularly NS4B and NS5A.[10,11] In addition, other studies reported that DCV or DCV-related compounds decrease mobility,[12] intracellular redistribution,[13,14] and/or clustering[5,12,15] of NS5A. Despite these remarkable findings, there is no clear consensus on the role, location, and kinetics of these events, possibly because of differences in experimental conditions. NS5A is an HCV RNA-binding protein[16,17] that mediates HCV RNA transfer to viral particles,[18] so it seems possible that altered NS5A intracellular localization and/or trafficking could prevent assembly of infectious particles.

We investigated the relationship between DCV-induced clustering of HCV proteins and inhibition of viral particle assembly. We studied the intracellular localization of HCV assembly and RC proteins along with HCV RNA(+) and RNA(−) species within HCV-infected cells at early time points after DCV exposure and compared these events with the production of infectious particles. We show that in addition to inhibiting DMV biogenesis, DCV prevents HCV assembly by blocking the transfer of viral genomes to virion assembly proteins. This leads to clustering of HCV proteins, likely because viral particles and RC vesicles cannot form and/or egress from the endoplasmic reticulum (ER) membranes. This dual mode of action of DCV could account for its extremely high potency in cell culture and, most likely, in patients.

Materials and Methods

Cell Culture and Reagents

Huh7.5 cells were grown in Dulbecco's modified minimal essential medium (Invitrogen, Cergy-Pontoise, France) supplemented with 100 U/mL penicillin, 100 μg/mL streptomycin, and 10% fetal bovine serum.

Expression Constructs

pFK-JFH1wt_dg, pFK-JFH1/J6/C-846_dg and pFK-Jc1-Y93H_dg plasmids[6,19] were kind gifts from R. Bartenschlager.

Cell-Culture–Derived Hepatitis C Virus Production and Titration

Cell-culture–derived HCV production procedures were described previously.[20] Supernatants infectivity titers were determined as focus-forming units per milliliter. Serial dilutions of supernatants were used to infect Huh7.5 cells, focus-forming units were determined 3 days post-infection by counting NS5A-immunostained foci.

Immunofluorescence and Confocal Microscopy Imaging

Huh7.5 cells grown on uncoated 14-mm-diameter glass coverslips were infected at multiplicity of infection (MOI) of 0.2. At indicated times post-infection, cells were washed with phosphate-buffered saline (PBS), fixed with 3% paraformaldehyde in PBS for 15 minutes, quenched with 50 mM NH_4Cl, and permeabilized with 0.1% Triton X-100 for 7 minutes. Fixed cells were then incubated for 1 hour with primary antibodies in 1% bovine serum albumin/PBS, washed and stained for 1 hour with the corresponding fluorescent Alexa-conjugated secondary antibody (Alexa-488, Alexa-555, and Alexa-647, Molecular Probes Europe BV, Leiden, The Netherlands) in 1% bovine serum albumin/PBS. Lipid droplets (LDs) were stained with 10 μg/mL Bodipy 493/503 (Molecular Probes) according to the manufacturer's instructions. Cells were washed 3 times with PBS, stained for nuclei with Hoechst (Molecular Probes) for 5 minutes when stated, washed, and mounted in Mowiol (Fluka, Buchs, Switzerland) before image acquisition with LSM-510 or LSM-710 confocal microscopes.

Combined Detection of Hepatitis C Virus RNA by Fluorescent In Situ Hybridization and Viral Proteins

Viral proteins were first immunostained as described. After a post-fixation step with 3% paraformaldehyde for 15 minutes and 3 washes with PBS, HCV RNA(+), and RNA(−) strands were detected using probe sets that target regions between nucleotide positions 3733-4870 and 4904–5911, respectively, in the JFH1 genome using QuantiGene ViewRNA ISH Cell Assay kit (Panomics/Affymetrix, Santa Clara, CA) according to the manufacturer's instructions, except for the protease digestion step that was omitted. Omission of protease digestion step did not affect detection of HCV RNA(+) or RNA(−) foci (data not shown). Nuclei staining, slide mounting, and acquisition were performed as described.

Structured Illumination Microscopy

Huh7.5 cells were grown on high precision cover glasses and infected (MOI = 0.2). At 72 hours post-infection, cells were fixed with 3% paraformaldehyde and stained as described. Cells were then mounted in Fluoromount-G (Southern Biotech, Birmingham, AL) before image acquisition with Elyra PS-1 microscope (Zeiss, Oberkochen, Germany). Images were reconstructed using the Zen 2012 Black software (Zeiss).

Image Analysis and Quantifications

Images were analyzed with the ImageJ software (imagj.nih.gov). For quantifications of structures, colocalized pixels were extracted with the ColocalizeRGB plugin with auto-thresholding and a pixel ratio between paired channels set to 50%. They were then segmented with the Watershed algorithm and quantified with the Analyze Particles function of ImageJ. Only structures with size >0.02 μm^2, which corresponds to half of the resolution limit of confocal laser scanning microscopy, were recorded. For quantification of structures apposed at the edge of LDs, an ImageJ macro was developed (for details, see Supplementary Results) to search for variation of max intensity in the neighborhood of each LD as an indicator of proximity. Structures distant from LDs by >3 pixels (approximately 205–207 nm) were considered as non-apposed at the edge of LDs. When stated, the Pearson's correlation coefficients were calculated by using the JACoP plugin.

Statistical Analysis

Significance values were calculated by applying the 2-tailed, unpaired Mann–Whitney test for image analyses and the paired t test for the quantification of viral RNA, core protein,

and infection assays, using the GraphPad Prism 6 software (GraphPad Software, La Jolla, CA). P values $<.05$ were considered statistically significant and the following denotations were used: $^{****}P \leq .0001$; $^{***}P \leq .001$; $^{**}P \leq .01$; $^{*}P \leq .05$; ns (not significant) $P > .05$.

Results

An NS5A Inhibitor Preventing Viral Assembly Induces Co-Clustering of Structural and Non-Structural Proteins

To understand the impact of DCV on viral particle assembly, first we confirmed and extended previous studies[4,5] indicating that, unlike the DCV-resistant NS5A-mutant Jc1-Y93H virus,[6] a 6-hour-long treatment with 1 nM DCV had no effect on intracellular HCV RNA (Supplementary Figure 1*A, left panels*) and core protein (Supplementary Figure 1*A, right panel*) levels in cells infected with Jc1 virus. In contrast, a longer treatment (24 hours) reduced Jc1 intracellular RNAs by >10-fold, in accordance with these former reports. As reported previously,[4,5] inhibition of infectivity was detectable from 2 hours after the initiation of DCV treatment (Supplementary Figure 2*A* and *B*). Upon a 6-hour-long treatment, the levels of both intracellular and extracellular infectious particles were reduced by approximately 13-fold and 4-fold, respectively, whereas Jc1-Y93H virus infectivity was not affected (Supplementary Figures 1*B* and *2A* and *B*). Finally, we found that DCV inhibited the production of physical particles (Supplementary Figure 1*C*), as judged by the inhibition of both secreted viral RNAs and core protein from infected cells. Altogether, these results indicated that the decrease of viral production via short-time DCV treatment is due to inhibition of viral assembly rather than egress of particles, whereas longer treatments inhibit both assembly and replication.

Because DCV alters NS5A intracellular distribution[5,12–15] and core colocalizes with several other HCV proteins in Jc1-infected cells, including E2, NS2, NS3, NS4B, and NS5A (Supplementary Figure 3), we next wondered whether DCV inhibits viral assembly by altering the association of structural proteins with non-structural proteins from RCs. We investigated by confocal microscopy the effect of short-time DCV treatments on HCV proteins that mark either component of viral particles[20]—core and E2 or RCs[10,21]—that is, NS5A (Figure 1) and NS4B (Figure 2). Importantly, punctate

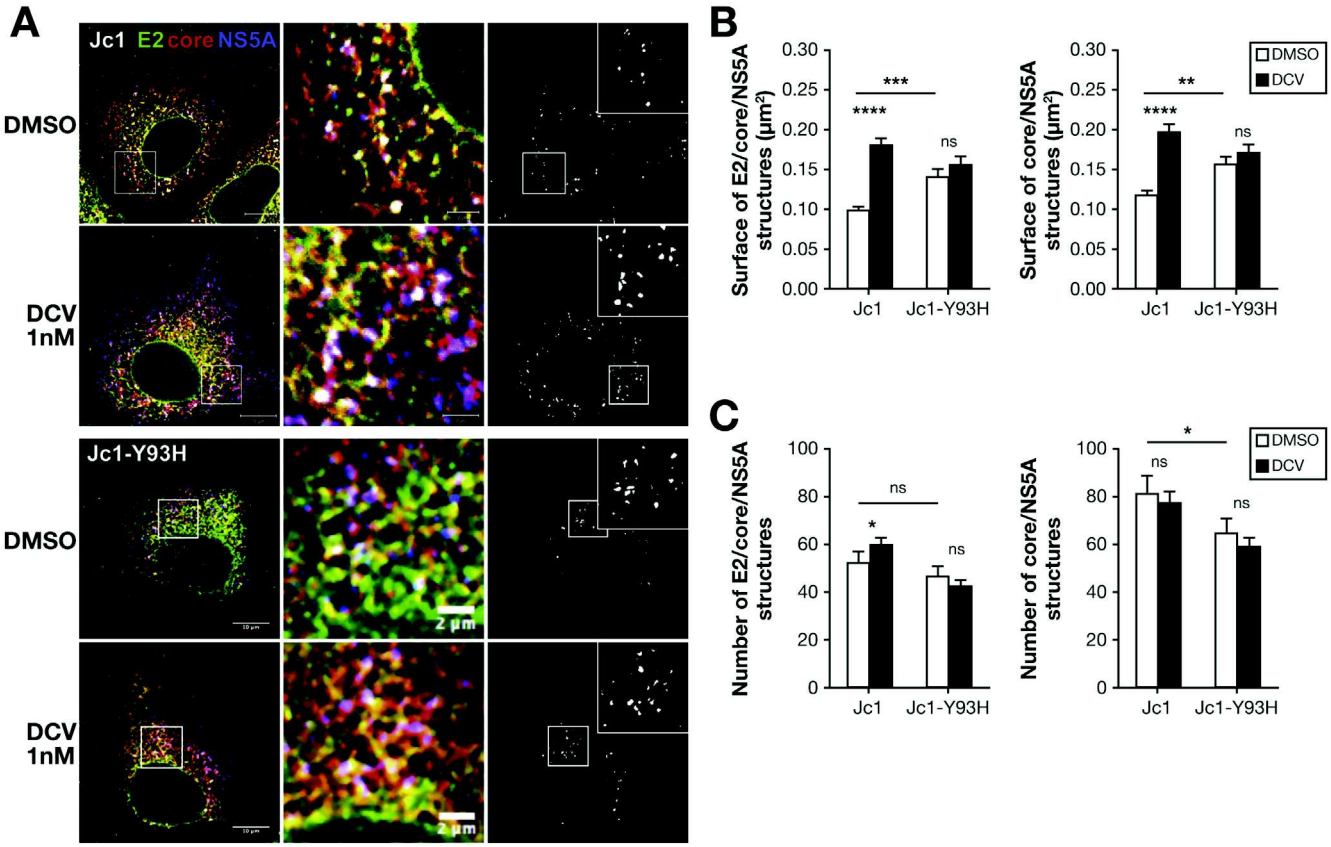

Figure 1. DCV induces the clustering of E2/core/NS5A structures. Huh7.5 cells infected with Jc1 or Jc1-Y93H viruses (MOI = 0.2) were incubated at 66 hours post-infection with 1 nM DCV or dimethyl sulfoxide (DMSO) for 6 hours. After staining for HCV E2, core, and NS5A proteins, colocalization of core (*red channel*) with E2 (*green channel*) and NS5A (*blue channel*) proteins was analyzed by confocal microscopy (*A*). Scale bars of *panels* and *zooms* from *squared area* represent 10 μm and 2 μm, respectively. Colocalized pixels (*white channel*) between *red*, *green*, and *blue* channels were extracted with the ColocalizeRGB plugin of ImageJ. The surface (*B*) and number (*C*) of E2/core/NS5A and core/NS5A structures were quantified with ImageJ. For each condition, 30–50 cells were quantified. $^{****}P \leq .0001$; $^{***}P \leq .001$; $^{**}P \leq .01$; $^{*}P \leq .05$; ns (not significant) $P > .05$.

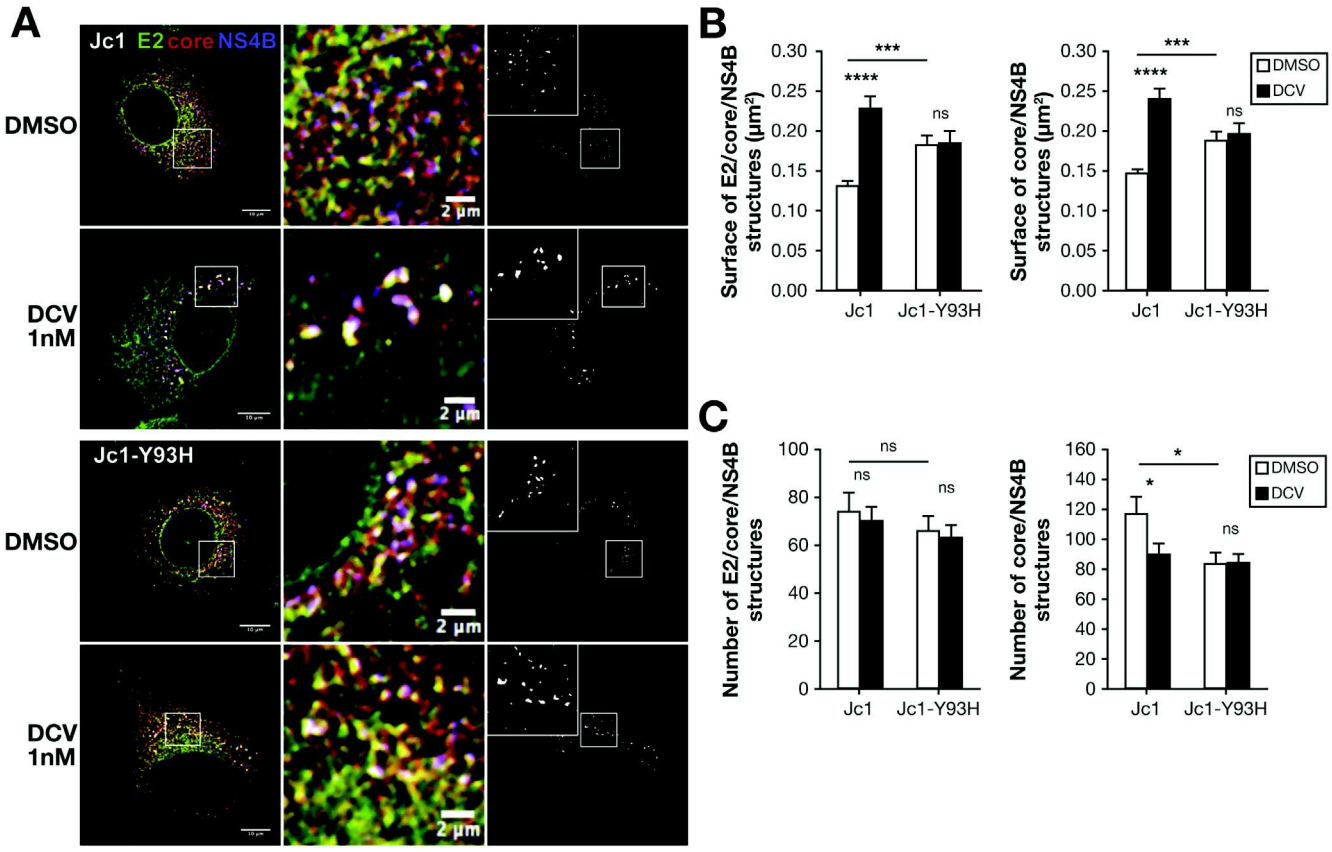

Figure 2. DCV induces the clustering of E2/core/NS4B structures. Cells were infected, treated, and analyzed as in Figure 1. Confocal analysis of core with E2 and NS4B, displayed as in Figure 1*A*, with NS4B instead of NS5A in the *blue channel* (*A*). The surface (*B*) and number (*C*) of E2/core/NS4B and core/NS4B structures were quantified with ImageJ. DMSO, dimethyl sulfoxide. ****$P \leq .0001$; ***$P \leq .001$; *$P \leq .05$; ns (not significant) $P > .05$.

structures colocalizing E2, core, and NS5A proteins were readily detected in Jc1-infected cells at 72 hours post-infection (see the extractions of E2/core/NS5A colocalization pixels in the *right panels* [*A*] of either Figure 1 or 2 and quantifications in *panels B–C*). Strikingly, after a 6-hour-long DCV treatment, they appeared approximately 85% bigger than without treatment (Figure 1*B*). Likewise, E2/core/NS4B punctate structures were also detected in Jc1-infected cells (Figure 2); yet, similar to E2/core/NS5A structures, their size steadily increased from 2 hours after DCV treatment (Supplementary Figure 2*C*) and was approximately 75% bigger than without DCV treatment after a 6-hour-long incubation (Figure 2*B*), although their number remained constant (Supplementary Figure 2*D*, Figure 2*C*). Of note, short-time DCV treatments from 18 hours post-infection also induced strong enlargements of both E2/core/NS5A and E2/core/NS4B punctate structures, by up to 3-fold (data not shown). These core/NS5A and core/NS4B structures clustering with E2 (Figures 1 and 2) likely gathered within combined structures, as indicated by the enlargement of punctae that included core, NS5A, and NS4B upon short-time DCV treatments (Supplementary Figure 4). Importantly, the Y93H DCV-resistant mutation abolished DCV-induced enlargement of all these structures (Figures 1 and 2, Supplementary Figure 2*C–D*), indicating that their alteration likely involved DCV effect on NS5A.

Finally, DCV treatment blocked NS5A hyper-phosphorylation, as reported by others,[22,23] which correlated with the co-clustering of structural and non-structural proteins and with the concomitant decrease of assembly of infectious viral particles (Supplementary Figures 5 and 2). As noted by others,[6,22] the Y93H DCV-resistant mutation altered DCV-mediated inhibition of NS5A hyper-phosphorylation (Supplementary Figure 5). As NS5A hyper-phosphorylation modulates NS5A functions in both replication and assembly,[8] these results further implied that DCV targeting of NS5A DI domain function(s) is pivotal for both steps.

Altogether, these results suggested that DCV acts shortly after administration to block viral assembly and results in the co-clustering of structural proteins with RC components.

In Absence of Daclatasvir Treatment, Structural and Nonstructural Proteins Colocalize Over Time Post-Infection Within Accruing Punctate Structures

Our results suggested that, rather than inducing novel structures, DCV expands or merges pre-existing structures colocalizing structural and nonstructural proteins. Accordingly, DCV did not modify the cellular localization and membrane association of E2, core, NS4B, and NS5A proteins,

as indicated by subcellular fractionation assays of infected cells that did not reveal changes in their fraction contents upon DCV treatment (Supplementary Figure 6*A*). Altogether, this prompted us to characterize such pre-existing structures, aiming at understanding the mode of action of DCV on HCV assembly inhibition.

Using super-resolution microscopy (3-dimensional structured illumination microscopy), we found that E2/core/NS4B dot structures gather NS4B part(s) and E2-dense parts, with core joining either areas (Figure 3*A*). Such structures might represent territories connecting the sites of replication and assembly. Therefore, to investigate their formation, they were characterized over time post-infection with the Jc1 virus comparatively to the JFH1 virus that produces 50−100-fold less infectious viral particles[20] despite identical replication rates.[19] At early time points post-infection (before 24 hours), core and NS4B appeared as punctate structures, whereas E2 was spread throughout the ER (Figure 4*A*, Supplementary Figure 7). Few dots of colocalization between core, E2, and NS4B were detected at early time points in both Jc1- and JFH1-infected cells; yet, their number increased subsequently. Specifically, from 24 hours to 72 hours post-infection, the number and size of E2/core/NS4B structures increased in Jc1-infected cells by approximately 20-fold and 3-fold, respectively (Figure 4*B,C*). This suggested that core progressively concentrates in areas including E2 and/or NS4B, and that the structures containing both structural proteins and components of RCs appear concomitantly. Comparatively, the number and size of E2/core/NS4B structures increased slowly in JFH1

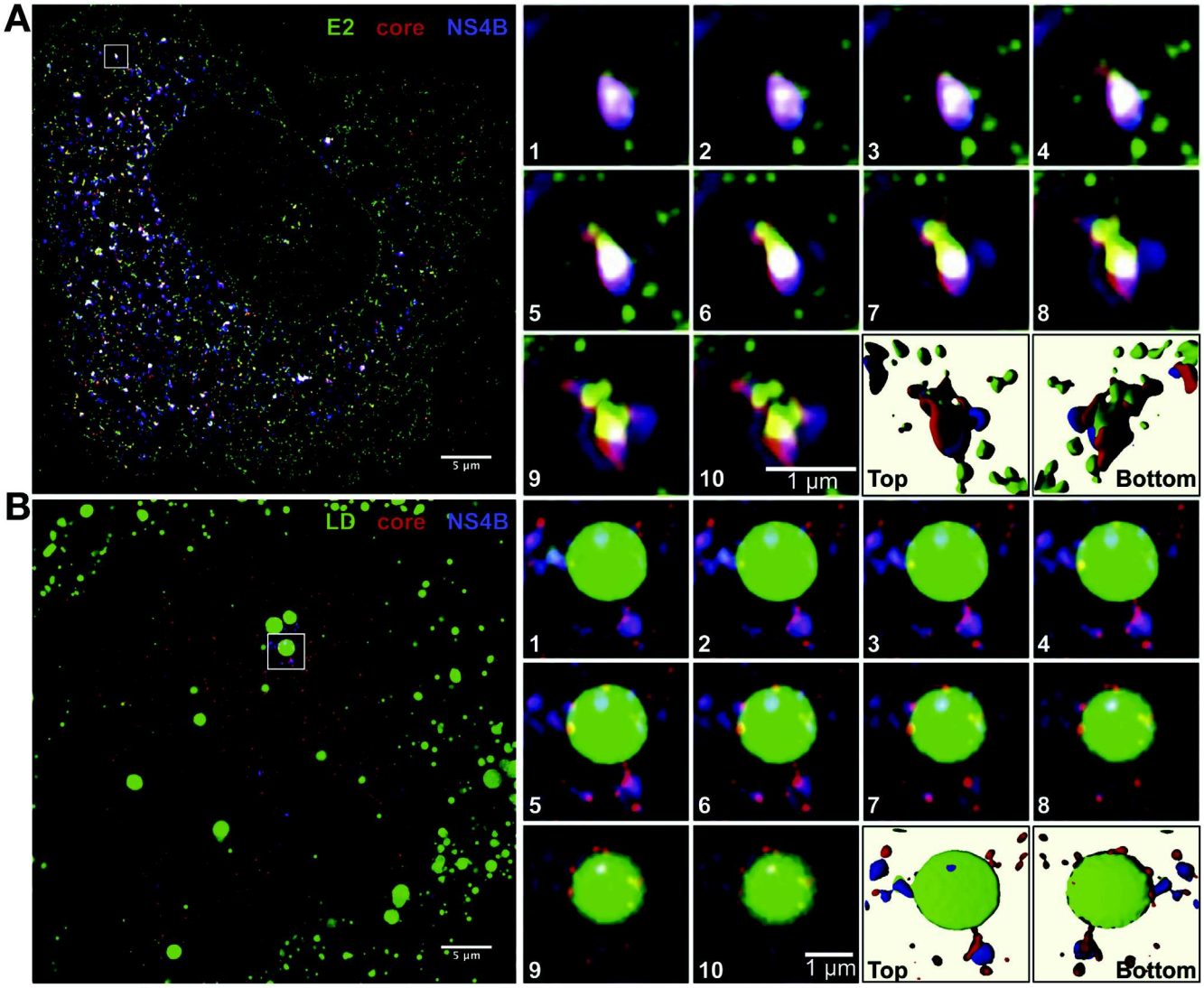

Figure 3. Three-dimensional structured illumination microscopy (3D-SIM) super-resolution imaging of E2/core/NS4B structures. Cells were infected with Jc1 virus (MOI = 0.2), treated for 24 hours with 20 µg/mL CHX at 48 hours post-infection, and fixed at 72 hours post-infection. Cells were stained for HCV E2, core, and NS4B proteins and for LDs. Colocalization of core (*red channel*) with E2 (*green channel*) and NS4B (*blue channel*) (*A*) or core with LDs (*green channel*) and NS4B (*blue channel*) (*B*) was analyzed by 3D-SIM. *Zooms* of typical structures are represented as individual stack from *top* to *bottom* (referred to as 1−10) and 3D reconstructions from Imaris software are shown. Scale bars of *panels* and *zooms* from *squared area* represent 5 µm and 1 µm, respectively.

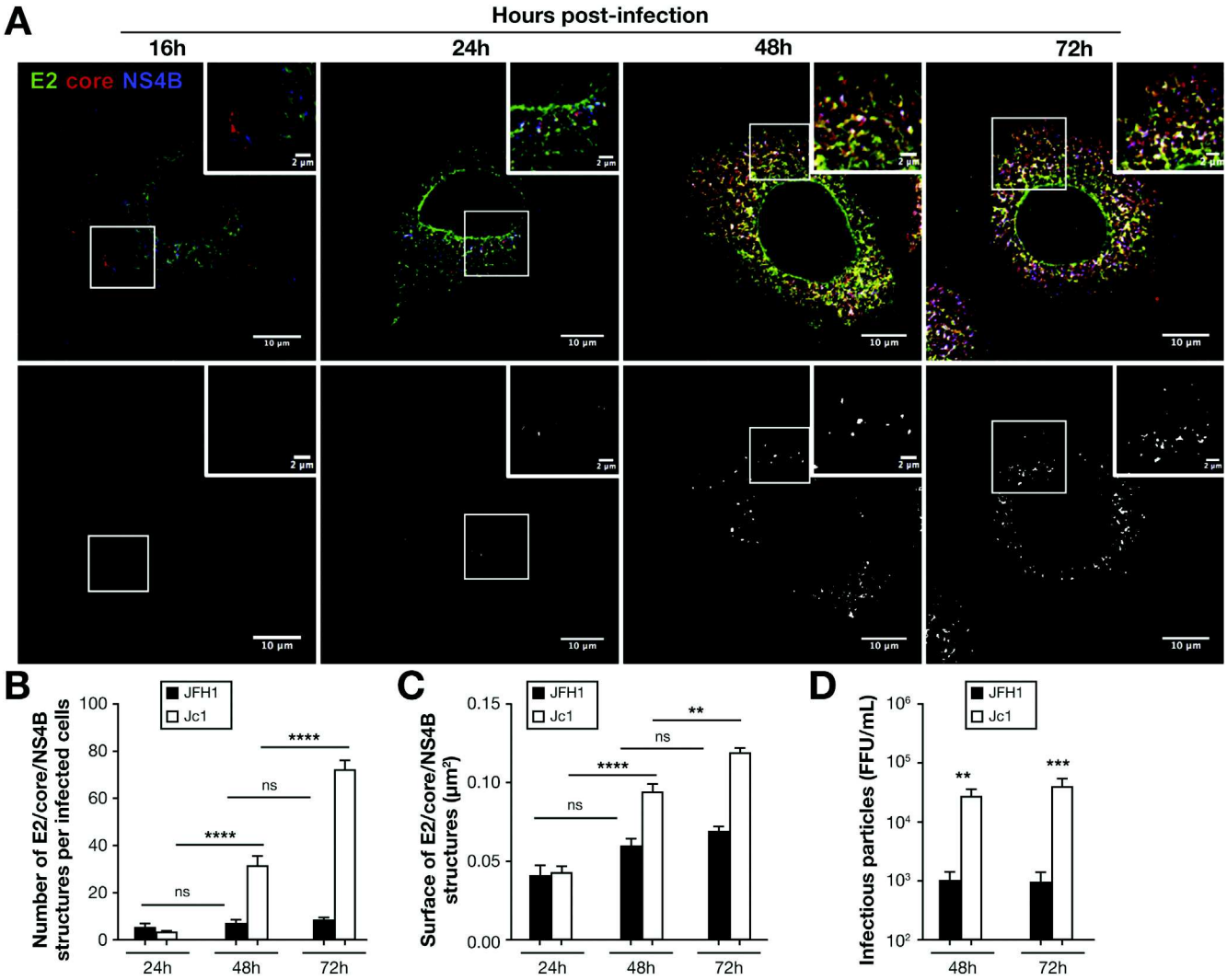

Figure 4. Structural proteins and NS4B colocalize within discrete structures. Cells infected with Jc1 or JFH1 viruses (MOI = 0.2) were fixed at the indicated time post-infection and were then stained for HCV E2, core, and NS4B proteins. The colocalization of core (*red channel*) with E2 (*green channel*) and NS4B (*blue channel*) was analyzed by confocal microscopy. A representative picture of Jc1-infected cells is presented (*A*). Scale bars of *panels* and *zooms* from *squared area* represent 10 μm and 2 μm, respectively. Colocalized pixels (*white channel*) between *red*, *green*, and *blue* channels were extracted with the ColocalizeRGB plugin of ImageJ (*second row*). The number (*B*) and size (*C*) of E2/core/NS4B structures were quantified with ImageJ. For each condition, 30–50 cells were quantified. The supernatants of infected cells were harvested at the indicated time post-infection and used to infect naïve Huh7.5 cells to determine virus infectivity (*D*). $^{****}P \leq .0001$; $^{***}P \leq .001$; $^{**}P \leq .01$; ns (not significant) $P > .05$.

virus-infected cells from 24 hours post-infection and were approximately 10-fold less frequent at 72 hours post-infection as compared to Jc1 (Figure 4*B*), in agreement with the lower production of infectious viral particles (Figure 4*D*). The appearance of E2/core/NS4B structures, which correlated with infectivity levels, suggested that they could represent RCs connected to viral particle assembly components or sites.

Daclatasvir Does Not Alter the Localization of Punctate Structures That Are Apposed to, But Not Associated With Lipid Droplets

Previous studies reported a differential accumulation of HCV core in 2 distinct intracellular areas in Jc1- vs JFH1-infected cells, that is, at the ER vs LDs,[20,24] respectively, which may reflect the dissimilar capacity of core from either virus to engage in assembly. Thus, aiming at better characterizing the initiation of HCV assembly, we compared core localization at different time points post-infection. At 16 hours post-infection, the core protein showed intracellular localization patterns as small and discrete punctae that were distributed uniformly (Supplementary Figure 8*A*). These structures were still observed at 24 hours post-infection for both viruses; yet, in JFH1-infected cells, core also became detectable at the surface of LDs. At later time points, from 48 hours post-infection, the core protein was found clearly redistributed following 2 different patterns, that is, as a reticular pattern in Jc1-infected cells vs surrounding LDs in JFH1-infected cells (Supplementary Figure 8*A*).

To determine how the initial core punctae were progressively redistributed in either pattern, we inhibited protein synthesis at 24 hours vs 48 hours post-infection by treating infected cells with cycloheximide (CHX) for 24 hours (Supplementary Figure 8*A*). After CHX treatment, the core protein of JFH1 virus was still observed as ring-like structures that completely surrounded >95% of the LDs, suggesting that the core protein initially present as discrete punctae progressively reached and accumulated at LD surface. In sharp contrast, the early-detected discrete core punctae persisted in CHX-treated Jc1-infected cells and enlarged by approximately 50% from 48 hours to 72 hours post-infection (Supplementary Figure 8*A* and *B*).

When we determined the localization of these core punctae in Jc1-infected cells, we found that they were not randomly distributed throughout the ER but rather, that a significant part, of approximately 40%, was apposed at the edge of LDs (Figure 5*A* and *B*), which represent specific sites where LDs are juxtaposed to the ER membrane and may gain their proteins.[25] As about 10% of LDs in Jc1-infected cells were surrounded by core protein compared to >95% in JFH1-infected cells (Figure 5*C*), this suggested that core-apposition at LD edges, rather than LD surface-association, promotes HCV early assembly steps. These findings implied that the core protein of Jc1 virus was not mobilized to or from the LD surface, but rather, was targeted and/or retained at ER membrane sites apposed to LDs. This also indicated that the reticular pattern detected at late time points post-infection in CHX-untreated cells reflected the progressive accrual and/or enlargement of core punctae (Supplementary Figure 8*A*). Altogether, these results suggested that the association of core on LD surface does not contribute to virion assembly, at least in a direct manner, and that, over time post-infection, the core protein of the highly infectious Jc1 virus progressively concentrates in large, LD edge-apposed punctate structures, which is concomitant to virus production.

It is expected from these findings that a part of the punctae in which core accumulated represented assembly sites. To characterize the connection of these dots with replication sites, we investigated the intracellular localization of core punctae colocalizing with the non-structural proteins revealed here, that is, NS5A and NS4B (Figures 1 and 2). Interestingly, both structures frequently localized (approximately 40%−55%) at the edge of LDs in Jc1-infected cells (Figure 5*D*). By super-resolution microscopy, we found that core/NS4B dotted structures apposed at LD edges exhibited a bipolar arrangement, separating by approximately 0.1 μm core on the one side and NS4B on the other side (Figure 3*B*). Importantly, a similarly high proportion of core/NS4B and core/NS5A structures remained apposed at the edges of LDs in infected cells treated or not

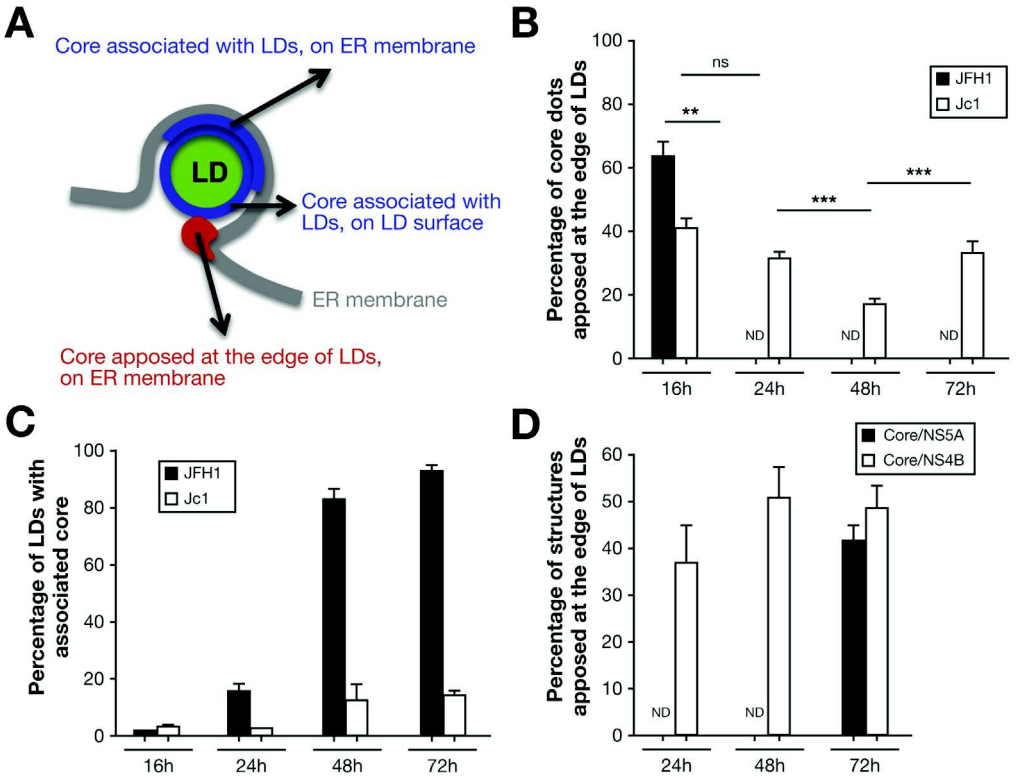

Figure 5. Characterization of HCV core structures within infected cells. A schematic representation distinguishing the different categories of core structures with regard to LD localization that were quantified (*A*). From images of Supplementary Figure 8*A*, the percentage of core punctate structures apposed at the edge of LDs (*B*) and the percentage of LDs with associated core either on ER membrane or on LD surface (*C*) were quantified using a macro developed with ImageJ (see Supplementary Results). The percentage of core/NS4B and core/NS5A punctate structures apposed at the edge of LDs in Jc1-infected cells (*D*) were quantified with ImageJ. ND, not determined. For each condition, 30−50 cells were quantified. ***$P \leq .001$; **$P \leq .01$; ns (not significant) $P > .05$.

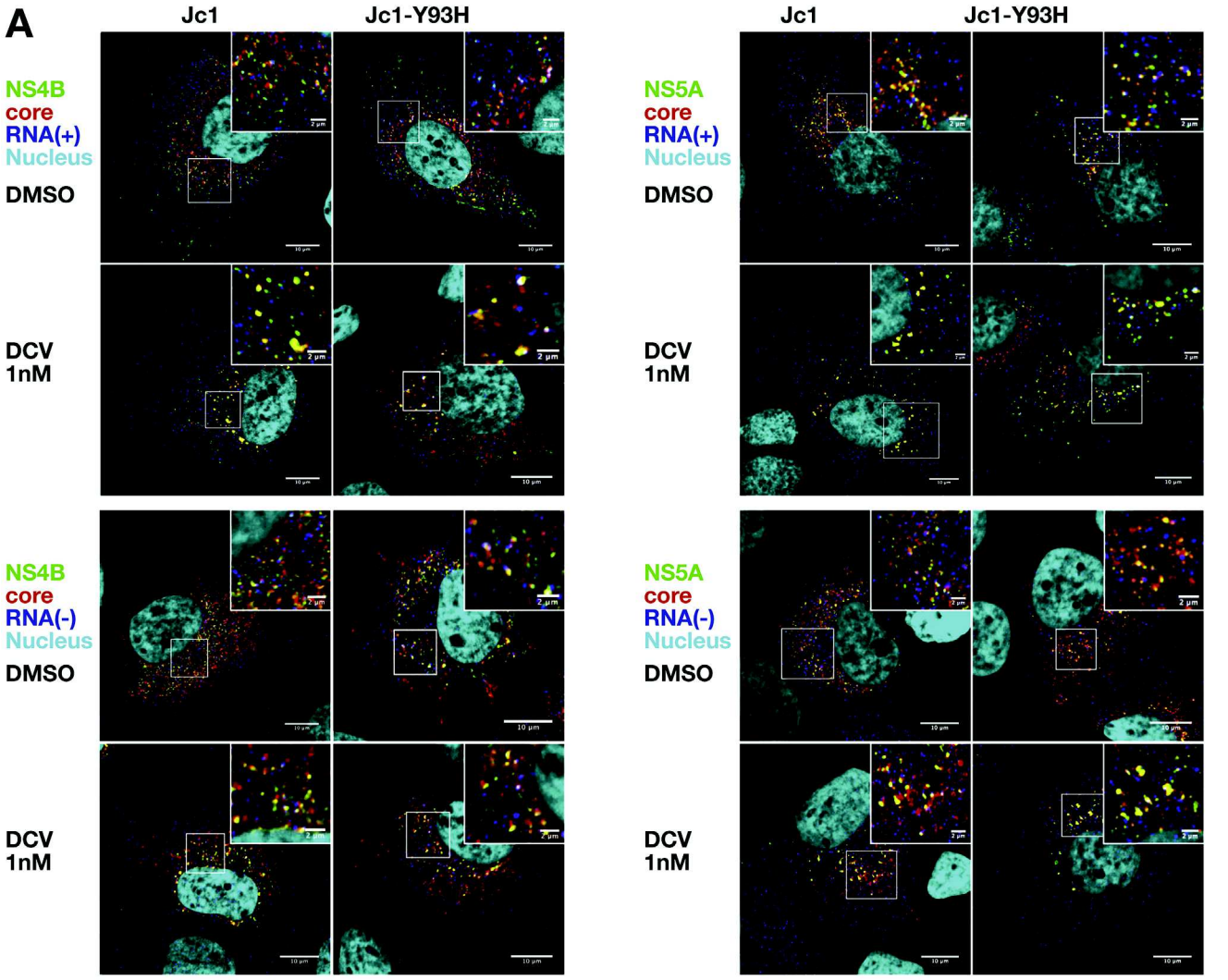
A
Jc1
Jc1-Y93H
NS4B
core
RNA(+)
Nucleus
DMSO
DCV
1nM
NS5A
core
RNA(+)
Nucleus
DMSO
DCV
1nM
NS4B
core
RNA(-)
Nucleus
DMSO
DCV
1nM
NS5A
core
RNA(-)
Nucleus
DMSO
DCV
1nM

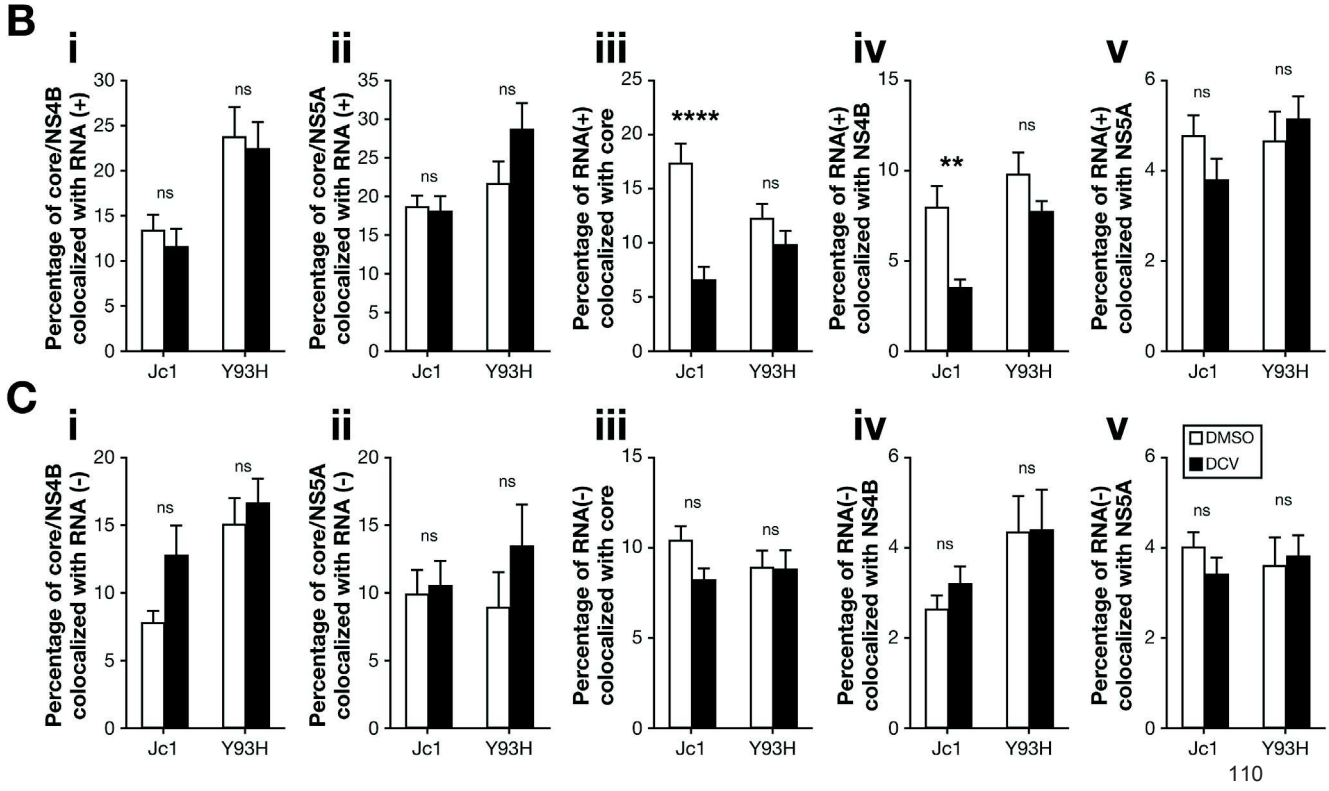
B
i
ii
iii
iv
v
Percentage of core/NS4B colocalized with RNA (+)
Percentage of core/NS5A colocalized with RNA (+)
Percentage of RNA(+) colocalized with core
Percentage of RNA(+) colocalized with NS4B
Percentage of RNA(+) colocalized with NS5A
ns
****
**
Jc1
Y93H
C
i
ii
iii
iv
v
Percentage of core/NS4B colocalized with RNA (-)
Percentage of core/NS5A colocalized with RNA (-)
Percentage of RNA(-) colocalized with core
Percentage of RNA(-) colocalized with NS4B
Percentage of RNA(-) colocalized with NS5A
DMSO
DCV
ns
Jc1
Y93H

with DCV (Supplementary Figure 6*B*), which further implied that DCV did not inhibit HCV assembly by altering localization of assembly proteins.

Daclatasvir Prevents Hepatitis C Virus Genome Transfer to Virus-Induced Structures That May Represent Assembly Platforms

At first sight, the increasing size of E2/core/NS4B structures during the infection course (Figure 4) seemingly contradicted the fact that DCV treatment could also induce their enlargement (Figure 2). As DCV inhibits viral particle assembly, we thought that this apparent paradox reflects the accumulation of proteins at assembly and RC sites. To test this hypothesis, we reasoned that impairing cellular assembly factors would similarly induce the expansion of E2/core/NS5A and/or E2/core/NS4B structures. Hence, we targeted diacylglycerol acyltransferase-1, a factor that regulates HCV assembly by attracting core and NS5A proteins onto the surface of the same LDs.[26,27] Upon diacylglycerol acyltransferase-1 down-regulation or chemical inhibition, which reduced infectivity by approximately 9-fold, we found that both E2/core/NS5A and/or E2/core/NS4B structures enlarged, by up to 2-fold (Supplementary Figure 9). In a similar manner, we surmised that, owing to the dual role of NS5A in replication vs packaging of HCV RNA,[8,18] the enlargement of either structure upon short-time DCV treatment (Figures 1 and 2) may reflect a loss of functional transition from HCV replication to assembly as caused by defective NS5A targeting of the viral genome to assembly components, ultimately resulting in their aggregation as inactive structures.

To further address this possibility, we wanted to investigate whether the viral genome and its replicative intermediate, that is, HCV RNA(+) and RNA(−) species, respectively, could be found within these structures and could be altered upon DCV treatment. We therefore combined immunofluorescence analysis to label core, NS4B, and NS5A proteins with fluorescence in situ hybridization to detect HCV RNA(+) and RNA(−) strands, which appeared as dots that could represent sites of translation, replication, viral assembly, or intracellular particles.[28] Importantly, both HCV RNA(+) and RNA(−) were detected within core/NS5A and core/NS4B structures, which suggested that they represent, at least partly, assembly structures connected with RCs (Figure 6*A*–*C*, *panels i* and *ii*). Interestingly, a 6-hour-long DCV treatment did not change the proportion of either protein structure colocalizing with both types of RNAs (Figure 6*A*–*C*, *panels i* and *ii*). However, when we quantified the number of RNA dots colocalizing with HCV protein dots in Jc1-infected cells, we found that such DCV treatment specifically decreased by up to 3-fold the proportion of HCV RNA(+) dots colocalizing with either core or NS4B punctae, whereas no changes were observed in Jc1-Y93H infected cells (Figure 6*A* and *B*, *panels iii* and *iv*). In contrast, the proportion of HCV RNA(+) dots colocalizing with NS5A structures remained unchanged (Figure 6*A* and *B*, *panel v*), implying that DCV-mediated NS5A inhibition acts downstream of NS5A/RNA interaction(s), in agreement with previous reports indicating that DCV does not inhibit HCV RNA binding to NS5A.[14,29] Finally, DCV did not change the proportion of HCV RNA(−) colocalizing with NS4B, NS5A, and core in either Jc1 or Jc1-Y93H–infected cells (Figure 6*A* and *C*). Together these observations suggest that DCV inhibited assembly by blocking the formation of active, that is, RNA(+) containing, assembly sites.

Discussion

Our results uncover novel features of DCV-mediated HCV inhibition that further our understanding of HCV assembly. We confirmed that DCV induces NS5A clustering, in line with previous studies.[5,12,15] Interestingly, we found that other HCV proteins, such as E2, core, and NS4B, gathered with these NS5A clusters (Figures 1 and 2, Supplementary Figure 4). We also found that the enlargement of these clusters upon short-time DCV treatments correlated with the reduction of viral particle assembly. As we will discuss, we propose that DCV-induced accretion of HCV proteins reflects the loss of functional association between HCV replication and assembly.

Connection Between Replication Complexes and Assembly Sites at Lipid Droplets Proximity

Overall, our imaging, biochemical, and functional data are congruent with a model previously proposed by others[21] wherein assembly sites are closely associated with RCs and LDs in a micro-environment favoring replication, mobilization, and protection of HCV RNA. First, by comparing the poorly infectious JFH1 virus vs the highly infectious Jc1 virus, we found that the occurrence and intracellular localization of E2/core/NS4B and E2/core/NS5A structures were intimately related to infectivity levels (Figure 4) and that such structures were frequently apposed at the edge of LDs, that is, close to the ER membrane, but were not associated around or at LD surface (Figure 5). Second, through time-course analysis of infection combined with translation inhibition assays (Supplementary Figure 8), we highlighted the progressive

Figure 6. DCV prevents the delivery of HCV RNA(+) to assembly sites. Cells infected with Jc1 or Jc1-Y93H viruses (MOI = 0.2) were incubated at 66 hours post-infection with 1 nM DCV or dimethyl sulfoxide (DMSO) for 6 hours. After staining for HCV core, NS4B, and NS5A proteins and nuclei, HCV RNA(+) and RNA(−) species were stained by fluorescent in situ hybridization. Colocalization of core (*red channel*) with NS4B or NS5A proteins (*green channel*) and HCV RNA(+) or RNA(−) strands (*blue channel*) was analyzed by confocal microscopy (*A*). Nuclei are represented as *cyan channel*. Scale bars of *panels* and *zooms* from *squared area* represent 10 μm and 2 μm, respectively. The proportion of core/NS4B and core/NS5A colocalizing with HCV RNA(+) (*B*) or RNA(−) (*C*), as well as the proportion of HCV RNA(+) (*B*) or RNA(−) (*C*) dots colocalizing with core, NS4B, or NS5A structures were quantified with ImageJ. For each condition, 30–50 cells were quantified. ****$P \leq .0001$; ***$P \leq .001$; **$P \leq .01$; *$P \leq .05$; ns (not significant) $P > .05$.

accumulation of core punctae at ER membranes, which ultimately appeared as a mesh distributed throughout the ER, and their rapid and strong colocalization with HCV glycoproteins. Third, we found that a significant proportion (approximately 15%−20%) of core/NS4B and core/NS5A structures contain HCV RNAs (Figure 6). Finally, our data underscored that the structures associating RNA(+), core, and E2 structural components (ie, representing, at least in part, assembly sites[28]) with RCs and LDs,[21] evolve in a very dynamic process both naturally and in response to specific inhibitors.

Daclatasvir Induces Clustering of Viral Proteins by Altering Both Assembly and Replication Complex Formation

We noticed that a high proportion (approximately 80%−85%) of core/NS4B and core/NS5A structures do not contain HCV RNAs. We propose that such structures may represent assembly sites for which functional linkage with RCs or, alternatively, viral RNA transfer to nascent virions, have waned or not occurred. Intuitively, one might expect that functional assembly sites would be difficult to seize, as they are necessarily transient, owing to release of assembled viral particles from such sites into the ER lumen and secretion by the cell. In addition, that HCV RNA seems rate-limiting for inducing functional assembly is congruent with other findings that functional RCs, represented by DMVs having a cytosol-oriented orifice allowing release of newly synthesized HCV RNA, account for <10%,[10] and that HCV RNA triggers viral particle envelopment.[18] Furthermore, HCV assembly is a poorly efficient process, in line with a general notion that the vast majority of structural proteins are not engaged or consummated in virions production. Accordingly, the progressive accumulation and enlargement of core-dotted structures appearing as a mesh in Jc1-infected cells (Supplementary Figure 8) likely revealed accretion of nonfunctional assembly sites or, corollary, of residual core proteins that have not engaged in assembled and/or released virions. In support of this view, we found that such core punctae do not arise from mobilization of LD-associated core, but rather from their multiplication throughout the ER (Supplementary Figure 8) while replication and translation progress, and from their enlargement after ER targeting.

In this respect, our unexpected finding that DCV accentuated the clustering and/or enlargement of core punctae concomitant to inhibition of assembly may likely reflect an accrued accumulation of nonfunctional assembly sites, that is, of core proteins not recruited or released as infectious viral particles. Furthermore, we observed that both E2/core/NS4B and E2/core/NS5A structures also enlarged upon DCV treatment, concomitant to assembly inhibition. Finally, inhibiting assembly by targeting diacylglycerol acyltransferase-1, which promotes localization of core and NS5A at LDs,[26,27] also resulted in enlargement of either structure (Supplementary Figure 9). However, these observations are not paradoxical if one considers that a majority of such structures are not functionally connected to ongoing assembly events. Indeed, expression of HCV proteins continuously raises several vesicle types that are formed from the ER membrane, particularly viral particles and DMVs. Therefore, the release of the 2 latter vesicles, respectively, within the ER lumen and the cytosol, as well as their turnover through secretion and/or degradation, requires an unceasing creation of areas forming novel assembly sites and RCs. In this regard, NS5A, which intersects cellular degradation machineries, for example, autophagy,[30] might be pivotal for DMV turnover.

Importantly, because the Y93H mutation in NS5A renders both assembly and DMV biogenesis events resistant to DCV,[6,9] it implies that DCV targets a mutual, specific NS5A function that inhibits both processes. Indeed, NS5A, in concert with CypA[9,31] and NS4B,[10,11,32,33] has the capacity to induce DMV biogenesis through binding of its AH N-terminal amphipathic helix on the ER membrane and, as proposed previously,[1,6,34–36] NS5A multimerization. Because DCV binds close to the amino-terminus of the DI domain of NS5A dimer, that is, at the junction of both DI subunits and their interface with the ER membrane,[1,6,7,35] DCV binding could perturb the positioning, orientation, or flexibility of the AH helix that anchors NS5A. This could alter the membranotropic properties of NS5A by altering its membrane binding, multimerization, and/or interaction with partners, which would explain DCV capacity to inhibit the formation of DMVs[6,9] and subsequent RNA synthesis and/or trafficking,[5] but also its lack of effect on replication within pre-existing DMVs.[9] Owing to the fast turnover of DMVs,[6] this inhibition would progressively lead to decay of HCV RNAs[5] by loss of newly formed DMVs. As a result, de novo−expressed nonstructural proteins would tend to accumulate because their lack of segregation as DMVs would enhance the clustering of NS5A[5,12,15] and NS5B,[12] as reported previously, but also of NS4B (this report) at ER membrane domains where DMVs form.

Daclatasvir Prevents Delivery of Viral Genomes to Assembly Sites

It is unlikely that inhibition of DMV biogenesis explains the nearly immediate effect of DCV on assembly of infectious particles.[4–6] However, another important finding of our study was that short-time DCV treatments that prevented HCV assembly strongly reduced the colocalization of core with HCV RNA(+) strand (Figure 6), which likely precluded formation of infectious particles (Supplementary Figure 1). Furthermore, because DCV had no effect on colocalization of viral RNA with core/NS4B and core/NS5A structures (Figure 6), we propose that, reminiscent of specific NS5A mutants in domain DIII that affect core/NS5A interaction,[18] this could be due to a lack of transfer of viral genomic RNA to assembling virions. Indeed, DCV-mediated inhibition of DMV formation[6,9] may not result, per se, in the blockage of HCV RNA packaging or transfer because RNA synthesis may not occur before DMVs become fully formed and active.[5] Rather, we propose that DCV restrains pre-existing, replication-active DMVs, that is, among those already present at the onset of DCV treatment, from

mediating this critical event in infectious particles assembly by targeting the same function of NS5A as described here, that is, its membranotropic properties. Indeed, transfer of HCV RNA from active DMVs to assembly sites would also be precluded if the membrane-binding properties of NS5A were altered for different, albeit not exclusive reasons. First, as NS5A is located both inside and outside DMVs,[37] such alterations would compromise the stability of DMV surface-associated NS5A, and, consequently, the gathering of replication-active DMVs at the vicinity of HCV particle assembly sites and/or of LDs, because this targeting depends on core and NS5A interaction[21,38,39] and is critical for mediating RNA transfer to the core protein.[18] Second, as NS5A is also distributed on LDs and ER membranes,[10,21,27] DCV-mediated disruption of NS5A membrane association on these interfaces may subsequently inhibit RNA transfer, which could require NS5A multimers to guide HCV RNA toward structural proteins, as proposed elsewhere.[1,6,34–36] Regardless of NS5A localization, this would explain why DCV did not alter RNA/NS5A colocalization (Figure 6), as DCV does not inhibit RNA/NS5A binding,[14,29] whereas perturbing NS5A multimers by DCV via either their disruption or altered membrane association would likely have a strong impact on RNA transfer and packaging in assembling virions. Third, DCV-induced perturbation of NS5A amino-terminus, which interacts with NS4B C-terminal domain,[40,41] may preclude NS4B packaging functions[42] and RNA transfer to core. In this respect, it is interesting to note that DCV treatment also strongly reduced the colocalization of NS4B and HCV RNA(+) strand (Figure 6). This likely reflects the role of NS4B in post-replication steps,[32,43] particularly the packaging function of its C-terminal domain,[42] which relies on both weak RNA binding capacity[44] and interaction with the DIII domain of NS5A that is involved in HCV assembly.[18,38,39,45]

Interestingly, enlarged E2/core/NS5A and E2/core/NS4B structures were observed for the Y93H DCV-resistant virus as compared to wild-type in absence of DCV (Figures 1 and 2). Nonetheless, RNA(+) dots readily localized with core or NS4B structures (Figure 6*B*), even in the presence of DCV (Supplementary Figure 1), congruent with efficient viral particle assembly of this mutant. Therefore, in line with the model discussed here, we propose that DCV-escape mutations may compensate altered membranotropic properties of NS5A and optimize interactions with NS4B (and/or other nonstructural proteins) in order to maintain efficient RNA targeting to assembly sites. Additional experiments will be required to validate this hypothesis.

In conclusion, our results indicate that DCV may inhibit HCV by preventing NS5A-mediated HCV RNA transfer to sites of virion assembly, in addition to other effects induced by this multifunctional protein.[8] This finding emphasizes the attractiveness of this class of inhibitors that targets 2 distinct steps of HCV cycle, that is, RNA replication and viral particle assembly. Furthermore, investigating the mode of action of DCV allowed further characterization of how replication and assembly are intimately linked and a specific function of NS5A in this respect.

Supplementary Material

Note: To access the supplementary material accompanying this article, visit the online version of *Gastroenterology* at www.gastrojournal.org, and at http://dx.doi.org/10.1053/j.gastro.2016.11.047.

References

1. Bartenschlager R, Lohmann V, Penin F. The molecular and structural basis of advanced antiviral therapy for hepatitis C virus infection. Nat Rev Microbiol 2013; 11:482–496.
2. Gotte M, Feld JJ. Direct-acting antiviral agents for hepatitis C: structural and mechanistic insights. Nat Rev Gastroenterol Hepatol 2016;13:338–351.
3. Gao M, Nettles RE, Belema M, et al. Chemical genetics strategy identifies an HCV NS5A inhibitor with a potent clinical effect. Nature 2010;465:96–100.
4. Guedj J, Dahari H, Rong L, et al. Modeling shows that the NS5A inhibitor daclatasvir has two modes of action and yields a shorter estimate of the hepatitis C virus half-life. Proc Natl Acad Sci U S A 2013;110:3991–3996.
5. McGivern DR, Masaki T, Williford S, et al. Kinetic analyses reveal potent and early blockade of hepatitis C virus assembly by NS5A inhibitors. Gastroenterology 2014;147:453–462 e7.
6. Berger C, Romero-Brey I, Radujkovic D, et al. Daclatasvir-like inhibitors of NS5A block early biogenesis of hepatitis C virus-induced membranous replication factories, independent of RNA replication. Gastroenterology 2014;147:1094–1105 e25.
7. Ascher DB, Wielens J, Nero TL, et al. Potent hepatitis C inhibitors bind directly to NS5A and reduce its affinity for RNA. Sci Rep 2014;4:4765.
8. Ross-Thriepland D, Harris M. Hepatitis C virus NS5A: enigmatic but still promiscuous 10 years on. J Gen Virol 2015;96:727–738.
9. Chatterji U, Bobardt M, Tai A, et al. Cyclophilin and NS5A inhibitors, but not other anti-hepatitis C virus (HCV) agents, preclude HCV-mediated formation of double-membrane-vesicle viral factories. Antimicrob Agents Chemother 2015;59:2496–2507.
10. Romero-Brey I, Merz A, Chiramel A, et al. Three-dimensional architecture and biogenesis of membrane structures associated with hepatitis C virus replication. PLoS Pathog 2012;8:e1003056.
11. Romero-Brey I, Berger C, Kallis S, et al. NS5A Domain 1 and Polyprotein cleavage kinetics are critical for induction of double-membrane vesicles associated with hepatitis C Virus replication. MBio 2015;6:e00759.
12. Chukkapalli V, Berger KL, Kelly SM, et al. Daclatasvir inhibits hepatitis C virus NS5A motility and hyperaccumulation of phosphoinositides. Virology 2015; 476:168–179.
13. Lee C, Ma H, Hang JQ, et al. The hepatitis C virus NS5A inhibitor (BMS-790052) alters the subcellular localization of the NS5A non-structural viral protein. Virology 2011; 414:10–18.
14. Targett-Adams P, Graham EJ, Middleton J, et al. Small molecules targeting hepatitis C virus-encoded NS5A

cause subcellular redistribution of their target: insights into compound modes of action. J Virol 2011; 85:6353–6368.
15. Reghellin V, Donnici L, Fenu S, et al. NS5A inhibitors impair NS5A-phosphatidylinositol 4-kinase IIIalpha complex formation and cause a decrease of phosphatidylinositol 4-phosphate and cholesterol levels in hepatitis C virus-associated membranes. Antimicrob Agents Chemother 2014;58:7128–7140.
16. Huang L, Hwang J, Sharma SD, et al. Hepatitis C virus nonstructural protein 5A (NS5A) is an RNA-binding protein. J Biol Chem 2005;280:36417–36428.
17. Foster TL, Belyaeva T, Stonehouse NJ, et al. All three domains of the hepatitis C virus nonstructural NS5A protein contribute to RNA binding. J Virol 2010; 84:9267–9277.
18. Zayas M, Long G, Madan V, et al. Coordination of hepatitis C virus assembly by distinct regulatory regions in nonstructural protein 5A. PLoS Pathog 2016; 12:e1005376.
19. Pietschmann T, Kaul A, Koutsoudakis G, et al. Construction and characterization of infectious intragenotypic and intergenotypic hepatitis C virus chimeras. Proc Natl Acad Sci U S A 2006;103:7408–7413.
20. Boson B, Granio O, Bartenschlager R, et al. A concerted action of hepatitis C virus p7 and nonstructural protein 2 regulates core localization at the endoplasmic reticulum and virus assembly. PLoS Pathog 2011;7:e1002144.
21. Miyanari Y, Atsuzawa K, Usuda N, et al. The lipid droplet is an important organelle for hepatitis C virus production. Nat Cell Biol 2007;9:1089–1097.
22. Qiu D, Lemm JA, O'Boyle DR 2nd, et al. The effects of NS5A inhibitors on NS5A phosphorylation, polyprotein processing and localization. J Gen Virol 2011; 92:2502–2511.
23. Fridell RA, Qiu D, Valera L, et al. Distinct functions of NS5A in hepatitis C virus RNA replication uncovered by studies with the NS5A inhibitor BMS-790052. J Virol 2011;85:7312–7320.
24. Shavinskaya A, Boulant S, Penin F, et al. The lipid droplet binding domain of hepatitis C virus core protein is a major determinant for efficient virus assembly. J Biol Chem 2007;282:37158–37169.
25. Boulant S, Targett-Adams P, McLauchlan J. Disrupting the association of hepatitis C virus core protein with lipid droplets correlates with a loss in production of infectious virus. J Gen Virol 2007;88:2204–2213.
26. Herker E, Harris C, Hernandez C, et al. Efficient hepatitis C virus particle formation requires diacylglycerol acyltransferase-1. Nat Med 2010;16:1295–1298.
27. Camus G, Herker E, Modi AA, et al. Diacylglycerol acyltransferase-1 localizes hepatitis C virus NS5A protein to lipid droplets and enhances NS5A interaction with the viral capsid core. J Biol Chem 2013;288:9915–9923.
28. Shulla A, Randall G. Spatiotemporal analysis of hepatitis C virus infection. PLoS Pathog 2015;11:e1004758.
29. Nag A, Robotham JM, Tang H. Suppression of viral RNA binding and the assembly of infectious hepatitis C virus particles in vitro by cyclophilin inhibitors. J Virol 2012; 86:12616–12624.
30. Kim N, Kim MJ, Sung PS, et al. Interferon-inducible protein SCOTIN interferes with HCV replication through the autolysosomal degradation of NS5A. Nat Commun 2016;7:10631.
31. Madan V, Paul D, Lohmann V, et al. Inhibition of HCV replication by cyclophilin antagonists is linked to replication fitness and occurs by inhibition of membranous web formation. Gastroenterology 2014;146:1361–1372 e1–e9.
32. Paul D, Romero-Brey I, Gouttenoire J, et al. NS4B self-interaction through conserved C-terminal elements is required for the establishment of functional hepatitis C virus replication complexes. J Virol 2011;85:6963–6976.
33. Gouttenoire J, Montserret R, Paul D, et al. Aminoterminal amphipathic alpha-helix AH1 of hepatitis C virus nonstructural protein 4B possesses a dual role in RNA replication and virus production. PLoS Pathog 2014; 10:e1004501.
34. Appel N, Schaller T, Penin F, et al. From structure to function: new insights into hepatitis C virus RNA replication. J Biol Chem 2006;281:9833–9836.
35. Lambert SM, Langley DR, Garnett JA, et al. The crystal structure of NS5A domain 1 from genotype 1a reveals new clues to the mechanism of action for dimeric HCV inhibitors. Protein Sci 2014;23:723–734.
36. Love RA, Brodsky O, Hickey MJ, et al. Crystal structure of a novel dimeric form of NS5A domain I protein from hepatitis C virus. J Virol 2009;83:4395–4403.
37. Paul D, Hoppe S, Saher G, et al. Morphological and biochemical characterization of the membranous hepatitis C virus replication compartment. J Virol 2013; 87:10612–10627.
38. Masaki T, Suzuki R, Murakami K, et al. Interaction of hepatitis C virus nonstructural protein 5A with core protein is critical for the production of infectious virus particles. J Virol 2008;82:7964–7976.
39. **Appel N, Zayas M**, Miller S, et al. Essential role of domain III of nonstructural protein 5A for hepatitis C virus infectious particle assembly. PLoS Pathog 2008;4:e1000035.
40. Biswas A, Treadaway J, Tellinghuisen TL. Interaction between non-structural proteins NS4B And NS5A is essential for proper NS5A localization and hepatitis C virus RNA replication. J Virol 2016;90:7205–7218.
41. David N, Yaffe Y, Hagoel L, et al. The interaction between the hepatitis C proteins NS4B and NS5A is involved in viral replication. Virology 2015;475:139–149.
42. Han Q, Manna D, Belton K, et al. Modulation of hepatitis C virus genome encapsidation by nonstructural protein 4B. J Virol 2013;87:7409–7422.
43. Jones DM, Patel AH, Targett-Adams P, et al. The hepatitis C virus NS4B protein can trans-complement viral RNA replication and modulates production of infectious virus. J Virol 2009;83:2163–2177.
44. **Einav S, Gerber D**, Bryson PD, et al. Discovery of a hepatitis C target and its pharmacological inhibitors by microfluidic affinity analysis. Nat Biotechnol 2008; 26:1019–1027.
45. Tellinghuisen TL, Foss KL, Treadaway JC, et al. Identification of residues required for RNA replication in domains II and III of the hepatitis C virus NS5A protein. J Virol 2008;82:1073–1083.

Author names in bold designate shared co-first authorship.

Received July 20, 2016. Accepted November 28, 2016.

Reprint requests
Address requests for reprints to: François-Loïc Cosset, PhD, International Center for Infectiology Research, Université de Lyon, Lyon, 21 Avenue Tony Garnier, Lyon 69365, France. e-mail: flcosset@ens-lyon.fr; fax: +33 472 72 81 37.

Acknowledgments
The authors are grateful to Ralf Bartenschlager for the gift of JFH1, Jc1, and Jc1-Y93H constructs, Charles Rice for the gift of Huh7.5 cells and 9E10 monoclonal NS5A antibody, Mishinori Kohara for the gift of NS4B antibody, Jane McKeating for the gift of 3/11 E2 antibody, and Colette Jolivet for the gift of core antibody. The authors thank François Penin for helpful comments and critical reading of the manuscript and Claire Lionnet and Elodie Chatre for excellent technical assistance with confocal microscopy.

The authors dedicate this paper to the memory of our colleague and friend Professor Christophe Terzian.

Marlène Dreux and François-Loïc Cosset contributed equally to this work.

Conflicts of interest
The authors disclose no conflicts.

Funding
This work was supported by the Agence Nationale de la Recherche sur le Sida et les Hépatites Virales (ANRS), European Research Council (ERC-2008-AdG-233130-HEPCENT), and LabEx Ecofect (ANR-11-LABX-0048).

Supplementary Materials and Methods

Antibodies and Reagents

Rabbit antiserum against calnexin (Sigma-Aldrich, Lyon, France), mouse anti−adipose differentiation-related protein (clone AP125; Progen, Heidelberg, Germany), mouse anti-Actin (clone AC74; Sigma-Aldrich), rabbit anti−diacylglycerol acyltransferase-1 (DGAT1) (clone H-255; Santa Cruz Biotechnology, Santa Cruz, CA), mouse anti-core 19D9D6 (kind gift from C. Jolivet, bioMérieux, Lyon, France), rat anti-E2 clone 3/11 (kind gift from J. McKeating, University of Birmingham, UK), mouse anti-NS5A 9E10 (kind gift from C. Rice, Rockefeller University, New York, NY), rabbit anti-NS4B (kind gift from M. Kohara, Tokyo Metropolitan Institute of Medical Science, Tokyo, Japan), DCV (BMS-790052; Selleck Chemicals, Houston, TX), A922500 (Sigma-Aldrich), CHX (Sigma-Aldrich), Mowiol 40-88 (Fluka), Bodipy 493/503 and Hoecsht 33342 (Molecular Probes Europe BV), Fluoromount-G (SouthernBiotech), Protease/phosphatase inhibitor cocktail (Cell Signaling Technology, Danvers, MA) was used according to manufacturer's instructions.

Inhibition of Diacylglycerol Acyltransferase-1

Down-regulation of DGAT1 was achieved using procedure described previously[1] via a small interfering RNA (5′-GAACCTCATCAAGTATGGCAT) expressed from a lentiviral vector (MISSION pLKO.1-puro vector with short-hairpin RNA insert TRCN0000036153; Sigma-Aldrich). DGAT1 expression was verified by Western blot analysis. Inhibition of DGAT1 was achieved using 150 μM A922500 inhibitor added at the time of infection for 72 hours.

Analysis of Intracellular and Extracellular RNA Levels

RNAs were isolated from cells and supernatant harvested in guanidinium thiocyanate citrate buffer (GTC), extracted by phenol/chloroform extraction, reverse transcribed (iScript cDNA synthesis kit; Bio-Rad, Hercules, CA), and quantified with the FastStart Universal SYBR Green Master kit (Roche Applied Science, Indianapolis, IN) on an Applied StepOne Real-Time PCR apparatus, as described previously.[2,3] The efficiency of extracellular RNA extraction and reverse transcription real-time quantitative polymerase chain reaction was controlled by the addition of carrier RNAs encoding in vitro transcripts of Xef1a (*Xenopus* transcription factor 1a) in supernatants diluted in GTC buffer. The sequences of the primers used for the reverse transcription real-time quantitative polymerase chain reaction were: HCV-specific primers (5′-CTGCGGAACCGGTGAGTA and 5′-TCAGGCAGTACCACAAGGC), glyceraldehyde-3-phosphate dehydrogenase−specific primers (5′-AGGTGAAGGTCGGAGTCAACG and 5′-TGGAAGATGGTGATGGGATTTC), and Xef1a-specific primers (5′-GACGTTGTCAC CGGGCACG and 5′-ACCAGGCATGGTGGTTACCTT TGC). Extracellular and intracellular HCV RNA levels were normalized for Xef1a and glyceraldehyde-3-phosphate dehydrogenase RNA levels, respectively.

Analysis of Intracellular and Extracellular Core Protein Levels

Infected cells were washed with PBS, trypsinized, and centrifuged for 5 minutes at 400×*g*. Cell pellets were resuspended in PBS and subjected to 4 cycles of freeze and thaw using liquid nitrogen. Samples were then centrifuged at 10,000×*g* for 10 minutes to remove cell debris. For the quantification of extracellular core protein levels, supernatants of infected cells were harvested and diluted in Dulbecco's modified minimal essential medium to obtain a final concentration of 5% bovine serum albumin. Core protein levels were then quantified with the HCV core Antigen Detection ELISA assay (XpressBio, Frederick, MD) according to manufacturer's instructions.

Subcellular Fractionation

Separation of different membrane compartments was achieved as described previously.[4] Huh7.5 cells were electroporated with in vitro−transcribed Jc1 RNA. Sixty-six hours post-electroporation, cells were washed 3 times and were incubated with 1 nM DCV or dimethyl sulfoxide for an additional 6 hours. Cells were then detached, washed in PBS, and homogenized in 1 volume of 10 mM HEPES-NaOH 10 mM (pH 7.8) (hypo-osmotic buffer). Cells were allowed to swell on ice for 20 minutes and were re-isolated by centrifugation at 800×*g* at 4°C for 5 minutes. The medium was returned to iso-osmoticity by removing two-thirds of the supernatant and adding one-third volume of 0.6 M sucrose and 10 mM HEPES-NaOH at pH 7.8 (hyper-osmotic buffer). Cells were disrupted by passaging 20 times through a 25-G needle and lysates were extracted from the nuclei by centrifugation at 13,000×*g* for 10 minutes at 4°C. Subcellular fractionation was performed in 3-step iodixanol gradients. Equal protein amounts of the post-nuclear extracts were mixed with 60% iodixanol to give a final concentration of 30%, the hypo-osmotic buffer was mixed with 60% iodixanol to generate 10% and 20% iodixanol solutions. Equal volumes of these 3 solutions were layered in SW60Ti centrifuge tubes and centrifuged at 50,000 rpm for 3 hours at 4°C. Twelve fractions were collected from the top and proteins were revealed by Western blotting.

Western Blotting

Infected cells were lysed in lysis buffer (20 mM Tris [pH 7.5], 1% Triton X100, 0.05% sodium dodecyl sulfate, 150 nM NaCL, 5‰ Na deoxycholate) supplemented with protease/phosphatase inhibitor cocktail (Cell Signaling Technology) and clarified from the nuclei by centrifugation at 13,000×*g* for 10 minutes at 4°C. Ten micrograms total proteins were separated by sodium dodecyl sulfate polyacrylamide gel electrophoresis, then transferred to polyvinylidene fluoride membranes (FluoroTrans W; Pall Corporation, Port Washington, NY) and revealed with specific monoclonal antibodies, followed by the addition of goat anti-mouse, anti-rat, or anti-rabbit immunoglobulin conjugated to peroxidase (Dako A/S, Glostrup, Denmark). The proteins of interest were revealed by enhanced chemiluminescence detection (SuperSignal West Pico

Chemiluminescent, Thermo Scientific, Logan, UT) as recommended by the manufacturer.

Supplementary Results

For quantification of structures apposed at the edge of LDs,[5] we developed an ImageJ macro that searches for variation of max intensity in the neighborhood of each LD as an indicator of proximity. The code of this macro is as can be found on pages e3-e5

Supplementary References

1. Lavillette D, Tarr AW, Voisset C, et al. Characterization of host-range and cell entry properties of hepatitis C virus of major genotypes and subtypes. Hepatology 2005; 41:265–274.
2. Calattini S, Fusil F, Mancip J, et al. Functional and biochemical characterization of hepatitis C virus (HCV) particles produced in a humanized liver mouse model. J Biol Chem 2015;290:23173–23187.
3. Dao Thi VL, Granier C, Zeisel MB, et al. Characterization of hepatitis C virus particle subpopulations reveals multiple usage of the scavenger receptor BI for entry steps. J Biol Chem 2012;287:31242–31257.
4. Boson B, Granio O, Bartenschlager R, et al. A concerted action of hepatitis C virus p7 and nonstructural protein 2 regulates core localization at the endoplasmic reticulum and virus assembly. PLoS Pathog 2011;7:e1002144.
5. Boulant S, Targett-Adams P, McLauchlan J. Disrupting the association of hepatitis C virus core protein with lipid droplets correlates with a loss in production of infectious virus. J Gen Virol 2007;88:2204–2213.

```
showMessage("The system will now search for variation of \nmax intensity in the
neighborhood of each vesicle\nas indicator of proximity\n\nThe integrated density
should increase dramatically too.");

//Image management
if (nImages==0) {
        exit("No images are open");
 }else{
        getDimensions(width, height, channels, slices, frames);
        if(channels>1)  run("Split Channels");
        titres=newArray(nImages);
        //setBatchMode(true);
        for (i=1; i<=nImages; i++) {
        selectImage(i);
        titres[i-1]=getTitle();
   }

dir=getDirectory("image");

Dialog.create("Parameters");
Dialog.addNumber("Number of dilatations", 3);
Dialog.addNumber("Max. variation of max intensity", 50);
Dialog.addNumber("Max. variation of integrated intensity", 2000);
Dialog.addNumber("Min. area for analysis", 0.02);
Dialog.addChoice("To dilate", titres);
Dialog.addChoice("Target", titres);
Dialog.addCheckbox("Save ROIs ?", 0);
Dialog.show();
n=Dialog.getNumber();
maxIntVar=Dialog.getNumber();
maxDenVar=Dialog.getNumber();
minArea=Dialog.getNumber();
toDilate=Dialog.getChoice();
target=Dialog.getChoice();
saveROI=Dialog.getCheckbox();


//Preparation and configuration
run("Set Measurements...", "area min integrated redirect=None decimal=3");
roiManager("reset");

//Removing of channels useless for this analysis and separation of channels
/*setSlice(2);
run("Delete Slice", "delete=channel");
run("Next Slice [>]");
run("Delete Slice", "delete=channel");
run("Split Channels");
*/
```

```
/* TODO add sequence of automatic selection of the cell
run("Next Slice [>]");
run("Gaussian Blur...", "sigma=20 slice");
setAutoThreshold("Percentile dark");
setAutoThreshold("Percentile dark");
run("Convert to Mask");
doWand(265, 252);
*/

//Automatic thresholding and  separation
selectImage(toDilate);

//Possibility to place a ROI around the cell
waitForUser("Place ROI around the cell to avoid\nexternal counting");

//ROI counting
selectImage(toDilate);
run("Analyze Particles...", "size="+minArea+"-Infinity circularity=0.00-1.00
show=Nothing add");

//Selection of the image carrying the information
selectImage(target);
//selectWindow("C1-Jc1LDcoreNS4B4.lsm");

//Highlighting of the counted area
roiManager("Show All without labels");

//Saving of the ROI

if(saveROI) roiManager("Save", "");

//Scanning of the ROI
for(i=0;i<roiManager("count");i++){
roiManager("Select", i);
        //Measure of the dilations
        j=1;
        while(j<=n){
                run("Measure");
                run("Enlarge...", "enlarge=1 pixel");
                j++;
                }//end of ROI measurement

                //Construction secondary tables
                //Table of max
                maxs=newArray(n);
                for(z=0;z<n;z++){
                        maxs[z]=getResult("Max", z);
                }
                /*Array.print(maxs);
```

```
		print(maxs[4]);
		Array.reverse(maxs);
		Array.print(maxs);
		print(maxs[4]);
		Array.getStatistics(maxs, min, max, mean, stdDev);
		print(stdDev);
		print(delta(maxs))
		*/

		//Table of integrated intensities
		intDen=newArray(n);
		for(y=0;y<n;y++){
			intDen[y]=getResult("RawIntDen", y);
		}

		//Decision of the positive character or not
	if((delta(maxs)>maxIntVar)||(delta(intDen)>maxDenVar)) {
	print("ROI "+i+1+"\tpositif");
	}else{
		print("ROI "+i+1+"\tnegatif");
	}
	 //if(deltaMax<threshold) the area of max intensity is close by
	 //if(deltaRawIntDen>threshold) progress thus closeness

	 //deletion of n first raws of the table
	 IJ.deleteRows(0, n-1);


}//end of the scanning of the ROI

function delta(a){
val=0;
for(i=1;i<a.length;i++){
	val=val+a[i]-a[i-1];
	}
return val;
}
```

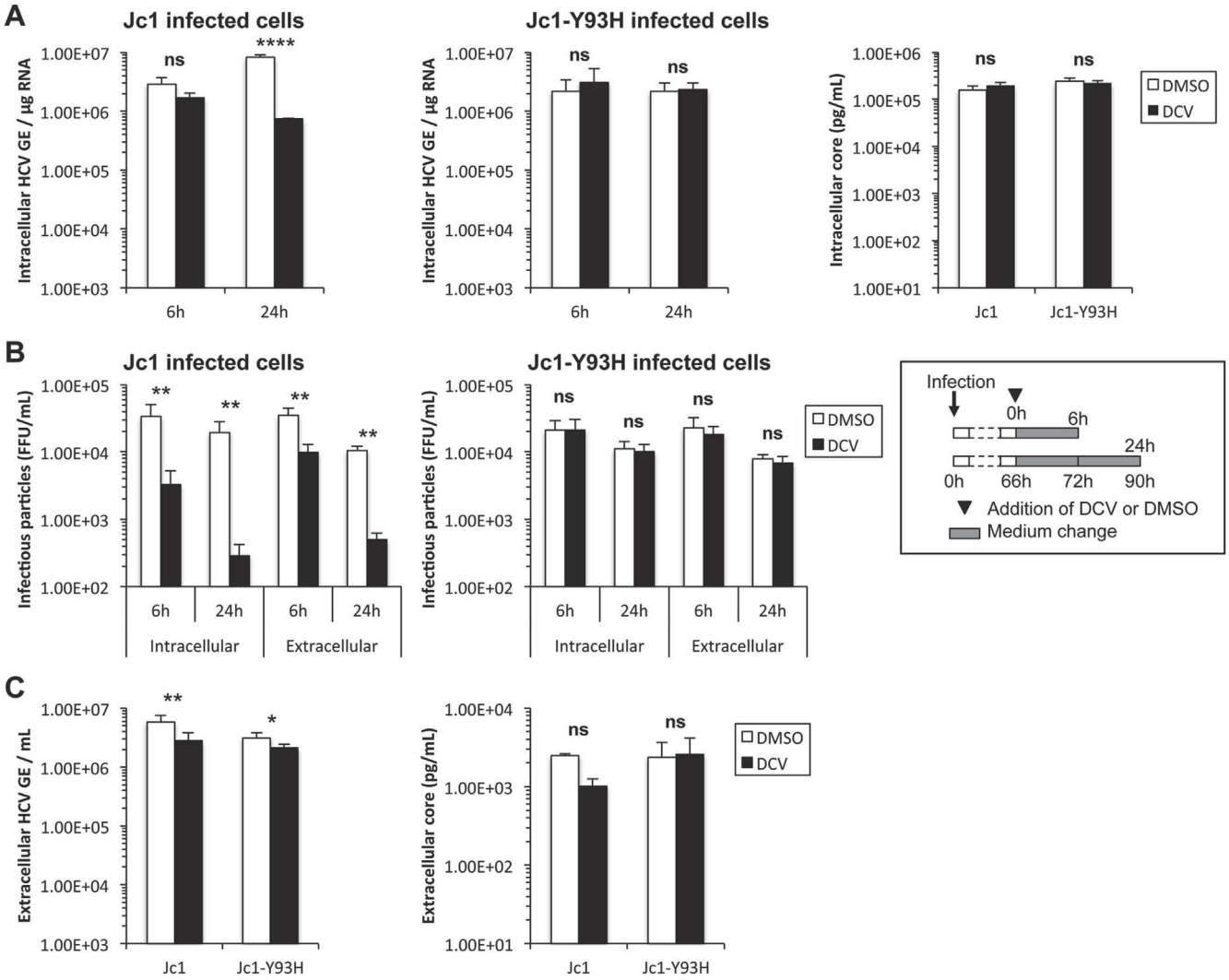

Supplementary Figure 1. DCV prevents HCV assembly. Huh7.5 cells infected with Jc1 or Jc1-Y93H viruses (MOI = 0.2) were incubated 66 hours post-infection with 1 nM DCV or dimethyl sulfoxide (DMSO) for 6 hours vs 24 hours, as outlined in the *boxed panel*. (*A*) The intracellular viral genomes (*left panels*) and core proteins (*right panel*) were quantified by reverse transcription quantitative polymerase chain reaction (RT-qPCR) and enzyme-linked immunosorbent assay (ELISA), respectively. (*B*) The intracellular or extracellular infectivity was determined from cell lysates or supernatants of infected cells, respectively. (*C*) The extracellular physical particles were analyzed by quantification of the release of viral RNA (*left panel*) or core protein (*right panel*) in the supernatant by RT-qPCR and ELISA, respectively. GE, genome equivalent. $^{****}P \leq .0001$; $^{***}P \leq .001$; $^{**}P \leq .01$; $^{*}P \leq .05$; ns (not significant) $P > .05$.

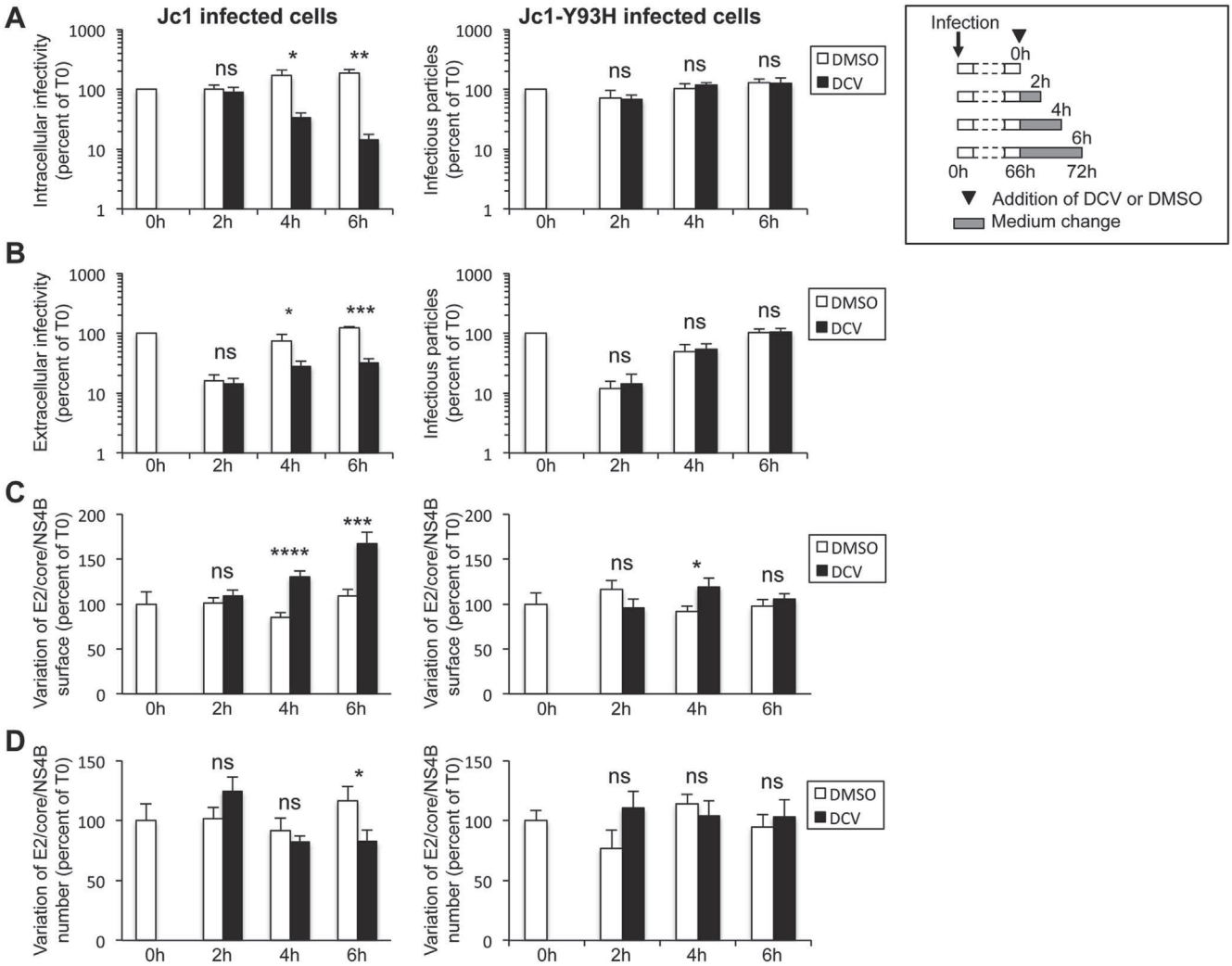

Supplementary Figure 2. HCV assembly inhibition by DCV correlates with clustering of structural proteins and NS4B. Huh7.5 cells were infected with Jc1 or Jc1-Y93H viruses at an MOI of 0.2. At 66 hours post-infection, cells were washed and incubated with 1 nM of DCV or dimethyl sulfoxide (DMSO) for the indicated time, as outlined in the *boxed panel*. (*A*) The intracellular and (*B*) extracellular infectivity were determined from cell lysates or supernatants of infected cells, respectively. (*C*) The size and (*D*) number of E2/core/NS4B structures were quantified with ImageJ. For each time point, results are expressed as percentage of the value at the initiation of DCV treatment (T0). For each condition, 30−50 cells were quantified. ****$P \leq .0001$; ***$P \leq .001$; **$P \leq .01$; *$P \leq .05$; ns (not significant) $P > .05$.

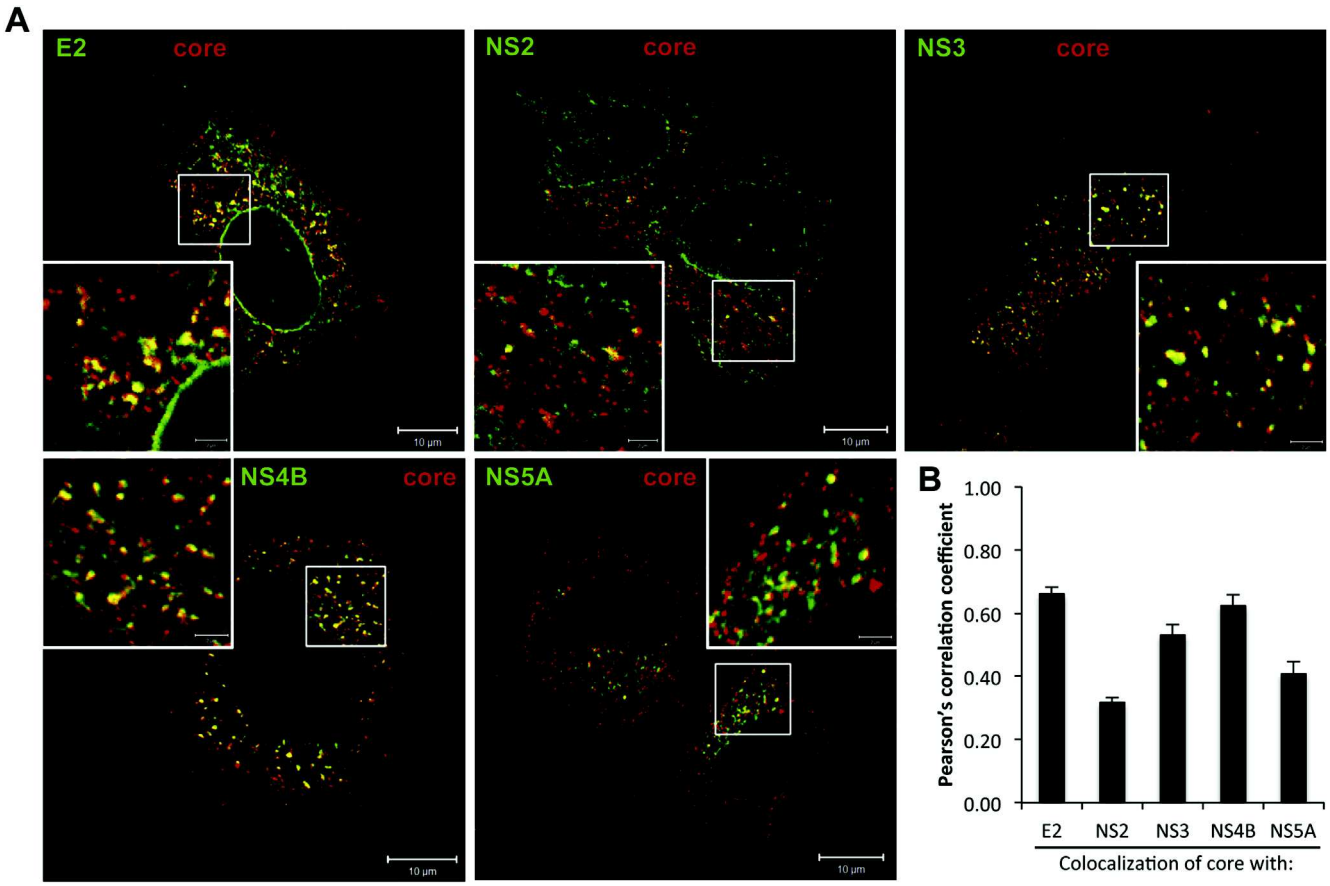

Supplementary Figure 3. Jc1 core punctate structures colocalize with E2 and elements of the replication complexes. Huh7.5 cells were infected with Jc1 virus at an MOI of 0.2, treated for 24 hours with 20 μg/mL CHX at 48 hours post-infection, and fixed at 72 hours post-infection. Cells were stained for HCV core and other viral proteins, as indicated. (*A*) Colocalization of core (*red channel*) with E2, NS2, NS3, NS4B, or NS5A (*green channel*) was analyzed by confocal microscopy. Scale bars of *panels* and *zooms* from *squared area* represent 10 μm and 2 μm, respectively. (*B*) The relative degree of colocalization of proteins was quantified by determining Pearson's correlation coefficients of 20 cells by using the JACoP plugin of ImageJ.

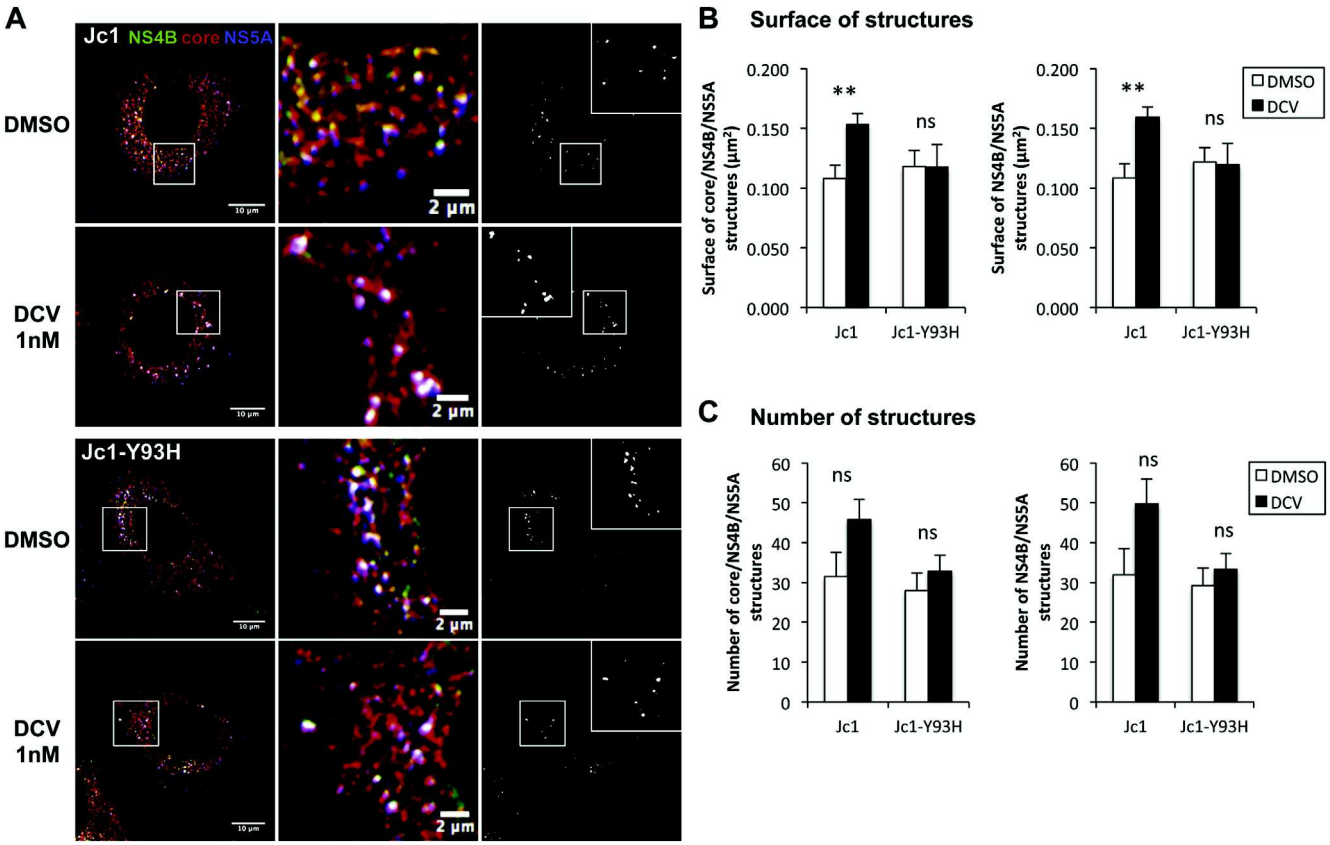

Supplementary Figure 4. DCV induces the clustering of core/NS4B/NS5A structures. Huh7.5 cells infected with Jc1 or Jc1-Y93H viruses (MOI = 0.2) were incubated at 66 hours post-infection with 1 nM DCV or dimethyl sulfoxide (DMSO) for 6 hours. (*A*) Cells were then stained for HCV core, NS4B, and NS5A proteins and the colocalization of core (*red channel*) with NS4B (*green channel*) and NS5A (*blue channel*) proteins were analyzed by confocal microscopy. Scale bars of *panels* and *zooms* from *squared area* represent 10 μm and 2 μm, respectively. Colocalized pixels (*white channel*) between *red*, *green*, and *blue* channels were extracted with the ColocalizeRGB plugin of ImageJ. (*B*) The surface and (*C*) number of core/NS4B/NS5A and NS4B/NS5A structures were quantified with ImageJ. For each condition, 30−50 cells were quantified. $^{****}P \leq .0001$; $^{***}P \leq .001$; $^{**}P \leq .01$; $^{*}P \leq .05$; ns (not significant) $P > .05$.

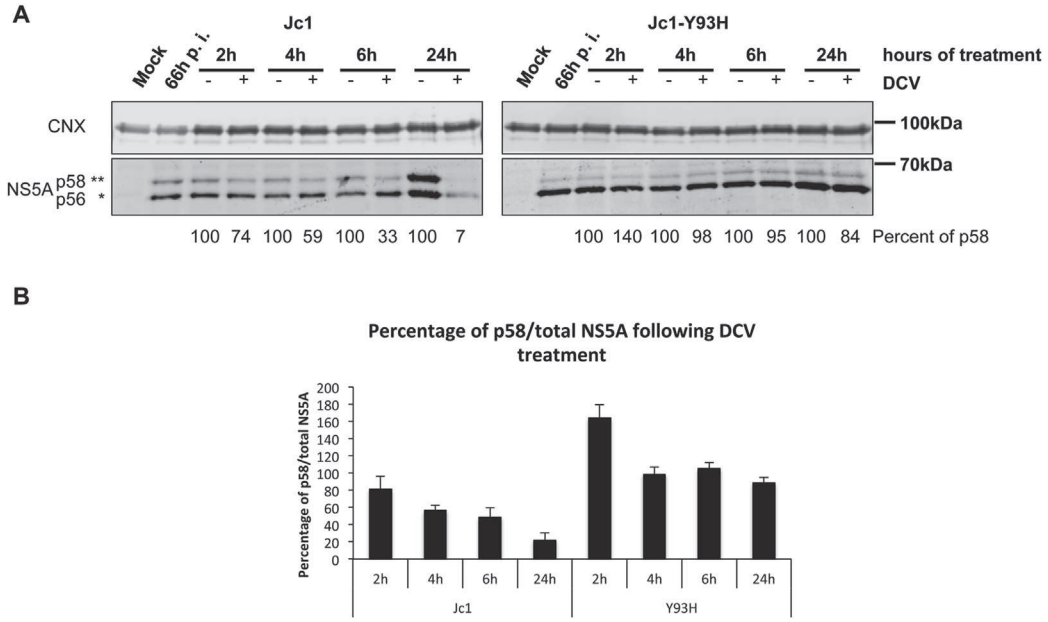

Supplementary Figure 5. Analysis of phosphorylated forms of NS5A. Huh7.5 cells were infected with Jc1 or Jc1-Y93H viruses at an MOI of 0.2. At 66 hours post-infection, cells were washed and incubated with 1 nM DCV or dimethyl sulfoxide (DMSO) for the indicated time. Infected cells were harvested at 2, 4, 6, or 24 hours after initiation of DCV treatment and expression of calnexin (CNX) and NS5A proteins was analyzed by Western blot. (*A*) A representative experiment is shown. The lower (*) and upper (**) NS5A bands correspond to basal (p56) and hyperphosphorylated (p58) forms of NS5A, respectively. The intensity of each band was quantified by densitometry with ImageJ. The ratio of p58/total NS5A normalized to the internal control calnexin (CNX) (designated % p58) is indicated below each lane. The values determined for mock-treated samples at each time point were set to 100%. (*B*) The means of the ratio of p58/total NS5A after DCV treatment from 3 independent experiments are shown.

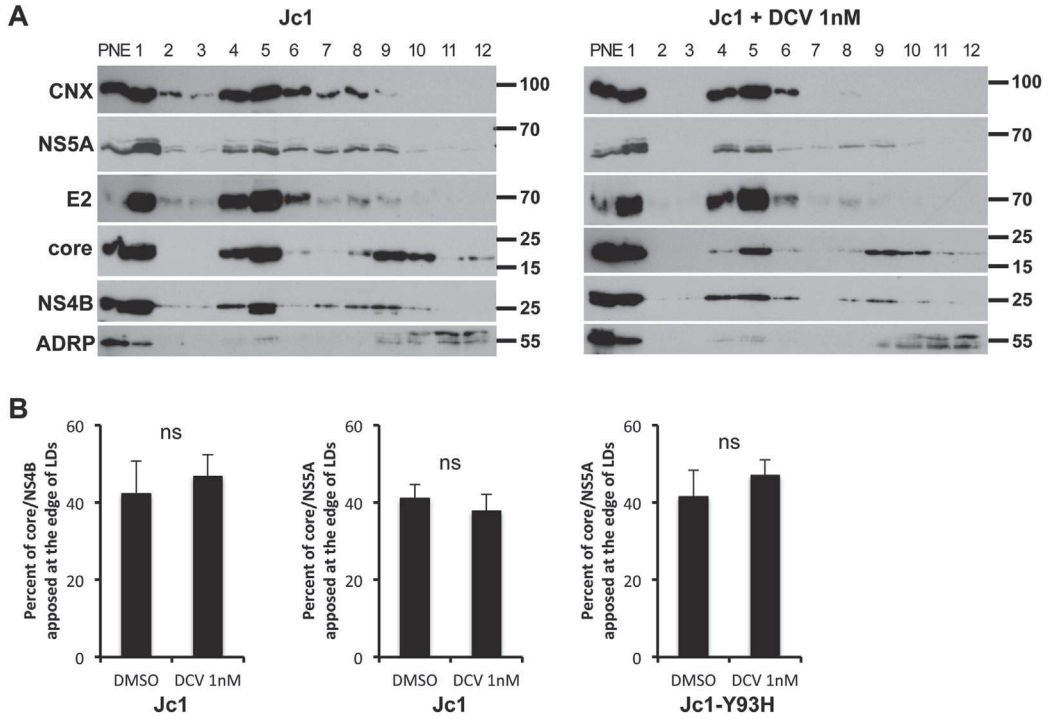

Supplementary Figure 6. Analysis of subcellular distribution of HCV proteins in Jc1-infected cells upon DCV treatment. (*A*) Huh7.5 cells transfected with Jc1 full-length genome RNA were incubated with 1 nM DCV or dimethyl sulfoxide (DMSO) at 66 hours post-transfection. Transfected cells were lysed at 6 hours after initiation of DCV treatment and were fractionated on iodixanol gradients. Each fraction was analyzed by Western blotting using antibodies against calnexin (CNX), HCV NS5A, E2, core and NS4B proteins, and adipose differentiation-related protein (ADRP). One-fiftieth of unfractionated post-nuclear extracts (PNE) were also analyzed. Results are representative of 5 independent experiments. (*B*) Huh7.5 cells were infected with Jc1 (*lefts panels*) or Jc1-Y93H (*right panel*) viruses at an MOI of 0.2. At 66 hours post-infection, infected cells were washed and incubated with 1 nM of DCV or DMSO. After 6 hours of DCV treatment, cells were fixed and then stained for HCV core, NS5A, and NS4B proteins and for LDs. Colocalization of core and NS4B or core and NS5A proteins with LDs was analyzed by confocal microscopy. The percentage of core/NS4B (*left panel*) or core/NS5A punctate structures apposed at the edges of LDs in Jc1 (*middle panel*) or Jc1-Y93H (*right panel*) infected cells were quantified with ImageJ. ns (not significant), $P > .05$.

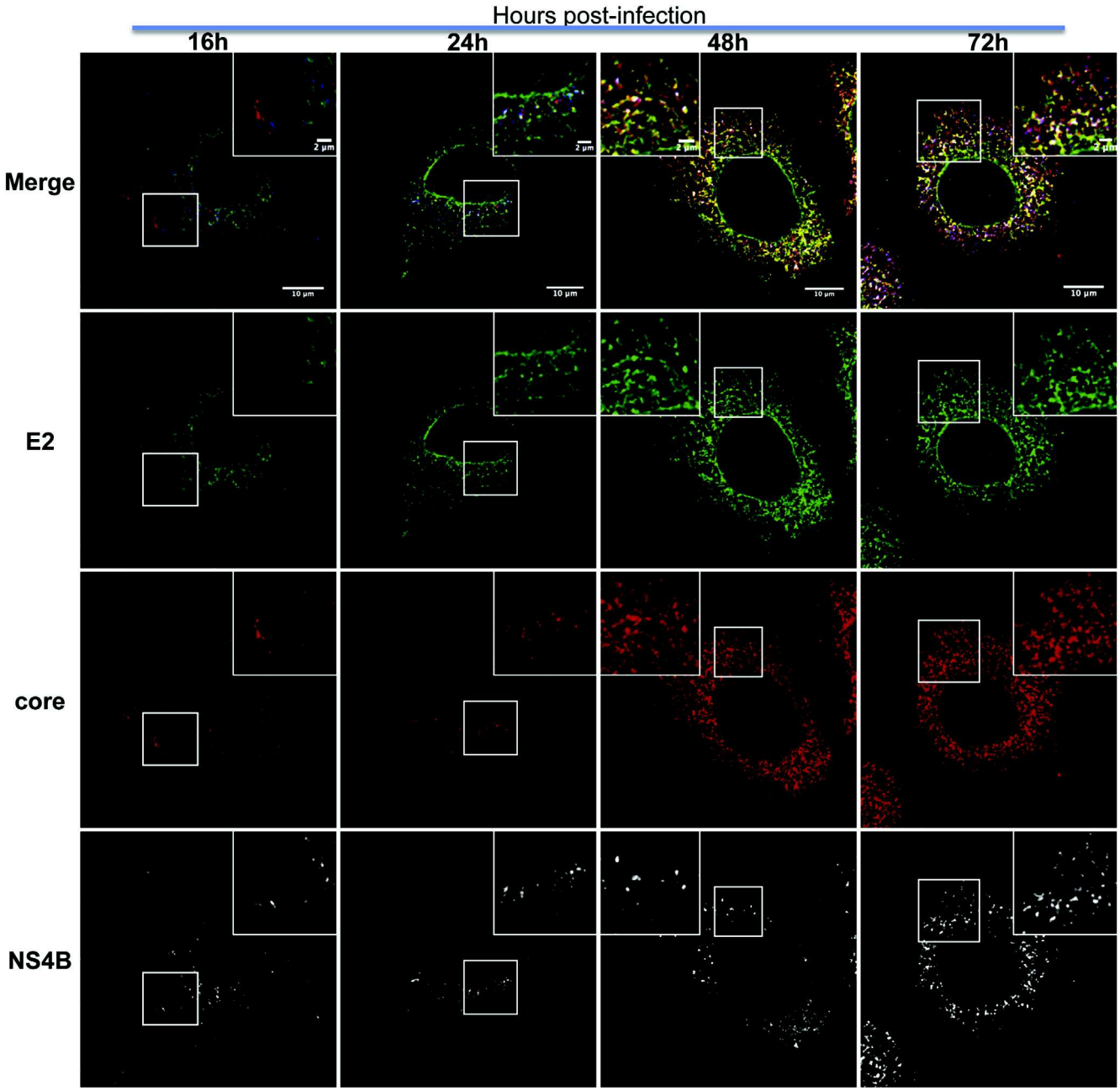

Supplementary Figure 7. Structural proteins and NS4B colocalize within discrete structures. Huh7.5 cells were infected with Jc1 at an MOI of 0.2 and were fixed at the indicated times post-infection. Cells were then stained for HCV E2, core, and NS4B proteins and the colocalization of core proteins with E2 and NS4B was analyzed by confocal microscopy. The merge of the 3 channels, as well as individual channels for E2, core, and NS4B proteins (*green*, *red*, and *white channel*, respectively) are represented. Scale bars of *panels* and *zooms* from *squared area* represent 10 μm and 2 μm, respectively.

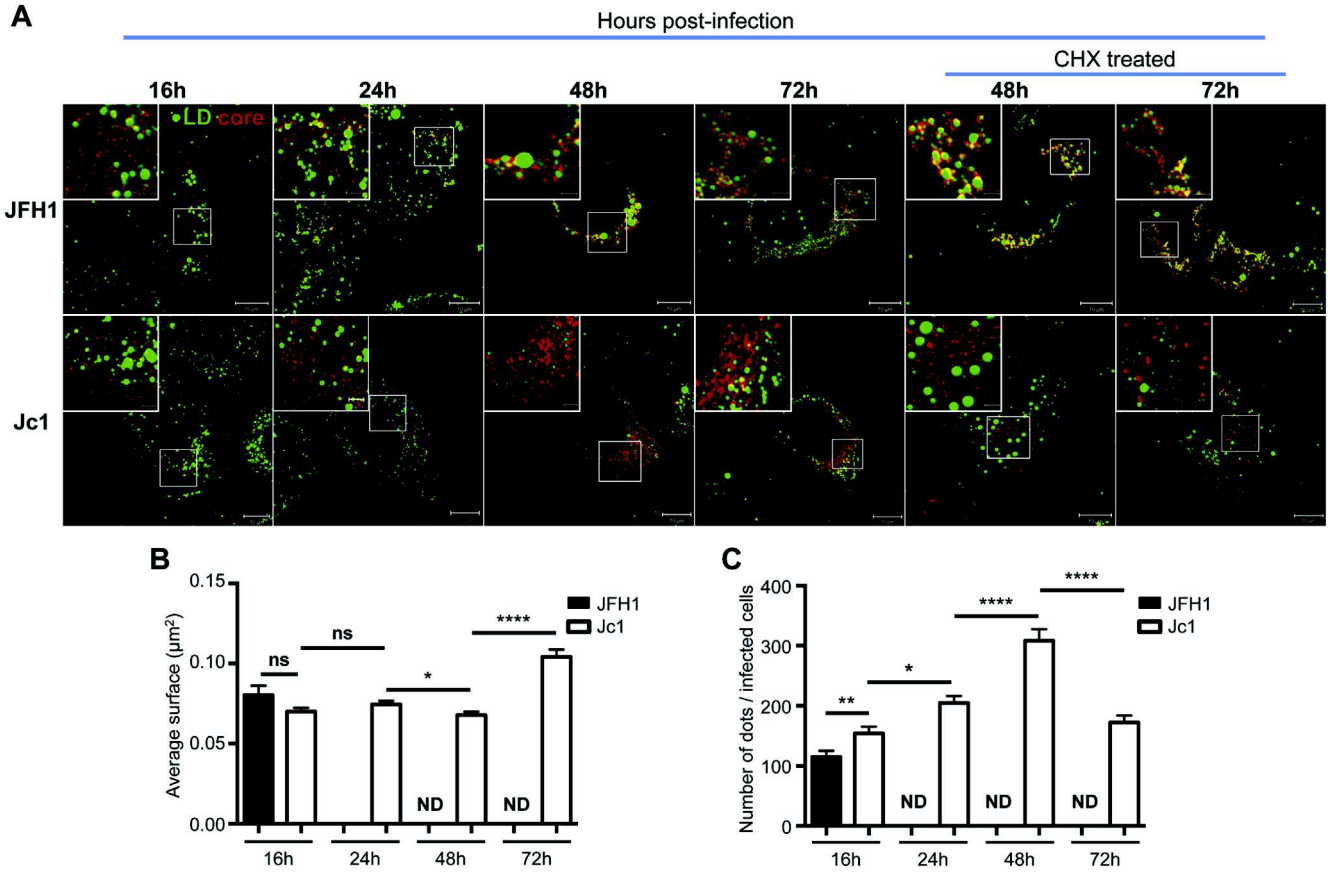

Supplementary Figure 8. Kinetics of HCV core distribution within infected cells. Huh7.5 cells were infected with JFH1 or Jc1 viruses at an MOI of 0.2 and cultured for the indicated time points with or without a 24-hour treatment with 20 μg/mL CHX from 24 hours or from 48 hours post-infection, as indicated. Cells were fixed at 16, 24, 48, or 72 hours post-infection, as indicated, and then stained for HCV core and LDs. (*A*) Colocalization of core protein (*red channel*) with LDs (*green channel*) was analyzed by confocal microscopy. Scale bars of *panels* and *zooms* from *squared area* represent 10 μm and 2 μm, respectively. (*B*) The size and (*C*) the number of core punctate structures in CHX-treated cells were quantified with ImageJ. For each condition, 30−50 cells were quantified. ****$P \leq .0001$; ***$P \leq .001$; **$P \leq .01$; *$P \leq .05$; ns (not significant) $P > .05$. ND, not determined.

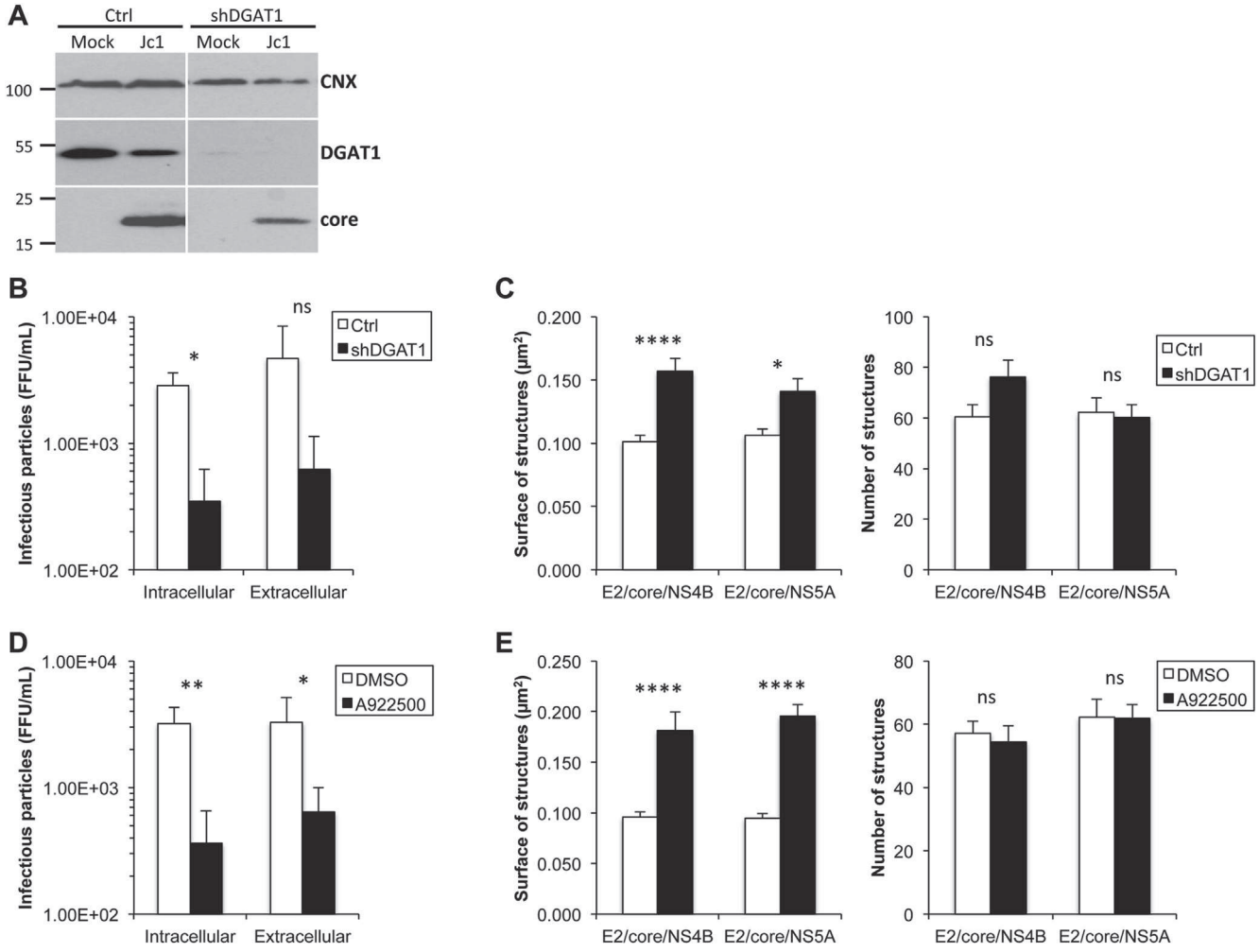

Supplementary Figure 9. DGAT1 down-regulation or inhibition induces the clustering of E2/core/NS4B and E2/core/NS5A structures. Huh7.5 cells were transduced with pLKO.1-puro empty vector (Ctrl) or with pLKO.1-puro vector with DGAT1 short-hairpin RNA (shDGAT1). Seven days post-transduction, down-regulated cells were infected with Jc1 virus at an MOI of 0.2. In separate experiments, Huh7.5 cells were infected with Jc1 virus at an MOI of 0.2 and treated with 150 μM of the DGAT1 inhibitor A922500 or dimethyl sulfoxide (DMSO). In both conditions, cells were fixed at 72 hours post-infection, stained for HCV E2, core and NS4B or NS5A proteins and the colocalization of core protein with E2 and NS4B or with E2 and NS5A was analyzed by confocal microscopy. (*A*) Expression of DGAT1 and calnexin (CNX) and core proteins at 72 hours post-infection was analyzed by Western blot. (*B*) The intracellular or extracellular infectivity were determined from cell lysates or supernatants of infected cells, respectively. (*C*) The surface (*left panel*) and the number (*right panel*) of E2/core/NS4B and E2/core/NS5A structures were quantified with ImageJ. (*D*) The intracellular or extracellular infectivity were determined from cell lysates or supernatants of infected cells, respectively. (*E*) The surface (*left panel*) and the number (*right panel*) of E2/core/NS4B and E2/core/NS5A structures were quantified with ImageJ. For each condition, 20 cells were quantified. $^{****}P \leq .0001$; $^{***}P \leq .001$; $^{**}P \leq .01$; $^{*}P \leq .05$; ns (not significant) $P > .05$.

IV- The amino-terminus of the hepatitis C virus (HCV) p7 viroporin and its cleavage from glycoprotein E2-p7 precursor determine specific infectivity and secretion levels of HCV particle types

Solène Denolly, Chloé Mialon, Thomas Bourlet, Fouzia Amirache, François Penin, Brett Lindenbach, Bertrand Boson, François-Loïc Cosset

Plos Pathogens 2017

PLOS | PATHOGENS

RESEARCH ARTICLE

The amino-terminus of the hepatitis C virus (HCV) p7 viroporin and its cleavage from glycoprotein E2-p7 precursor determine specific infectivity and secretion levels of HCV particle types

Solène Denolly[1], Chloé Mialon[1], Thomas Bourlet[2], Fouzia Amirache[1], François Penin[3], Brett Lindenbach[4], Bertrand Boson[1], François-Loïc Cosset[1]*

1 CIRI–International Center for Infectiology Research, Team EVIR, Inserm, U1111, Université Claude Bernard Lyon 1, CNRS, UMR5308, Ecole Normale Supérieure de Lyon, Univ Lyon, Lyon, France, **2** GIMAP, EA 3064, Faculté de Médecine, Université de Saint-Etienne, Univ Lyon, Saint Etienne, France, **3** IBCP—Institut de Biologie et Chimie des Protéines, MMSB, UMR 5086, CNRS, Univ Lyon, Lyon, France, **4** Department of Microbial Pathogenesis, Yale School of Medicine, New Haven, CT, United States of America

* flcosset@ens-lyon.fr

Citation: Denolly S, Mialon C, Bourlet T, Amirache F, Penin F, Lindenbach B, et al. (2017) The amino-terminus of the hepatitis C virus (HCV) p7 viroporin and its cleavage from glycoprotein E2-p7 precursor determine specific infectivity and secretion levels of HCV particle types. PLoS Pathog 13(12): e1006774. https://doi.org/10.1371/journal.ppat.1006774

Editor: Aleem Siddiqui, University of California, San Diego, UNITED STATES

Received: July 21, 2017

Accepted: November 27, 2017

Published: December 18, 2017

Data Availability Statement: All relevant data are within the paper and its Supporting Information files.

Funding: This work was supported by the French "Agence Nationale de la Recherche sur le SIDA et les hépatites virales" (http://www.anrs.fr), the European Research Council (ERC-2008-AdG-233130-HEPCENT) and the LabEx Ecofect (ANR-11-LABX-0048) (http://ecofect.universite-lyon.fr/)

Abstract

Viroporins are small transmembrane proteins with ion channel activities modulating properties of intracellular membranes that have diverse proviral functions. Hepatitis C virus (HCV) encodes a viroporin, p7, acting during assembly, envelopment and secretion of viral particles (VP). HCV p7 is released from the viral polyprotein through cleavage at E2-p7 and p7-NS2 junctions by signal peptidase, but also exists as an E2p7 precursor, of poorly defined properties. Here, we found that ectopic p7 expression in HCVcc-infected cells reduced secretion of particle-associated E2 glycoproteins. Using biochemical assays, we show that p7 dose-dependently slows down the ER-to-Golgi traffic, leading to intracellular retention of E2, which suggested that timely E2p7 cleavage and p7 liberation are critical events to control E2 levels. By studying HCV mutants with accelerated E2p7 processing, we demonstrate that E2p7 cleavage controls E2 intracellular expression and secretion levels of nucleocapsid-free subviral particles and infectious virions. In addition, our imaging data reveal that, following p7 liberation, the amino-terminus of p7 is exposed towards the cytosol and coordinates the encounter between NS5A and NS2-based assembly sites loaded with E1E2 glycoproteins, which subsequently leads to nucleocapsid envelopment. We identify punctual mutants at p7 membrane interface that, by abrogating NS2/NS5A interaction, are defective for transmission of infectivity owing to decreased secretion of core and RNA and to increased secretion of non/partially-enveloped particles. Altogether, our results indicate that the retarded E2p7 precursor cleavage is essential to regulate the intracellular and secreted levels of E2 through p7-mediated modulation of the cell secretory pathway and to unmask critical novel assembly functions located at p7 amino-terminus.

to FLC. SD was supported by a fellowship of the French "Agence Nationale de la Recherche sur le SIDA et les hépatites virales" (http://www.anrs.fr). The funders had no role in study design, data collection and analysis, decision to publish, or preparation of the manuscript.

Competing interests: The authors have declared that no competing interests exist.

Author summary

Viroporins are small transmembrane viral proteins with ion channel activities modulating properties of intracellular membranes, which impacts several fundamental biological processes such as trafficking, ion fluxes as well as connections and exchanges between organelles. Hepatitis C virus (HCV) encodes a viroporin, p7, acting during assembly, envelopment and secretion of viral particles. HCV p7 is produced by cleavage from the HCV polyprotein but also exists as an E2p7 precursor, of poorly defined properties. In this study, we have explored how the retarded cleavage between E2 glycoprotein and p7 viroporin could regulate their functions associated to virion assembly and/or perturbation of cellular membrane processes. Specifically, we demonstrate that p7 is able to regulate the cell secretory pathway, which induces the intracellular retention of HCV glycoproteins and favors assembly of HCV particles. Our study also identifies a novel assembly function located at p7 amino-terminus that is unmasked through E2p7-regulated processing and that controls the infectivity of different types of released viral particles. Altogether, our results underscore a critical post-translational control of assembly and secretion of HCV particles that governs their specific infectivity.

Introduction

Hepatitis C virus (HCV) infection is a major cause of chronic liver diseases worldwide. With 180 million people persistently infected, chronic HCV infection induces liver diseases such as liver cirrhosis and hepatocellular carcinoma. Although new direct antiviral agents are now able to eradicate the virus in most patients, no protective vaccine currently exists against HCV and it remains major challenges in basic, translational and clinical research [1, 2].

HCV is a plus-strand RNA enveloped virus. Its genome is translated as a single polyprotein that is processed by cellular and viral proteases in 10 mature viral proteins [3] consisting of: i) an assembly module (core-E1-E2-p7-NS2) encompassing the capsid protein (core) as well as the E1 and E2 surface glycoproteins that are incorporated in viral particles, and the p7 and NS2 proteins that support virion assembly, and ii) a replication module encompassing the nonstructural proteins NS3, NS4A, NS4B, NS5A and NS5B that are sufficient to support viral RNA replication but that also contribute to virion production through ill-defined processes. As HCV proteins arise from a shared polyprotein, several post-translational modifications control their expression rates within infected cells. In addition, at least three precursors, *i.e.*, tandem proteins with delayed cleavage, are also detected and may implement functions different than their cognate individual proteins. They consist of immature core protein, associated to the D3 trans-membrane peptide, whose removal allows core targeting to lipid droplets (LDs) [4, 5]; NS4B-5A, which promotes the formation of replication vesicles [6]; and E2p7 [7–11], whose properties are explored in this report.

Assembly of viral particles occurs at endoplasmic reticulum (ER)-derived membranes in close proximity to LDs and virus replication complexes [12], with NS2 and p7 being key players in gathering virion components [13–17]. Particularly, NS2 associates with E1E2 glycoproteins and NS3 as well as with NS5A, which interacts with HCV RNA and core [18–20] and promotes genome encapsidation. Virion assembly begins with the formation of a nucleocapsid, formed by core/RNA complex, and is coupled with its envelopment and acquisition of the E1E2 glycoproteins as well as lipids and apolipoproteins [18, 21]. The pathway of secretion of virions remains to be elucidated and may occur through a non-canonical route [22, 23]. Of note, HCV produces different types of particles in addition to infectious virions, including

nucleocapsid-free subviral particles [24, 25], E2-containing exosome vesicles [26, 27], naked nucleocapsids [28], and a range of more or less lipidated infectious viral particles [29]; yet, the regulation of their production is poorly understood.

The p7 protein is a small, 63 amino-acid-long protein, consisting of a "hairpin-like" topology involving three helices inducing two trans-membrane segments connected by a hydrophilic, positively-charged cytosolic loop [30–32], though alternative folds and topologies have been proposed [33–35], *e.g.*, with the p7 C-terminus exposed to the cytosol [33]. As it is able to form an ion channel in either hexameric or heptameric form [30, 35, 36] exhibiting a funnel- or flower-like shape [35, 37], it was classified as a viroporin, like M2 of influenza virus [38]. Importantly, p7 is dispensable for replication but essential for both assembly and secretion of infectious particles [11]. First, p7 modulates the formation of NS2 complexes with E2, NS3 and NS5A [9, 13, 14, 16, 39], allowing clustering of assembly components and regulation of early assembly events. Second, p7 allows, in concert with NS2, the regulation of core localization at lipid droplets *vs*. ER-derived membranes [17], from where viral particles are released in the secretory pathway. Third, p7 modulates the envelopment of nascent virions [40]. Fourth, p7 may regulate the pH of some intracellular compartments, which could be essential for the protection and secretion of infectious particles [41, 42].

A recent study indicated that residues of the first helix of p7 that are predicted to point toward the channel pore are important for assembly [10]. Noteworthy, viroporin ion channel activities modulate properties of intracellular membranes and, thereby, impacts several fundamental biological processes such as trafficking, ion fluxes as well as connections and exchanges between organelles [38, 43]. While several biophysical studies showed that p7 can change ionic gradients in reconstituted membrane assays *in vitro* [30, 44–47], few reports have addressed the relevance of such properties *in cellulo* [41, 42, 48, 49], although, by analogy with viroporins from alternative viruses, this may have diverse proviral functions [38]. For example, the 2B viroporin from coxsackievirus modulates calcium homeostasis, which leads to the suppression of apoptotic host cell responses [50]. Likewise, p7 may promote immune evasion by antagonizing the antiviral IFN function [51].

Interestingly, while p7 is released from the viral polyprotein through cleavage at E2-p7 and p7-NS2 junctions by the cellular signal peptidase [7, 52], it also exists in infected cells as an E2p7 precursor of poorly defined properties [7–11]. Intriguingly, virus mutants that exhibit either only E2p7 precursor (*i.e.*, using a point mutation in E2-p7 cleavage site) or, conversely, no E2p7 expression (*i.e.*, using an IRES sequence between E2 and p7) are both impaired for production of infectious particles [9, 14, 39, 53], suggesting that timely liberation of E2 and/or p7 are critical events for assembly/release of HCV particles.

Here, we explored how the retarded cleavage between E2 and p7 could regulate their functions associated to virion assembly and/or perturbation of cellular membrane processes. We demonstrate that p7 is able to regulate the cell secretory pathway, which induces intracellular retention of HCV glycoproteins, and to control release of nucleocapsid-free subviral and infectious viral particles. Specifically, through biochemical, imaging and functional analysis of a series of mutant viruses with modified E2-p7 junction as well as through p7 transcomplementation assays, our data uncover different mechanisms by which p7 regulates the proportion of different types of secreted HCV particles and determines their specific infectivity.

Results

HCV p7 inhibits the cell secretory pathway and induces E2 intracellular retention

As HCV p7 is released through inefficient E2p7 cleavage, we first sought to address its function by increasing its expression levels in HCV-infected cells. We found that co-expression of

individual p7 with JFH1 HCVcc RNAs in Huh7.5 hepatoma cells decreased the levels of extracellular particle- associated E2 proteins, resulting in *ca*. 3-fold reduced secretion (Fig 1A).

Since some viroporins from alternative viruses alter the canonical secretory pathway [38, 43], we then asked whether p7 could impact the secretion of VSV-G tsO45 (VSV-Gts), a temperature-dependent folding mutant of VSV-G glycoprotein commonly used as model cargo of protein secretion [54]. At 40˚C, this protein remains unfolded, resulting in its accumulation in the ER, whereas its folding can be restored at 32˚C, which allowed its transfer from the ER to the Golgi and then the plasma membrane (Fig 1C). We transfected in Huh-7.5 cells VSV-Gts with p7 constructs from different HCV strains and using different signal peptide configurations, which resulted in *ca*. 60% of cells co-expressing both proteins among the transfected cells (Fig 1B). As monitored by flow cytometry analysis, p7 co-expression significantly reduced the kinetics and levels of VSV-Gts cell surface expression at permissive temperature of 32˚C (Fig 1C).

Next, to address how p7 alters traffic through the secretory pathway, we measured the resistance of intracellular VSV-Gts to endoH digestion, used as a marker of ER-to-Golgi traffic [54, 55]. While at 0h, all VSV-Gts glycans remained endoH-sensitive, reflecting ER retention at 40˚C, they progressively became resistant to endoH cleavage upon 1-3h incubation at 32˚C (Fig 1D–1F), underscoring VSV-Gts transfer to the Golgi apparatus. Importantly, p7 co-expression resulted in dose-dependent decrease of the kinetics of VSV-Gts endoH-resistance (Fig 1D–1F), in a manner similar to influenza virus M2 (Fig 1E), indicating that p7 slowed down the rate of VSV-Gts ER-to-Golgi traffic or, alternatively, favored its retention in the ER. We noticed that p7 proteins from different HCV genotypes/strains mediated this effect (Fig 1E) with that of H77 strain appearing less efficient for inhibiting Golgi transfer. We also found that p7 associated to its own signal-peptide, *i.e*., the E2 amino-terminus (ΔE2p7 construct), induced the strongest VSV-Gts ER retention.

We then thought that p7-mediated alteration of the secretory pathway could induce the retention of HCV glycoproteins at ER membranes, which may favor assembly of HCV particles [21]. Thus, we expressed E1E2 glycoproteins, alone or with p7, to promote their secretion in the cell supernatant as subviral particles (SVP), *i.e*., nucleocapsid-free enveloped particles [24], that peaked at a buoyant density of *ca*. 1.05–1.06 g/ml (Fig 1G). As detected by E2 immunoblots from the pellets after ultracentrifugation of the cell supernatants (Fig 1H and 1I), we found that p7 co-expression induced up to 60% increase of E2 intracellular expression and concomitant 55% decrease of SVP release (Fig 1H). This resulted in a *ca*. 2–3 fold reduced E2 secretion (Fig 1I), which, combined with the results of Fig 1A, indicates that p7 can induce the retention of HCV glycoproteins.

p7 N-terminal alterations that accelerate E2p7 cleavage inhibit HCV infectivity

By controlling the release of free p7, E2p7 cleavage efficiency may adjust the levels of p7 expression, which could regulate the extent by which p7 slows down the cell secretory pathway and, concomitantly, the traffic and thus secretion of HCV E2 glycoproteins (Fig 1A, 1H and 1I). Hence, we introduced mutations at the E2-p7 junction in Jc1 and/or JFH1 viruses in order to design HCVcc mutants that exhibit increased E2p7 cleavage scores (Fig 2A), as predicted by SignalP method (http://www.cbs.dtu.dk/services/SignalP/). This strategy was preferred over the use of an IRES sequence between E2 and p7, as reported before [9, 10, 14], because it induces a natural, *i.e*., signal peptidase-mediated liberation of p7 from the HCV polyprotein. First, we inserted linkers of various sizes at the N-terminus of p7 (HAHALp7 and ASGGSp7 viruses), which left p7 sequence unchanged; the former linker consisting of a double HA tag

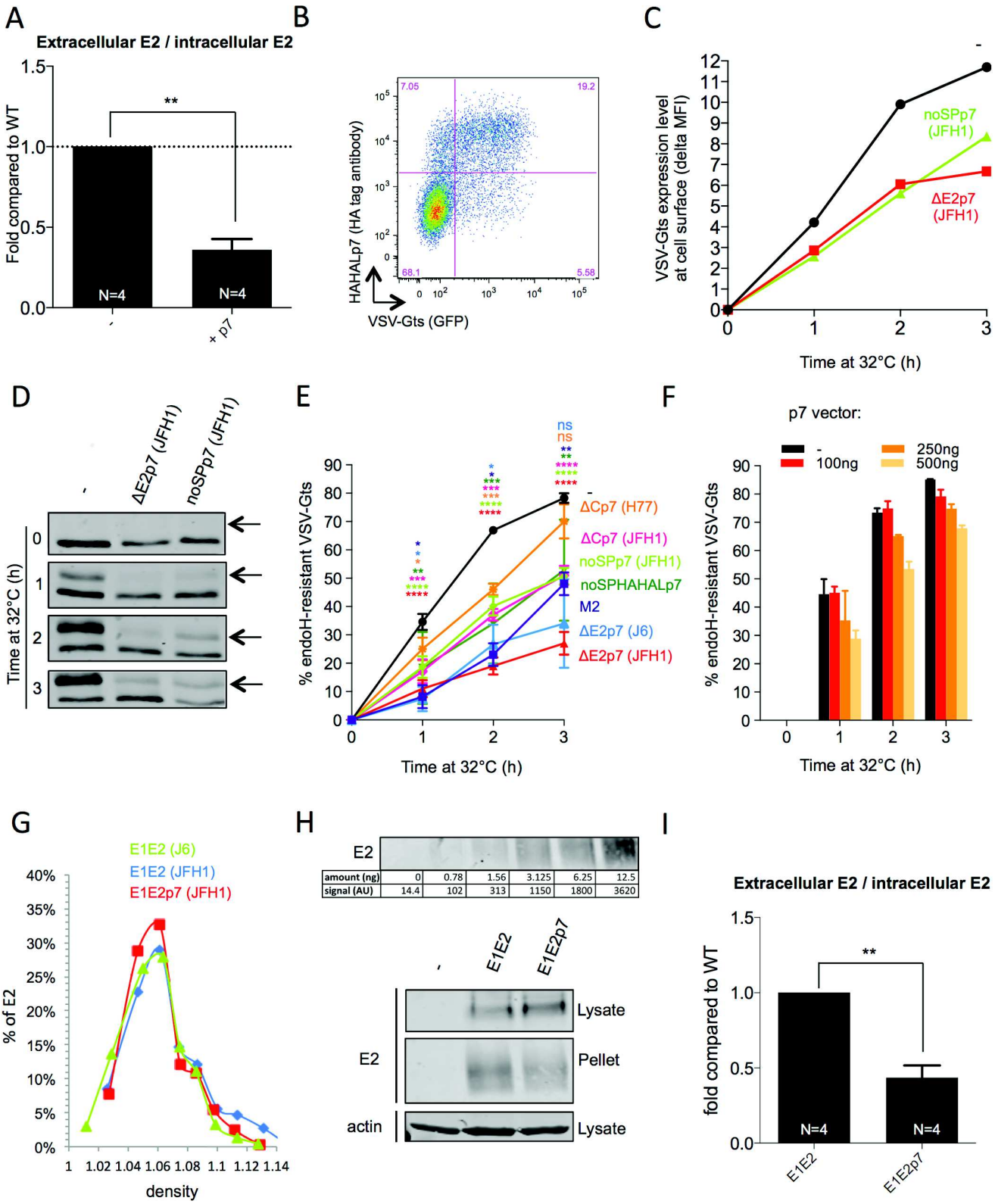

Fig 1. HCV p7 inhibits the cell secretory pathway. (A) Ratio of extra- *vs.* intra-cellular HCV E2 glycoprotein determined by western blot analysis of cell lysates and of pellets of ultracentrifuged supernatants from Huh7.5 cells co-electroporated with Jc1 HCVcc RNAs and p7-expression (+ p7)

or control (-) vectors, at 72h post-electroporation. (**B**) Intracellular expression of VSV-Gts-GFP fusion protein (VSV-Gts) and HA-tagged p7 assessed by flow cytometry, at 24h post-transfection. **(C)** Cell surface expression of VSV-Gts assessed by flow cytometry, using the 41A1 mAb directed against VSV-G ectodomain, after co-transfection of Huh7.5 cells with vectors encoding VSV-Gts and p7 (JFH1) expressed with the end of E2 (ΔE2p7) or no signal peptide (noSPp7). Transfected cells were grown overnight at 40˚C, which maintains VSV-Gts unfolded and results in its accumulation in the ER. Cells were then incubated for different periods of time (0h, 1h, 2h and/or 3h, as indicated) at 32˚C, which allows restoration of its folding and thus, its secretion. The values represent the variations of the mean fluorescence intensity (delta MFI) of cell surface-expressed VSV-Gts relative to time 0h at 32˚C. **(D)** Representative western blot analysis of cell lysates co-expressing VSV-Gts and p7, digested with endoH glycosidase. Cells were grown overnight at 40˚C and lysed at different time points after incubation at 32˚C. The endoH-resistant VSV-Gts species (arrows) indicates proteins that traffic to and beyond the Golgi apparatus. **(E)** Quantification of western blot from independent experiments performed as described in (**D**) after co-transfection of VSVG-ts with different p7 or with influenza H7N1 M2 [97] protein-expressing constructs, as indicated. The values indicate the mean percentages of endoH-resistant VSV-Gts relative to total VSV-Gts for each time point. (**F**) p7 dose-dependence induction of endoH-resistance of VSV-Gts. **(G)** Representation of HCV E2 glycoprotein profile (expressed as percentage of total E2) in 3–40% iodixanol density gradients of subviral particles (SVP) produced after transduction of Huh7.5 cells with lentiviral vectors allowing the expression of either E1E2 or E1E2p7 proteins from J6 and/or JFH1 viruses. **(H)** Representative western blot of E2 detected with 3/11 antibodies in lysates and pellets of ultracentrifuged supernatants from cells producing SVPs (JFH1 strain). A range of dilutions of sE2 purified to homogeneity were run in parallel to the same western blot shown here. The intensity of E2 signals and the amounts of E2 are indicated. **(I)** Ratio of extra- *vs*. intra-cellular HCV E2 glycoprotein determined by quantification of western blots from independent experiments as described in (**H**). Data represent mean values ± SEM. The numbers of experiments performed are indicated below the graphs.

https://doi.org/10.1371/journal.ppat.1006774.g001

allowing the detection of p7 [56]. Second, we introduced a substitution at position 2 of p7 (p7-L2S). Third, we generated p7 mutants having insertions of a single residue, either a threonine (p7-T2) at position 2 [8] or an alanine (Ap7) at position 1 of p7 (Fig 2A). None of these mutations–termed hereafter p7 ATMI (Amino-Terminus Membrane Interface) mutants, introduced before the first p7 helix (shown as grey box in Fig 2A) [30, 35, 36], are expected to change p7 structure or opening of its channel pore, as shown by molecular modeling (S1 Fig). Of note, we could not identify mutations at E2 carboxy-terminus that accelerated E2p7 cleavage. Finally, we also introduced a control mutation abrogating E2p7 cleavage (E2-A367R; Fig 2A) [9].

Next, we investigated the rate of E2p7 cleavage by treating lysates of Huh-7.5 cells expressing mutant virus RNAs with EndoH to remove E2 glycans, which improved E2 *vs*. E2p7 electrophoretic separation (Fig 2B and 2C). Except for the E2-A367R mutant that was not cleaved, as expected, all mutants displayed almost complete E2p7 cleavage, which compared to the *ca*. 40% and 50% uncleaved E2p7 precursor detected with parental Jc1 and JFH1 viruses, respectively. Using a HA-tag antibody to reveal the HAHALp7 protein, we confirmed that the accelerated cleavage detected for the JFH1 HAHALp7 and Jc1 HAHALp7 viruses induced the release of p7 at the expected molecular size with poor if not undetectable E2p7 (*i.e.*, E2HAHALp7) expression (Fig 2D), though such analysis could not be extended to the other p7 ATMI mutants owing to the unavailability of antibodies against native p7. In addition, as previously reported [8, 11], we also detected small amounts of E2p7NS2 precursor for both wt and mutant viruses (Fig 2D; S2A Fig).

Interestingly, when we investigated the infectivity of these mutant viruses, we found that, relative to parental viruses, the p7 ATMI mutant viruses had decreased extracellular infectivity, by *ca*. 3-fold to over 100-fold (Fig 2E), depending on the p7 modifications and the virus backbones (Fig 2A). Particularly, the Ap7 insertion and the p7-L2S substitution mutants in JFH1 virus induced *ca*. 3- and 10-fold decreased infectivity, respectively, whereas the p7-T2, ASGGSp7, and HAHALp7 JFH1 insertion mutants exhibited complete loss of infectivity (Fig 2E). Likewise, the Jc1 HAHALp7 mutant virus displayed a 10–20 fold reduced infectivity, as compared to parental virus (Fig 2E). Similar defects were observed for intracellular infectivity (Fig 2E), indicating that these p7 ATMI mutant viruses were not impaired at the stage of secretion of viral particles. Finally, we found that co-expression of wt p7 (though not mutant p7 such as HAHALp7) restored the production of both extracellular and intracellular infectious particles to levels detected for wt viruses (Fig 2F and 2G; S2B Fig). Hence, since all p7 ATMI

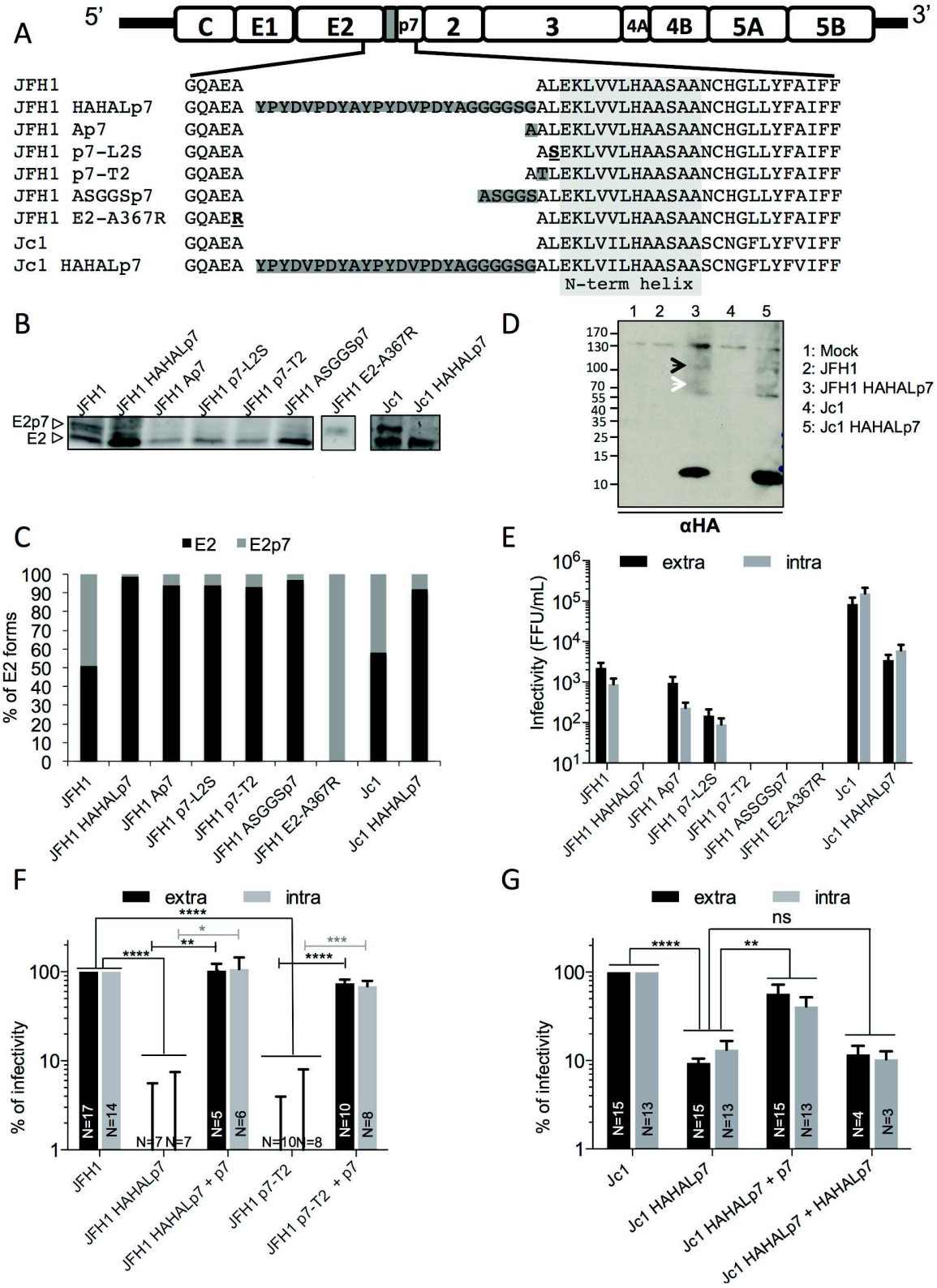

Fig 2. HCVcc mutants with modified p7 amino-termini prevent infectivity. (A) Schematic representation of JFH1 and Jc1 HCVcc mutants in E2-p7 junction. The first helix of p7 is shown in the light grey box. The insertions of residues are shown in dark

grey and the substitutions are underlined. (**B-D**) Western blot analysis of Huh7.5 cells electroporated with RNAs from HCVcc viruses encoding wild-type or E2p7 cleavage mutants. **(B)** At 72h post-electroporation, cells were lysed and digested with endoH glycosidase before western blotting using 3/11 antibodies against E2. **(C)** The relative ratios of E2p7 precursors *vs*. free E2 species are indicated. **(D)** The HAHALp7 protein and the E2HAHALp7 (white arrows) and E2HAHALp7NS2 (black arrows) precursors were revealed using an HA tag antibody in lysates of cells electroporated with the indicated HCVcc constructs. **(E)** The extracellular (black) and intracellular (grey) infectivity levels for all mutants are represented. **(F)** The extracellular (black) and intracellular (grey) infectivity levels, normalized after determining the proportion of HCV-positive virus producer cells (see Fig 3A), of JFH1 HAHALp7 or p7-T2 mutant viruses expressed alone or with wild-type p7 (+ p7) are represented relative to infectivity of parental JFH1 virus. **(G)** The extracellular (black) and intracellular (grey) infectivity levels, normalized by determining the proportion of HCV-positive virus producer cells, of Jc1 HAHALp7 mutant virus expressed alone or with wild-type p7 or HAHALp7, as indicated, are represented relative to infectivity of parental Jc1 virus. Data are displayed as means ± SEM. The numbers of experiments performed are indicated below the graphs.

https://doi.org/10.1371/journal.ppat.1006774.g002

mutants displayed nearly complete E2p7 cleavage (Fig 2B and 2C) and since HAHALp7 co-expressed with mutant viruses did not restore infectivity (Fig 2G), these results indicated that the integrity of the N-terminal end of p7 itself is crucial for assembly of infectious particles.

Thus, in the subsequent experiments, we compared more particularly the Jc1 HAHALp7 virus to its parental Jc1 counterpart since this mutant retained some infectivity levels, which allowed us to further characterize this novel phenotype; yet, the most salient results described below could be extended to the other p7 ATMI mutant viruses (see supplemental figure set).

p7 modulates the expression and secretion of HCV particle components

Since p7 ATMI mutant viruses displayed augmented E2p7 cleavage rates (Fig 2), we wondered whether they had altered E2 expression levels. As compared to wt viruses, we observed a 2–3 fold increased intracellular expression of total E2 (*i.e.*, free E2 + E2p7) for all mutant viruses exhibiting increased E2p7 cleavage (Fig 3A–3C; S3A Fig). No modification of E2 half-life could be detected for mutant *vs*. wt virus (S3C Fig). Specifically, taking into account that *ca*. 40% E2 was detected as E2p7 precursor for wt JC1 virus (Fig 2B and 2C), we estimated that the actual ratio of free E2 expression for mutant *vs*. wt viruses is *ca*. 4–5 fold. We also found that core expression was increased by *ca*. 1.5–2 fold (Fig 3B and 3D; S3B Fig), whereas expression levels of NS2 and NS5A non-structural proteins (Fig 3B and 3D) were unchanged. As similar results were obtained for all p7 ATMI mutant viruses, this indicated that these mutations modulated the expression levels of structural proteins without altering viral replication and/or translation. Importantly, co-expression of either wt p7 or HAHALp7 did not revert E2 expression to wt levels (Fig 3B and 3C), which indicated that increased E2p7 cleavage (rather that p7 N-terminus modification *per se*) induce up-regulation of E2 glycoproteins.

Next, we hypothesized that the increased expression of structural proteins could be due to a blockage of their secretion, which may also explain the losses of mutant virus infectivity (Fig 2E–2G). Thus, we quantified the total secretion of virion components, *i.e*., E2 glycoproteins, core and viral RNAs, in the supernatants of cells expressing p7 ATMI mutant virus relative to wt virus (Fig 4). Using immuno-precipitation (IP) assays of cell supernatants with GNA lectins, which bind glycans present on HCV E1E2 glycoproteins [57], we detected a *ca*. 4–5 fold increased secretion of E2 protein (Fig 4A), which matched the 4–5 fold elevated levels of intracellular free E2 (Fig 3C, combined with Fig 2B and 2C). Although the ratio of extracellular *vs*. total intracellular E2 expression levels indicated a 2–3 fold difference between wild-type and mutant viruses (Fig 4D), taking into account that 40% of intracellular E2 species were in the form of non-secreted E2p7, we deduced identical ratios of extracellular *vs*. intracellular free E2 for wt and mutant viruses. Similar results were obtained for the other p7 ATMI mutants (S4A Fig), suggesting that the increased E2 secretion from cells expressing the p7 ATMI mutant viruses is directly linked to the augmented intracellular E2 expression. As co-expression of p7

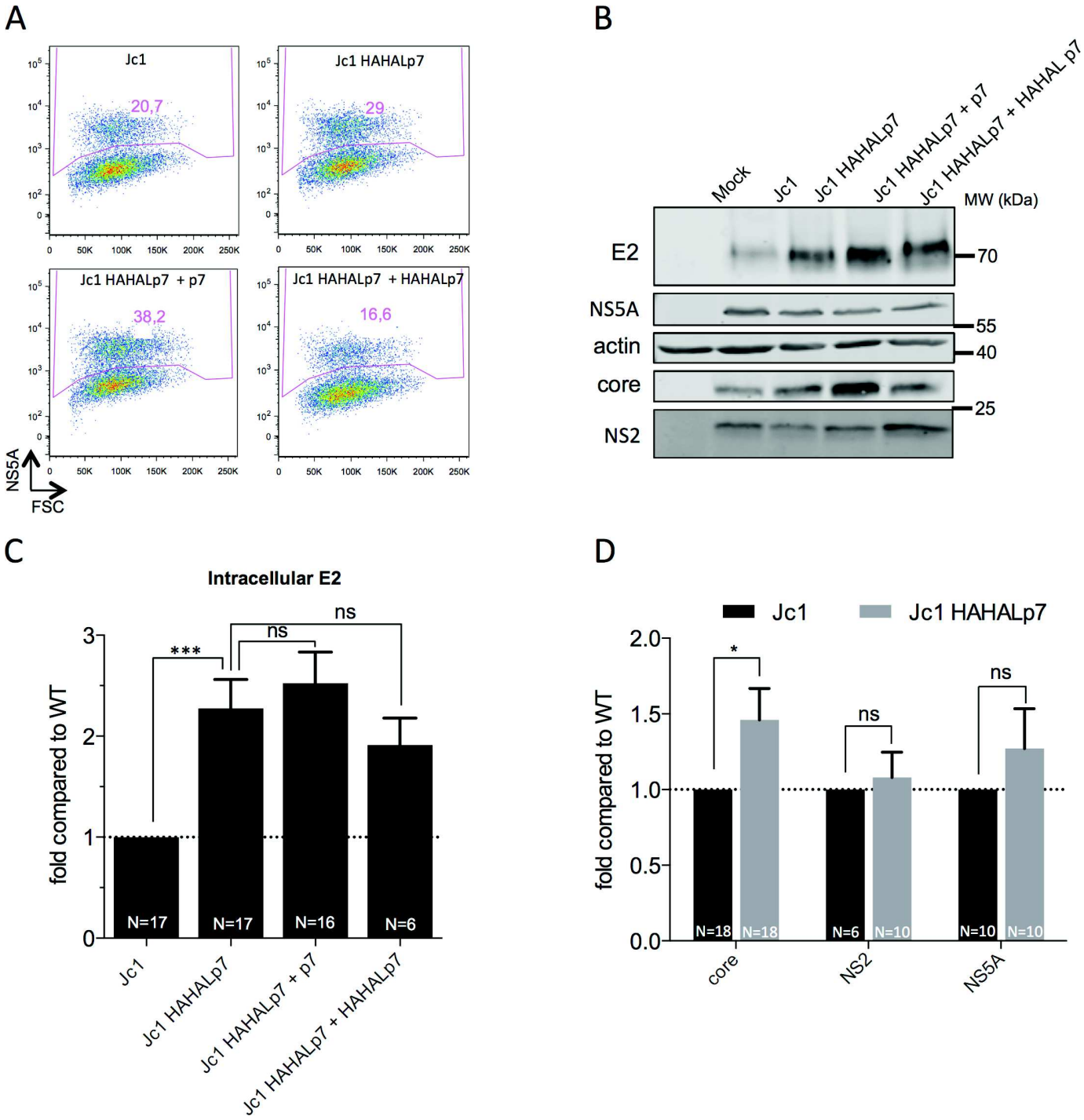

Fig 3. p7 ATMI mutant viruses increase the expression levels of HCV structural proteins. Huh7.5 cells were electroporated with RNAs from parental or Jc1 HAHALp7 mutant viruses expressed alone or with wild-type p7 or HAHALp7. Analyses were performed at 72h post-electroporation. Results obtained with other p7 ATMI mutant viruses are shown in S3 Fig. **(A)** Flow cytometry analysis of HCVcc-expressing cells with NS5A antibody used to determine the proportion of HCV-positive virus producer cells. **(B)** Representative western blot analysis of cell lysates using antibodies against the indicated proteins. **(C)** Quantification of intracellular E2 levels. **(D)** Quantification of intracellular levels of core, NS2 and NS5A proteins. **(C-D)** Proteins were quantified and normalized after determining the proportion of HCV-positive virus producer cells (as determined in (**A**)) and the amounts of cellular actin. The values are displayed relative to expression of E2, core, NS2 and NS5A in Jc1 HCVcc RNA-electroporated cells. Data represent mean values ± SEM. The numbers of experiments performed are indicated below the graphs.

https://doi.org/10.1371/journal.ppat.1006774.g003

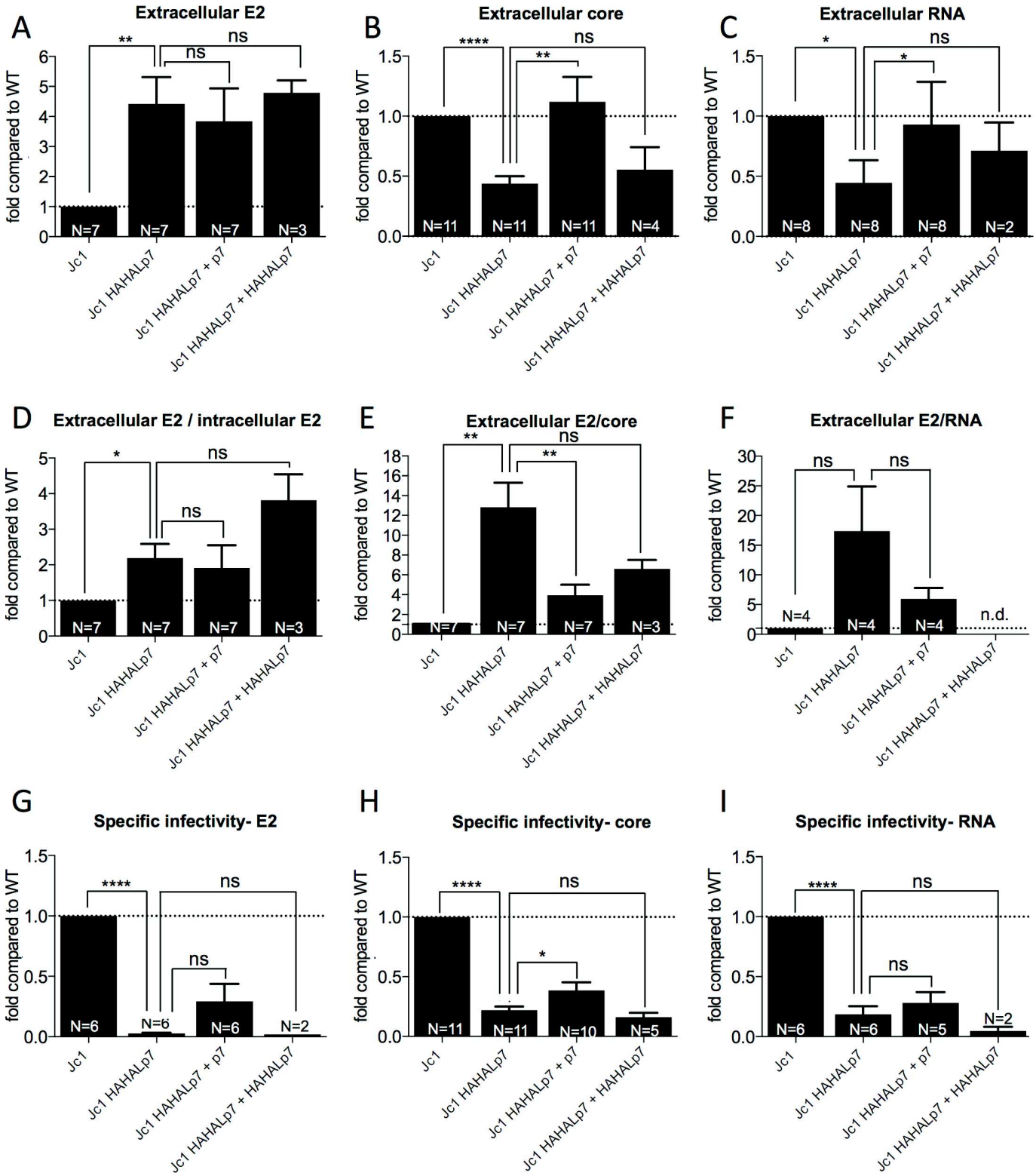

Fig 4. p7 ATMI mutant viruses display increased E2 secretion and decreased RNA and core secretion. Huh7.5 cells were electroporated with RNAs from parental or Jc1 HAHALp7 mutant HCVcc viruses expressed alone or with wild-type p7 or HAHALp7. Analyses were performed at 72h post-electroporation. All data are normalized by percentage of HCV-positive virus producer cells obtained as in Fig 3A. Results obtained with other p7 ATMI

mutant viruses are shown in S4 Fig and S5 Fig. (**A**) Levels of secreted E2 determined by quantitative western blot following GNA lectin pull down of cell supernatants. (**B**) Levels of secreted core as determined by CMIA (Chemiluminescent Microparticle ImmunoAssay). (**C**) Levels of secreted HCV RNAs as determined by RT-qPCR. (**D**) Ratio of extracellular E2 to intracellular E2. (**E**) Ratio of extracellular E2 to extracellular core. (**F**) Ratio of extracellular E2 to extracellular HCV RNA. (**G**) Specific infectivity relative to E2 amounts. (**H**) Specific infectivity relative to core amounts. (**I**) Specific infectivity relative to RNA amounts. All values are displayed relative to infectivity and expression of E2, core or RNA values determined in the supernatants of Jc1 virus-electroporated cells (**A-I**). Data represent mean values ± SEM. The numbers of experiments performed are indicated below the graphs.

https://doi.org/10.1371/journal.ppat.1006774.g004

in trans did not significantly restore E2 expression (Fig 3C) and secretion (Fig 4A and 4D) to wt levels, this indicated that the delayed cleavage of E2p7 is essential for the control of intracellular and extracellular E2 levels.

Strikingly, in contrast to E2, we observed that the p7 ATMI mutant viruses had decreased secretion of both core and viral RNAs in the cell supernatants, by *ca*. 2–5 fold (Fig 4B and 4C; S4B and S4C Fig). Furthermore, we found that wt p7 restored normal secretion levels of nucleocapsid components (Fig 4B and 4C; S4D Fig) though not those of E2 glycoproteins (Fig 4A). This indicated that viruses harboring p7 ATMI mutations display differential alterations of pathways leading to trafficking and/or secretion of viral glycoproteins *vs*. nucleocapsid components, *i.e*., HCV core and RNA. Finally, since mutant p7, *e.g*., HAHALp7, co-expression did not restore normal secretion levels of core and RNA (Fig 4B and 4C), these results indicated that p7 itself, rather than its cleavage from E2, modulates the secretion of viral nucleocapsids.

Altogether, our results suggest that altered p7 expression, as induced by accelerated cleavage and release from E2 as well as by its N-terminal modification, influence the proportion of secreted virion components. Indeed, relative to core and/or viral RNAs, a 15–25 fold higher expression of HCV glycoproteins was detected in the supernatants of cells infected with Jc1 HAHALp7 virus as compared to wt virus (Fig 4E and 4F).

Interestingly, we found that the p7 ATMI mutant viruses exhibited strongly decreased specific infectivity relative to their content in core protein or viral RNA, from 4–5 fold for Jc1 HAHALp7 virus (Fig 4H and 4I) to over 50-fold for other mutants (S5A and S5B Fig). Likewise, relative to E2 glycoprotein, the specific infectivity of the Jc1 HAHALp7 virus was decreased by *ca*. 35-fold, as compared to the parental virus (Fig 4G). Importantly, co-expression of wt p7, but not of ATMI mutant p7, restored (though not completely), the specific infectivity of the mutant viruses (Fig 4G–4I; S5C Fig). Altogether, this pointed out to altered ratios of different secreted forms of HCV-derived particles incorporating these components or, alternatively, altered composition of the viral particles themselves.

p7 controls secretion levels of HCV-derived particles

To demonstrate if the viral components were secreted in particulate forms, we centrifuged the supernatants of infected-cells in conditions allowing sedimentation of particles. We detected in the pellets a *ca*. 3-fold increase of E2 levels (Fig 5A; S6A Fig) and a 2–3 fold decrease of both core and RNA (Fig 5C) while comparing Jc1 HAHALp7 mutant *vs*. parental viruses. This augmentation of secreted particle-associated E2 levels could be detected for all p7 ATMI mutant viruses (S6B Fig). Interestingly, we also observed an increased secretion of E1-containing particles (S6A Fig), likely owing to secretion of HCV glycoproteins as E1E2 heterodimers. Furthermore, ectopic expression of wt p7 restored wt levels of particle-associated HCV glycoproteins, core and RNA (Fig 5A and 5C). Since ectopically-expressed ATMI mutant p7 did not rescue the above levels (Fig 5C), this indicated that p7 N-terminus modifications rather than accelerated E2p7 cleavage induced changes in secretion levels of mutant viral particles, perhaps by altering the ratios between SVPs and (infectious) viral particles.

Then, we aimed at characterizing the different types and proportions of secreted particles for wt *vs*. p7 ATMI mutant viruses.

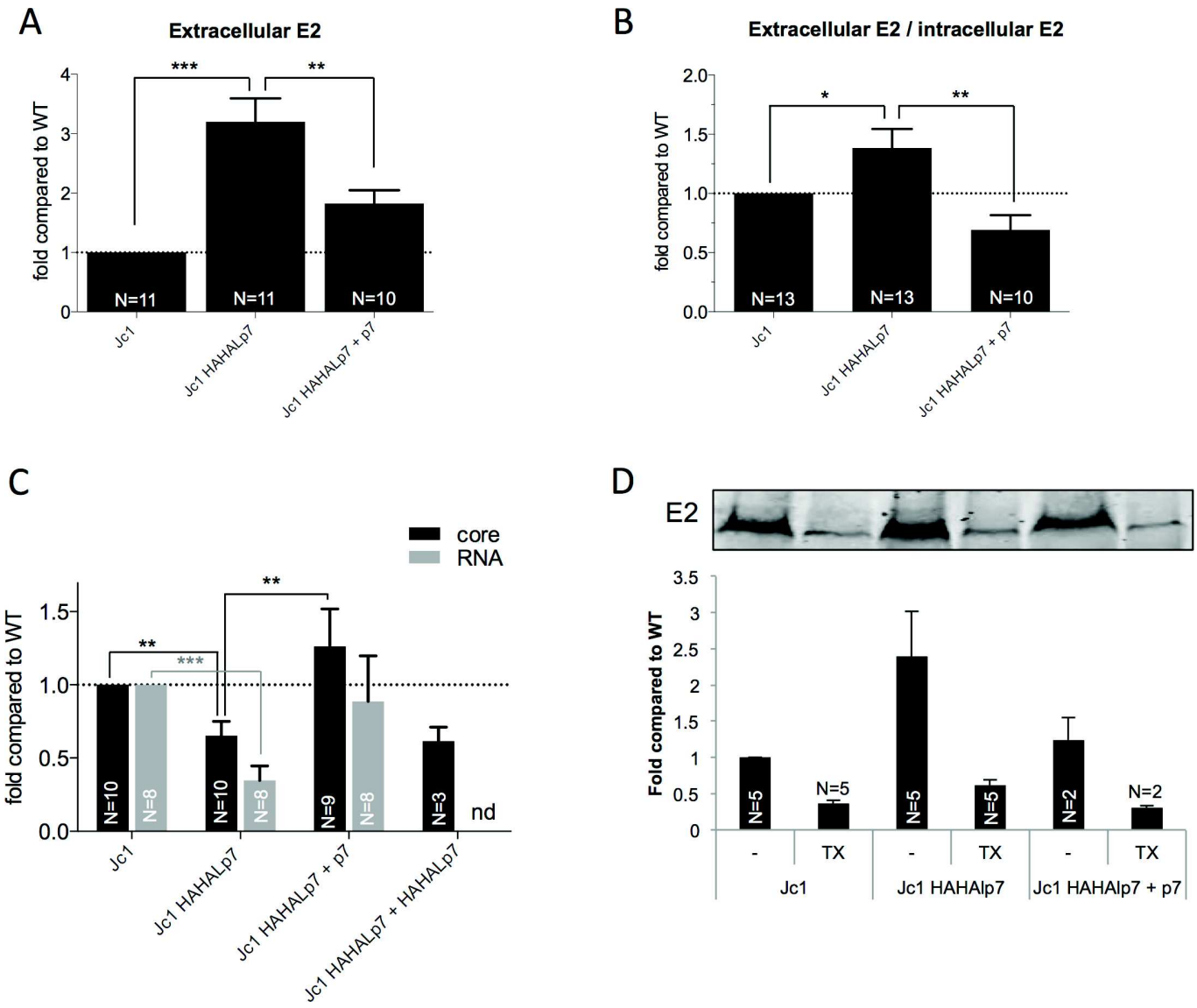

Fig 5. p7 ATMI mutant viruses modulate levels of particle-associated viral components. Huh7.5 cells were electroporated with RNAs from parental *vs*. Jc1 HAHALp7 mutant viruses expressed alone or with wild-type p7 or HAHALp7, as indicated. Analyses were performed at 72h post-electroporation and normalized by percentage of HCV-positive virus producer cells obtained as in Fig 3A. Results obtained with other p7 ATMI mutant viruses are shown in S6 Fig. (**A**) Levels of E2 in pellets from ultracentrifuged cell supernatants. (**B**) Ratio of E2 in pellets *vs*. intracellular E2. **(C)** Levels of core and HCV RNA present in the pellets of ultracentrifuged cell supernatants as determined by CMIA and RT-qPCR, respectively. **(D)** Cell supernatants were incubated with 1% Triton X-100 (TX) or left untreated (-) before ultracentrifugation and analysis of E2 present in the pellets analyzed by quantitative western blot. All values are displayed relative to E2, core or RNA values determined in the pellet of supernatants from Jc1 virus-electroporated cells (**A-D**). Data represent mean values ± SEM. The numbers of experiments performed are indicated below the graphs.

https://doi.org/10.1371/journal.ppat.1006774.g005

First, to confirm that E2 detected in the pellets of ultracentrifuged cell supernatants was secreted as particles, we treated the supernatants of virus-expressing cells with Triton-X100 before ultracentrifugation. We found that such treatment decreased the presence of E2 in the pellets for both wt and mutant viruses (Fig 5D; S6C Fig), hence indicating that a substantial part of secreted E2 proteins were in a sediment form, likely vesicular.

Second, since the p7 ATMI mutant viruses secreted higher E2 amounts with poorer infectivity compared to wt viruses (Fig 4G), we quantified the association of their glycoproteins with other virion components, *i.e*., core and RNA. When we pulled down E2 using GNA lectins, we found a 5–6 fold decreased association of core and RNA with E2 (Fig 6A). Moreover, ectopic expression of wt p7, though not mutant p7, restored, though partially, the association of E2 with viral core and genome (Fig 6A).

Finally, we investigated the degree of envelopment of the secreted core proteins within a lipid bilayer. Hence, we treated the supernatants of virus-expressing cells with proteinase K and subsequently determined the amounts of proteinase K-resistant core, which indicates its full protection by a lipid membrane or, conversely, its secretion as naked or badly enveloped core particles. Interestingly, as compared to their corresponding parental viruses, we detected decreased amounts of membrane-protected core for Jc1 HAHALp7 virus and, more dramatically, for JFH1 HAHALp7 virus (Fig 6B), which correlated with their respective losses of infectivity (Fig 2E–2G). Furthermore, we found that co-expression of wt p7, though not mutant p7, restored the lipid membrane envelopment of their secreted core proteins to almost wt levels (Fig 6B).

Altogether, these results pointed out to a disruption induced by p7 amino-terminus changes of the degree of association between HCV glycoproteins, viral envelopes and nucleocapsids, which could be due to an excess of E2 *vs*. core and RNA forms secreted independently, such as SVPs *vs*. naked/partially enveloped core particles, respectively, or, alternatively, to an increased density of E2 glycoproteins on the surface of secreted viral particles.

To investigate this further, we separated virus sub-populations using buoyant density-gradient fractionation. Jc1 and JFH1 HCVcc physical particles had more than 90% of viral RNA and 95% of core protein in fractions of densities of 1.10–1.15 g/ml, with a peak at 1.11 g/ml (Fig 6C; S7A–S7C Fig). As shown before [58–62], core and RNA could also be detected at higher densities (to up to 1.36 g/ml) and at lower densities, until 1.02 g/ml (S7 Fig). Jc1 HCVcc particles had more than 80% of their infectivity in fractions of densities of 1.08–1.13 g/ml, with a peak at 1.11 g/ml (Fig 6C; S7A and S7B Fig), in agreement with recent reports [57, 60–64]. Lastly, we found that E2 glycoproteins were detected in lower density fractions, with *ca*. 90% in fractions of densities of 1.03–1.08 g/ml and a peak at 1.05–1.06 g/ml (Fig 6C; S7A Fig) representing SVPs (Fig 1G). Importantly, less than 10% of E2 could be detected at densities of 1.08–1.15 g/ml, in which physical and infectious particles were prominent and corresponded to enveloped viral particles.

Interestingly, the density profile of Jc1 HAHALp7 virus was qualitatively similar to that of wt virus (Fig 6C; S7A and S7B Fig) and did not reveal any alteration of the distribution of the different types of particles along the gradient. However, quantitatively, we found the same alterations of the ratios of E2, core, RNA and infectivity in the different fractions for the mutant *vs*. parental virus (S7A Fig), as compared to unfractionated viral particles (Fig 5A and 5C). Specifically, 2–3 fold augmented E2 levels were detected in the SVP fractions of 1.03–1.08 densities (S7A Fig). Likewise, 2–3 fold reduced core or RNA levels were detected in all fractions whereas infectious titers were decreased by *ca*. 10-fold in these fractions (S7A Fig). Furthermore, we found that, whatever the density, the co-expression of Jc1 HAHALp7 virus with ectopic p7 restored wt infectivity concomitantly to restoration of the wt levels of core and RNA (S7B Fig).

Finally, we found that the loss of infectivity was accentuated for the JFH1 HAHALp7 virus, which displays a stronger phenotype than the Jc1 HAHALp7 virus (Fig 2E–2G), in fractions of densities of 1.08–1.15 g/ml containing most viral particles (Fig 6C; S7C Fig). Particularly, while core levels were reduced by *ca*. 2–3 fold for both Jc1 HAHALp7 and JFH1 HAHALp7, 6-

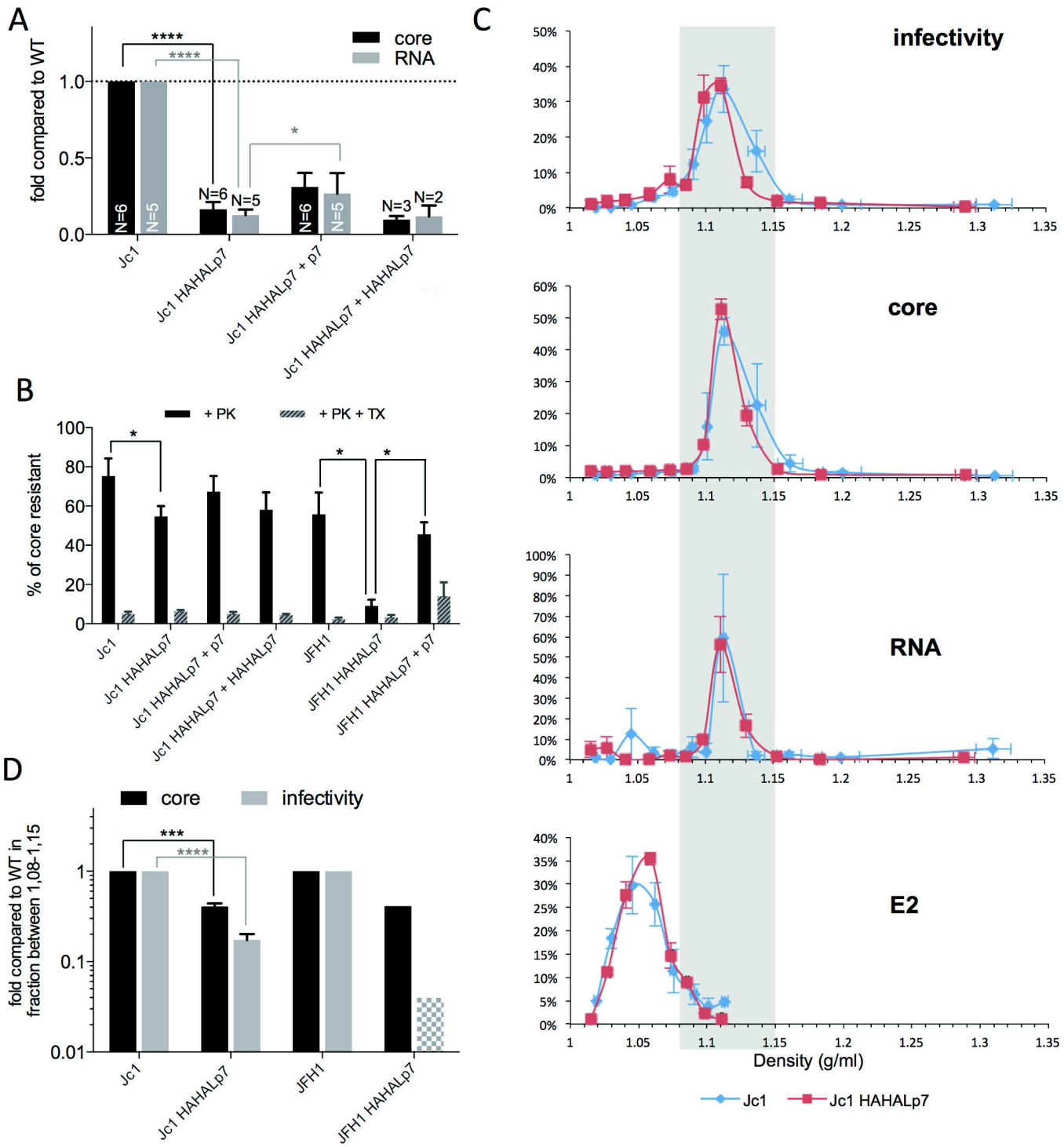

Fig 6. p7 ATMI mutant viruses induce secretion of viral particles with impaired envelopment. Huh7.5 cells were electroporated with RNAs from parental *vs.* Jc1 HAHALp7 or JFH1 HAHALp7 mutant viruses expressed alone or with wild-type p7 or HAHALp7, as indicated. Analyses were performed at 72h post-electroporation. **(A)** Levels of core and RNA following GNA pull down of cell supernatants, as determined by CMIA and RT-qPCR, respectively, and normalized by the amounts of immuno-precipitated E2. The values are displayed relative to association of core or RNAs to E2 pulled-down from the supernatants of Jc1 virus-electroporated cells. **(B)** Cell supernatants were digested with proteinase K (+ PK) with (+ TX) or without pre-treatment with Triton X-100 and the residual amounts of core (*i.e.*, lipid membrane-protected core) were determined by CMIA. The values are displayed relative to non-treated conditions. **(C)** Analysis of density gradients of cell supernatants. Infectivity, core, RNA, and E2 were measured in

each fraction and expressed as percentage of the sum of fractions. Examples of raw data of infectivity can be found in S7A–S7C Fig. **(D)** Infectivity and core of the indicated viruses were measured in pooled fractions of densities of 1.08–1.15 g/ml and represented as data normalized by values obtained with parental viruses. The grey shaded area represents values below the sensitivity threshold of the experiments. Data represent mean values ± SEM.

https://doi.org/10.1371/journal.ppat.1006774.g006

and over 100-fold reductions of infectivity levels were detected for the Jc1 HAHALp7 and JFH1 HAHALp7 mutant viruses, respectively, relative to parental viruses (Fig 6D).

Altogether, these results suggested that the p7 N-terminus controls both the secretion and the specific infectivity of secreted virus particles, likely *via* a process involving the completion of their envelopment, as indicated by the PK-sensitivity of core from secreted p7 ATMI mutant particles.

p7 amino-terminal alterations impair NS2, NS5A and E2 interactions required for envelopment of infectious particles

We then aimed at dissecting how p7 modulates the composition of viral particles by addressing HCV assembly mechanisms, from intracellular clustering of virion components to their envelopment.

First, since the HCV virion assembly rate is linked to core subcellular localization [17, 65–67] and since p7 alters this event in concert with NS2 [17, 40], we investigated by confocal microscopy analysis whether core from p7 ATMI mutant viruses could be relocated from lipid droplets to ER membranes, where envelopment and release of viral particles occur [3, 21]. While individually expressed Jc1 core had predominant distribution around lipid droplets, as previously described [17], its co-expression with either wt p7 or HAHALp7 protein induced full targeting at ER membranes (S8A Fig). Similar results were obtained with full-length viruses, since no difference between Jc1 and Jc1 HAHALp7 viruses could be detected regarding the prevalent ER-localization of their core proteins (S8B Fig). These data indicated that the p7 ATMI mutations and/or the accelerated E2p7 cleavage did not prevent p7-mediated early assembly events leading to core targeting to the ER membrane, but rather, impaired later assembly events.

Using HA-tag antibodies, we confirmed that HAHALp7 and core co-localized at the ER in cells infected with the Jc1 HAHALp7 virus (Fig 7A), as reported before [56]. Interestingly, we found that HAHALp7 and core co-localization could also be detected in infected cells treated with 5μg/ml digitonin (Fig 7A and 7C), which permeabilizes plasma but not ER membranes [68, 69]. Similar results were also obtained with JFH1 HAHALp7 virus as well as with HAHALp7 expressed individually, with or without signal peptide (S9A–S9C Fig). Since E2/core co-localization could be detected in Triton-treated cells but not in digitonin-treated cells (Fig 7B and 7C; S9A–S9C Fig), as expected owing to the luminal exposition of E2 ectodomain, these results indicated that the N-terminus of HAHALp7 points towards the cytosol. Note that these results do not exclude that p7 may also adopt the reverse topology, *i.e.*, with N- and C-termini exposed toward the luminal side of the ER [70].

We then investigated the sites of HCV assembly, which are represented by ER-derived areas where structural and non-structural viral proteins co-cluster with HCV RNA [66]. As compared to parental virus, we did not find significantly altered clustering of core, E2, NS4B, and NS5A for the Jc1 HAHALp7 virus (Fig 8A and 8B), suggesting identical rates of early assembly events. Likewise, we did not observe strong differences in the number of core structures co-localizing at assembly sites with HCV positive strand RNA for wt *vs*. mutant viruses (Fig 8C and 8D). Altogether, these results indicated that the initiation of early assembly events, *i.e.*, allowing clustering of the HCV structural components at the ER membrane, were not impaired by p7 ATMI mutations.

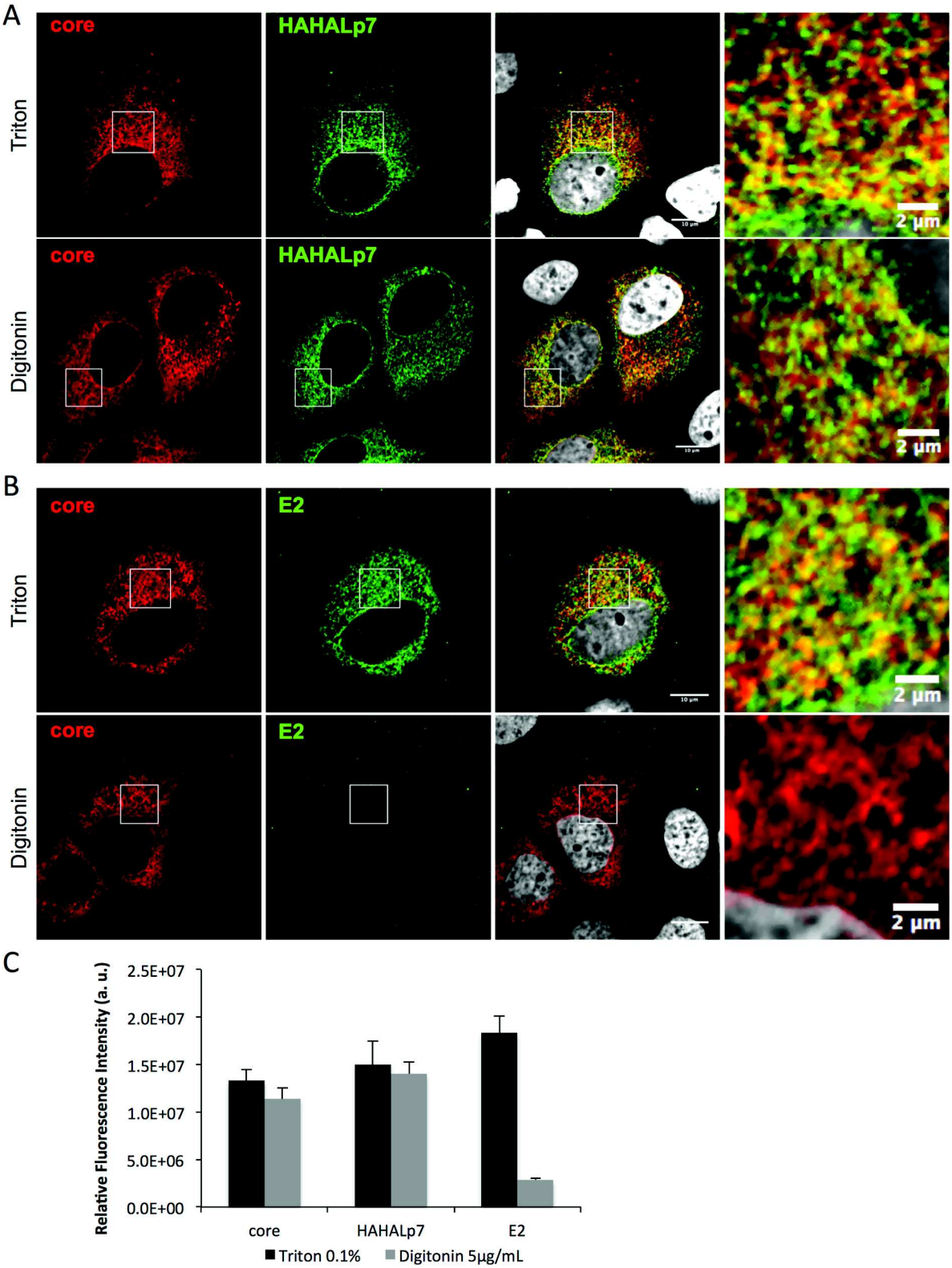

Fig 7. Co-localization of p7 ATMI mutant and E2 with core protein in HCVcc infected cells. Confocal microscopy analysis of Huh7.5 cells infected with Jc1 HAHALp7 virus. At 72h post-infection, cells were fixed, permeabilized with either Triton X-100 or

Digitonin, as indicated, and stained for HCV core (red), HAHALp7 (green) (**A**), E2 (green) (**B**) and nuclei (grey). The relative fluorescence intensity (arbitrary units) of each channel (**C**) was quantified by using ImageJ.

https://doi.org/10.1371/journal.ppat.1006774.g007

Next, since the NS2 non-structural protein is thought to serve as a scaffold for gathering virion assembly components through its interaction with E1E2 [9, 13–16, 71] and since p7 regulates this association [9, 14, 39], we tested if our p7 ATMI mutants had impaired E1E2/NS2 association. Using confocal microscopy, we did not detect altered co-localization of core, E2 and NS2 (Fig 9A and 9B), further highlighting that the assembly sites of viral particles were not grossly changed. However, when we analyzed E1 and NS2 co-immuno-precipitation with E2 antibodies, although the E1/E2 association was unchanged (Fig 9C), we detected a 3–4 fold decreased association of E2 with NS2 for p7 ATMI mutant *vs*. wt viruses (Fig 9E; S10A Fig). These results indicated that, relative to wt virus, the higher amounts of intracellular HCV glycoproteins detected for the p7 ATMI mutant viruses (Fig 3B and 3C; S3 Fig; S7 Fig) were not associated to NS2. This implied that only a fraction of the up-regulated E2 levels interact with the NS2 assembly platform, and suggested that part of the pool of HCV glycoproteins not associated to NS2 or to assembly sites induce the formation of SVPs. Thus, we performed the reverse co-immuno-precipitation with NS2 antibodies to more directly address interactions between assembly proteins at assembly sites. Strikingly, when we analyzed E1 and E2 co-immuno-precipitation with NS2, we found *ca*. 2–3 fold increased E1E2 association to NS2 in cells expressing Jc1 (Fig 9F) or JFH1 (Fig 9D; S10B Fig) p7 ATMI mutant viruses, as compared to parental viruses. Furthermore, these altered interactions with NS2 were reversed upon ectopic expression of wt p7 (Fig 9D; S10B Fig). Thus, since ectopically-expressed p7 did not restore wt intracellular E2 expression (Fig 3C) and since NS2 expression was unchanged for the mutant virus compared to wt (Fig 3D), this indicated that p7 N-terminus modulates NS2 association with HCV glycoproteins.

Finally, since NS5A interacts with HCV RNA [72, 73] and core [18, 19] as well as with NS2 [13, 15], which likely transfers core and HCV RNA to assembly sites or to nascent viral particles [18–20], we investigated NS2 association with NS5A. No significantly altered co-localization of core, E2, NS2 and NS5A could be detected while comparing mutant *vs*. parental viruses (Fig 10A–10D), again underscoring the proximity of these different factors at assembly sites that appeared unaltered qualitatively. However, as compared to parental virus, we found a reduced NS5A co-immuno-precipitation with NS2 in cells expressing the Jc1 HAHALp7 or other p7 ATMI mutant viruses (Fig 10E; S9C Fig), which was restored upon co-expression with wt p7 (Fig 10E).

Altogether, these results suggested that the p7 amino-terminus determines the fine-tuning of the interactions between HCV glycoproteins, NS5A and NS2 required for envelopment of viral particles at assembly platforms.

Discussion

We report here novel functions of the HCV p7 viroporin, which appears to modulate i) the cell secretory pathway, ii) the assembly and proportion of different secreted HCV-derived particle forms, including SVPs, partially enveloped core particles and infectious virions, and iii) the specific infectivity of the latter type of particles. Overall, our results provide novel insights in the properties of p7, particularly regarding the role of its junction segment with E2 and its retarded cleavage from E2. This distinguishes different functions of p7 between those that only depend on delayed E2p7 cleavage from those that reveal the role played by the p7 amino-terminus itself in envelopment and production of infectious viral particles.

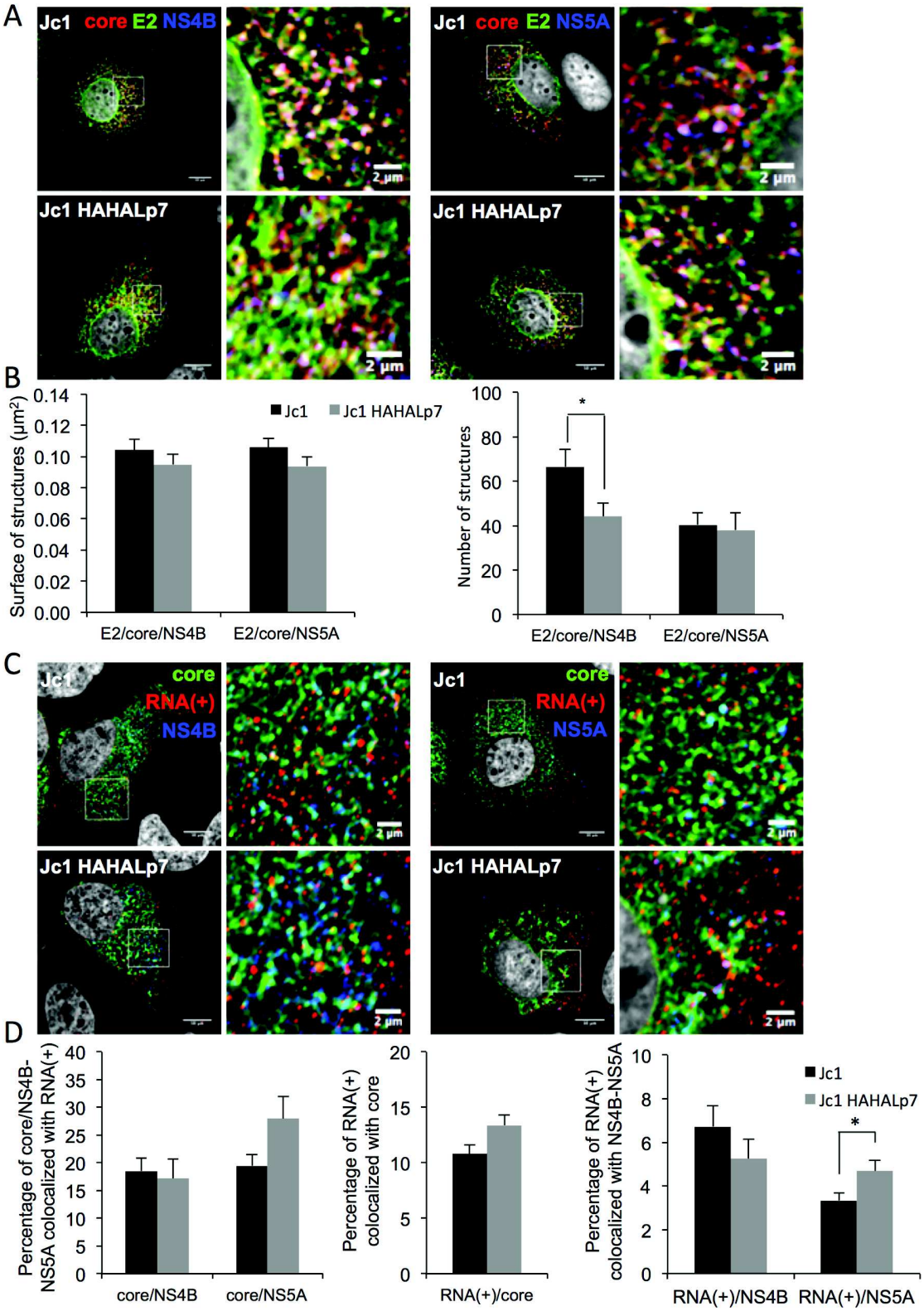

Fig 8. p7 ATMI mutant viruses do not alter E2, core, NS4B, NS5A and HCV RNA(+) clustering. (A) Confocal microscopy of Huh7.5 cells infected with Jc1 or Jc1 HAHALp7 viruses. At 72h post-infection, cells were fixed and stained for

HCV core (red), E2 (green), NS4B (blue, left panels), NS5A (blue, right panels) and nuclei (grey). **(B)** Quantification of size (left) and number (right) of co-localized core/E2/NS4B or core/E2/NS5A structures. (**C**) Confocal microscopy of Huh7.5 expressing Jc1 or Jc1 HAHALp7 viruses. At 72h post-infection, cells were fixed and stained for HCV core (green), NS4B (blue, left panels), NS5A (blue, right panels) and nuclei (grey). HCV RNA(+) were stained by FISH (red). **(D)** Quantification of percentage of core/NS4B or core/NS5A structures co-localizing with RNA(+) (left), of RNA(+) co-localizing with core (middle), or of RNA(+) co-localizing with NS4B/NS5A structures. Scale bars of panels and zooms from squared area represent 10μm and 2μm, respectively. For each condition, over 20 cells were quantified.

https://doi.org/10.1371/journal.ppat.1006774.g008

E2p7 cleavage rate regulates E2 intracellular levels

Because of their intrinsic capacity to be routed to the cell surface, owing to their localization in the cell secretory pathway, the traffic and distribution of envelope glycoproteins need to be controlled, by *e.g*., retention in specific intracellular compartments, in order to avoid immune detection of infected cells. Moreover, as these glycoproteins are synthesized in the ER lumen, counteracting ER stress activation in infected cells is important to avoid subsequent cell death. Since HCV proteins are expressed from a polyprotein, implying that all proteins are initially expressed at the same rate, its well-ordered cleavage may regulate the stability and functions of some proteins, such as for E2 and p7 that coexist with a E2p7 precursor (Fig 2) of ill-defined functions [7–11]. Here, by designing mutants at E2-p7 junction, we show that the augmentation of E2p7 cleavage, which is mediated by signal peptidase [7, 52], induced an up-regulation of the levels of E2 in infected cells, by *ca*. 4–5 fold.

This original phenotype is not caused by increased rates of replication or translation of such mutant viruses, judging from similar levels of viral RNAs or of non-structural proteins, respectively, for mutant *vs*. wt viruses. That both short peptide extensions and single alanine insertion before p7 structure induced E2p7 increased cleavage and E2 up-regulation at similar levels (Figs 2C and 3C; S3A Fig) argued against the possibility that p7 N-terminal modifications could *per se* change E2 expression. Consistently, co-expression of wt p7 with these mutant viruses did not restore wt E2 intracellular levels (Fig 3C).

Different possibilities may explain how E2p7 processing could modulate E2 expression. On the one hand, liberated E2 could be stabilized by its partners, such as *e.g*., E1 [74, 75] or SPCS1 [71]. On the other hand, E2 and E2p7 could activate or block different degradation pathways, such as autophagy or proteasome/lysosome. Indeed, HCV glycoproteins are known to be activators of the unfolded protein response (UPR) in HCV-infected cells [76]. Finally, it is also possible that the amounts of free p7, which are likely higher for the p7 ATMI mutant viruses, may regulate these degradation pathways. In support of these assumptions, a previous study [77] indicated that a mutation of p7 reported to block cleavage between E2 and p7 (p7-R(K)GR33-35AAA) [9, 11, 13] induced E2 degradation. Likewise, mutants abrogating E2p7 cleavage, such as E2-A367R (Fig 2) as well as p7-A1W, p7-E3W, p7-K4W, p7-A10W or p7-S12W [10], exhibited poor E2p7 expression despite wt rates of replication, relative to parental viruses. Further studies will be necessary to clarify this issue.

Processing of E2p7 modulates E2 targeting to NS2 assembly platform

Regulation of the intracellular quantities of surface glycoproteins as well as their recruitment at virion assembly sites is crucial for production of infectious particles, which require optimal E1E2 incorporation levels to mediate entry into cells. Several cellular factors promoting the different steps of HCV assembly have been identified [3] and include factors allowing initial core and NS5A targeting at the LDs [78–82], HCV particle assembly [71, 83], or fission of enveloped nucleocapsids [84, 85]. As for viral factors, NS2 gathers assembly components at ER-localized sites near LDs and replication complexes [13, 15, 16, 86], at detergent-resistant membranes (DRM) areas [9, 39]. Specifically, NS2 interaction with E2 and E1 as well as with

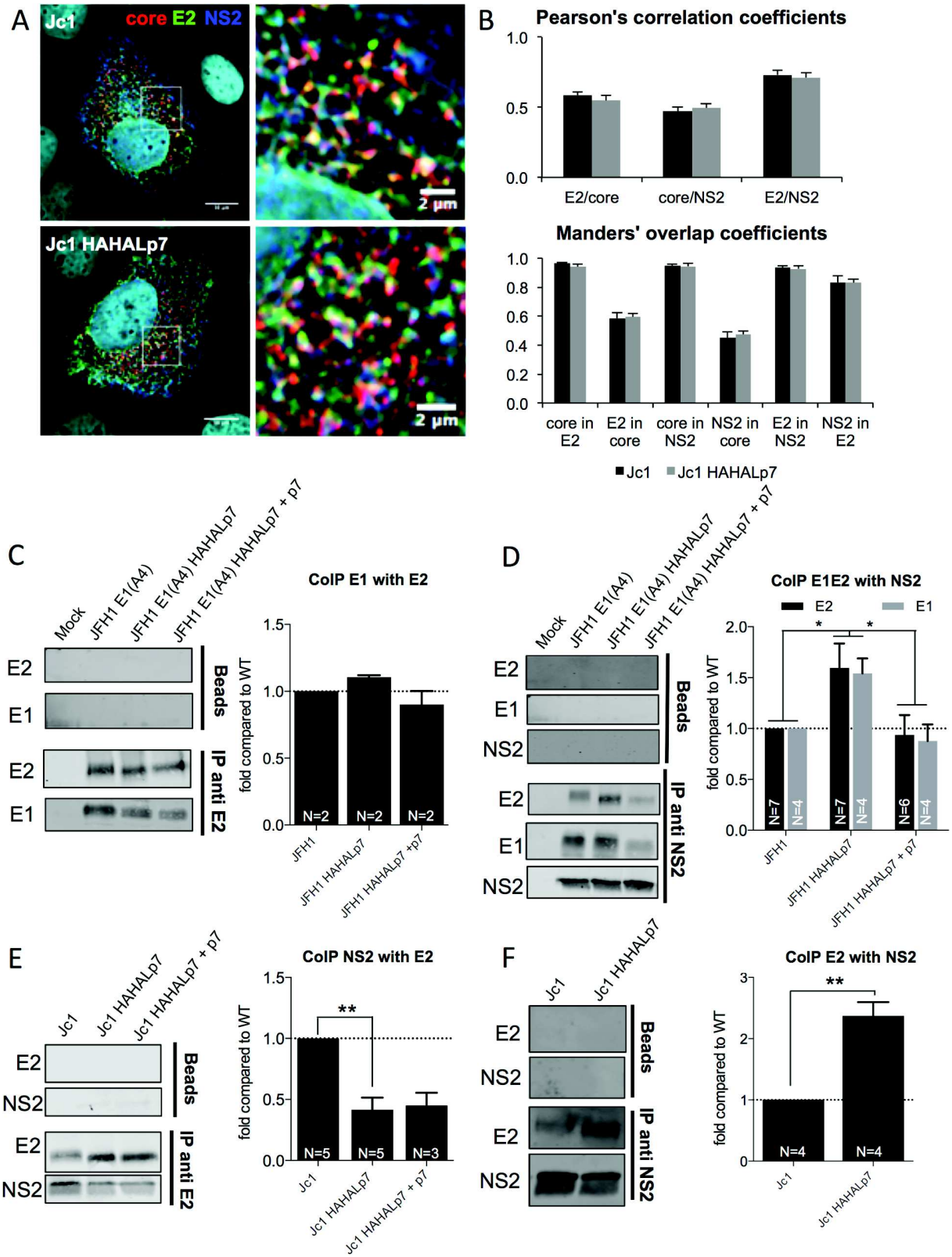
A
Jc1
core E2 NS2
2 µm
Jc1 HAHALp7
2 µm
B
Pearson's correlation coefficients
1.0
0.5
0.0
E2/core
core/NS2
E2/NS2
Manders' overlap coefficients
1.0
0.8
0.6
0.4
0.2
0.0
core in E2
E2 in core
core in NS2
NS2 in core
E2 in NS2
NS2 in E2
Jc1
Jc1 HAHALp7
C
Mock
JFH1 E1(A4)
JFH1 E1(A4) HAHALp7
JFH1 E1(A4) HAHALp7 + p7
E2
E1
Beads
E2
E1
IP anti E2
CoIP E1 with E2
fold compared to WT
1.5
1.0
0.5
0.0
N=2
N=2
N=2
JFH1
JFH1 HAHALp7
JFH1 HAHALp7 +p7
D
Mock
JFH1 E1(A4)
JFH1 E1(A4) HAHALp7
JFH1 E1(A4) HAHALp7 + p7
E2
E1
NS2
Beads
E2
E1
NS2
IP anti NS2
CoIP E1E2 with NS2
E2
E1
fold compared to WT
2.0
1.5
1.0
0.5
0.0
*
*
N=7
N=4
N=7
N=4
N=6
N=4
JFH1
JFH1 HAHALp7
JFH1 HAHALp7 + p7
E
Jc1
Jc1 HAHALp7
Jc1 HAHALp7 + p7
E2
NS2
Beads
E2
NS2
IP anti E2
CoIP NS2 with E2
fold compared to WT
1.5
1.0
0.5
0.0
**
N=5
N=5
N=3
Jc1
Jc1 HAHALp7
Jc1 HAHALp7 + p7
F
Jc1
Jc1 HAHALp7
E2
NS2
Beads
E2
NS2
IP anti NS2
CoIP E2 with NS2
fold compared to WT
3
2
1
0
**
N=4
N=4
Jc1
Jc1 HAHALp7

Fig 9. p7 ATMI mutant viruses alter NS2 and E2 association. Huh7.5 cells expressing RNAs from parental *vs.* Jc1 HAHALp7 or JFH1 HAHALp7 mutant viruses expressed alone or with wild-type p7 were analyzed at 72h. For immuno-precipitation, cell lysates were incubated with protein A/G agarose beads after pre-treatment, or not (beads), with NS2 or E2 antibodies. Immuno-precipitated complexes were eluted and analyzed by quantitative western blot. (**A**) Confocal microscopy of Huh7.5 cells expressing Jc1 or Jc1 HAHALp7 viruses and stained for HCV core (red), E2 (green) and NS2 (blue). (**B**) Co-localization analysis from (**A**), displaying the Pearson's correlation coefficients and the Manders' overlap coefficients, as indicated. **(C)** Representative western blot of E1 proteins co-immuno-precipitated with E2 antibodies (left). The levels of co-immuno-precipitated E1 proteins are normalized to the amount of immuno-precipitated E2 from JFH1 or JFH1 HAHALp7 virus-expressing cells (right). (**D**) Representative western blot of E1 and E2 proteins co-immuno-precipitated with NS2 antibodies (left). The levels of co-immuno-precipitated E1 and E2 proteins are normalized to the amount of immuno-precipitated NS2 in JFH1 or JFH1 HAHALp7 virus-expressing cells (right). Note that we used the JFH1 E1(A4) and JFH1 E1(A4) HAHALp7 viruses to detect E1 in these CoIP experiments. (**E**) Representative western blot of NS2 proteins co-immuno-precipitated with E2 antibodies (left). The levels of co-immuno-precipitated NS2 proteins are normalized to the amount of immuno-precipitated E2 from Jc1 or Jc1 HAHALp7 virus-expressing cells (right) **(F)** Representative western blot of E2 proteins co-immuno-precipitated with NS2 antibodies (left). The levels of co-immuno-precipitated E2 proteins are normalized to the amount of immuno-precipitated NS2 in Jc1 or Jc1 HAHALp7 virus-expressing cells. Data represent mean values ± SEM. The values are displayed relative to co-immuno-precipitation assays from JFH1 or Jc1 virus-expressing cells. The numbers of experiments performed are indicated below the graphs.

https://doi.org/10.1371/journal.ppat.1006774.g009

other viral factors—p7, NS3 and NS5A, is believed to be key for virion biogenesis [9, 13–15, 71, 84]. Yet, independent of this capture mechanism, E1E2 glycoproteins have the intrinsic capacity to induce SVP formation (Fig 1) [24], which implies a competition for their recruitment at the assembly sites of infectious particles. Noteworthy, E2/NS2 interaction depends on SPCS1, one of the 5 subunits of signal peptidase, and abrogation of E2/NS2/SPCS1 triple interaction *via* SPCS1 silencing markedly reduced HCV assembly [71].

Our co-IP assays indicated that increasing E2p7 cleavage, concomitantly with augmented E2 expression and SVP formation, stimulated the interaction between E1E2 and NS2 (Fig 9D and 9F; S10B Fig). A first, simple possibility to explain this stronger E1E2/NS2 association may involve the increase of E2 intracellular expression, which, incidentally, would lead to greater opportunities for E2/NS2 association. A second possibility could involve either a concentration of SPCS1 at the vicinity of E2 and NS2, as a result of SPCS1 recruitment by the signal peptidase complex during E2p7 and p7NS2 processing, or, alternatively, of a preferential interaction of cleaved, liberated E2 with SPCS1 and hence, with NS2. However, both possibilities would be difficult to reconcile with the finding that wt p7 co-expression, which did not restore wt E2 intracellular levels (Fig 3C), restored normal levels of E1E2/NS2 interaction (Fig 9D and 9F; S10B Fig). A third possibility is that the alteration of p7 N-terminus in our E2-p7 junction mutants may affect NS2 capacity to interact with some of its other partners, as discussed below. Unexpectedly, our results indicated that the increased E1E2/NS2 interaction correlated with reduced formation of infectious particles, in agreement with lowered secretion of nucleocapsids (Fig 5C). In this respect, it is likely that a loss of viral particle formation would translate in an increase of E2 density on NS2 platforms (Fig 9D and 9F) because E2 would not be consummated in assembled and released virions.

Processing of E2p7 uncovers novel p7 assembly functions

Our results indicate that the p7 N-terminus also determines HCV infectivity by controlling the secretion of enveloped *vs.* naked/partially enveloped core particles (Fig 6B and 6D). This is in agreement with a previous report showing that p7 regulates the envelopment of nascent viral particles [40]. A recent study indicated that the first helix of p7 harbors a key determinant of HCV infectivity (*e.g.*, V6, H9, S12), as underscored by mutagenesis of these residues pointing toward the p7 channel pore [10]. Intriguingly, we reveal here for the first time, a novel determinant at the extreme amino-terminal end of p7, *i.e.*, before its first helix (S1 Fig), that strongly modulates infectivity (Fig 2) and the relative amounts of enveloped *vs.* non/partially-enveloped core particles (Fig 6B). Furthermore, we demonstrate that changes in this amino-terminal p7

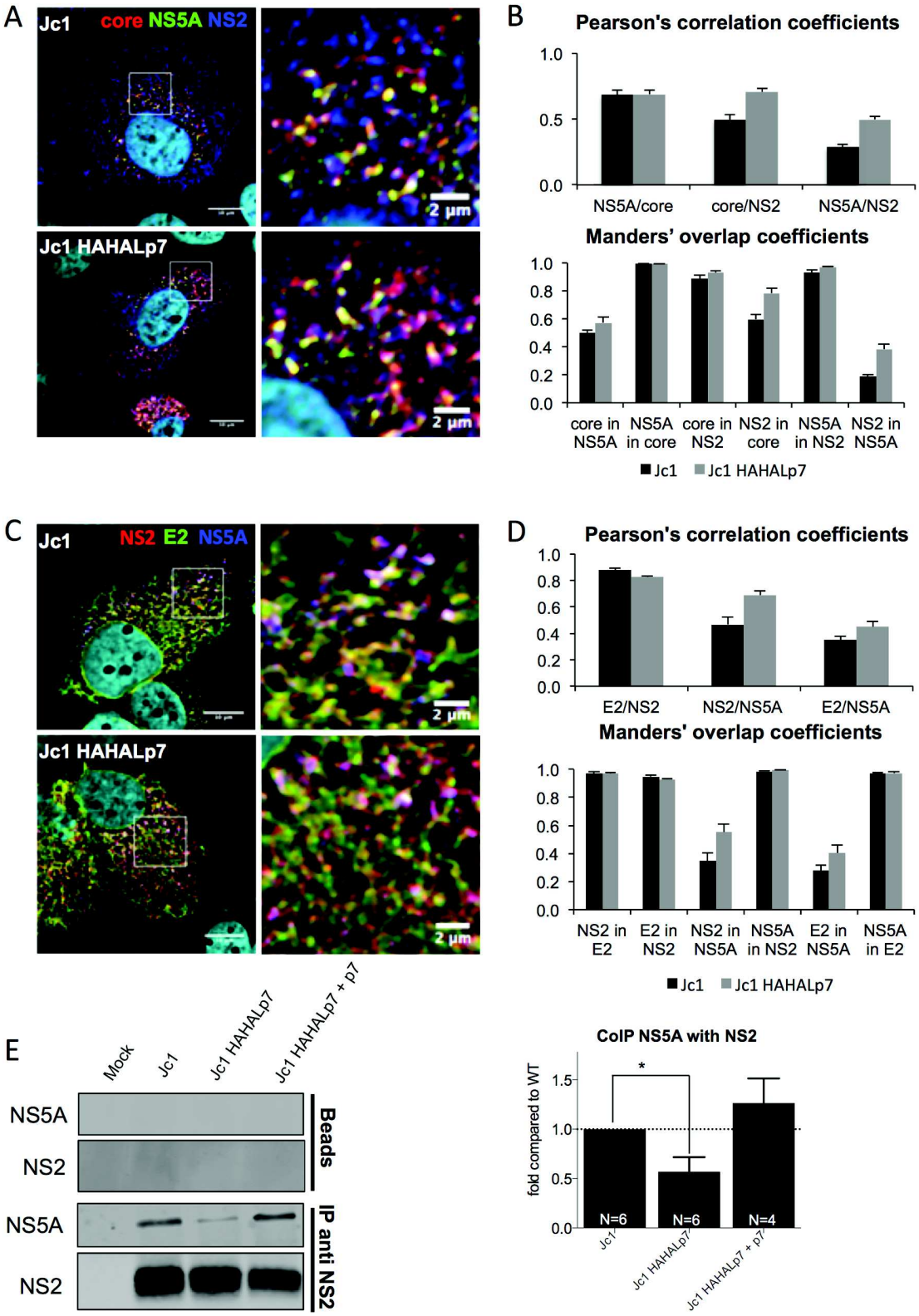

Fig 10. HCVcc mutants with modified p7 amino-terminus impair NS2 and NS5A association. Huh7.5 cells expressing RNAs from parental *vs.* Jc1 HAHALp7 mutant viruses expressed alone or with wild-type p7 were analyzed at 72h. (**A**)

Confocal microscopy of Huh7.5 cells expressing Jc1 or Jc1 HAHALp7 viruses and stained for HCV core (red), NS5A (green) and NS2 (blue). (**B**) Co-localization analysis from (**A**), displaying the Pearson's correlation coefficients and the Manders' overlap coefficients, as indicated. (**C**) Confocal microscopy of Huh7.5 cells expressing Jc1 or Jc1 HAHALp7 viruses and stained for HCV NS2 (red), E2 (green) and NS5A (blue). (**D**) Co-localization analysis from (**C**), displaying the Pearson's correlation coefficients and the Manders' overlap coefficients, as indicated. (**E**) Cell lysates were incubated with protein A/G agarose beads after pre-treatment, or not (beads), with NS2 antibodies. Immuno-precipitated complexes were eluted and analyzed by quantitative western blot (see representative western blot to the left). The graphs show the levels of NS5A proteins co-immuno-precipitated by NS2 antibodies normalized to the amount of immuno-precipitated NS2 in Jc1 or Jc1 HAHALp7 virus-expressing cells. The values are displayed relative to association of NS5A to NS2 immuno-precipitated from Jc1 virus-expressing cells. Data represent mean values ± SEM. The numbers of experiments performed are indicated below the graphs.

https://doi.org/10.1371/journal.ppat.1006774.g010

determinant (p7 ATMI mutants), *via e.g.*, short peptide extensions, single amino-acid insertions or substitutions that did not alter p7 structure (S1 Fig), induced a stronger reduction of infectivity (Fig 2) than of secretion of enveloped core particles (Fig 6D), resulting in reduced specific infectivity of the mutants, by 4- to over 50-fold depending on ATMI mutant types (Fig 4G–4I; S5 Fig.

Envelopment of viral particles pertains to a series of events that likely occur rapidly once two components, *i.e.*, surface glycoproteins and nucleocapsids, encounter at assembly sites following mobilization from their respective storage pools, *i.e.*, respectively, NS2 platforms apposed to LDs [9, 39] and LDs/replication complexes [12]. Such events are difficult to catch experimentally, because they are transient by nature as they lead to quick release of assembled viral particle from such assembly sites within the ER lumen. How HCV core and RNA are transferred from LD surface to ER assembly sites to initiate the release of infectious, enveloped viral particles remains poorly defined [3, 87], although it involves concerted actions of p7 and NS2 [17] and of NS5A [18, 20]. Accordingly, previously described assembly-defective mutants, such as p7-KR33/35QQ and core-C69-72A [40], Δp7 [65] or ΔE1E2 and NS5A-Δ2328–2435 [20], display strong core-LD accumulation, which correlates with their loss of infectivity. Strikingly, in contrast to these previous assembly mutants but similar to parental viruses, our Jc1 p7 ATMI mutants readily targeted core at the ER membrane (S8 Fig) despite reduced infectivity and did not significantly alter the co-clustering of structural and non-structural proteins with HCV RNA (Figs 8–10), both of which events previously shown to be critical for achieving efficient assembly [17, 65, 66]. Moreover, as shown by others, p7 regulates NS2 subcellular localization at punctate sites near LDs and its association with DRMs along with other viral proteins, including core, E2, and NS3 [9, 16, 39, 86]; yet, while other assembly-defective virus mutants, such as the p7-KR33/35QQ and p7-KR33/35AA in these previous reports, disrupted NS2 localization and/or E2/NS2 association, the p7 ATMI mutants displayed increased E1E2/NS2 interaction, compared to parental viruses. Along with the finding that our mutants exhibited wt capacity to slow down the cell secretory pathway (Fig 1E), this underscores that the ATMI class of p7 mutants retains most p7 properties and inhibits viral assembly though a novel mechanism.

Our results imply an envelopment defect caused by inadequate mobilization and/or transfer of core and RNA at E1E2-containing NS2 assembly platforms. This is reflected by our findings that such p7 ATMI mutants exhibited altered E1E2/NS2 and NS2/NS5A interactions (Figs 9 and 10) but also that failure to mediate correct particle envelopment resulted in secretion of partially enveloped, proteinase K-sensitive core particles (Fig 6B). Since co-expression of our mutant viruses with wt p7 restored the above alterations to almost normal levels, this questions about the role of p7 N-terminus in this mechanism and raises the possibility that it regulates core and RNA transfer to assembly sites and/or to assembling viral particles (Fig 11). Interestingly, a previous report suggested that p7 genetically interacts with some regions of NS2 as

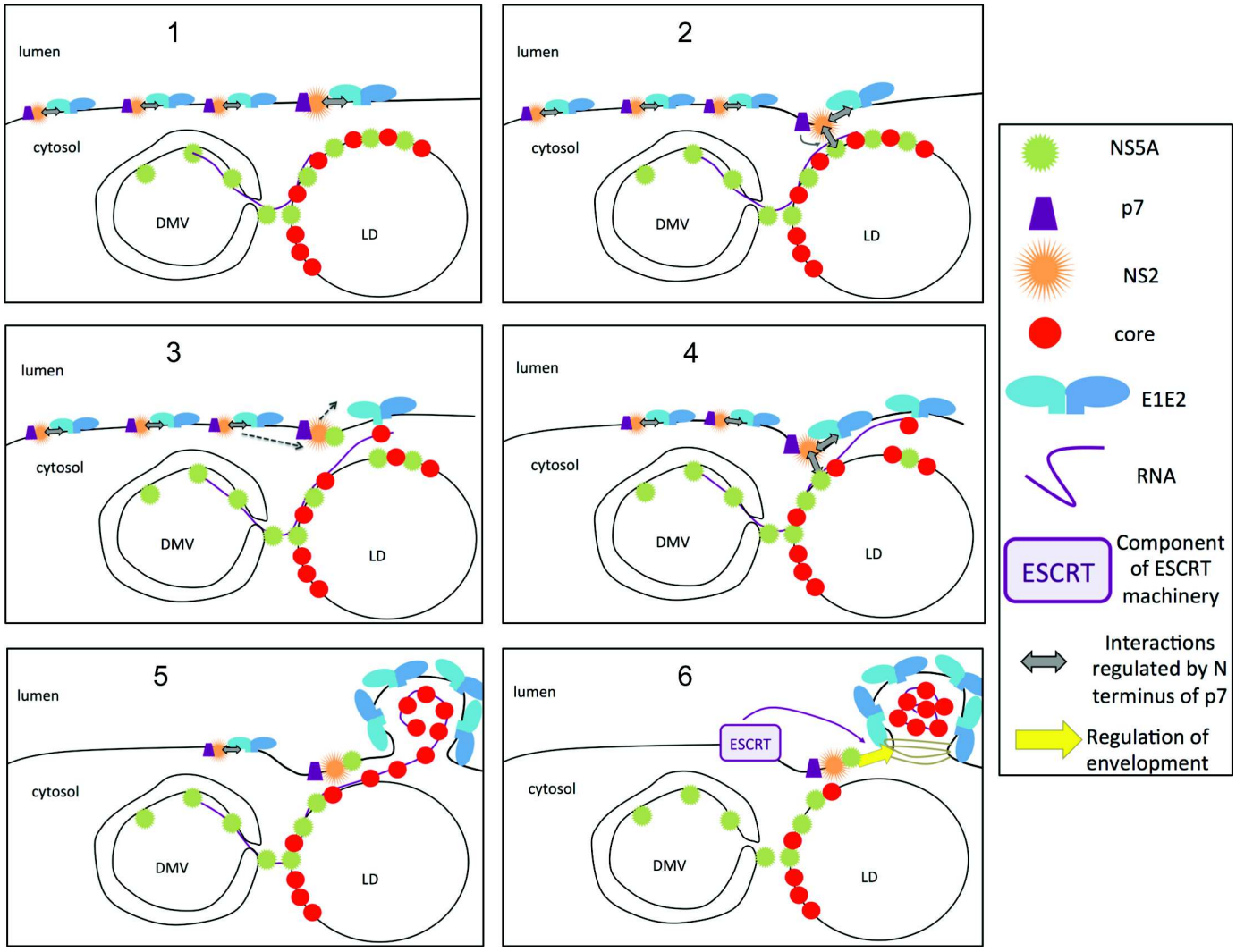

Fig 11. Model of p7 role in assembly and envelopment of HCV particles. (**1**) HCV assembly takes place at the ER membrane close to HCV replication complexes-containing double membrane vesicles (DMV) and to cytosolic lipid droplets (LD) harboring core and NS5A at their surface. Upon translation of the HCV genome, E1E2p7NS2 complexes form and accumulate at the ER membrane. (**2**) p7, *via* its N-terminal extremity, regulates (thin grey arrow) the interaction of NS2 with NS5A. (**3**) This interaction may allow the release of E1E2 from E1E2p7NS2 complexes at the assembly site of nascent viral particles on the one hand and co-recruitment of core and RNA to E1E2 on the other hand. Subsequently, the E1E2-free p7NS2NS5A complex leaves whereas a new E1E2p7NS2 complex reaches the assembly area (dotted arrows). (**4**) The process is reiterated with p7 from incoming E1E2p7NS2 complexes regulating the encountering of NS2 and NS5A, which leads to the further release of E1E2 and core/RNA that accumulate at the assembly site. (**5**) The process is repeated until the formation of a viral particle that buds in the ER lumen. (**6**) The NS2NS5A complex, regulated by p7, may recruit ESCRT components to induce scission of the nascent particle until full envelopment and egress.

https://doi.org/10.1371/journal.ppat.1006774.g011

well as of NS5A [88], strengthening the notion of a functional dialog between p7, NS2 and NS5A. Our findings that the N-terminus of HA-tagged p7 points towards the cytosol (Fig 7) support the likelihood that it mediates critical interactions with cytosolic factors promoting assembly. A possibility is that modifications of p7 N-terminal surface, before the first p7 helix (S1 Fig), disrupted such interactions (Fig 11). In this respect, co-localization and association of NS2 with NS5A, which is decreased upon p7 deletion or alterations [13, 16], is thought as a crucial event mediating core/RNA transfer to assembly sites [18, 20, 66]. Thus, since our mutant viruses did not display altered co-localization of these assembly factors, it is likely that

NS2 complexes formed with p7 ATMI mutants failed to efficiently mediate the encountering of nucleocapsids with NS2-bound viral surface components and/or to induce the release of fully enveloped, infectious viral particles. Why such failure resulted in a proportional release of partially enveloped core particles (Fig 6B *vs*. Fig 6D), which could be similar to those that have been detected in the serum of infected patients [28], is intriguing. It raises the possibility that the transfer of core and RNA to E1E2 glycoproteins liberated from NS2 complexes at assembly sites is associated to the recruitment of a mechanism that closes nascent particles (Fig 11). Such a mechanism, which likely involves components of the ESCRT pathway, as previously described for HCV [84, 85], could be disrupted by p7 ATMI mutants is such a way that, rather than being correctly closed, the budding membrane capsule would detach, allowing escape of imperfectly enveloped nucleocapsids in the ER lumen, which could explain their reduced specific infectivity. Indeed, as p7 ATMI mutants impair the interaction between NS2 and NS5A, this may prevent the recruitment of HRS, an ESCRT-0 component that interacts with p7, NS2 and NS5A [84] and subsequently, of all ESCRT components required for correct envelopment.

Free p7 slows down the cell secretory pathway

Our data indicate that the regulation of the amounts of free p7 could modulate the production of viral particles. Indeed, we found that p7, which localizes at the ER (Fig 7) [89] slows down the cell secretory pathway in a dose-dependent manner, likely at the stage of ER-Golgi transport (Fig 1). While this property is not intuitive, given that HCV, like other *Flaviviridae*, is thought to exit the cells through the secretion pathway [90], this could either induce the concentration of its glycoproteins at virion assembly sites in the ER lumen through their active retention or reflect the cooptation of another pathway of secretion for HCV particles [22, 23]. Furthermore, as HCV glycoproteins can be secreted as SVPs independently of other viral proteins (Fig 1G) [24], this feedback loop may ensure that excess glycoproteins, arising from their release upon E2p7 cleavage, could be appropriately controlled so as to prevent activation of immune responses. Additionally, as indicated by the delayed transport of VSV-Gts used as a model cargo (Fig 1B–1F), it is possible that p7 expression could alter the secretion of cellular proteins such as, *e.g*., immune effectors, as shown for viroporins of other viruses [43, 91].

The mechanism used by p7 to slow down the secretion of glycoproteins needs further investigation. Viroporins of alternative viruses have previously been involved in modulation of the secretory pathway, though through a variety of mechanisms [38]. For example, the M2 protein from influenza virus has a direct effect on late steps of plasma membrane delivery by delaying late Golgi transport, which indirectly affects the efficiency of earlier transport steps by altering the ionic content of the Golgi apparatus and the endosomes [92, 93]. Alternatively, Coxsackievirus 2B proteins modify ER membranes, which inhibits protein processing and sorting by decreasing calcium homeostasis in ER and Golgi [43]. Likewise, p7 can change ionic gradients in both reconstituted membrane assays *in vitro* [30, 44–47] and *in cellulo* [41, 42], which could affect anterograde transport and/or modify intracellular compartments.

In conclusion, our report underscores the function of E2p7 delayed processing in modulating i) the intracellular E2 levels, ii) the retention of E2 through the slowing down of the secretion pathway, and iii) the unmasking of functions of p7 amino-terminus in assembly and envelopment.

Materials and methods

Cell culture and reagents

Huh7.5 cells (kind gift of C Rice, Rockefeller University, New York, USA) and 293T kidney (ATCC CRL-1573) cells were grown in Dulbecco's modified minimal essential medium

(DMEM, Invitrogen, France) supplemented with 100U/ml of penicillin, 100μg/ml of streptomycin, and 10% fetal bovine serum.

Plasmids and constructs

pFK-JFH1wt_dg, pFK-JFH1/J6/C-846_dg plasmids encoding full-length JFH1 and Jc1 HCV [94] were kind gifts from R Bartenschlager (Heidelberg University, Germany). pFK-JFH1J6 XbaIC-846HAHA-L-p7_dg encoding a Jc1 virus with the HAHALp7 linker peptide between E2 and p7 [56] was kindly provided by T Pietschmann (Twincore, Germany). JFH1 virus-derived constructs encoding the p7-T2, p7-L2S, Ap7 and ASGGSp7, HAHALp7, and E2-A367R mutants were derived from the pFK-JFH1wt_dg plasmid. The E1 glycoprotein was also point-mutated in the pFK-JFH1wt_dg and pFK-JFH1 HAHALp7 constructs to introduce the A4 epitope, resulting in plasmids encoding JFH1 E1(A4) and JFH1 E1(A4) HAHALp7 viruses, respectively [57]. Constructs were created by PCR mutagenesis (oligonucleotide sequences are available upon request).

The plasmid pEGFP-N3-VSV-Gts was a kind gift from K Konan (Albany Medical College, USA). The plasmids encoding noSPp7 (JFH1), ΔE2p7 (JFH1), ΔCp7 (JFH1), ΔCp7 (H77), ΔE2p7 (J6), ΔE2HAHALp7 (JFH1), and noSPHAHALp7 (JFH1) allow individual expression of wt, variant or mutant p7 under different signal peptide configurations. The plasmids pTG 13077-HCV-ΔC-E1-E2-J6, pTG 13077-HCV-ΔC-E1-E2-JFH1 and pTG 13077-HCV-ΔC-E1-E2-p7-JFH1 contain retroviral vector genomes encoding E1E2 and/or E1E2p7 proteins from J6 and JFH1 viruses.

All constructs were expressed in Huh7.5 cells using procedures reported before [17].

Antibodies

Mouse anti-actin (clone AC74, Sigma-Aldrich), mouse anti-E1 A4 (kind gift from HB Greenberg), rat anti-HA (clone 3F10, Roche), mouse anti core C7-50 (Thermo Fisher Scientific), rat anti-E2 clone 3/11 (kind gift from J McKeating), mouse anti-NS2 6H6 and mouse anti-NS5A 9E10 (kind gift from C Rice), rabbit anti-NS2 (kind gift from B Lindenbach), human anti-E2 AR3A (kind gift from M Law), mouse anti-GFP (Roche), anti-VSV-G 41A1, mouse anti-E2 antibody AP33 (kind gift from A Patel) were used according to the providers' instructions.

VSV-Gts analysis

Huh7.5 cells were seeded 16h prior to transfection with pEGFP-N3-VSV-Gts and p7-encoding plasmids using GeneJammer transfection reagent (Agilent). Medium was changed 4h post-transfection and cells were incubated overnight at 40˚C. 24h post-transfection, cells were chased at 32˚C. For western blot analysis, cells were lysed at indicated time points in wells cooled on ice before clarification and western blot analysis. For flow cytometry analysis, cells were harvested and put in suspension at 32˚C. At indicated time points, cells were fixed with 3% paraformaldehyde.

Purification of soluble E2 (JFH1)

The plasmid popol-ΔE1sE2 (JFH1)-H6 (kind gift from Epixis SA) encoding soluble E2 (JFH1) with a 6xHis tag was used to purify E2 in order to assess the sensitivity of E2 quantifications by western blots. 293T cells grown in 10 cm-plates were transfected with 15μg of popol-ΔE1sE2 (JFH1)-H6. 16h post-transfection, the medium was replaced by OptiMEM. 24h and 48h later, supernatant was harvested and purified using a HisTrap column. Fractions were pooled and

then dialyzed. A sample was analyzed by SDS-PAGE. Concentration of sE2 was obtained by measurement of OD at 280nm and purity was analyzed by LC-MS/MS.

Production of lentivirals vectors

HEK293T cells were seeded 24h prior to transfection with VSV-G plasmid, pTG-5349 packaging plasmid, and either pTG 13077-HCV-ΔC-E1-E2-JFH1, pTG 13077-HCV-ΔC-E1-E2-J6 or pTG 13077-HCV-ΔC-E1-E2-p7-JFH1 plasmids using calcium phosphate precipitation. Medium was replaced 16h post-transfection. Vector supernatants were harvested 24h later, filtered through a 0.45 μm filter, and were titrated by flow cytometry using AP33 antibody against E2.

Production of SVPs

Lentiviral vectors were used to transduce Huh7.5 cells (MOI = 2). 72h post-transduction, cell supernatants were centrifuged at 25,000 rpm for 4h at 4˚C using SW41 rotor and Optima L-90 centrifuge (Beckman). Pellets were suspended in PBS prior to use for western blot analysis.

For gradient analysis, 1 ml of supernatant concentrated 40x by Vivaspin columns (MW cut-off 100-kDa (Sartorius)) was loaded on iodixanol density gradients. 12 fractions were collected from the top and used for refractive index measurement and precipitation of proteins before western blot analysis.

Production of HCVcc particles and quantifications of virion components

Methods for *in vitro* transcription of HCV RNA and its electroporation into Huh-7.5 cells have been described [17, 61]. When p7 was co-expressed with viral RNA, 2μg of plasmid DNA encoding p7 or control DNA were co-electroporated with 10μg of viral RNA.

To determine the percentage of HCV-positive producer cells following electroporation, cells were fixed and stained using Cytofix/Cytoperm (BD) according to manufacturer's instructions. NS5A staining was achieved with 9E10 antibody (kind gift from C. Rice, Rockefeller University, New York, USA) and cells were analyzed using MacsQuant VYB (Milteny Biotech).

Electroporated cells were counted and 100,000 cells were lysed in lysis buffer (20 mM Tris [pH 7.5], 1% Triton X-100, 0.05% sodium dodecyl sulfate, 150 nM NaCL, 5‰ Na deoxycholate) supplemented with protease/phosphatase inhibitor cocktail (Roche) and clarified from the nuclei by centrifugation at 13,000×*g* for 10 min at 4˚C for quantitative western blot analysis (see below).

HCV core protein was also quantified by CMIA—Chemiluminescent Microparticle ImmunoAssay (Architect, Abott). The extracellular E2 protein was quantified by Western Blot after precipitation of E2-containing cell supernatants with Galanthus Nivalis lectins (GNA) bound to agarose beads (Vector Laboratories). The extracellular HCV RNAs were quantified as described previously [61]. Infectivity titers were determined as focus-forming units per milliliter [17]. Serial dilutions of supernatants were used to infect Huh7.5 cells and focus-forming units were determined 3 days post-infection by counting NS5A-immunostained foci. For determining intracellular infectivity, electroporated cells were washed with PBS, harvested with Versene and centrifuged for 4 min at 400xg. Cell pellets were suspended in medium and subjected to 4 cycles of freeze and thaw, using liquid nitrogen.

For purification of particles, supernatants were harvested and filtered through a 0.45μm filter and centrifuged at 25,000 rpm for 1h45 at 4˚C with a SW41 rotor and Optima L-90 centrifuge (Beckman). Pellets were resuspended in PBS prior to use for western blot to quantify E2 or for quantification of core and RNAs.

Proteinase K digestion assays

Viral supernatants were i) left untreated, ii) treated with Proteinase K (PK, 50 μg/mL) in 10x PK buffer as described in [84] for 1h on ice, or iii) pre-treated with Triton X-100 5min at room temperature prior to treatment with PK. PK activity was stopped by adding 10 mM PMSF and protease inhibitors cocktail (Roche). The core protein was quantified with CMIA.

Iodixanol density gradient of HCVcc particles

1mL of viral supernatant was loaded on top of a 3–40% continuous iodixanol gradient (Optiprep, Axis Shield). Gradients were centrifuged for 16h at 4˚C in Optima L-90 centrifuge (Beckman). 16 fractions of 750 μl were collected from the top and used for refractive index measurement infectivity titration, core quantification and RNA quantification, as described above. For E2 protein analysis, HCV particles were produced in OptiMEM (Invitrogen) and concentrated 40x by Vivaspin molecular weight cutoff 100-kDa columns (Sartorius). 1 ml of concentrated virus suspension was loaded on density gradients. 12 fractions were collected from the top and used for refractive index measurement, titration, core quantification and RNA quantification, as described above. The remaining volumes of fractions were used for protein precipitation with 4 volumes of acidified acetone/methanol buffer and left at -20˚C overnight. Proteins were pelleted at 16,000xg for 15min and dried before resuspension in lysate buffer, denaturation in Laemmli buffer, and Western Blot analysis.

Deglycosylation with endoglycosidase H

Endoglycosidase Hf (Endo-Hf; NEB) treatment was performed according to the manufacturer's recommendations. Briefly, protein samples were mixed to denaturing glycoprotein buffer and heated at 100˚C for 5 min. Subsequently, 1,000 units of Endo-Hf were added to samples in a final volume of 25 μl and the reaction mixtures were incubated for 1 h at 37˚C, before western blot analysis.

Western blot analysis

Proteins obtained in total lysates or after digestion or immunoprecipitation, were denatured in Laemmli buffer at 95˚C for 5min and were separated by sodium dodecyl sulfate polyacrylamide gel electrophoresis, then transferred to nitrocellulose membrane and revealed with specific primary antibodies, followed by the addition of IRdye secondary antibodies (Li-Cor Biosciences), followed by imaging with an Odyssey infrared imaging system CLx (Li-Cor Biosciences).

Co-immuno-precipitation assays

For NS2/E2 interaction, 1 million electroporated cells were lysed with buffer (50 mM Tris-Cl (pH 7.5), 150 mM NaCl, 1% Nonidet P-40, 1% sodium deoxycholate, and 0.1% SDS). Lysates were cleared by centrifugation at 16,000xg for 10 min at 4˚C and were incubated overnight at 4˚C with AR3A antibody against HCV E2 or with rabbit NS2 antibody. Protein A/G-coated agarose beads were added to samples for 2h at room temperature. Immune complexes were then washed and eluted with Laemmli buffer for 5 min at 95˚C before western blot analysis.

For NS2/NS5A interaction, 1 million electroporated cells were cross-linked with 1mM dithiobis(succinimidyl propionate) (DSP) (ThermoFisher) 30min at room temperature. Tris (pH 7.5) was added up to 200 mM to quench unreacted DSP. Cells were resuspended in lysis buffer (50mM Tris pH 7.4, 150mM NaCl, 1mM EDTA, 0.5% n-dodecyl-β-maltoside) and treated as for NS2/E2 interaction with incubation with rabbit NS2 antibody.

Immuno-fluorescence (IF) and confocal microscopy imaging

Experimental procedures were previously described [66]. Briefly, Huh7.5 cells grown on glass coverslips and were infected at MOI of 0.2. 72h post-infection, cells were washed with PBS, fixed with 3% paraformaldehyde in PBS for 15min, quenched with 50mM NH_4Cl and permeabilized with 0.1% Triton X-100. Fixed cells were then incubated with primary antibodies in 1% BSA/PBS, washed and stained with the corresponding fluorescent Alexa-conjugated secondary antibody (Alexa-488, Alexa-555 and Alexa-647, Molecular Probes) in 1% BSA/PBS. LDs were stained with 10μg/mL Bodipy 493/503 (Molecular Probes) according to the manufacturer's instructions. Cells were washed with PBS, stained for nuclei with Hoechst (Molecular Probes) and mounted with Mowiol 4–88 (Sigma-Aldrich) prior to image acquisition with LSM-710 (Zeiss) confocal microscope. When stated, the combined detection of HCV RNA by FISH and viral proteins was done as previously described [66].

For digitonin permeabilization, the staining procedure was the same except that cells were permeabilized with 5μg/ml Digitonin (Sigma-Aldrich) for 10 min. Cells permeabilized with Triton X-100 were acquired first; then, cells permeabilized with Digitonin were acquired in order to use the same laser settings.

Image analysis and quantifications

Images were analyzed and quantified with the ImageJ software as previously described [66]. The Pearson's and Manders' correlation coefficients were calculated by using the JACoP plugin [95]. For the Digitonin *vs*. Triton permeabilization experiments, the relative fluorescence intensity of each channel was quantified by using the integrated density measurement of ImageJ software.

Molecular modeling of p7 hexamers

Three-dimensional homology models of p7 hexamers and their mutants were constructed using the NMR/MD p7 model of Chandler and colleagues [36] and the NMR p7 structure of OuYang and colleagues [35] (PDB accession number 2M6X) as templates. Models of p7 were constructed with the Swiss-Model automated protein structure homology modeling server (http://www.expasy.org/spdbv/ [96]) using the HCV JFH1 strain p7 sequence as input. JFH1 p7 homology model derived from OuYang et al. was directly obtained as a hexamer by the automated procedure. For JFH1 p7 homology model derived from Chandler et al., raw amino-acid sequence of p7 from strain JFH1 was first loaded in Swiss-PdbViewer software [96] and fitted to the NMR/MD p7 hexamer model [36] before submission for model building to Swiss-Model using the SwissModel Project Mode. All p7 JFH1 mutants were constructed using the latter protocol, *i.e*., fitting of the raw amino-acid sequence of p7 mutants to wild type hexamer models from the JFH1 strain. Coordinates of homology models derived from the automated model building were used without further minimization or manual manipulation. For mutants Ap7 and ASGGSp7 exhibiting N-terminal extensions, additional residues were added manually assuming a random conformation and were minimized using Swiss-PDB Viewer tools.

Statistical analysis

Significance values were calculated by applying the paired t-test using the GraphPad Prism 6 software (GraphPad Software, USA). For confocal analysis, a two-tailed, unpaired Mann-Whitney test was applied. P values under 0.05 were considered statistically significant and the following denotations were used: ****, $P \leq 0.0001$; ***, $P \leq 0.001$; **, $P \leq 0.01$; *, $P \leq 0.05$; ns (not significant), $P > 0.05$.

Supporting information

S1 Fig. Molecular modeling of p7 ATMI mutant structures. Comparison of three-dimensional homology molecular models of p7 structures using the NMR/MD model in POPC [36] and the NMR model in DPC [35]. The first amino-acid positions are represented in blue, second positions in red, third positions in green. Single amino acid insertions are represented in orange whereas larger insertions are represented in violet.
(TIFF)

S2 Fig. Transcomplementation of p7 ATMI mutant viruses with wt p7. Huh7.5 cells were electroporated with RNAs from parental or p7 ATMI mutant viruses, as indicated. At 72h post-electroporation, expression analyses were performed. (**A**) NS2, HAHALp7, E2, E2p7 as well as E2HAHALp7 (white arrows) and E2p7NS2 and E2HAHALp7NS2 (black arrows) precursors were revealed using anti-E2, anti-NS2 and HA antibodies, as indicated. (**B**) The infectivity levels of JFH1-derived p7 ATMI mutant viruses expressed alone (black bars) or with wild-type p7 (hatched bars) are represented.
(TIFF)

S3 Fig. p7 ATMI mutant viruses accelerating E2p7 cleavage have increased expression levels of E2 and core proteins. Huh7.5 cells were electroporated with RNAs from parental or p7 ATMI mutant viruses, as indicated. At 72h post-electroporation, expression analyses were performed and determined by quantitative western blot. (**A**) Levels of intracellular E2 for the JFH1-derived p7 ATMI mutant viruses. (**B**) Levels of intracellular core for the same mutant viruses. Proteins in (**A**) and (**B**) were quantified and normalized after determining the proportion of HCV-positive virus producer cells and the amounts of cellular actin (see Fig 3A). (**C**) Huh7.5 cells were electroporated with RNAs from parental or Jc1 HAHALp7 mutant virus. At 72h post-electroporation, cells were treated with cycloheximide (100μg/mL) and brefeldin A (1μg/mL). At the indicated time points, cells were counted and the same amounts of cells were lysed. Levels of E2 were determined by quantitative Western blot. The values are displayed relative to expression of E2 and core in JFH1 HCVcc virus-electroporated cells (**A**, **B**) or relative to time 0h post-addition of the drugs (**C**). Data represent mean values ± SEM. The number of experiments performed are indicated below the graphs.
(TIFF)

S4 Fig. p7 ATMI mutant viruses display increased secretion of E2 but decreased secretion of core proteins and RNA. Huh7.5 cells were electroporated with RNAs from parental or JFH1 mutant viruses expressed alone or with wild-type p7. At 72h post-electroporation, analyses were performed and normalized after determining the proportion of HCV-positive virus producer cells (see Fig 3A). (**A**) Levels of secreted E2 determined by quantitative western blot following GNA lectin pull down of cell supernatants. (**B**) Levels of secreted HCV RNAs as determined by RT-qPCR. (**C, D**) Levels of secreted core as determined by CMIA for JFH1 HAHALp7 or JFH1 p7-T2 mutant viruses alone or with WT p7 (**D**) and for other JFH1-derived p7 ATMI mutants (**C**). All values are displayed relative to expression of E2, core or RNA values determined in the supernatants of JFH1 virus-electroporated cells (**A-C**). Data represent mean values ± SEM. The number of experiments performed are indicated below the graphs.
(TIFF)

S5 Fig. p7 ATMI mutant viruses exhibit decreased specific infectivity. Huh7.5 cells were electroporated with RNAs from parental or JFH1 mutant viruses expressed alone or with wild-type p7. At 72h post-electroporation, infectivity, and RNA and core secretion analyses were performed. (**A**) Specific infectivity relative to RNA amounts for all JFH1-derived p7 ATMI

mutant viruses. (**B**) Specific infectivity relative to core amounts for all JFH1-derived p7 ATMI mutants. (**C**) Specific infectivity relative to core amounts for JFH1 HAHALp7 or JFH1 p7-T2 mutant viruses expressed alone or with wild-type p7. Values are displayed relative to expression of specific infectivity in the supernatants of JFH1-electroporated cells. Data represent mean values ± SEM. The number of experiments performed are indicated below the graphs.
(TIFF)

S6 Fig. p7 ATMI mutant viruses have increased secretion of particle-associated E2 proteins. Huh7.5 cells were electroporated with RNAs from parental or JFH1 mutant viruses expressed alone or with wild-type p7. At 72h post-electroporation, quantitative western blot analyses were performed. (**A**) Level of E2 and E1 in pellet for the JFH1 HAHALp7 mutant virus relative to parental virus. (**B**) Level of E2 in pellets from ultracentrifuged cell supernatants for all p7 ATMI mutants. (**C**) Aliquots of supernatant from cells expressing JFH1 or JFH1 HAHALp7 viruses were incubated for 1hr with 1% Triton X-100 or left untreated before ultracentrifugation and analysis of E2 in the pellets by quantitative western blot. Proteins in (**A**) were quantified and normalized after determining the proportion of HCV-positive virus producer cells. Values are displayed relative to expression of E2 or E1 in the pellets of supernatants from JFH1 virus-electroporated cells. Data represent mean values ± SEM. The number of experiments performed are indicated below the graphs.
(TIFF)

S7 Fig. Representative density gradient analysis of p7 ATMI mutant viruses in Jc1 or JFH1 HCVcc backbones. Huh7.5 cells were electroporated with RNAs from parental *vs*. Jc1 HAHALp7 (**A**), JFH1 HAHALp7 (**C**) viruses expressed alone or with wild-type p7 (**B**). At 72h post-electroporation supernatants were collected and layered on iodixanol buoyant density gradients. (**A**) Representative gradient profiles of Jc1 and Jc1 HAHALp7 viruses. The levels of E2, core, infectivity, and viral RNAs were quantified and normalized after determining the proportion of HCV-positive virus producer cells (see Fig 3A). (**B**) Representative gradient profiles of Jc1 and Jc1 HAHALp7 viruses expressed with or without wt p7. The levels of core and infectivity were quantified and normalized after determining the proportion of HCV-positive virus producer cells (see Fig 3A). (**C**) Representative gradient profiles of JFH1 and JFH1 HAHALp7. The core, E2 and E1 proteins and infectivity were measured in each fraction and expressed of percentages of the sum of fractions.
(TIFF)

S8 Fig. p7 ATMI mutant viruses do not alter the intracellular localization of core. At 72h post-transfection or post-infection, cells were fixed and stained for HCV core (red), LD (green, left panels), calnexin (green, right panels) and nuclei (blue). (**A**) Confocal microscopy analysis of Huh7.5 cells transfected with constructs expressing J6 core alone or in combination with wt p7 or HAHALp7. (**B**) Confocal microscopy of Huh7.5 infected with Jc1 or Jc1 HAHALp7 viruses.
(TIFF)

S9 Fig. Co-localization of p7 ATMI mutant and E2 with core protein. At 72h post-electroporation or transfection, cells were fixed, permeabilized with either Triton X-100 or Digitonin, as indicated, and stained for HCV core (red), HAHALp7 (green), E2 (green) and nuclei (grey). (**A**) Confocal microscopy analysis of Huh7.5 electroporated with JFH1 HAHALp7 virus RNAs. (**B**) Confocal microscopy analysis of Huh7.5 cells transfected with core-E1E2 and noSPHAHALp7 expression constructs. (**C**) Confocal microscopy analysis of Huh7.5 cells transfected with core-E1E2 and ΔE2HAHALp7 expression constructs. The relative

fluorescence intensity of each channel was quantified by using ImageJ.
(PDF)

S10 Fig. p7 ATMI mutants impair NS2 association with E2 and NS5A. Huh7.5 cells expressing RNAs from parental or JFH1-derived p7 ATMI mutant viruses expressed alone or with wild-type p7 were analyzed at 72h. **(A)** Levels of NS2 proteins co-immuno-precipitated by E2 antibodies normalized to the amount of immuno-precipitated E2 proteins. (**B**) Levels of E2 proteins co-immuno-precipitated by NS2 antibodies normalized to the amount of immuno-precipitated E2 proteins. **(C)** Levels of NS5A proteins co-immuno-precipitated by NS2 antibodies normalized to the amount of immuno-precipitated NS2 proteins. The values are displayed relative to co-immuno-precipitated E2, NS5A or NS2 in JFH1 virus-expressing cells. Data represent mean values ± SEM. The number of experiments performed are indicated below the graphs.
(TIFF)

Acknowledgments

We are grateful to Ralf Bartenschlager for the gift of JFH1 and Jc1 HCVcc constructs, Harry Greenberg for the A4 anti-E1 antibody, Colette Jolivet for the core antibody, Mishinori Kohara for the NS4B antibody, Konan Kouacou for the VSV-Gts construct, Mansun Law for the AR3A E2 antibody, Jane McKeating for the 3/11 E2 antibody, Arvin Patel for the AP33 E2 antibody, Thomas Pietschmann for the Jc1 HAHALp7 construct, and Charles Rice for the Huh7.5 cells and 9E10 NS5A and 6H6 NS2 monoclonal antibodies.

We thank Ali Amara and Denis Gerlier for stimulating discussions and helpful comments.

We acknowledge the contribution of SFR Biosciences (UMS3444/CNRS, US8/Inserm, ENS de Lyon, UCBL) facilities: LBI-PLATIM-Microscopy (Claire Lionnet and Elodie Chatre), PSF Protein Science (Véronique Senty-Segault and Frédéric Delolme), ANIRA-Cytometry, and ANIRA-Genetic Analysis for excellent technical assistance and support. We than Didier Décimo for support with the BSL3 facility. We thank Omran Allatif for guidance with the statistical analysis.

Author Contributions

Conceptualization: Solène Denolly, Bertrand Boson, François-Loïc Cosset.

Formal analysis: Solène Denolly, Chloé Mialon, François Penin, Bertrand Boson, François-Loïc Cosset.

Funding acquisition: François-Loïc Cosset.

Investigation: Solène Denolly, Chloé Mialon, Thomas Bourlet, Fouzia Amirache, Bertrand Boson.

Methodology: Solène Denolly, Chloé Mialon, Thomas Bourlet, Fouzia Amirache, François Penin, Brett Lindenbach, Bertrand Boson, François-Loïc Cosset.

Project administration: François-Loïc Cosset.

Resources: Brett Lindenbach, François-Loïc Cosset.

Supervision: Bertrand Boson, François-Loïc Cosset.

Validation: Solène Denolly, François-Loïc Cosset.

Writing – original draft: Solène Denolly, Bertrand Boson, François-Loïc Cosset.

Writing – review & editing: Solène Denolly, Bertrand Boson, François-Loïc Cosset.

References

1. Pawlotsky JM. The end of the hepatitis C burden: Really? Hepatology. 2016; 64(5):1404–7. https://doi.org/10.1002/hep.28758 PMID: 27486957.
2. Moradpour D, Grakoui A, Manns MP. Future landscape of hepatitis C research—Basic, translational and clinical perspectives. J Hepatol. 2016; 65(1 Suppl):S143–55. https://doi.org/10.1016/j.jhep.2016.07.026 PMID: 27641984.
3. Dubuisson J, Cosset FL. Virology and cell biology of the hepatitis C virus life cycle: an update. J Hepatol. 2014; 61(1 Suppl):S3–S13. https://doi.org/10.1016/j.jhep.2014.06.031 PMID: 25443344.
4. Targett-Adams P, Hope G, Boulant S, McLauchlan J. Maturation of hepatitis C virus core protein by signal peptide peptidase is required for virus production. J Biol Chem. 2008; 283(24):16850–9. https://doi.org/10.1074/jbc.M802273200 PMID: 18424431.
5. McLauchlan J, Lemberg MK, Hope G, Martoglio B. Intramembrane proteolysis promotes trafficking of hepatitis C virus core protein to lipid droplets. EMBO J. 2002; 21(15):3980–8. https://doi.org/10.1093/emboj/cdf414 PMID: 12145199; PubMed Central PMCID: PMCPMC126158.
6. Romero-Brey I, Berger C, Kallis S, Kolovou A, Paul D, Lohmann V, et al. NS5A Domain 1 and Polyprotein Cleavage Kinetics Are Critical for Induction of Double-Membrane Vesicles Associated with Hepatitis C Virus Replication. mBio. 2015; 6:e00759–15. https://doi.org/10.1128/mBio.00759-15 PMID: 26152585
7. Lin C, Lindenbach BD, Pragai BM, McCourt DW, Rice CM. Processing in the hepatitis C virus E2-NS2 region: identification of p7 and two distinct E2-specific products with different C termini. J Virol. 1994; 68(8):5063–73. PMID: 7518529; PubMed Central PMCID: PMCPMC236449.
8. Carrère-Kremer S, Montpellier C, Lorenzo L, Brulin B, Cocquerel L, Belouzard S, et al. Regulation of Hepatitis C Virus Polyprotein Processing by Signal Peptidase Involves Structural Determinants at the p7 Sequence Junctions. Journal of Biological Chemistry. 2004; 279:41384–92. https://doi.org/10.1074/jbc.M406315200 PMID: 15247249
9. Shanmugam S, Yi M. The Efficiency of E2-p7 Processing Modulates the Production of Infectious Hepatitis C Virus. Journal of Virology. 2013. https://doi.org/10.1128/JVI.01807-13 PMID: 23946462
10. Scull MA, Schneider WM, Flatley BR, Hayden R, Fung C, Jones CT, et al. The N-terminal Helical Region of the Hepatitis C Virus p7 Ion Channel Protein Is Critical for Infectious Virus Production. PLoS Pathogens. 2015; 11:e1005297. https://doi.org/10.1371/journal.ppat.1005297 PMID: 26588073.
11. Steinmann E, Penin F, Kallis S, Patel AH, Bartenschlager R, Pietschmann T. Hepatitis C Virus p7 Protein Is Crucial for Assembly and Release of Infectious Virions. PLoS Pathog. 2007; 3:e103. https://doi.org/10.1371/journal.ppat.0030103 PMID: 17658949
12. Miyanari Y, Atsuzawa K, Usuda N, Watashi K, Hishiki T, Zayas M, et al. The lipid droplet is an important organelle for hepatitis C virus production. Nat Cell Biol. 2007; 9(9):1089–97. https://doi.org/10.1038/ncb1631 PMID: 17721513.
13. Ma Y, Anantpadma M, Timpe JM, Shanmugam S, Singh SM, Lemon SM, et al. Hepatitis C Virus NS2 Protein Serves as a Scaffold for Virus Assembly by Interacting with both Structural and Nonstructural Proteins. Journal of Virology. 2011; 85:86–97. https://doi.org/10.1128/JVI.01070-10 PMID: 20962101
14. Stapleford KA, Lindenbach BD. Hepatitis C virus NS2 coordinates virus particle assembly through physical interactions with the E1-E2 glycoprotein and NS3-NS4A enzyme complexes. J Virol. 2011; 85(4):1706–17. https://doi.org/10.1128/JVI.02268-10 PMID: 21147927; PubMed Central PMCID: PMCPMC3028914.
15. Jirasko V, Montserret R, Lee JY, Gouttenoire J, Moradpour D, Penin F, et al. Structural and Functional Studies of Nonstructural Protein 2 of the Hepatitis C Virus Reveal Its Key Role as Organizer of Virion Assembly. PLoS Pathog. 2010; 6:e1001233. https://doi.org/10.1371/journal.ppat.1001233 PMID: 21187906
16. Popescu CI, Callens N, Trinel D, Roingeard P, Moradpour D, Descamps V, et al. NS2 protein of hepatitis C virus interacts with structural and non-structural proteins towards virus assembly. PLoS Pathog. 2011; 7(2):e1001278. https://doi.org/10.1371/journal.ppat.1001278 PMID: 21347350; PubMed Central PMCID: PMCPMC3037360.
17. Boson B, Granio O, Bartenschlager R, Cosset F-L. A Concerted Action of Hepatitis C Virus P7 and Nonstructural Protein 2 Regulates Core Localization at the Endoplasmic Reticulum and Virus Assembly. PLoS Pathog. 2011; 7:e1002144. https://doi.org/10.1371/journal.ppat.1002144 PMID: 21814513
18. Zayas M, Long G, Madan V, Bartenschlager R. Coordination of Hepatitis C Virus Assembly by Distinct Regulatory Regions in Nonstructural Protein 5A. PLoS Pathog. 2016; 12(1):e1005376. https://doi.org/10.1371/journal.ppat.1005376 PMID: 26727512; PubMed Central PMCID: PMCPMC4699712.
19. Masaki T, Suzuki R, Murakami K, Aizaki H, Ishii K, Murayama A, et al. Interaction of hepatitis C virus nonstructural protein 5A with core protein is critical for the production of infectious virus particles. J

Virol. 2008; 82(16):7964–76. https://doi.org/10.1128/JVI.00826-08 PMID: 18524832; PubMed Central PMCID: PMCPMC2519576.

20. Appel N, Zayas M, Miller S, Krijnse-Locker J, Schaller T, Friebe P, et al. Essential role of domain III of nonstructural protein 5A for hepatitis C virus infectious particle assembly. PLoS Pathog. 2008; 4(3): e1000035. https://doi.org/10.1371/journal.ppat.1000035 PMID: 18369481; PubMed Central PMCID: PMCPMC2268006.

21. Vieyres G, Dubuisson J, Pietschmann T. Incorporation of hepatitis C virus E1 and E2 glycoproteins: the keystones on a peculiar virion. Viruses. 2014; 6(3):1149–87. https://doi.org/10.3390/v6031149 PMID: 24618856; PubMed Central PMCID: PMCPMC3970144.

22. Mankouri J, Walter C, Stewart H, Bentham M, Park WS, Heo WD, et al. Release of Infectious Hepatitis C Virus from Huh7 Cells Occurs via a trans-Golgi Network-to-Endosome Pathway Independent of Very-Low-Density Lipoprotein Secretion. J Virol. 2016; 90(16):7159–70. https://doi.org/10.1128/JVI.00826-16 PMID: 27226379; PubMed Central PMCID: PMCPMC4984645.

23. Bayer K, Banning C, Bruss V, Wiltzer-Bach L, Schindler M. Hepatitis C Virus Is Released via a Noncanonical Secretory Route. J Virol. 2016; 90(23):10558–73. https://doi.org/10.1128/JVI.01615-16 PMID: 27630244; PubMed Central PMCID: PMCPMC5110177.

24. Icard V, Diaz O, Scholtes C, Perrin-Cocon L, Ramière C, Bartenschlager R, et al. Secretion of Hepatitis C Virus Envelope Glycoproteins Depends on Assembly of Apolipoprotein B Positive Lipoproteins. PLoS ONE. 2009; 4:e4233. https://doi.org/10.1371/journal.pone.0004233 PMID: 19156195

25. Scholtes C, Ramiere C, Rainteau D, Perrin-Cocon L, Wolf C, Humbert L, et al. High plasma level of nucleocapsid-free envelope glycoprotein-positive lipoproteins in hepatitis C patients. Hepatology. 2012; 56(1):39–48. Epub 2012/02/01. https://doi.org/10.1002/hep.25628 PMID: 22290760.

26. Masciopinto F, Giovani C, Campagnoli S, Galli-Stampino L, Colombatto P, Brunetto M, et al. Association of hepatitis C virus envelope proteins with exosomes. European Journal of Immunology. 2004; 34:2834–42. https://doi.org/10.1002/eji.200424887 PMID: 15368299

27. Ramakrishnaiah V, Thumann C, Fofana I, Habersetzer F, Pan Q, Ruiter PEd, et al. Exosome-mediated transmission of hepatitis C virus between human hepatoma Huh7.5 cells. Proceedings of the National Academy of Sciences. 2013; 110:13109–13. https://doi.org/10.1073/pnas.1221899110 PMID: 23878230

28. Maillard P, Krawczynski K, Nitkiewicz J, Bronnert C, Sidorkiewicz M, Gounon P, et al. Nonenveloped nucleocapsids of hepatitis C virus in the serum of infected patients. J Virol. 2001; 75(17):8240–50. https://doi.org/10.1128/JVI.75.17.8240-8250.2001 PMID: 11483769; PubMed Central PMCID: PMCPMC115068.

29. Bartenschlager R, Penin F, Lohmann V, Andre P. Assembly of infectious hepatitis C virus particles. Trends Microbiol. 2011; 19(2):95–103. https://doi.org/10.1016/j.tim.2010.11.005 PMID: 21146993.

30. Montserret R, Saint N, Vanbelle C, Salvay AG, Simorre JP, Ebel C, et al. NMR structure and ion channel activity of the p7 protein from hepatitis C virus. J Biol Chem. 2010; 285(41):31446–61. https://doi.org/10.1074/jbc.M110.122895 PMID: 20667830; PubMed Central PMCID: PMCPMC2951219.

31. Foster TL, Thompson GS, Kalverda AP, Kankanala J, Bentham M, Wetherill LF, et al. Structure-guided design affirms inhibitors of hepatitis C virus p7 as a viable class of antivirals targeting virion release. Hepatology. 2014; 59(2):408–22. https://doi.org/10.1002/hep.26685 PMID: 24022996; PubMed Central PMCID: PMCPMC4298801.

32. Cook GA, Dawson LA, Tian Y, Opella SJ. Three-dimensional structure and interaction studies of hepatitis C virus p7 in 1,2-dihexanoyl-sn-glycero-3-phosphocholine by solution nuclear magnetic resonance. Biochemistry. 2013; 52(31):5295–303. https://doi.org/10.1021/bi4006623 PMID: 23841474; PubMed Central PMCID: PMCPMC3855088.

33. Isherwood BJ, Patel AH. Analysis of the processing and transmembrane topology of the E2p7 protein of hepatitis C virus. J Gen Virol. 2005; 86(Pt 3):667–76. https://doi.org/10.1099/vir.0.80737-0 PMID: 15722527.

34. Madan V, Bartenschlager R. Structural and Functional Properties of the Hepatitis C Virus p7 Viroporin. Viruses. 2015; 7(8):4461–81. https://doi.org/10.3390/v7082826 PMID: 26258788; PubMed Central PMCID: PMCPMC4576187.

35. OuYang B, Xie S, Berardi MJ, Zhao X, Dev J, Yu W, et al. Unusual architecture of the p7 channel from hepatitis C virus. Nature. 2013; 498(7455):521–5. https://doi.org/10.1038/nature12283 PMID: 23739335; PubMed Central PMCID: PMCPMC3725310.

36. Chandler DE, Penin F, Schulten K, Chipot C. The p7 protein of hepatitis C virus forms structurally plastic, minimalist ion channels. PLoS Comput Biol. 2012; 8(9):e1002702. https://doi.org/10.1371/journal.pcbi.1002702 PMID: 23028296; PubMed Central PMCID: PMCPMC3447957.

37. Luik P, Chew C, Aittoniemi J, Chang J, Wentworth P Jr., Dwek RA, et al. The 3-dimensional structure of a hepatitis C virus p7 ion channel by electron microscopy. Proc Natl Acad Sci U S A. 2009; 106

(31):12712–6. https://doi.org/10.1073/pnas.0905966106 PMID: 19590017; PubMed Central PMCID: PMCPMC2722341.

38. Nieto-Torres JL, Verdia-Baguena C, Castano-Rodriguez C, Aguilella VM, Enjuanes L. Relevance of Viroporin Ion Channel Activity on Viral Replication and Pathogenesis. Viruses. 2015; 7(7):3552–73. https://doi.org/10.3390/v7072786 PMID: 26151305; PubMed Central PMCID: PMCPMC4517115.

39. Shanmugam S, Saravanabalaji D, Yi M. Detergent-resistant membrane association of NS2 and E2 during hepatitis C virus replication. J Virol. 2015; 89(8):4562–74. https://doi.org/10.1128/JVI.00123-15 PMID: 25673706; PubMed Central PMCID: PMCPMC4442399.

40. Gentzsch J, Brohm C, Steinmann E, Friesland M, Menzel N, Vieyres G, et al. Hepatitis C Virus p7 is Critical for Capsid Assembly and Envelopment. PLoS Pathog. 2013; 9:e1003355. https://doi.org/10.1371/journal.ppat.1003355 PMID: 23658526

41. Wozniak AL, Griffin S, Rowlands D, Harris M, Yi M, Lemon SM, et al. Intracellular proton conductance of the hepatitis C virus p7 protein and its contribution to infectious virus production. PLoS Pathog. 2010; 6(9):e1001087. https://doi.org/10.1371/journal.ppat.1001087 PMID: 20824094; PubMed Central PMCID: PMCPMC2932723.

42. Bentham MJ, Foster TL, McCormick C, Griffin S. Mutations in hepatitis C virus p7 reduce both the egress and infectivity of assembled particles via impaired proton channel function. J Gen Virol. 2013; 94 (Pt 10):2236–48. https://doi.org/10.1099/vir.0.054338-0 PMID: 23907396.

43. de Jong AS, de Mattia F, Van Dommelen MM, Lanke K, Melchers WJ, Willems PH, et al. Functional analysis of picornavirus 2B proteins: effects on calcium homeostasis and intracellular protein trafficking. J Virol. 2008; 82(7):3782–90. https://doi.org/10.1128/JVI.02076-07 PMID: 18216106; PubMed Central PMCID: PMCPMC2268507.

44. Griffin SD, Beales LP, Clarke DS, Worsfold O, Evans SD, Jaeger J, et al. The p7 protein of hepatitis C virus forms an ion channel that is blocked by the antiviral drug, Amantadine. FEBS Lett. 2003; 535(1–3):34–8. PMID: 12560074.

45. Steinmann E, Pietschmann T. Hepatitis C virus p7-a viroporin crucial for virus assembly and an emerging target for antiviral therapy. Viruses. 2010; 2(9):2078–95. https://doi.org/10.3390/v2092078 PMID: 21994720; PubMed Central PMCID: PMCPMC3185753.

46. StGelais C, Foster TL, Verow M, Atkins E, Fishwick CW, Rowlands D, et al. Determinants of hepatitis C virus p7 ion channel function and drug sensitivity identified in vitro. J Virol. 2009; 83(16):7970–81. https://doi.org/10.1128/JVI.00521-09 PMID: 19493992; PubMed Central PMCID: PMCPMC2715780.

47. Pavlovic D, Neville DC, Argaud O, Blumberg B, Dwek RA, Fischer WB, et al. The hepatitis C virus p7 protein forms an ion channel that is inhibited by long-alkyl-chain iminosugar derivatives. Proc Natl Acad Sci U S A. 2003; 100(10):6104–8. https://doi.org/10.1073/pnas.1031527100 PMID: 12719519; PubMed Central PMCID: PMCPMC156333.

48. Breitinger U, Farag NS, Ali NKM, Breitinger HA. Patch-Clamp Study of Hepatitis C p7 Channels Reveals Genotype-Specific Sensitivity to Inhibitors. Biophys J. 2016; 110(11):2419–29. Epub 2016/06/09. https://doi.org/10.1016/j.bpj.2016.04.018 PMID: 27276260; PubMed Central PMCID: PMCPMC4906147.

49. Farag NS, Breitinger U, El-Azizi M, Breitinger HG. The p7 viroporin of the hepatitis C virus contributes to liver inflammation by stimulating production of Interleukin-1beta. Biochim Biophys Acta. 2017; 1863 (3):712–20. Epub 2016/12/17. https://doi.org/10.1016/j.bbadis.2016.12.006 PMID: 27979709.

50. Campanella M, de Jong AS, Lanke KW, Melchers WJ, Willems PH, Pinton P, et al. The coxsackievirus 2B protein suppresses apoptotic host cell responses by manipulating intracellular Ca2+ homeostasis. J Biol Chem. 2004; 279(18):18440–50. https://doi.org/10.1074/jbc.M309494200 PMID: 14976205.

51. Qi H, Chu V, Wu NC, Chen Z, Truong S, Brar G, et al. Systematic identification of anti-interferon function on hepatitis C virus genome reveals p7 as an immune evasion protein. Proc Natl Acad Sci U S A. 2017; 114(8):2018–23. Epub 2017/02/06. https://doi.org/10.1073/pnas.1614623114 PMID: 28159892; PubMed Central PMCID: PMCPMC5338388.

52. Hijikata M, Kato N, Ootsuyama Y, Nakagawa M, Shimotohno K. Gene mapping of the putative structural region of the hepatitis C virus genome by in vitro processing analysis. Proc Natl Acad Sci U S A. 1991; 88(13):5547–51. PMID: 1648221; PubMed Central PMCID: PMCPMC51914.

53. Jones CT, Murray CL, Eastman DK, Tassello J, Rice CM. Hepatitis C virus p7 and NS2 proteins are essential for production of infectious virus. J Virol. 2007; 81(16):8374–83. https://doi.org/10.1128/JVI.00690-07 PMID: 17537845; PubMed Central PMCID: PMCPMC1951341.

54. Konan KV, Giddings TH Jr., Ikeda M, Li K, Lemon SM, Kirkegaard K. Nonstructural protein precursor NS4A/B from hepatitis C virus alters function and ultrastructure of host secretory apparatus. J Virol. 2003; 77(14):7843–55. https://doi.org/10.1128/JVI.77.14.7843-7855.2003 PMID: 12829824; PubMed Central PMCID: PMCPMC161946.

55. Rothman JE, Lodish HF. Synchronised transmembrane insertion and glycosylation of a nascent membrane protein. Nature. 1977; 269(5631):775–80. PMID: 200844.

56. Vieyres G, Brohm C, Friesland M, Gentzsch J, Wolk B, Roingeard P, et al. Subcellular localization and function of an epitope-tagged p7 viroporin in hepatitis C virus-producing cells. J Virol. 2013; 87 (3):1664–78. https://doi.org/10.1128/JVI.02782-12 PMID: 23175364; PubMed Central PMCID: PMCPMC3554161.

57. Vieyres G, Thomas X, Descamps V, Duverlie G, Patel AH, Dubuisson J. Characterization of the envelope glycoproteins associated with infectious hepatitis C virus. J Virol. 2010; 84(19):10159–68. https://doi.org/10.1128/JVI.01180-10 PMID: 20668082; PubMed Central PMCID: PMCPMC2937754.

58. Gastaminza P, Kapadia SB, Chisari FV. Differential biophysical properties of infectious intracellular and secreted hepatitis C virus particles. J Virol. 2006; 80(22):11074–81. https://doi.org/10.1128/JVI.01150-06 PMID: 16956946; PubMed Central PMCID: PMCPMC1642172.

59. Lindenbach BD, Meuleman P, Ploss A, Vanwolleghem T, Syder AJ, McKeating JA, et al. Cell culture-grown hepatitis C virus is infectious in vivo and can be recultured in vitro. Proc Natl Acad Sci U S A. 2006; 103(10):3805–9. https://doi.org/10.1073/pnas.0511218103 PMID: 16484368; PubMed Central PMCID: PMCPMC1533780.

60. Bankwitz D, Steinmann E, Bitzegeio J, Ciesek S, Friesland M, Herrmann E, et al. Hepatitis C virus hypervariable region 1 modulates receptor interactions, conceals the CD81 binding site, and protects conserved neutralizing epitopes. J Virol. 2010; 84(11):5751–63. https://doi.org/10.1128/JVI.02200-09 PMID: 20357091; PubMed Central PMCID: PMCPMC2876602.

61. Calattini S, Fusil F, Mancip J, Dao Thi VL, Granier C, Gadot N, et al. Functional and Biochemical Characterization of Hepatitis C Virus (HCV) Particles Produced in a Humanized Liver Mouse Model. The Journal of biological chemistry. 2015; 290(38):23173–87. https://doi.org/10.1074/jbc.M115.662999 PMID: 26224633; PubMed Central PMCID: PMC4645586.

62. Dao Thi VL, Granier C, Zeisel MB, Guerin M, Mancip J, Granio O, et al. Characterization of hepatitis C virus particle subpopulations reveals multiple usage of the scavenger receptor BI for entry steps. J Biol Chem. 2012; 287(37):31242–57. https://doi.org/10.1074/jbc.M112.365924 PMID: 22767607; PubMed Central PMCID: PMCPMC3438956.

63. Merz A, Long G, Hiet MS, Brugger B, Chlanda P, Andre P, et al. Biochemical and morphological properties of hepatitis C virus particles and determination of their lipidome. J Biol Chem. 2011; 286(4):3018–32. https://doi.org/10.1074/jbc.M110.175018 PMID: 21056986; PubMed Central PMCID: PMCPMC3024796.

64. Podevin P, Carpentier A, Pene V, Aoudjehane L, Carriere M, Zaidi S, et al. Production of infectious hepatitis C virus in primary cultures of human adult hepatocytes. Gastroenterology. 2010; 139(4):1355–64. https://doi.org/10.1053/j.gastro.2010.06.058 PMID: 20600021.

65. Shavinskaya A, Boulant S, Penin F, McLauchlan J, Bartenschlager R. The Lipid Droplet Binding Domain of Hepatitis C Virus Core Protein Is a Major Determinant for Efficient Virus Assembly. Journal of Biological Chemistry. 2007; 282:37158–69. https://doi.org/10.1074/jbc.M707329200 PMID: 17942391

66. Boson B, Denolly S, Turlure F, Chamot C, Dreux M, Cosset F-L. Daclatasvir Prevents Hepatitis C Virus Infectivity by Blocking Transfer of the Viral Genome to Assembly Sites. Gastroenterology. 2017; 152:895–907.e14. https://doi.org/10.1053/j.gastro.2016.11.047 PMID: 27932311

67. Yan Y, He Y, Boson B, Wang X, Cosset FL, Zhong J. A Point Mutation in the N-Terminal Amphipathic Helix alpha0 in NS3 Promotes Hepatitis C Virus Assembly by Altering Core Localization to the Endoplasmic Reticulum and Facilitating Virus Budding. J Virol. 2017; 91(6). https://doi.org/10.1128/JVI.02399-16 PMID: 28053108; PubMed Central PMCID: PMCPMC5331820.

68. DiGiuseppe S, Keiffer TR, Bienkowska-Haba M, Luszczek W, Guion LG, Muller M, et al. Topography of the Human Papillomavirus Minor Capsid Protein L2 during Vesicular Trafficking of Infectious Entry. J Virol. 2015; 89(20):10442–52. https://doi.org/10.1128/JVI.01588-15 PMID: 26246568; PubMed Central PMCID: PMCPMC4580179.

69. Lange Y. Disposition of intracellular cholesterol in human fibroblasts. J Lipid Res. 1991; 32(2):329–39. PMID: 2066666.

70. Carrere-Kremer S, Montpellier-Pala C, Cocquerel L, Wychowski C, Penin F, Dubuisson J. Subcellular localization and topology of the p7 polypeptide of hepatitis C virus. J Virol. 2002; 76(8):3720–30. https://doi.org/10.1128/JVI.76.8.3720-3730.2002 PMID: 11907211; PubMed Central PMCID: PMCPMC136108.

71. Suzuki R, Matsuda M, Watashi K, Aizaki H, Matsuura Y, Wakita T, et al. Signal Peptidase Complex Subunit 1 Participates in the Assembly of Hepatitis C Virus through an Interaction with E2 and NS2. PLoS Pathog. 2013; 9:e1003589. https://doi.org/10.1371/journal.ppat.1003589 PMID: 24009510

72. Huang L, Hwang J, Sharma SD, Hargittai MR, Chen Y, Arnold JJ, et al. Hepatitis C virus nonstructural protein 5A (NS5A) is an RNA-binding protein. J Biol Chem. 2005; 280(43):36417–28. https://doi.org/10.1074/jbc.M508175200 PMID: 16126720.

73. Foster TL, Belyaeva T, Stonehouse NJ, Pearson AR, Harris M. All three domains of the hepatitis C virus nonstructural NS5A protein contribute to RNA binding. J Virol. 2010; 84(18):9267–77. https://doi.org/10.1128/JVI.00616-10 PMID: 20592076; PubMed Central PMCID: PMCPMC2937630.

74. Deleersnyder V, Pillez A, Wychowski C, Blight K, Xu J, Hahn YS, et al. Formation of native hepatitis C virus glycoprotein complexes. J Virol. 1997; 71(1):697–704. Epub 1997/01/01. PMID: 8985401; PubMed Central PMCID: PMCPMC191102.

75. Dubuisson J, Hsu HH, Cheung RC, Greenberg HB, Russell DG, Rice CM. Formation and intracellular localization of hepatitis C virus envelope glycoprotein complexes expressed by recombinant vaccinia and Sindbis viruses. J Virol. 1994; 68(10):6147–60. Epub 1994/10/01. PMID: 8083956; PubMed Central PMCID: PMCPMC237034.

76. Mohl B-P, Tedbury PR, Griffin S, Harris M. Hepatitis C Virus-Induced Autophagy Is Independent of the Unfolded Protein Response. Journal of Virology. 2012; 86:10724–32. https://doi.org/10.1128/JVI.01667-12 PMID: 22837205

77. Atoom AM, Jones DM, Russell RS. Evidence suggesting that HCV p7 protects E2 glycoprotein from premature degradation during virus production. Virus Research. 2013; 176:199–210. https://doi.org/10.1016/j.virusres.2013.06.008 PMID: 23816605

78. Camus G, Herker E, Modi AA, Haas JT, Ramage HR, Farese RV Jr., et al. Diacylglycerol acyltransferase-1 localizes hepatitis C virus NS5A protein to lipid droplets and enhances NS5A interaction with the viral capsid core. J Biol Chem. 2013; 288(14):9915–23. https://doi.org/10.1074/jbc.M112.434910 PMID: 23420847; PubMed Central PMCID: PMCPMC3617291.

79. Herker E, Harris C, Hernandez C, Carpentier A, Kaehlcke K, Rosenberg AR, et al. Efficient hepatitis C virus particle formation requires diacylglycerol acyltransferase-1. Nat Med. 2010; 16(11):1295–8. https://doi.org/10.1038/nm.2238 PMID: 20935628; PubMed Central PMCID: PMCPMC3431199.

80. Salloum S, Wang H, Ferguson C, Parton RG, Tai AW. Rab18 binds to hepatitis C virus NS5A and promotes interaction between sites of viral replication and lipid droplets. PLoS Pathog. 2013; 9(8):e1003513. https://doi.org/10.1371/journal.ppat.1003513 PMID: 23935497; PubMed Central PMCID: PMCPMC3731246.

81. Dansako H, Hiramoto H, Ikeda M, Wakita T, Kato N. Rab18 is required for viral assembly of hepatitis C virus through trafficking of the core protein to lipid droplets. Virology. 2014; 462–463:166–74. https://doi.org/10.1016/j.virol.2014.05.017 PMID: 24997429.

82. Neveu G, Barouch-Bentov R, Ziv-Av A, Gerber D, Jacob Y, Einav S. Identification and targeting of an interaction between a tyrosine motif within hepatitis C virus core protein and AP2M1 essential for viral assembly. PLoS Pathog. 2012; 8(8):e1002845. https://doi.org/10.1371/journal.ppat.1002845 PMID: 22916011; PubMed Central PMCID: PMCPMC3420927.

83. Backes P, Quinkert D, Reiss S, Binder M, Zayas M, Rescher U, et al. Role of annexin A2 in the production of infectious hepatitis C virus particles. J Virol. 2010; 84(11):5775–89. https://doi.org/10.1128/JVI.02343-09 PMID: 20335258; PubMed Central PMCID: PMCPMC2876593.

84. Barouch-Bentov R, Neveu G, Xiao F, Beer M, Bekerman E, Schor S, et al. Hepatitis C Virus Proteins Interact with the Endosomal Sorting Complex Required for Transport (ESCRT) Machinery via Ubiquitination To Facilitate Viral Envelopment. MBio. 2016; 7(6). https://doi.org/10.1128/mBio.01456-16 PMID: 27803188; PubMed Central PMCID: PMCPMC5090039.

85. Tamai K, Shiina M, Tanaka N, Nakano T, Yamamoto A, Kondo Y, et al. Regulation of hepatitis C virus secretion by the Hrs-dependent exosomal pathway. Virology. 2012; 422(2):377–85. https://doi.org/10.1016/j.virol.2011.11.009 PMID: 22138215.

86. Tedbury P, Welbourn S, Pause A, King B, Griffin S, Harris M. The subcellular localization of the hepatitis C virus non-structural protein NS2 is regulated by an ion channel-independent function of the p7 protein. J Gen Virol. 2011; 92(Pt 4):819–30. https://doi.org/10.1099/vir.0.027441-0 PMID: 21177929; PubMed Central PMCID: PMCPMC3133701.

87. Falcon V, Acosta-Rivero N, Gonzalez S, Duenas-Carrera S, Martinez-Donato G, Menendez I, et al. Ultrastructural and biochemical basis for hepatitis C virus morphogenesis. Virus Genes. 2017; 53(2):151–64. https://doi.org/10.1007/s11262-017-1426-2 PMID: 28233195.

88. Gouklani H, Beyer C, Drummer H, Gowans EJ, Netter HJ, Haqshenas G. Identification of specific regions in hepatitis C virus core, NS2 and NS5A that genetically interact with p7 and co-ordinate infectious virus production. J Viral Hepat. 2013; 20(4):e66–71. https://doi.org/10.1111/jvh.12004 PMID: 23490391.

89. Haqshenas G, Mackenzie JM, Dong X, Gowans EJ. Hepatitis C virus p7 protein is localized in the endoplasmic reticulum when it is encoded by a replication-competent genome. J Gen Virol. 2007; 88(Pt 1):134–42. https://doi.org/10.1099/vir.0.82049-0 PMID: 17170445.

90. Coller KE, Heaton NS, Berger KL, Cooper JD, Saunders JL, Randall G. Molecular determinants and dynamics of hepatitis C virus secretion. PLoS Pathog. 2012; 8(1):e1002466. https://doi.org/10.1371/journal.ppat.1002466 PMID: 22241992; PubMed Central PMCID: PMCPMC3252379.

91. Cornell CT, Kiosses WB, Harkins S, Whitton JL. Coxsackievirus B3 proteins directionally complement each other to downregulate surface major histocompatibility complex class I. J Virol. 2007; 81 (13):6785–97. https://doi.org/10.1128/JVI.00198-07 PMID: 17442717; PubMed Central PMCID: PMCPMC1933326.

92. Henkel JR, Weisz OA. Influenza virus M2 protein slows traffic along the secretory pathway. pH perturbation of acidified compartments affects early Golgi transport steps. J Biol Chem. 1998; 273(11):6518–24. PMID: 9497387.

93. Sakaguchi T, Leser GP, Lamb RA. The ion channel activity of the influenza virus M2 protein affects transport through the Golgi apparatus. J Cell Biol. 1996; 133(4):733–47. PMID: 8666660; PubMed Central PMCID: PMCPMC2120830.

94. Pietschmann T, Kaul A, Koutsoudakis G, Shavinskaya A, Kallis S, Steinmann E, et al. Construction and characterization of infectious intragenotypic and intergenotypic hepatitis C virus chimeras. Proceedings of the National Academy of Sciences. 2006; 103:7408–13. https://doi.org/10.1073/pnas.0504877103 PMID: 16651538

95. Bolte S, Cordelieres FP. A guided tour into subcellular colocalization analysis in light microscopy. J Microsc. 2006; 224(Pt 3):213–32. https://doi.org/10.1111/j.1365-2818.2006.01706.x PMID: 17210054.

96. Biasini M, Bienert S, Waterhouse A, Arnold K, Studer G, Schmidt T, et al. SWISS-MODEL: modelling protein tertiary and quaternary structure using evolutionary information. Nucleic Acids Res. 2014; 42 (Web Server issue):W252–8. https://doi.org/10.1093/nar/gku340 PMID: 24782522; PubMed Central PMCID: PMCPMC4086089.

97. Szecsi J, Boson B, Johnsson P, Dupeyrot-Lacas P, Matrosovich M, Klenk HD, et al. Induction of neutralising antibodies by virus-like particles harbouring surface proteins from highly pathogenic H5N1 and H7N1 influenza viruses. Virol J. 2006; 3:70. https://doi.org/10.1186/1743-422X-3-70 PMID: 16948862; PubMed Central PMCID: PMCPMC1569823.

Model:
Chandler et al., 2012

Model:
OuYang et al., 2013

JFH1

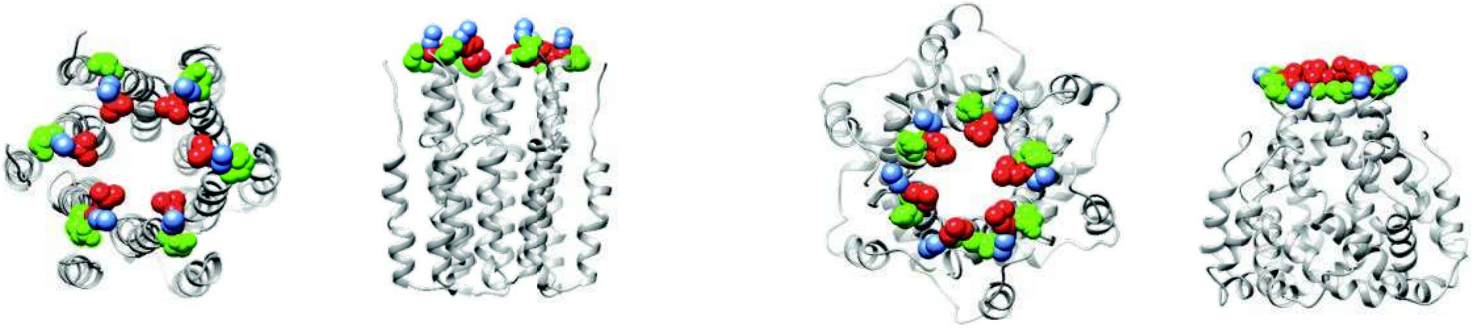

JFH1 Ap7

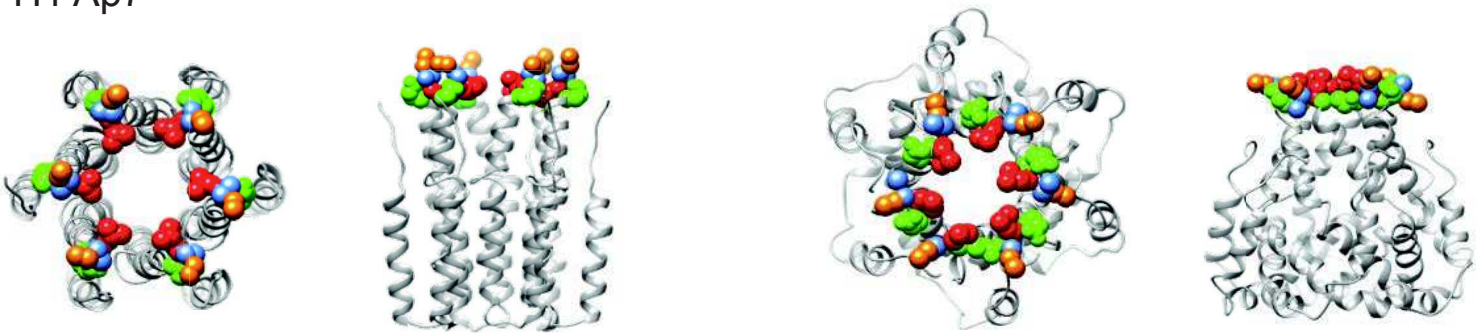

JFH1 p7-L2S

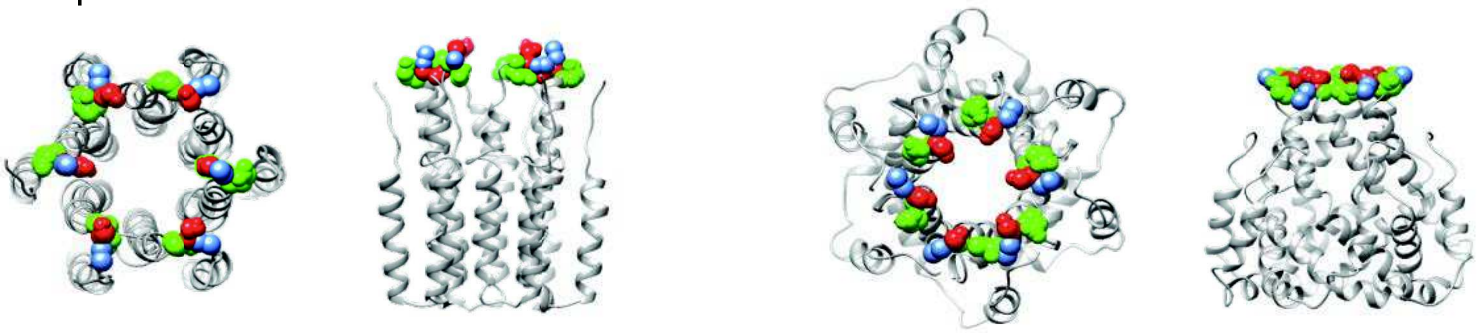

JFH1 p7-T2

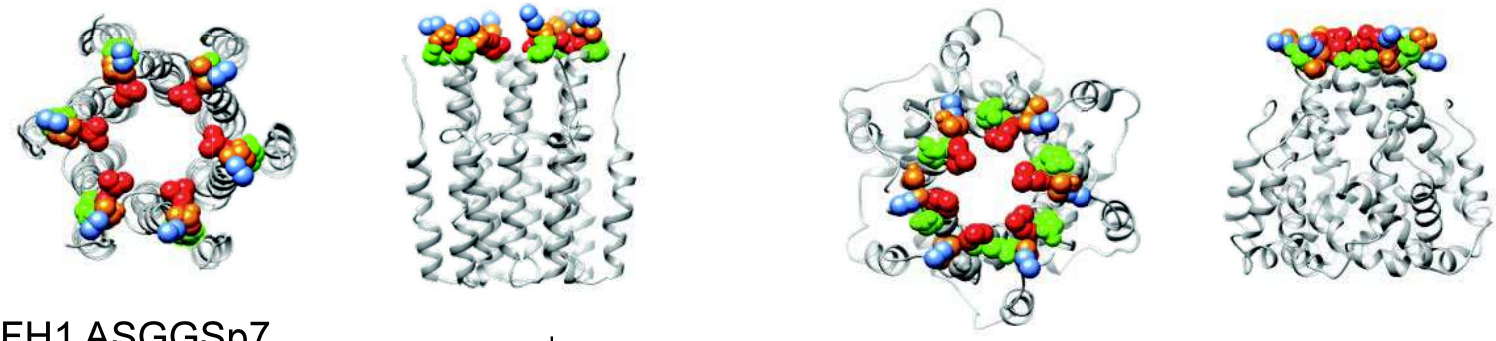

JFH1 ASGGSp7

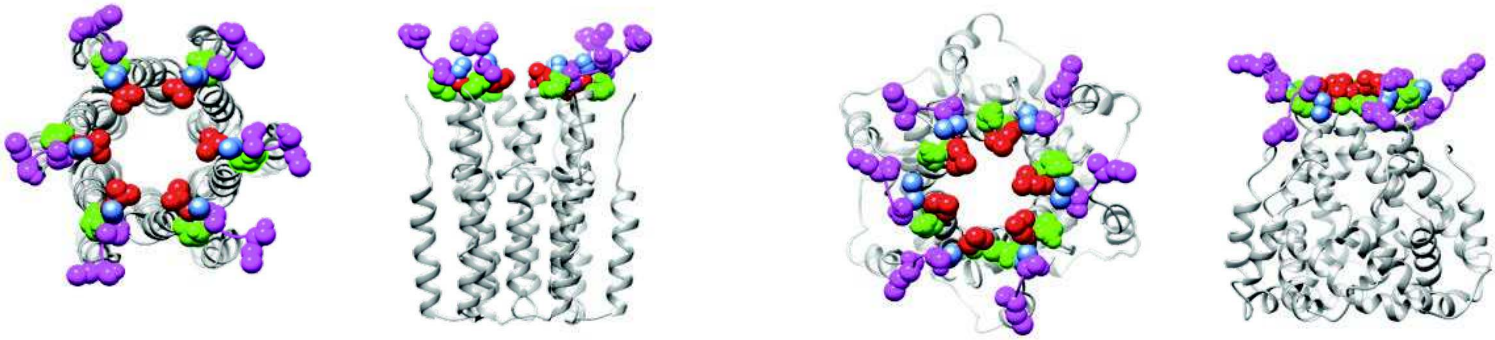

S1 Figure: Denolly et al., 2017

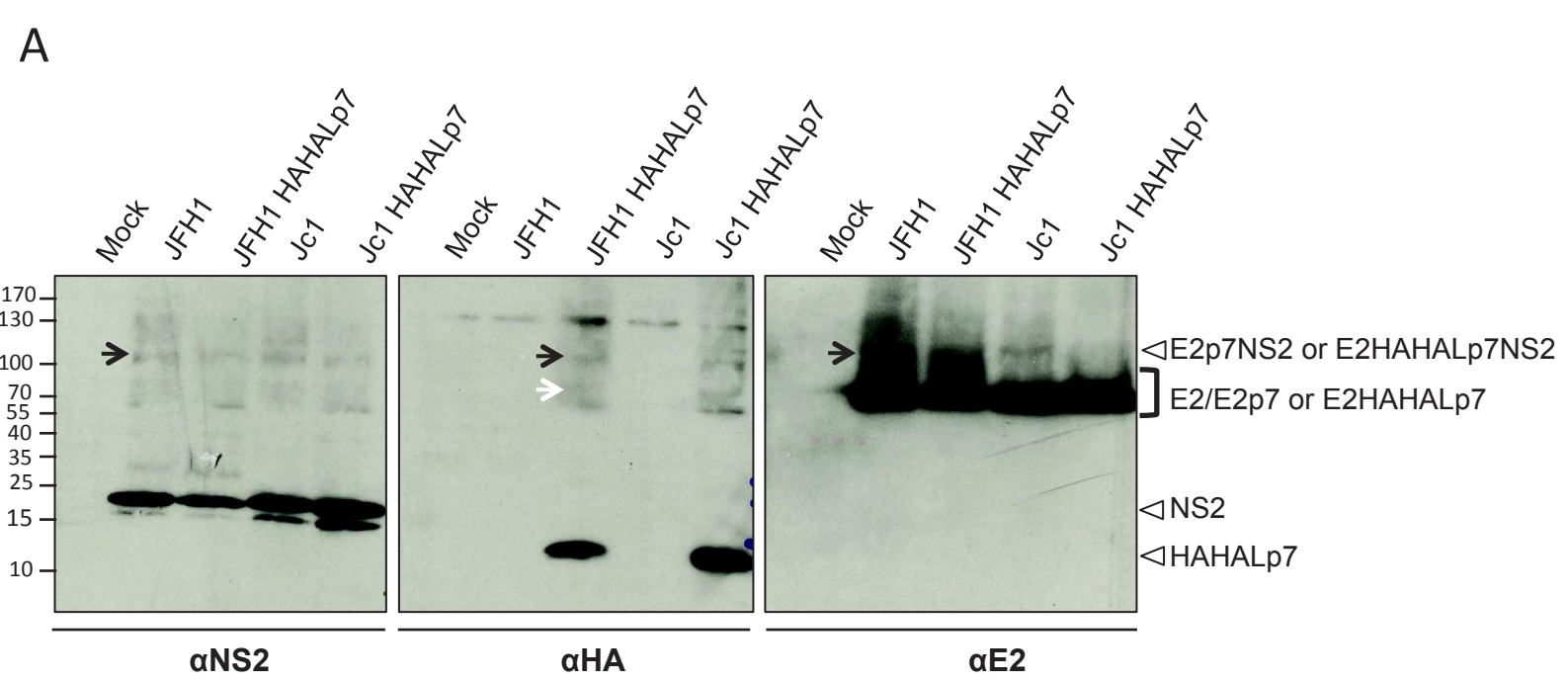

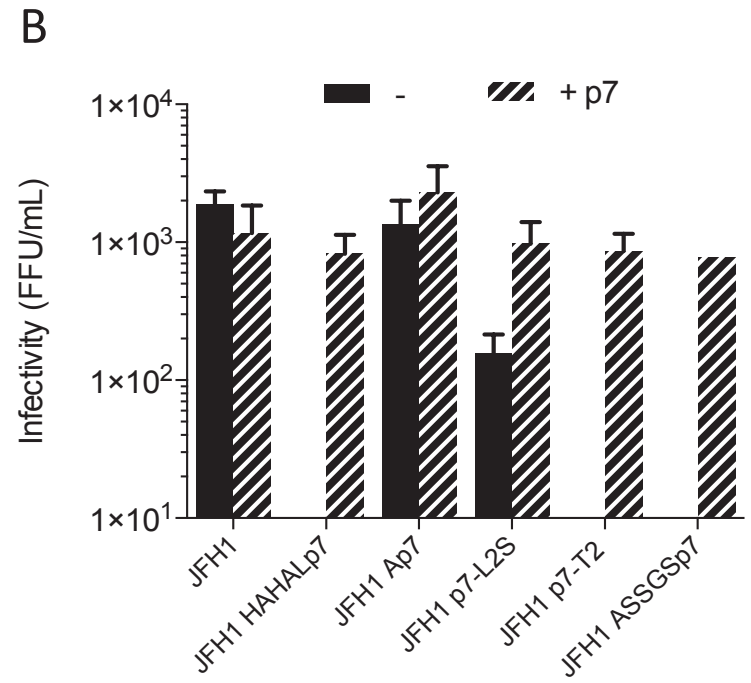

S2 Figure: Denolly et al., 2017

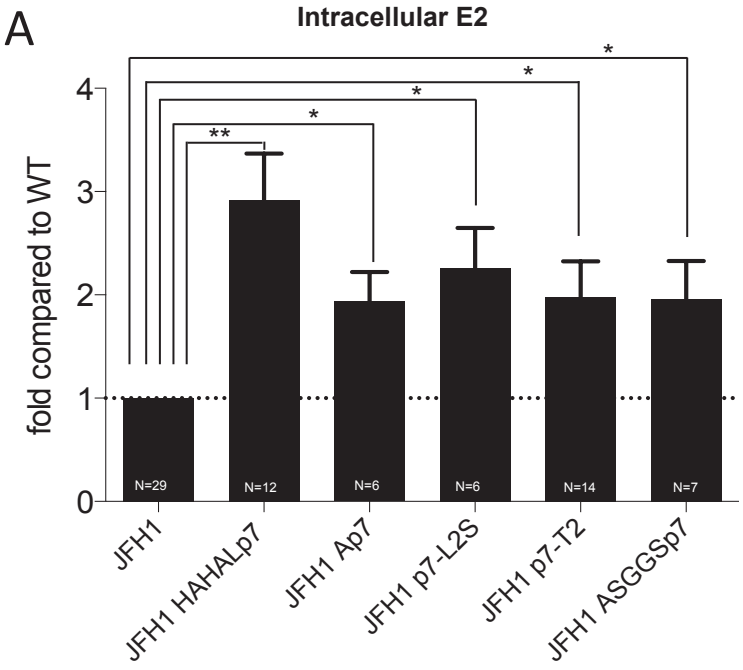

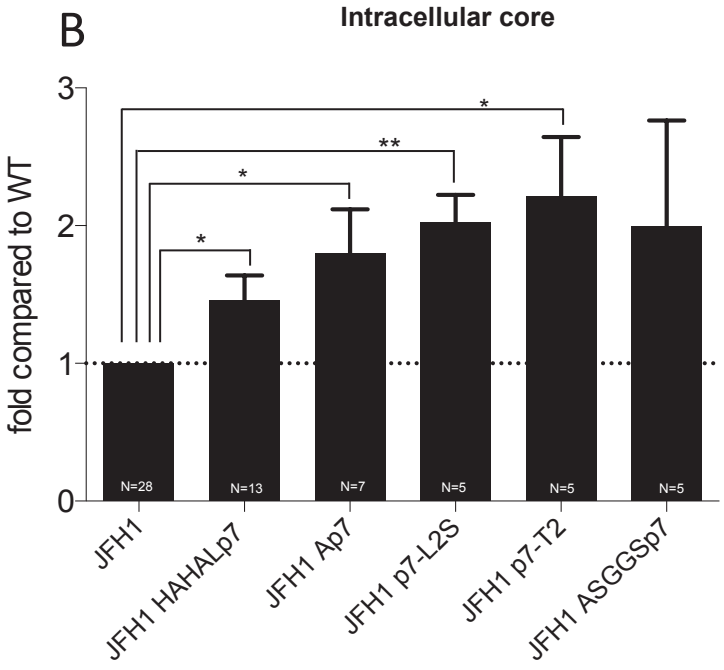

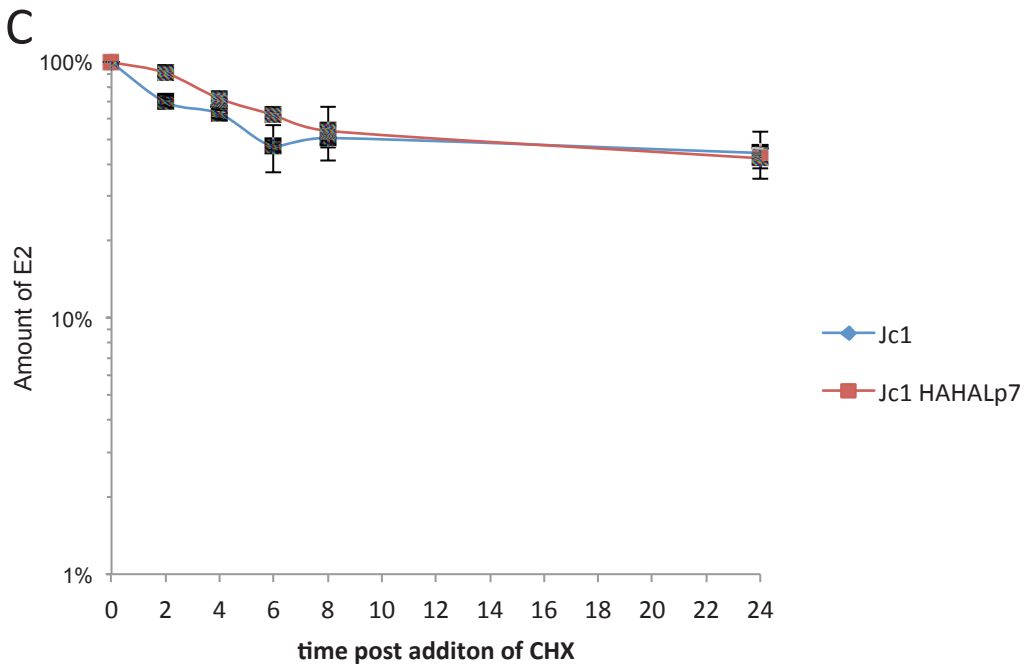

S3 Figure: Denolly et al., 2017

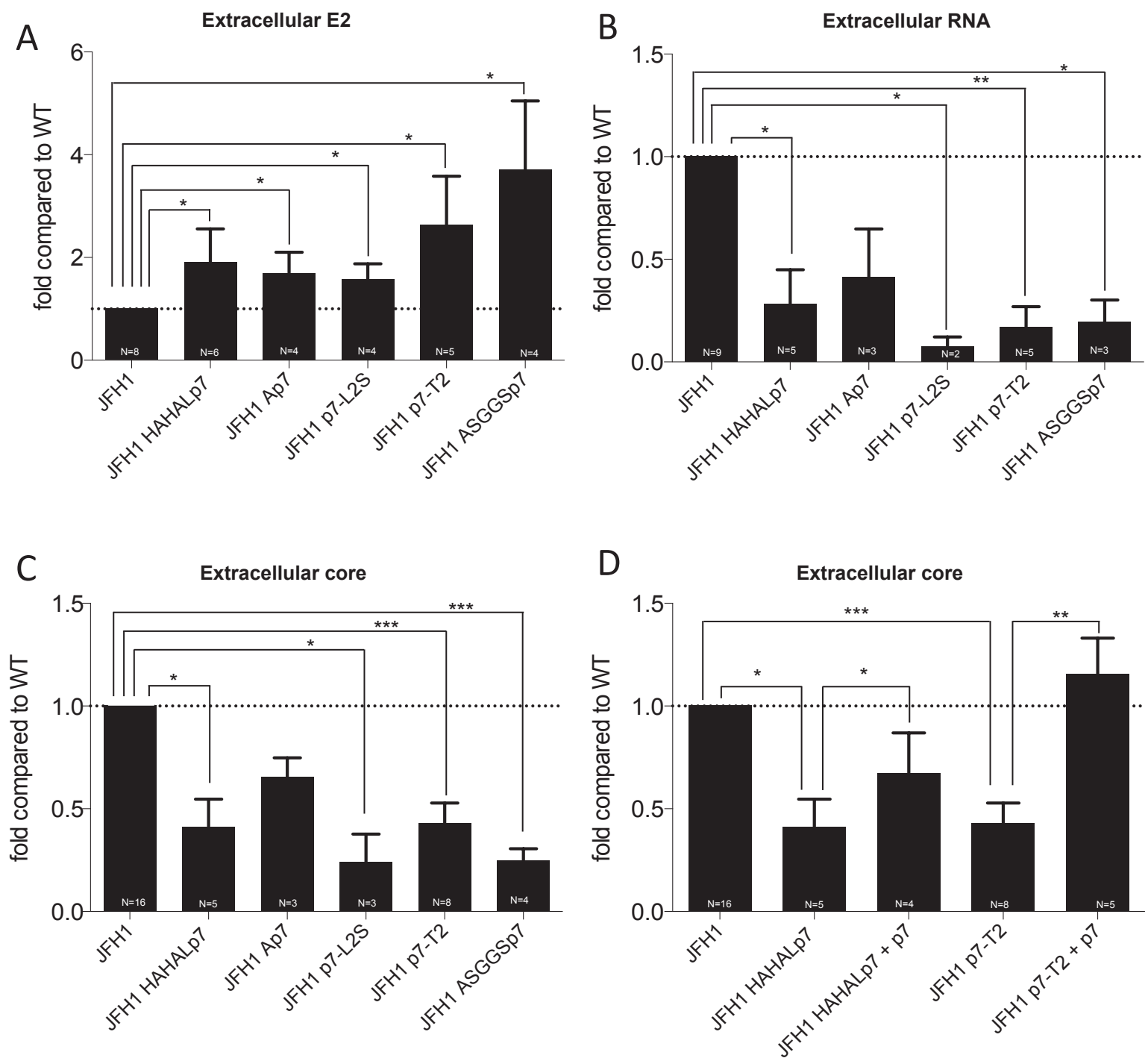

S4 Figure: Denolly et al., 2017

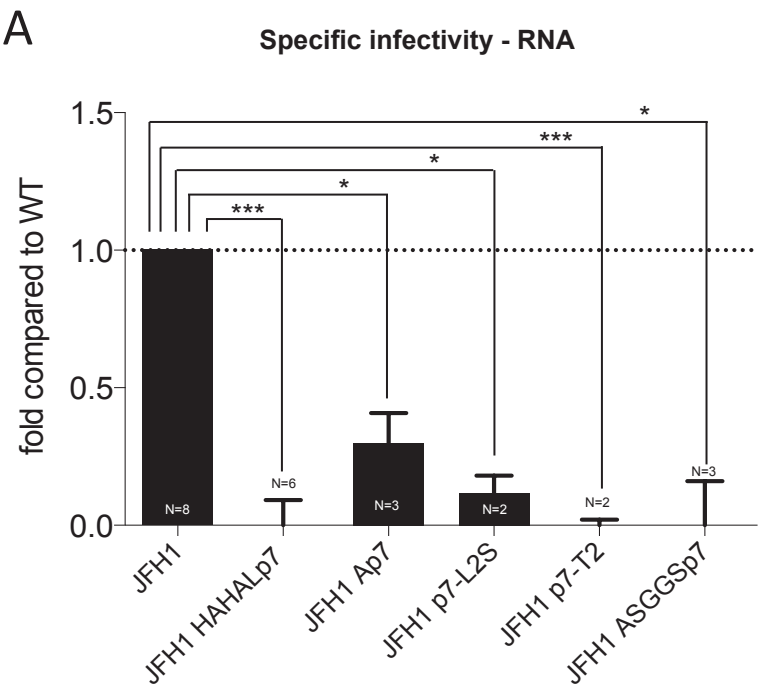

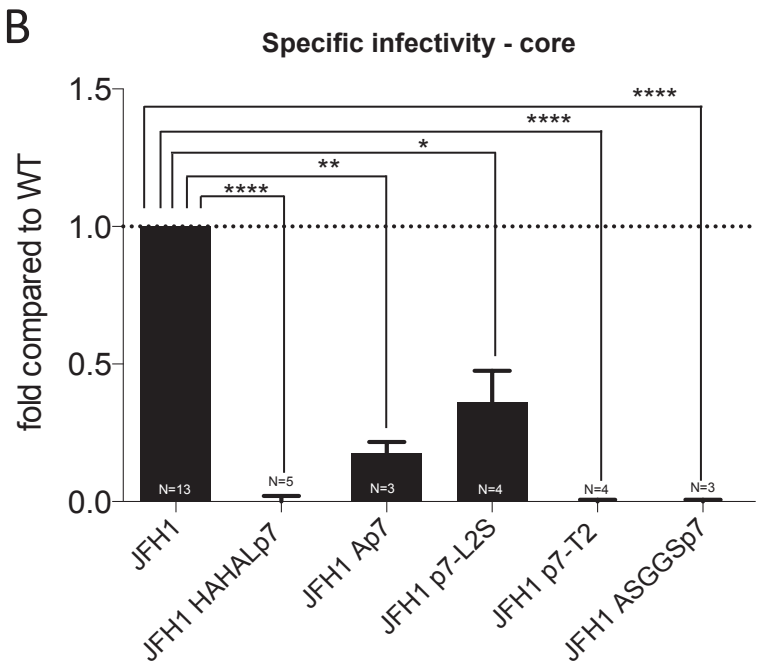

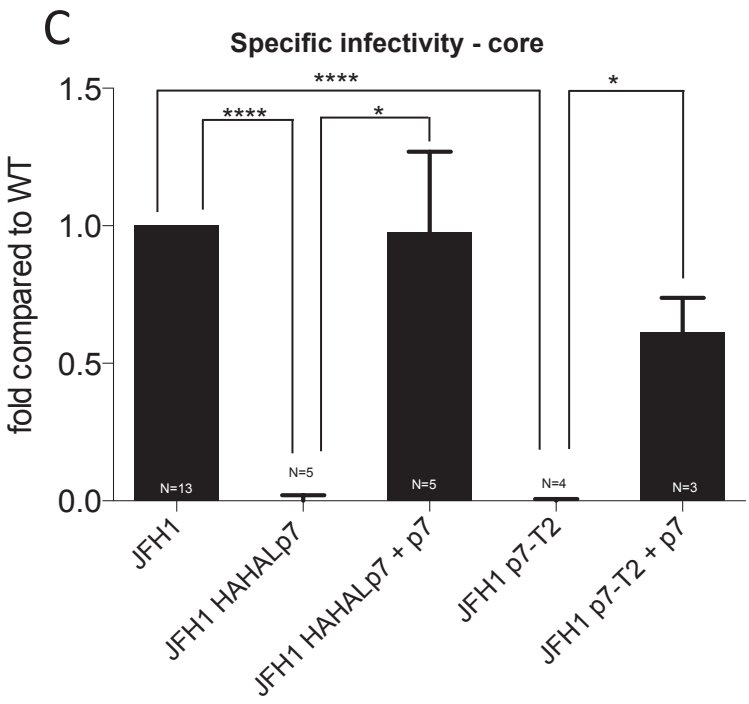

S5 Figure: Denolly et al., 2017

A

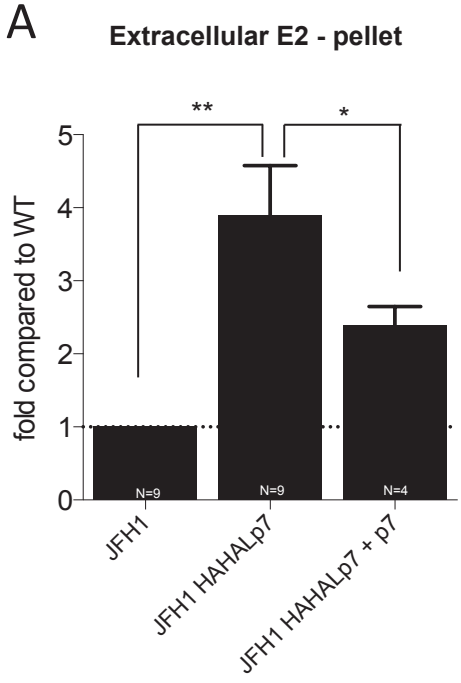

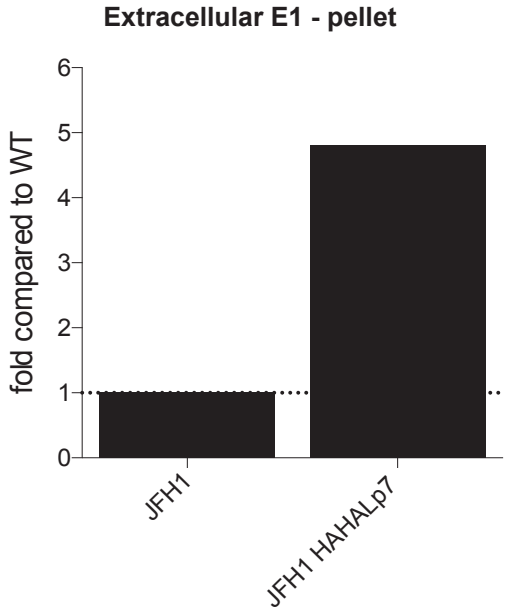

C

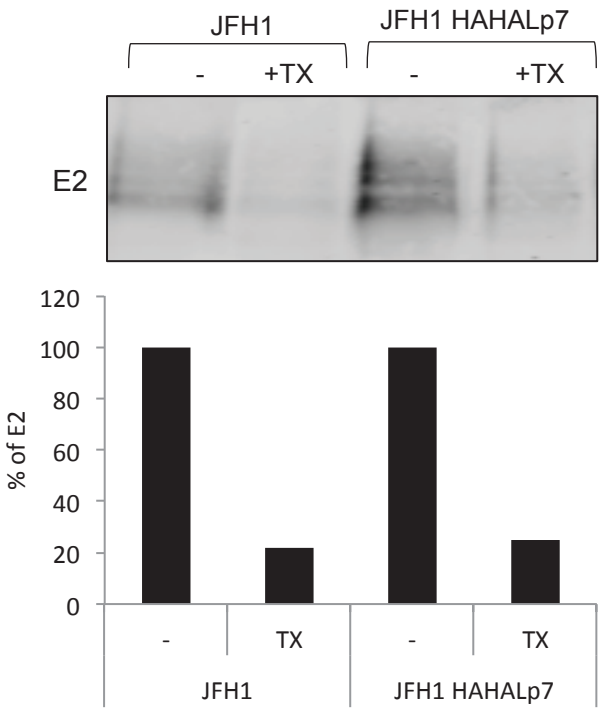

B

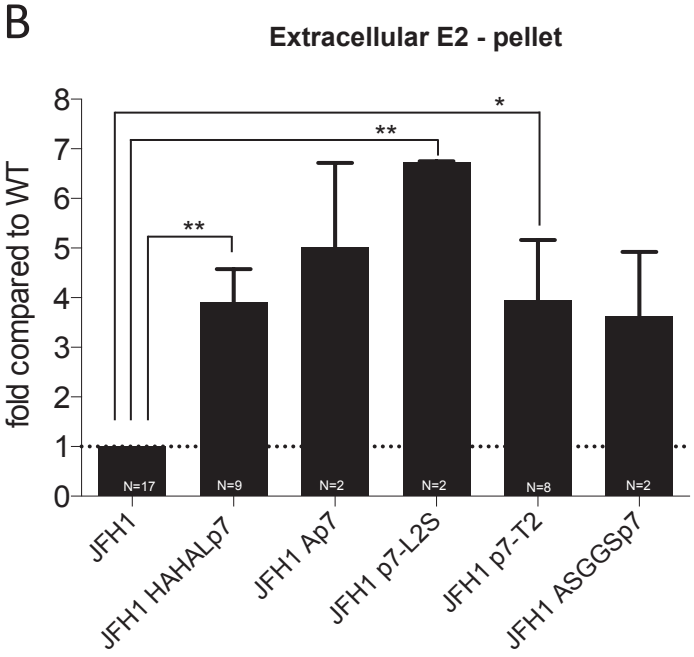

S6 Figure: Denolly et al., 2017

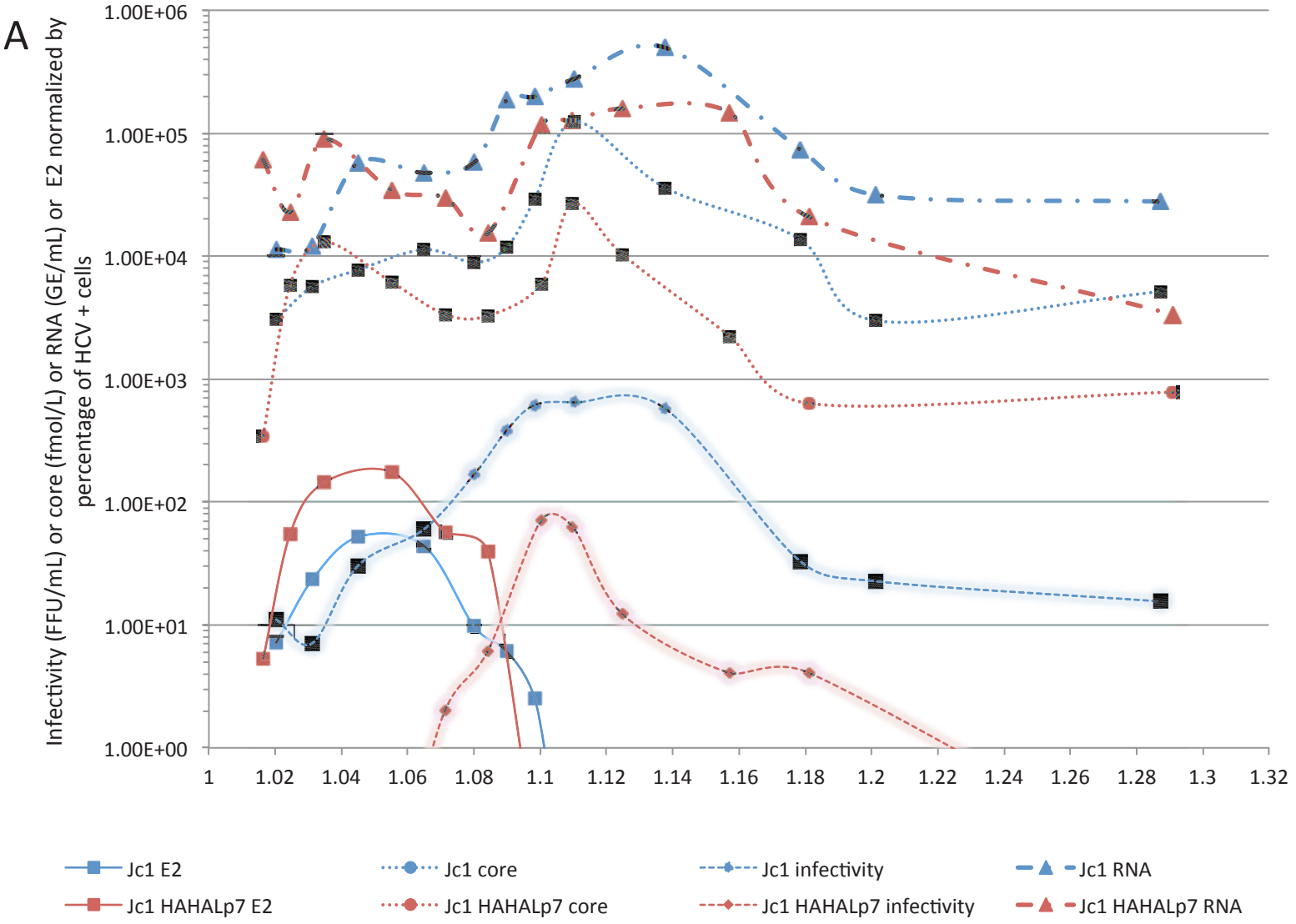

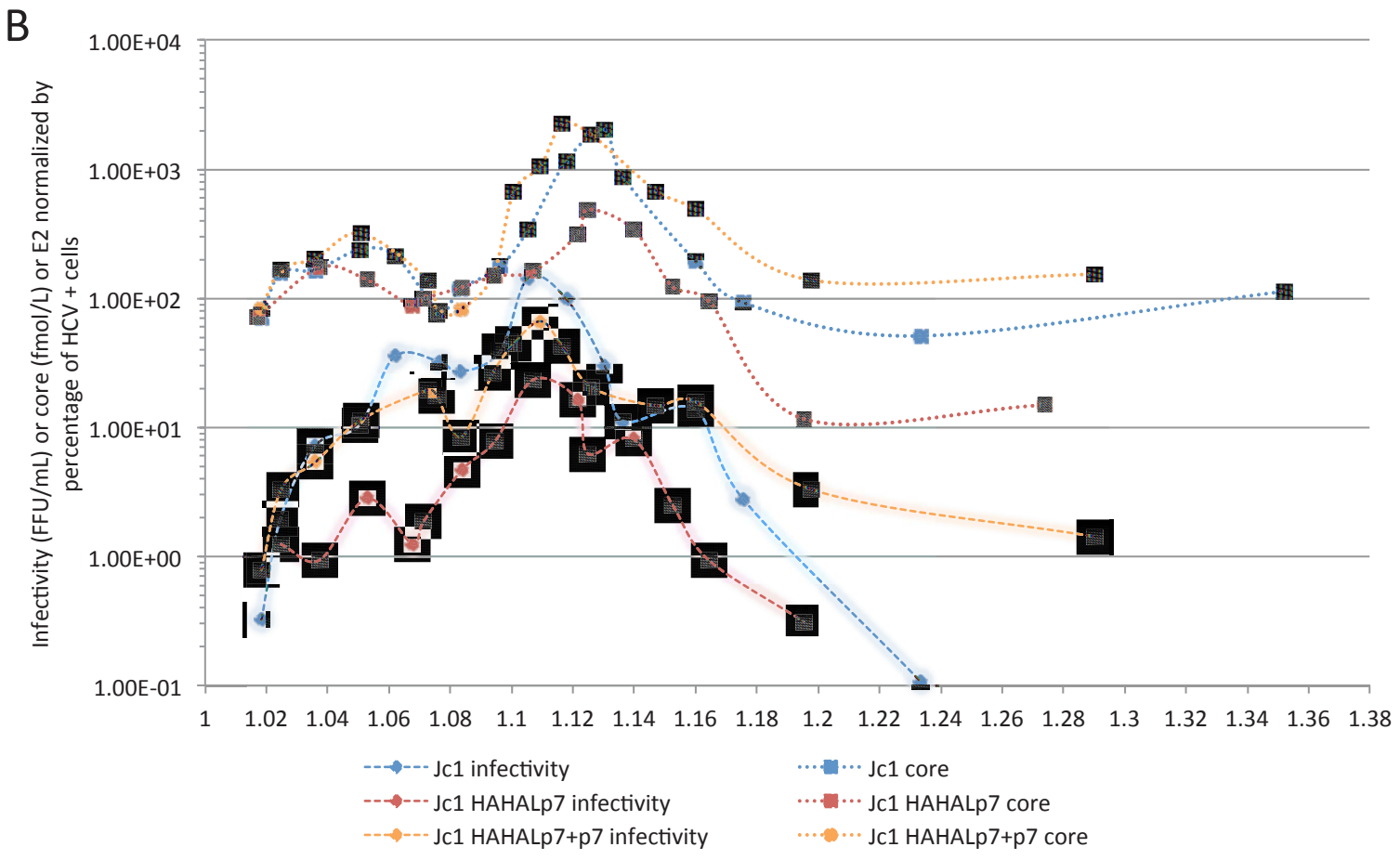

S7 Figure: Denolly et al., 2017

C

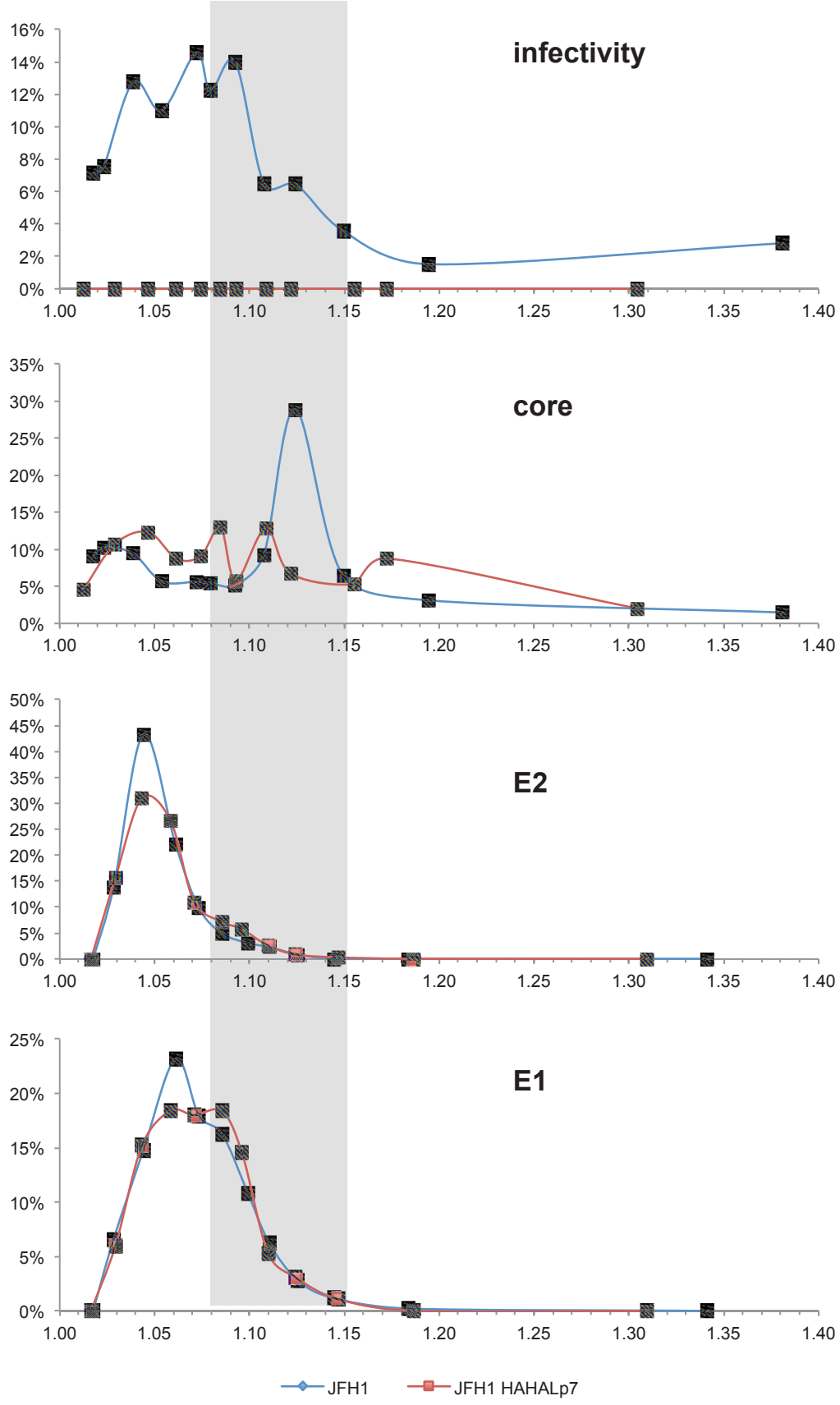

S7 Figure: Denolly et al., 2017

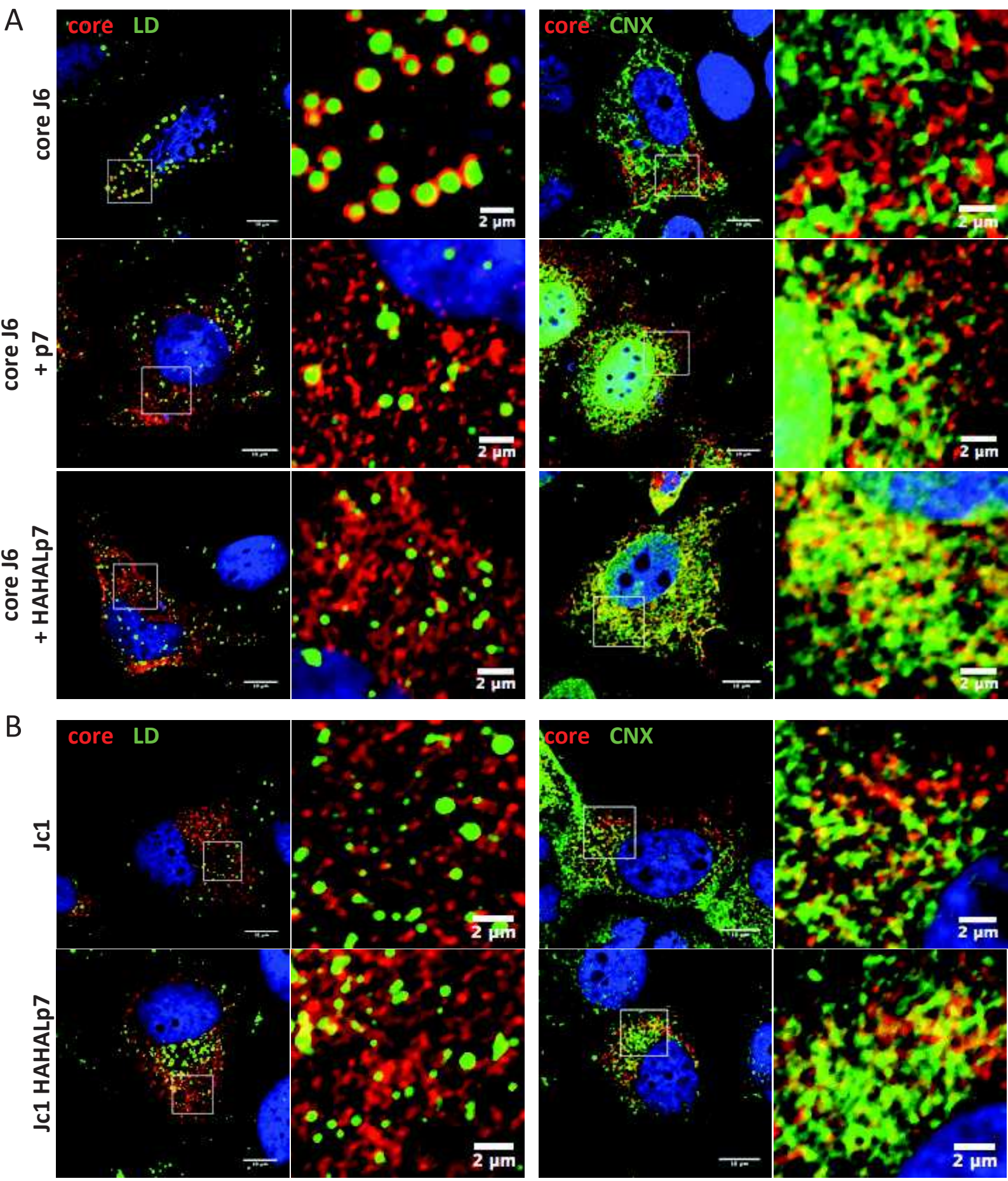

S8 Figure: Denolly et al., 2017

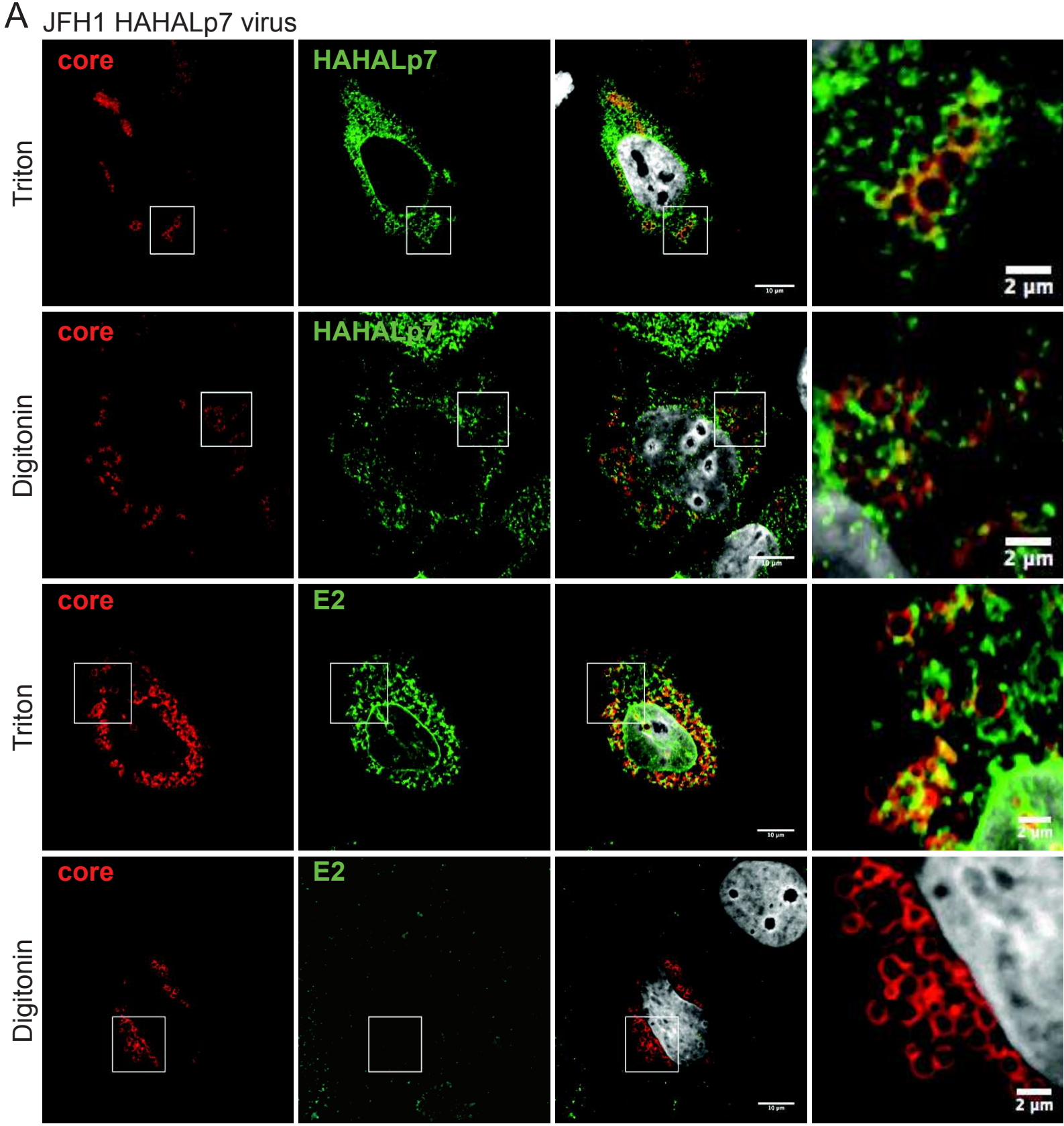

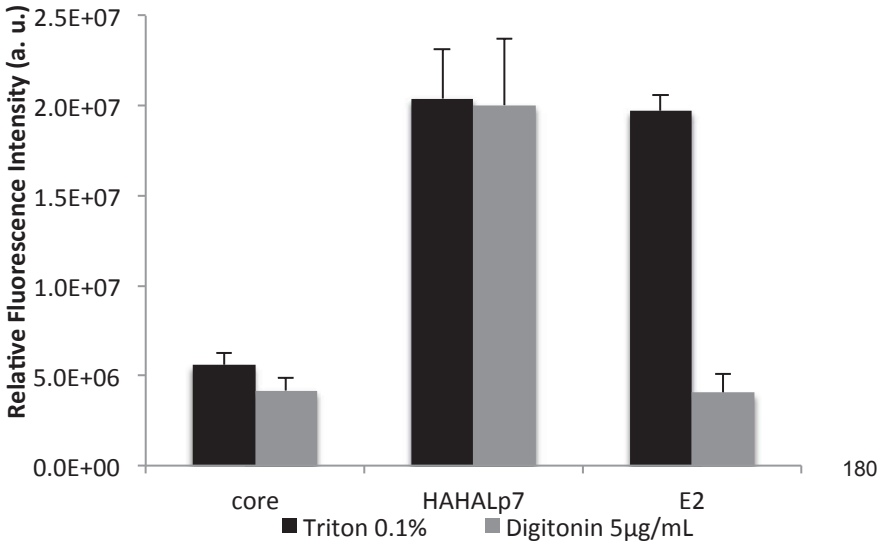

S9 Figure : Denolly et al., 2017

B C-E1E2 + noSPHAHALp7

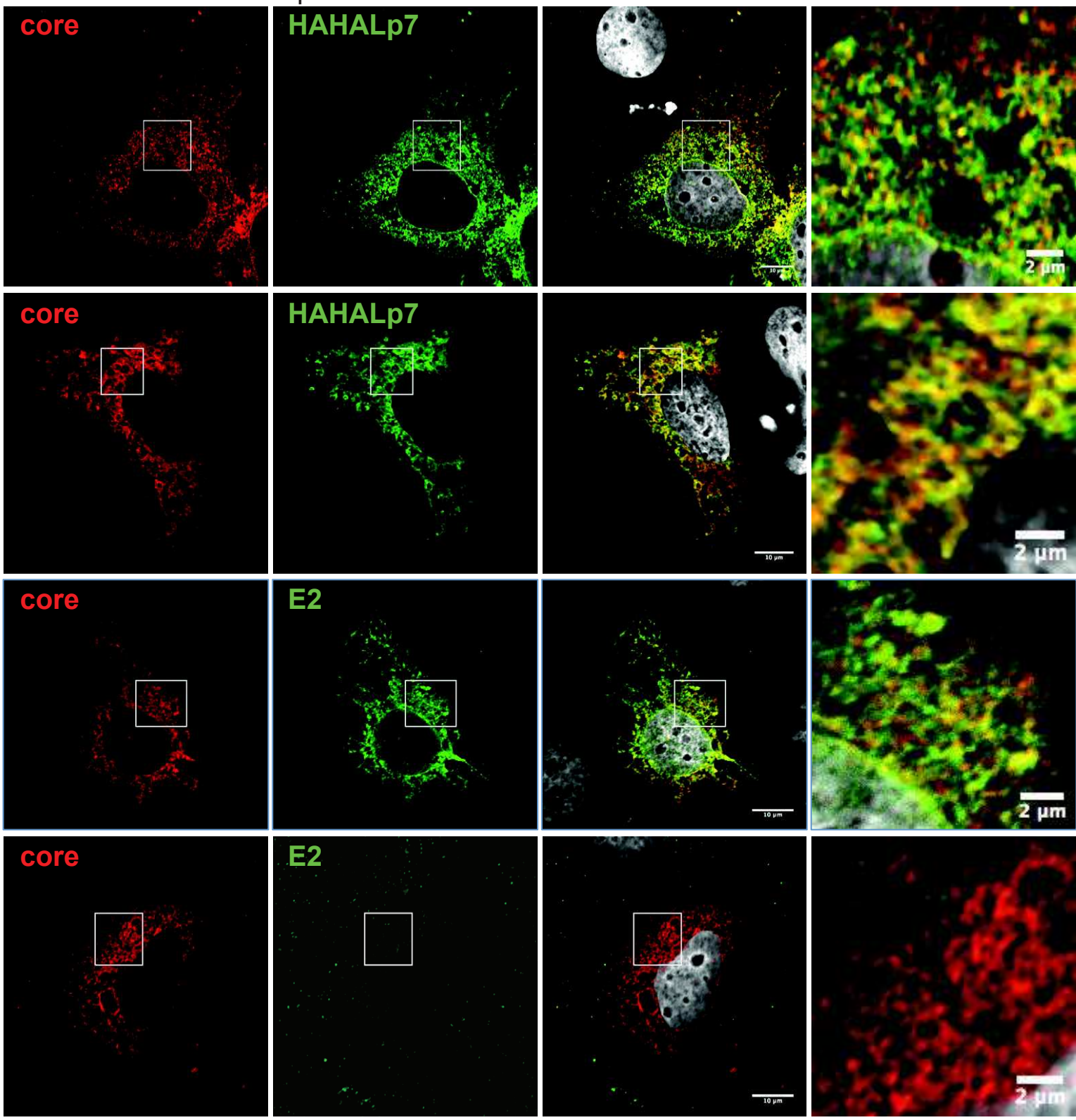

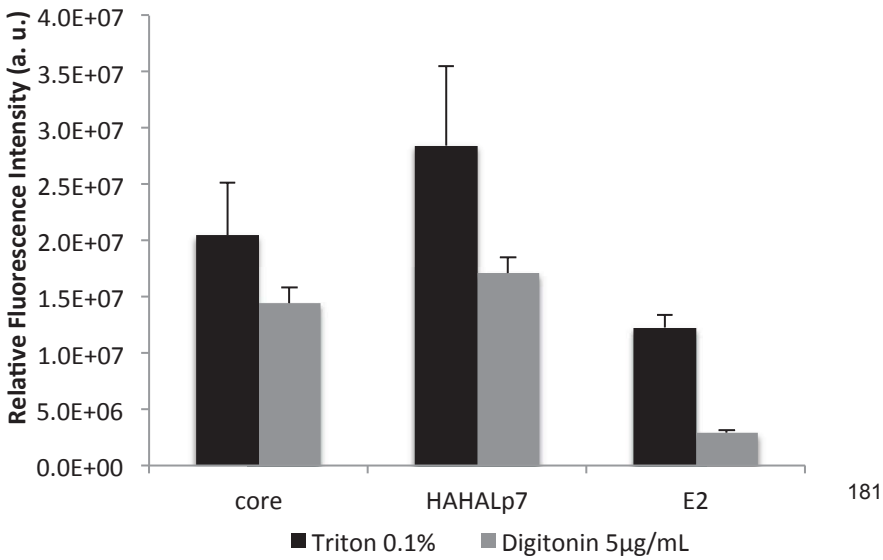

S9 Figure : Denolly et al., 2017

C C-E1E2 + ΔE2HAHALp7

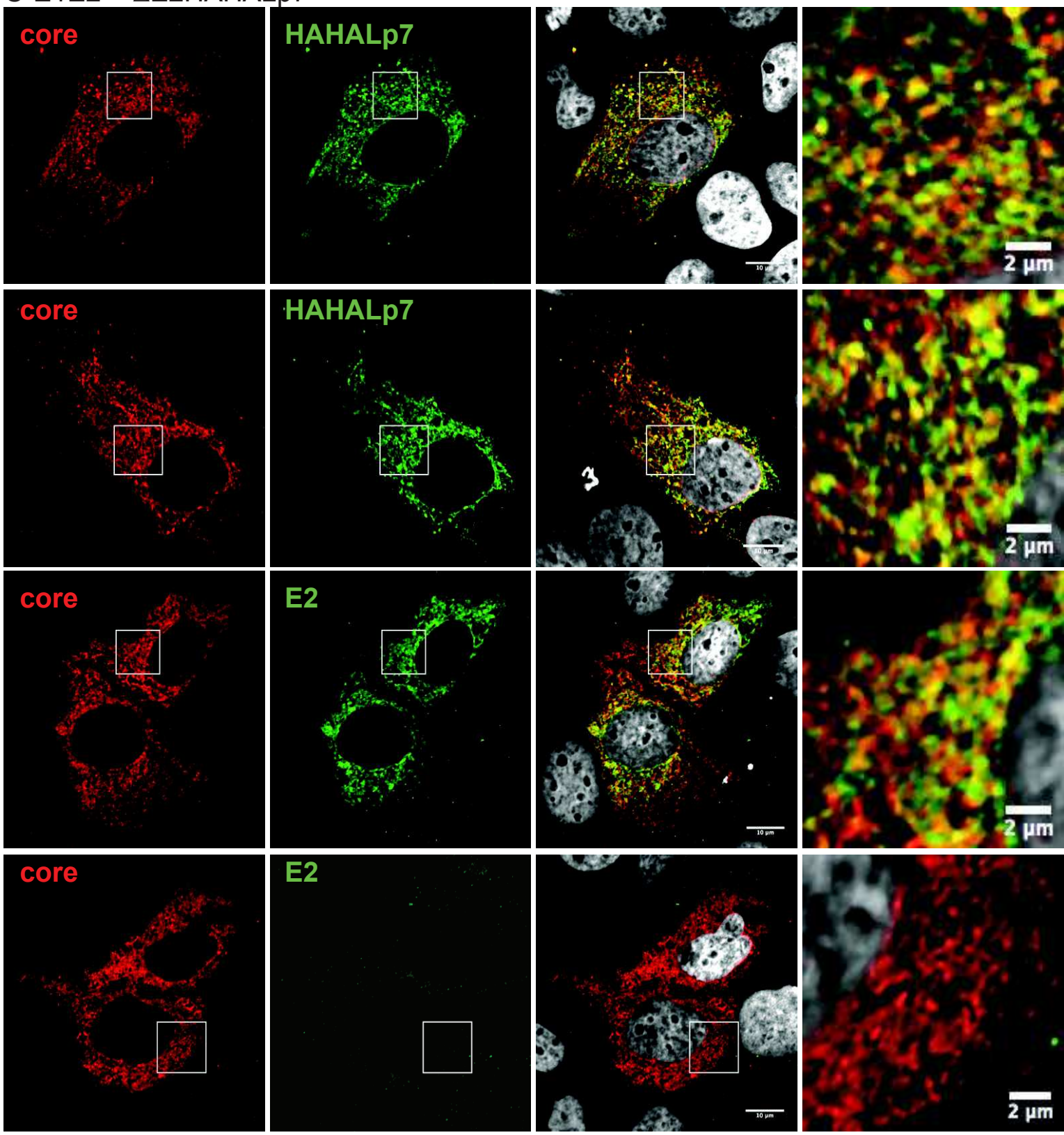

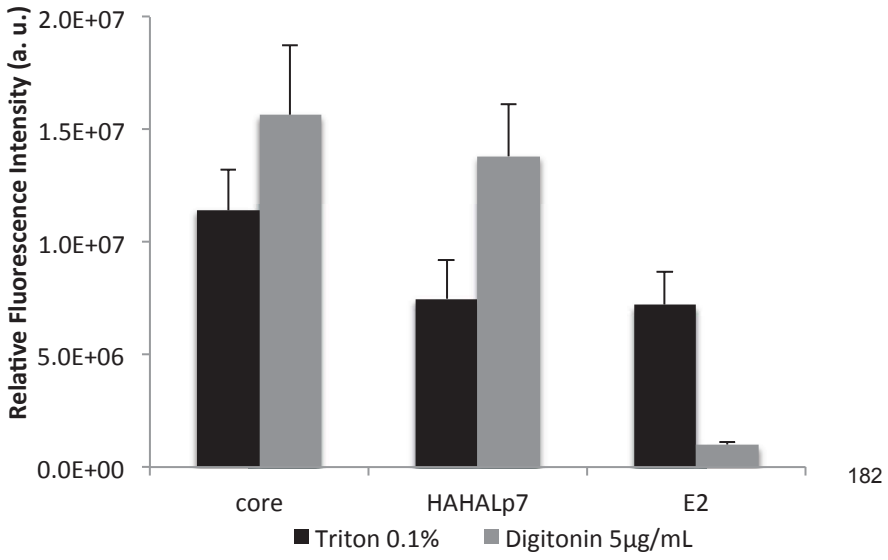

S9 Figure : Denolly et al., 2017

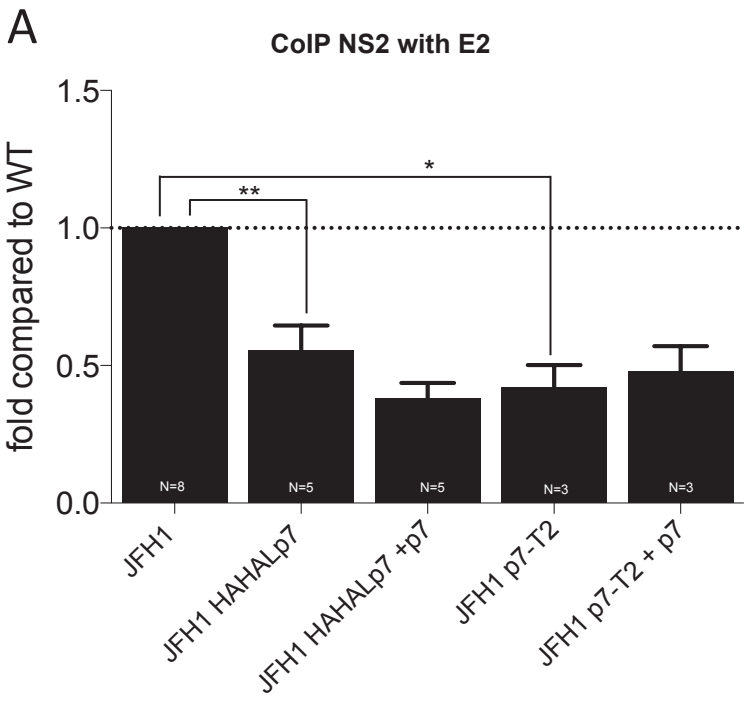

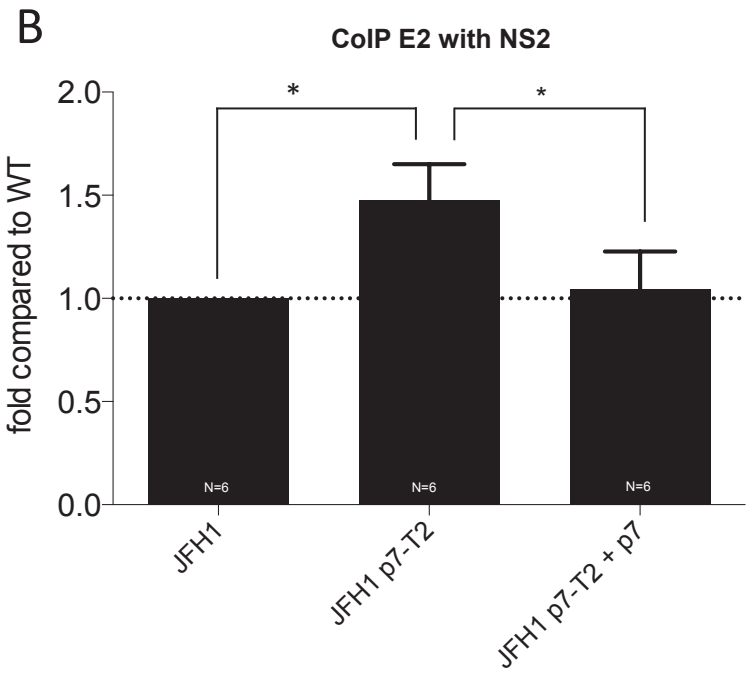

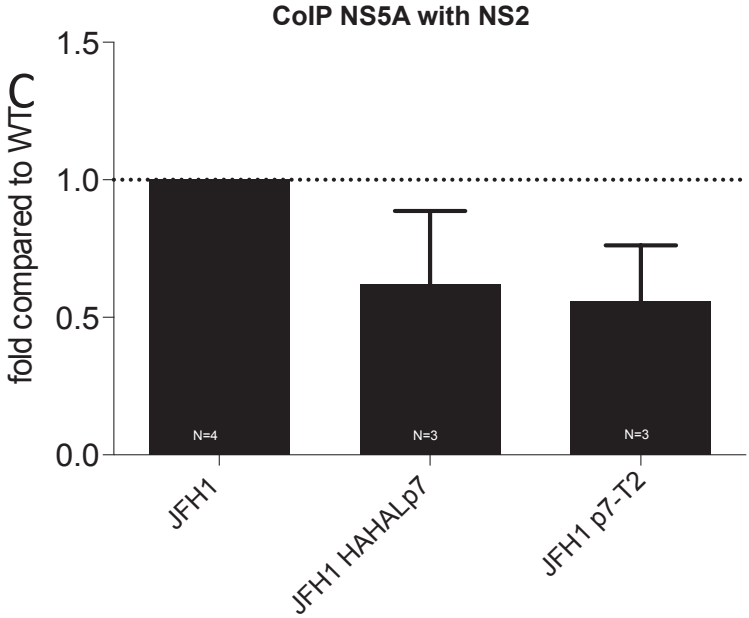

S10 Figure: Denolly et al., 2017

V- A serum protein factor mediates lipid acquisition by HCV particles in the extracellular milieu

Solène Denolly, Christelle Granier, Nelly Fontaine, Bruno Pozzetto, Thomas Bourlet, Maryse Guérin, François-Loïc Cosset

In Preparation

A serum protein factor mediates lipid acquisition by HCV particles in the extracellular milieu

Short title: HCV virion lipid acquisition occurs post-secretion

Authors: Solène Denolly[1], Christelle Granier[1], Nelly Fontaine[1], Bruno Pozzetto[2], Thomas Bourlet[2], Maryse Guérin[3], and François-Loïc Cosset[1]

[1]CIRI – Centre International de Recherche en Infectiologie, Univ Lyon, Université Claude Bernard Lyon 1, Inserm, U1111, CNRS, UMR5308, ENS Lyon, F-69007, Lyon, France.
[2]GIMAP, EA 3064, Faculté de Médecine, Université de Saint-Etienne, Univ Lyon, F-42023, Saint Etienne, France.
[3]Inserm, Sorbonne-Université, Research Unit of Cardiovascular, Metabolism and Nutrition Diseases UMR_S1166-ICAN, Paris, F-75013, France.

Grant support: This work was supported by the French “Agence Nationale de la Recherche sur le SIDA et les hépatites virales” (ANRS), the European Research Council (ERC-2008-AdG-233130-HEPCENT) and the LabEx Ecofect (ANR-11-LABX-0048) of the “Université de Lyon”, within the program "Investissements d'Avenir" (ANR-11-IDEX-0007) operated by the French National Research Agency (ANR). SD was supported by a fellowship of the ANRS.

Abbreviations: FCS, fetal calf serum; FFU, focus-forming unit; GE, genome equivalent; HCV, hepatitis C virus; HDL, high-density lipoproteins; HS, human serum; HSA, human serum albumin; LDL, low-density; LVP, lipo-viro-particle; RNA, ribonucleic acid; VLDL, very-low-density lipoprotein.

Correspondence: François-Loïc Cosset. CIRI – International Center for Infectiology Research. E-mail: flcosset@ens-lyon.fr

Disclosures: The authors disclose no conflicts.

Author contributions: Study concept and design: SD, FLC. Acquisition of data: CG, NF, TB, MG, SD. Analysis and interpretation of data: SD, CG, NF, MG, FLC. Drafting of the manuscript: SD, FLC. Material support: BP.

Abstract

BACKGROUND & AIMS: Hepatitis C virus (HCV) particles detected in sera from infected patients display heterogeneous forms of low buoyant densities (<1.08), highlighting their lipidation *via* association with apoB-containing lipoproteins, which was proposed to occur during assembly or secretion from infected hepatocytes. However, the mechanisms inducing this association remain poorly defined and, intriguingly, most HCVcc particles secreted from cultured cells exhibit higher density (>1.08) and are not/poorly apoB-associated.

METHODS: We produced HCVcc particles of Jc1 or H77 strains from Huh-7.5 hepatoma cells cultured in 10%-fetal calf serum (FCS) standard conditions *vs*. in serum-free or human serum (HS) conditions before analyzing their density profiles comparatively to patient-virus. We also characterized serum-free medium-produced wild-type and Jc1/H77 HVR1-swapped mutant HCVcc particles incubated with either serum type or with purified lipoproteins.

RESULTS: Compared to serum-free or FCS conditions, production with HS redistributed most HCVcc infectious particles to low-density or very-low-density (<1.04) ranges. In addition, short-time incubation with HS was sufficient to shift HCVcc physical particles to low-density fractions, in time- and dose-dependent manners, which increased their specific infectivity and induced apoB-association. Moreover, as compared to Jc1, we detected higher levels of H77 HCVcc infectious particles in very-low-density fractions, which could be unambiguously attributed to strain-specific features of HVRI sequence. Finally, all three lipoprotein classes, *i.e.*, very-low-density, low-density and high-density lipoproteins, could synergistically induce lipidation of HCV particles; yet, this required additional non-lipid serum factor(s) that include albumin.

CONCLUSIONS: The association of HCV particles with lipids may occur in the extracellular milieu. The lipidation level depends on serum composition as well as on HVRI-specific properties.

Keywords: *Hepatitis C virus; Lipoprotein; Lipidation; Serum; Infectivity*

Abstract: 260/260
Intro: 676/700
Materiel/ Methods: 776/800
Results: 1834/1900
Discussion: 1590/1600
Legends: 835/1000
References: 1370/1000
TOTAL: 7081/7000

Introduction

Hepatitis C virus (HCV) infection is a major cause of chronic liver diseases worldwide, such as liver cirrhosis and hepatocellular carcinoma. Although direct antiviral agents (DAA) are now able to eradicate the virus in most patients, no preventive vaccine currently exists against HCV and it remains major challenges in basic, translational and clinical research(Bartenschlager et al., 2018). As DAAs are only curative, the development of a protective vaccine remains an important goal, though this requires a deeper knowledge of the structure of HCV particles. Indeed, the HCV virion exhibits unusually heterogeneous particles in morphology, size and properties(Lindenbach & Rice, 2013). The immunocapture of particles with antibodies against surface proteins revealed particles of 50-80nm that do not display a symmetrical arrangement(Andre et al., 2002, Catanese et al., 2013, Merz et al., 2011, Piver et al., 2017). HCV particles harbor two envelope glycoproteins, E1 and E2, inserted on a membranous envelope that surrounds a nucleocapsid, composed of a core protein multimer and a positive-strand RNA viral genome; yet, the arrangement of the structural proteins onto the virion surface remains elusive and there is currently no clear model of HCV particles topology.

A most remarkable property of HCV is the particularly low buoyant density of viral particles, coined lipo-viro-particles (LVP)(Andre et al., 2002). In sera from infected patients and experimentally-infected chimpanzees, most HCV particles are found in densities between 1.00 and 1.10(Andre et al., 2002, Lindenbach et al., 2006, Nielsen et al., 2006). This is mainly due to the particular lipid compositions of virions that are distinct from that of other enveloped viruses. Indeed, *in vivo*, patient-derived HCV particles contain neutral lipids such as triglycerides or cholesterol esters and are associated with circulating apolipoproteins such as apoC-I, apoE and apoB(Andre et al., 2002, Diaz et al., 2006, Nielsen et al., 2006, Thomssen et al., 1992); the latter one being the major structural component of low-density lipoproteins (LDL) and very-low-density lipoproteins (VLDL). Importantly, injection of HCV particles in experimentally-infected animals revealed that the inoculum of low-density is the most infectious(Bradley et al., 1991).

One of the bottleneck of HCV characterization is the lack of infectivity of particles retrieved from infected patients(Bartenschlager et al., 2018, Steenbergen et al., 2013), which prevents unravelling the properties of this striking virus/lipid interaction. To overcome this, several experimental cellular models have been designed, including a most prominent one, the cell culture-grown HCV model (HCVcc) that is usually produced from Huh-7.5 hepatoma cells(Lindenbach et al., 2005, Pietschmann et al., 2006). While HCVcc infectious particles have heterogeneous density profile, between 1.00 and >1.17, they have poor specific infectivity in the low-density fractions(Dao Thi et al., 2012, Gastaminza et al., 2006,

Lindenbach et al., 2005, Merz et al., 2011), which is thought to reflect their incomplete lipidation. Indeed, while HCVcc particles are associated with apoC-I(Dreux et al., 2007a, Meunier et al., 2008) and apoE(Chang et al., 2007, Jiang & Luo, 2009), their association with apoB is variably detected(Boyer et al., 2014, Catanese et al., 2013, Huang et al., 2007, Jiang & Luo, 2009, Merz et al., 2011, Steenbergen et al., 2013).

The difference of lipidation between HCVcc and patient-derived HCV particles has been attributed to a defective lipoprotein metabolism pathway in Huh-7 cells that prevents the formation of fully lipidated VLDLs(Calattini et al., 2015, Meex et al., 2011, Podevin et al., 2010, Steenbergen et al., 2013, Yamamoto et al., 1987). HCVcc particles grown in primary human hepatocytes (PHH), which produce normal VLDLs, have higher specific infectivity owing to the viral RNA peak that coincides with the fractions of highest infectivity; yet, they display densities between 1.07 and 1.11(Podevin et al., 2010), which is higher than that of patient-derived HCV. Likewise, HCV particles grown *in vivo* in PHH-xenograft mouse models that release normal levels of human apoB and apoE display coincident viral RNA and infectivity peaks at 1.06-1.11(Calattini et al., 2015, Lindenbach et al., 2006), which, again, are above those detected for patient-derived HCV.

While the study of HCVcc has provided tremendous progresses in the knowledge of HCV and its interactions with host cells, culminating with the design of new DAAs regimen that can efficiently eradicate HCV in most patients, many aspects of HCV biology are not completely resolved because of the lack of models that fully mimic the conformation of authentic HCV particles. Furthermore, as the morphology of LPVs is poorly-defined and as lipoprotein-association is thought to shape their surface and induce neutralization resistance(Andre et al., 2002, Catanese et al., 2013, Dao Thi et al., 2012, Grove et al., 2008, Nielsen et al., 2006), elucidating their structure would improve the design of rational vaccine candidates.

Here, by studying HCVcc production *in vitro* with media of defined serum conditions, we demonstrate that short time incubation of HCVcc particles with human serum can induce full conversion of apoB-defective infectious virions to apoB-containing, low- or very-low-density particles, which augments their specific infectivity. We also reveal that besides lipoproteins, specific serum factors are required to allow extracellular maturation of HCV virions, hence showing that a major determinant that imprints lipidation of particles is serum itself, likely at a post-secretion step.

Materials and Methods

Cell culture and Reagents.

Huh-7.5 cells (kind gift from C. Rice) were grown in DMEM (Invitrogen) supplemented with 100U/ml penicillin, 100µg/ml streptomycin and 10% fetal calf serum (FCS).
For preparation of human serum (HS), blood from healthy donors retrieved from the national blood collection was incubated on ice for 2h and centrifuged at 4,000rpm for 20min, and the supernatants were harvested and stored at -80°C. The HS used in this study, consisting in pools of 4 specimens from different donors, contained, on average, 0.38g/L cholesterol-VLDL, 0.93g/L cholesterol-LDL and 0.47g/L cholesterol-HDL (Supplementary Figure 7A), which is in the range of normal HS (https://www.cholesterolmenu.com/cholesterol-levels-chart/).
The lipoprotein-deficient serum (LPDS), corresponding to HS fractions of density >1.24, was prepared from HS by a two-step ultracentrifugation procedure using a Beckman TL100 centrifuge. Briefly, the density of HS was adjusted to 1.063 g/ml by addition of dry KBr powder and centrifuged at 100,000 rpm for 3h30 at 15°C. The fraction of density >1.063 was harvested and its density was increased to 1.24 by adding KBR. The LPDS fraction was subsequently obtained after a second ultracentrifugation at 100,000rpm for 12h at 15°C and dialyzed exhaustively against PBS before use. The quality of LPDS was assessed by measurement of apoB, apoE and human serum albumin (HSA) (Supplementary Figure 7B).
VLDLs, LDLs, HDLs and HSA (fraction V) purified from HS (Sigma-Aldrich) were used for reconstitution experiments, at amounts corresponding to that of 10% HS typically used in this study.

Patients' serum specimens.

Blood samples were collected from HCV-infected patients in Saint Etienne's University hospitals in January-June 2016. Written informed consent was obtained from each patient to use sera samples for anonymous research purposes.
All blood samples were HCV antibody-positive as determined using the Architect anti-HCV assay (Abbott). HCV RNA was genotyped by using the TRUGENE HCV-5′NC genotyping kit designed to identify the HCV genotypes (Siemens Healthcare Diagnostics).

Plasmids.

Plasmid pFK-H77/JFH1/HQL(EVIR)(Dao Thi et al., 2012) and pFK-JFH1/J6/C-846_dg(Pietschmann et al., 2006) plasmids (kind gifts from R. Bartenschlager) were used to produce HCVcc particles. Recombinant forms of either construct were engineered using synthetic genes and restriction digestions to swap amino-acids 1-27 of E2 (HVR1) between Jc1 and H77 sequences, generating the pFK-H77/JFH1/HQL-HVRI(Jc1) and pFK-JFH1/J6/C-846-HVRI(H77) plasmids.

HCVcc production.

Methods for *in vitro* transcription of HCV RNA and electroporation into Huh-7.5 cells were described previously(Denolly et al., 2017). For production experiments, HCVcc-producer cells were grown in OptiMEM (Invitrogen) only or in OptiMEM supplemented with 10% FCS or HS. For incubation experiments, HCVcc-producer cells were grown in OptiMEM and the harvested virions were incubated with either serum-free or with FCS- or HS-containing OptiMEM. To determine intracellular infectivity, electroporated cells were washed with PBS, harvested with versene and centrifuged for 4min at 400xg. Cell pellets were suspended in OptiMEM and subjected to 4 freeze/thaw cycles in liquid nitrogen.

Iodixanol density-gradient fractionation.

1ml of HCVcc particle-containing supernatant passed through 0.45-µm pore-size filters was loaded on top of a 3–40% continuous iodixanol gradient (Optiprep, Axis Shield). Gradients were centrifuged for 16h at 4°C in Optima L-90 centrifuge (Beckman). Sixteen fractions of 750µl were collected from the top and used for refractive index measurement, infectivity titration, core and RNA quantification, as described below.

Infectivity titration, core quantification and RNA quantifications.

Infectivity titers of cell supernatants or intracellular virus samples were determined as detailed previously(Denolly et al., 2017). Serial dilutions of supernatants or fractions were used to infect Huh-7.5 cells and focus-forming units were determined 72h post-infection by counting NS5A-immunostained foci.

HCV core protein was quantified by CMIA - Chemiluminescent Microparticle ImmunoAssay (Architect i2000, Abbott Diagnostics). HCV RNAs were extracted (TRI Reagent®, Euromedex), reverse transcribed (iScript cDNA synthesis kit, Bio-Rad), and quantified (FastStart Universal SYBR Green Master kit, Roche Applied Science) on an Applied StepOne Real-Time PCR apparatus. HCV-specific primers (5′-TCTGCGGAACCGGTGAGTA and 5′-TCAGGCAGTACCACAAGGC). As an internal control of extraction, an exogenous RNA from the linearized Triplescript plasmid pTRI-Xef (Invitrogen) was added into the supernatant prior to extraction and quantified with specific primers (5′-CGACGTTGTCACCGGGCACG and 5′-ACCAGGCATGGTGGTTACCTTTGC).

Co-immunoprecipitation of apolipoproteins and viral RNAs.

100µl of HCVcc supernatants or patient sera were precleared for 1h at 4°C with 40µl of protein A/G agarose beads and incubated overnight at 4°C with 15µl goat anti-apoB (AB742, Millipore) or control goat IgG under continuous agitation. The complexes were incubated for 2h at room temperature with 40µl of protein A/G agarose beads. The immune complexes

were washed three times in PBS and beads were re-suspended in Tri-Reagent for RNA extraction.

Statistical analysis.

Significance values were calculated by applying the paired t-test using the GraphPad Prism 6 software (GraphPad Software). P-values under 0.05 were considered statistically significant and the following denotations were used: ****, P≤0.0001; ***, P≤0.001; **, P≤0.01; *, P≤0.05; ns (not significant), P>0.05. All data were represented as means ± SEM.

Results

Serum composition of culture media dictates HCV particle density.

HCV particles isolated from HCV-infected patient sera exhibited low buoyant densities (Figure 1A), with most viral RNAs detected at densities <1.08, reflecting their lipidation state(Andre et al., 2002, Lindenbach et al., 2006, Nielsen et al., 2006). Since HCVcc particles are typically produced from Huh-7.5 cells grown with 10% FCS, we hypothesized that the species origin and composition of serum used in culture media may influence virion density. Whereas infectious HCV particles produced for 72h in serum-free media were poorly lipidated (Figure 1B), with <10% infectivity in fractions below 1.08 (see examples of raw density profiles in Supplementary Figure 1), 38% of the infectivity of particles grown in FCS-containing media were shifted to low-density fractions, yet with less than 8% of infectivity detected below 1.04 (Figure 1B). Strikingly, HCVcc particles produced with 10% HS exhibited >80% of infectivity at densities <1.08 and *ca*. 60% at density <1.04 (Figure 1B). Importantly, the density shifts of infectivity correlated with of viral RNA- and core-containing particles (Figure 1C; Supplementary Figure 1A-C), indicating that HCV physical particles become lipidated when produced in the presence of serum, with a major effect of HS. Similar results were obtained when using different individual or pools of normal HS and when applying shorter production times (data not shown).

We extended these results obtained with genotype 2a to H77 HCVcc (genotype 1a) (Figure 2A; Supplementary Figure 1D-F). Interestingly, H77 HCVcc particles grown with serum shifted to lower densities than Jc1 particles. Indeed, compared to Jc1, H77 HCVcc infectious particles were detected in higher proportions in densities <1.08 [60% (H77) *vs*. 38% (Jc1)] when produced with FCS, and, strikingly, peaked at lower densities: 1.02-1.09 (H77) *vs*. 1.06-1.09 (Jc1) and 1.00-1.03 (H77) *vs*. 1.03-1.06 (Jc1) when produced with FCS and HS, respectively (Figures 2A *vs*. 1B). Likewise, compared to serum-free production, the amounts of H77 HCVcc physical particles produced in serum-containing medium were increased by

>10-fold in the low-density fractions, with higher increases of viral RNAs for particles produced in HS than for FCS (Figure 2B) and for H77 than for Jc1 HCVcc particles (Figures 2B *vs*. 1C). Altogether, these results indicated that HCV-specific sequences influence the lipidation level of viral particles.

Lipidation of HCV particles occurs post-egress and enhances specific infectivity.

The poorly lipidated profile of HCVcc particles produced in serum-free conditions suggested that the extracellular milieu imprints virion composition. Accordingly, when we investigated Jc1 and H77 intracellular particles, we found that they had identical density profiles with almost no infectivity in fractions <1.08 whether the virus-producer culture medium contained serum or not (Figures 1D and 2C). This suggested that the acquisition of the low-density profile of HCVcc particles occurs at the step of virion secretion and/or after secretion in the extracellular milieu.

To test the latter possibility, we incubated Jc1 and H77 HCVcc particles produced in serum-free conditions in media containing 10% HS or FCS *vs*. no serum for 6h (Figure 3; Supplementary Figure 2 for examples of raw data). We found that this incubation procedure could reproduce the lipidation observed in the HCVcc production protocol (Figure 3 *vs*. Figures 1 and 2). Indeed, we found that Jc1 or H77 viruses incubated with HS shifted *ca*. 90% of infectivity in densities <1.08 (Figure 3A,C), which correlated with a shift of physical particles in these low-density fractions (Figure 3B,D; Supplementary Figure 2B,E). Again, more marked shifts of both infectious and physical particles were detected for virus incubation in HS- rather than in FCS-containing media, implying the presence of species-specific lipidation factor(s). Moreover, a stronger lipidation was observed for H77 particles as compared to Jc1 particles (Figure 3C,D *vs*. 3A,B), with 50% *vs*. 20% of infectivity in densities below 1.04 for H77 *vs*. Jc1 viruses. In agreement with the above results, purified intracellular particles incubated with serum-containing media readily shifted to low-density fractions, again with a more marked shift for HS rather than FCS and for H77 virus rather than Jc1 (Figure 3E-G).

To corroborate these results, we incubated viral particles purified from fractions of densities of 1.08-1.14 with HS-containing *vs*. serum-free media before subjecting them to a second density-gradient analysis (Figure 4A). We found that incubation with HS shifted >75% of infectious particles to low-density fractions (Figure 4B).

Altogether, these results indicated that acquisition of lipids could occur after virion egress and that incubation of poorly lipidated viral particles change virion structure and/or composition through their lipidation.

While displacement of HCV particles to low-density fractions upon HS-incubation resulted in strongly reduced infectivity in fractions of density 1.08-1.14 (Figure 3A,C; Figure 4B), the levels of viral RNAs in these fractions remained abundant (Figure 3B,D; Supplementary Figure 2), likely reflecting that most viral RNAs and/or particles in these densities are not infectious. In contrast, in low-density fractions, the comparison of the shifts of infectivity *vs*. physical particles suggested that HS-incubation of Jc1 and H77 viruses increased more readily the infectivity than the viral RNA quantities (Figure 3: panels A *vs*. B and panels C *vs.* D). Accordingly, the ratio of infectivity to viral RNAs calculated in each fraction steadily increased once viruses acquired lower densities (Supplementary Figure 3), with respectively 14-fold and 25-fold mean augmentations for HS-incubated Jc1 and H77 particles compared to serum-free incubation in fractions below <1.04 (Figure 4C,D), and likewise for fractions of densities of 1.04-1.08. This indicated that lipidation modifies the specific infectivity of HCV particles upon their shift to low-densities and render the particles more infectious.

Time and serum dose-dependent HCV virions lipidation leads to apoB-association.

The higher infectivity detected in low-density fractions for viral particles produced for 72h with HS-containing media compared to viruses incubated for 6h with HS (Figure 3 *vs*. Figures 1 and 2) suggested that virion lipidation occurs in a time-dependent manner. Upon incubation with HS for different periods of time, we found that the lipidation of both Jc1 and H77 HCVcc particles (Figure 5A-C; Supplementary Figure 4 for examples of raw data of infectivity, core and RNA levels) progressively increased in fractions of densities between 1.04-1.08, reaching a transient maximum at *ca*. 4-6h incubation, after which the infectious particles in these densities decreased but steadily accumulated in the very-low-density fractions (<1.04). These results suggested that lipidation of HCV particles is a continuous process that occurs over time post-secretion from producer cells.

Next, we sought to determine whether serum concentration influences the lipidation levels of HCVcc particles. As shown in Figure 5D-F (Supplementary Figure 5 for raw data), we found that incubation of HCVcc particles with increasing HS doses gradually shifted infectivity and physical particles, reaching nearly 100% infectivity in low-density fractions upon incubation with 50% HS. These results indicated that acquisition of lipids depends on the amounts of sera and underscored a limiting serum factor responsible for lipidation of HCV particles at a post-egress step.

Since HS-incubated HCVcc particles reached densities close to those of HCV-infected patients (Figure 1A), we wondered if the former viruses were associated to apoB, as observed *in vivo*(Andre et al., 2002, Diaz et al., 2006, Nielsen et al., 2006, Thomssen et al., 1992). When we quantified the viral RNAs after co-immuno-precipitation assays with apoB antibodies, we found a strong enrichment of viral RNAs for HCVcc particles incubated with

HS, reaching values comparable to those detected for patient sera (Figure 5G). This indicated that the low-density profile of HCV particles incubated with HS reflects their association with apoB, suggesting that upon HS-incubation, HCV infectious particles interact with apoB-containing lipoproteins in a manner similar to patient-derived virus.

HVRI sequence of HCV E2 glycoprotein determines lipidation of viral particles.

Since Jc1 and H77 viruses displayed different lipidation levels and rates (Figure 5A-C), we sought to investigate which viral determinant could influence virion lipidation. We found that swapping the H77 HVRI sequence in Jc1 virus (Figure 6A) induced stronger lipidation of the resulting Jc1_HVR1_H77 recombinant particles as compared to parental Jc1 virus, with an increase of over 5-6 fold of both infectious (Figure 6B,D; Supplementary Figure 6A) and physical (Figure 6F; Supplementary Figure 6B) particles detected in fractions of densities below 1.04 upon HS-incubation. Interestingly, the lipidation of this recombinant virus was higher than that of parental H77 virus itself, with over two-fold more infectious particles detected in such fractions (80% *vs*. 40%; Figure 6B,D *vs*. Figure 6C,E; Supplementary Figure 6A *vs*. 6C), correlating with the higher shift of physical particles (6-7 fold *vs*. 2.5-fold; Figure 6F,G; Supplementary Figure 6B,D). Conversely, compared to parental H77 virus, swapping the Jc1 HVRI sequence decreased the lipidation of the resulting H77_HVR1_Jc1 recombinant particles upon HS-incubation, as shown by the reduction of *ca*. 40-fold of the percentage of infectious particles detected in fractions of densities below 1.04 (Figure 5C,E; Supplementary Figure 6C). Altogether, these results indicated that HVRI is a key viral determinant regulating the lipidation of viral particles in an HCV strain-dependent manner.

HSA is a serum factor that promotes HCV particle lipidation by apoB-containing lipoproteins.

That HS could more efficiently induce lipidation of viral particles as compared to FCS (Figures 1-3) indicated that either serum type might differ in HCV-specific lipidation factor(s). Indeed, when we quantified the lipoproteins composition of sera used in our experiments, we found that compared to HS, FCS displayed 6-7 folds lower amounts of both HDLs and LDLs, and no VLDLs (Supplementary Figure 7A). Thus, we sought to characterize serum factors, including lipoproteins, that could modulate lipidation of HCV particles.

To determine which lipoprotein class is important for lipidation of viral particles, we depleted lipoproteins from HS to generate a LPDS with >100-fold decreased apoB levels, despite normal HSA levels (Supplementary Figure 7B), indicating effective removal of lipoproteins. Next, we incubated Jc1 HCVcc particles produced in serum-free conditions with LPDS or with purified HSA *vs*. with different lipoprotein types, *i.e.,* VLDL, LDL or HDL, before density-gradient analysis. We found that incubation with either LPDS or HSA only did not grossly

change the lipidation profile of viral particles (Figure 7A; Supplementary Figure 7C), suggesting that lipoproteins present in serum are likely the source of virion lipidation. Conversely, incubation of HCVcc particles with purified VLDLs, LDLs or HDLs at physiological concentrations did not significantly change their lipidation profiles, indicating that a serum protein component could be required for virus lipidation by either lipoprotein type. Confirming this hypothesis, we found that HCVcc incubation with LPDS added to lipoproteins shifted the viral particles to low-densities, with >50% of infectivity detected below 1.08 (Figure 7A; Supplementary Figure 7C). Furthermore, the incubation of HCVcc particles with LPDS and combinations of HDL and VLDL or LDL induced full lipidation, similar to that detected with HS-incubation (Figure 7B; Supplementary Figure 7C). Similar results were obtained with H77 HCVcc particles (data not shown).

Finally, while searching for serum factors promoting HCV lipidation, we found that blocking serum lipoprotein-modification factors such as cholesteryl ester transfer protein (CETP) and lecithin-cholesterol acyltransferase (LCAT) did not change HS-induced virion low-density (Supplementary Figure 8), thus ruling out their involvement in HCV lipidation. In contrast, we found that HSA added to VLDL and LDL could induce HCV particle lipidation (Figure 7A; Supplementary Figure 7C).

Altogether, these results indicated that lipoproteins are the main source of HCV lipidation, which requires additional serum component(s) that include HSA.

Discussion

The overall organization of HCV particles form(s) remains elusive. *In vivo*, HCV particles are associated to apoB, the major structural and non-exchangeable component of VLDLs and LDLs. This may explain the particularly low buoyant density of HCV LVPs, *i.e.* ≤1.08 (Figure 1A), which is significantly lower than those of other enveloped viruses, including the HCV-related flaviviruses(Lindenbach & Rice, 2013). Indeed, the lipidomics of purified HCVcc particles confirmed that their lipid content is related to that of serum lipoproteins(Merz et al., 2011). Several studies proposed that HCV particle production from hepatocytes depends on cellular factors controlling biosynthesis of VLDLs, suggesting that the interaction of virions with serum lipoproteins begins at the steps of their assembly and secretion processes during which immature particles are converted to mature virions by lipidation and incorporation of some apolipoproteins(Andre et al., 2002, Boyer et al., 2014, Catanese et al., 2013, Chang et al., 2007, Dao Thi et al., 2012, Diaz et al., 2006, Dreux et al., 2007a, Gastaminza et al., 2006, Huang et al., 2007, Jiang & Luo, 2009, Lee et al., 2014, Lindenbach et al., 2005, Lindenbach et al., 2006, Merz et al., 2011, Meunier et al., 2008, Nielsen et al., 2006,

Steenbergen et al., 2013, Thomssen et al., 1992). Yet, while there is a strong consensus indicating that the exchangeable apolipoprotein apoE is necessary at an early assembly step to promote envelopment, lipidation and/or release of viral particles, some studies suggests that apoB may not be required to promote these initial steps (reviewed in(Lindenbach & Rice, 2013)). This is intriguing because apoB is essential for VLDL biogenesis(Lehner et al., 2012) and because HCV retrieved from patients can be readily immuno-precipitated with antibodies against apoB(Nielsen et al., 2006, Thomssen et al., 1992) (Figure 5G). One orthodox explanation is that the Huh-7.5 hepatoma cells that efficiently support HCVcc production *in vitro*(Lindenbach et al., 2005, Pietschmann et al., 2006) lack many properties of hepatocytes, such as the ability to produce normal VLDLs(Calattini et al., 2015, Meex et al., 2011, Podevin et al., 2010, Steenbergen et al., 2013, Yamamoto et al., 1987). That Huh-7.5 cells produce under-lipidated, VLDL-like particles would thus explain why the HCVcc particles they produce have a higher buoyant density and lower specific infectivity than HCV produced *in vivo*(Andre et al., 2002, Lindenbach et al., 2006, Nielsen et al., 2006) or from primary hepatocytes(Calattini et al., 2015, Lindenbach et al., 2006, Podevin et al., 2010). However, when HepG2 hepatoma cells, which are thought to represent more mature hepatocytes than Huh-7 cells, are induced to produce normal, apoB-containing VLDLs, they yield infectious viral particles that are biophysically and biochemically similar to those produced from Huh-7.5 cells(Jammart et al., 2013).

Since this and other evidence(Lindenbach & Rice, 2013) showed that there is no clear correlation between the ability of cells that replicate HCV to secrete apoB or VLDLs and their capacity to produce LVPs, we thought to investigate the possibility that LVP formation *in vivo* could derive from a post-secretion interaction between extracellular HCV particles and VLDLs or other lipoproteins. Our results indicate that while Huh-7.5 cells grown in serum-free medium produce very-poorly lipidated, if not completely immature HCV particles of intermediate density (>1.08), the maturation to fully-lipidated, apoB-containing infectious virions of low-density can be rapidly induced once they encounter in the extracellular milieu the appropriate serum conditions that exhibit physiologic concentrations of lipoproteins. These results do not disrepute that *in vivo* or in normal hepatocytes as well as in long-term HS-induced metabolically-adapted hepatoma cells as proposed previously(Gastaminza et al., 2006, Huang et al., 2007, Steenbergen et al., 2013), HCV maturation may occur during transit through the cell secretory pathway, where virions may associate or fuse with apoB-containing lipoproteins precursors and/or luminal, apoE-containing lipid droplets(Lehner et al., 2012). However, they imply that a major factor of lipid-imprinting of HCV particles is the environment provided by the extracellular milieu and/or the serum characteristics.

Our data reveal that lipidation of viral particles requires interaction(s) with defined serum lipoproteins but also involves additional, presumably non-lipid serum factor(s) such as HSA (Figure 7). Concerning the lipoprotein type allowing lipidation of viral particles, our results indicate that all principal lipoprotein classes, *i.e.*, VLDL, LDL and HDL, could induce lipidation *in vitro*, upon short time incubation with HCV particles in the presence of LPDS, with an additive effect when either VLDL or LDL was combined with HDL. While these results are consistent with the strong lipidation induced by HS (this report), in contrast to FCS that contains at least 6-fold lower concentrations of either lipoprotein (Supplementary Figure 7A), they raise the question of the nature of the interaction between lipoproteins and viral particles, and of its outcome in terms of HCV virion morphology. LVP structures harboring different lipoprotein components may indeed be formed by transfer of lipids, through their spontaneous release/exchange or *via* fusion ("single-particle" model), or, alternatively, by transient or stable virion association with lipoproteins ("two-particle" model)(Lindenbach & Rice, 2013).

Although direct evidence by electron microscopy is missing in favor of the latter model(Andre et al., 2002, Catanese et al., 2013, Gastaminza et al., 2010, Merz et al., 2011, Piver et al., 2017), perhaps owing to its transient or unstable state, our results argue for this model since lipidation of cell-free viral particles upon short time treatment with HS induced their association with apoB, a non-exchangeable apolipoprotein (Figure 5G). Other arguments for this morphological model are that *in vivo*, HCV particles may associate with apoB48-containing chylomicrons(Diaz et al., 2006), although HCV is not produced by enterocytes, and that they exhibit rapid though transient postprandial shifts in buoyant density upon lipid-rich diet in HCV-infected patients(Felmlee et al., 2010). Yet, this evidence does not rule out the alternative and/or nonexclusive possibility that viral particles may mimic lipoproteins and thus, exchange or uptake their lipids just as lipoproteins do between themselves. Accordingly, it was previously reported that apoliproteins can be exchanged or transferred from cells, lipoproteins or serum itself to infectious particles(Bankwitz et al., 2017, Chang et al., 2007, Dreux et al., 2007a, Meunier et al., 2008, Yang et al., 2016). Thus, as LVPs contain specific subsets of apoliproteins(Andre et al., 2002, Catanese et al., 2013, Merz et al., 2011), this may regulate the exchange and/or transfer of lipids with lipoproteins, which could modify their inner neutral lipid content, as inferred from the lipidation state and infectivity of viral particles that are altered upon treatment with lipoprotein lipase and/or hepatic triglyceride lipase(Shimizu et al., 2011). In this respect, our HS-incubation kinetics (Figure 5), suggesting that lipidation of infectious particles is progressive over time, may argue for the "single-particle" model of HCV structure, sharing with a lipoprotein particle its envelope that is continuously remodeled upon interactions with lipoproteins. Since HCV

particle lipidation can be induced by different types of lipoproteins (Figure 7), we surmise that the mode of lipoprotein association or of lipidation mechanism varies accordingly.
Importantly, our results reveal that lipidation of viral particles by lipoproteins requires additional serum factor(s), since incubation with VLDL, LDL and HDL could induce the low-density shift of HCV virions only in the presence of LPDS. We were unable to block lipidation of viral particles by inhibitors of CETP and LCAT that promote lipid transfer to lipoproteins and maturation (Supplementary Figure 8), hence discarding these candidate factors. Yet, we found that HSA, added to VLDL or LDL, induced lipidation of viral particles. This indicated that HSA is one of the serum co-factors mediating LVP formation, perhaps by bridging lipoproteins and virions or by favoring lipid efflux(Sankaranarayanan et al., 2013).

Our results indicate that the HVRI domain of the E2 glycoprotein plays a major role in the lipidation process and accounts for the differential lipidation sensitivities of Jc1 *vs*. H77 HCVcc particles. HVR1 remains an intriguing determinant of E2 that modulates i) the conformation of E2 by concealing the CD81-binding site(Dao Thi et al., 2012, Roccasecca et al., 2003) and the accessibility to cross-neutralizing epitopes that target virus-CD81 interaction(Bankwitz et al., 2010, Bartosch et al., 2005, Dreux et al., 2006); ii) the recruitment and/or conformation of apolipoproteins such as apoC1(Dreux et al., 2007a) and apoE(Bankwitz et al., 2014) to viral particles; and iii) the interaction of virions with lipoproteins, which promotes HDL-mediated enhancement of their infectivity(Bartosch et al., 2005, Dreux et al., 2007a, Dreux et al., 2009a, Dreux et al., 2006, Lavillette et al., 2005a) and their lipidation profiles(Bankwitz et al., 2014, Dao Thi et al., 2012, Prentoe et al., 2011, Prentoe et al., 2014). While HVR1 deletion shifts the density of particles to a homogenous intermediate density of 1.11(Bankwitz et al., 2010, Dao Thi et al., 2012, Prentoe et al., 2011) that corresponds to the density of the non-lipidated particles of our study, it is interesting that simple HVR1 swaps between H77 and Jc1 HCVcc reconstituted the differential lipidation profiles of either parental virus. This suggests that, in contrast to its role in the concealment of CD81-binding site that is modulated in concert with other residues in both E1 and E2(Bankwitz et al., 2010), HVR1 seems relatively autonomous to organize the lipidation profile of the virus to which it belongs, in a strain-specific manner.
The reasons why HCV is lipidated *in vivo* raise different and fascinating scenarios. First, in agreement with previous reports indicating that lipidated viruses exhibit strain-dependent usage of different lipoprotein receptors acting as cell entry factors(Prentoe et al., 2014), including SR-BI(Bankwitz et al., 2010, Calattini et al., 2015, Dao Thi et al., 2012, Prentoe et al., 2014), LDLr(Prentoe et al., 2014) and VLDLr(Ujino et al., 2016, Yamamoto et al., 2016), by driving both lipidation and apolipoprotein display, HVR1 plasticity may dictate the set of receptors used during entry steps. Second, lipidation may contribute to shielding cross-

neutralizing epitopes(Andre et al., 2002, Catanese et al., 2013, Dao Thi et al., 2012, Grove et al., 2008, Nielsen et al., 2006), although recent studies with HCVcc indicated that neutralization efficiency of different genotypes seemed independent of virus density(Prentoe et al., 2011) and that the main E2 target of such cross-neutralizing antibodies is concealed by HVR1, whether or not the virus particles are lipidated(Bankwitz et al., 2010, Bartosch et al., 2005, Dreux et al., 2006). Accordingly, it will be of high interest to investigate neutralization resistance using HS-treated HCVcc virus, which is fully lipidated, rather than HCVcc produced in the standard (FCS) conditions used in these previous studies. Indeed, it is possible that lipidation allows viral particles to access, following a first step of entry induced by lipoprotein receptors, to a protected environment into which they can subsequently and safely interact with CD81 in a putative neutralizing antibody-free sanctuary where further steps of cell penetration can be promoted. A third scenario, which is also consistent with the latter one, is that the usage of lipoprotein receptors increases the specific infectivity of viral particles. Indeed, lipidation of viral particles, which shift them to low or very-low densities, is accompanied by their increased specific infectivity (Figure 4C,D). This could provide a positive selection for eliciting HVR1 variants that drive full lipidation. The varying specific infectivity according to virion density could thus reflect the differential efficiency of cell entry pathways depending on the lipidation status of the particles, which would influence binding and usage of specific lipoprotein receptors. Finally, it is also possible that lipidation increases the stability and/or infectivity of particles by protecting them from degradation(Steenbergen et al., 2013).

In conclusion, our results indicate that HCV particles acquire their neutral lipids from the extracellular milieu, which requires both lipoproteins and serum protein factors as well as HVR1 determinants. Overall, these findings allow developing simple and useful culture conditions to produce infectious HCV particles that resemble those retrieved from chronically-infected patients, which may facilitate structural and functional investigations but also the rationale design of a much-needed vaccine.

Supplementary Material

To access the supplementary material accompanying this article, visit the online version of Gastroenterology at www.gastrojournal.org, and at …
Supplementary Material includes eight Supplementary Figures.

Literature cited

1. Bartenschlager R, Baumert TF, Bukh J, et al. Critical challenges and emerging opportunities in hepatitis C virus research in an era of potent antiviral therapy: Considerations for scientists and funding agencies. Virus Res 2018;248:53-62
2. Lindenbach BD, Rice CM. The ins and outs of hepatitis C virus entry and assembly. Nat Rev Microbiol 2013;11:688-700
3. Piver E, Boyer A, Gaillard J, et al. Ultrastructural organisation of HCV from the bloodstream of infected patients revealed by electron microscopy after specific immunocapture. Gut 2017;66:1487-1495
4. Catanese MT, Uryu K, Kopp M, et al. Ultrastructural analysis of hepatitis C virus particles. Proc Natl Acad Sci U S A 2013;110:9505-10
5. Merz A, Long G, Hiet MS, et al. Biochemical and morphological properties of hepatitis C virus particles and determination of their lipidome. J Biol Chem 2011;286:3018-32
6. Andre P, Komurian-Pradel F, Deforges S, et al. Characterization of low- and very-low-density hepatitis C virus RNA-containing particles. J Virol 2002;76:6919-28
7. Nielsen SU, Bassendine MF, Burt AD, et al. Association between hepatitis C virus and very-low-density lipoprotein (VLDL)/LDL analyzed in iodixanol density gradients. J Virol 2006;80:2418-28
8. Lindenbach BD, Meuleman P, Ploss A, et al. Cell culture-grown hepatitis C virus is infectious in vivo and can be recultured in vitro. Proc Natl Acad Sci U S A 2006;103:3805-9
9. Thomssen R, Bonk S, Propfe C, et al. Association of hepatitis C virus in human sera with beta-lipoprotein. Med Microbiol Immunol 1992;181:293-300
10. Diaz O, Delers F, Maynard M, et al. Preferential association of Hepatitis C virus with apolipoprotein B48-containing lipoproteins. J Gen Virol 2006;87:2983-91
11. Bradley D, McCaustland K, Krawczynski K, et al. Hepatitis C virus: buoyant density of the factor VIII-derived isolate in sucrose. J Med Virol 1991;34:206-8
12. Steenbergen RH, Joyce MA, Thomas BS, et al. Human serum leads to differentiation of human hepatoma cells, restoration of very-low-density lipoprotein secretion, and a 1000-fold increase in HCV Japanese fulminant hepatitis type 1 titers. Hepatology 2013;58:1907-17
13. Lindenbach BD, Evans MJ, Syder AJ, et al. Complete replication of hepatitis C virus in cell culture. Science 2005;309:623-6
14. Pietschmann T, Kaul A, Koutsoudakis G, et al. Construction and characterization of infectious intragenotypic and intergenotypic hepatitis C virus chimeras. Proceedings of the National Academy of Sciences 2006;103:7408-7413
15. Dao Thi VL, Granier C, Zeisel MB, et al. Characterization of hepatitis C virus particle subpopulations reveals multiple usage of the scavenger receptor BI for entry steps. J Biol Chem 2012;287:31242-57
16. Gastaminza P, Kapadia SB, Chisari FV. Differential biophysical properties of infectious intracellular and secreted hepatitis C virus particles. J Virol 2006;80:11074-81
17. Meunier JC, Russell RS, Engle RE, et al. Apolipoprotein c1 association with hepatitis C virus. J Virol 2008;82:9647-56
18. Dreux M, Boson B, Ricard-Blum S, et al. The exchangeable apolipoprotein APOC-I promotes membrane fusion of hepatitis C virus. J Biol Chem 2007;282:32357-32369

19. Chang KS, Jiang J, Cai Z, et al. Human apolipoprotein e is required for infectivity and production of hepatitis C virus in cell culture. J Virol 2007;81:13783-93
20. Jiang J, Luo G. Apolipoprotein E but not B is required for the formation of infectious hepatitis C virus particles. J Virol 2009;83:12680-91
21. Boyer A, Dumans A, Beaumont E, et al. The association of hepatitis C virus glycoproteins with apolipoproteins E and B early in assembly is conserved in lipoviral particles. J Biol Chem 2014;289:18904-13
22. Huang H, Sun F, Owen DM, et al. Hepatitis C virus production by human hepatocytes dependent on assembly and secretion of very low-density lipoproteins. Proc Natl Acad Sci U S A 2007;104:5848-53
23. Meex SJ, Andreo U, Sparks JD, et al. Huh-7 or HepG2 cells: which is the better model for studying human apolipoprotein-B100 assembly and secretion? J Lipid Res 2011;52:152-8
24. Podevin P, Carpentier A, Pene V, et al. Production of infectious hepatitis C virus in primary cultures of human adult hepatocytes. Gastroenterology 2010;139:1355-64
25. Calattini S, Fusil F, Mancip J, et al. Functional and Biochemical Characterization of Hepatitis C Virus (HCV) Particles Produced in a Humanized Liver Mouse Model. J Biol Chem 2015;290:23173-87
26. Yamamoto T, Takahashi S, Moriwaki Y, et al. A newly discovered apolipoprotein B-containing high-density lipoprotein produced by human hepatoma cells. Biochim Biophys Acta 1987;922:177-83
27. Grove J, Nielsen S, Zhong J, et al. Identification of a residue in hepatitis C virus E2 glycoprotein that determines scavenger receptor BI and CD81 receptor dependency and sensitivity to neutralizing antibodies. J Virol 2008;82:12020-9
28. Denolly S, Mialon C, Bourlet T, et al. The amino-terminus of the hepatitis C virus (HCV) p7 viroporin and its cleavage from glycoprotein E2-p7 precursor determine specific infectivity and secretion levels of HCV particle types. PLoS Pathog 2017;13:e1006774
29. Lee JY, Acosta EG, Stoeck IK, et al. Apolipoprotein E likely contributes to a maturation step of infectious hepatitis C virus particles and interacts with viral envelope glycoproteins. J Virol 2014;88:12422-37
30. Lehner R, Lian J, Quiroga AD. Lumenal lipid metabolism: implications for lipoprotein assembly. Arterioscler Thromb Vasc Biol 2012;32:1087-93
31. Jammart B, Michelet M, Pecheur EI, et al. Very-low-density lipoprotein (VLDL)-producing and hepatitis C virus-replicating HepG2 cells secrete no more lipoviroparticles than VLDL-deficient Huh7.5 cells. J Virol 2013;87:5065-80
32. Gastaminza P, Dryden KA, Boyd B, et al. Ultrastructural and biophysical characterization of hepatitis C virus particles produced in cell culture. J Virol 2010;84:10999-1009
33. Felmlee DJ, Sheridan DA, Bridge SH, et al. Intravascular transfer contributes to postprandial increase in numbers of very-low-density hepatitis C virus particles. Gastroenterology 2010;139:1774-83, 1783 e1-6
34. Yang Z, Wang X, Chi X, et al. Neglected but Important Role of Apolipoprotein E Exchange in Hepatitis C Virus Infection. J Virol 2016;90:9632-9643
35. Bankwitz D, Doepke M, Hueging K, et al. Maturation of secreted HCV particles by incorporation of secreted ApoE protects from antibodies by enhancing infectivity. J Hepatol 2017;67:480-489

36. Shimizu Y, Hishiki T, Ujino S, et al. Lipoprotein component associated with hepatitis C virus is essential for virus infectivity. Current Opinion in Virology 2011;1:19-26
37. Sankaranarayanan S, de la Llera-Moya M, Drazul-Schrader D, et al. Serum albumin acts as a shuttle to enhance cholesterol efflux from cells. J Lipid Res 2013;54:671-6
38. Roccasecca R, Ansuini H, Vitelli A, et al. Binding of the hepatitis C virus E2 glycoprotein to CD81 is strain specific and is modulated by a complex interplay between hypervariable regions 1 and 2. J Virol 2003;77:1856-67
39. Bartosch B, Verney G, Dreux M, et al. An interplay between hypervariable region 1 of the hepatitis C virus E2 glycoprotein, the scavenger receptor BI, and high-density lipoprotein promotes both enhancement of infection and protection against neutralizing antibodies. J Virol 2005;79:8217-29
40. Dreux M, Pietschmann T, Granier C, et al. High density lipoprotein inhibits hepatitis C virus-neutralizing antibodies by stimulating cell entry via activation of the scavenger receptor BI. J Biol Chem 2006;281:18285-95
41. Bankwitz D, Steinmann E, Bitzegeio J, et al. Hepatitis C virus hypervariable region 1 modulates receptor interactions, conceals the CD81 binding site, and protects conserved neutralizing epitopes. J Virol 2010;84:5751-63
42. Bankwitz D, Vieyres G, Hueging K, et al. Role of hypervariable region 1 for the interplay of hepatitis C virus with entry factors and lipoproteins. J Virol 2014;88:12644-55
43. Dreux M, Dao Thi VL, Fresquet J, et al. Receptor complementation and mutagenesis reveal SR-BI as an essential HCV entry factor and functionally imply its intra- and extra-cellular domains. PLoS Pathog 2009;5:e1000310
44. Lavillette D, Morice Y, Germanidis G, et al. Human Serum Facilitates Hepatitis C Virus Infection, and Neutralizing Responses Inversely Correlate with Viral Replication Kinetics at the Acute Phase of Hepatitis C Virus Infection. Journal of Virology 2005;79:6023-6034
45. Prentoe J, Jensen TB, Meuleman P, et al. Hypervariable region 1 differentially impacts viability of hepatitis C virus strains of genotypes 1 to 6 and impairs virus neutralization. J Virol 2011;85:2224-34
46. Prentoe J, Serre SB, Ramirez S, et al. Hypervariable region 1 deletion and required adaptive envelope mutations confer decreased dependency on scavenger receptor class B type I and low-density lipoprotein receptor for hepatitis C virus. J Virol 2014;88:1725-39
47. Ujino S, Nishitsuji H, Hishiki T, et al. Hepatitis C virus utilizes VLDLR as a novel entry pathway. Proc Natl Acad Sci U S A 2016;113:188-93
48. Yamamoto S, Fukuhara T, Ono C, et al. Lipoprotein Receptors Redundantly Participate in Entry of Hepatitis C Virus. PLoS Pathog 2016;12:e1005610

Author names in bold designate shared co-first authorship

Acknowledgments

We are grateful to Ralf Bartenschlager for the gift of JFH1 and Jc1 HCVcc constructs, and Charles Rice for the Huh7.5 cells and 9E10 NS5A monoclonal antibody.
We acknowledge the contribution of SFR Biosciences (UMS3444/CNRS, US8/Inserm, ENS de Lyon, UCBL) ANIRA-Genetic Analysis facility for excellent technical assistance and support. We thank Didier Décimo for support with the BSL3 facility.

Figures legends

Figure 1: Serum conditions dictate the density of extracellular HCV particles.
Density-gradient analysis of viral particles from HCV-infected patients (**A**) and HCVcc (**B-D**). Representative examples of gradient analysis are shown (right panels) and expressed as percentages of HCV RNA or infectivity, as indicated. The values from different gradients are regrouped in 3 categories of density (left panels). (**A**) Repartition of viral RNAs derived from sera of HCV-infected patients. HCV genotypes (Gt) and viral loads (log copies/mL) are indicated. (**B, C**) Extracellular and (**D**) intracellular Jc1 HCVcc particles were produced for 72h without serum (blue) *vs*. with 10% FCS (green) or 10% HS (red).

Figure 2: Lipidation of HCV particles is HCV genotype-independent.
Density-gradient analysis of H77 HCVcc particles. Representative examples of gradient analysis are shown (right panels) and expressed as percentages of HCV RNA or infectivity, as indicated. The values from different gradients are regrouped in 3 categories of density (left panels). (**A, B**) Extracellular and (**C**) intracellular particles were produced for 72h without serum (blue) *vs*. with 10% FCS (green) or 10% HS (red).

Figure 3: Lipidation of HCV particles occurs in the extracellular medium.
Jc1 (red) or H77 (blue) HCVcc particles produced for 72h in serum-free medium were incubated for 6h without serum *vs*. with 10% FCS or 10% HS. (**A-D**) Representative density-gradient analysis of extracellular HCVcc particles are shown (central panels) and expressed as percentages of infectivity. The values from different gradients are regrouped in 3 categories of density and displayed for infectivity (left panels in **A** and **C**) or HCV RNAs (**B, D**). (**E-G**) Representative density-gradient analysis of intracellular Jc1 and H77 HCVcc particles are shown (**E, F**) and expressed as percentages of infectivity. (**G**) The values from different gradients are regrouped in 3 categories of density and displayed for infectivity values of fractions of density <1.14.

Figure 4: Lipidation increase the specific infectivity of HCV particles.
(**A**) Schematic representation of experiment. Jc1 HCVcc particles produced in serum-free medium were layered on a first density-gradient (grey). Fractions of densities between 1.08-1.14, containing 80% of infectivity (grey bars in **B**), were pooled and incubated for 6h without serum (blue) *vs*. with 10% HS (red) before being layered on a second density-gradient. Each secondary fraction was then used to infect naïve cells. (**B**) Percentage of infectivity of extracellular particles treated as described in (**A**) and regrouped in three categories of density. The results of the first gradient (grey bars) and of the secondary gradients (blue and

red bars) are shown on the same graph. (**C, D**) Specific infectivity of Jc1 (**C**) and H77 (**D**) HCVcc particles produced in serum-free medium and incubated for 6h without serum (blue) *vs*. with 10% HS (red) normalized to serum-free condition. The mean values of means specific infectivity from fractions of different gradients are regrouped in 3 categories of density.

Figure 5: Lipidation of secreted HCV particles is time- and dose-dependent, and induces apoB-association.

(**A, B**) Representative density-gradient analysis of infectivity of Jc1 (**A**) and H77 (**B**) HCVcc particles produced in serum-free medium and incubated for different times with 10% HS, expressed as percentages of infectivity. (**C**) The values from different gradients are regrouped in 3 categories of density and displayed for Jc1 (red) and H77 (blue) particles produced and incubated as in (**A**) or (**B**). The results of HCVcc production for 72h in HS-containing medium are shown here for sake of comparison (dotted lines). (**D**) Representative density-gradient analysis of infectivity of Jc1 HCVcc particles produced in serum-free medium and incubated in 0%, 2%, 10% or 50% HS, and expressed as percentages of infectivity. The values of infectivity (**E**) or of RNA (**F**) from different gradients are regrouped in 3 categories of density. (**G**) Percentage of viral RNAs relative to input RNA co-immuno-precipitated with control (grey) or apoB (black) antibodies that were incubated with sera from patient-derived HCV or with Jc1 HCVcc produced without serum and incubated for 6h with 10% HS, 10% FCS or without serum, as indicated.

Figure 6: The HVRI determinant of HCV E2 regulates lipidation of HCV particles.

(**A**) Schematic representation of recombinant genomes generated by swapping HVRI domains between Jc1 and H77 HCVcc sequences. (**B, C**) Representative density-gradient analysis of infectivity of Jc1 (red) or Jc1_HVRI_H77 (brown) (**B**) or of H77 (blue) or H77_HVRI_Jc1 (purple) (**C**) HCVcc particles produced in serum-free medium and incubated for 6h without serum *vs*. with 10% HS, expressed as percentages of infectivity. The values of infectivity (**D, E**) and HCV RNAs (**F, G**) from different gradients are regrouped in 3 categories of density and displayed for Jc1 (red) or Jc1_HVRI_H77 (brown) (**D, F**) or H77 (blue) or H77_HVRI_Jc1 (purple) (**E, G**) HCVcc particles.

Figure 7: Lipoproteins and a serum protein are required for lipidation of HCV particles.

(**A, B**) Percentage of infectivity of Jc1 HCVcc particles produced in serum-free medium and incubated for 6h without serum *vs*. with the indicated factors at concentrations equivalent to the 10% HS used here. The data show the results from density-gradient analysis that were regrouped in three categories of density.

Supplementary Figures legends

Figure S1: Serum conditions dictate the density of extracellular HCVcc particles.
Extracellular Jc1 (**A-C**) or H77 (**D-F**) HCVcc particles were produced for 72h in serum-free medium (blue) *vs*. with 10% FCS (green) or 10% HS (red) and layered on density-gradients. The data show representative density-gradient analysis of infectivity (**A, D**), HCV RNA titers (**B, E**) and core concentrations (**C, F**).

Figure S2: Lipidation of HCVcc occurs in the extracellular medium.
Extracellular (**A, B, D, E**) or intracellular (**C, F**) Jc1 (red) or H77 (blue) HCVcc particles produced in serum-free medium were incubated for 6h without serum (full lines) *vs*. 10% FCS (large dotted lines) or 10% HS (small dotted lines) and were layered on density-gradients. The data show representative density-gradient analysis of extracellular infectivity (**A, D**) and HCV RNA titers (**B, E**) and of intracellular infectivity **(C, F)**.

Figure S3: Lipidation increase the specific infectivity of HCV particles.
Extracellular Jc1 (**A**) or H77 (**B**) HCVcc particles produced in serum-free medium were incubated for 6h without serum (blue) *vs*. 10% HS (red). The data show the means specific infectivity determined in fractions from several density-gradient analyses.

Figure S4: Lipidation of secreted HCV particles is time-dependent.
Extracellular Jc1 **(A-C)** or H77 **(D-E)** HCVcc particles produced in serum-free medium were incubated for different times with 10% HS and were layered on density-gradients. The data show representative density-gradient analysis of extracellular infectivity (**A, D**), HCV RNA titers (**B, E**) and core concentrations **(C)**.

Figure S5: Lipidation of secreted HCV particles is dose-dependent.
Extracellular Jc1 HCVcc particles produced in serum-free medium were incubated for 6h with different doses of HS and were layered on density-gradients. The data show representative density-gradient analysis of infectivity (**A**) and HCV RNA titers (**B**).

Figure S6: The HVRI determinant of HCV E2 regulates lipidation of viral particles.
Extracellular Jc1 (red) or Jc1_HVRI_H77 (brown) (**A, B**) H77 (blue) or H77_HVRI_Jc1 (purple) (**C, D**) HCVcc particles produced in serum-free medium were incubated for 6h without serum *vs*. with 10% HS and were layered on density-gradients. The data show representative density-gradient analysis of infectivity (**A, C**) and HCV RNA titers (**B, D**).

Figure S7: Lipoproteins and a protein of serum are required for lipidation of particles.
Quantification of VLDL-, LDL- and HDL-cholesterol contents in HS (red) and FCS (green) samples used in this study **(A)**. Quantification of apoB, human serum albumin (HSA) or apoE in HS, LPDS, and Huh-7.5 cell-conditioned OPTIMEM medium **(B)**. Extracellular Jc1 HCVcc particles produced in serum-free medium were incubated for 6h with the indicated factors and were layered on density-gradients. For each conditions, the boxes represent the densities for which infectivity was found above 20% of total infectivity. The central lines in each box represent the density of the maximum of infectivity **(C)**.

Figure S8: Enzymatic activities of CETP and LCAT are not involved in lipidation of viral particles.
CETP (cholesteryl ester transfer protein) in HS was inhibited with 2µM torcetrapib. Analysis of CETP activity in HS in presence or not of inhibitor for 6h **(A)**. Density-gradient analysis of infectivity of Jc1 or H77 HCVcc extracellular particles produced without serum and incubated 6h with 10% HS in presence or not of torcetrapib **(B)**. LCAT (lecithin-cholesterol acyltransferase) in HS was inhibited with 2mM DNTB. Analysis of LCAT activity, measured as the level of formation of cholesterol ester in presence or not of DNTB (5,5-dithiobis-2-nitrobenzoic acid) **(C)**. Density-gradient analysis of infectivity of Jc1 or H77 HCVcc extracellular particles produced without serum and incubated 6h with 10% HS in presence or not of DNTB **(D)**.

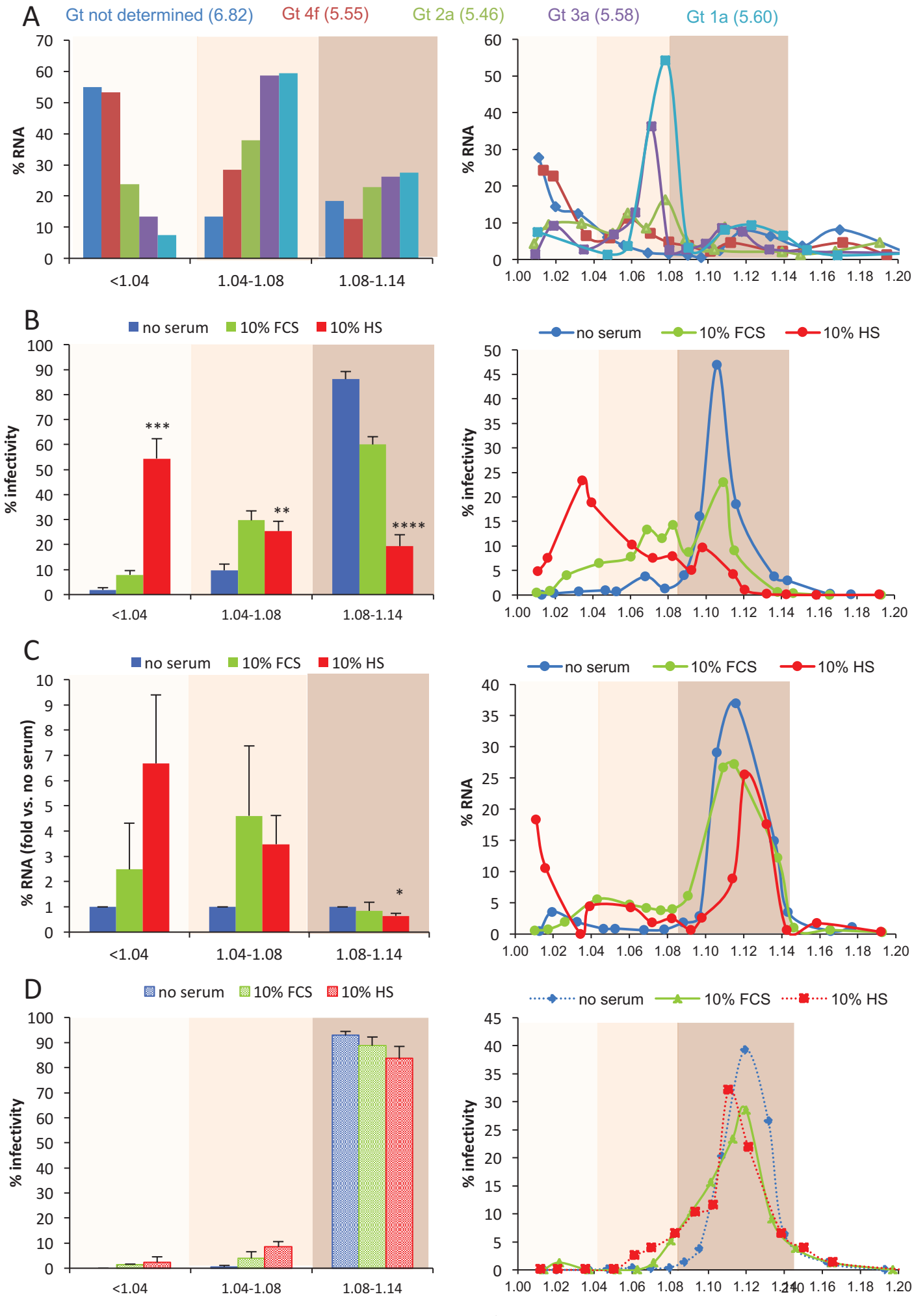
A
Gt not determined (6.82)
Gt 4f (5.55)
Gt 2a (5.46)
Gt 3a (5.58)
Gt 1a (5.60)
% RNA
<1.04
1.04-1.08
1.08-1.14
B
no serum
10% FCS
10% HS
% infectivity
***
**
****
C
% RNA (fold vs. no serum)
*
D

Figure1

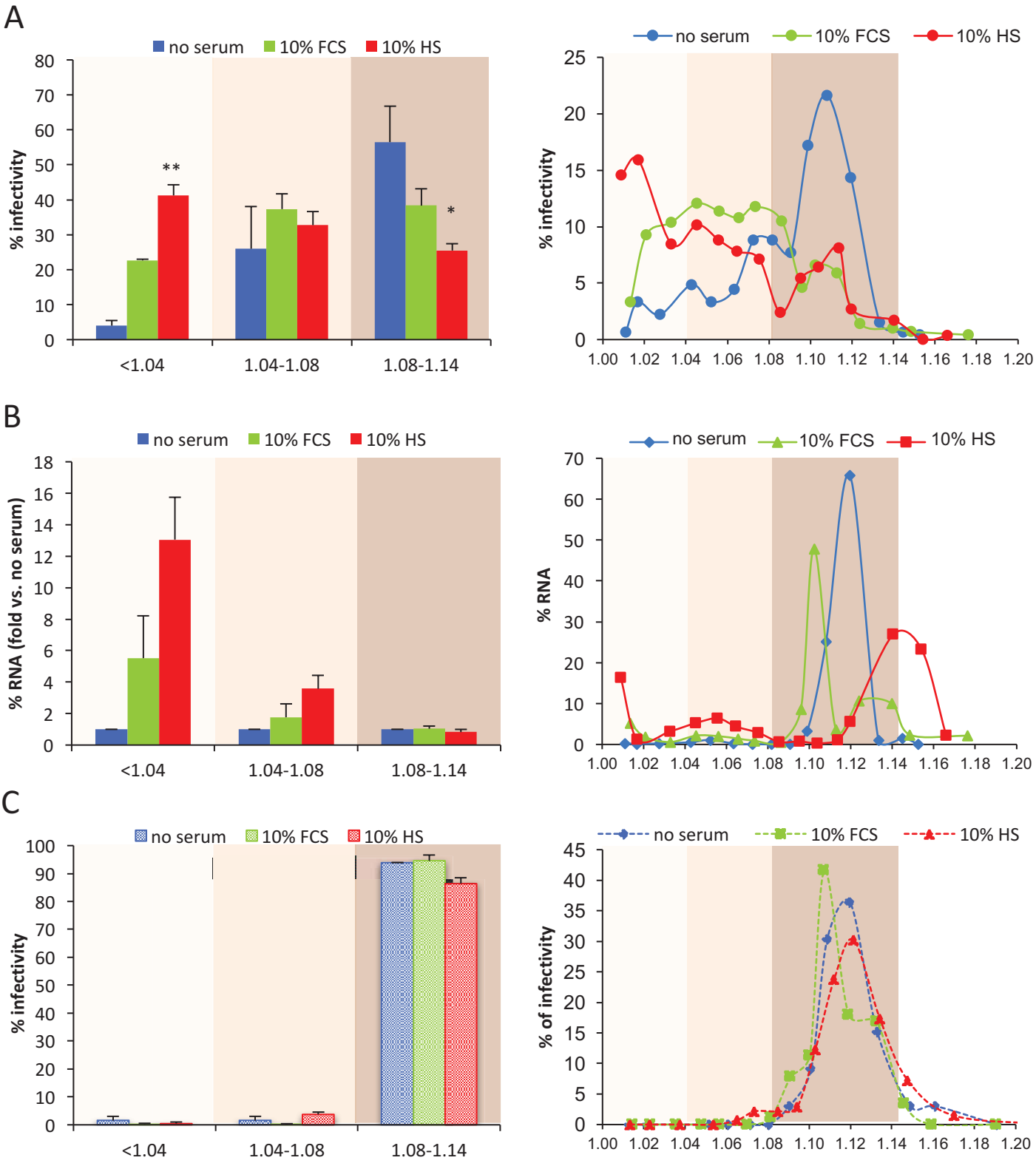
A
no serum
10% FCS
10% HS
% infectivity
**
*
<1.04
1.04-1.08
1.08-1.14
B
% RNA (fold vs. no serum)
% RNA
C
% infectivity
% of infectivity

Figure 2

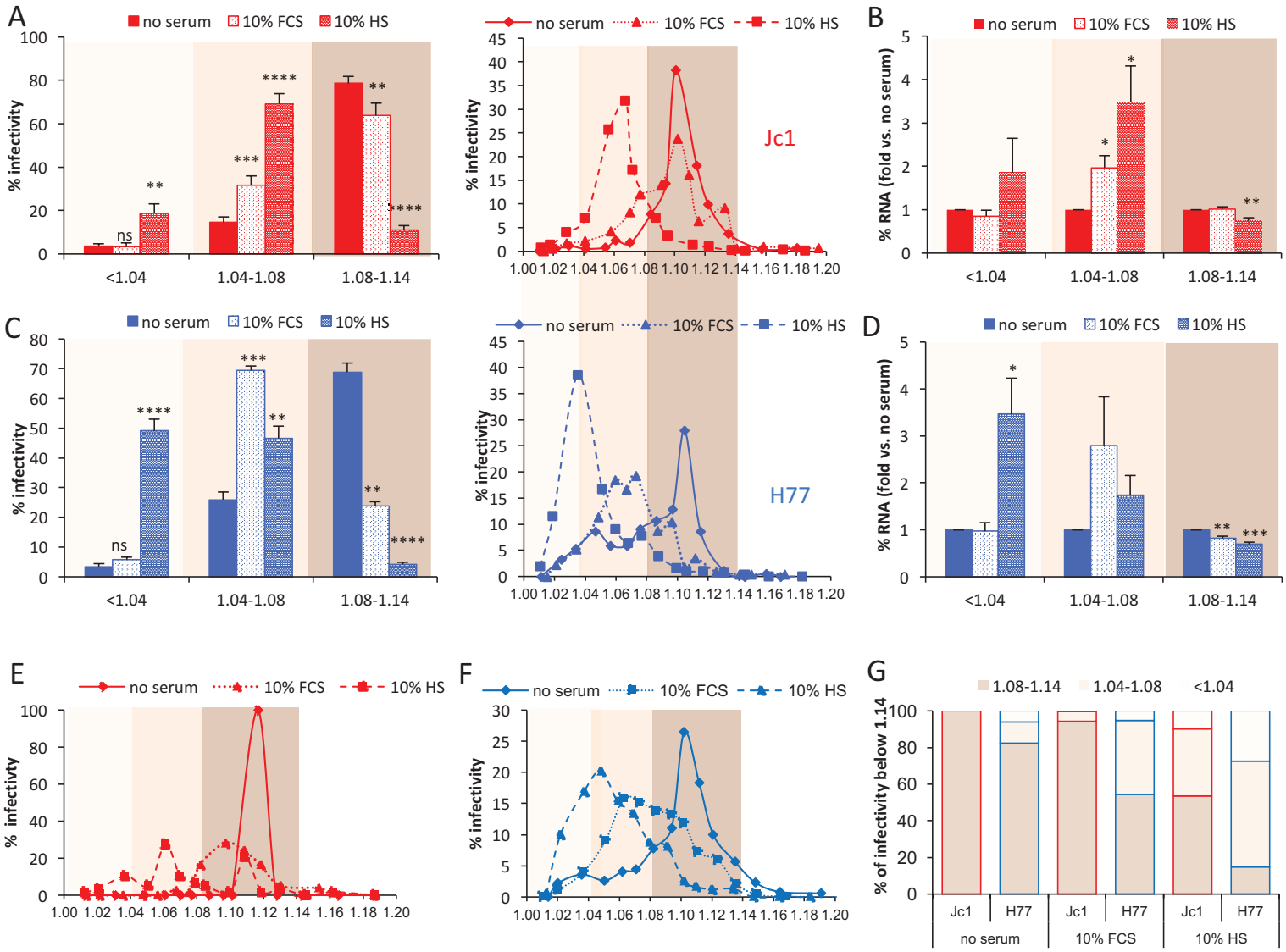
A
no serum
10% FCS
10% HS
% infectivity
ns
**
***
****
**
****
<1.04
1.04-1.08
1.08-1.14
Jc1
1.00 1.02 1.04 1.06 1.08 1.10 1.12 1.14 1.16 1.18 1.20
B
% RNA (fold vs. no serum)
*
*
**
C
H77
D
E
% infectivty
F
G
% of infectivity below 1.14
Jc1
H77
no serum
10% FCS
10% HS

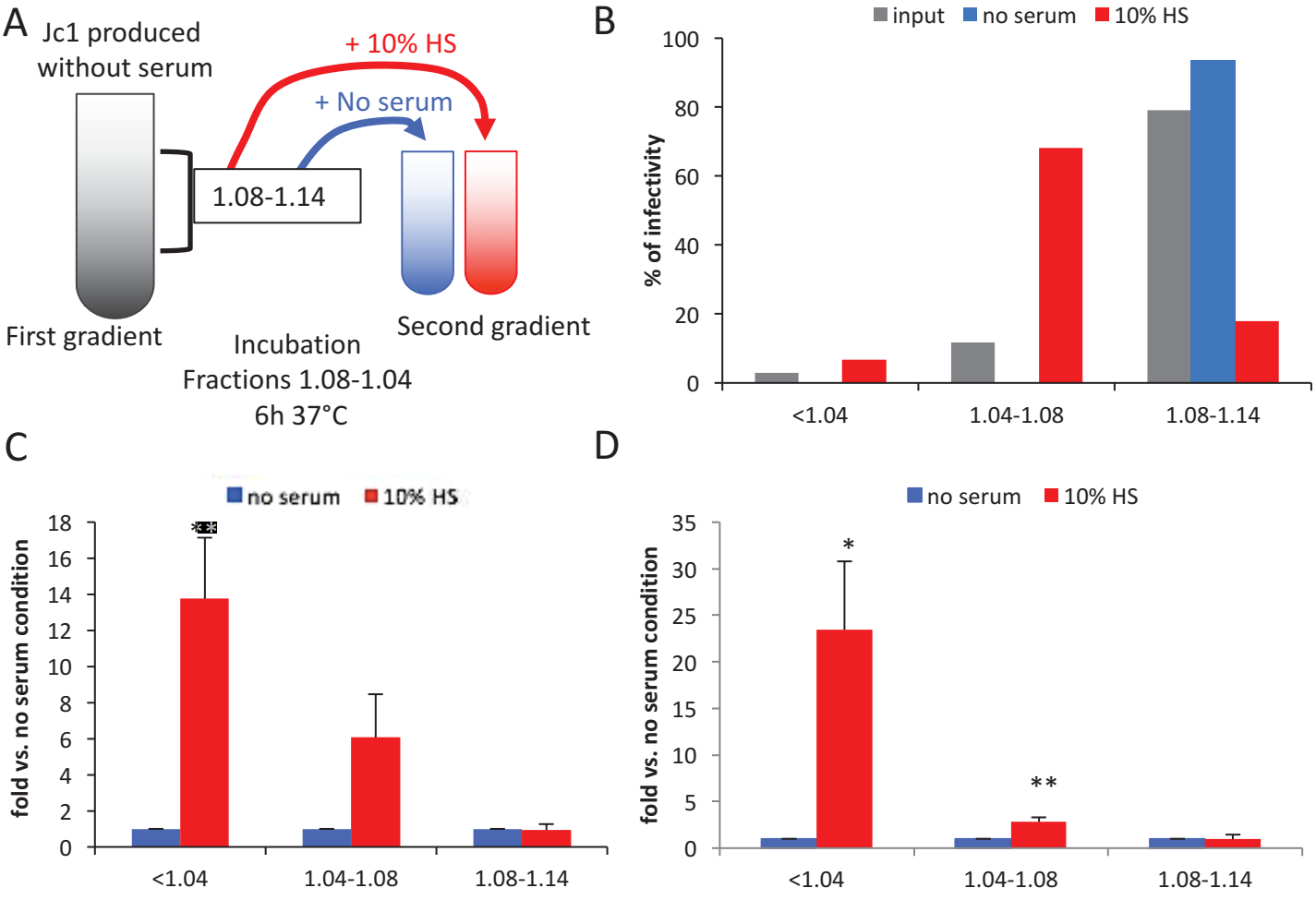
A
Jc1 produced without serum
+ 10% HS
+ No serum
1.08-1.14
First gradient
Incubation
Fractions 1.08-1.04
6h 37°C
Second gradient
B
input
no serum
10% HS
% of infectivity
100
80
60
40
20
0
<1.04
1.04-1.08
1.08-1.14
C
no serum
10% HS
fold vs. no serum condition
18
16
14
12
10
8
6
4
2
0
*
<1.04
1.04-1.08
1.08-1.14
D
no serum
10% HS
fold vs. no serum condition
35
30
25
20
15
10
5
0
*
**
<1.04
1.04-1.08
1.08-1.14

Figure 4

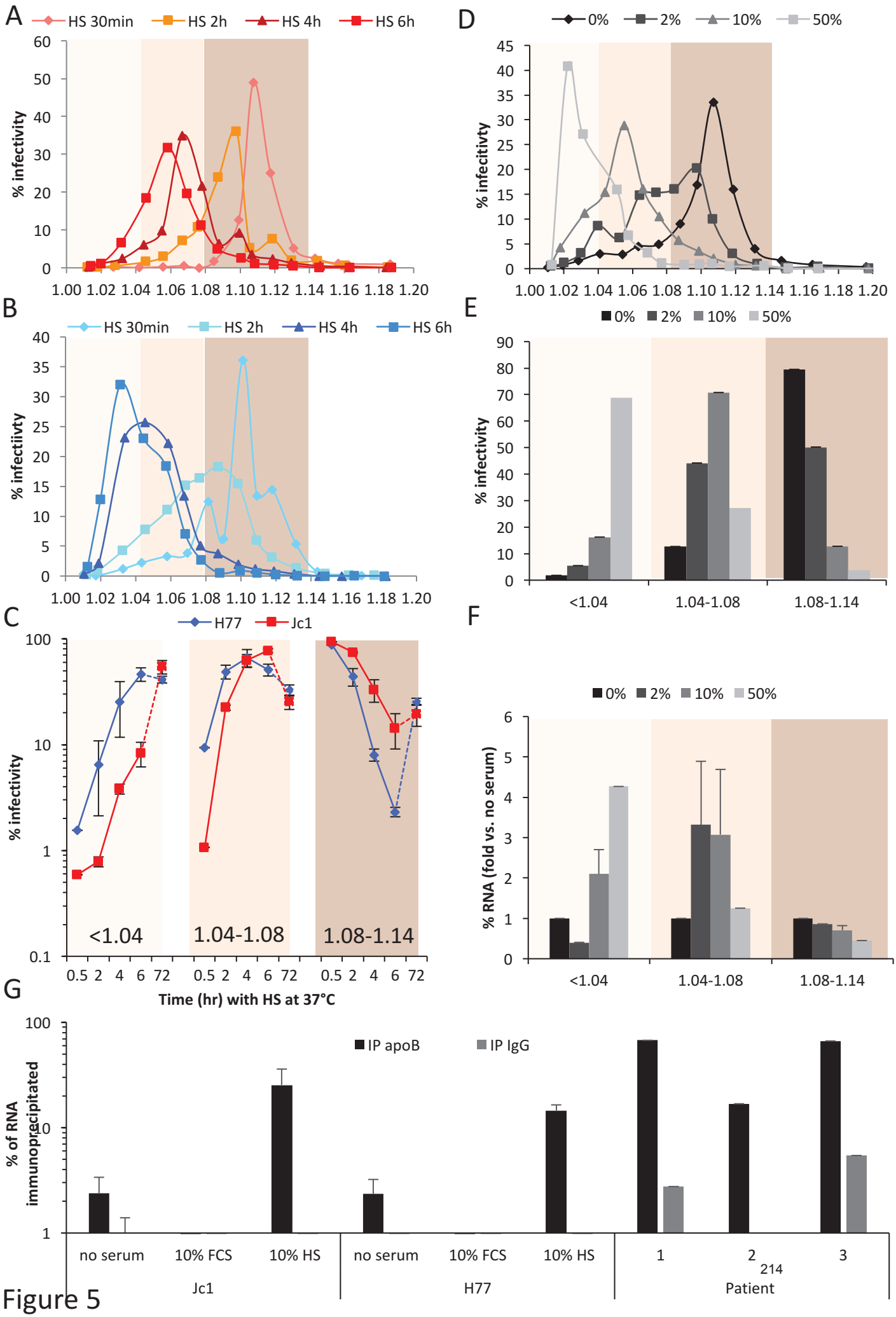
A
HS 30min
HS 2h
HS 4h
HS 6h
% infectivity
B
% infectiivty
C
H77
Jc1
% infectivity
<1.04
1.04-1.08
1.08-1.14
Time (hr) with HS at 37°C
D
0%
2%
10%
50%
% infecitivty
E
% infectivity
F
% RNA (fold vs. no serum)
G
IP apoB
IP IgG
% of RNA immunoprecipitated
no serum
10% FCS
10% HS
Jc1
H77
1
2
3
214
Patient

Figure 5

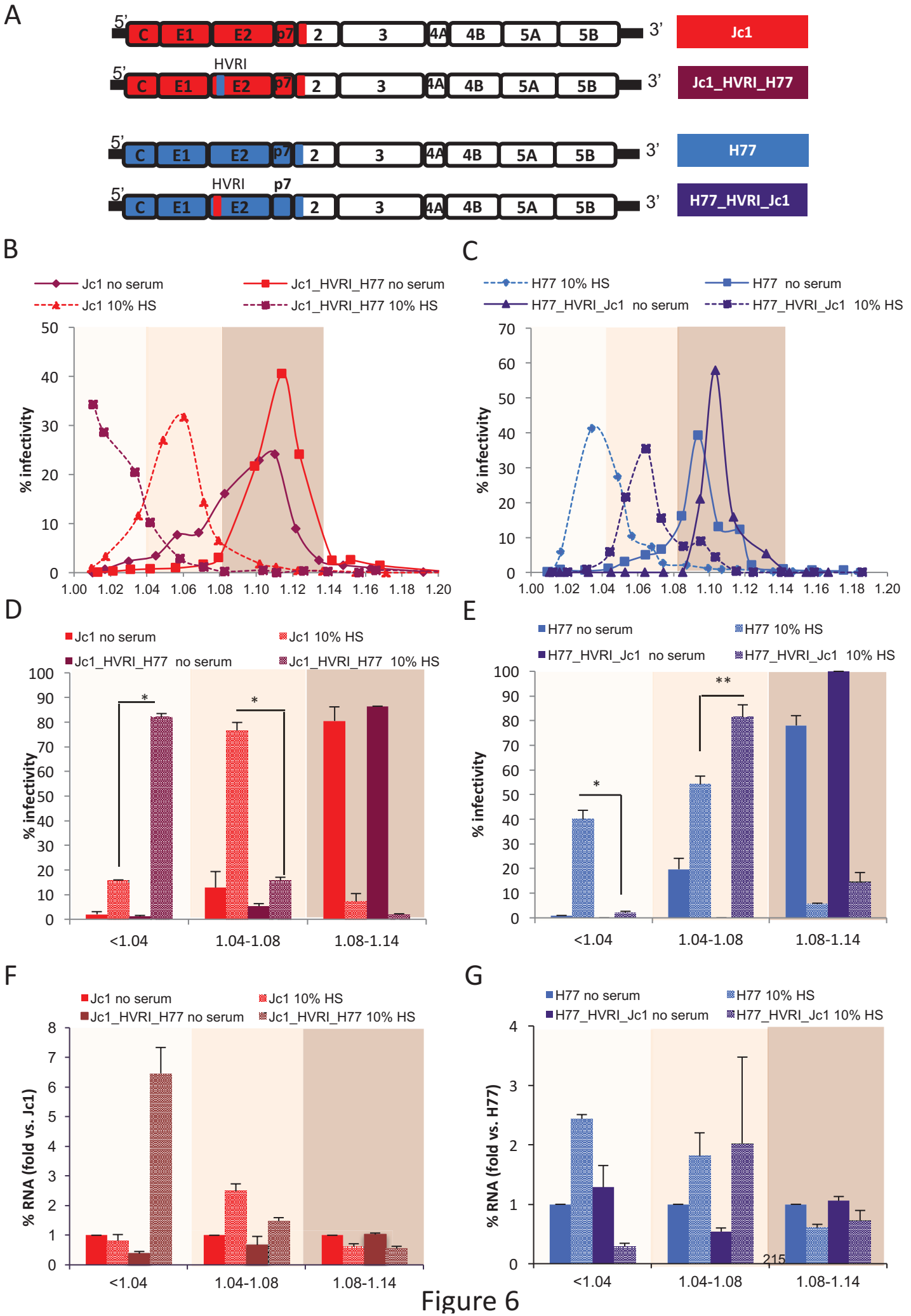
A
5'
C
E1
E2
p7
2
3
4A
4B
5A
5B
3'
Jc1
HVRI
Jc1_HVRI_H77
H77
H77_HVRI_Jc1
B
Jc1 no serum
Jc1_HVRI_H77 no serum
Jc1 10% HS
Jc1_HVRI_H77 10% HS
% infectivity
C
H77 10% HS
H77 no serum
H77_HVRI_Jc1 no serum
H77_HVRI_Jc1 10% HS
D
Jc1_HVRI_H77 no serum
Jc1_HVRI_H77 10% HS
<1.04
1.04-1.08
1.08-1.14
E
H77 no serum
H77 10% HS
F
% RNA (fold vs. Jc1)
G
% RNA (fold vs. H77)
215

Figure 6

A

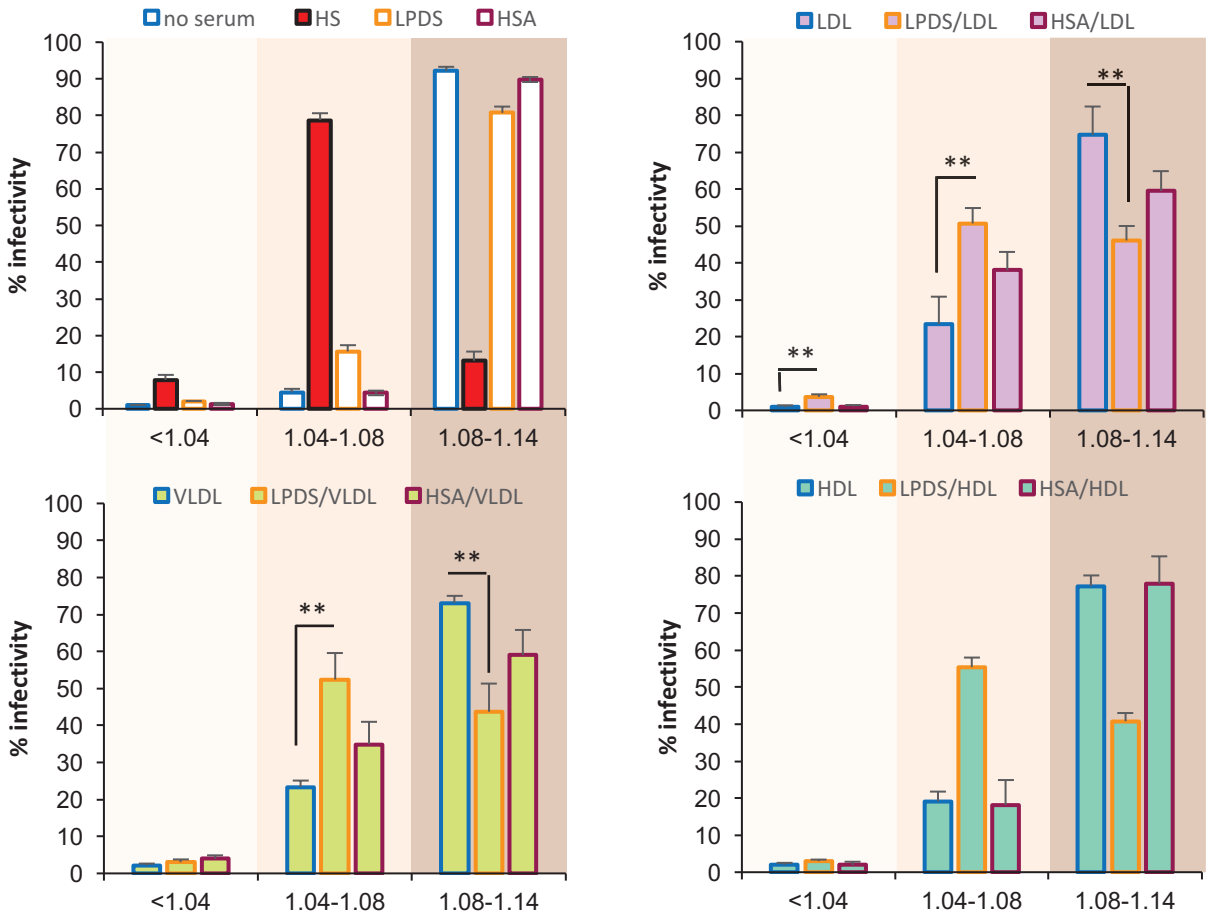
no serum
HS
LPDS
HSA
% infectivity
<1.04
1.04-1.08
1.08-1.14
LDL
LPDS/LDL
HSA/LDL
**
VLDL
LPDS/VLDL
HSA/VLDL
HDL
LPDS/HDL
HSA/HDL

B

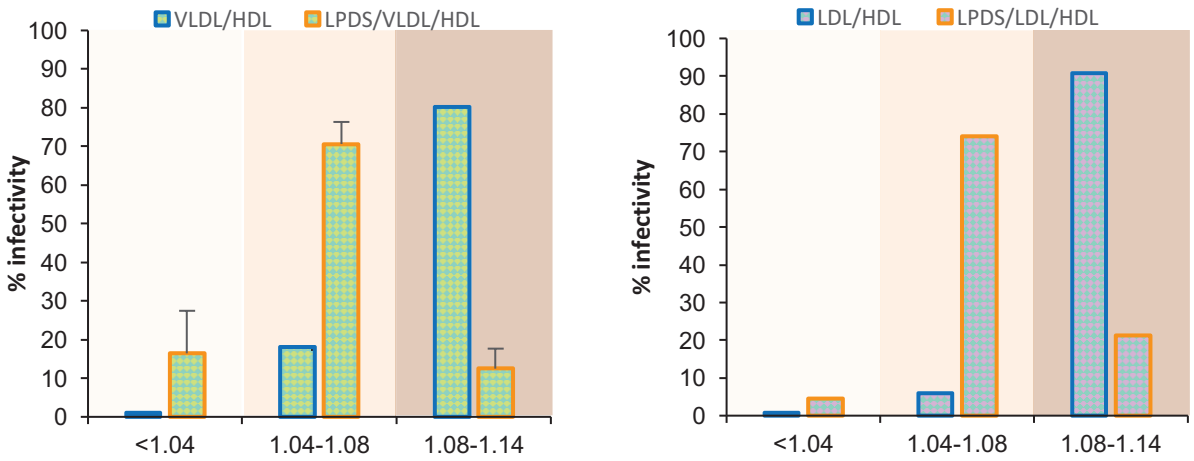
VLDL/HDL
LPDS/VLDL/HDL
LDL/HDL
LPDS/LDL/HDL
% infectivity
<1.04
1.04-1.08
1.08-1.14

Figure 7

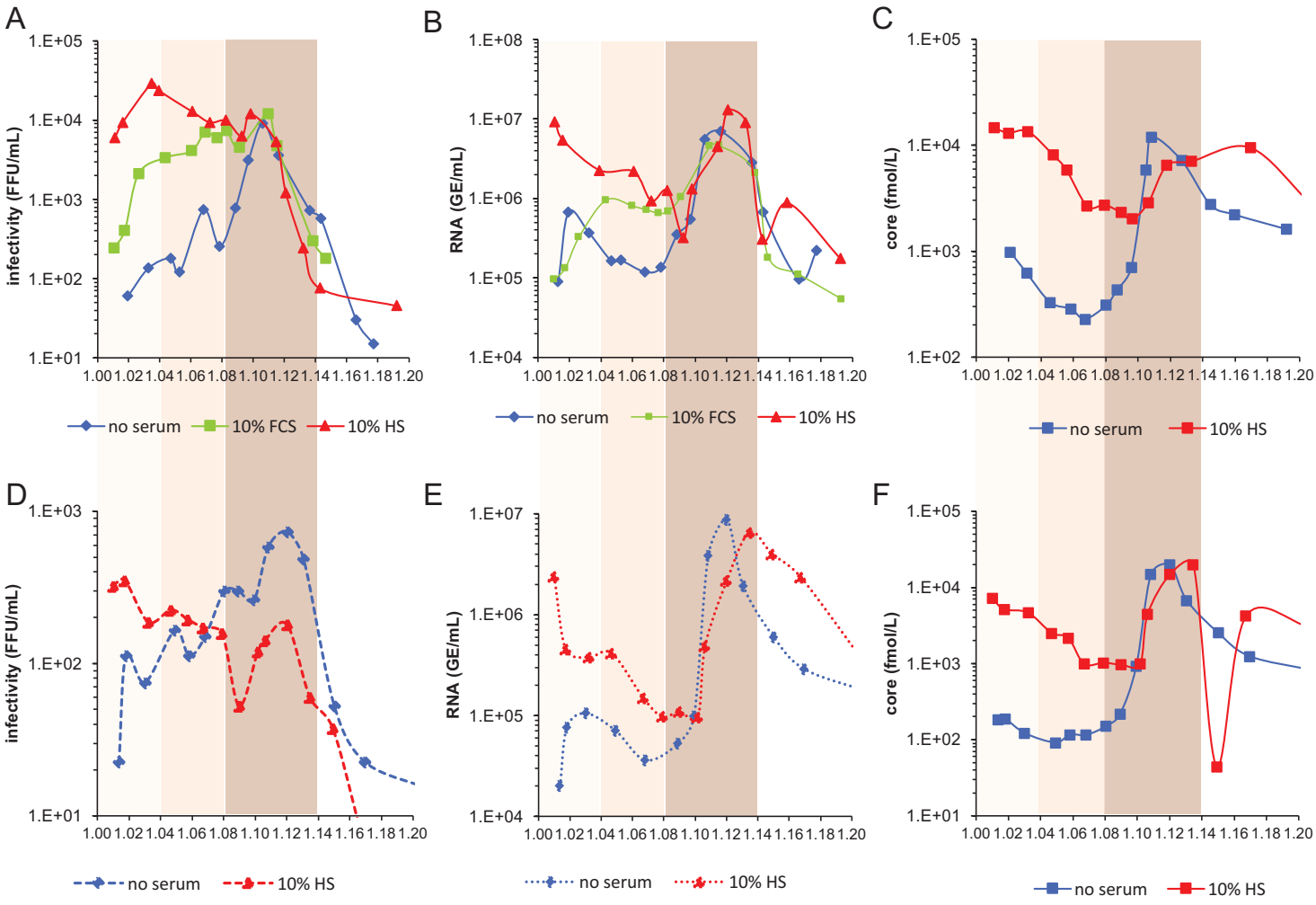

Supplementary Figure 1

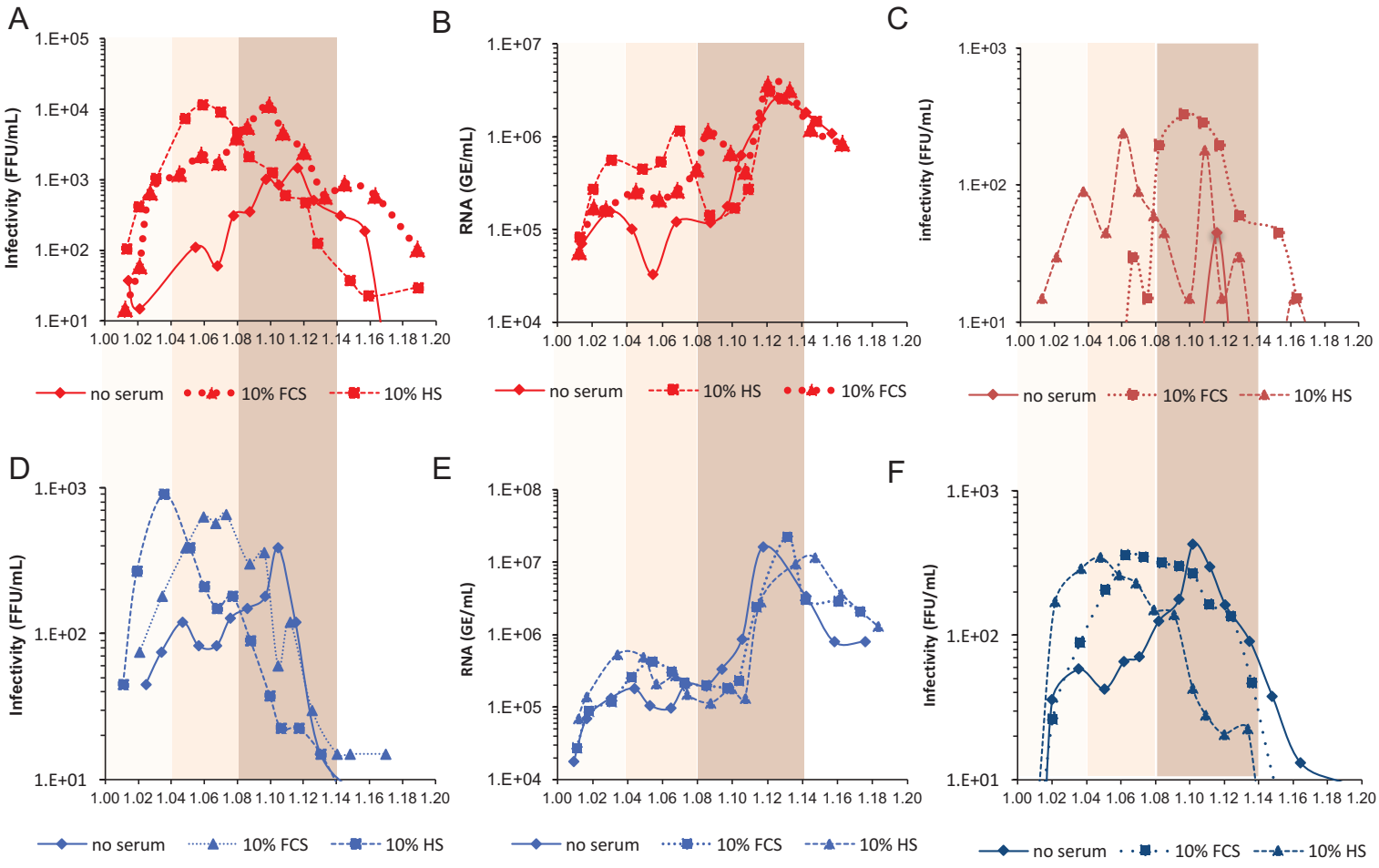

Supplementary Figure 2

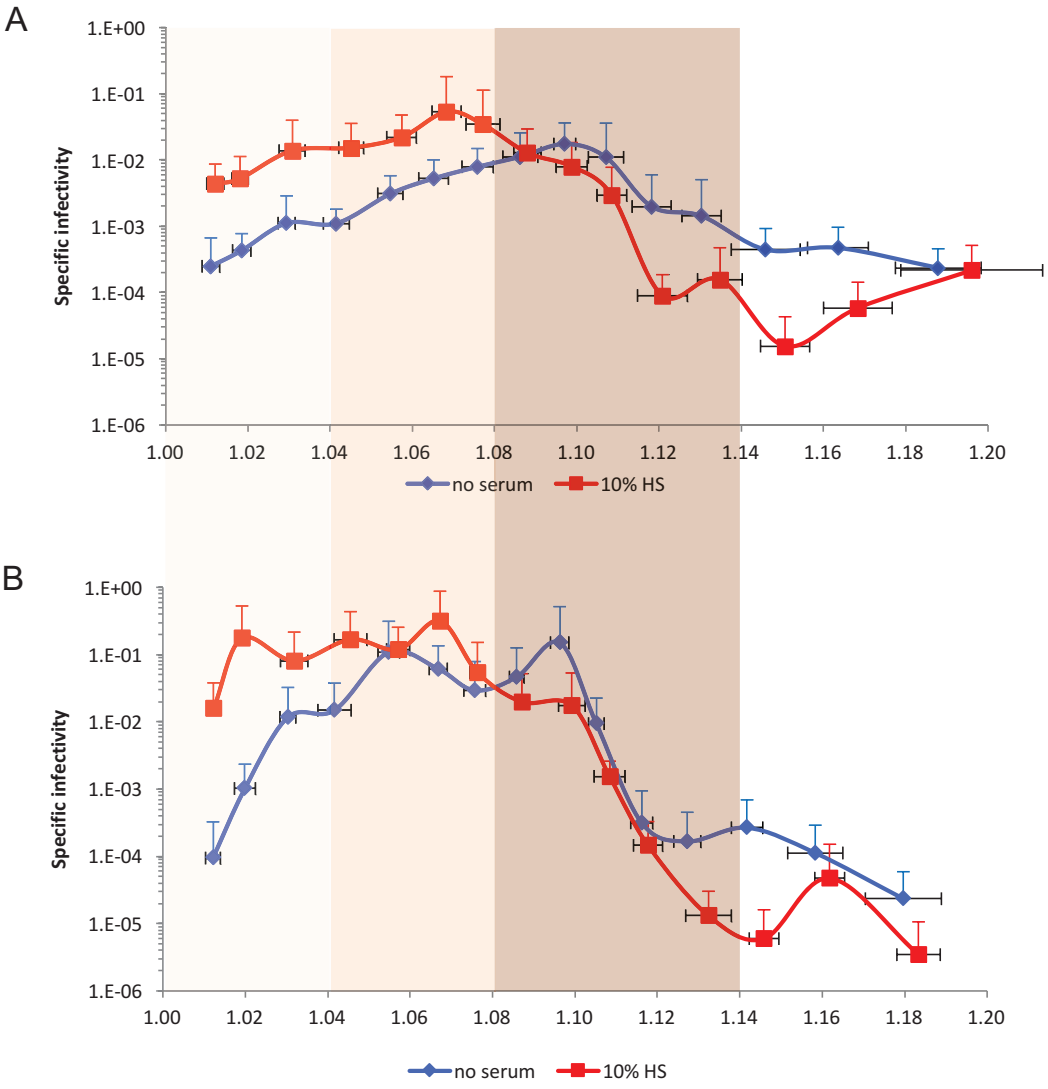

Supplementary Figure 3

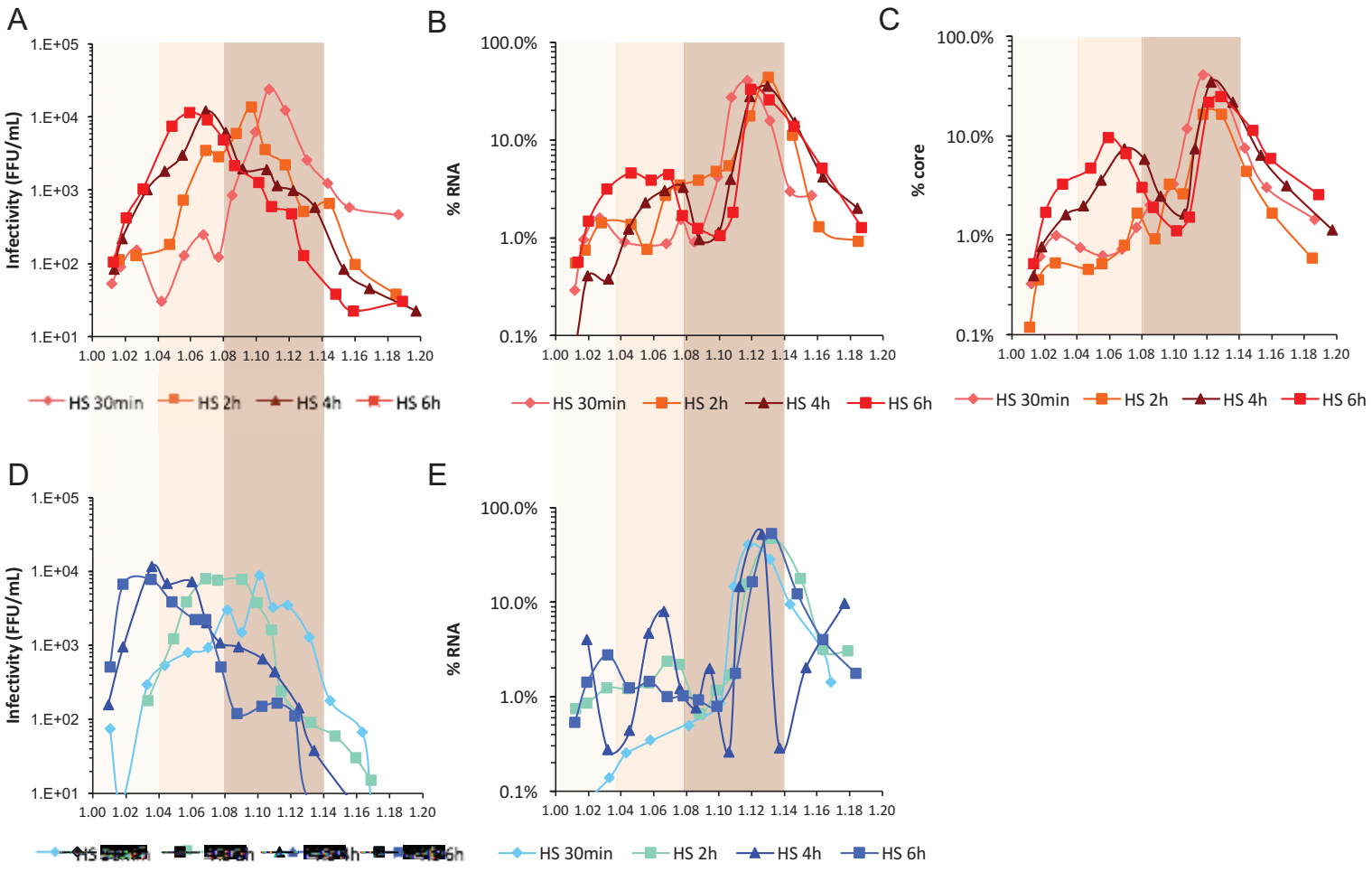

Supplementary Figure 4

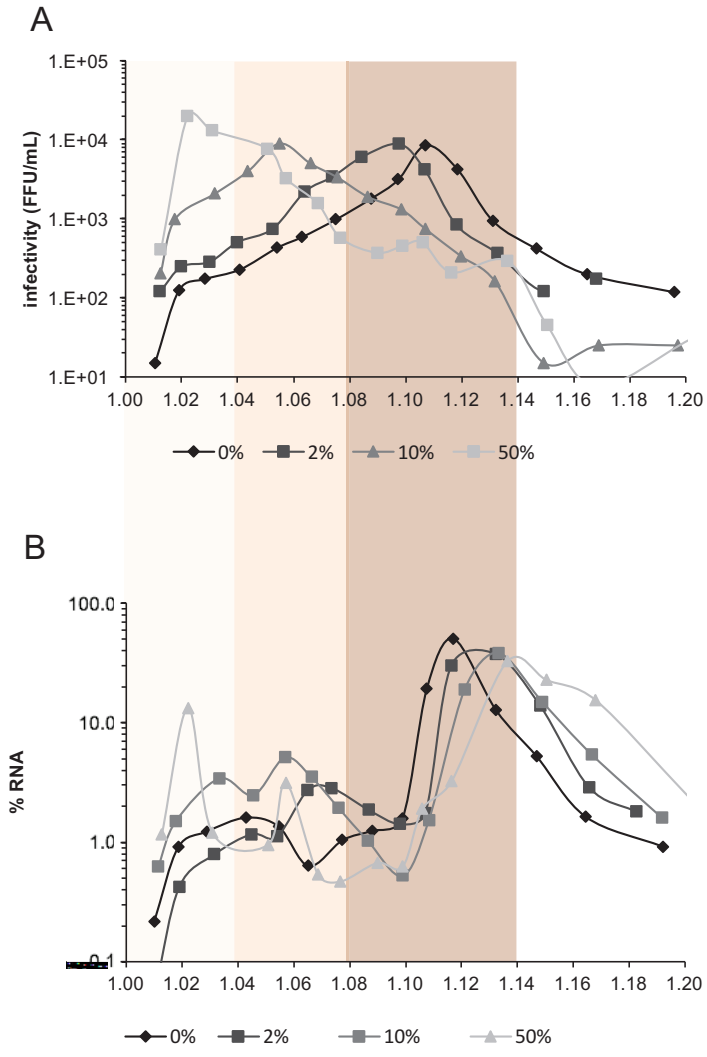

Supplementary Figure 5

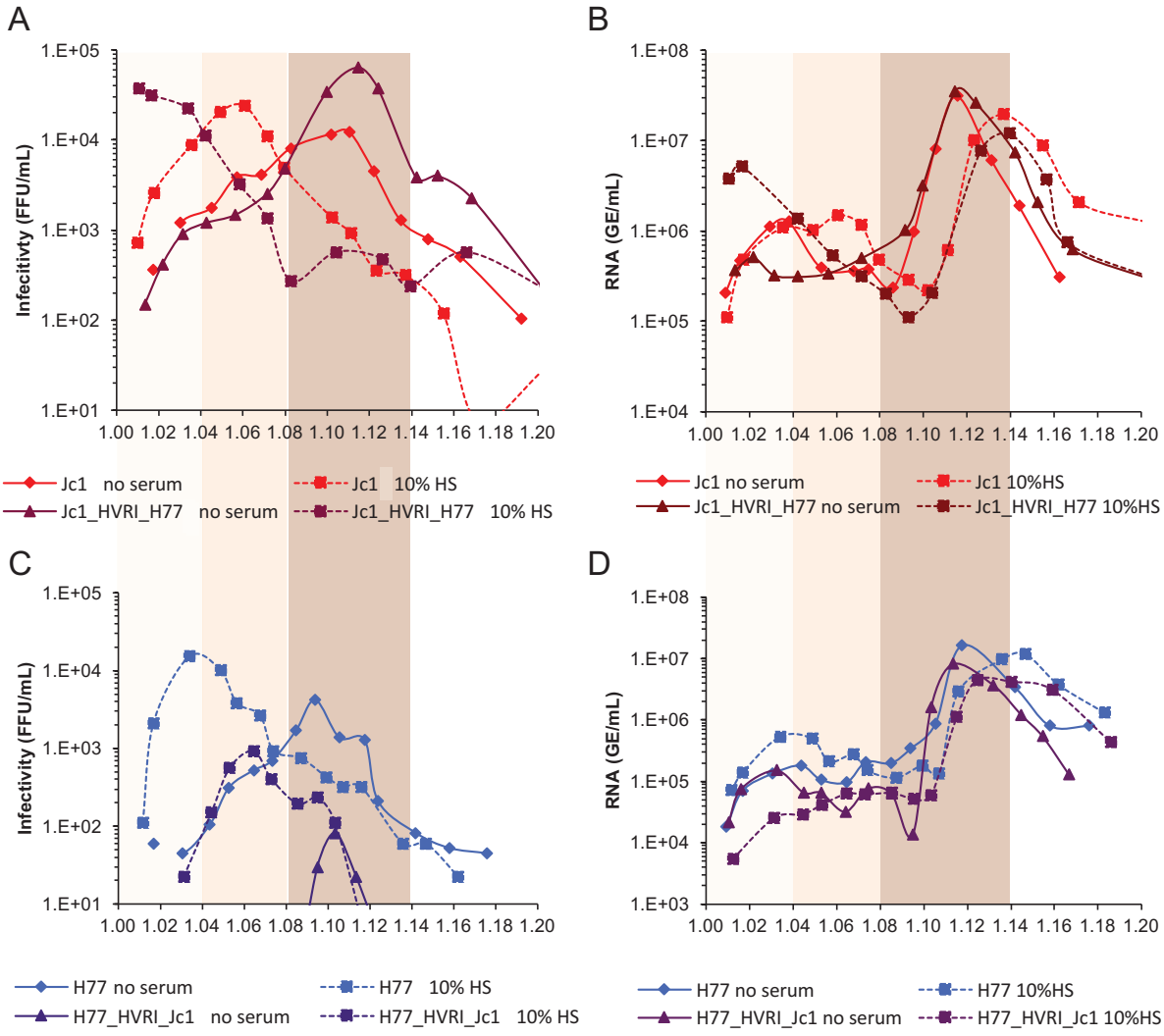

Supplementary Figure 6

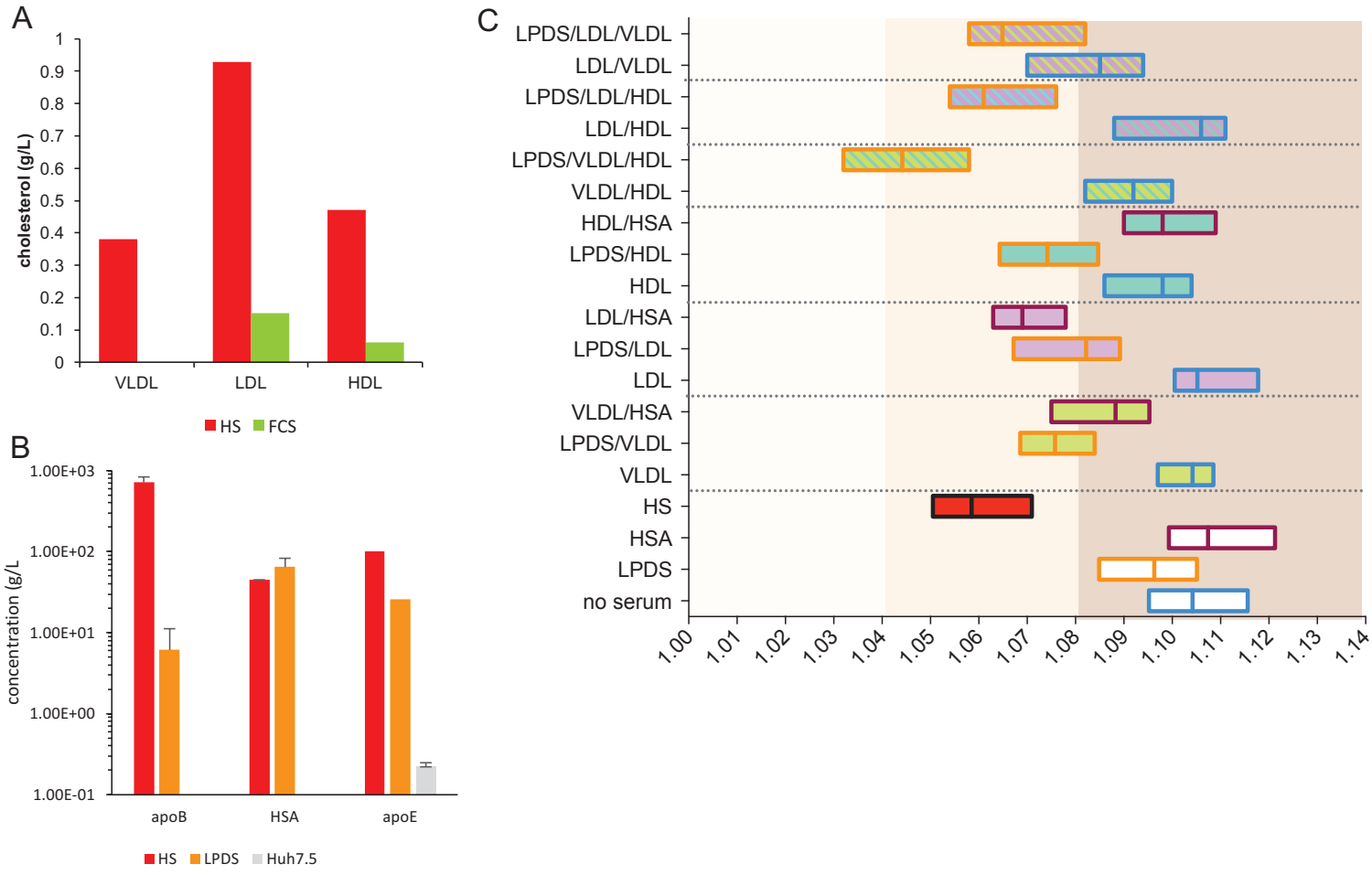

Supplementary Figure 7

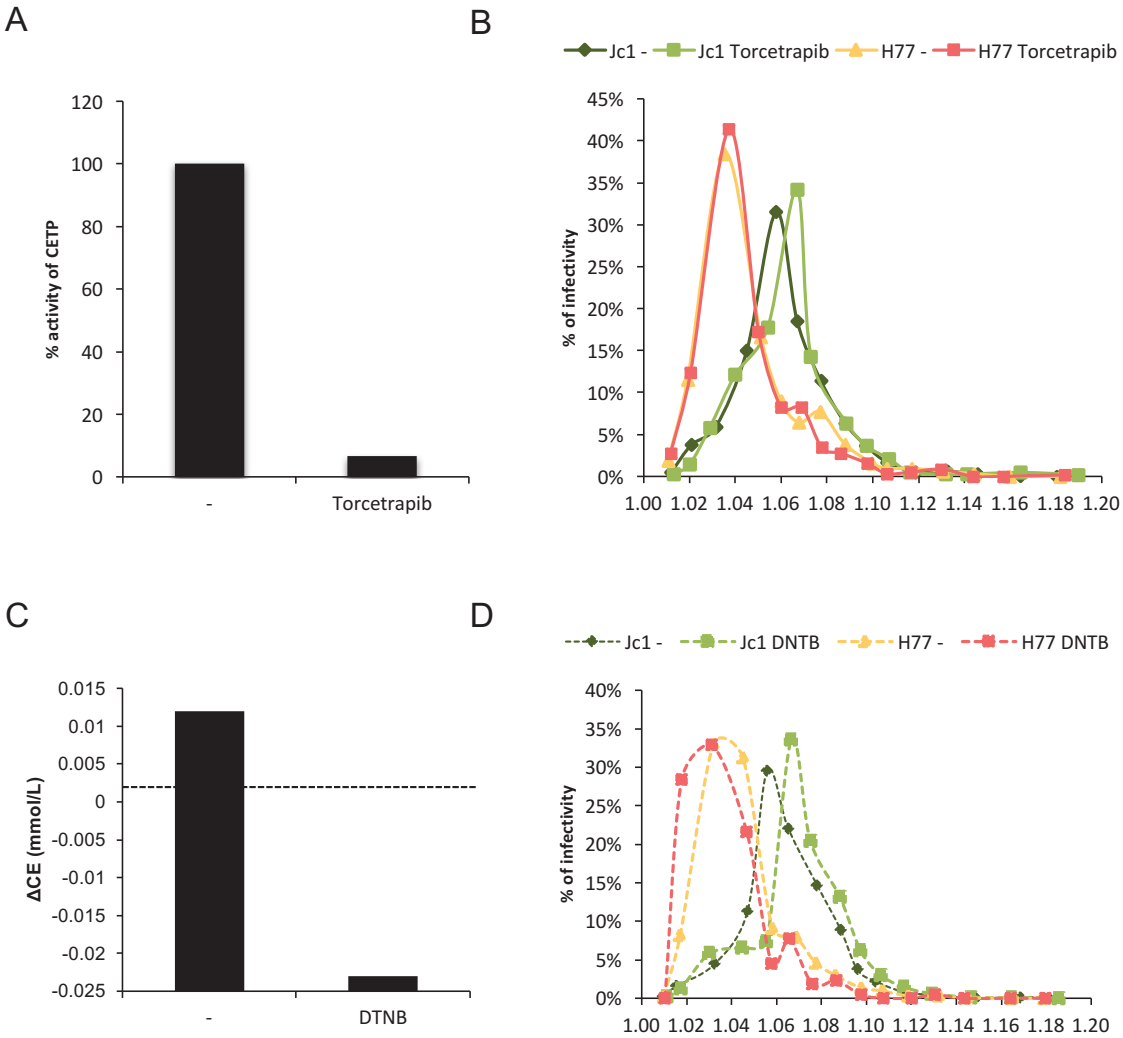

Supplementary Figure 8

CONCLUSIONS & PERSPECTIVES

The work of my PhD thesis has mainly focused on the mechanisms of assembly of HCV particles. A major interest of my projects has concerned the study of the role of p7 in these events. The HCV p7 protein, known as a viroporin (see part IV in Introduction section of this document), is a pleiotropic viral factor that plays a role at different steps of the early and late stages of the viral cycle as summarized below (Figure 46).

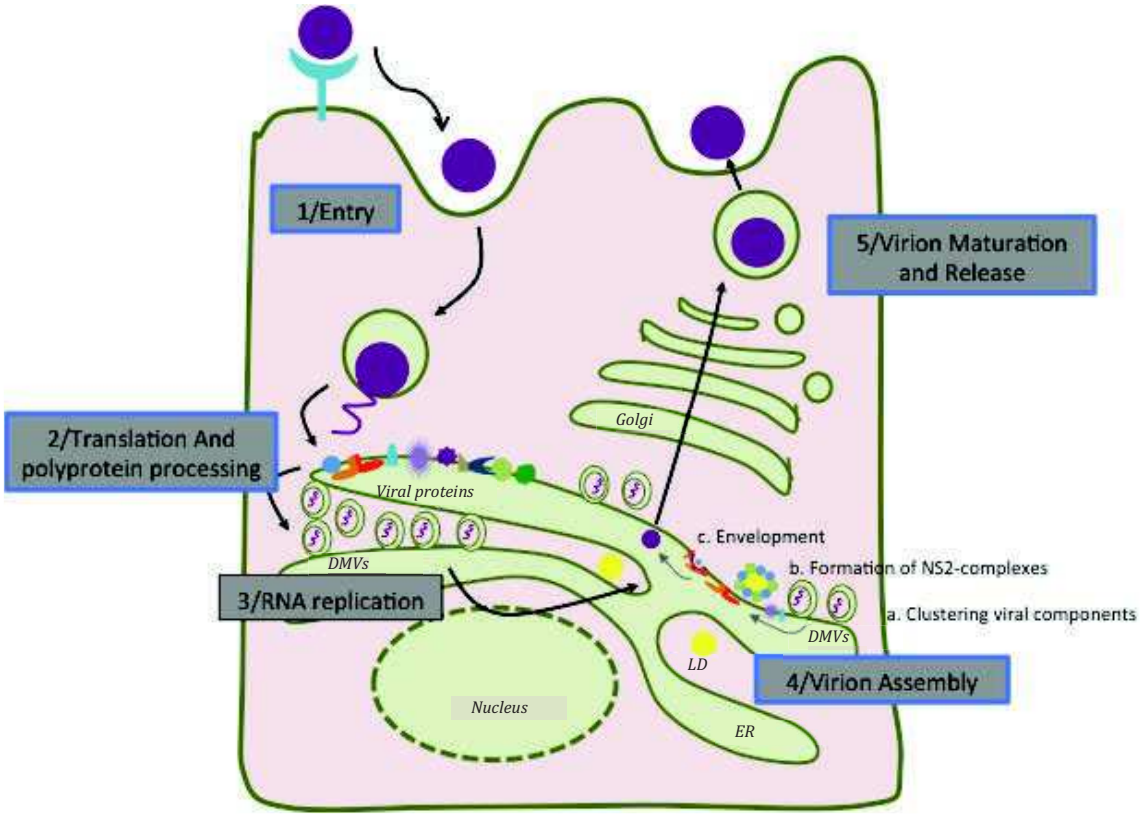

Figure 47. Involvement of p7 in HCV life cycle. Viral particle in violet enter the cell through receptors binding followed by endocytosis and fusion of viral membrane with endosomal membrane. Viral genome is then translated in a polyprotein that is then matured in ten proteins. Viral replication occurs in double membrane vesicles (DMV) closed to ER membrane. Assembly occurs in the ER lumen closed to lipid droplets (LD) and DMV. Finally, particles are secreted outside the cells. In blue, the steps in which p7 could be involved.

Some indirect results reported a possible role of p7 in HCV entry (figure 47 (1)) by acting at the surface of viral particles (Griffin et al., 2008) like for the M2 viroporin of influenza virus (reviewed in (Manzoor et al., 2017)). However, the involvement of p7 in HCV entry remains controversial since there is no evidence for the presence of p7 in particles from proteomics analysis of HCV particles (Lussignol et al., 2016) or from attempts to neutralize infectivity of a virus encoding a tagged p7 (Vieyres et al., 2013).
On our side, we highlighted that p7 and its E2p7 precursor are involved in the regulation of the level of expression of E2 (2). This is discussed in part II below.
Major functions of p7 reside at the level of assembly of infectious particles (figure 47 (4)). First, a previous study of our laboratory indicated that p7 is involved in the regulation of the localization of core at the ER membrane *vs.* the lipid droplet (LD) (Boson et al., 2011). This event might represent a starting point for initiation of the clustering of viral structural proteins with non-structural proteins, which reflects the functional connection of assembly sites with replication complexes (4a). We found that

these events are inhibited by some NS5A inhibitors such as daclatasvir, as discussed in part IV. Second, p7 is required to allow and/or modulate the formation and localization of NS2-based complexes (4b), a key event for assembly of viral particles that promotes the recruitment of E1E2 glycoproteins with nucleocapsids components at specific sites of the ER (Ma et al., 2011, Shanmugam & Yi, 2013, Stapleford & Lindenbach, 2011). Third, complementing previous results of others (Gentzsch et al., 2013), we also detailed the involvement of p7 in envelopment and scission of particles (4c). These latter events, *i.e*., p7-regulation of viral particle formation and its envelopment, are discussed in part I.
Regarding the late steps of HCV life cycle, p7 also seems to act in virion maturation and release (figure 47 (5)). Indeed, previous reports indicated that p7 is involved in secretion of HCV particles (Bentham et al., 2013, Steinmann et al., 2007) as well as in cell-cell transmission (Meredith et al., 2013), though the mechanisms still remain poorly-defined. It was also proposed that p7 could modulate the sensitivity of infectious particles to acid pH in a HCV strain-dependent manner, hence preventing premature activation of membrane fusion (Atkins et al., 2014). Here, we showed that p7 regulates the cell secretory pathway, which could facilitate the assembly and secretion of HCV particles, but also help preventing the activation of immune pathways, as discussed in part III.
Finally, the secretion of HCV particles is still poorly defined and has been linked to the acquisition of lipids concomitantly to their assembly and maturation (reviewed in (Lavie & Dubuisson, 2017). Thus, a part of my work has also focused on the lipidation mechanisms of particles, as discussed in parts V and VI.

I- New insights in the model of HCV assembly

In a joint study with Bertrand Boson of our team, we focused our efforts on the unravelling of the mechanisms allowing the clustering of viral components (Figure 47; 4a), which are key to functionally connect HCV RNA replication to formation of the viral nucleocapsid. Indeed, viral RNAs need to be exported from their site of synthesis, *i.e.,* the replication complexes, and imported to the assembly sites in order to form infectious particles. In the case of HCV, NS5A is a major protein involved in this connection between replication and assembly (Zayas et al., 2016); it is an RNA-binding protein (Foster et al., 2010, Huang et al., 2005) and it is able to interact with core (Appel et al., 2008, Masaki et al., 2008). As shown in part I of the Results section of this document, we found that the core and E2 structural proteins, in association with viral RNAs, co-cluster with some non-structural proteins, including NS5A and NS4B; hence indicating the close proximity of assembly sites and replication complexes. In addition, we showed that these clusters localize close to lipid droplets. Finally, through the use of an inhibitor of NS5A, we found that this protein is the main viral factor involved in the transfer of viral RNA to assembly sites. Note that these considerations are further discussed (see part IV below).

The second part of the Results section of this document addressed later steps of HCV assembly, *i.e.*, post-clustering of non-structural and structural HCV assembly components. We showed how p7, through its amino-terminal extremity, regulates critical interactions allowing virion formation, which were previously described to engage cross-talks between NS2 and NS3, NS5A and/or E1E2 (Jirasko et al., 2010, Ma et al., 2011, Popescu et al., 2011, Shanmugam & Yi, 2013, Stapleford & Lindenbach, 2011). Indeed, NS2 complexes are thought to act as a platform for HCV assembly, likely by allowing the connection of the virion surface glycoproteins, E1 and E2, with core and RNA. Since NS5A is able to interact with core and viral RNA (Tellinghuisen et al., 2008b), p7 might modulate the encountering of the nucleocapsid with E1E2 and then the envelopment and scission of particles. We identified some mutations, named p7 ATMI (Amino-Terminus Membrane Interface) mutants, abrogating NS2/NS5A interactions. The resulting virus mutant genomes are defective for transmission of infectivity owing to decreased secretion of core and RNA and to increased secretion of non/partially-enveloped particles. Overall, these results led us to extend and provide molecular details on the current model of HCV assembly (Dubuisson & Cosset, 2014). As shown in Figure 48, which is derived from the contributions of several others groups (Dubuisson & Cosset, 2014), we propose the following revisions of the HCV assembly steps, on the basis of our experimental results.

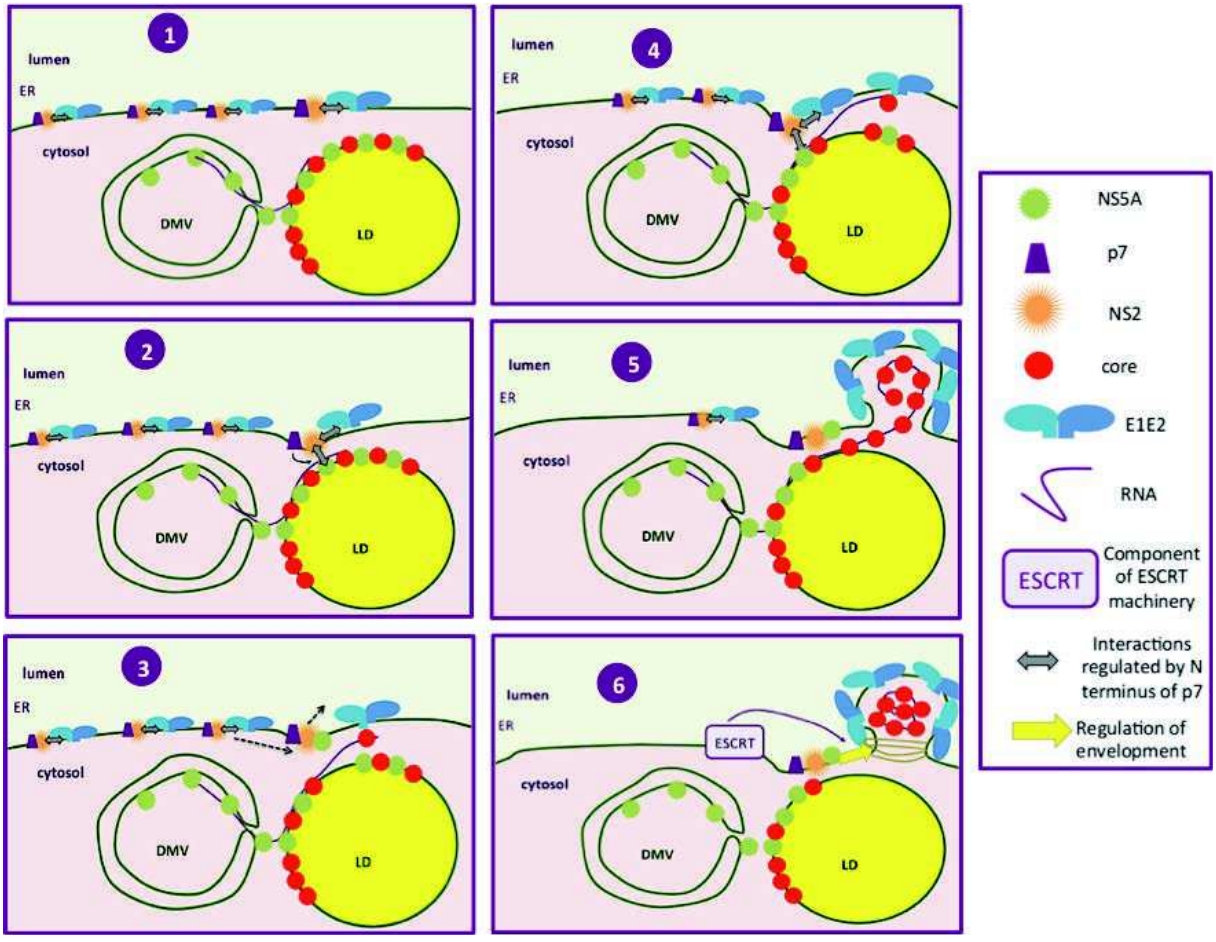

Figure 48: Proposition for a revised model of HCV assembly. See the text for more details.

(**1**) HCV assembly takes place at the ER membrane close to HCV replication complexes-containing double membrane vesicles (DMV) and to cytosolic lipid droplets (LD) harboring core and NS5A at their surface (Appel et al., 2008, Masaki et al., 2008, Miyanari et al., 2007). The DMV is represented separated from the ER membrane for sake of clarity but the same mechanism could occur with DMVs attached to the ER membrane. Upon translation of the HCV genome, E1E2p7NS2 complexes form and accumulate at the ER membrane (Jirasko et al., 2010, Ma et al., 2011, Popescu et al., 2011, Shanmugam et al., 2015, Shanmugam & Yi, 2013).
(**2**) p7, *via* its N-terminal extremity, regulates (thin grey arrow) the interaction of NS2 with NS5A (large grey arrow).
(**3**) This interaction may allow the release of E1E2 glycoproteins from E1E2p7NS2 complexes at the assembly site of nascent viral particles, on the one hand, and the co-recruitment of core and RNA to E1E2 glycoproteins, on the other hand. This switch of interactions could be the result of a conformational change of NS2 mediated by p7. Subsequently, the E1E2-free p7NS2NS5A complex leaves the assembly area whereas a new E1E2p7NS2 complex reaches this site (dotted arrows).
(**4**) The process is reiterated with p7 from incoming E1E2p7NS2 complexes regulating the encountering of NS2 and NS5A, which leads to the further release of E1E2 and core/RNA that accumulate at the assembly site.
(**5**) The process is repeated until the formation of a viral particle that buds in the ER lumen.
(**6**) The NS2NS5A complex, regulated by p7, may recruit ESCRT components to induce scission of the nascent particle until full envelopment and egress. Supporting this hypothesis, it was shown that ESCRT proteins modulate HCV assembly (see part V.1.2.1 in Introduction) and, more specifically, that NS2 and NS5A could interact with HRS, a member of ESCRT-0 complex (Barouch-Bentov et al., 2016).

Note that according to this model and unlike the current topological model of p7 (Carrere-Kremer et al., 2002), the p7 amino-terminus would need to be positioned at an interface of the p7 hexamer that faces NS5A, with p7 second transmembrane apposed to that of NS2, as proposed elsewhere (Cook et al., 2013). Disruption of this interface, like with the amino-terminal extensions of p7 ATMI mutants described in our work, would tend to disrupt an interaction of the E1E2p7NS2 complexes with NS5A, RNA and core, which would explain the reduced secretion of viral particles (Denolly et al., 2017). While it remains difficult to experimentally prove such a cytosolic orientation of wt p7, owing to the lack of suitable antibodies, our results of mutant p7 topology obtained with differential membrane permeabilization of cells expressing p7 ATMI mutants unambiguously show that either expressed alone or in the context of the HCV polyprotein, at least a part of such modified p7 may adopt this topology. This is also consistent with previous results (Isherwood & Patel, 2005) .

It remains intriguing why a large part of the viral particles released by these p7 ATMI mutants seem partially enveloped, as indicated by their increased susceptibility to

protease K digestion. This suggests that p7 could participate to a complex that recruits a cellular pathway of scission, such as the ESCRT pathway as proposed by other groups (Ariumi et al., 2011, Barouch-Bentov et al., 2016, Corless et al., 2010, Tamai et al., 2012). Specifically, several HCV proteins were shown to interact with HRS (Barouch-Bentov et al., 2016) the primary component of the ESCRT complexes that induces scission of several types of vesicles and that is exploited by numerous virus types to induce envelopment of their particles. Of note, p7 was shown to interact with HRS in a complementation assay (Barouch-Bentov et al., 2016), *i.e., via* expression of single proteins fused with fragment of luciferase allowing its luminescence activity only when the two fragments are in close proximity. These data, indicating an interaction between the two proteins, are also consistent with a cytosolic orientation of its amino-terminal end. Further investigations are required to investigate the role of the HCV proteins in the activation of the ESCRT pathway.
Another possibility could be the direct involvement of p7 in scission itself. Indeed, a recent study indicated that p7 could mediate membrane-membrane adhesion (Lee et al., 2016). Thus, since the M2 viroporin of avian influenza virus (AIV) was shown to mediate the scission of infectious influenza particles(Rossman et al., 2010) through a mechanisms involving membrane-membrane adhesion (Figure 49), it is therefore possible to imagine a similar mechanism for HCV envelopment.

Both hypothesis, *i.e.*, activation of the ESCRT pathway and direct scission mechanism, are highly interesting to explore and we are currently trying to get more details on the mechanisms of scission and envelopment.
As for the possibility that p7 and other non-structural proteins could induce the recruitment of the ESCRT complex (Barouch-Bentov et al., 2016), we propose to investigate the effect of the down-regulation of ESCRT proteins such as HRS in the quality of envelopment of viral particles, as measured by the protection of core to proteinase K digestion in the same way we did with our p7 ATMI mutants (Denolly et al., 2017) .
Another aspect of the HCV assembly process that remains not fully understood is the involvement of cellular proteins in the clustering of viral proteins and the transfer of viral RNA from replication complexes to assembly sites. Indeed, several factors have been already described for their involvement of HCV assembly such as *e.g.*, DGAT1, Rab proteins (see part V.2 in Introduction Section); yet, their precise role remains poorly described. Thus, we are currently studying the effect of down-regulation of some of these factors in the clustering of core, E2 and NS5A or NS4B.

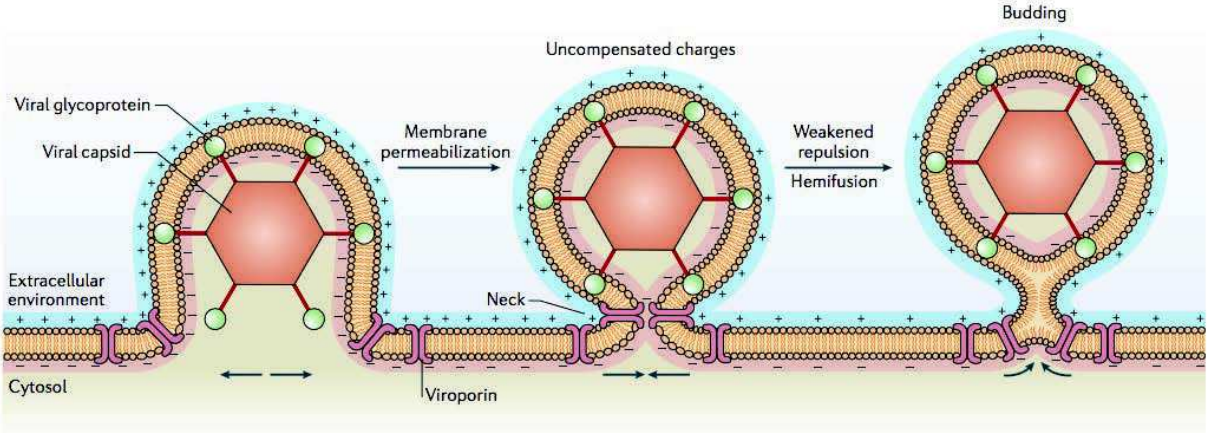

Figure 49: Model of a viroporin promoting viral budding at the plasma membrane. Viroporins can alter membrane permeability by conducting the flux of different ion across the membrane in favor of their concentration gradients, which could reduce the transmembrane potential. This would induce the depolarization of the membrane and induce the budding and scission of the particles. Adapted from (Nieva et al., 2012)

II- Role of the regulation of the cleavage between E2 and p7

During our study of p7 in the context of p7 ATMI mutant viruses, we also highlighted that the modulation of cleavage between E2 and p7 is key for the regulation of p7 function, on the one hand, and for the regulation of E2 expression levels, on the other hand (Denolly et al., 2017). Importantly, several studies underscore that the regulation of protein cleavage is a significant mechanism used by different virus types to modulate some of their functions. For example, regulated cleavage is important for the maturation of glycoproteins such as those from DENV or IAV. Likewise, alphaviruses express a polyprotein in which ordered and/or partial cleavage has been shown to be important for the switch between synthesis of (-) RNA vs. (+) RNA. (Viral precursors are reviewed in (Yost & Marcotrigiano, 2013)).

In the case of HCV, the precursors for several of its proteins have been described, such as E2p7, core with its domain III, which regulates core intracellular localization, as well as the NS4B-NS5A precursor known to be involved in the formation of DMVs (Romero-Brey et al., 2015a). Here, we focused our studies on the properties of the E2p7 precursor. Interestingly, we showed that E2p7 mutants that display increased cleavage showed up to 6-fold E2 increased amounts in infected cells, which modifies the ratio of E1E2 sub-viral particles (SVP) *vs*. viral particles (Denolly et al., 2017). Yet, the mechanism explaining how increased E2p7 cleavage modulates the level of E2 has remained elusive, though different possibilities could explain the above, such as the modification of the rates of either translation, secretion or degradation. We excluded the possibility of increased retention of E2 in the ER or the secretory pathway since higher E2 levels were detected in the supernatant of infected cells. Likewise, we excluded the possibility of increased rates of replication or translation of the mutant HCV genomes

since we observed no difference in the expression levels of viral RNAs or of non-structural proteins, which are produced from the same polyprotein that for E2.
Because of their intrinsic capacity to be routed to the cell surface, owing to their localization in the cell secretory pathway, the traffic and distribution of envelope glycoproteins as well as their SVPs need to be controlled, by *e.g.*, retention in specific intracellular compartments, in order to avoid immune detection of infected cells. Moreover, these glycoproteins are synthesized in the ER lumen, implying that counteracting ER stress activation is important to avoid cell death. Viruses have evolved different strategies to alleviate ER stress (Jheng et al., 2014). Since HCV proteins are expressed from a polyprotein, indicating that its proteins are initially expressed at the same rate, we propose that the delayed cleavage between E2 and p7 could be a way to regulate the function and stability of E2.

Different possibilities may explain how E2p7 processing could modulate E2 expression and we discuss below some of these possibilities as well as preliminary results of experiments aimed to address them. First, we hypothesized that E2p7 and E2 could have a different stability and/or could differentially activate pathways of degradation such as autophagy or proteasome, for example, as it is known that HCV glycoproteins activate the unfolded protein response (UPR) in HCV-infected cells (Mohl et al., 2012). To test this, we blocked proteasomal/lysosomal degradation pathway, using MG132 and bafilomycin A1. We compared wild-type virus (with balanced E2p7 *vs*. E2 and p7 individual expression) *vs*. p7 ATMI virus mutant (with full E2p7 cleavage) and E2-A367R mutant virus (in which E2p7 cleavage is blocked). Our preliminary results (Figure 49) show that E2p7 is not degraded through lysosomal or proteasome degradation pathways. Unexpectedly, a slightly decreased E2 expression of up to 40% for both wt and p7 ATMI mutant viruses was observed when proteasomal degradation was blocked, which raises the possibility of a E2-destabilizing protein (*i.e.,* upon blocking of proteasomal degradation, the level of this protein is up-regulated, which increases E2 degradation). Additionally, these results show increased E2 levels upon bafilomycin A1 treatment, again for both wt and p7 ATMI mutant viruses, which indicates, first, that part of E2 turnover is controlled by lysosomal degradation and second, that this mechanism is not at play in increased intracellular E2 expression for the p7 ATMI mutant viruses (Figure 50). Consistently, we found that cycloheximide (CHX) treatment did not reveal differences between wt and p7 ATMI mutant viruses for intracellular E2 degradation (Denolly et al., 2017).
On the other hand, we may also propose that liberated E2 could be stabilized by its partner such as E1 or NS2 (Jirasko et al., 2010, Ma et al., 2011, Popescu et al., 2011, Shanmugam et al., 2015, Shanmugam & Yi, 2013), or *via* a subunit of the signal peptidase SPCS1 with which E2NS2 complex interacts (Suzuki et al., 2013). This latter interaction seems a very interesting possibility to address since, being part of the complex of the cellular signal peptidase (SP) (Paetzel et al., 2002), SPCS1 is directly linked to modulation of SP cleavage efficiency (Fang et al., 1996). Thus, we could propose that since SP cleaves E2p7 (as well as other blocks of the HCV polyprotein such as p7NS2),

the SPCS1 subunit remains associated to E2 and NS2 (and perhaps p7) after cleavage and induces a greater stability of E2 that explains our results.
Finally, it is also possible that the amounts of free p7 may regulate these degradation pathways. In support of these assumptions, a previous study (Atoom et al., 2013) indicated that a mutation of p7 reported to decrease cleavage between E2 and p7 (p7-R(K)GR33-35AAA) (Ma et al., 2011, Shanmugam & Yi, 2013, Steinmann et al., 2007) induced E2 degradation. Likewise, mutants abrogating E2p7 cleavage, such as E2-A367R (see part II in Results sections) as well as p7-A1W, p7-E3W, p7-K4W, p7-A10W or p7-S12W (Scull et al., 2015), exhibited poor E2p7 expression despite wt rates of replication, relative to parental viruses.
The unravelling of the mechanism underlying E2 upregulation upon increased E2-p7 cleavage will need additional experiments in order to provide a broader picture.

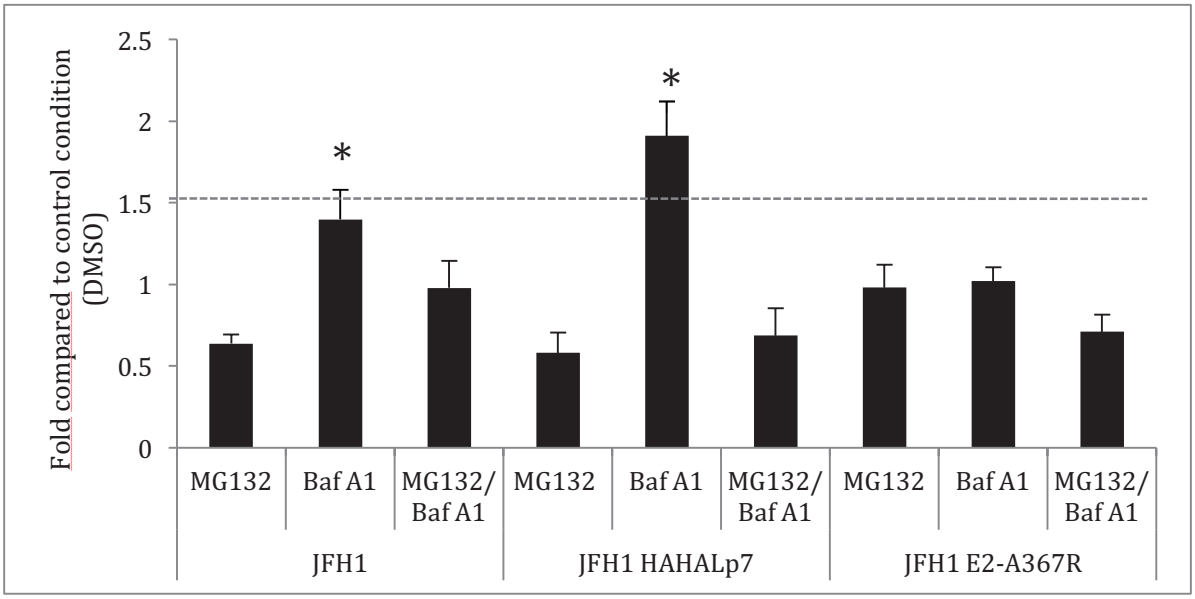

Figure 50. Effect of inhibition of proteasome or autophagy on expression level of E2 or E2p7. Huh7.5 cells were electroporated with RNAs from parental or JFH1 HAHALp7 or JFH1 E2-A367R mutant HCVcc viruses. At 56h post electroporation cells were treated either with Bafilomycin A1 (100uM) or MG132 (40uM) alone or in combination for 16h. Control cells were treated with DMSO. At 72h post electroporation cells were counted and the same amounts of cells were lysed. Level of E2 was determined by quantitative western blot. Data represent mean values ± SEM.

III- HCV p7 and inhibition of cell secretory pathway

Besides its role in assembly, we also revealed a new function of p7. Indeed, we demonstrated that free p7, which localizes at the ER (Bentham et al., 2013, Griffin et al., 2005, Haqshenas et al., 2007, Vieyres et al., 2013), is able to slow down the cell secretory pathway in a dose-dependent manner, likely at the stage of ER-Golgi transition which induces a specific retention of HCV glycoproteins in a wild-type virus infection context. This property is not intuitive since HCV, like other *Flaviviridae*, is thought to exit the cells through the secretion pathway (Coller et al., 2012). Yet, this function could be a way for the virus to induce the retention of E1E2 at assembly sites in the ER lumen as suggested by the notion that HCV glycoproteins are also secreted as SVPs (Denolly et al., 2017, Icard et al., 2009) independently of the other viral proteins. It could also reflect the cooptation of an alternative pathway of secretion for HCV particles, in agreement with an emerging notion that the secretion of virions may occur through a non-canonical route (Bayer et al., 2016, Mankouri et al., 2016). Alternatively, this function could provide a feedback loop that may ensures that excess glycoproteins, arising from their release upon E2p7 cleavage, could be appropriately controlled so as to prevent activation of immune responses. Additionally, as indicated by the delayed transport of VSV-Gts used as a model cargo (Denolly et al., 2017), it is possible that p7 expression could alter the secretion of cellular proteins such as, *e.g.,* immune effectors, as shown for viroporins of other viruses (Cornell et al., 2007, de Jong et al., 2008). In this respect, it was recently shown that p7 may promote immune evasion by antagonizing the antiviral functions induced by IFN upregulation (Qi et al., 2017).

The mechanism used by p7 to slow down the secretion of glycoproteins needs further investigation. The viroporins of alternative viruses have previously been involved in modulation of the secretory pathway, though through a variety of mechanisms (Nieto-Torres et al., 2015). For example, the M2 protein from influenza virus has a direct effect on late steps of plasma membrane delivery by delaying late Golgi transport, which indirectly affects the efficiency of earlier transport steps by altering the ionic content of the Golgi apparatus and the endosomes (Henkel & Weisz, 1998, Sakaguchi et al., 1996). Alternatively, Coxsackievirus 2B proteins modify ER membranes, which inhibits protein processing and sorting by decreasing calcium homeostasis in ER and Golgi (de Jong et al., 2008). Likewise, p7 can change ionic gradients in both reconstituted membrane assays *in vitro* (Griffin et al., 2003, Montserret et al., 2010, Pavlovic et al., 2003, Steinmann & Pietschmann, 2010, StGelais et al., 2009) and *in cellulo* (Bentham et al., 2013, Wozniak et al., 2010), which could affect anterograde transport and/or modify intracellular compartments. We therefore speculated that p7 could also act through its ion channel activity. Our preliminary results addressed this possibility by studying several mutants and/or inhibitors of p7 (Figure 51). We found that p7 mutants that may have altered pore functioning, *i.e.*, p7-A1W, p7-V6W, p7-H9W and p7-A10W(Scull et al., 2015) or p7-R33Q/R35Q (Steinmann et al., 2007) could slow down the cell secretory pathway using the VSV-Gts secretion assay like for the wt p7 (Figure 51A). Likewise, the

HCV p7 and influenza M2 inhibitor, rimantadine (StGelais et al., 2007) did not affect p7 capacity to decrease VSV-Gts trafficking whereas it affected that of M2 (Figure 51B) as well as the infectivity of HCV (Figure 51C).

Overall, these unpublished results argue against a role of the ion channel function of p7 in the regulation of the cell secretory pathway. Further investigations are hence required to investigate the involved mechanism, such the possibility that p7 specifically interact with cellular proteins involved in secretion of glycoproteins (*e.g.*, adaptor proteins,…).

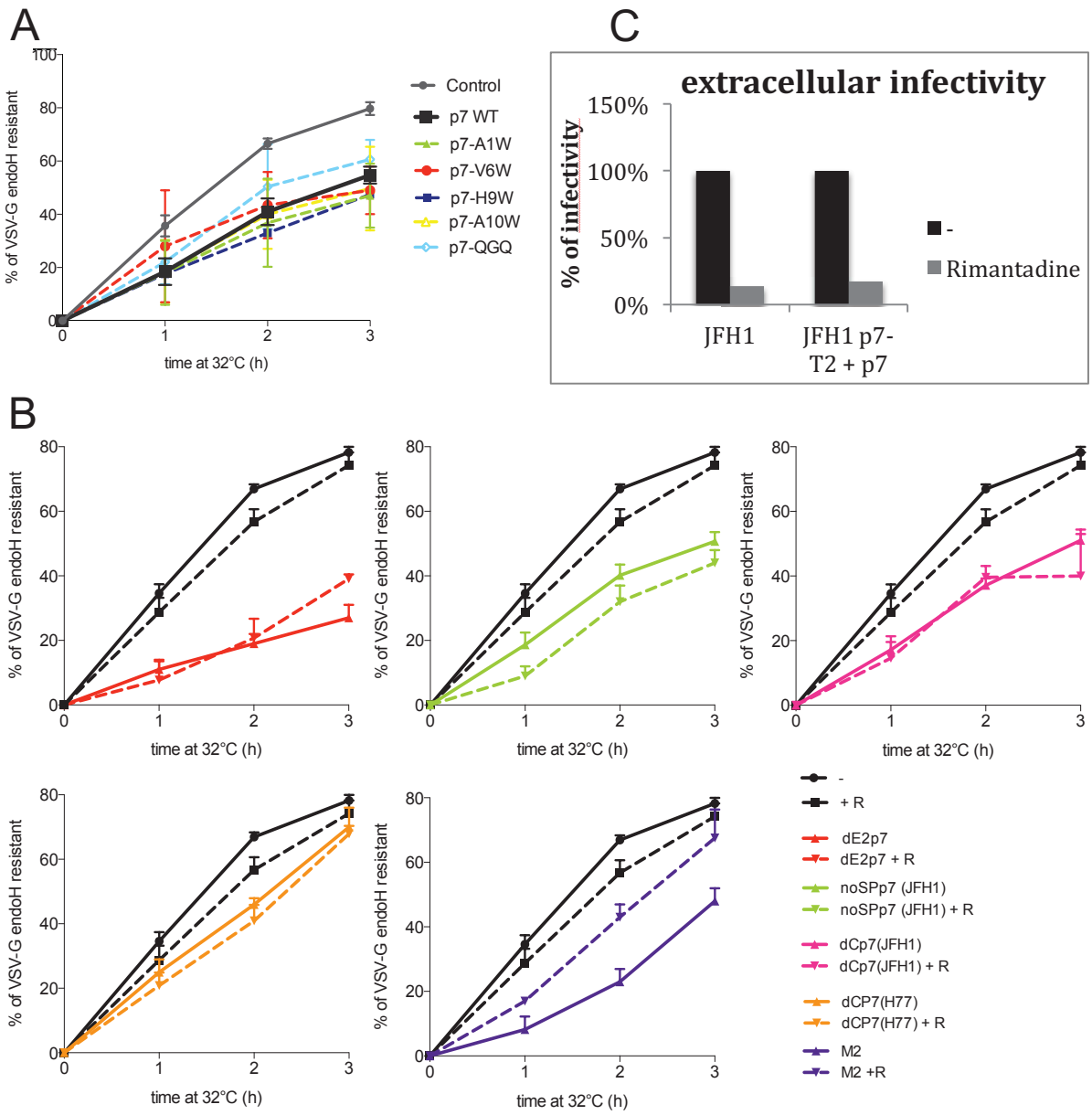

Figure 51. The ion channel activity of p7 is not involved in the delayed trafficking of glycoproteins. (**A**) Huh7.5 cells were transfected with vectors encoding VSV-Gts and p7 (JFH1) wild-type or harboring A1W, V6W, H9W, A10W or KR33/35QQ (QGQ) mutations. Transfected cells were grown overnight at 40°C, which maintains VSV-Gts unfolded and results in its accumulation in the ER. Cells were then incubated for different periods of time (0h, 1h, 2h and/or 3h, as indicated) at 32°C, which allows restoration of its folding and thus, its secretion. Quantification of western blot of cell lysates digested with endoH, from independent experiments. (**B**) Huh7.5 were transfected with vectors encoding VSV-Gts and p7 from different genotypes, as indicated or H7N1 M2, as in figure 1E. Transfected cells were grown overnight at 40°C in presence of rimantadine (50µM). Cells were then incubated for different periods of times (0h, 1h, 2h and/or 3h, as indicated) at 32°C. Quantifications of western blot of cell lysates digested with endoH, from independent experiments, conditions with rimantadine (R) were represented in dotted lines. (**C**) Electroporated cells with either JFH1 wild-type or p7-T2 mutant expressed with wild-type p7, were treated with rimantadine (50µM) for 24h at 48h post electroporation or left untreated. Supernatants were harvested and used to infect naïve cells.

IV- Mode of action of daclatasvir on HCV assembly

Our study on the clustering of structural and non-structural HCV assembly components (see Part I of the Results section of this document) allowed us to highlight how daclatasvir (DCV), an inhibitor of NS5A, inhibits HCV assembly before inhibiting HCV replication (Boson et al., 2017). First, having extended previous results of other groups indicating that DCV induces NS5A clustering (Chukkapalli et al., 2015, McGivern et al., 2014, Reghellin et al., 2014), we showed that other HCV proteins, such as E2, core and NS4B, are gathered with NS5A clusters upon short DCV treatment of infected cells. We found that the enlargement of these clusters reflects the loss of the functional connection between replication complexes and assembly sites. Furthermore, we showed that DCV prevents the NS5A-mediated transfer of the viral genome from replication complexes to assembly sites, which inhibits the formation of the nucleocapsid.
Based on these results, we proposed the following model for mode of action of DCV in assembly inhibition (Figure 52).

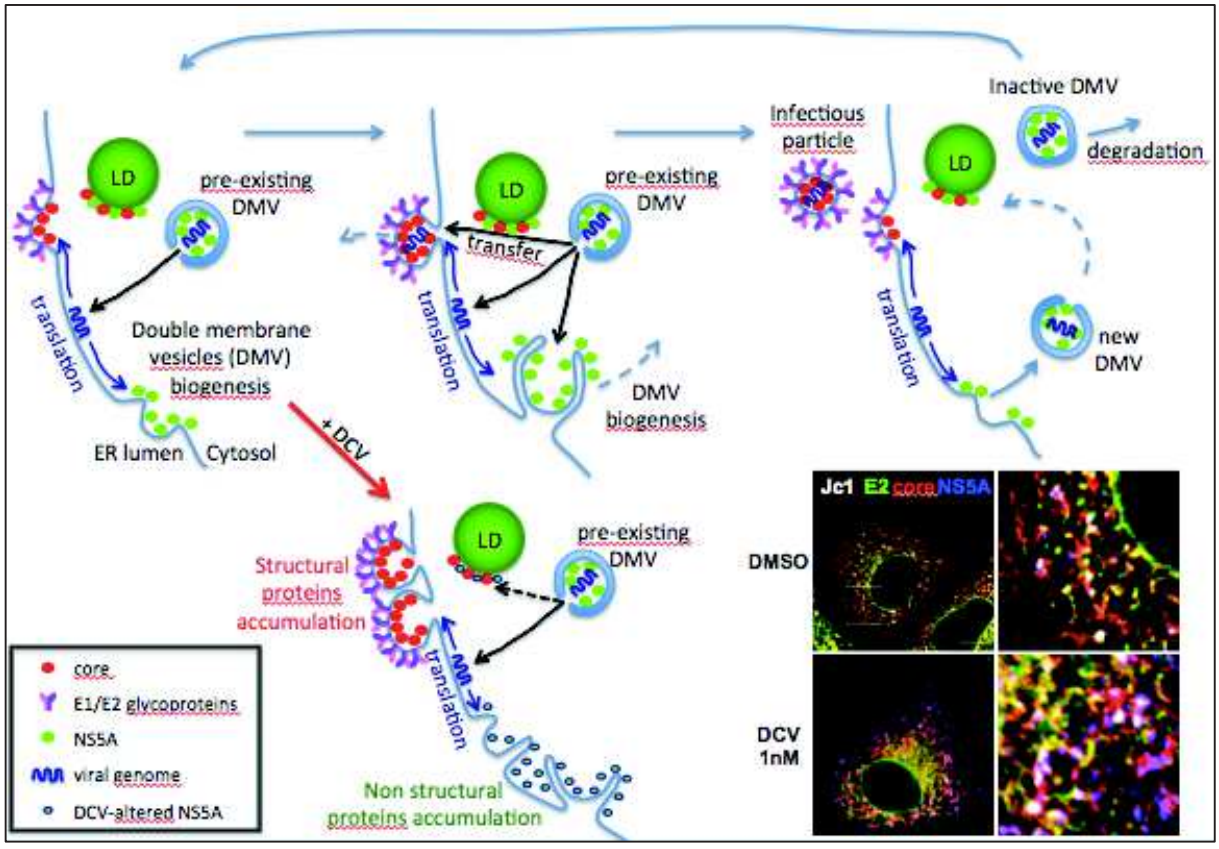

Figure 52 : Mode of action of DCV. See text below for details

In the absence of DCV, the double-membrane vesicles (DMVs), which are HCV-induced membrane structures, replicate the viral genome and produce viral RNAs that are translated as a polyprotein. Upon maturation of the latter protein by proteolysis, the Core, E1 and E2 structural proteins accumulate and induce assembly sites while the

non-structural proteins induce the formation of new DMVs, with NS5A and/or NS4B-NS5A precursor playing a key role in their biogenesis (Romero-Brey et al., 2015a) . At the same time, the viral genome is encapsidated in the assembling viral particles through its transfer from DMVs that depends on NS5A and, probably, its localization on the surface of the lipid droplets (LDs) (Appel et al., 2008, Miyanari et al., 2007). The nascent viral particles are then enveloped, matured and released *via* the secretion pathway (see Part I of this Discussion section). New DMVs become also individualized from their site of biogenesis and replace old DMVs that become rapidly inactive. The system is thus more or less in equilibrium and returns to the initial situation.

However, in the presence of DCV, disruption of the membranotropic properties of NS5A could prevent its correct folding and thus positioning, hence preventing the formation of new DMVs and of virus particles. Indeed, transfer of HCV RNA from active DMVs to assembly sites could be affected by the defect in membrane-binding properties of NS5A for different reasons. First, as NS5A is located both inside and outside DMVs (Paul et al., 2013), such alterations could perturb the stability of NS5A at the surface of DMV and thus prevent the gathering of DMVs to assembly sites. Second, DCV could disrupt NS5A-association with ER or LD interface, which may inhibits RNA transfer as this likey requires NS5A multimers to guide HCV RNA as proposed by others (Appel et al., 2008, Bartenschlager et al., 2013, Berger et al., 2014, Love et al., 2009). As a result, DCV induces the accumulation and clustering of viral both structural and non-structural proteins at the sites of DMV biogenesis and of viral particle assembly. Ultimately, the system shuts off because there are no new DMVs required for replication the viral genome, which explains the delayed effect of DCV on HCV RNA replication.

Further investigations are required to investigate how DCV could alter membranotropic properties of NS5A.

V- Model of lipidation of particles

Our study (see Part III in Results section) allowed us to demonstrate that lipidation of HCV particles, and thus the formation of lipo-viro-particles (LVP), could be induced once poorly lipidated particles, produced from Huh7.5 cells (such as grown in serum-free medium), encounter appropriate extracellular serum and media conditions that exhibit physiologic concentrations of VLDLs and other lipoproteins. These results are important in several regards, not only as they allow to provide further details on the mechanisms of lipidation but also because they raise a new and unique way to mimic patients' particles composition from *in vitro*-produced virions.

The overall organization of HCV particles form(s) remains elusive. *In vivo*, HCV particles are associated to apoB, the major structural protein component of VLDLs and LDLs. This may explain the particularly low buoyant density of HCV virions, of ≤1.10, which is significantly lower than those of other enveloped viruses, including the HCV-related flaviviruses. Indeed, the lipid profiling of purified HCVcc particles confirmed that their

lipid content is similar to that of serum lipoproteins, although they could not be assigned to a specific lipoprotein class (Merz et al., 2011).

Several studies have proposed that HCV particle production depends on cellular factors controlling assembly and release of VLDLs, indicating that the interaction of virus particles with serum lipoproteins begins at early steps of their assembly and egress processes during which immature particles are converted to mature virions by lipidation and incorporation of some apolipoproteins (Felmlee et al., 2013). While there is a strong consensus indicating that the small, exchangeable apolipoprotein apoE is necessary at an early step to promote envelopment, lipidation and/or release of viral particles, some studies suggests that apoB may not be required to promote these initial steps (reviewed in (Lindenbach & Rice, 2013)). This is intriguing because apoB is essential for VLDL assembly and because HCV retrieved from patients can be readily immuno-precipitated with antibodies against apoB. One orthodox explanation is that the cell line that efficiently supports HCVcc experiments *in vitro*, the Huh-7.5 hepatoma, lacks many properties of hepatocytes, such as the ability to produce normal serum lipoproteins VLDL (Icard et al., 2009, Merz et al., 2011). That Huh-7.5 cells produce under-lipidated, VLDL-like particles would thus explain why the HCVcc particles they produce have a higher buoyant density and lower specific infectivity than HCV produced *in vivo* or from primary hepatocytes (Calattini et al., 2015, Lindenbach et al., 2006, Podevin et al., 2010). However, when HepG2 hepatoma cells, that are thought to represent more mature hepatocytes than Huh7 cells, are induced to produce normal, apoB-containing VLDLs, they yield infectious viral particles that are biophysically and biochemically similar to those produced from Huh7.5 cells (Jammart et al., 2013). Altogether these evidences showed that there is no correlation between the ability of cells that replicate HCV to secrete VLDLs and their capacity to produce LVPs, reinforcing our results that lipidation of particles produced in Huh7.5 cells could happen in the extracellular medium. Yet, these results do not disrepute that *in vivo* or in normal hepatocytes, HCV particles maturation may occur during transit through the secretory pathway where they may associate or fuse with apoB-containing lipoproteins precursors and/or luminal, apoE-containing lipid droplets as proposed previously (Lehner et al., 2012). Importantly, they imply that a major factor of lipid-imprinting of HCV particles is the environment provided by the extracellular milieu and/or the serum characteristics.

Our data also unravel that lipidation of viral particles combines virion interaction(s) with defined serum lipoproteins but also requires an additional, presumably non-lipid serum factor (see below). Concerning the lipoprotein type allowing lipidation of viral particles, our results indicate that all principal lipoprotein classes, *i.e.*, VLDL, LDL and HDL, could mediate the lipidation effect *in vitro*, upon short time incubation with HCV particles in the presence of lipoproteins depleted serum (LPDS), with an additive effect when either lipoprotein type was combined with one another. While these results are consistent with the strong lipidation induced by human serum (HS), in contrast to fetal calf serum (FCS) than contains at least 6-fold lower concentrations of either lipoprotein,

they raise the question of the nature of the interaction between lipoproteins and viral particles, and of its outcome in terms of HCV virion morphology. Hybrid viral structures harboring different lipoprotein components may indeed be formed by transfer of lipids, through their spontaneous release/exchange or *via* fusion, or, alternatively, by transient or stable virion association with lipoproteins. Although direct evidence by electron microscopy are missing in favor of the latter "two (or more)-particle" model (Catanese et al., 2013, Gastaminza et al., 2010, Merz et al., 2011, Piver et al., 2017) (Figure 53, left) perhaps owing to its transient or unstable state, our results argue for this model since full lipidation of viral particles, inducing their association with the non-exchangeable apoB apolipoprotein could be readily observed upon short time treatment of cell-free HCV virions with HS or purified lipoproteins. In addition, the additive effects of virion lipidation observed after combination with different lipoprotein types could reflect the fact that, since lipoproteins have different sizes (VLDL and chylomicron being the larger ones), the best geometrical solution to maximize virion interaction with lipoproteins is to combine different types of lipoprotein particles. The other arguments for this morphological model are that *in vivo*, HCV particles may associate with apoB48-containing chylomicrons (Diaz et al., 2006), which are not produced by hepatocytes, and that they exhibit rapid though transient postprandial shifts in buoyant density upon lipid-rich diet in HCV-infected patients (Felmlee et al., 2010).

Yet, all this evidence does not rule out the alternative and/or nonexclusive possibility that viral particles may mimic lipoproteins and thus, exchange or uptake their lipids just as lipoproteins do between themselves. Indeed, it was previously reported by different groups that apoliproteins could be exchanged or transferred from lipoproteins, serum itself or extracellular milieu to infectious particles (Bankwitz et al., 2017, Dreux et al., 2007b, Yang et al., 2016). Thus, as LVPs contain specific subsets of apoliproteins (Andre et al., 2002, Catanese et al., 2013, Merz et al., 2011), this may regulate the exchange and/or transfer of lipids with lipoproteins, which could modify their inner lipid content. In this respect, our HS-incubation kinetics that suggested that lipidation of infectious particles is progressive over time, argues for the "single-particle" model (Figure 53, right) of HCV structure, sharing an envelope with a lipoprotein particle that is continuously modified upon interactions with lipoproteins. Since HCV particle lipidation can be induced by different types of lipoproteins, we surmise that the mode of lipoprotein association or of lipidation mechanism may vary accordingly.

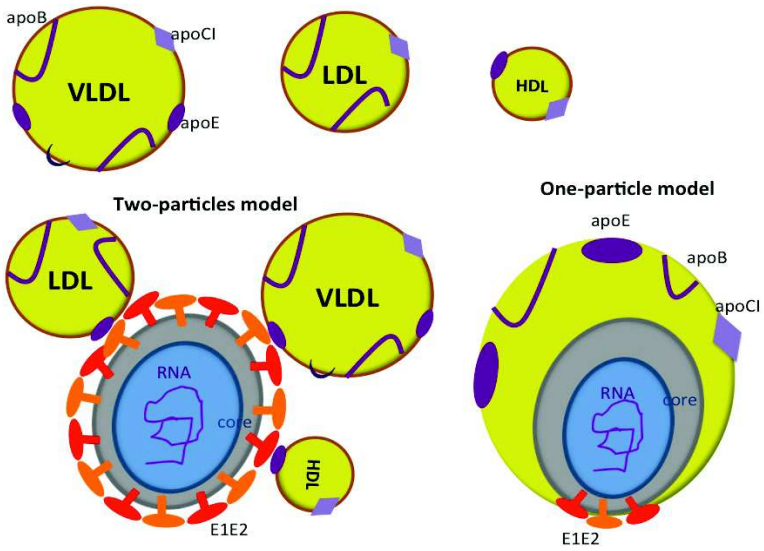

Figure 53: Lipoproteins and models of HCV particles

A major difficulty in the study of the 'one' *vs*. 'two' particles models is the secretion of different types of non-infectious particles, at least in *in vitro* conditions of virus production. Indeed, as shown in the part II of the Results section, we confirmed and extended that HCV induces the secretion of SVPs, *i.e.*, particles incorporating only E1 and E2 (Icard et al., 2009). These particles are not yet well described but we confirmed that they exhibit low densities (Denolly et al., 2017). Besides SVPs, HCV was found to secrete naked nucleocapsids in patient sera (Maillard et al., 2001), though we were not able to detect them in the supernatants of HCVcc-produced Huh7.5 cells. Yet, the most intriguing finding remains the secretion of a huge amount of viral RNA that is not associated with infectivity. Indeed, the incubation of particles with HS allows a shift of all infectious particles in low-density fractions, due to their lipidation; yet, only a marginal part of viral RNAs become associated to these low-density viruses, indicating that a large amount of RNA-containing particles is not able to be lipidated. Accordingly, it has been well described that HCV secretes exosomes (Longatti et al., 2015, Masciopinto et al., 2004, Ramakrishnaiah et al., 2013), which are difficult to separate from HCV infectious particles. Such exosomes may contain viral RNAs and could also harbor E1E2 glycoproteins at their surface.

Our results combined with previous studies (Dao Thi et al., 2012, Gastaminza et al., 2006) also indicate that besides the viral RNAs, a large population of core protein is not associated with infectious particles, which suggests that both core and RNA could be associated with alternative types of particles that remain to be determined. These non-infectious particles could be naked nucleocapsids, *i.e.*, not associated with glycoproteins or, alternatively, could exhibit a defect in the formation in the nucleocapsids, resulting in an impairment at the level of entry. Interestingly, the major peak of viral RNAs of HCVcc found in gradient, *i.e.*, between densities 1.10-1.12, is generally not observed in HCV patients' sera, suggesting that such particles could be an artifact of Huh7.5 cells.

Finally, and importantly, our results reveal that lipidation of viral particles by lipoproteins requires a serum factor, likely different of lipoproteins, since only in the presence of LPDS could incubation with VLDL, LDL and HDL induce the low-density shift of HCV virions. Although the lipidation state and infectivity of viral particles can be altered upon treatment with lipoprotein lipase (LPL) and hepatic triglyceride lipase (HTGL) (Shimizu et al., 2011), we were unable to block lipidation of viral particles by serum lipid transfer enzymes such as CETP and LCAT that promote lipid transfer. Yet, we found that HSA, added to VLDL or LDL, induced lipidation of viral particles. This indicated that HSA is one of the serum co-factors mediating LVP formation, perhaps by bridging lipoproteins and virions or by favoring lipid efflux VI- Key role of the Hypervariable Region I (HVR1) of E2 in the lipidation process

Our results indicate that the HVRI domain of the E2 glycoprotein plays a major role in the lipidation process and accounts for the differential lipidation sensitivities of Jc1 *vs*. H77 HCVcc particles. HVRI remains an intriguing determinant of E2 that modulates i) conformation of E2 by concealing the CD81 binding site (Bartosch et al., 2003, Dao Thi et al., 2012, Roccasecca et al., 2003) and the accessibility to cross-neutralizing epitopes that target virus-CD81 interaction (Bankwitz et al., 2010, Bartosch et al., 2005, Dreux et al., 2006); ii) the recruitment to and/or conformation on viral particles of apolipoproteins such as ApoCI and ApoE(Bankwitz et al., 2014, Dreux et al., 2007b); iii) the interaction of viral particles with lipoproteins, which promotes HDL-mediated enhancement of their infectivity (Bartosch et al., 2005, Dreux et al., 2007b, Dreux et al., 2009b, Dreux et al., 2006, Lavillette et al., 2005b) and their lipidation profiles (Bankwitz et al., 2014, Dao Thi et al., 2012, Prentoe et al., 2011, Prentoe et al., 2014). While deletion of HVRI shifts the density of particles to a homogenous intermediate density of 1.11(Bankwitz et al., 2010, Dao Thi et al., 2012, Prentoe et al., 2011) that corresponds to the density of non-lipidated particles of our study, it is interesting that simple swaps of HVRI sequences between H77 and Jc1 HCVcc could reconstitute the differential lipidation profiles of either parental virus. This confirms that HVRI harbors key residue involved in lipidation. However, we observed that HVRI of H77 induce a stronger lipidation of viral particles when swapped in Jc1 virus compared to the parental H77 HCVcc virus, suggesting that HVRI might act in concert with other residues in E1 and E2. Moreover, it has been shown that HVRI modulates the conformation of virion-incorporated apoliproteins, such as ApoE (Bankwitz et al., 2014), whether these factors are inherited by the virus-producer cells (Boyer et al., 2014, Lee et al., 2014) or subsequent to virion release (Bankwitz et al., 2017, Dreux et al., 2007b, Yang et al., 2016). Thus, in agreement with the findings of others that lipidated viruses exhibit strain-dependent usage of different cell entry factors that act as lipoprotein receptors (Prentoe et al., 2014), one possibility is that HVRI plasticity can drive both lipidation and apolipoprotein display, which in return dictates the set of lipoprotein receptors used at an early step of entry. The extended lipidation state detected with HCVcc particles incubated with human serum, which bear seemingly identical features as those of virus retrieved from patients with respect to their ApoB content, is expected to reinforce the

usage of different lipoprotein receptors including SR-BI (Bankwitz et al., 2010, Calattini et al., 2015, Dao Thi et al., 2012, Prentoe et al., 2014), LDLr (Prentoe et al., 2014), and likely VLDLr (Ujino et al., 2016, Yamamoto et al., 2016) .

The requirement of HCV for selecting its unusually high number of entry receptors is unclear. One possibility is that the usage of lipoprotein receptors correlates with a lipidation state that contribute to shielding cross-neutralizing epitopes, as inferred from previous studies. However, a recent study indicated that the IC50 of cross-neutralizing antibodies were, in general, not dependent on virus density(Prentoe et al., 2011). Moreover, the main E2 target of such cross-neutralizing antibodies, likely the CD81 binding site, is concealed by HVRI, whether or not the virus particles are lipidated (Bankwitz et al., 2010, Dreux et al., 2006). A second possibility is that lipidation of viral particles allow the viral particles to access, following a first step of entry induced by lipoprotein receptors, to a protected environment into which it can subsequently and safely interact with CD81 in a putative neutralizing antibody-free sanctuary to promote the further steps of cell penetration. A third possibility, which also fits well with the latter hypothesis, is that the usage of lipoprotein receptors increases the specific infectivity of viral particles. Accordingly, lipidation of viral particles, which shift them to low or very-low densities, is accompanied by their increased specific infectivity that could provide a positive selection for selecting the HVRI variants that drive full lipidation. The varied specific infectivity detected depending on virion density could reflect the differential efficiency of pathways of entry into cells depending on the lipidation status of the particles and their corresponding recepties. Indeed, it was shown that particles can bind to VLDL-R as well as SRBI or LDL-R and the use of these different receptors depend on the density of the particles (Prentoe et al., 2014, Yamamoto et al., 2016). It is also possible that the lipidation may increase the stability of particles by protecting them from degradation.

REFERENCES

Ahmad J, Eng FJ, Branch AD (2011) HCV and HCC: clinical update and a review of HCC-associated viral mutations in the core gene. Semin Liver Dis 31: 347-55

Ai LS, Lee YW, Chen SS (2009) Characterization of hepatitis C virus core protein multimerization and membrane envelopment: revelation of a cascade of core-membrane interactions. J Virol 83: 9923-39

Aizawa Y, Seki N, Nagano T, Abe H (2015) Chronic hepatitis C virus infection and lipoprotein metabolism. World J Gastroenterol 21: 10299-313

Alagona P, Jr. (2010) Fenofibric acid: a new fibrate approved for use in combination with statin for the treatment of mixed dyslipidemia. Vasc Health Risk Manag 6: 351-62

Albecka A, Belouzard S, Op de Beeck A, Descamps V, Goueslain L, Bertrand-Michel J, Terce F, Duverlie G, Rouille Y, Dubuisson J (2012) Role of low-density lipoprotein receptor in the hepatitis C virus life cycle. Hepatology 55: 998-1007

Aldabe R, Barco A, Carrasco L (1996) Membrane permeabilization by poliovirus proteins 2B and 2BC. J Biol Chem 271: 23134-7

Ali N, Tardif KD, Siddiqui A (2002) Cell-free replication of the hepatitis C virus subgenomic replicon. J Virol 76: 12001-7

Amako Y, Tsukiyama-Kohara K, Katsume A, Hirata Y, Sekiguchi S, Tobita Y, Hayashi Y, Hishima T, Funata N, Yonekawa H, Kohara M (2010) Pathogenesis of hepatitis C virus infection in Tupaia belangeri. J Virol 84: 303-11

Andre P, Komurian-Pradel F, Deforges S, Perret M, Berland JL, Sodoyer M, Pol S, Brechot C, Paranhos-Baccala G, Lotteau V (2002) Characterization of low- and very-low-density hepatitis C virus RNA-containing particles. J Virol 76: 6919-28

Appel N, Zayas M, Miller S, Krijnse-Locker J, Schaller T, Friebe P, Kallis S, Engel U, Bartenschlager R (2008) Essential role of domain III of nonstructural protein 5A for hepatitis C virus infectious particle assembly. PLoS Pathog 4: e1000035

Ariumi Y, Kuroki M, Maki M, Ikeda M, Dansako H, Wakita T, Kato N (2011) The ESCRT system is required for hepatitis C virus production. PLoS One 6: e14517

Arzumanyan A, Reis HM, Feitelson MA (2013) Pathogenic mechanisms in HBV- and HCV-associated hepatocellular carcinoma. Nat Rev Cancer 13: 123-35

Ashfaq UA, Javed T, Rehman S, Nawaz Z, Riazuddin S (2011) Lysosomotropic agents as HCV entry inhibitors. Virol J 8: 163

Atkins E, Tatineni R, Li H, Gretch D, Harris M, Griffin S (2014) The stability of secreted, acid-labile H77/JFH-1 hepatitis C virus (HCV) particles is altered by patient isolate genotype 1a p7 sequences. Virology 448: 117-24

Atoom AM, Jones DM, Russell RS (2013) Evidence suggesting that HCV p7 protects E2 glycoprotein from premature degradation during virus production. Virus Research 176: 199-210

Bamberger MJ, Lane MD (1990) Possible role of the Golgi apparatus in the assembly of very low density lipoprotein. Proc Natl Acad Sci U S A 87: 2390-4

Bankwitz D, Doepke M, Hueging K, Weller R, Bruening J, Behrendt P, Lee JY, Vondran FWR, Manns MP, Bartenschlager R, Pietschmann T (2017) Maturation of secreted HCV particles by incorporation of secreted ApoE protects from antibodies by enhancing infectivity. J Hepatol 67: 480-489

Bankwitz D, Steinmann E, Bitzegeio J, Ciesek S, Friesland M, Herrmann E, Zeisel MB, Baumert TF, Keck ZY, Foung SK, Pecheur EI, Pietschmann T (2010) Hepatitis C virus hypervariable region 1 modulates receptor interactions, conceals the CD81 binding site, and protects conserved neutralizing epitopes. J Virol 84: 5751-63

Bankwitz D, Vieyres G, Hueging K, Bitzegeio J, Doepke M, Chhatwal P, Haid S, Catanese MT, Zeisel MB, Nicosia A, Baumert TF, Kaderali L, Pietschmann T (2014) Role of hypervariable region 1 for the interplay of hepatitis C virus with entry factors and lipoproteins. J Virol 88: 12644-55

Barba G, Harper F, Harada T, Kohara M, Goulinet S, Matsuura Y, Eder G, Schaff Z, Chapman MJ, Miyamura T, Brechot C (1997) Hepatitis C virus core protein shows a cytoplasmic localization and associates to cellular lipid storage droplets. Proc Natl Acad Sci U S A 94: 1200-5

Barouch-Bentov R, Neveu G, Xiao F, Beer M, Bekerman E, Schor S, Campbell J, Boonyaratanakornkit J, Lindenbach B, Lu A, Jacob Y, Einav S (2016) Hepatitis C Virus Proteins Interact with the Endosomal Sorting Complex Required for Transport (ESCRT) Machinery via Ubiquitination To Facilitate Viral Envelopment. MBio 7

Barretto N, Uprichard SL (2014) Hepatitis C virus Cell-to-cell Spread Assay. Bio Protoc 4

Bartenschlager R, Ahlborn-Laake L, Mous J, Jacobsen H (1994) Kinetic and structural analyses of hepatitis C virus polyprotein processing. J Virol 68: 5045-55

Bartenschlager R, Baumert TF, Bukh J, Houghton M, Lemon SM, Lindenbach BD, Lohmann V, Moradpour D, Pietschmann T, Rice CM, Thimme R, Wakita T (2018) Critical challenges and emerging opportunities in hepatitis C virus research in an era of potent antiviral therapy: Considerations for scientists and funding agencies. Virus Res 248: 53-62

Bartenschlager R, Lohmann V, Penin F (2013) The molecular and structural basis of advanced antiviral therapy for hepatitis C virus infection. Nat Rev Microbiol 11: 482-96

Bartosch B, Dubuisson J, Cosset FL (2003) Infectious hepatitis C virus pseudo-particles containing functional E1-E2 envelope protein complexes. J Exp Med 197: 633-42

Bartosch B, Verney G, Dreux M, Donot P, Morice Y, Penin F, Pawlotsky JM, Lavillette D, Cosset FL (2005) An interplay between hypervariable region 1 of the hepatitis C virus E2 glycoprotein, the scavenger receptor BI, and high-density lipoprotein promotes both enhancement of infection and protection against neutralizing antibodies. J Virol 79: 8217-29

Baumert TF, Ito S, Wong DT, Liang TJ (1998) Hepatitis C virus structural proteins assemble into viruslike particles in insect cells. J Virol 72: 3827-36

Baumert TF, Vergalla J, Satoi J, Thomson M, Lechmann M, Herion D, Greenberg HB, Ito S, Liang TJ (1999) Hepatitis C virus-like particles synthesized in insect cells as a potential vaccine candidate. Gastroenterology 117: 1397-407

Bayer K, Banning C, Bruss V, Wiltzer-Bach L, Schindler M (2016) Hepatitis C Virus Is Released via a Noncanonical Secretory Route. J Virol 90: 10558-10573

Beaumont E, Patient R, Hourioux C, Dimier-Poisson I, Roingeard P (2013) Chimeric hepatitis B virus/hepatitis C virus envelope proteins elicit broadly neutralizing antibodies and constitute a potential bivalent prophylactic vaccine. Hepatology 57: 1303-13

Benedicto I, Gondar V, Molina-Jimenez F, Garcia-Buey L, Lopez-Cabrera M, Gastaminza P, Majano PL (2015) Clathrin mediates infectious hepatitis C virus particle egress. J Virol 89: 4180-90

Benedicto I, Molina-Jimenez F, Bartosch B, Cosset FL, Lavillette D, Prieto J, Moreno-Otero R, Valenzuela-Fernandez A, Aldabe R, Lopez-Cabrera M, Majano PL (2009) The tight junction-associated protein occludin is required for a postbinding step in hepatitis C virus entry and infection. J Virol 83: 8012-20

Benga WJ, Krieger SE, Dimitrova M, Zeisel MB, Parnot M, Lupberger J, Hildt E, Luo G, McLauchlan J, Baumert TF, Schuster C (2010) Apolipoprotein E interacts with hepatitis C virus nonstructural protein 5A and determines assembly of infectious particles. Hepatology 51: 43-53

Bentham MJ, Foster TL, McCormick C, Griffin S (2013) Mutations in hepatitis C virus p7 reduce both the egress and infectivity of assembled particles via impaired proton channel function. J Gen Virol 94: 2236-48

Berger C, Romero-Brey I, Radujkovic D, Terreux R, Zayas M, Paul D, Harak C, Hoppe S, Gao M, Penin F, Lohmann V, Bartenschlager R (2014) Daclatasvir-like inhibitors of NS5A block early biogenesis of hepatitis C virus-induced membranous replication factories, independent of RNA replication. Gastroenterology 147: 1094-105 e25

Berriot-Varoqueaux N, Aggerbeck LP, Samson-Bouma M, Wetterau JR (2000) The role of the microsomal triglygeride transfer protein in abetalipoproteinemia. Annu Rev Nutr 20: 663-97

Bichmann L, Wang YT, Fischer WB (2014) Docking assay of small molecule antivirals to p7 of HCV. Comput Biol Chem 53PB: 308-317

Bility MT, Curtis A, Su L (2014) A chimeric mouse model to study immunopathogenesis of HCV infection. Methods Mol Biol 1213: 379-88

Billerbeck E, de Jong Y, Dorner M, de la Fuente C, Ploss A (2013) Animal models for hepatitis C. Curr Top Microbiol Immunol 369: 49-86

Bishop JR, Schuksz M, Esko JD (2007) Heparan sulphate proteoglycans fine-tune mammalian physiology. Nature 446: 1030-7

Bissig KD, Le TT, Woods NB, Verma IM (2007) Repopulation of adult and neonatal mice with human hepatocytes: a chimeric animal model. Proc Natl Acad Sci U S A 104: 20507-11

Bissig KD, Wieland SF, Tran P, Isogawa M, Le TT, Chisari FV, Verma IM (2010) Human liver chimeric mice provide a model for hepatitis B and C virus infection and treatment. J Clin Invest 120: 924-30

Biswas A, Treadaway J, Tellinghuisen TL (2016) Interaction between Nonstructural Proteins NS4B and NS5A Is Essential for Proper NS5A Localization and Hepatitis C Virus RNA Replication. J Virol 90: 7205-18

Blanchard E, Belouzard S, Goueslain L, Wakita T, Dubuisson J, Wychowski C, Rouille Y (2006) Hepatitis C virus entry depends on clathrin-mediated endocytosis. J Virol 80: 6964-72

Boson B, Denolly S, Turlure F, Chamot C, Dreux M, Cosset F-L (2017) Daclatasvir Prevents Hepatitis C Virus Infectivity by Blocking Transfer of the Viral Genome to Assembly Sites. Gastroenterology 152: 895-907.e14

Boson B, Granio O, Bartenschlager R, Cosset F-L (2011) A Concerted Action of Hepatitis C Virus P7 and Nonstructural Protein 2 Regulates Core Localization at the Endoplasmic Reticulum and Virus Assembly. PLoS Pathog 7: e1002144

Boulant S, Targett-Adams P, McLauchlan J (2007) Disrupting the association of hepatitis C virus core protein with lipid droplets correlates with a loss in production of infectious virus. J Gen Virol 88: 2204-13

Boulant S, Vanbelle C, Ebel C, Penin F, Lavergne JP (2005) Hepatitis C virus core protein is a dimeric alpha-helical protein exhibiting membrane protein features. Journal of Virology 79: 11353-11365

Boyer A, Dumans A, Beaumont E, Etienne L, Roingeard P, Meunier JC (2014) The association of hepatitis C virus glycoproteins with apolipoproteins E and B early in assembly is conserved in lipoviral particles. J Biol Chem 289: 18904-13

Bradley D, McCaustland K, Krawczynski K, Spelbring J, Humphrey C, Cook EH (1991) Hepatitis C virus: buoyant density of the factor VIII-derived isolate in sucrose. J Med Virol 34: 206-8

Bressanelli S, Tomei L, Roussel A, Incitti I, Vitale RL, Mathieu M, De Francesco R, Rey FA (1999) Crystal structure of the RNA-dependent RNA polymerase of hepatitis C virus. Proc Natl Acad Sci U S A 96: 13034-9

Brimacombe CL, Grove J, Meredith LW, Hu K, Syder AJ, Flores MV, Timpe JM, Krieger SE, Baumert TF, Tellinghuisen TL, Wong-Staal F, Balfe P, McKeating JA (2011) Neutralizing antibody-resistant hepatitis C virus cell-to-cell transmission. J Virol 85: 596-605

Brohm C, Steinmann E, Friesland M, Lorenz IC, Patel A, Penin F, Bartenschlager R, Pietschmann T (2009) Characterization of determinants important for hepatitis C virus p7 function in morphogenesis by using trans-complementation. J Virol 83: 11682-93

Bukong TN, Momen-Heravi F, Kodys K, Bala S, Szabo G (2014) Exosomes from hepatitis C infected patients transmit HCV infection and contain replication competent viral RNA in complex with Ago2-miR122-HSP90. PLoS Pathog 10: e1004424

Cai H, Yao W, Li L, Li X, Hu L, Mai R, Peng T (2016) Cell-death-inducing DFFA-like Effector B Contributes to the Assembly of Hepatitis C Virus (HCV) Particles and Interacts with HCV NS5A. Sci Rep 6: 27778

Calattini S, Fusil F, Mancip J, Dao Thi VL, Granier C, Gadot N, Scoazec JY, Zeisel MB, Baumert TF, Lavillette D, Dreux M, Cosset FL (2015) Functional and Biochemical Characterization of Hepatitis C Virus (HCV) Particles Produced in a Humanized Liver Mouse Model. J Biol Chem 290: 23173-87

Camus G, Herker E, Modi AA, Haas JT, Ramage HR, Farese RV, Jr., Ott M (2013) Diacylglycerol acyltransferase-1 localizes hepatitis C virus NS5A protein to lipid droplets and enhances NS5A interaction with the viral capsid core. J Biol Chem 288: 9915-23

Carrasco L (1978) Membrane leakiness after viral infection and a new approach to the development of antiviral agents. Nature 272: 694-9

Carrere-Kremer S, Montpellier-Pala C, Cocquerel L, Wychowski C, Penin F, Dubuisson J (2002) Subcellular localization and topology of the p7 polypeptide of hepatitis C virus. J Virol 76: 3720-30

Catanese MT, Dorner M (2015) Advances in experimental systems to study hepatitis C virus in vitro and in vivo. Virology 479-480: 221-33

Catanese MT, Uryu K, Kopp M, Edwards TJ, Andrus L, Rice WJ, Silvestry M, Kuhn RJ, Rice CM (2013) Ultrastructural analysis of hepatitis C virus particles. Proc Natl Acad Sci U S A 110: 9505-10

Cavrois M, De Noronha C, Greene WC (2002) A sensitive and specific enzyme-based assay detecting HIV-1 virion fusion in primary T lymphocytes. Nat Biotechnol 20: 1151-4

Cerino A, Bissolati M, Cividini A, Nicosia A, Esumi M, Hayashi N, Mizuno K, Slobbe R, Oudshoorn P, Silini E, Asti M, Mondelli MU (1997) Antibody responses to the hepatitis C virus E2 protein: relationship to viraemia and prevalence in anti-HCV seronegative subjects. J Med Virol 51: 1-5

Chan ST, Ou JJ (2017) Hepatitis C Virus-Induced Autophagy and Host Innate Immune Response. Viruses 9

Chandler DE, Penin F, Schulten K, Chipot C (2012) The p7 protein of hepatitis C virus forms structurally plastic, minimalist ion channels. PLoS Comput Biol 8: e1002702

Chang KS, Jiang J, Cai Z, Luo G (2007) Human apolipoprotein e is required for infectivity and production of hepatitis C virus in cell culture. J Virol 81: 13783-93

Chatel-Chaix L, Melancon P, Racine ME, Baril M, Lamarre D (2011) Y-box-binding protein 1 interacts with hepatitis C virus NS3/4A and influences the equilibrium between viral RNA replication and infectious particle production. J Virol 85: 11022-37

Chen X, Van Valkenburgh C, Fang H, Green N (1999) Signal peptides having standard and nonstandard cleavage sites can be processed by Imp1p of the mitochondrial inner membrane protease. J Biol Chem 274: 37750-4

Chi X, Niu Y, Cheng M, Liu X, Feng Y, Zheng F, Fan J, Li X, Jin Q, Zhong J, Li YP, Yang W (2016) Identification of a Potent and Broad-Spectrum Hepatitis C Virus Fusion Inhibitory Peptide from the E2 Stem Domain. Sci Rep 6: 25224

Choo QL, Richman KH, Han JH, Berger K, Lee C, Dong C, Gallegos C, Coit D, Medina-Selby R, Barr PJ, et al. (1991) Genetic organization and diversity of the hepatitis C virus. Proc Natl Acad Sci U S A 88: 2451-5

Chukkapalli V, Berger KL, Kelly SM, Thomas M, Deiters A, Randall G (2015) Daclatasvir inhibits hepatitis C virus NS5A motility and hyper-accumulation of phosphoinositides. Virology 476: 168-79

Clarke D, Griffin S, Beales L, Gelais CS, Burgess S, Harris M, Rowlands D (2006) Evidence for the formation of a heptameric ion channel complex by the hepatitis C virus p7 protein in vitro. J Biol Chem 281: 37057-68

Clayton RF, Owsianka A, Aitken J, Graham S, Bhella D, Patel AH (2002) Analysis of antigenicity and topology of E2 glycoprotein present on recombinant hepatitis C virus-like particles. J Virol 76: 7672-82

Cocquerel L, Duvet S, Meunier JC, Pillez A, Cacan R, Wychowski C, Dubuisson J (1999) The transmembrane domain of hepatitis C virus glycoprotein E1 is a signal for static retention in the endoplasmic reticulum. J Virol 73: 2641-9

Cocquerel L, Kuo CC, Dubuisson J, Levy S (2003) CD81-dependent binding of hepatitis C virus E1E2 heterodimers. J Virol 77: 10677-83

Cocquerel L, Op de Beeck A, Lambot M, Roussel J, Delgrange D, Pillez A, Wychowski C, Penin F, Dubuisson J (2002) Topological changes in the transmembrane domains of hepatitis C virus envelope glycoproteins. EMBO J 21: 2893-902

Coller KE, Heaton NS, Berger KL, Cooper JD, Saunders JL, Randall G (2012) Molecular determinants and dynamics of hepatitis C virus secretion. PLoS Pathog 8: e1002466

Cook GA, Dawson LA, Tian Y, Opella SJ (2013) Three-dimensional structure and interaction studies of hepatitis C virus p7 in 1,2-dihexanoyl-sn-glycero-3-phosphocholine by solution nuclear magnetic resonance. Biochemistry 52: 5295-303

Corless L, Crump CM, Griffin SD, Harris M (2010) Vps4 and the ESCRT-III complex are required for the release of infectious hepatitis C virus particles. J Gen Virol 91: 362-72

Cornell CT, Kiosses WB, Harkins S, Whitton JL (2007) Coxsackievirus B3 proteins directionally complement each other to downregulate surface major histocompatibility complex class I. J Virol 81: 6785-97

Cucuianu M, Coca M, Hancu N (2007) Reverse cholesterol transport and atherosclerosis. A mini review. Rom J Intern Med 45: 17-27

Cun W, Jiang J, Luo G (2010) The C-terminal alpha-helix domain of apolipoprotein E is required for interaction with nonstructural protein 5A and assembly of hepatitis C virus. J Virol 84: 11532-41

Da Costa D, Turek M, Felmlee DJ, Girardi E, Pfeffer S, Long G, Bartenschlager R, Zeisel MB, Baumert TF (2012) Reconstitution of the entire hepatitis C virus life cycle in nonhepatic cells. J Virol 86: 11919-25

Dahari H, Feinstone SM, Major ME (2010) Meta-analysis of hepatitis C virus vaccine efficacy in chimpanzees indicates an importance for structural proteins. Gastroenterology 139: 965-74

Dalbey RE, Lively MO, Bron S, van Dijl JM (1997) The chemistry and enzymology of the type I signal peptidases. Protein Sci 6: 1129-38

Dallinga-Thie GM, Franssen R, Mooij HL, Visser ME, Hassing HC, Peelman F, Kastelein JJ, Peterfy M, Nieuwdorp M (2010) The metabolism of triglyceride-rich lipoproteins revisited: new players, new insight. Atherosclerosis 211: 1-8

Dansako H, Hiramoto H, Ikeda M, Wakita T, Kato N (2014) Rab18 is required for viral assembly of hepatitis C virus through trafficking of the core protein to lipid droplets. Virology 462-463: 166-74

Dao Thi VL, Granier C, Zeisel MB, Guerin M, Mancip J, Granio O, Penin F, Lavillette D, Bartenschlager R, Baumert TF, Cosset FL, Dreux M (2012) Characterization of hepatitis C virus particle subpopulations reveals multiple usage of the scavenger receptor BI for entry steps. J Biol Chem 287: 31242-57

de Jong AS, de Mattia F, Van Dommelen MM, Lanke K, Melchers WJ, Willems PH, van Kuppeveld FJ (2008) Functional analysis of picornavirus 2B proteins: effects on calcium homeostasis and intracellular protein trafficking. J Virol 82: 3782-90

Denolly S, Cosset FL (2017) A master regulator of tight junctions involved in hepatitis C virus entry and pathogenesis. Hepatology 65: 1756-1758

Denolly S, Mialon C, Bourlet T, Amirache F, Penin F, Lindenbach B, Boson B, Cosset FL (2017) The amino-terminus of the hepatitis C virus (HCV) p7 viroporin and its cleavage from glycoprotein E2-p7 precursor determine specific infectivity and secretion levels of HCV particle types. PLoS Pathog 13: e1006774

Diao J, Pantua H, Ngu H, Komuves L, Diehl L, Schaefer G, Kapadia SB (2012) Hepatitis C virus induces epidermal growth factor receptor activation via CD81 binding for viral internalization and entry. J Virol 86: 10935-49

Diaz O, Delers F, Maynard M, Demignot S, Zoulim F, Chambaz J, Trepo C, Lotteau V, Andre P (2006) Preferential association of Hepatitis C virus with apolipoprotein B48-containing lipoproteins. J Gen Virol 87: 2983-91

Doedens JR, Kirkegaard K (1995) Inhibition of cellular protein secretion by poliovirus proteins 2B and 3A. EMBO J 14: 894-907

Dorner M, Horwitz JA, Donovan BM, Labitt RN, Budell WC, Friling T, Vogt A, Catanese MT, Satoh T, Kawai T, Akira S, Law M, Rice CM, Ploss A (2013) Completion of the entire hepatitis C virus life cycle in genetically humanized mice. Nature 501: 237-41

Dorner M, Horwitz JA, Robbins JB, Barry WT, Feng Q, Mu K, Jones CT, Schoggins JW, Catanese MT, Burton DR, Law M, Rice CM, Ploss A (2011) A genetically humanized mouse model for hepatitis C virus infection. Nature 474: 208-11

Douam F, Lavillette D, Cosset FL (2015) The mechanism of HCV entry into host cells. Prog Mol Biol Transl Sci 129: 63-107

Dreux M, Boson B, Ricard-Blum S, Molle J, Lavillette D, Bartosch B, Pecheur EI, Cosset FL (2007a) The exchangeable apolipoprotein APOC-I promotes membrane fusion of hepatitis C virus. J Biol Chem 282: 32357-32369

Dreux M, Boson B, Ricard-Blum S, Molle J, Lavillette D, Bartosch B, Pecheur EI, Cosset FL (2007b) The exchangeable apolipoprotein ApoC-I promotes membrane fusion of hepatitis C virus. J Biol Chem 282: 32357-69

Dreux M, Dao Thi VL, Fresquet J, Guerin M, Julia Z, Verney G, Durantel D, Zoulim F, Lavillette D, Cosset* FL, Bartosch* B (2009a) Receptor complementation and

mutagenesis reveal SR-BI as an essential HCV entry factor and functionally imply its intra- and extra-cellular domains. PLoS pathogens 5: e1000310

Dreux M, Garaigorta U, Boyd B, Decembre E, Chung J, Whitten-Bauer C, Wieland S, Chisari FV (2012) Short-range exosomal transfer of viral RNA from infected cells to plasmacytoid dendritic cells triggers innate immunity. Cell Host Microbe 12: 558-70

Dreux M, Gastaminza P, Wieland SF, Chisari FV (2009b) The autophagy machinery is required to initiate hepatitis C virus replication. Proc Natl Acad Sci U S A 106: 14046-51

Dreux M, Pietschmann T, Granier C, Voisset C, Ricard-Blum S, Mangeot PE, Keck Z, Foung S, Vu-Dac N, Dubuisson J, Bartenschlager R, Lavillette D, Cosset FL (2006) High density lipoprotein inhibits hepatitis C virus-neutralizing antibodies by stimulating cell entry via activation of the scavenger receptor BI. J Biol Chem 281: 18285-95

Drummer HE, Boo I, Maerz AL, Poumbourios P (2006) A conserved Gly436-Trp-Leu-Ala-Gly-Leu-Phe-Tyr motif in hepatitis C virus glycoprotein E2 is a determinant of CD81 binding and viral entry. J Virol 80: 7844-53

Drummer HE, Boo I, Poumbourios P (2007) Mutagenesis of a conserved fusion peptide-like motif and membrane-proximal heptad-repeat region of hepatitis C virus glycoprotein E1. J Gen Virol 88: 1144-8

Drummer HE, Maerz A, Poumbourios P (2003) Cell surface expression of functional hepatitis C virus E1 and E2 glycoproteins. FEBS Lett 546: 385-90

Dubuisson J (2000) Folding, assembly and subcellular localization of hepatitis C virus glycoproteins. Curr Top Microbiol Immunol 242: 135-48

Dubuisson J, Cosset FL (2014) Virology and cell biology of the hepatitis C virus life cycle: an update. J Hepatol 61: S3-S13

Earnest-Silveira L, Christiansen D, Herrmann S, Ralph SA, Das S, Gowans EJ, Torresi J (2016) Large scale production of a mammalian cell derived quadrivalent hepatitis C virus like particle vaccine. J Virol Methods 236: 87-92

Eckel RH (1989) Lipoprotein lipase. A multifunctional enzyme relevant to common metabolic diseases. N Engl J Med 320: 1060-8

Einav S, Gerber D, Bryson PD, Sklan EH, Elazar M, Maerkl SJ, Glenn JS, Quake SR (2008) Discovery of a hepatitis C target and its pharmacological inhibitors by microfluidic affinity analysis. Nat Biotechnol 26: 1019-27

El Omari K, Iourin O, Kadlec J, Sutton G, Harlos K, Grimes JM, Stuart DI (2014) Unexpected structure for the N-terminal domain of hepatitis C virus envelope glycoprotein E1. Nat Commun 5: 4874

Elgner F, Donnerhak C, Ren H, Medvedev R, Schreiber A, Weber L, Heilmann M, Ploen D, Himmelsbach K, Finkernagel M, Klingel K, Hildt E (2016) Characterization of alpha-

taxilin as a novel factor controlling the release of hepatitis C virus. Biochem J 473: 145-55

Estes C, Abdel-Kareem M, Abdel-Razek W, Abdel-Sameea E, Abuzeid M, Gomaa A, Osman W, Razavi H, Zaghla H, Waked I (2015) Economic burden of hepatitis C in Egypt: the future impact of highly effective therapies. Aliment Pharmacol Ther 42: 696-706

Evans EA, Gilmore R, Blobel G (1986) Purification of microsomal signal peptidase as a complex. Proc Natl Acad Sci U S A 83: 581-5

Evans MJ, von Hahn T, Tscherne DM, Syder AJ, Panis M, Wolk B, Hatziioannou T, McKeating JA, Bieniasz PD, Rice CM (2007) Claudin-1 is a hepatitis C virus co-receptor required for a late step in entry. Nature 446: 801-5

Ewart GD, Mills K, Cox GB, Gage PW (2002) Amiloride derivatives block ion channel activity and enhancement of virus-like particle budding caused by HIV-1 protein Vpu. Eur Biophys J 31: 26-35

Ewart GD, Sutherland T, Gage PW, Cox GB (1996) The Vpu protein of human immunodeficiency virus type 1 forms cation-selective ion channels. Journal of Virology 70: 7108-7115

Fahmy AM, Labonte P (2017) The autophagy elongation complex (ATG5-12/16L1) positively regulates HCV replication and is required for wild-type membranous web formation. Sci Rep 7: 40351

Failla C, Tomei L, De Francesco R (1994) Both NS3 and NS4A are required for proteolytic processing of hepatitis C virus nonstructural proteins. J Virol 68: 3753-60

Fang H, Panzner S, Mullins C, Hartmann E, Green N (1996) The homologue of mammalian SPC12 is important for efficient signal peptidase activity in Saccharomyces cerevisiae. J Biol Chem 271: 16460-5

Farci P, Alter HJ, Shimoda A, Govindarajan S, Cheung LC, Melpolder JC, Sacher RA, Shih JW, Purcell RH (1996) Hepatitis C virus-associated fulminant hepatic failure. N Engl J Med 335: 631-4

Farci P, Alter HJ, Wong DC, Miller RH, Govindarajan S, Engle R, Shapiro M, Purcell RH (1994) Prevention of hepatitis C virus infection in chimpanzees after antibody-mediated in vitro neutralization. Proc Natl Acad Sci U S A 91: 7792-6

Farci P, Shimoda A, Coiana A, Diaz G, Peddis G, Melpolder JC, Strazzera A, Chien DY, Munoz SJ, Balestrieri A, Purcell RH, Alter HJ (2000) The outcome of acute hepatitis C predicted by the evolution of the viral quasispecies. Science 288: 339-44

Farquhar MJ, Hu K, Harris HJ, Davis C, Brimacombe CL, Fletcher SJ, Baumert TF, Rappoport JZ, Balfe P, McKeating JA (2012) Hepatitis C virus induces CD81 and claudin-1 endocytosis. J Virol 86: 4305-16

Feingold KR, Grunfeld C (2000) Introduction to Lipids and Lipoproteins. In Endotext, De Groot LJ, Chrousos G, Dungan K, Feingold KR, Grossman A, Hershman JM, Koch C, Korbonits M, McLachlan R, New M, Purnell J, Rebar R, Singer F, Vinik A (eds) South Dartmouth (MA):

Felmlee DJ, Hafirassou ML, Lefevre M, Baumert TF, Schuster C (2013) Hepatitis C virus, cholesterol and lipoproteins--impact for the viral life cycle and pathogenesis of liver disease. Viruses 5: 1292-324

Felmlee DJ, Sheridan DA, Bridge SH, Nielsen SU, Milne RW, Packard CJ, Caslake MJ, McLauchlan J, Toms GL, Neely RD, Bassendine MF (2010) Intravascular transfer contributes to postprandial increase in numbers of very-low-density hepatitis C virus particles. Gastroenterology 139: 1774-83, 1783 e1-6

Feneant L, Potel J, Francois C, Sane F, Douam F, Belouzard S, Calland N, Vausselin T, Rouille Y, Descamps V, Baumert TF, Duverlie G, Lavillette D, Hober D, Dubuisson J, Wychowski C, Cocquerel L (2015) New Insights into the Understanding of Hepatitis C Virus Entry and Cell-to-Cell Transmission by Using the Ionophore Monensin A. J Virol 89: 8346-64

Fletcher NF, Sutaria R, Jo J, Barnes A, Blahova M, Meredith LW, Cosset FL, Curbishley SM, Adams DH, Bertoletti A, McKeating JA (2014) Activated macrophages promote hepatitis C virus entry in a tumor necrosis factor-dependent manner. Hepatology 59: 1320-30

Flint M, Maidens C, Loomis-Price LD, Shotton C, Dubuisson J, Monk P, Higginbottom A, Levy S, McKeating JA (1999) Characterization of hepatitis C virus E2 glycoprotein interaction with a putative cellular receptor, CD81. J Virol 73: 6235-44

Fofana I, Xiao F, Thumann C, Turek M, Zona L, Tawar RG, Grunert F, Thompson J, Zeisel MB, Baumert TF (2013) A novel monoclonal anti-CD81 antibody produced by genetic immunization efficiently inhibits Hepatitis C virus cell-cell transmission. PLoS One 8: e64221

Foster TL, Belyaeva T, Stonehouse NJ, Pearson AR, Harris M (2010) All three domains of the hepatitis C virus nonstructural NS5A protein contribute to RNA binding. J Virol 84: 9267-77

Foster TL, Thompson GS, Kalverda AP, Kankanala J, Bentham M, Wetherill LF, Thompson J, Barker AM, Clarke D, Noerenberg M, Pearson AR, Rowlands DJ, Homans SW, Harris M, Foster R, Griffin S (2014) Structure-guided design affirms inhibitors of hepatitis C virus p7 as a viable class of antivirals targeting virion release. Hepatology 59: 408-22

Fukuhara T, Kambara H, Shiokawa M, Ono C, Katoh H, Morita E, Okuzaki D, Maehara Y, Koike K, Matsuura Y (2012) Expression of microRNA miR-122 facilitates an efficient replication in nonhepatic cells upon infection with hepatitis C virus. J Virol 86: 7918-33

Fukuhara T, Tamura T, Ono C, Shiokawa M, Mori H, Uemura K, Yamamoto S, Kurihara T, Okamoto T, Suzuki R, Yoshii K, Kurosu T, Igarashi M, Aoki H, Sakoda Y, Matsuura Y (2017) Host-derived apolipoproteins play comparable roles with viral secretory

proteins Erns and NS1 in the infectious particle formation of Flaviviridae. PLoS Pathog 13: e1006475

Fukuhara T, Wada M, Nakamura S, Ono C, Shiokawa M, Yamamoto S, Motomura T, Okamoto T, Okuzaki D, Yamamoto M, Saito I, Wakita T, Koike K, Matsuura Y (2014) Amphipathic alpha-helices in apolipoproteins are crucial to the formation of infectious hepatitis C virus particles. PLoS Pathog 10: e1004534

Gan SW, Surya W, Vararattanavech A, Torres J (2014) Two different conformations in hepatitis C virus p7 protein account for proton transport and dye release. PLoS One 9: e78494

Gao M, Nettles RE, Belema M, Snyder LB, Nguyen VN, Fridell RA, Serrano-Wu MH, Langley DR, Sun JH, O'Boyle DR, 2nd, Lemm JA, Wang C, Knipe JO, Chien C, Colonno RJ, Grasela DM, Meanwell NA, Hamann LG (2010) Chemical genetics strategy identifies an HCV NS5A inhibitor with a potent clinical effect. Nature 465: 96-100

Garrone P, Fluckiger AC, Mangeot PE, Gauthier E, Dupeyrot-Lacas P, Mancip J, Cangialosi A, Du Chene I, LeGrand R, Mangeot I, Lavillette D, Bellier B, Cosset FL, Tangy F, Klatzmann D, Dalba C (2011) A prime-boost strategy using virus-like particles pseudotyped for HCV proteins triggers broadly neutralizing antibodies in macaques. Sci Transl Med 3: 94ra71

Gastaminza P, Cheng G, Wieland S, Zhong J, Liao W, Chisari FV (2008) Cellular determinants of hepatitis C virus assembly, maturation, degradation, and secretion. J Virol 82: 2120-9

Gastaminza P, Dryden KA, Boyd B, Wood MR, Law M, Yeager M, Chisari FV (2010) Ultrastructural and biophysical characterization of hepatitis C virus particles produced in cell culture. J Virol 84: 10999-1009

Gastaminza P, Kapadia SB, Chisari FV (2006) Differential biophysical properties of infectious intracellular and secreted hepatitis C virus particles. J Virol 80: 11074-81

Gentzsch J, Brohm C, Steinmann E, Friesland M, Menzel N, Vieyres G, Perin PM, Frentzen A, Kaderali L, Pietschmann T (2013) Hepatitis C Virus p7 is Critical for Capsid Assembly and Envelopment. PLoS Pathog 9: e1003355

Giang E, Dorner M, Prentoe JC, Dreux M, Evans MJ, Bukh J, Rice CM, Ploss A, Burton DR, Law M (2012) Human broadly neutralizing antibodies to the envelope glycoprotein complex of hepatitis C virus. Proc Natl Acad Sci U S A 109: 6205-10

Goffard A, Dubuisson J (2003) Glycosylation of hepatitis C virus envelope proteins. Biochimie 85: 295-301

Gondar V, Molina-Jimenez F, Hishiki T, Garcia-Buey L, Koutsoudakis G, Shimotohno K, Benedicto I, Majano PL (2015) Apolipoprotein E, but Not Apolipoprotein B, Is Essential for Efficient Cell-to-Cell Transmission of Hepatitis C Virus. J Virol 89: 9962-73

Gordon DA, Jamil H (2000) Progress towards understanding the role of microsomal triglyceride transfer protein in apolipoprotein-B lipoprotein assembly. Biochim Biophys Acta 1486: 72-83

Gottwein JM, Scheel TK, Callendret B, Li YP, Eccleston HB, Engle RE, Govindarajan S, Satterfield W, Purcell RH, Walker CM, Bukh J (2010) Novel infectious cDNA clones of hepatitis C virus genotype 3a (strain S52) and 4a (strain ED43): genetic analyses and in vivo pathogenesis studies. J Virol 84: 5277-93

Gottwein JM, Scheel TK, Hoegh AM, Lademann JB, Eugen-Olsen J, Lisby G, Bukh J (2007) Robust hepatitis C genotype 3a cell culture releasing adapted intergenotypic 3a/2a (S52/JFH1) viruses. Gastroenterology 133: 1614-26

Gottwein JM, Scheel TK, Jensen TB, Lademann JB, Prentoe JC, Knudsen ML, Hoegh AM, Bukh J (2009) Development and characterization of hepatitis C virus genotype 1-7 cell culture systems: role of CD81 and scavenger receptor class B type I and effect of antiviral drugs. Hepatology 49: 364-77

Gouttenoire J, Montserret R, Paul D, Castillo R, Meister S, Bartenschlager R, Penin F, Moradpour D (2014) Aminoterminal amphipathic alpha-helix AH1 of hepatitis C virus nonstructural protein 4B possesses a dual role in RNA replication and virus production. PLoS Pathog 10: e1004501

Grakoui A, Wychowski C, Lin C, Feinstone SM, Rice CM (1993) Expression and identification of hepatitis C virus polyprotein cleavage products. J Virol 67: 1385-95

Griffin S, Clarke D, McCormick C, Rowlands D, Harris M (2005) Signal peptide cleavage and internal targeting signals direct the hepatitis C virus p7 protein to distinct intracellular membranes. J Virol 79: 15525-36

Griffin S, Stgelais C, Owsianka AM, Patel AH, Rowlands D, Harris M (2008) Genotype-dependent sensitivity of hepatitis C virus to inhibitors of the p7 ion channel. Hepatology 48: 1779-90

Griffin SD, Beales LP, Clarke DS, Worsfold O, Evans SD, Jaeger J, Harris MP, Rowlands DJ (2003) The p7 protein of hepatitis C virus forms an ion channel that is blocked by the antiviral drug, Amantadine. FEBS Lett 535: 34-8

Griffin SD, Harvey R, Clarke DS, Barclay WS, Harris M, Rowlands DJ (2004) A conserved basic loop in hepatitis C virus p7 protein is required for amantadine-sensitive ion channel activity in mammalian cells but is dispensable for localization to mitochondria. J Gen Virol 85: 451-61

Grompe M, al-Dhalimy M, Finegold M, Ou CN, Burlingame T, Kennaway NG, Soriano P (1993) Loss of fumarylacetoacetate hydrolase is responsible for the neonatal hepatic dysfunction phenotype of lethal albino mice. Genes Dev 7: 2298-307

Grompe M, Lindstedt S, al-Dhalimy M, Kennaway NG, Papaconstantinou J, Torres-Ramos CA, Ou CN, Finegold M (1995) Pharmacological correction of neonatal lethal hepatic dysfunction in a murine model of hereditary tyrosinaemia type I. Nat Genet 10: 453-60

Grove J, Nielsen S, Zhong J, Bassendine MF, Drummer HE, Balfe P, McKeating JA (2008) Identification of a residue in hepatitis C virus E2 glycoprotein that determines scavenger receptor BI and CD81 receptor dependency and sensitivity to neutralizing antibodies. J Virol 82: 12020-9

Gu M, Rice CM (2010) Three conformational snapshots of the hepatitis C virus NS3 helicase reveal a ratchet translocation mechanism. Proc Natl Acad Sci U S A 107: 521-8

Guedj J, Dahari H, Uprichard SL, Perelson AS (2013) The hepatitis C virus NS5A inhibitor daclatasvir has a dual mode of action and leads to a new virus half-life estimate. Expert Rev Gastroenterol Hepatol 7: 397-9

Guevin C, Manna D, Belanger C, Konan KV, Mak P, Labonte P (2010) Autophagy protein ATG5 interacts transiently with the hepatitis C virus RNA polymerase (NS5B) early during infection. Virology 405: 1-7

Gusarova V, Brodsky JL, Fisher EA (2003) Apolipoprotein B100 exit from the endoplasmic reticulum (ER) is COPII-dependent, and its lipidation to very low density lipoprotein occurs post-ER. J Biol Chem 278: 48051-8

Gusarova V, Seo J, Sullivan ML, Watkins SC, Brodsky JL, Fisher EA (2007) Golgi-associated maturation of very low density lipoproteins involves conformational changes in apolipoprotein B, but is not dependent on apolipoprotein E. J Biol Chem 282: 19453-62

Hagen N, Bayer K, Rosch K, Schindler M (2014) The intraviral protein interaction network of hepatitis C virus. Mol Cell Proteomics 13: 1676-89

Haid S, Pietschmann T, Pecheur EI (2009) Low pH-dependent hepatitis C virus membrane fusion depends on E2 integrity, target lipid composition, and density of virus particles. J Biol Chem 284: 17657-67

Hajarizadeh B, Grebely J, Dore GJ (2013) Epidemiology and natural history of HCV infection. Nat Rev Gastroenterol Hepatol 10: 553-62

Han Q, Manna D, Belton K, Cole R, Konan KV (2013) Modulation of hepatitis C virus genome encapsidation by nonstructural protein 4B. J Virol 87: 7409-22

Handley MA, Paddock S, Dall A, Panganiban AT (2001) Association of Vpu-binding protein with microtubules and Vpu-dependent redistribution of HIV-1 Gag protein. Virology 291: 198-207

Hansen MD, Johnsen IB, Stiberg KA, Sherstova T, Wakita T, Richard GM, Kandasamy RK, Meurs EF, Anthonsen MW (2017) Hepatitis C virus triggers Golgi fragmentation and

autophagy through the immunity-related GTPase M. Proc Natl Acad Sci U S A 114: E3462-E3471

Haqshenas G, Mackenzie JM, Dong X, Gowans EJ (2007) Hepatitis C virus p7 protein is localized in the endoplasmic reticulum when it is encoded by a replication-competent genome. J Gen Virol 88: 134-42

Harak C, Meyrath M, Romero-Brey I, Schenk C, Gondeau C, Schult P, Esser-Nobis K, Saeed M, Neddermann P, Schnitzler P, Gotthardt D, Perez-Del-Pulgar S, Neumann-Haefelin C, Thimme R, Meuleman P, Vondran FW, Francesco R, Rice CM, Bartenschlager R, Lohmann V (2016) Tuning a cellular lipid kinase activity adapts hepatitis C virus to replication in cell culture. Nat Microbiol 2: 16247

Harding C, Heuser J, Stahl P (1984) Endocytosis and intracellular processing of transferrin and colloidal gold-transferrin in rat reticulocytes: demonstration of a pathway for receptor shedding. Eur J Cell Biol 35: 256-63

Harris HJ, Davis C, Mullins JG, Hu K, Goodall M, Farquhar MJ, Mee CJ, McCaffrey K, Young S, Drummer H, Balfe P, McKeating JA (2010) Claudin association with CD81 defines hepatitis C virus entry. J Biol Chem 285: 21092-102

Harris HJ, Farquhar MJ, Mee CJ, Davis C, Reynolds GM, Jennings A, Hu K, Yuan F, Deng H, Hubscher SG, Han JH, Balfe P, McKeating JA (2008) CD81 and claudin 1 coreceptor association: role in hepatitis C virus entry. J Virol 82: 5007-20

Heim MH (2013) 25 years of interferon-based treatment of chronic hepatitis C: an epoch coming to an end. Nat Rev Immunol 13: 535-42

Heim MH, Thimme R (2014) Innate and adaptive immune responses in HCV infections. J Hepatol 61: S14-25

Helle F, Goffard A, Morel V, Duverlie G, McKeating J, Keck ZY, Foung S, Penin F, Dubuisson J, Voisset C (2007) The neutralizing activity of anti-hepatitis C virus antibodies is modulated by specific glycans on the E2 envelope protein. J Virol 81: 8101-11

Helle F, Vieyres G, Elkrief L, Popescu CI, Wychowski C, Descamps V, Castelain S, Roingeard P, Duverlie G, Dubuisson J (2010) Role of N-linked glycans in the functions of hepatitis C virus envelope proteins incorporated into infectious virions. J Virol 84: 11905-15

Henkel JR, Popovich JL, Gibson GA, Watkins SC, Weisz OA (1999) Selective perturbation of early endosome and/or trans-Golgi network pH but not lysosome pH by dose-dependent expression of influenza M2 protein. J Biol Chem 274: 9854-60

Henkel JR, Weisz OA (1998) Influenza virus M2 protein slows traffic along the secretory pathway. pH perturbation of acidified compartments affects early Golgi transport steps. J Biol Chem 273: 6518-24

Herker E, Harris C, Hernandez C, Carpentier A, Kaehlcke K, Rosenberg AR, Farese RV, Jr., Ott M (2010) Efficient hepatitis C virus particle formation requires diacylglycerol acyltransferase-1. Nat Med 16: 1295-8

Herker E, Ott M (2012) Emerging role of lipid droplets in host/pathogen interactions. J Biol Chem 287: 2280-7

Hishiki T, Shimizu Y, Tobita R, Sugiyama K, Ogawa K, Funami K, Ohsaki Y, Fujimoto T, Takaku H, Wakita T, Baumert TF, Miyanari Y, Shimotohno K (2010) Infectivity of hepatitis C virus is influenced by association with apolipoprotein E isoforms. J Virol 84: 12048-57

Honda M, Ping LH, Rijnbrand RC, Amphlett E, Clarke B, Rowlands D, Lemon SM (1996) Structural requirements for initiation of translation by internal ribosome entry within genome-length hepatitis C virus RNA. Virology 222: 31-42

Horner SM, Gale M, Jr. (2013) Regulation of hepatic innate immunity by hepatitis C virus. Nat Med 19: 879-88

Hsu K, Han J, Shinlapawittayatorn K, Deschenes I, Marban E (2010) Membrane Potential Depolarization as a Triggering Mechanism for Vpu-Mediated HIV-1 Release. Biophys J 99: 1718-1725

Hsu M, Zhang J, Flint M, Logvinoff C, Cheng-Mayer C, Rice CM, McKeating JA (2003) Hepatitis C virus glycoproteins mediate pH-dependent cell entry of pseudotyped retroviral particles. Proc Natl Acad Sci U S A 100: 7271-6

Huang H, Sun F, Owen DM, Li W, Chen Y, Gale M, Jr., Ye J (2007) Hepatitis C virus production by human hepatocytes dependent on assembly and secretion of very low-density lipoproteins. Proc Natl Acad Sci U S A 104: 5848-53

Huang L, Hwang J, Sharma SD, Hargittai MR, Chen Y, Arnold JJ, Raney KD, Cameron CE (2005) Hepatitis C virus nonstructural protein 5A (NS5A) is an RNA-binding protein. J Biol Chem 280: 36417-28

Hueging K, Doepke M, Vieyres G, Bankwitz D, Frentzen A, Doerrbecker J, Gumz F, Haid S, Wolk B, Kaderali L, Pietschmann T (2014) Apolipoprotein E codetermines tissue tropism of hepatitis C virus and is crucial for viral cell-to-cell transmission by contributing to a postenvelopment step of assembly. J Virol 88: 1433-46

Hui AY, Friedman SL (2003) Molecular basis of hepatic fibrosis. Expert Rev Mol Med 5: 1-23

Hui JM, Sud A, Farrell GC, Bandara P, Byth K, Kench JG, McCaughan GW, George J (2003) Insulin resistance is associated with chronic hepatitis C virus infection and fibrosis progression [corrected]. Gastroenterology 125: 1695-704

Hussain MM, Bakillah A, Nayak N, Shelness GS (1998) Amino acids 430-570 in apolipoprotein B are critical for its binding to microsomal triglyceride transfer protein. J Biol Chem 273: 25612-5

Hutagalung AH, Novick PJ (2011) Role of Rab GTPases in membrane traffic and cell physiology. Physiol Rev 91: 119-49

Hyser JM, Collinson-Pautz MR, Utama B, Estes MK (2010) Rotavirus disrupts calcium homeostasis by NSP4 viroporin activity. MBio 1

Icard V, Diaz O, Scholtes C, Perrin-Cocon L, Ramiere C, Bartenschlager R, Penin F, Lotteau V, Andre P (2009) Secretion of hepatitis C virus envelope glycoproteins depends on assembly of apolipoprotein B positive lipoproteins. PLoS One 4: e4233

Isherwood BJ, Patel AH (2005) Analysis of the processing and transmembrane topology of the E2p7 protein of hepatitis C virus. J Gen Virol 86: 667-76

Ishido S, Fujita T, Hotta H (1998) Complex formation of NS5B with NS3 and NS4A proteins of hepatitis C virus. Biochem Biophys Res Commun 244: 35-40

Jackel-Cram C, Babiuk LA, Liu Q (2007) Up-regulation of fatty acid synthase promoter by hepatitis C virus core protein: genotype-3a core has a stronger effect than genotype-1b core. J Hepatol 46: 999-1008

Jammart B, Michelet M, Pecheur EI, Parent R, Bartosch B, Zoulim F, Durantel D (2013) Very-low-density lipoprotein (VLDL)-producing and hepatitis C virus-replicating HepG2 cells secrete no more lipoviroparticles than VLDL-deficient Huh7.5 cells. J Virol 87: 5065-80

Jensen TB, Gottwein JM, Scheel TK, Hoegh AM, Eugen-Olsen J, Bukh J (2008) Highly efficient JFH1-based cell-culture system for hepatitis C virus genotype 5a: failure of homologous neutralizing-antibody treatment to control infection. J Infect Dis 198: 1756-65

Jheng JR, Ho JY, Horng JT (2014) ER stress, autophagy, and RNA viruses. Front Microbiol 5: 388

Jiang J, Luo G (2009) Apolipoprotein E but not B is required for the formation of infectious hepatitis C virus particles. J Virol 83: 12680-91

Jirasko V, Montserret R, Appel N, Janvier A, Eustachi L, Brohm C, Steinmann E, Pietschmann T, Penin F, Bartenschlager R (2008) Structural and functional characterization of nonstructural protein 2 for its role in hepatitis C virus assembly. J Biol Chem 283: 28546-62

Jirasko V, Montserret R, Lee JY, Gouttenoire J, Moradpour D, Penin F, Bartenschlager R (2010) Structural and Functional Studies of Nonstructural Protein 2 of the Hepatitis C Virus Reveal Its Key Role as Organizer of Virion Assembly. PLoS Pathog 6: e1001233

Jonas A (2000) Lecithin cholesterol acyltransferase. Biochim Biophys Acta 1529: 245-56

Jones CT, Murray CL, Eastman DK, Tassello J, Rice CM (2007) Hepatitis C virus p7 and NS2 proteins are essential for production of infectious virus. J Virol 81: 8374-83

Jones DM, Atoom AM, Zhang X, Kottilil S, Russell RS (2011) A genetic interaction between the core and NS3 proteins of hepatitis C virus is essential for production of infectious virus. J Virol 85: 12351-61

Jones DM, Patel AH, Targett-Adams P, McLauchlan J (2009) The hepatitis C virus NS4B protein can trans-complement viral RNA replication and modulates production of infectious virus. J Virol 83: 2163-77

Jopling CL, Yi M, Lancaster AM, Lemon SM, Sarnow P (2005) Modulation of hepatitis C virus RNA abundance by a liver-specific MicroRNA. Science 309: 1577-81

Kalita MM, Griffin S, Chou JJ, Fischer WB (2015) Genotype-specific differences in structural features of hepatitis C virus (HCV) p7 membrane protein. Biochim Biophys Acta 1848: 1383-92

Kapoor A, Simmonds P, Gerold G, Qaisar N, Jain K, Henriquez JA, Firth C, Hirschberg DL, Rice CM, Shields S, Lipkin WI (2011) Characterization of a canine homolog of hepatitis C virus. Proc Natl Acad Sci U S A 108: 11608-13

Kato T, Furusaka A, Miyamoto M, Date T, Yasui K, Hiramoto J, Nagayama K, Tanaka T, Wakita T (2001) Sequence analysis of hepatitis C virus isolated from a fulminant hepatitis patient. J Med Virol 64: 334-9

Kaul A, Woerz I, Meuleman P, Leroux-Roels G, Bartenschlager R (2007) Cell culture adaptation of hepatitis C virus and in vivo viability of an adapted variant. J Virol 81: 13168-79

Kendal AP, Klenk HD (1991) Amantadine inhibits an early, M2 protein-dependent event in the replication cycle of avian influenza (H7) viruses. Arch Virol 119: 265-73

Khan AG, Whidby J, Miller MT, Scarborough H, Zatorski AV, Cygan A, Price AA, Yost SA, Bohannon CD, Jacob J, Grakoui A, Marcotrigiano J (2014) Structure of the core ectodomain of the hepatitis C virus envelope glycoprotein 2. Nature 509: 381-4

Kienzle C, von Blume J (2014) Secretory cargo sorting at the trans-Golgi network. Trends Cell Biol 24: 584-93

Klein KC, Dellos SR, Lingappa JR (2005) Identification of residues in the hepatitis C virus core protein that are critical for capsid assembly in a cell-free system. J Virol 79: 6814-26

Kong L, Giang E, Nieusma T, Kadam RU, Cogburn KE, Hua Y, Dai X, Stanfield RL, Burton DR, Ward AB, Wilson IA, Law M (2013) Hepatitis C virus E2 envelope glycoprotein core structure. Science 342: 1090-4

Kulinski A, Rustaeus S, Vance JE (2002) Microsomal triacylglycerol transfer protein is required for lumenal accretion of triacylglycerol not associated with ApoB, as well as for ApoB lipidation. J Biol Chem 277: 31516-25

Lam AM, Frick DN (2006) Hepatitis C virus subgenomic replicon requires an active NS3 RNA helicase. J Virol 80: 404-11

Lavie M, Dubuisson J (2017) Interplay between hepatitis C virus and lipid metabolism during virus entry and assembly. Biochimie 141: 62-69

Lavillette D, Bartosch B, Nourrisson D, Verney G, Cosset FL, Penin F, Pecheur EI (2006) Hepatitis C virus glycoproteins mediate low pH-dependent membrane fusion with liposomes. J Biol Chem 281: 3909-17

Lavillette D, Morice Y, Germanidis G, Donot P, Soulier A, Pagkalos E, Sakellariou G, Intrator L, Bartosch B, Pawlotsky J-M, Cosset F-L (2005a) Human Serum Facilitates Hepatitis C Virus Infection, and Neutralizing Responses Inversely Correlate with Viral Replication Kinetics at the Acute Phase of Hepatitis C Virus Infection. Journal of Virology 79: 6023-6034

Lavillette D, Pecheur EI, Donot P, Fresquet J, Molle J, Corbau R, Dreux M, Penin F, Cosset FL (2007) Characterization of fusion determinants points to the involvement of three discrete regions of both E1 and E2 glycoproteins in the membrane fusion process of hepatitis C virus. J Virol 81: 8752-65

Lavillette D, Tarr AW, Voisset C, Donot P, Bartosch B, Bain C, Patel AH, Dubuisson J, Ball JK, Cosset FL (2005b) Characterization of host-range and cell entry properties of the major genotypes and subtypes of hepatitis C virus. Hepatology 41: 265-74

Law JL, Chen C, Wong J, Hockman D, Santer DM, Frey SE, Belshe RB, Wakita T, Bukh J, Jones CT, Rice CM, Abrignani S, Tyrrell DL, Houghton M (2013) A hepatitis C virus (HCV) vaccine comprising envelope glycoproteins gpE1/gpE2 derived from a single isolate elicits broad cross-genotype neutralizing antibodies in humans. PLoS One 8: e59776

Ledford AS, Weinberg RB, Cook VR, Hantgan RR, Shelness GS (2006) Self-association and lipid binding properties of the lipoprotein initiating domain of apolipoprotein B. J Biol Chem 281: 8871-6

Lee GY, Lee S, Lee HR, Yoo YD (2016) Hepatitis C virus p7 mediates membrane-to-membrane adhesion. Biochim Biophys Acta 1861: 1096-1101

Lee JY, Acosta EG, Stoeck IK, Long G, Hiet MS, Mueller B, Fackler OT, Kallis S, Bartenschlager R (2014) Apolipoprotein E likely contributes to a maturation step of infectious hepatitis C virus particles and interacts with viral envelope glycoproteins. J Virol 88: 12422-37

LeFevre ML, Force USPST (2014) Screening for hepatitis B virus infection in nonpregnant adolescents and adults: U.S. Preventive Services Task Force recommendation statement. Ann Intern Med 161: 58-66

Lehner R, Lian J, Quiroga AD (2012) Lumenal lipid metabolism: implications for lipoprotein assembly. Arterioscler Thromb Vasc Biol 32: 1087-93

Li H, Atkins E, Bruckner J, McArdle S, Qiu WC, Thomassen LV, Scott J, Shuhart MC, Livingston S, Townshend-Bulson L, McMahon BJ, Harris M, Griffin S, Gretch DR (2012a) Genetic and functional heterogeneity of the hepatitis C virus p7 ion channel during natural chronic infection. Virology 423: 30-7

Li Q, Sodroski C, Lowey B, Schweitzer CJ, Cha H, Zhang F, Liang TJ (2016) Hepatitis C virus depends on E-cadherin as an entry factor and regulates its expression in epithelial-to-mesenchymal transition. Proc Natl Acad Sci U S A 113: 7620-5

Li X, Jiang H, Qu L, Yao W, Cai H, Chen L, Peng T (2014) Hepatocyte nuclear factor 4alpha and downstream secreted phospholipase A2 GXIIB regulate production of infectious hepatitis C virus. J Virol 88: 612-27

Li YP, Ramirez S, Jensen SB, Purcell RH, Gottwein JM, Bukh J (2012b) Highly efficient full-length hepatitis C virus genotype 1 (strain TN) infectious culture system. Proc Natl Acad Sci U S A 109: 19757-62

Lin C, Lindenbach BD, Pragai BM, McCourt DW, Rice CM (1994a) Processing in the hepatitis C virus E2-NS2 region: identification of p7 and two distinct E2-specific products with different C termini. J Virol 68: 5063-73

Lin C, Pragai BM, Grakoui A, Xu J, Rice CM (1994b) Hepatitis C virus NS3 serine proteinase: trans-cleavage requirements and processing kinetics. J Virol 68: 8147-57

Lin K, Perni RB, Kwong AD, Lin C (2006) VX-950, a novel hepatitis C virus (HCV) NS3-4A protease inhibitor, exhibits potent antiviral activities in HCv replicon cells. Antimicrob Agents Chemother 50: 1813-22

Lindenbach BD, Evans MJ, Syder AJ, Wolk B, Tellinghuisen TL, Liu CC, Maruyama T, Hynes RO, Burton DR, McKeating JA, Rice CM (2005) Complete replication of hepatitis C virus in cell culture. Science 309: 623-6

Lindenbach BD, Meuleman P, Ploss A, Vanwolleghem T, Syder AJ, McKeating JA, Lanford RE, Feinstone SM, Major ME, Leroux-Roels G, Rice CM (2006) Cell culture-grown hepatitis C virus is infectious in vivo and can be recultured in vitro. Proc Natl Acad Sci U S A 103: 3805-9

Lindenbach BD, Pragai BM, Montserret R, Beran RK, Pyle AM, Penin F, Rice CM (2007) The C terminus of hepatitis C virus NS4A encodes an electrostatic switch that regulates NS5A hyperphosphorylation and viral replication. J Virol 81: 8905-18

Lindenbach BD, Rice CM (2013) The ins and outs of hepatitis C virus entry and assembly. Nat Rev Microbiol 11: 688-700

Liu Z, Zhang X, Yu Q, He JJ (2014) Exosome-associated hepatitis C virus in cell cultures and patient plasma. Biochem Biophys Res Commun 455: 218-22

Lohmann V (2013) Hepatitis C virus RNA replication. Curr Top Microbiol Immunol 369: 167-98

Lohmann V, Korner F, Koch J, Herian U, Theilmann L, Bartenschlager R (1999a) Replication of subgenomic hepatitis C virus RNAs in a hepatoma cell line. Science 285: 110-3

Lohmann V, Overton H, Bartenschlager R (1999b) Selective stimulation of hepatitis C virus and pestivirus NS5B RNA polymerase activity by GTP. J Biol Chem 274: 10807-15

Longatti A, Boyd B, Chisari FV (2015) Virion-independent transfer of replication-competent hepatitis C virus RNA between permissive cells. J Virol 89: 2956-61

Lorenz IC, Marcotrigiano J, Dentzer TG, Rice CM (2006) Structure of the catalytic domain of the hepatitis C virus NS2-3 protease. Nature 442: 831-5

Love RA, Brodsky O, Hickey MJ, Wells PA, Cronin CN (2009) Crystal structure of a novel dimeric form of NS5A domain I protein from hepatitis C virus. J Virol 83: 4395-403

Lu W, Zheng BJ, Xu K, Schwarz W, Du L, Wong CK, Chen J, Duan S, Deubel V, Sun B (2006) Severe acute respiratory syndrome-associated coronavirus 3a protein forms an ion channel and modulates virus release. Proc Natl Acad Sci U S A 103: 12540-5

Luik P, Chew C, Aittoniemi J, Chang J, Wentworth P, Jr., Dwek RA, Biggin PC, Venien-Bryan C, Zitzmann N (2009) The 3-dimensional structure of a hepatitis C virus p7 ion channel by electron microscopy. Proc Natl Acad Sci U S A 106: 12712-6

Lupberger J, Zeisel MB, Xiao F, Thumann C, Fofana I, Zona L, Davis C, Mee CJ, Turek M, Gorke S, Royer C, Fischer B, Zahid MN, Lavillette D, Fresquet J, Cosset FL, Rothenberg SM, Pietschmann T, Patel AH, Pessaux P et al. (2011) EGFR and EphA2 are host factors for hepatitis C virus entry and possible targets for antiviral therapy. Nat Med 17: 589-95

Luscombe CA, Huang Z, Murray MG, Miller M, Wilkinson J, Ewart GD (2010) A novel Hepatitis C virus p7 ion channel inhibitor, BIT225, inhibits bovine viral diarrhea virus in vitro and shows synergism with recombinant interferon-alpha-2b and nucleoside analogues. Antiviral Res 86: 144-53

Lussignol M, Kopp M, Molloy K, Vizcay-Barrena G, Fleck RA, Dorner M, Bell KL, Chait BT, Rice CM, Catanese MT (2016) Proteomics of HCV virions reveals an essential role for the nucleoporin Nup98 in virus morphogenesis. Proc Natl Acad Sci U S A 113: 2484-9

Ma Y, Anantpadma M, Timpe JM, Shanmugam S, Singh SM, Lemon SM, Yi M (2011) Hepatitis C Virus NS2 Protein Serves as a Scaffold for Virus Assembly by Interacting with both Structural and Nonstructural Proteins. Journal of Virology 85: 86-97

Ma Y, Yates J, Liang Y, Lemon SM, Yi M (2008) NS3 helicase domains involved in infectious intracellular hepatitis C virus particle assembly. J Virol 82: 7624-39

Madan V, Bartenschlager R (2015) Structural and Functional Properties of the Hepatitis C Virus p7 Viroporin. Viruses 7: 4461-81

Maillard P, Krawczynski K, Nitkiewicz J, Bronnert C, Sidorkiewicz M, Gounon P, Dubuisson J, Faure G, Crainic R, Budkowska A (2001) Nonenveloped nucleocapsids of hepatitis C virus in the serum of infected patients. J Virol 75: 8240-50

Mailly L, Robinet E, Meuleman P, Baumert TF, Zeisel MB (2013) Hepatitis C virus infection and related liver disease: the quest for the best animal model. Front Microbiol 4: 213

Mankouri J, Walter C, Stewart H, Bentham M, Park WS, Heo WD, Fukuda M, Griffin S, Harris M (2016) Release of Infectious Hepatitis C Virus from Huh7 Cells Occurs via a trans-Golgi Network-to-Endosome Pathway Independent of Very-Low-Density Lipoprotein Secretion. J Virol 90: 7159-70

Manns MP, Buti M, Gane E, Pawlotsky JM, Razavi H, Terrault N, Younossi Z (2017) Hepatitis C virus infection. Nat Rev Dis Primers 3: 17006

Manzoor R, Igarashi M, Takada A (2017) Influenza A Virus M2 Protein: Roles from Ingress to Egress. Int J Mol Sci 18

Margeridon-Thermet S, Shafer RW (2010) Comparison of the Mechanisms of Drug Resistance among HIV, Hepatitis B, and Hepatitis C. Viruses 2: 2696-739

Martin DN, Uprichard SL (2013) Identification of transferrin receptor 1 as a hepatitis C virus entry factor. Proc Natl Acad Sci U S A 110: 10777-82

Masaki T, Suzuki R, Murakami K, Aizaki H, Ishii K, Murayama A, Date T, Matsuura Y, Miyamura T, Wakita T, Suzuki T (2008) Interaction of hepatitis C virus nonstructural protein 5A with core protein is critical for the production of infectious virus particles. J Virol 82: 7964-76

Masciopinto F, Giovani C, Campagnoli S, Galli-Stampino L, Colombatto P, Brunetto M, Yen TS, Houghton M, Pileri P, Abrignani S (2004) Association of hepatitis C virus envelope proteins with exosomes. Eur J Immunol 34: 2834-42

Matsumura T, Hu Z, Kato T, Dreux M, Zhang YY, Imamura M, Hiraga N, Juteau JM, Cosset FL, Chayama K, Vaillant A, Liang TJ (2009) Amphipathic DNA polymers inhibit hepatitis C virus infection by blocking viral entry. Gastroenterology 137: 673-81

McGivern DR, Masaki T, Williford S, Ingravallo P, Feng Z, Lahser F, Asante-Appiah E, Neddermann P, De Francesco R, Howe AY, Lemon SM (2014) Kinetic analyses reveal potent and early blockade of hepatitis C virus assembly by NS5A inhibitors. Gastroenterology 147: 453-62 e7

McLauchlan J, Lemberg MK, Hope G, Martoglio B (2002) Intramembrane proteolysis promotes trafficking of hepatitis C virus core protein to lipid droplets. EMBO J 21: 3980-8

Medvedev R, Ploen D, Spengler C, Elgner F, Ren H, Bunten S, Hildt E (2017) HCV-induced oxidative stress by inhibition of Nrf2 triggers autophagy and favors release of viral particles. Free Radic Biol Med 110: 300-315

Meex SJ, Andreo U, Sparks JD, Fisher EA (2011) Huh-7 or HepG2 cells: which is the better model for studying human apolipoprotein-B100 assembly and secretion? J Lipid Res 52: 152-8

Mercer DF, Schiller DE, Elliott JF, Douglas DN, Hao C, Rinfret A, Addison WR, Fischer KP, Churchill TA, Lakey JR, Tyrrell DL, Kneteman NM (2001) Hepatitis C virus replication in mice with chimeric human livers. Nat Med 7: 927-33

Meredith LW, Zitzmann N, McKeating JA (2013) Differential effect of p7 inhibitors on hepatitis C virus cell-to-cell transmission. Antiviral Res 100: 636-9

Merz A, Long G, Hiet MS, Brugger B, Chlanda P, Andre P, Wieland F, Krijnse-Locker J, Bartenschlager R (2011) Biochemical and morphological properties of hepatitis C virus particles and determination of their lipidome. J Biol Chem 286: 3018-32

Meuleman P, Libbrecht L, De Vos R, de Hemptinne B, Gevaert K, Vandekerckhove J, Roskams T, Leroux-Roels G (2005) Morphological and biochemical characterization of a human liver in a uPA-SCID mouse chimera. Hepatology 41: 847-56

Meunier JC, Russell RS, Engle RE, Faulk KN, Purcell RH, Emerson SU (2008) Apolipoprotein c1 association with hepatitis C virus. J Virol 82: 9647-56

Meylan E, Curran J, Hofmann K, Moradpour D, Binder M, Bartenschlager R, Tschopp J (2005) Cardif is an adaptor protein in the RIG-I antiviral pathway and is targeted by hepatitis C virus. Nature 437: 1167-72

Minola E, Prati D, Suter F, Maggiolo F, Caprioli F, Sonzogni A, Fraquelli M, Paggi S, Conte D (2002) Age at infection affects the long-term outcome of transfusion-associated chronic hepatitis C. Blood 99: 4588-91

Miyanari Y, Atsuzawa K, Usuda N, Watashi K, Hishiki T, Zayas M, Bartenschlager R, Wakita T, Hijikata M, Shimotohno K (2007) The lipid droplet is an important organelle for hepatitis C virus production. Nat Cell Biol 9: 1089-97

Mohl B-P, Tedbury PR, Griffin S, Harris M (2012) Hepatitis C Virus-Induced Autophagy Is Independent of the Unfolded Protein Response. Journal of Virology 86: 10724-10732

Montserret R, Saint N, Vanbelle C, Salvay AG, Simorre JP, Ebel C, Sapay N, Renisio JG, Bockmann A, Steinmann E, Pietschmann T, Dubuisson J, Chipot C, Penin F (2010) NMR structure and ion channel activity of the p7 protein from hepatitis C virus. J Biol Chem 285: 31446-61

Moradpour D, Englert C, Wakita T, Wands JR (1996) Characterization of cell lines allowing tightly regulated expression of hepatitis C virus core protein. Virology 222: 51-63

Moradpour D, Penin F, Rice CM (2007) Replication of hepatitis C virus. Nat Rev Microbiol 5: 453-63

Moreno C, Berg T, Tanwandee T, Thongsawat S, Van Vlierberghe H, Zeuzem S, Lenz O, Peeters M, Sekar V, De Smedt G (2012) Antiviral activity of TMC435 monotherapy in patients infected with HCV genotypes 2-6: TMC435-C202, a phase IIa, open-label study. J Hepatol 56: 1247-53

Mortimer BC, Beveridge DJ, Martins IJ, Redgrave TG (1995) Intracellular localization and metabolism of chylomicron remnants in the livers of low density lipoprotein receptor-deficient mice and apoE-deficient mice. Evidence for slow metabolism via an alternative apoE-dependent pathway. J Biol Chem 270: 28767-76

Morton RE, Greene DJ (1997) Suppression of lipid transfer inhibitor protein activity by oleate. A novel mechanism of cholesteryl ester transfer protein regulation by plasma free fatty acids. Arterioscler Thromb Vasc Biol 17: 3041-8

Mousseau G, Kota S, Takahashi V, Frick DN, Strosberg AD (2011) Dimerization-driven interaction of hepatitis C virus core protein with NS3 helicase. J Gen Virol 92: 101-11

Nahmias Y, Goldwasser J, Casali M, van Poll D, Wakita T, Chung RT, Yarmush ML (2008) Apolipoprotein B-dependent hepatitis C virus secretion is inhibited by the grapefruit flavonoid naringenin. Hepatology 47: 1437-45

Neil SJ, Sandrin V, Sundquist WI, Bieniasz PD (2007) An interferon-alpha-induced tethering mechanism inhibits HIV-1 and Ebola virus particle release but is counteracted by the HIV-1 Vpu protein. Cell Host Microbe 2: 193-203

Netter HJ, Macnaughton TB, Woo WP, Tindle R, Gowans EJ (2001) Antigenicity and immunogenicity of novel chimeric hepatitis B surface antigen particles with exposed hepatitis C virus epitopes. J Virol 75: 2130-41

Neufeldt CJ, Joyce MA, Levin A, Steenbergen RH, Pang D, Shields J, Tyrrell DL, Wozniak RW (2013) Hepatitis C virus-induced cytoplasmic organelles use the nuclear transport machinery to establish an environment conducive to virus replication. PLoS Pathog 9: e1003744

Neveu G, Barouch-Bentov R, Ziv-Av A, Gerber D, Jacob Y, Einav S (2012) Identification and targeting of an interaction between a tyrosine motif within hepatitis C virus core protein and AP2M1 essential for viral assembly. PLoS Pathog 8: e1002845

Nielsen SU, Bassendine MF, Burt AD, Martin C, Pumeechockchai W, Toms GL (2006) Association between hepatitis C virus and very-low-density lipoprotein (VLDL)/LDL analyzed in iodixanol density gradients. J Virol 80: 2418-28

Nieto-Torres JL, Verdia-Baguena C, Castano-Rodriguez C, Aguilella VM, Enjuanes L (2015) Relevance of Viroporin Ion Channel Activity on Viral Replication and Pathogenesis. Viruses 7: 3552-73

Nieva JL, Madan V, Carrasco L (2012) Viroporins: structure and biological functions. Nat Rev Microbiol 10: 563-74

Ogata N, Alter HJ, Miller RH, Purcell RH (1991) Nucleotide sequence and mutation rate of the H strain of hepatitis C virus. Proc Natl Acad Sci U S A 88: 3392-6

Okamoto K, Mori Y, Komoda Y, Okamoto T, Okochi M, Takeda M, Suzuki T, Moriishi K, Matsuura Y (2008) Intramembrane processing by signal peptide peptidase regulates the membrane localization of hepatitis C virus core protein and viral propagation. J Virol 82: 8349-61

Op De Beeck A, Voisset C, Bartosch B, Ciczora Y, Cocquerel L, Keck Z, Foung S, Cosset FL, Dubuisson J (2004) Characterization of functional hepatitis C virus envelope glycoproteins. J Virol 78: 2994-3002

Orland JR, Wright TL, Cooper S (2001) Acute hepatitis C. Hepatology 33: 321-7

Ostrowski M, Carmo NB, Krumeich S, Fanget I, Raposo G, Savina A, Moita CF, Schauer K, Hume AN, Freitas RP, Goud B, Benaroch P, Hacohen N, Fukuda M, Desnos C, Seabra MC, Darchen F, Amigorena S, Moita LF, Thery C (2010) Rab27a and Rab27b control different steps of the exosome secretion pathway. Nat Cell Biol 12: 19-30; sup pp 1-13

Out R, Kruijt JK, Rensen PC, Hildebrand RB, de Vos P, Van Eck M, Van Berkel TJ (2004) Scavenger receptor BI plays a role in facilitating chylomicron metabolism. J Biol Chem 279: 18401-6

OuYang B, Xie S, Berardi MJ, Zhao X, Dev J, Yu W, Sun B, Chou JJ (2013) Unusual architecture of the p7 channel from hepatitis C virus. Nature 498: 521-5

Owen DM, Huang H, Ye J, Gale M, Jr. (2009) Apolipoprotein E on hepatitis C virion facilitates infection through interaction with low-density lipoprotein receptor. Virology 394: 99-108

Owsianka A, Clayton RF, Loomis-Price LD, McKeating JA, Patel AH (2001) Functional analysis of hepatitis C virus E2 glycoproteins and virus-like particles reveals structural dissimilarities between different forms of E2. J Gen Virol 82: 1877-83

Owsianka AM, Tarr AW, Keck ZY, Li TK, Witteveldt J, Adair R, Foung SK, Ball JK, Patel AH (2008) Broadly neutralizing human monoclonal antibodies to the hepatitis C virus E2 glycoprotein. J Gen Virol 89: 653-9

Owsianka AM, Timms JM, Tarr AW, Brown RJ, Hickling TP, Szwejk A, Bienkowska-Szewczyk K, Thomson BJ, Patel AH, Ball JK (2006) Identification of conserved residues in the E2 envelope glycoprotein of the hepatitis C virus that are critical for CD81 binding. J Virol 80: 8695-704

Paetzel M, Karla A, Strynadka NC, Dalbey RE (2002) Signal peptidases. Chem Rev 102: 4549-80

Pan BT, Teng K, Wu C, Adam M, Johnstone RM (1985) Electron microscopic evidence for externalization of the transferrin receptor in vesicular form in sheep reticulocytes. J Cell Biol 101: 942-8

Park SH, Rehermann B (2014) Immune responses to HCV and other hepatitis viruses. Immunity 40: 13-24

Patel AH, Wood J, Penin F, Dubuisson J, McKeating JA (2000) Construction and characterization of chimeric hepatitis C virus E2 glycoproteins: analysis of regions critical for glycoprotein aggregation and CD81 binding. J Gen Virol 81: 2873-83

Patient R, Hourioux C, Vaudin P, Pages JC, Roingeard P (2009) Chimeric hepatitis B and C viruses envelope proteins can form subviral particles: implications for the design of new vaccine strategies. N Biotechnol 25: 226-34

Paul D, Hoppe S, Saher G, Krijnse-Locker J, Bartenschlager R (2013) Morphological and biochemical characterization of the membranous hepatitis C virus replication compartment. J Virol 87: 10612-27

Paul D, Madan V, Bartenschlager R (2014) Hepatitis C virus RNA replication and assembly: living on the fat of the land. Cell Host Microbe 16: 569-79

Paul D, Romero-Brey I, Gouttenoire J, Stoitsova S, Krijnse-Locker J, Moradpour D, Bartenschlager R (2011) NS4B self-interaction through conserved C-terminal elements is required for the establishment of functional hepatitis C virus replication complexes. J Virol 85: 6963-76

Pavlovic D, Fischer W, Hussey M, Durantel D, Durantel S, Branza-Nichita N, Woodhouse S, Dwek RA, Zitzmann N (2005) Long alkylchain iminosugars block the HCV p7 ion channel. Adv Exp Med Biol 564: 3-4

Pavlovic D, Neville DC, Argaud O, Blumberg B, Dwek RA, Fischer WB, Zitzmann N (2003) The hepatitis C virus p7 protein forms an ion channel that is inhibited by long-alkyl-chain iminosugar derivatives. Proc Natl Acad Sci U S A 100: 6104-8

Pecheur EI, Lavillette D, Alcaras F, Molle J, Boriskin YS, Roberts M, Cosset FL, Polyak SJ (2007) Biochemical mechanism of hepatitis C virus inhibition by the broad-spectrum antiviral arbidol. Biochemistry 46: 6050-9

Perez-Berna AJ, Moreno MR, Guillen J, Bernabeu A, Villalain J (2006) The membrane-active regions of the hepatitis C virus E1 and E2 envelope glycoproteins. Biochemistry 45: 3755-68

Perin PM, Haid S, Brown RJ, Doerrbecker J, Schulze K, Zeilinger C, von Schaewen M, Heller B, Vercauteren K, Luxenburger E, Baktash YM, Vondran FW, Speerstra S, Awadh A, Mukhtarov F, Schang LM, Kirschning A, Muller R, Guzman CA, Kaderali L et al. (2016) Flunarizine prevents hepatitis C virus membrane fusion in a genotype-dependent manner by targeting the potential fusion peptide within E1. Hepatology 63: 49-62

Pestka JM, Zeisel MB, Blaser E, Schurmann P, Bartosch B, Cosset FL, Patel AH, Meisel H, Baumert J, Viazov S, Rispeter K, Blum HE, Roggendorf M, Baumert TF (2007) Rapid induction of virus-neutralizing antibodies and viral clearance in a single-source outbreak of hepatitis C. Proc Natl Acad Sci U S A 104: 6025-30

Pham TM, Tran SC, Lim YS, Hwang SB (2017) Hepatitis C Virus-Induced Rab32 Aggregation and Its Implications for Virion Assembly. J Virol 91

Pietschmann T, Kaul A, Koutsoudakis G, Shavinskaya A, Kallis S, Steinmann E, Abid K, Negro F, Dreux M, Cosset F-L, Bartenschlager R (2006) Construction and characterization of infectious intragenotypic and intergenotypic hepatitis C virus chimeras. Proceedings of the National Academy of Sciences 103: 7408-7413

Pileri P, Uematsu Y, Campagnoli S, Galli G, Falugi F, Petracca R, Weiner AJ, Houghton M, Rosa D, Grandi G, Abrignani S (1998) Binding of hepatitis C virus to CD81. Science 282: 938-41

Pinto LH, Dieckmann GR, Gandhi CS, Papworth CG, Braman J, Shaughnessy MA, Lear JD, Lamb RA, DeGrado WF (1997) A functionally defined model for the M2 proton channel of influenza A virus suggests a mechanism for its ion selectivity. Proc Natl Acad Sci U S A 94: 11301-6

Piver E, Boyer A, Gaillard J, Bull A, Beaumont E, Roingeard P, Meunier JC (2017) Ultrastructural organisation of HCV from the bloodstream of infected patients revealed by electron microscopy after specific immunocapture. Gut 66: 1487-1495

Ploen D, Hafirassou ML, Himmelsbach K, Sauter D, Biniossek ML, Weiss TS, Baumert TF, Schuster C, Hildt E (2013) TIP47 plays a crucial role in the life cycle of hepatitis C virus. J Hepatol 58: 1081-8

Ploss A, Evans MJ, Gaysinskaya VA, Panis M, You H, de Jong YP, Rice CM (2009) Human occludin is a hepatitis C virus entry factor required for infection of mouse cells. Nature 457: 882-6

Podevin P, Carpentier A, Pene V, Aoudjehane L, Carriere M, Zaidi S, Hernandez C, Calle V, Meritet JF, Scatton O, Dreux M, Cosset FL, Wakita T, Bartenschlager R, Demignot S, Conti F, Rosenberg AR, Calmus Y (2010) Production of infectious hepatitis C virus in primary cultures of human adult hepatocytes. Gastroenterology 139: 1355-64

Popescu CI, Callens N, Trinel D, Roingeard P, Moradpour D, Descamps V, Duverlie G, Penin F, Heliot L, Rouille Y, Dubuisson J (2011) NS2 protein of hepatitis C virus interacts with structural and non-structural proteins towards virus assembly. PLoS Pathog 7: e1001278

Post JJ, Pan Y, Freeman AJ, Harvey CE, White PA, Palladinetti P, Haber PS, Marinos G, Levy MH, Kaldor JM, Dolan KA, Ffrench RA, Lloyd AR, Rawlinson WD, Hepatitis CI, Transmission in Prisons Study G (2004) Clearance of hepatitis C viremia associated with cellular immunity in the absence of seroconversion in the hepatitis C incidence and transmission in prisons study cohort. J Infect Dis 189: 1846-55

Poynard T, Bedossa P (1997) Age and platelet count: a simple index for predicting the presence of histological lesions in patients with antibodies to hepatitis C virus. METAVIR and CLINIVIR Cooperative Study Groups. J Viral Hepat 4: 199-208

Premkumar A, Wilson L, Ewart GD, Gage PW (2004) Cation-selective ion channels formed by p7 of hepatitis C virus are blocked by hexamethylene amiloride. FEBS Lett 557: 99-103

Prentoe J, Jensen TB, Meuleman P, Serre SB, Scheel TK, Leroux-Roels G, Gottwein JM, Bukh J (2011) Hypervariable region 1 differentially impacts viability of hepatitis C virus strains of genotypes 1 to 6 and impairs virus neutralization. J Virol 85: 2224-34

Prentoe J, Serre SB, Ramirez S, Nicosia A, Gottwein JM, Bukh J (2014) Hypervariable region 1 deletion and required adaptive envelope mutations confer decreased dependency on scavenger receptor class B type I and low-density lipoprotein receptor for hepatitis C virus. J Virol 88: 1725-39

Puig-Basagoiti F, Fukuhara T, Tamura T, Ono C, Uemura K, Kawachi Y, Yamamoto S, Mori H, Kurihara T, Okamoto T, Aizaki H, Matsuura Y (2016) Human Cathelicidin Compensates for the Role of Apolipoproteins in Hepatitis C Virus Infectious Particle Formation. J Virol 90: 8464-77

Qi H, Chu V, Wu NC, Chen Z, Truong S, Brar G, Su SY, Du Y, Arumugaswami V, Olson CA, Chen SH, Lin CY, Wu TT, Sun R (2017) Systematic identification of anti-interferon function on hepatitis C virus genome reveals p7 as an immune evasion protein. Proc Natl Acad Sci U S A 114: 2018-2023

Raboisson P, Lin TI, Kock H, Vendeville S, Vreken WV, McGowan D, Tahri A, Hu L, Lenz O, Delouvroy F, Surleraux D, Wigerinck P, Nilsson M, Rosenquist S, Samuelsson B, Simmen K (2008) Discovery of novel potent and selective dipeptide hepatitis C virus NS3/4A serine protease inhibitors. Bioorg Med Chem Lett 18: 5095-100

Rabouille C (2017) Pathways of Unconventional Protein Secretion. Trends Cell Biol 27: 230-240

Raghava S, Giorda KM, Romano FB, Heuck AP, Hebert DN (2011) The SV40 late protein VP4 is a viroporin that forms pores to disrupt membranes for viral release. PLoS Pathog 7: e1002116

Raiborg C, Stenmark H (2009) The ESCRT machinery in endosomal sorting of ubiquitylated membrane proteins. Nature 458: 445-52

Ramakrishnaiah V, Thumann C, Fofana I, Habersetzer F, Pan Q, de Ruiter PE, Willemsen R, Demmers JA, Stalin Raj V, Jenster G, Kwekkeboom J, Tilanus HW, Haagmans BL, Baumert TF, van der Laan LJ (2013) Exosome-mediated transmission of hepatitis C virus between human hepatoma Huh7.5 cells. Proc Natl Acad Sci U S A 110: 13109-13

Ramirez S, Li YP, Jensen SB, Pedersen J, Gottwein JM, Bukh J (2014) Highly efficient infectious cell culture of three hepatitis C virus genotype 2b strains and sensitivity to lead protease, nonstructural protein 5A, and polymerase inhibitors. Hepatology 59: 395-407

Reed KE, Grakoui A, Rice CM (1995) Hepatitis C virus-encoded NS2-3 protease: cleavage-site mutagenesis and requirements for bimolecular cleavage. J Virol 69: 4127-36

Reghellin V, Donnici L, Fenu S, Berno V, Calabrese V, Pagani M, Abrignani S, Peri F, De Francesco R, Neddermann P (2014) NS5A inhibitors impair NS5A-phosphatidylinositol 4-kinase IIIalpha complex formation and cause a decrease of phosphatidylinositol 4-phosphate and cholesterol levels in hepatitis C virus-associated membranes. Antimicrob Agents Chemother 58: 7128-40

Reiss S, Rebhan I, Backes P, Romero-Brey I, Erfle H, Matula P, Kaderali L, Poenisch M, Blankenburg H, Hiet MS, Longerich T, Diehl S, Ramirez F, Balla T, Rohr K, Kaul A, Buhler S, Pepperkok R, Lengauer T, Albrecht M et al. (2011) Recruitment and activation of a lipid kinase by hepatitis C virus NS5A is essential for integrity of the membranous replication compartment. Cell Host Microbe 9: 32-45

Ren H, Elgner F, Himmelsbach K, Akhras S, Jiang B, Medvedev R, Ploen D, Hildt E (2017) Identification of syntaxin 4 as an essential factor for the hepatitis C virus life cycle. Eur J Cell Biol 96: 542-552

Roccasecca R, Ansuini H, Vitelli A, Meola A, Scarselli E, Acali S, Pezzanera M, Ercole BB, McKeating J, Yagnik A, Lahm A, Tramontano A, Cortese R, Nicosia A (2003) Binding of the hepatitis C virus E2 glycoprotein to CD81 is strain specific and is modulated by a complex interplay between hypervariable regions 1 and 2. J Virol 77: 1856-67

Romero-Brey I, Berger C, Kallis S, Kolovou A, Paul D, Lohmann V, Bartenschlager R (2015a) NS5A Domain 1 and Polyprotein Cleavage Kinetics Are Critical for Induction of Double-Membrane Vesicles Associated with Hepatitis C Virus Replication. MBio 6: e00759

Romero-Brey I, Berger C, Kallis S, Kolovou A, Paul D, Lohmann V, Bartenschlager R (2015b) NS5A Domain 1 and Polyprotein Cleavage Kinetics Are Critical for Induction of Double-Membrane Vesicles Associated with Hepatitis C Virus Replication. mBio 6: e00759-15

Romero-Brey I, Merz A, Chiramel A, Lee JY, Chlanda P, Haselman U, Santarella-Mellwig R, Habermann A, Hoppe S, Kallis S, Walther P, Antony C, Krijnse-Locker J, Bartenschlager R (2012) Three-dimensional architecture and biogenesis of membrane structures associated with hepatitis C virus replication. PLoS Pathog 8: e1003056

Rosa D, Campagnoli S, Moretto C, Guenzi E, Cousens L, Chin M, Dong C, Weiner AJ, Lau JY, Choo QL, Chien D, Pileri P, Houghton M, Abrignani S (1996) A quantitative test to estimate neutralizing antibodies to the hepatitis C virus: cytofluorimetric assessment of envelope glycoprotein 2 binding to target cells. Proc Natl Acad Sci U S A 93: 1759-63

Rossman JS, Jing X, Leser GP, Lamb RA (2010) Influenza virus M2 protein mediates ESCRT-independent membrane scission. Cell 142: 902-13

Russell RS, Kawaguchi K, Meunier JC, Takikawa S, Faulk K, Bukh J, Purcell RH, Emerson SU (2009) Mutational analysis of the hepatitis C virus E1 glycoprotein in retroviral pseudoparticles and cell-culture-derived H77/JFH1 chimeric infectious virus particles. J Viral Hepat 16: 621-32

Sainz B, Jr., Barretto N, Martin DN, Hiraga N, Imamura M, Hussain S, Marsh KA, Yu X, Chayama K, Alrefai WA, Uprichard SL (2012) Identification of the Niemann-Pick C1-like 1 cholesterol absorption receptor as a new hepatitis C virus entry factor. Nat Med 18: 281-5

Sakaguchi T, Leser GP, Lamb RA (1996) The ion channel activity of the influenza virus M2 protein affects transport through the Golgi apparatus. J Cell Biol 133: 733-47

Salloum S, Wang H, Ferguson C, Parton RG, Tai AW (2013) Rab18 binds to hepatitis C virus NS5A and promotes interaction between sites of viral replication and lipid droplets. PLoS Pathog 9: e1003513

Sankaranarayanan S, de la Llera-Moya M, Drazul-Schrader D, Phillips MC, Kellner-Weibel G, Rothblat GH (2013) Serum albumin acts as a shuttle to enhance cholesterol efflux from cells. J Lipid Res 54: 671-6

Santantonio T, Wiegand J, Gerlach JT (2008) Acute hepatitis C: current status and remaining challenges. J Hepatol 49: 625-33

Scarselli E, Ansuini H, Cerino R, Roccasecca RM, Acali S, Filocamo G, Traboni C, Nicosia A, Cortese R, Vitelli A (2002) The human scavenger receptor class B type I is a novel candidate receptor for the hepatitis C virus. EMBO J 21: 5017-25

Scheel TK, Gottwein JM, Jensen TB, Prentoe JC, Hoegh AM, Alter HJ, Eugen-Olsen J, Bukh J (2008) Development of JFH1-based cell culture systems for hepatitis C virus genotype

4a and evidence for cross-genotype neutralization. Proc Natl Acad Sci U S A 105: 997-1002

Schmitt M, Scrima N, Radujkovic D, Caillet-Saguy C, Simister PC, Friebe P, Wicht O, Klein R, Bartenschlager R, Lohmann V, Bressanelli S (2011) A comprehensive structure-function comparison of hepatitis C virus strain JFH1 and J6 polymerases reveals a key residue stimulating replication in cell culture across genotypes. J Virol 85: 2565-81

Schubert U, FerrerMontiel AV, OblattMontal M, Henklein P, Strebel K, Montal M (1996) Identification of an ion channel activity of the Vpu transmembrane domain and its involvement in the regulation of virus release from HIV-1-infected cells. Febs Letters 398: 12-18

Scull MA, Schneider WM, Flatley BR, Hayden R, Fung C, Jones CT, van de Belt M, Penin Fo, Rice CM (2015) The N-terminal Helical Region of the Hepatitis C Virus p7 Ion Channel Protein Is Critical for Infectious Virus Production. PLoS Pathogens 11: e1005297

Segrest JP, Jones MK, Dashti N (1999) N-terminal domain of apolipoprotein B has structural homology to lipovitellin and microsomal triglyceride transfer protein: a "lipid pocket" model for self-assembly of apob-containing lipoprotein particles. J Lipid Res 40: 1401-16

Segrest JP, Jones MK, De Loof H, Brouillette CG, Venkatachalapathi YV, Anantharamaiah GM (1992) The amphipathic helix in the exchangeable apolipoproteins: a review of secondary structure and function. J Lipid Res 33: 141-66

Shanmugam S, Saravanabalaji D, Yi M (2015) Detergent-resistant membrane association of NS2 and E2 during hepatitis C virus replication. J Virol 89: 4562-74

Shanmugam S, Yi M (2013) The Efficiency of E2-p7 Processing Modulates the Production of Infectious Hepatitis C Virus. Journal of Virology

Sharma NR, Mateu G, Dreux M, Grakoui A, Cosset FL, Melikyan GB (2011) Hepatitis C virus is primed by CD81 protein for low pH-dependent fusion. J Biol Chem 286: 30361-76

Shavinskaya A, Boulant S, Penin F, McLauchlan J, Bartenschlager R (2007) The Lipid Droplet Binding Domain of Hepatitis C Virus Core Protein Is a Major Determinant for Efficient Virus Assembly. Journal of Biological Chemistry 282: 37158-37169

Shelness GS, Sellers JA (2001) Very-low-density lipoprotein assembly and secretion. Curr Opin Lipidol 12: 151-7

Shi Q, Jiang J, Luo G (2013) Syndecan-1 serves as the major receptor for attachment of hepatitis C virus to the surfaces of hepatocytes. J Virol 87: 6866-75

Shimakami T, Yamane D, Jangra RK, Kempf BJ, Spaniel C, Barton DJ, Lemon SM (2012) Stabilization of hepatitis C virus RNA by an Ago2-miR-122 complex. Proc Natl Acad Sci U S A 109: 941-6

Shimizu Y, Hishiki T, Ujino S, Sugiyama K, Funami K, Shimotohno K (2011) Lipoprotein component associated with hepatitis C virus is essential for virus infectivity. Current Opinion in Virology 1: 19-26

Shirota Y, Luo H, Qin W, Kaneko S, Yamashita T, Kobayashi K, Murakami S (2002) Hepatitis C virus (HCV) NS5A binds RNA-dependent RNA polymerase (RdRP) NS5B and modulates RNA-dependent RNA polymerase activity. J Biol Chem 277: 11149-55

Shrivastava S, Devhare P, Sujijantarat N, Steele R, Kwon YC, Ray R, Ray RB (2015) Knockdown of Autophagy Inhibits Infectious Hepatitis C Virus Release by the Exosomal Pathway. J Virol 90: 1387-96

Simmonds P, Bukh J, Combet C, Deleage G, Enomoto N, Feinstone S, Halfon P, Inchauspe G, Kuiken C, Maertens G, Mizokami M, Murphy DG, Okamoto H, Pawlotsky JM, Penin F, Sablon E, Shin IT, Stuyver LJ, Thiel HJ, Viazov S et al. (2005) Consensus proposals for a unified system of nomenclature of hepatitis C virus genotypes. Hepatology 42: 962-73

Sir D, Kuo CF, Tian Y, Liu HM, Huang EJ, Jung JU, Machida K, Ou JH (2012) Replication of hepatitis C virus RNA on autophagosomal membranes. J Biol Chem 287: 18036-43

Smith BD, Morgan RL, Beckett GA, Falck-Ytter Y, Holtzman D, Teo CG, Jewett A, Baack B, Rein DB, Patel N, Alter M, Yartel A, Ward JW, Centers for Disease C, Prevention (2012) Recommendations for the identification of chronic hepatitis C virus infection among persons born during 1945-1965. MMWR Recomm Rep 61: 1-32

Sofia MJ, Bao D, Chang W, Du J, Nagarathnam D, Rachakonda S, Reddy PG, Ross BS, Wang P, Zhang HR, Bansal S, Espiritu C, Keilman M, Lam AM, Steuer HM, Niu C, Otto MJ, Furman PA (2010) Discovery of a beta-d-2'-deoxy-2'-alpha-fluoro-2'-beta-C-methyluridine nucleotide prodrug (PSI-7977) for the treatment of hepatitis C virus. J Med Chem 53: 7202-18

Sourisseau M, Michta ML, Zony C, Israelow B, Hopcraft SE, Narbus CM, Parra Martin A, Evans MJ (2013) Temporal analysis of hepatitis C virus cell entry with occludin directed blocking antibodies. PLoS Pathog 9: e1003244

Spahn CM, Kieft JS, Grassucci RA, Penczek PA, Zhou K, Doudna JA, Frank J (2001) Hepatitis C virus IRES RNA-induced changes in the conformation of the 40s ribosomal subunit. Science 291: 1959-62

Stapleford KA, Lindenbach BD (2011) Hepatitis C virus NS2 coordinates virus particle assembly through physical interactions with the E1-E2 glycoprotein and NS3-NS4A enzyme complexes. J Virol 85: 1706-17

Stauffer S, Feng Y, Nebioglu F, Heilig R, Picotti P, Helenius A (2014) Stepwise priming by acidic pH and a high K+ concentration is required for efficient uncoating of influenza A virus cores after penetration. J Virol 88: 13029-46

Steenbergen RH, Joyce MA, Thomas BS, Jones D, Law J, Russell R, Houghton M, Tyrrell DL (2013) Human serum leads to differentiation of human hepatoma cells, restoration of very-low-density lipoprotein secretion, and a 1000-fold increase in HCV Japanese fulminant hepatitis type 1 titers. Hepatology 58: 1907-17

Steinhauer DA, Domingo E, Holland JJ (1992) Lack of evidence for proofreading mechanisms associated with an RNA virus polymerase. Gene 122: 281-8

Steinmann E, Doerrbecker J, Friesland M, Riebesehl N, Ginkel C, Hillung J, Gentzsch J, Lauber C, Brown R, Frentzen A, Pietschmann T (2013) Characterization of hepatitis C virus intra- and intergenotypic chimeras reveals a role of the glycoproteins in virus envelopment. J Virol 87: 13297-306

Steinmann E, Penin F, Kallis S, Patel AH, Bartenschlager R, Pietschmann T (2007) Hepatitis C Virus p7 Protein Is Crucial for Assembly and Release of Infectious Virions. PLoS Pathog 3: e103

Steinmann E, Pietschmann T (2010) Hepatitis C virus p7-a viroporin crucial for virus assembly and an emerging target for antiviral therapy. Viruses 2: 2078-95

StGelais C, Foster TL, Verow M, Atkins E, Fishwick CW, Rowlands D, Harris M, Griffin S (2009) Determinants of hepatitis C virus p7 ion channel function and drug sensitivity identified in vitro. J Virol 83: 7970-81

StGelais C, Tuthill TJ, Clarke DS, Rowlands DJ, Harris M, Griffin S (2007) Inhibition of hepatitis C virus p7 membrane channels in a liposome-based assay system. Antiviral Res 76: 48-58

Stillemark-Billton P, Beck C, Boren J, Olofsson SO (2005) Relation of the size and intracellular sorting of apoB to the formation of VLDL 1 and VLDL 2. J Lipid Res 46: 104-14

Sundaram M, Yao Z (2010) Recent progress in understanding protein and lipid factors affecting hepatic VLDL assembly and secretion. Nutr Metab (Lond) 7: 35

Suzuki R, Matsuda M, Watashi K, Aizaki H, Matsuura Y, Wakita T, Suzuki T (2013) Signal Peptidase Complex Subunit 1 Participates in the Assembly of Hepatitis C Virus through an Interaction with E2 and NS2. PLoS Pathog 9: e1003589

Swadling L, Capone S, Antrobus RD, Brown A, Richardson R, Newell EW, Halliday J, Kelly C, Bowen D, Fergusson J, Kurioka A, Ammendola V, Del Sorbo M, Grazioli F, Esposito ML, Siani L, Traboni C, Hill A, Colloca S, Davis M et al. (2014) A human vaccine strategy based on chimpanzee adenoviral and MVA vectors that primes, boosts, and sustains functional HCV-specific T cell memory. Sci Transl Med 6: 261ra153

Takikawa S, Ishii K, Aizaki H, Suzuki T, Asakura H, Matsuura Y, Miyamura T (2000) Cell fusion activity of hepatitis C virus envelope proteins. J Virol 74: 5066-74

Tamai K, Shiina M, Tanaka N, Nakano T, Yamamoto A, Kondo Y, Kakazu E, Inoue J, Fukushima K, Sano K, Ueno Y, Shimosegawa T, Sugamura K (2012) Regulation of hepatitis C virus secretion by the Hrs-dependent exosomal pathway. Virology 422: 377-85

Tanaka T, Kuroda K, Ikeda M, Wakita T, Kato N, Makishima M (2013) Hepatitis C virus NS4B targets lipid droplets through hydrophobic residues in the amphipathic helices. J Lipid Res 54: 881-92

Tanji Y, Hijikata M, Hirowatari Y, Shimotohno K (1994a) Hepatitis C virus polyprotein processing: kinetics and mutagenic analysis of serine proteinase-dependent cleavage. J Virol 68: 8418-22

Tanji Y, Hijikata M, Hirowatari Y, Shimotohno K (1994b) Identification of the domain required for trans-cleavage activity of hepatitis C viral serine proteinase. Gene 145: 215-9

Tedbury P, Welbourn S, Pause A, King B, Griffin S, Harris M (2011) The subcellular localization of the hepatitis C virus non-structural protein NS2 is regulated by an ion channel-independent function of the p7 protein. J Gen Virol 92: 819-30

Tellinghuisen TL, Foss KL, Treadaway J (2008a) Regulation of hepatitis C virion production via phosphorylation of the NS5A protein. PLoS Pathog 4: e1000032

Tellinghuisen TL, Foss KL, Treadaway JC, Rice CM (2008b) Identification of residues required for RNA replication in domains II and III of the hepatitis C virus NS5A protein. J Virol 82: 1073-83

Thimme R, Binder M, Bartenschlager R (2012) Failure of innate and adaptive immune responses in controlling hepatitis C virus infection. FEMS Microbiol Rev 36: 663-83

Thimme R, Bukh J, Spangenberg HC, Wieland S, Pemberton J, Steiger C, Govindarajan S, Purcell RH, Chisari FV (2002) Viral and immunological determinants of hepatitis C virus clearance, persistence, and disease. Proc Natl Acad Sci U S A 99: 15661-8

Thimme R, Oldach D, Chang KM, Steiger C, Ray SC, Chisari FV (2001) Determinants of viral clearance and persistence during acute hepatitis C virus infection. J Exp Med 194: 1395-406

Thomssen R, Bonk S, Propfe C, Heermann KH, Kochel HG, Uy A (1992) Association of hepatitis C virus in human sera with beta-lipoprotein. Med Microbiol Immunol 181: 293-300

Tillmann HL, Thompson AJ, Patel K, Wiese M, Tenckhoff H, Nischalke HD, Lokhnygina Y, Kullig U, Gobel U, Capka E, Wiegand J, Schiefke I, Guthoff W, Grungreiff K, Konig I, Spengler U, McCarthy J, Shianna KV, Goldstein DB, McHutchison JG et al. (2010) A polymorphism near IL28B is associated with spontaneous clearance of acute hepatitis C virus and jaundice. Gastroenterology 139: 1586-92, 1592 e1

Timpe JM, Stamataki Z, Jennings A, Hu K, Farquhar MJ, Harris HJ, Schwarz A, Desombere I, Roels GL, Balfe P, McKeating JA (2008) Hepatitis C virus cell-cell transmission in hepatoma cells in the presence of neutralizing antibodies. Hepatology 47: 17-24

Tiwari S, Siddiqi SA (2012) Intracellular trafficking and secretion of VLDL. Arterioscler Thromb Vasc Biol 32: 1079-86

Tong X, Chase R, Skelton A, Chen T, Wright-Minogue J, Malcolm BA (2006) Identification and analysis of fitness of resistance mutations against the HCV protease inhibitor SCH 503034. Antiviral Res 70: 28-38

Tong Y, Zhu Y, Xia X, Liu Y, Feng Y, Hua X, Chen Z, Ding H, Gao L, Wang Y, Feitelson MA, Zhao P, Qi ZT (2011) Tupaia CD81, SR-BI, claudin-1, and occludin support hepatitis C virus infection. J Virol 85: 2793-802

Torresi J (2017) The Rationale for a Preventative HCV Virus-Like Particle (VLP) Vaccine. Front Microbiol 8: 2163

Tscherne DM, Jones CT, Evans MJ, Lindenbach BD, McKeating JA, Rice CM (2006) Time- and temperature-dependent activation of hepatitis C virus for low-pH-triggered entry. J Virol 80: 1734-41

Tsukiyama-Kohara K, Iizuka N, Kohara M, Nomoto A (1992) Internal ribosome entry site within hepatitis C virus RNA. J Virol 66: 1476-83

Ujino S, Nishitsuji H, Hishiki T, Sugiyama K, Takaku H, Shimotohno K (2016) Hepatitis C virus utilizes VLDLR as a novel entry pathway. Proc Natl Acad Sci U S A 113: 188-93

Van Damme N, Guatelli J (2008) HIV-1 Vpu inhibits accumulation of the envelope glycoprotein within clathrin-coated, Gag-containing endosomes. Cell Microbiol 10: 1040-57

van Greevenbroek MM, de Bruin TW (1998) Chylomicron synthesis by intestinal cells in vitro and in vivo. Atherosclerosis 141 Suppl 1: S9-16

Vanwolleghem T, Libbrecht L, Hansen BE, Desombere I, Roskams T, Meuleman P, Leroux-Roels G (2010) Factors determining successful engraftment of hepatocytes and susceptibility to hepatitis B and C virus infection in uPA-SCID mice. J Hepatol 53: 468-76

Vieyres G, Brohm C, Friesland M, Gentzsch J, Wolk B, Roingeard P, Steinmann E, Pietschmann T (2013) Subcellular localization and function of an epitope-tagged p7 viroporin in hepatitis C virus-producing cells. J Virol 87: 1664-78

Vieyres G, Dubuisson J, Pietschmann T (2014) Incorporation of hepatitis C virus E1 and E2 glycoproteins: the keystones on a peculiar virion. Viruses 6: 1149-87

Vieyres G, Thomas X, Descamps V, Duverlie G, Patel AH, Dubuisson J (2010) Characterization of the envelope glycoproteins associated with infectious hepatitis C virus. J Virol 84: 10159-68

Vogt DA, Camus G, Herker E, Webster BR, Tsou CL, Greene WC, Yen TS, Ott M (2013) Lipid droplet-binding protein TIP47 regulates hepatitis C Virus RNA replication through interaction with the viral NS5A protein. PLoS Pathog 9: e1003302

von Hahn T, Yoon JC, Alter H, Rice CM, Rehermann B, Balfe P, McKeating JA (2007) Hepatitis C virus continuously escapes from neutralizing antibody and T-cell responses during chronic infection in vivo. Gastroenterology 132: 667-78

von Heijne G, Steppuhn J, Herrmann RG (1989) Domain structure of mitochondrial and chloroplast targeting peptides. Eur J Biochem 180: 535-45

Wahid A, Helle F, Descamps V, Duverlie G, Penin F, Dubuisson J (2013) Disulfide bonds in hepatitis C virus glycoprotein E1 control the assembly and entry functions of E2 glycoprotein. J Virol 87: 1605-17

Wakita T, Pietschmann T, Kato T, Date T, Miyamoto M, Zhao Z, Murthy K, Habermann A, Krausslich HG, Mizokami M, Bartenschlager R, Liang TJ (2005) Production of infectious hepatitis C virus in tissue culture from a cloned viral genome. Nat Med 11: 791-6

Walker CM (2017) Designing an HCV vaccine: a unique convergence of prevention and therapy? Curr Opin Virol 23: 113-119

Wang H, Perry JW, Lauring AS, Neddermann P, De Francesco R, Tai AW (2014) Oxysterol-binding protein is a phosphatidylinositol 4-kinase effector required for HCV replication membrane integrity and cholesterol trafficking. Gastroenterology 146: 1373-85 e1-11

Wang L, Kim JY, Liu HM, Lai MMC, Ou JJ (2017) HCV-induced autophagosomes are generated via homotypic fusion of phagophores that mediate HCV RNA replication. PLoS Pathog 13: e1006609

Wang N, Silver DL, Costet P, Tall AR (2000) Specific binding of ApoA-I, enhanced cholesterol efflux, and altered plasma membrane morphology in cells expressing ABC1. J Biol Chem 275: 33053-8

Wasan KM, Brocks DR, Lee SD, Sachs-Barrable K, Thornton SJ (2008) Impact of lipoproteins on the biological activity and disposition of hydrophobic drugs: implications for drug discovery. Nat Rev Drug Discov 7: 84-99

Washburn ML, Bility MT, Zhang L, Kovalev GI, Buntzman A, Frelinger JA, Barry W, Ploss A, Rice CM, Su L (2011) A humanized mouse model to study hepatitis C virus infection, immune response, and liver disease. Gastroenterology 140: 1334-44

Watashi K, Ishii N, Hijikata M, Inoue D, Murata T, Miyanari Y, Shimotohno K (2005) Cyclophilin B is a functional regulator of hepatitis C virus RNA polymerase. Mol Cell 19: 111-22

Wharton SA, Belshe RB, Skehel JJ, Hay AJ (1994) Role of Virion M2 Protein in Influenza-Virus Uncoating - Specific Reduction in the Rate of Membrane-Fusion between Virus and Liposomes by Amantadine. Journal of General Virology 75: 945-948

Whitfield T, Miles AJ, Scheinost JC, Offer J, Wentworth P, Jr., Dwek RA, Wallace BA, Biggin PC, Zitzmann N (2011) The influence of different lipid environments on the structure and function of the hepatitis C virus p7 ion channel protein. Mol Membr Biol 28: 254-64

Wiley TE, Brown J, Chan J (2002) Hepatitis C infection in African Americans: its natural history and histological progression. Am J Gastroenterol 97: 700-6

Willey RL, Maldarelli F, Martin MA, Strebel K (1992) Human immunodeficiency virus type 1 Vpu protein induces rapid degradation of CD4. J Virol 66: 7193-200

Wilson EM, Bial J, Tarlow B, Bial G, Jensen B, Greiner DL, Brehm MA, Grompe M (2014) Extensive double humanization of both liver and hematopoiesis in FRGN mice. Stem Cell Res 13: 404-12

Wilson JA, Zhang C, Huys A, Richardson CD (2011) Human Ago2 is required for efficient microRNA 122 regulation of hepatitis C virus RNA accumulation and translation. J Virol 85: 2342-50

Wilson L, Gage P, Ewart G (2006) Hexamethylene amiloride blocks E protein ion channels and inhibits coronavirus replication. Virology 353: 294-306

Witteveldt J, Evans MJ, Bitzegeio J, Koutsoudakis G, Owsianka AM, Angus AG, Keck ZY, Foung SK, Pietschmann T, Rice CM, Patel AH (2009) CD81 is dispensable for hepatitis C virus cell-to-cell transmission in hepatoma cells. J Gen Virol 90: 48-58

Wozniak AL, Griffin S, Rowlands D, Harris M, Yi M, Lemon SM, Weinman SA (2010) Intracellular proton conductance of the hepatitis C virus p7 protein and its contribution to infectious virus production. PLoS Pathog 6: e1001087

Wu X, Zhou M, Huang LS, Wetterau J, Ginsberg HN (1996) Demonstration of a physical interaction between microsomal triglyceride transfer protein and apolipoprotein B during the assembly of ApoB-containing lipoproteins. J Biol Chem 271: 10277-81

Wu YJ, Xu MY, Lu LG (2014) Clinical Advances in Fibrosis Progression of Chronic Hepatitis B and C. J Clin Transl Hepatol 2: 222-7

Yamaguchi J, Gamble MV, Conlon D, Liang JS, Ginsberg HN (2003) The conversion of apoB100 low density lipoprotein/high density lipoprotein particles to apoB100 very low density lipoproteins in response to oleic acid occurs in the endoplasmic reticulum and not in the Golgi in McA RH7777 cells. J Biol Chem 278: 42643-51

Yamamoto S, Fukuhara T, Ono C, Uemura K, Kawachi Y, Shiokawa M, Mori H, Wada M, Shima R, Okamoto T, Hiraga N, Suzuki R, Chayama K, Wakita T, Matsuura Y (2016) Lipoprotein Receptors Redundantly Participate in Entry of Hepatitis C Virus. PLoS Pathog 12: e1005610

Yamamoto T, Takahashi S, Moriwaki Y, Hada T, Higashino K (1987) A newly discovered apolipoprotein B-containing high-density lipoprotein produced by human hepatoma cells. Biochim Biophys Acta 922: 177-83

Yan Y, He Y, Boson B, Wang X, Cosset FL, Zhong J (2017) A Point Mutation in the N-Terminal Amphipathic Helix alpha0 in NS3 Promotes Hepatitis C Virus Assembly by Altering Core Localization to the Endoplasmic Reticulum and Facilitating Virus Budding. J Virol 91

Yang Z, Wang X, Chi X, Zhao F, Guo J, Ma P, Zhong J, Niu J, Pan X, Long G (2016) Neglected but Important Role of Apolipoprotein E Exchange in Hepatitis C Virus Infection. J Virol 90: 9632-9643

Yao H, Ye J (2008) Long chain acyl-CoA synthetase 3-mediated phosphatidylcholine synthesis is required for assembly of very low density lipoproteins in human hepatoma Huh7 cells. J Biol Chem 283: 849-54

Yi M, Ma Y, Yates J, Lemon SM (2007) Compensatory mutations in E1, p7, NS2, and NS3 enhance yields of cell culture-infectious intergenotypic chimeric hepatitis C virus. J Virol 81: 629-38

Yonezawa A, Cavrois M, Greene WC (2005) Studies of ebola virus glycoprotein-mediated entry and fusion by using pseudotyped human immunodeficiency virus type 1 virions: involvement of cytoskeletal proteins and enhancement by tumor necrosis factor alpha. J Virol 79: 918-26

Yost SA, Marcotrigiano J (2013) Viral precursor polyproteins: keys of regulation from replication to maturation. Curr Opin Virol 3: 137-42

Zahid MN, Turek M, Xiao F, Thi VL, Guerin M, Fofana I, Bachellier P, Thompson J, Delang L, Neyts J, Bankwitz D, Pietschmann T, Dreux M, Cosset FL, Grunert F, Baumert TF, Zeisel MB (2013) The postbinding activity of scavenger receptor class B type I mediates initiation of hepatitis C virus infection and viral dissemination. Hepatology 57: 492-504

Zayas M, Long G, Madan V, Bartenschlager R (2016) Coordination of Hepatitis C Virus Assembly by Distinct Regulatory Regions in Nonstructural Protein 5A. PLoS Pathog 12: e1005376

Zhang M, Gaschen B, Blay W, Foley B, Haigwood N, Kuiken C, Korber B (2004) Tracking global patterns of N-linked glycosylation site variation in highly variable viral glycoproteins: HIV, SIV, and HCV envelopes and influenza hemagglutinin. Glycobiology 14: 1229-46

Zhang X, Wang T, Dai X, Zhang Y, Jiang H, Zhang Q, Liu F, Wu K, Liu Y, Zhou H, Wu J (2016) Golgi protein 73 facilitates the interaction of hepatitis C virus NS5A with apolipoprotein E to promote viral particle secretion. Biochem Biophys Res Commun 479: 683-689

Zhong J, Gastaminza P, Cheng G, Kapadia S, Kato T, Burton DR, Wieland SF, Uprichard SL, Wakita T, Chisari FV (2005) Robust hepatitis C virus infection in vitro. Proc Natl Acad Sci U S A 102: 9294-9

Zona L, Lupberger J, Sidahmed-Adrar N, Thumann C, Harris HJ, Barnes A, Florentin J, Tawar RG, Xiao F, Turek M, Durand SC, Duong FH, Heim MH, Cosset FL, Hirsch I, Samuel D, Brino L, Zeisel MB, Le Naour F, McKeating JA et al. (2013) HRas signal transduction promotes hepatitis C virus cell entry by triggering assembly of the host tetraspanin receptor complex. Cell Host Microbe 13: 302-13

ANNEXES

I- A Master Regulator of Tight Junctions Involved in Hepatitis C Virus Entry and Pathogenesis

Solène Denolly and François-Loïc Cosset

Hepatology 2017

HEPATOLOGY

AASLD
AMERICAN ASSOCIATION FOR THE STUDY OF LIVER DISEASES

HEPATOLOGY *ELSEWHERE* | HEPATOLOGY, VOL. 65, NO. 5, 2017

A Master Regulator of Tight Junctions Involved in Hepatitis C Virus Entry and Pathogenesis

Hepatitis C virus (HCV) entry in hepatocytes is a complex and multistep process. HCV particles interact with attachment factors and receptors on the cell surface. Attachment is mediated by heparan sulfate proteoglycans, syndecan-1/4, the scavenger receptor class B type I (SR-BI), and, possibly, the low-density lipoprotein and very low-density lipoprotein receptors. At least four receptors and coreceptors, including SR-BI, the tetraspanin CD81, and the tight junction (TJ) proteins claudin-1 (CLDN1) and occludin (OCLN), mediate subsequent cell penetration steps comprising receptor engagement, internalization and trafficking of endocytosed viral particles, and fusion between viral and endosomal membranes.[1] Several factors are also necessary at postattachment steps, comprising AP2-associated protein kinase-1 and cyclin G-associated kinase but also sodium taurocholate cotransporting polypeptide, epidermal growth factor receptor (EGFR), ephrin receptor A2, and associated guanosine triphosphatase H-Ras. Other proteins, such as cholesterol transporter Niemann-Pick C1-like 1 and iron-uptake receptor transferrin receptor 1, modulate HCV entry; however, their precise roles remain to be determined. Although many cellular factors involved in HCV entry have been identified, how their action is coordinated during this crucial step of infection remains ill-defined. Indeed, HCV entry is a slow process that requires the recruitment of several actors at the site of entry and/or within the cell surface. It is likely that additional factors involved in this complex conundrum need to be discovered in order to fully understand the mechanism(s) of HCV entry. In a recent report, using an unbiased, genome-wide small interfering RNA screen followed by integrative functional genomics and systems virology approaches, Li et al. revealed E-cadherin as a novel piece of the HCV entry puzzle.[2] Of particular interest, the authors highlighted its involvement as an original entry factor, neither as a viral receptor nor as a postbinding factor, but rather as a master regulator of the distribution of some HCV receptor components on the cell surface (Fig. 1).

E-cadherin is an essential component of adherens junctions (AJ) that mediate cell–cell adhesion in epithelia. AJs initiate cell–cell contacts and are responsible for the maintenance of the contacts, in contrast to TJs, which regulate the paracellular pathway for the movement of ions and solutes in between cells. Interestingly, using functional assays with cell culture–produced HCV/HCV pseudoparticles from several genotypes, Li et al. demonstrated that either down-regulation of E-cadherin beforehand or preincubation of cells with an E-cadherin antibody were able to inhibit HCV infection.[2] Specifically, they showed that in cells grown to high density, i.e., forming cell–cell contacts, E-cadherin depletion induced drastically reduced cell-surface distribution of the TJ membrane proteins CLDN1 and OCLN. Overall, this seminal finding will help us to understand the involvement of TJs in HCV entry. Indeed, whether and how TJs play a role during viral entry remains controversial, several years after the identification of CLDN1 and OCLN as coreceptors. It was first assumed that HCV particles could migrate to TJs for inducing their internalization; yet firm evidence to substantiate this hypothesis is lacking, and *in vitro* HCV can infect hepatoma cells that are not fully polarized and thus exhibit no complete TJs. It was later demonstrated that engagement of HCV glycoproteins with CD81 activates multiple signaling pathways,[3] including EGFR stimulation,[4] which induces rearrangement of the actin cytoskeleton and subsequent lateral diffusion of CD81 on the plasma membrane, and interaction of CD81 with CLDN1.[5] CD81–CLDN1 association occurs at the basolateral membrane of polarized hepatoma cells with minimal association in TJ-associated CLDN1 pools and is an essential event allowing viral particle internalization, which is consistent with HCV entry into the liver from sinusoidal blood through the basal membrane of hepatocytes. In contrast to CLDN1, the role of OCLN is still enigmatic, and there is no evidence for the importance of its localization in TJs during HCV entry. However, a recent study reported that

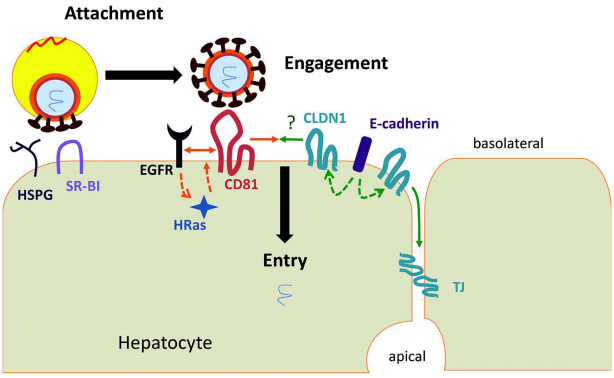

FIG. 1. E-cadherin mediates HCV entry. Following attachment to the cell surface, which is mediated by different molecules, including heparan sulfate proteoglycans and SR-BI, the E2 surface glycoprotein harbored by HCV particles interacts with CD81 (engagement), which promotes activation of EGFR and associated guanosine triphosphatases such as H-Ras and allows CD81 lateral mobility and subsequent association with CLDN1 (small orange arrows), leading to internalization of virions and to cell entry. On the other hand, it is proposed that E-cadherin regulates a pool of available CLDN1 molecules for their TJ localization or surface distribution (green arrows). Hence, depletion of E-cadherin or its blocking, through, e.g., antibodies, would inhibit CLDN1 redistribution and, possibly, its capacity to associate to CD81. Abbreviation: HSPG, heparan sulfate proteoglycan.

activated intrahepatic macrophages that produce tumor necrosis factor-α may promote HCV entry into polarized hepatoma cells through relocalization of OCLN at the basolateral membrane and increase of the lateral diffusion rates of CD81,[6] which also argues against a role of TJs *per se* in HCV entry.

The precise role of E-cadherin in HCV entry remains to be defined as it does not regulate the expression levels of the four major cellular factors, SR-BI, CLDN, OCLN, and CD81; it does not mediate virion binding to the cell surface; and it does not modulate internalization of viral particles.[2] Importantly, Li et al. showed that E-cadherin down-regulation disrupts cell-surface localization of CLDN1 and OCLN without affecting the localization of zonula occludens-1, an intracellular TJ protein that interacts with CLDN1 and OCLN, thus underlining a highly specific cellular mechanism co-opted by HCV. Intriguingly, they found that E-cadherin antibodies could readily prevent HCV infection without altering CLDN1 cell surface distribution, which suggested unrelated inhibition mechanisms. Yet, in polarized Madin-Darby canine kidney cells, E-cadherin down-regulation had little effect on the integrity of preformed TJs but rather impaired rebuilding of TJs after their disassembly,[7] which suggests the existence of different pools and/or functions of TJ proteins. Thus, it is possible that E-cadherin depletion, which has pleiotropic effects beyond inducing loss of AJs, prevents the recruitment of CLDN1 and OCLN from a pool of available molecules before they are targeted to their final localization, i.e., within TJs, and that these unaffected molecules are precisely those mediating HCV entry functions. Ultimately, E-cadherin down-regulation would induce the cell-surface redistribution of CLDN1 and OCLN, in contrast to zonula occludens-1; yet this delayed event may not be related to cell entry inhibition of incoming virus. Accordingly, E-cadherin antibodies, which were added just before infection,[2] may block E-cadherin–mediated co-optation of these TJ-free CLDN1 and OCLN molecules, which, hence, would prevent their functions in HCV entry, for example, the above-described critical CD81–CLDN1 association, in a manner independent of their role in TJ formation. Consequently, E-cadherin, by co-opting CLDN1 and OCLN to the site of cell entry and/or their recruitment in a receptor complex, may control entry of viral particles (Fig. 1).

Another interesting observation in the report by Li et al. is that soon after the establishment of infection, HCV induces loss of E-cadherin expression and leads to induction of epithelial-to-mesenchymal transition markers.[2] Interestingly, they found that HCV expression triggers epithelial-to-mesenchymal transition through activation of transforming growth factor-β signaling, which induces the loss of E-cadherin and, consequently, prevents correct localization of OCLN and CLDN1.[2] These results may explain previous observations indicating that the altered localization of OCLN and CLDN1 was induced by HCV glycoprotein expression.[8] Indeed, connections between EGFR and E-cadherin have been reported.[9] Specifically, EGFR activation leads to phosphorylation of cytoplasmic linker molecules, such as β-catenin, which, among other downstream signaling events, induces the disruption of AJs and promotes cell migration. Because HCV activates EGFR, through interaction of its surface glycoproteins with CD81,[4] this signaling may alter the interaction of E-cadherin with its partners, leading to disruption of the TJ barrier function, which could potentially affect hepatic functions.

Overall, the induction of epithelial-to-mesenchymal transition could represent a mechanism co-opted by HCV, which by modulating the localization of

CLDN1 and OCLN, limits the effect of superinfection of already infected cells and contributes to pathogenesis.

Solène Denolly, M.S.
François-Loïc Cosset, Ph.D.
CIRI–International Center for Infectiology Research
Team EVIR
Inserm, U1111, Université Claude Bernard Lyon-1
CNRS UMR5308, Ecole Normale Supérieure de Lyon
Université de Lyon
Lyon, France

REFERENCES

1) Dubuisson J, Cosset F-L. Virology and cell biology of the hepatitis C virus life cycle—an update. J Hepatol 2014;61(1 Suppl.):S3-S13.
2) Li Q, Sodroski C, Lowey B, Schweitzer CJ, Cha H, Zhang F, et al. Hepatitis C virus depends on E-cadherin as an entry factor and regulates its expression in epithelial-to-mesenchymal transition. Proc Natl Acad Sci USA 2016;113:7620-7625.
3) Brazzoli M, Bianchi A, Filippini S, Weiner A, Zhu Q, Pizza M, et al. CD81 is a central regulator of cellular events required for hepatitis C virus infection of human hepatocytes. J Virol 2008;82:8316-8329.
4) Diao J, Pantua H, Ngu H, Komuves L, Diehl L, Schaefer G, et al. Hepatitis C virus induces epidermal growth factor receptor activation via CD81 binding for viral internalization and entry. J Virol 2012;86:10935-10949.
5) **Zona L**, **Lupberger J**, Sidahmed-Adrar N, Thumann C, Harris HJ, Barnes A, et al. HRas signal transduction promotes hepatitis C virus cell entry by triggering assembly of the host tetraspanin receptor complex. Cell Host Microbe 2013;13:302-313.
6) Fletcher NF, Sutaria R, Jo J, Barnes A, Blahova M, Meredith LW, et al. Activated macrophages promote hepatitis C virus entry in a tumor necrosis factor–dependent manner. HEPATOLOGY 2014;59:1320-1330.
7) Capaldo CT, Macara IG. Depletion of E-cadherin disrupts establishment but not maintenance of cell junctions in Madin-Darby canine kidney epithelial cells. Mol Biol Cell 2007;18:189-200.
8) Benedicto I, Molina-Jiménez F, Barreiro O, Maldonado-Rodríguez A, Prieto J, Moreno-Otero R, et al. Hepatitis C virus envelope components alter localization of hepatocyte tight junction–associated proteins and promote occludin retention in the endoplasmic reticulum. HEPATOLOGY 2008;48:1044-1053.
9) Hoschuetzky H, Aberle H, Kemler R. Beta-catenin mediates the interaction of the cadherin–catenin complex with epidermal growth factor receptor. J Cell Biol 1994;127:1375-1380.

Author names in bold designate shared co-first authorship.

View this article online at wileyonlinelibrary.com.
DOI 10.1002/hep.29066
Potential conflict of interest: Nothing to report.

Fibrosis Evaluation by Transient Elastography in Alcoholic Liver Disease: Is the Histological Scoring System Impacting Cutoff Values?

Alcohol is one of the of the main causes of liver cirrhosis, which is responsible for 15% of all alcohol-attributable deaths. Most patients are diagnosed with alcoholic liver disease (ALD) at the cirrhotic stage when symptoms of decompensation and/or acute-on-chronic liver injury due to alcoholic hepatitis are obvious. In contrast, in patients with compensated ALD, cirrhosis or septal fibrosis may also be prevalent, but patients are mostly asymptomatic or present nonspecific symptoms, which explains why this serious condition is overlooked by physicians. In general, patients with compensated ALD have received only limited medical attention in the past.

Advanced fibrosis is one of the major factors that determine prognosis in ALD, as in most other chronic liver diseases; and the adverse impact of cirrhosis on outcome is well established. Five-year survival rates for patients with alcoholic cirrhosis are comparable to those of patients with breast, prostate, or colon cancer. However, less advanced fibrosis, as seen in ALD with central hyaline necrosis and presence of fibrous septa with collagen and elastic fibers, and alcoholic steatohepatitis are also risk factors for disease progression and associated with adverse prognosis.[1] Therefore, the diagnosis of earlier stages of fibrosis is important because patients at risk can be identified and given abstinence counseling to prevent the development of cirrhosis and hepatic decompensation. The diagnosis of hepatic fibrosis, traditionally achieved by histological evaluation, is now increasingly made by noninvasive methods including serum biomarkers of fibrosis or liver stiffness-elasticity based imaging techniques, including transient elastography, acoustic radiation force impulse imaging, shear wave elastography, and magnetic resonance elastography. These methods have been mainly evaluated in patients with viral hepatitis and nonalcoholic fatty liver disease but less frequently in ALD and allow a risk-free, repeatable, and quick assessment of liver fibrosis, sparing the necessity of liver biopsy for many.

II- Membrane fusion assays for studying entry hepatitis C virus into cells

Solène Denolly, François-Loïc Cosset and Natalia Freitas

Chapter to Methods in Molecular Biology - HCV Protocols

Submitted

Membrane fusion assays for studying entry hepatitis C virus into cells

Solène Denolly, François-Loïc Cosset* and Natalia Freitas

CIRI – International Center for Infectiology Research, Team EVIR, Inserm, U1111, Université Claude Bernard Lyon 1, CNRS, UMR5308, Ecole Normale Supérieure de Lyon, Univ Lyon, F-69007, Lyon, France.

*** Corresponding author**
E-mail: flcosset@ens-lyon.fr

Abstract

The membrane fusion properties of HCV envelope glycoproteins can be evaluated using several assays. Fusion assays generally require contacts between glycoproteins expressed on a donor membrane, such as those from a cell or a viral particle, and an acceptor membrane, that may or may not express cognate viral receptor, such as those from an indicator cell or a liposome. In this chapter, we describe three well-established methods in the field, that use either cell surface expression of glycoproteins, HCV pseudo-particles (HCVpp) or cell culture-grown HCV (HCVcc) particles for donor membrane, and cells or liposomes as acceptor membrane in which specific components can be included to monitor and quantify fusion. We provide details of cell-cell fusion assay, virus-liposome fusion assay and finally virus-plasma membrane fusion assay. We also describe inhibitors that can block HCV envelope membrane fusion.

Key words: fusion, hepatitis C, liposomes, inhibitors, plasma membrane, cell-cell fusion

1 Introduction

HCV entry is a complex process that is not fully understood. Entry begins by attachment of viral particles to several receptors including HSPGs and SR-BI. This allows the clustering of particles with CD81 and their lateral diffusion and interactions with Claudin-1 and other co-factors (Douam et al., 2015), which is followed by their endocytosis and internalization. The last step of entry is the fusion of viral membrane with that of the host cell. This last step allows the release of the genome in the cytosol and the initiation of virus replication. This process includes conformational changes of the fusion proteins at low endosomal pH, which induce insertion of a fusion peptide into the host membrane, lipid mixing of external membrane leaflets and finally full fusion of the two membranes.

As this fusion step is critical for the infection, it has been studied since many years. It was first studied by using some peptides derived from HCV glycoproteins, allowing determining putative fusion peptides (Perez-Berna et al., 2006). Cell-cell fusion assays were then developed (Takikawa et al., 2000) as for other viruses, based on the expression of glycoproteins at the cell surface of donor cells and a reporter gene expressed only after fusion with indicator cells. Although HCV does not induce formation of syncytia in this assay, the measurement of reporter gene allowed determining that fusion occurs at optimal pH of *ca*. 5 and requires both E1 and E2 glycoproteins. The development of HCV pseudoparticles (HCVpp) (Bartosch et al., 2003) allowed the study of fusion of HCV glycoproteins at the surface of particles instead of cell surface. This was determined using liposome fusion assays (Lavillette et al., 2006) that confirmed the requirement of both glycoproteins for inducing membrane fusion at pH 5.5, but also allowed the discovery of specific determinants in either glycoprotein that govern fusion (Lavillette et al., 2007). The study of fusion of fully infectious HCV particles, HCVcc, was developed later and is based on the fusion of viral particles at the plasma membrane (Tscherne et al., 2006), as previously achieved for other viruses, or with liposomes. Again, these assays confirmed the dependency of acid pH and for both E1E2 glycoproteins in cell entry. These three fusion assays were also used to find inhibitors of membrane fusion that block cell entry and infection.

According to findings obtained with these assays, membrane fusion of HCV particles might occur in the endosome compartment and requires its acidic environment. Interestingly, the optimal pH values required for membrane fusion is dependent of the assay used, indicating that this crucial step for HCV entry is complex and may require additional factors. As the study of membrane fusion *in cellulo* is technically difficult to achieve and there is still no assay for studying fusion of HCV particles in endosomes of hepatoma cells, it is clear that the assays described below, individually, are not perfect. However, their combined study could allow better understanding of this critical step and the discovery of new HCV drugs. Here we describe these three assays as well as previously described fusion inhibitors.

2 Materials

2.1 Cell-cell fusion assay

2.1.1 Cells lines

1. Donor cells: HEK-293T cells.
2. Indicator cells: typically cells that are permissive to HCV replication such as Huh-7, Huh7.5 cells transiently or stably expressing HIV-1 transactivator Tat protein. Huh7-Lunet cells expressing high levels of human CD81 can also be used.

2.1.2 Cell culture

1. Common cell culture solutions and equipment.
2. Additional solutions: Non-enzymatic cell dissociation reagent Versene 1:5000 (1X) solution.
3. Recommended cell culture media: Dulbecco’s modified Eagle’s medium (DMEM) supplemented with 10% fetal bovine serum and 1% Pen-Strep antibiotics solution.

2.1.3 Transfection reagents

1. JetPEI (Polyplus-transfection Inc.) for transfection of donor HEK-293T cells.
2. GeneJammer (Agilent) for transitory transfection of indicator cells.

2.1.4 Plasmid DNA for transfection

1. Luciferase reporter system, which consists in a pLTR-luc plasmid containing a fragment of HIV-1 long terminal repeat (LTR) driving luciferase expression in donor cells upon transactivation by HIV-1 Tat (Lavillette et al., 2007), as provided in acceptor cells by plasmid LXSN-Tat (Lavillette et al., 2007), upon cell-cell fusion.
2. Constructs expressing HCV glycoproteins consists of *e.g.*, plasmid phCMV-H77-wt expressing wild type E1E2 from genotype 1a strain H77, or alternative/mutated HCV glycoproteins, under control of the CMV promoter (Bartosch et al., 2003). Optionally, plasmid pGFP encoding green fluorescent protein (GFP) can be used to access transfection efficiency.
3. Controls plasmids such as plasmid phCMV, also called "empty vector" that does not contain any DNA sequences encoding for viral glycoproteins and is used as negative control to establish the background levels of cell-cell fusion assay.
4. Constructs such as plasmids phCMV-HA and phCMV-NA encoding the fowl plaque virus hemagglutinin and neuraminidase, respectively, or phCMV-VSVg expressing the vesicular stomatitis virus glycoprotein, which are used as positive controls of the cell-cell fusion assay. Both HA/NA and VSVg glycoproteins display maximum activity at pH5.

2.1.5 Buffers

1. 1X DPBS.
2. 1X Fusion Buffer (135 mM NaCl, 15 mM sodium citrate, 10 mM MES and 5 mM HEPES). First prepare a 10X concentrated Fusion Buffer by weighting 15.8 g of NaCl (M.W. 58.44 g/mol), 8.8 g of sodium citrate (M.W. 294.1 g/mol), 3.9 g of morpholineethanesulfonic acid (MES; M.W. 195.2 g/mol) and 2.3 g of HEPES (M.W. 238.1 g/mol) and dissolving all components in 200 ml of molecular biology grade water. To prepare 1X Fusion Buffer simply dilute 5ml of the 10X concentrated Fusion Buffer in 40 ml of water. Measure the pH using a calibrated pH meter and adjust the pH to the desired value. Use a 1N NaOH solution to adjust pH values above 5 and 37% HCl solution for fusion buffer pH 5 or below. After obtaining the desired pH add water to a final volume of 50 ml and sterilize the solution by filtration using 0,20 μm filter units.
3. 5X Passive Lysis buffer (Promega): Prepare a 1X working solution by diluting the 5X concentrated stock in molecular biology grade water and pre-chill the 1X lysis buffer at 4°C.
4. Firefly Luciferase reagent: First prepare 1L of Firefly Buffer (25mM Tricine buffer, pH 7.8, 5mM $MgSO_4$, 0.5mM EDTA, pH 8.0, 5mM DTT and 0.5mM ATP). Make 100ml aliquots, keep one vial to reconstitute firefly luciferase substrate mix and freeze the remaining tubes. In order to prepare Firefly Luciferase substrate mix, resuspend 50mg of D-Luciferin sodium salt (Synchem OHG) and 25mg of Coenzyme A sodium salt hydrate (Sigma) in 100 ml of Firefly Buffer. After reconstitution, this solution should be protected from light but can undergo several freeze/ thaw cycles.

2.1.6 Special equipment

1. Multimode plate reader like Mithras LB 940 or equivalent.

2.2 Virus-liposome fusion assay

2.2.1 HCV particles

1. HCVpp, β-lactamase HIV based HCV pseudoparticles or HCVcc particles (for a detailed protocol of HCVpp and HCVcc production see Chapter…). A protocol for production of β-lactamase HIV based HCV pseudoparticles can be found in (Lavillette et al., 2006).
2. Control particles devoid of envelope (negative control).
3. Pseudoparticles harboring alternative envelope virus glycoproteins used as positive or negative controls for acid pH sensitivity, such as HApp or MLVpp, respectively.

2.2.2 Reagents and materials

1. Phosphatidylcholine from egg yolk (PC, 99% pure; Sigma).
2. Cholesterol (chol, 99% pure; Sigma).
3. Sphingomyelin (SM, 99% pure; Sigma).
4. Triton X-100.
5. Octadecyl rhodamine B chloride (R_{18}; Molecular Probes).
6. Beta-Lactamase Substrate CCF2-FA; free acid (Invitrogen).
7. Polycarbonate filters.

2.2.3 Equipment

1. SLM Aminco 8000 spectrofluorimeter or equivalent.

2.3 Virus-plasma membrane fusion assay

2.3.1 Cell lines

1. Target cells: Huh7.5 or derivatives (Huh7-Lunet/hCD81).

2.3.2 Cell culture

1. Classical medium for target cell culture: for example, DMEM supplemented with 100U/ml of penicillin, 100µg/ml of streptomycin, and 10% fetal bovine serum.
2. Incubator for cell culture at 37°C, 5% CO_2.
3. Six-well plates.

2.3.3 HCV particles

1. HCVcc particles containing a luciferase reporter genome (see Chapter… for production).

2.3.4 Reagents

1. Inhibitor of endosomal acidification: Bafilomycin A1 (Sigma-Aldrich, CAS 88899-55-2) or Concanamycin A (Sigma-Aldrich 80890-47-7). Dissolve the powder in DMSO and stored the solutions at -20°C. A stock solution could be made at 25µM and 5µM for bafilomycin A1 and concanamycin A, respectively.
2. Ice cold DPBS.
3. Pre-warmed citric buffer (pH7 or pH5): 15mM citric acid, 150 mM NaCl. For 100mL, weight 288.2mg of citric acid and 876.6mg of NaCl and dissolve all components in

100mL of molecular biology grade water. Measure pH using a calibrated pH meter and adjust pH to the desired value (either 7 or 5). Use 1N of NaOH or HCl to adjust pH (*see* **Note 1**). Just before the assay, pre-warm buffer at 37°C.

4. Passive lysis buffer: see **section 2.1.5** for the recipe.
5. Luciferase reagent: see **section 2.1.5** for the recipe.
6. Multimode plate reader like Mithras LB 940 or equivalent.

2.4 Fusion inhibitors

A list of HCV fusion inhibitors described in previous studies is provided in Table 1. They can be used as controls in fusion experiments.

3 Methods

3.1 Cell-cell fusion assay

Cell-cell fusion assays typically consist in transient overexpression of viral glycoproteins in one cell type (donor cells) and co-culture (co-cultivation) with a second cell type that expresses viral receptors (indicator cells). Viral glycoproteins mediated cell-cell fusion is quantified by measuring the transcriptional activation of a reporter gene such as luciferase under the control of the HIV-1 3' long terminal repeat (LTR) in donor cells by the HIV-1 transactivator Tat produced in indicator cells. Fusion of the two cell types results in cytoplasmic content mixing between donor cells and indicator cells, allowing the expression of luciferase, which is measured upon cell lysis (see **Fig. 1**). This method allows investigating the direct role of the viral envelope proteins in membrane fusion independently of virus RNA replication and virion production. This is particularly advantageous when identifying fusion determinants and/or characterizing E1E2 point mutations that may significantly affect other steps of HCV life cycle and/or impair viral particle production. Nevertheless, this assay relies on efficient viral glycoproteins expression and transport to the cell surface, which should be properly monitored for cell-cell fusion normalization. Importantly, this assay can be easily employed to screen for anti-HCV compounds that specifically inhibit HCV entry.

In the following protocol Huh7-Tat indicator cells are generated by transient transfection of Huh-7 cells with the plasmid LXSN-Tat. Alternatively, stably transfected Huh-7 cell lines expressing Tat can also be used.

1. Day 1- Cells seeding for transient transfection. Approximately 24 hours before transfection seed $3x10^5$ HEK-293 T cells and $5x10^5$ Huh7 cells per well in a six-well plate (see **Notes 2 and 3**).
2. Day 2- Transient transfection of donor and indicator cells. 24 hours after cell seeding replace the culture media by adding 1 ml of fresh pre-warmed *media* and return cells to CO2 incubator while preparing transfection mixes. Co-transfect HEK-293T donor cells using JetPEI transfection reagent following the manufacturer's instructions with

3 μg of phCMV-H77-wt, empty vector or positive control plasmids and 50 ng of LTR-luc per well. Routinely, a JetPEI to DNA ratio of 2:1 is used but further optimization of transfection conditions is advisable to obtain maximum transfection efficiencies (see **Note 4**). 6 to 8 hours after transfection replace the culture media by adding 1 to 2 ml of fresh pre-warmed *media and incubate cells for 24 hours.*
In parallel, transfect Huh7 cells using GeneJammer transfection reagent following the manufacturer's instructions with 2 μg of LXSN-Tat per well and incubate cells for 24 hours without replacing the culture media (see **Notes 5 and 6**).

3. Day 3- Co-cultures of donor and indicator cells. Following a 24-hour incubation dissociate transfected HEK-293 T cells from the wells using Versene dissociation reagent and suspend them in DMEM medium. Count cells and seed them in a 12-well plate at a density of $1x10^5$ cells/well. Swirl the plates to spread the cells evenly and return them to the incubator. Let them attach, and repeat cell dissociation with the indicator cells (Huh7-Tat). Cell attachment takes usually less than 2 hours but should be checked by microscopy. Count Huh7-Tat cells and adjust cell density to $2x10^5$ cells/ml. Aspirate culture media from HEK-293 T cells and seed $2x10^5$ Huh7-Tat cells/well (1 ml) on the top of the donor cells. HEK-293 T cells detach very easily; therefore, extra care should be taken during media replacement. Return the co-cultures to the incubator for a period of 24 hours (see **Note 7**).
4. Day 4- pH shock. To initiate fusion, remove the media from the co-cultures and rinse the wells carefully once with 1X Fusion Buffer adjusted to the desired pH, at room temperature. Replace the 1X Fusion Buffer by fresh 1X Fusion Buffer and incubate for 3 to 5 min. After pH shock, remove 1X Fusion buffer and replace it by 1 ml of pre-warmed media. Repeat media exchange one more time and return the co-cultures to the incubator. Incubate the co-cultures for a period of 24 hours.
5. Day 5- Luciferase quantification. 24 hours after pH shock remove the media from the co-cultures and wash once with 1X DPBS. Add 175 μl of 1X Passive Lysis buffer pre-chilled at 4°C per well and incubate for 30 min with agitation at 4°C. Transfer the cell lysates to 1.5 ml eppendorf tubes and centrifuge the samples at maximum speed for 5 min at 4°C to remove cell debris. Transfer the supernatants to new tubes and freeze the cell lysates at -80°C or proceed with Luciferase quantification assay.
6. For Luciferase quantification assay aliquot 30 μl of each supernatant into a 96-well black plate.
7. Detect Luciferase luminescence using Mithras LB940 luminescence reader with integrated injectors (Bertold Technologies, Germany) after automatic addition of firefly luciferase reagent (substrate).

3.2 Virus-liposome fusion assay

Hemifusion/fusion lipid mixing assays have been invaluable tools in characterizing the biochemical properties of viral fusion steps, including the pH and the lipid species dependences. Sphingomyelin, together with cholesterol was shown to enhance HCVcc fusion using a liposome fusion assay (Haid et al., 2009). Lipid mixing kinetics between the virus and

the liposomes is monitored by measuring changes in fluorescence upon dilution of fluorescent lipid dyes such as R_{18}, incorporated into either the liposomes or the viral particles (see **Fig. 2**). Discrimination between hemifusion and complete lipid fusion with internal content mixing between viral particles and liposomes can be achieved by labeling the liposomes with CCF2 and incorporating β-lactamase (BlaM) into the core of HIV-1-based HCVpp. CCF2 is a fluorogenic substrate of BlaM composed of two moieties, a coumarin derivative and fluorescein, that upon contents mixing between pseudoparticles and liposomes is cleaved by BlaM resulting in a shift of the fluorescence spectrum of CCF2. BlaM is expressed as a chimeric protein encoding BlaM fused to the N-terminus of the HIV-1 viral protein R (Vpr).
HCVpp with incorporated BlaM-Vpr may also be used in entry/fusion assays *in cellulo*. However, this method have not been yet tested or published for HCV despite having been well described for HIV (Cavrois et al., 2002) and Ebola virus (Yonezawa et al., 2005) (*see* **Note 8**).

3.2.1 PC, PC:chol, PC:chol:SM liposomes preparation and R_{18} labeling

1. Dissolve the different components of liposomes (different lipids) individually in chloroform. To prepare PC, PC:chol (70:30 molar ratio) and PC:chol:SM (65:30:5 molar ratio) containing liposomes mix the dissolved lipids in chloroform in the required molar proportion.
2. Add R_{18} in ethanol at self-quenching concentrations, equivalent to approximately 5mol% relative to the phospholipid content of the liposome. Incubate the mixture for 1 hour in the dark at room temperature and allow the lipids to dry by vacuum evaporation for 30 min. Alternatively to liposome labeling; R_{18} can be incorporated into HCVpp.
3. Hydrate the lipid film in PBS 1X pH 7.4.
4. Conduct 5 freeze/thaw cycles (liquid nitrogen and 37°C, respectively). The vesicle suspension is then sized to 100 nm diameter vesicles by extrusion through polycarbonate filters.

3.2.2 HCVpp/liposome lipid mixing

1. Pipette different volumes (5 to 40 µl) of HCVpp or HCVcc in PBS (pH 7.4) to a 37°C –thermostable cuvette.
2. Add R_{18}-labeled liposomes (final lipid concentration of 15 µM) and incubate the mixtures at 37°C for 10 min to allow temperature equilibration.
3. Decrease the pH to 5 by adding an appropriate volume of diluted HCl to the cuvette and record the fusion kinetics on an SLM Aminco 8000 spectrofluorimeter over a 30-min period, with and excitation wavelength at 560 nm and an emission wavelength at 590 nm.
4. Add 0.1% Triton X-100 (final concentration, vol/vol) and measure the maximal R_{18} quenching.

3.2.3 CCF2-FA liposome preparation

1. Resuspend the lipid film into 100 µM CCF2-FA solution in 25 mM HEPES, 150 mM NaCl pH 7.5.
2. Remove unincorporated CCF2 by gel filtration using PD-10 columns.

3. Mix CCF2 loaded liposomes (150 μM phospholipid and 25 μM CCF2 final) with BlaM HIV core-based HCVpp.
4. After temperature equilibration at 37°C, decrease the pH to 5 by adding an appropriate volume of diluted HCl to the cuvette and record the fusion kinetics on an SLM Aminco 8000 spectrofluorimeter over a 30-min time period, with and excitation wavelength at 409 nm and an emission wavelength between 420 and 560 nm.

3.3 Virus-plasma membrane fusion assay

This assay allows the study of fusion of viral particles *in cellulo* has two main advantages: the use of HCVcc particles and the use of cells as target, rather than liposomes. The use of inhibitors of acidification of endosomes prevents viral entry and membrane fusion by the normal route through acidified endosomes, which is technically difficult to investigate. It was previously demonstrated that viral particles have to be primed by receptor interactions and that fusion can only occur after 1h incubation of viral particles with cells (*see* **Fig. 3**) as compared to other viruses that can directly fuse after binding to the cells. In contrast to the other above-described assays, this assay requires the uncoating of the viral genome and subsequent viral genome translation and replication, meaning that this assay is not directly related to fusion; thus, results obtained with this assay should be confirmed with other assays to ensure that fusion is the step that is really involved.

1. *Day 1*. Seed target cells in a six-well plate at 7-8x10^5 cells/well (*see* **Note 9**).
2. *Day 2*. Treat target cells with bafilomcyin A1 (25 nM) or concanamycin A (5 nM) for 1h at 37°C (*see* **Note 10**). For that add 1.5 mL of cell culture medium + 1.5 μL of stock solution of inhibitor per well.
3. Infect target cells in presence of bafilomcyin A1 or concanamycin A for 2h at 4°C (*see* **Note 11**). For that remove medium and replace it with ice-cold medium containing viral particles + inhibitors at the final concentration of 25 nM for bafilomycin A1 and 5 nM for concanamycin A1.
4. Wash cells with cold DPBS twice (*see* **Note 12**).
5. Incubate cells with medium containing bafilomcyin A1 or concanamycin A for 1h at 37°C (*see* **Note 13)**. For that add 1.5mL of cell culture medium + 1.5 μL of stock solution of inhibitor per well.
6. Incubate cells for 5minutes at 37°C with warm citric acid buffer (*see* **Note 14**). For that remove medium, wash with cold DPBS, add 1.5 mL/well of warm citric acid buffer and incubate cells 5min at 37°C. After that remove buffer and wash with medium.
7. Add fresh medium in presence of bafilomcyin A1 or concanamycin A for 3h at 37°C (*see* **Note 15**). For that add 1.5 mL of cell culture medium + 1.5 μL of stock solution of inhibitor per well.
8. Change medium and add 1.5mL cell culture medium per well.
9. Incubate cells at 37°C for 24h (*see* **Note 16**).
10. *Day* 3. Harvest cells and measure luciferase at 24h (*see* **Note 16**). Remove media from the cells and wash once with DPBS. Add 350 μL of 1X passive lysis buffer at 4°C per well and incubate for 30min with agitation at 4°C. Transfer the cell lysates to

a tube and centrifuge the samples at maximum speed for 5min at 4°C. Transfer the supernatant to a new tube and aliquot 30 µL of each supernatant into a 96-well black pate. Freeze the cell lysates at -80°C or proceed with luciferase quantification assay.

11. Detect luciferase luminescence using a luminescence reader with integrated injectors after automatic addition of firefly luciferase reagent.

3.4 Fusion inhibitors

Several drugs/compounds have been shown to modulate HCV infection by affecting viral membrane fusion. These molecules can be applied in combination with the different fusion assays described above to further characterize viral membrane fusion. Furthermore, fusion assays are powerful tools that can be used for screening and characterizing new antivirals that target virus entry. Fusion inhibitors are a diverse group of molecules that display different mechanisms of action but ultimately interfere with the required conformational changes of fusion peptides during virus fusion (**Table 1**). In this section, we provide examples of fusion inhibitors previously used in combination with the three fusion methods described.

3.4.1 Arbidol

The broad-spectrum antiviral arbidol has been shown to inhibit efficiently HCV membrane fusion in liposome fusion assays, either using HCVpp or cell-culture HCVcc (Haid et al., 2009, Pecheur et al., 2007). The extent of fusion inhibition was shown to be directly proportional to arbidol concentration, with some variations among genotypes. Fusion of HCVpp coated with E1E2 of genotype 1a was totally abolished at 1 µg/ml, while 6 µg/ml were required to block fusion of genotype 1b. For genotype 2a, HCVpp fusion was still observed using 6 µg/ml of arbidol, which is equivalent to 11.3 µM (Pecheur et al., 2007). The concentration of arbidol able to inhibit fusion of genotype 2a HCVcc by 50% (IC50) was determined to be 2 µg/ml (Haid et al., 2009).

1. Dissolve ARB first in 100% ethanol and then dilute ARB to a final concentration of 100 mM in water.
2. Pre-incubate ARB in the desired concentration for 2 min with either HCVpp or 15µM of R_{18}-labeled liposomes at 37°C in buffer at neutral pH.
3. Then, add the R_{18}-labeled liposomes or HCVpp to the mixture and start fusion by decreasing the pH to 5.0.
4. Monitor lipid mixing as described before.

3.4.2 Human monoclonal antibody CBH-5

CBH-5 against an epitope within E2, with neutralizing activity against HCVpp harboring diverse HCV genotypes (Owsianka et al., 2008), was shown to exert a dose-dependent inhibition of HCVcc fusion using liposome fusion assays (Perin et al., 2016). It was determined that 25 µg/ml of CBH-5 completely abrogates E1E2 mediated fusion and 5 µg/ml was estimated to inhibit 50% of the fusion activity.

1. Incubate HCVcc with increasing concentrations of CBH-5 in cell suspension buffer (0.85% (w/v) NaCl, 10 mM Tricine-NaOH, pH 7.4) for 15 min at pH 7.4.
2. Then, add the liposomes, induce fusion and monitor lipid mixing.

3.4.3 Amphipathic DNA polymers (APs)

Phosphorothioate oligonucleotides (PS-ONs) inhibit HCV infection of different genotypes without affecting replication or attachment. HCVpp fusion with liposomes was significantly inhibited when 10 nM of PS-ONs was incubated with HCVpp before the addition of R_{18}-labeled liposomes (Chi et al., 2016).

3.4.4 Fusion peptide inhibitors

Recently, a peptide library screening that covered the entire E1E2 amino acid sequence led to the identification of a peptide-based fusion inhibitor derived from the E2 stem domain, amino acids 671 to 705, with an anti-E1E2 fusion EC_{50} value of 734,2±9,3 nM in cell-cell fusion assays (Chi et al., 2016).

1. Add the peptide fusion inhibitor at a final concentration of 5 μM to the co-cultures, after pH shock.

3.4.5 Flunarizine

In the plasma membrane assay HCV can only access cells by exogenous acidification since endosomal acidification is prevented by continuous presence of bafilomycin A or concanamycin A as described. Alternatively, chloroquine or ammonium chloride can be used instead of bafilomycin A or concanamycin A.

Using this setting, it was observed that flunarizine reduces HCV infection when added after HCVcc inoculation and before the pH shock (Perin et al., 2016).

4 Notes

1. Buffer at pH 7 is used as a negative control (to set the background level) since no fusion occurs at this pH.
2. Prior to transfection cells can be detached with 0,05% Trypsin-EDTA (1X) solution, although after transfection it is highly recommended to detach cells using a non-enzymatic cell dissociation reagent such as Versene 1:5000 (1X) solution.
3. Calculate the number of wells and plates required taken into account that each pH condition should be tested at least in duplicate and extra cells might be required to seed co-cultures at different ratios.
4. When performing multiple *transfections* with the same plasmids combinations it is recommended to *prepare* a master *mix* of transfection complexes.
5. GFP reporter vector can be added to the transfection mixes, 5% of the total amount in μg of plasmid DNA used for transfection, for determination of *transfection efficiency.*
6. The described Luciferase reporter system works well in HEK-293 T and Huh7 cells. However, if using different cell lines, it is recommended to check the activity of the HIV-1 3' LTR promoter/Tat inducible system before performing cell-cell fusion assays. This can be achieved by simply co-transfecting both donor and indicator cells with 50 ng of LTR-luc and 2 μg of LXSN-Tat and measure luciferase activity after cell lysis.
7. Different ratios donor to indicator cells should be tested in order to maximize contacts between adjacent donor and indicator cells. For cell-cell fusion optimization we recommend to compare luciferase activity between ratios donor to indicator cells of 1:2, 1:5 and 5:1.

8. After infection with HCVpp containing BlaM-Vpr at 37°C for 1h-3h, cells are washed in CO_2-indpendent medium and loaded with CCF2-AM dye at room temperature for 1h. After two additional washes, the BlaM reaction is allowed to develop for 7h at room temperature in CO_2-independent medium supplemented with 10% FBS and 2.5 mM probenecid, a nonspecific inhibitor of anion transport, without antibiotics. Finally, cells are washed twice with PBS and fixed in a 1.2% paraformaldehyde solution prior to analysis. The change in emission fluorescence of CCF2 after cleavage by BlaM-Vpr is monitored by flow cytometer (520 nm before cleavage and 447 nm after upon excitation at 409 nm).
9. Density of cells should be adjusted depending of cell types and time of measurement of luciferase.
10. This pre-treatment allows inhibition of acidification of endosomes.
11. This step allows binding of particles. Concentrations of particles should be high and could be adjusted depending on the strain used. It is essential to put the same amounts of particles for all the conditions tested, especially when mutants are compared.
12. Temperature of DPBS is important to prevent internalization of particles. This step is used to remove unbound particles.
13. This step allows the priming of glycoproteins. Indeed, unlike other viruses like VSV or Semliki Forest virus, HCV requires additional step(s) to activate the pH-dependent fusion of glycoproteins (Tscherne et al., 2006). This step could be skipped to have an additional negative control.
14. This step triggers fusion. Incubation with citric acid buffer at pH7 is used as a negative control. Temperature of buffer is important for the quality of the assay and buffer at 37°C should be used to allow fusion of cells.
15. The analysis was made at 24 h post infection in (Tscherne et al., 2006) or 48 h post infection in (Perin et al., 2016). Since luciferase is a very sensitive way to detect infection, the result of this assay should be detected as soon as possible after infection to prevent the possibility of replication, assembly, secretion or second round of infection. High amounts of particles could help to reduce the time of analysis.

Acknowledgement

Our work is supported by the French “Agence Nationale de la Recherche sur le SIDA et les hépatites virales” (ANRS), the European Research Council (ERC-2008-AdG-233130-HEPCENT) and the LabEx Ecofect (ANR-11-LABX-0048).

Figure 1: Schematic representation of cell-cell fusion assay. See Methods for further details.

Figure 2: Schematic representation of virus-liposome fusion assay. See Methods for further details.

Figure 3: Schematic representation of virus-plasma membrane fusion assay. See Methods for further details.

References

1. Douam F, Lavillette D, Cosset FL (2015) The mechanism of HCV entry into host cells. Prog Mol Biol Transl Sci 129:63-107.
2. Perez-Berna AJ, Moreno MR, Guillen J, Bernabeu A, Villalain J (2006) The membrane-active regions of the hepatitis C virus E1 and E2 envelope glycoproteins. Biochemistry 45:3755-3768.
3. Takikawa S, Ishii K, Aizaki H, Suzuki T, Asakura H, Matsuura Y *et al.* (2000) Cell fusion activity of hepatitis C virus envelope proteins. J Virol 74:5066-5074.
4. Bartosch B, Dubuisson J, Cosset FL (2003) Infectious hepatitis C virus pseudo-particles containing functional E1-E2 envelope protein complexes. J Exp Med 197:633-642.
5. Lavillette D, Bartosch B, Nourrisson D, Verney G, Cosset FL, Penin F *et al.* (2006) Hepatitis C virus glycoproteins mediate low pH-dependent membrane fusion with liposomes. J Biol Chem 281:3909-3917.
6. Lavillette D, Pecheur EI, Donot P, Fresquet J, Molle J, Corbau R *et al.* (2007) Characterization of fusion determinants points to the involvement of three discrete regions of both E1 and E2 glycoproteins in the membrane fusion process of hepatitis C virus. J Virol 81:8752-8765.
7. Tscherne DM, Jones CT, Evans MJ, Lindenbach BD, McKeating JA, Rice CM (2006) Time- and temperature-dependent activation of hepatitis C virus for low-pH-triggered entry. J Virol 80:1734-1741.
8. Haid S, Pietschmann T, Pecheur EI (2009) Low pH-dependent hepatitis C virus membrane fusion depends on E2 integrity, target lipid composition, and density of virus particles. J Biol Chem 284:17657-17667.
9. Cavrois M, De Noronha C, Greene WC (2002) A sensitive and specific enzyme-based assay detecting HIV-1 virion fusion in primary T lymphocytes. Nat Biotechnol 20:1151-1154.
10. Yonezawa A, Cavrois M, Greene WC (2005) Studies of ebola virus glycoprotein-mediated entry and fusion by using pseudotyped human immunodeficiency virus type 1 virions: involvement of cytoskeletal proteins and enhancement by tumor necrosis factor alpha. J Virol 79:918-926.
11. Pecheur EI, Lavillette D, Alcaras F, Molle J, Boriskin YS, Roberts M *et al.* (2007) Biochemical mechanism of hepatitis C virus inhibition by the broad-spectrum antiviral arbidol. Biochemistry 46:6050-6059.
12. Owsianka AM, Tarr AW, Keck ZY, Li TK, Witteveldt J, Adair R *et al.* (2008) Broadly neutralizing human monoclonal antibodies to the hepatitis C virus E2 glycoprotein. J Gen Virol 89:653-659.
13. Perin PM, Haid S, Brown RJ, Doerrbecker J, Schulze K, Zeilinger C *et al.* (2016) Flunarizine prevents hepatitis C virus membrane fusion in a genotype-dependent manner by targeting the potential fusion peptide within E1. Hepatology 63:49-62.
14. Chi X, Niu Y, Cheng M, Liu X, Feng Y, Zheng F *et al.* (2016) Identification of a Potent and Broad-Spectrum Hepatitis C Virus Fusion Inhibitory Peptide from the E2 Stem Domain. Sci Rep 6:25224.
15. Matsumura T, Hu Z, Kato T, Dreux M, Zhang YY, Imamura M *et al.* (2009) Amphipathic DNA polymers inhibit hepatitis C virus infection by blocking viral entry. Gastroenterology 137:673-681.
16. Ashfaq UA, Javed T, Rehman S, Nawaz Z, Riazuddin S (2011) Lysosomotropic agents as HCV entry inhibitors. Virol J 8:163.

Table 1. HCV fusion inhibitors.

Drug/Compound	Application	Results	Concentration range	Mode of action	References
Arbidol (ARB)	HCVpp-HCVcc/Liposome fusion	Dose-dependent inhibition of HCVpp- and HCVcc-mediated lipid fusion	0.1-6 μg/ml (11.3 μM)	Membrane association	(Pecheur et al., 2007) (Haid et al., 2009)
Monoclonal antibody CBH-5 directed to an epitope in E2	HCVcc/Liposome fusion	Dose-dependent inhibition of HCVcc-mediated lipid fusion	1-25 μg/ml	Blocks E2 binding to CD81 (Owsianka et al., 2008)	(Haid et al., 2009)
Amphipathic DNA polymers	HCVcc/Liposome fusion	Inhibition of the rate and maximum extent of lipid fusion	1-10 nM	Target HCV postbinding step by an unknown mechanism	(Matsumura et al., 2009)
Peptide fusion inhibitor from E2 stem domain (E27)	Cell-cell fusion	Dose- dependent inhibition of E1E2 mediated membrane fusion	EC_{50} of 734.2±9,3 nM	Interfere with E1E2 heterodimerization	(Chi et al., 2016)
Flunarizine	Plasma membrane fusion	Reduction of HCV infection	10 μM	Targets the potential fusion peptide within E1	(Perin et al., 2016)
Concanamycin A (ConA), bafilomycin A (BafA1)	Plasma membrane fusion assay	Block HCVpp and HCVcc fusion at the endosomes	25-50 nM BafA1 5 nM ConA	Inhibitors of vacuolar ATPases that that disturb endosome acidification	(Perin et al., 2016)
Chloroquine, ammonium chloride	Plasma membrane fusion assay	Block HCVpp fusion at the endosomes (Ashfaq et al., 2011)	EC_{50} of 50 μM Chloroquine and 10 mM NH_4Cl	Weak bases that neutralize the pH of endosomes	(Perin et al., 2016)

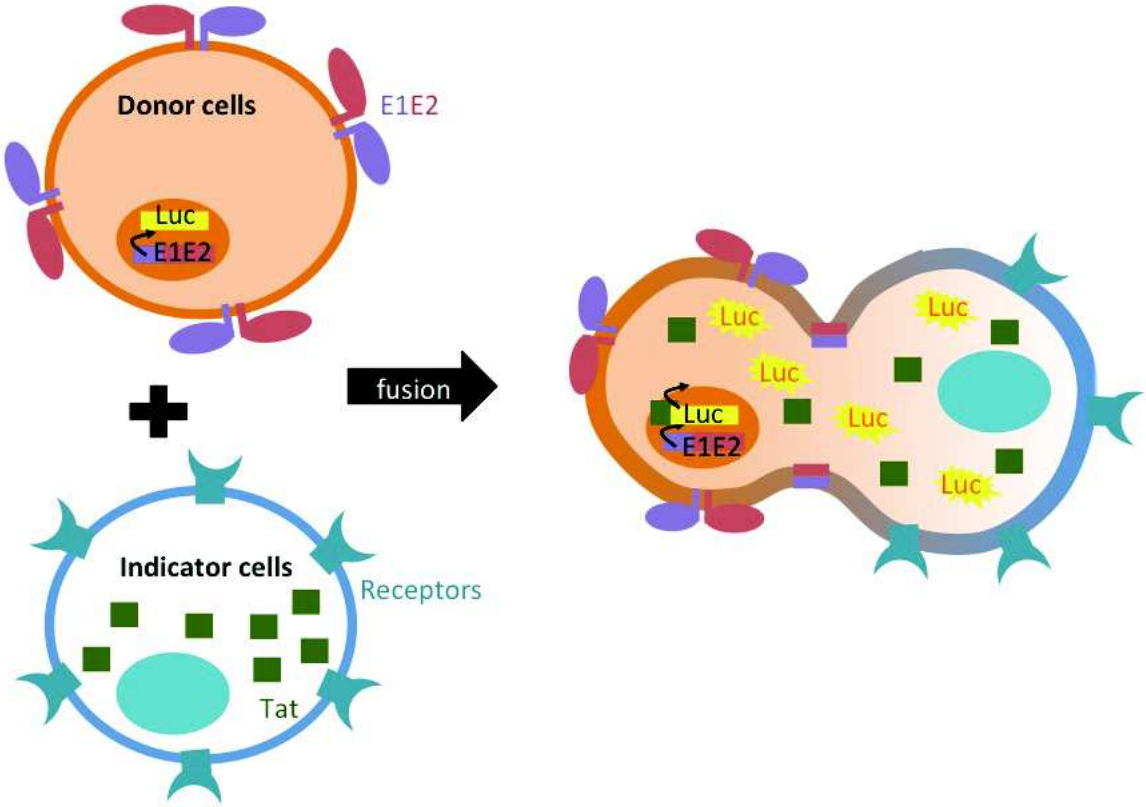
Donor cells
E1E2
Luc
E1E2
fusion
Indicator cells
Receptors
Tat
Luc
Luc
Luc
Luc
Luc
Luc
E1E2

Figure 1

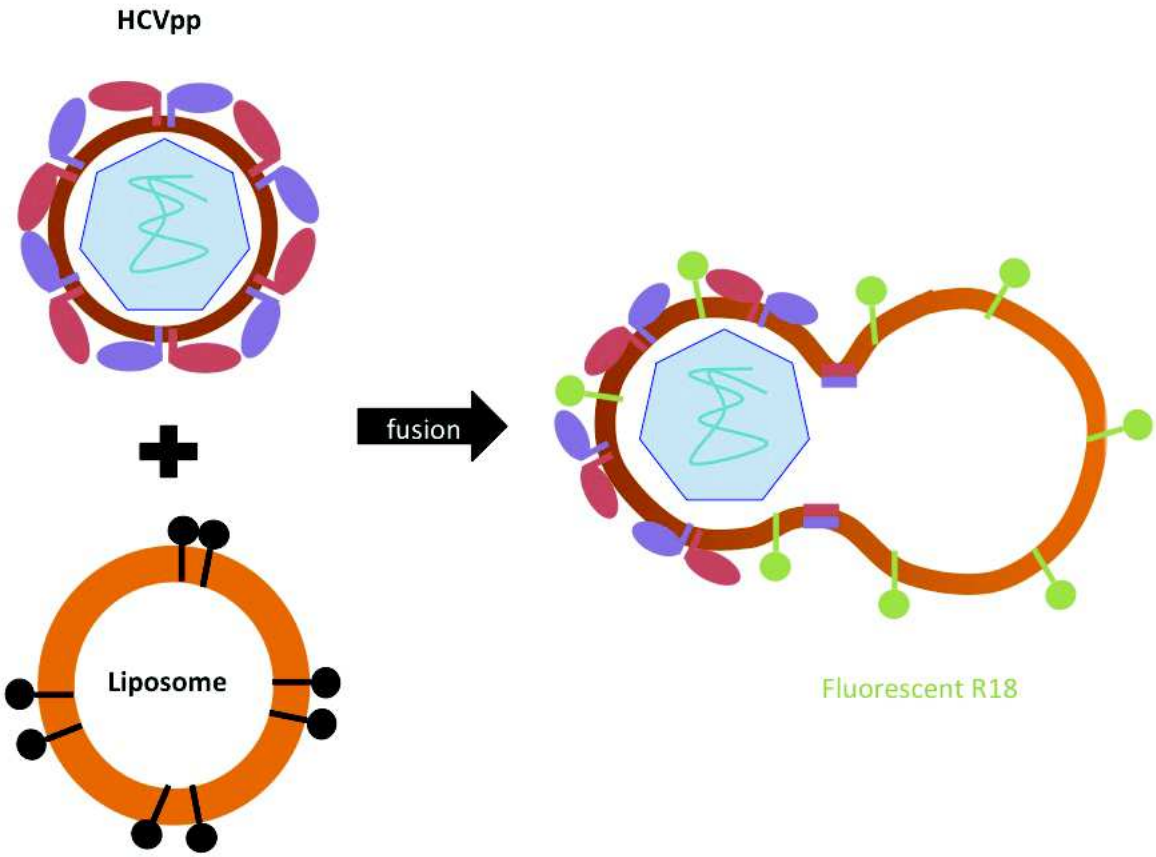

Figure 2

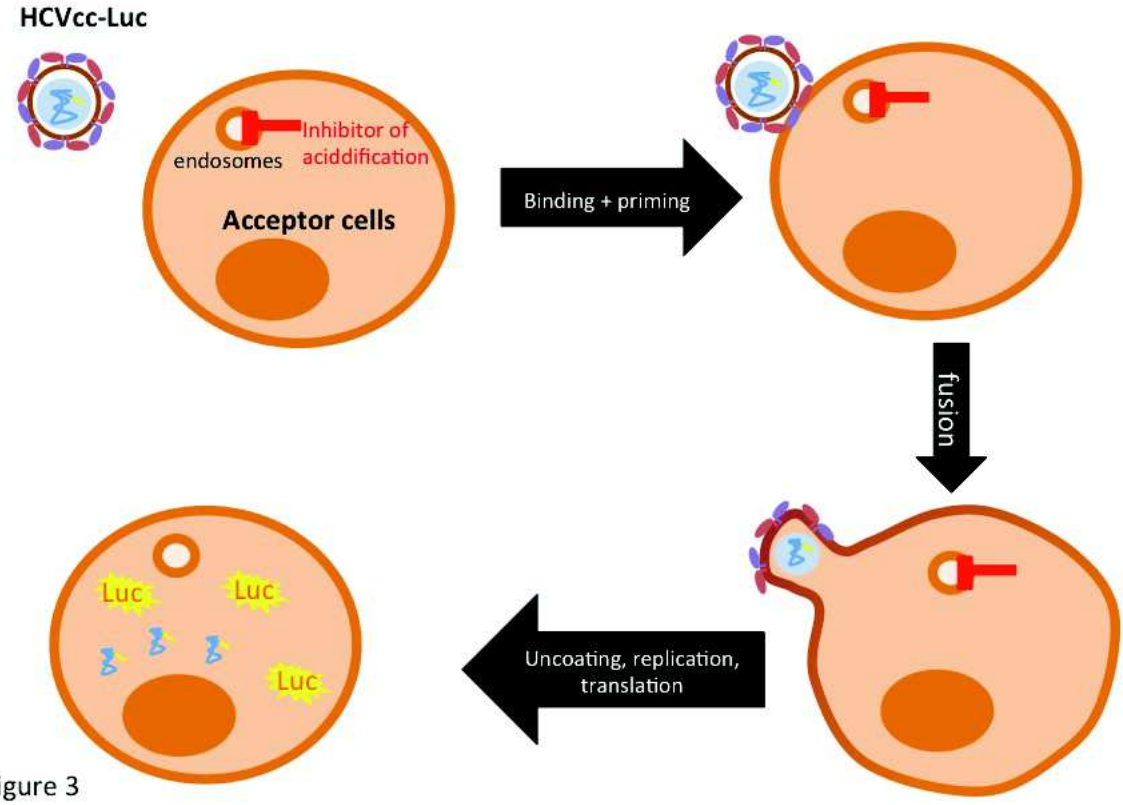
HCVcc-Luc
Inhibitor of
endosomes
aciddification
Acceptor cells
Binding + priming
fusion
Uncoating, replication,
translation
Luc
Luc
Luc

Figure 3